Pelagic Biodiversity and Ecophysiology of Copepods in the Eastern Atlantic Ocean

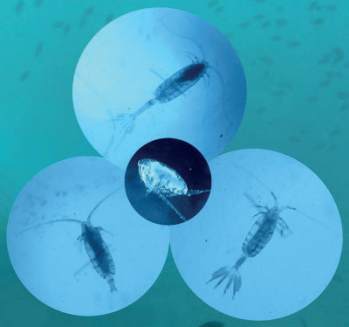

– Latitudinal and Bathymetric Aspects

Maya Bode

February 2016

GLOMAR
BreMarE Bremen Marine Ecology Centre for Research & Education
Universität Bremen
SENCKENBERG world of biodiversity
AWI

Pelagic Biodiversity and Ecophysiology of Copepods in the Eastern Atlantic Ocean – Latitudinal and Bathymetric Aspects

Maya Bode

Dissertation zur Erlangung des akademischen Grades eines Doktors der Naturwissenschaften (Dr. rer. nat.)

Bre**M**ar**E** Institut

(**B**remen **M**arine **E**cology, Centre for Research & Education)

Marine Zoologie

Fachbereich Biologie/Chemie

Universität Bremen

Februar 2016

CONTENTS

LIST OF ABBREVIATIONS

ANOSIM	Analysis of similarity
BCIR	Benguela Current influenced region
C	Carbon
Chl *a*	Chlorophyll *a*
CO_2	Carbon dioxide
COI	Cytochrome c oxidase subunit I
CTD	Conductivity-temperature-depth-profiler
DM	Dry mass
DVM	Diel vertical migration
FA	Fatty acid
Falc	Fatty alcohol
FAME	Fatty acid methyl ester
MALDI-TOF MS	Matrix-assisted laser desorption/ionization time-of-flight mass spectrometry
MDS	Multi-dimensional scaling
MOCNESS	Multiple opening/closing net and environmental sensing system
N_2	Nitrogen
NBC	Northern Benguela Current upwelling system
OM	Organic matter
OMZ	Oxygen minimum zone
OVM	Ontogenetic vertical migration
PCA	Principal component analysis
SBC	Southern Benguela Current upwelling system
SST	Sea surface temperature
SSS	Sea surface salinity
STNA	Subtropical North Atlantic
STSA	Subtropical South Atlantic
TFA	Total fatty acid
TFalc	Total fatty alcohol
TL	Total lipid
TNA	Tropical North Atlantic
TP	Trophic position/level
WE	Wax ester

SUMMARY

Pelagic copepods play a key role in marine food webs as they transfer energy from lower to higher trophic levels and are responsible for the cycling and flux of a substantial amount of organic matter. In order to reliably model ecosystem processes such as the contribution of different ecosystems to the carbon cycle, it is essential to understand the dynamics of community composition, distributional patterns and ecological roles of various key species. Copepod communities are usually characterized by strong latitudinal and bathymetric gradients. Their biodiversity is mainly regulated by environmental parameters, biological interactions and species-specific ecophysiological performances. However, major driving mechanisms generating high biodiversity are still poorly understood, especially in the deep pelagic sea.

The present thesis provides detailed information on distributional patterns, community structure and diversity of copepods in four major oceanic provinces of the tropical and subtropical eastern Atlantic, i.e. the subtropical North Atlantic (STNA), the tropical North Atlantic (TNA), the subtropical South Atlantic (STSA), a region influenced by the Benguela Current (BCIR), and additionally a coastal region of the northern Benguela Current upwelling system (NBC). The analysis of community structure was combined with ecophysiological characteristics, i.e. trophodynamics and metabolic demands of key species, to investigate trophic and spatial niche separations, food requirements and the role of copepods in mediating vertical carbon flux from the euphotic zone down to 2000 m.

Copepod abundance and biomass decreased exponentially with increasing depth, while community structure was generally more affected by depth rather than by regional differences. Highest copepod diversity was usually found in the mesopelagic zone. Thus, the twilight zone seemed to provide certain preconditions, which maintained an even higher biodiversity than found in epipelagic tropical layers. Yet, the abundance of certain key species differed between the hydrographic provinces. Also interannual and seasonal variability were observed in the NBC. For example, copepod abundance was generally lower and dominated by the oceanic species *Nannocalanus minor* during years with low spring to late summer temperature gradients, thus, less pronounced upwelling in spring and only moderate warm-water intrusions in late summer. In contrast, years with strong upwelling in spring and intensive warm-water intrusions in later summer were characterized by generally higher copepod abundances, dominated by the typical

upwelling species *Calanoides carinatus* and *Metridia lucens*, suggesting a strong link between zooplankton distribution and physical forcing.

Grazing impact of copepods was highly variable between stations and depth layers, especially in the epi- to mesopelagic zone, while diel vertical migrants such as *Pleuromamma* spp. enhanced vertical flux to deeper layers especially in the BCIR. Copepod community consumption ranged between 202 and >604 mg C m^{-2} d^{-1}, with highest ingestion rates in the TNA, where larger calanoids such as *Undinula vulgaris*, *Neocalanus gracilis, N. minor* and *Euchaeta marina* prevailed in the epipelagic zone. The total net loss rate of particulate organic carbon (POC) through copepod communities varied from 21% to 65% of surface primary production. In total, 75-90% of POC ingested by copepods was consumed by calanoids. However, the relative contribution of cyclopoids (mostly Oncaeidae) increased with depth. The impact of copepod communities on incoming POC fluxes decreased below 1000 m and POC resources reaching the bathypelagic zone were far from being fully exploited by copepods. In total, net loss rates due to copepod communities within the bathypelagic zone (1000-2000 m) varied from 11% to 22% of incoming POC, depending on the region.

Based on biomarker approaches, i.e. fatty acid and stable isotope analyses, most copepods were classified as omnivorous with carnivory/herbivory indices (CI) of ~0.5 and trophic positions (TP) of ~ 2.5, or as carnivorous with CIs ≥ 0.7 and TPs ≥ 2.9. Herbivorous copepods showed typical CIs of ≤ 0.3. Combining lipid storage profiles, trophic biomarker analyses and metabolic demands revealed a large variety of life-cycle adaptations and/or differences of dietary preferences in tropical and subtropical copepod species, which often coincided with their regional and/or vertical distributional ranges.

Accurate species identification at high taxonomic levels is crucial in ecological studies. Therefore, the applicability and potential of proteomic fingerprinting using matrix-assisted laser desorption/ionization time-of-flight mass spectrometry (MALDI-TOF MS) was evaluated as a cost- and time-efficient method not only to identify adult and juvenile closely related copepods but also to quantify specimens in net samples. An integrated taxonomic approach combining morphology, DNA sequence analyses and proteomic fingerprinting using MALDI-TOF MS was applied to investigate species richness and ontogenetic vertical distribution of the ecologically important, but often little noted deep-sea copepod family Spinocalanidae. In total, 40 putative spinocalanid species were identified, while only 28 species could be discriminated based on distinct morphological characters. Thus, species richness of Spinocalanidae was largely

underestimated. Even putative cryptic species, e.g. in the *Spinocalanus dispar* species complex, were discriminated based on protein mass spectra. Applying MALDI-TOF MS for abundance analysis yielded fine-scale spatial niches as well as ontogenetic vertical partitioning of some species of this deep-living copepod family.

To establish predictive models and integrate mesozooplankton into biogeochemical models, metabolic demands of key species and energy transfers, as well as major drivers of zooplankton biomass and community composition have to be assessed. This requires higher taxonomic, spatial and temporal resolution of distributional patterns and community structure combined with ecophysiological aspects of key species. New time- and cost-efficient molecular techniques such as the MALDI-TOF MS may allow copepod studies in much greater efficiency and detail. This will shed new light on biodiversity, plankton dynamics, phylogeographic patterns and vertical habitat partitioning, which is particularly promising for taxonomically challenging copepod groups such as cryptic species, juvenile stages and fragile deep-sea species.

ZUSAMMENFASSUNG

Copepoden spielen eine Schlüsselrolle in marinen Nahrungsnetzen, da sie niedrigere und höhere trophischen Ebenen miteinander verbinden. Durch Prozesse wie Nahrungsaufnahme, Atmung, Ausscheidung und tägliche oder ontogenetische Vertikalwanderungen haben sie einen wesentlichen Einfluss auf den marinen Kohlenstoffzyklus. Um verlässlich Ökosystemprozesse und deren Veränderungen - wie den Beitrag zum Kohlenstoffffluss - vorhersagen zu können, ist das Verständnis über die Dynamik der Gemeinschaftszusammensetzung und über die ökologischen Funktionen relevanter Schlüsselarten verschiedener Ökosysteme unerlässlich. Die Artenzusammensetzung und der Artenreichtum pelagischer Copepoden sind generell abhängig von geographischen und vertikalen Gradienten. Die Biodiversität dieser Gemeinschaften wird hauptsächlich durch Umweltfaktoren, biologische Interaktionen und artspezifische ökologische Leistungs- und Anpassungsmechanismen reguliert. Die treibenden Kräfte hoher Artenvielfalt sind jedoch vor allem in der Tiefsee bisher wenig verstanden.

Die vorliegende Studie stellt detaillierte Daten über Verbreitungsmuster, Gemeinschaftsstrukturen und Diversität von Copepoden in vier ozeanischen Regionen des tropischen und subtropischen, östlichen Atlantiks zur Verfügung: Dem subtropischen Nordatlantik (STNA), dem tropischen Nordatlantik (TNA), dem subtropischen Südatlantik (STSA), einer durch den Benguela-Strom beeinflussten Region (BCIR), sowie einer Küstenregion des nördlichen Benguela-Auftriebsgebietes (NBC). Eine Kombination von hochauflösenden Gemeinschaftsanalysen mit ökophysiologischen Parametern, wie Ernährungsstrategien und Stoffwechselraten relevanter Schlüsselarten, ermöglichte es, artspezifische Lebensstrategien und die Aufteilung in trophische und räumliche Nischen nachzuvollziehen und außerdem die Rolle der Copepoden-Gemeinschaften und bestimmter Schlüsselarten im vertikalen Kohlenstoffffluss von der euphotischen Zone bis in tiefe Wasserschichten von bis zu 2000 m zu ermitteln.

Sowohl Abundanz als auch Biomasse der Copepoden nahmen mit zunehmender Tiefe exponentiell ab. Im Allgemeinen war die Diversität der Copepoden in der mesopelagischen Zone am höchsten; während die pelagische Tiefsee generell eine höhere Biodiversität aufwies als das Epipelagial. Unterschiede in der Artzusammensetzung waren vor allem auf die Tiefe und weniger auf verschiedene Regionen zurückzuführen. Dennoch unterschied sich die Abundanz einiger Schlüsselarten in verschiedenen hydrographischen Regionen. Auch saisonale und

zwischenjährliche Varianzen im NBC wurden beobachtet. In Jahren mit weniger stark ausgeprägtem Auftrieb im Frühjahr und einem eher gemäßigten Warmwasser-Einstrom im Spätsommer, also mit geringen Frühjahr- bis Sommertemperaturgradienten, war die Häufigkeit der Copepoden generell niedriger und dominiert von der ozeanischen Art *Nannocalanus minor.* Im Gegensatz dazu waren die Abundanzen in Jahren mit starkem Auftrieb im Frühjahr und intensivem Warmwasser-Einstrom im Spätsommer höher, wobei die typischen Auftriebsarten *Calanoides carinatus* und *Metridia lucens* die Copepoden-Gemeinschaft dominierten. Dies weist auf einen starken Zusammenhang zwischen der Verteilung und Artzusammensetzung der Copepoden und physikalischen Kräften innerhalb der Wassersäule hin.

Der Fraßeinfluss der Copepoden variierte - insbesondere in der epi- und mesopelagischen Zone - stark zwischen den verschiedenen Stationen und Tiefenstufen. Vor allem im BCIR erhöhten tägliche Vertikalwanderer wie z.B. *Pleuromamma* spp. den vertikalen Transport von organischem Material in tiefere Schichten. Der tägliche Kohlenstoffbedarf der Copepoden-Gemeinschaften reichte von 202 bis >604 mg C m^{-2} d^{-1}. Die Konsumraten waren am höchsten im TNA, wo größere calanoide Arten wie z.B. *Undinula vulgaris*, *Neocalanus gracilis, N. minor* und *Euchaeta marina* vermehrt in der epipelagischen Zone auftraten. Die Nettoverlustrate von partikulärem organischem Kohlenstoff (POC) durch die Copepoden-Gemeinschaft variierte von 21% bis 65% der Primärproduktion an der Oberfläche. Insgesamt wurden 75% bis 90% des von den Copepoden aufgenommenen POC von calanoiden Copepoden konsumiert. Der Anteil von cyclopoiden Copepoden (vor allem Oncaeidae) stieg jedoch mit zunehmender Tiefe an. Unterhalb von 1000 m nahm der Einfluss der Copepoden-Gemeinschaft auf eingehende POC-Flüsse ab. Folglich wurden ankommende POC-Ressourcen im bathypelagischem Bereich (1000-2000 m) nur relativ wenig von den Copepoden genutzt. In dieser Zone betrug der Nettoverlust - je nach Region - nur noch 11% bis 22% des ankommenden POC.

Anhand von Biomarkeransätzen (Fettsäuren und stabilen Isotopen) wurden die meisten Copepoden als omnivor mit einem carnivor/herbivor-Verhältnis (Cl) von ~0.5 und einer trophischen Stufe (TP) von ~2.5, oder als carnivor mit Cls ≥ 0.7 und TPs ≥ 2.9 eingestuft. Herbivore Copepoden wiesen typischerweise Cls von ≤ 0.3 auf. Der Vergleich von Lipidspeicherungsmustern, trophischen Biomarkeranalysen und Stoffwechselraten enthüllte eine große Vielfalt an Lebensstrategien und/oder Nahrungspräferenzen der tropischen und subtropischen Copepodenarten. Unterschiede gingen meist mit Differenzen in ihrer regionalen oder vertikalen Verteilung einher.

Eine präzise Bestimmung von Organismen auf Artniveau ist ein wesentlicher Bestandteil ökologischer Planktonstudien. Daher wurde getestet, ob proteomisches Fingerprinting mit Hilfe von Matrix-unterstützter Laser-Desorptions/Ionisations (MALDI) Time-of-Flight (TOF) Massenspektrometrie (MS) dazu geeignet ist, nahverwandte Arten und schwer identifizierbare juvenile Copepoden effizient zu identifizieren und schließlich in Netzfängen zu quantifizieren. Um Artidentifizierungsmethoden direkt zu vergleichen, wurden morphologische und molekulare Analysen wie proteomisches Fingerprinting und DNA-Sequenzanalysen zusammen angewendet, um das Artenreichtum und die ontogenetische Vertikalverteilung der ökologisch wertvollen, aber oft vernachlässigten Copepoden-Familie Spinocalanidae, in Tiefsee zu untersuchen. Insgesamt konnten mit Hilfe des MALDI-TOF MS Verfahrens 40 vermeintliche spinocalanide Arten identifiziert werden, während nur 28 Arten allein auf Grund ihrer morphologischen Merkmale unterschieden werden konnten. Folglich wurde der Artenreichtum dieser Tiefseefamilie bisher erheblich unterschätzt. Sogar vermeintlich kryptische Arten - z.B. innerhalb des *Spinocalanus dispar* Artenkomplexes - konnten anhand artspezifischer Proteinmassenfingerprints unterschieden werden. Mit Hilfe der schnellen und kostengünstigen MALDI-TOF MS Methode wurden schließlich taxonomisch und räumlich hochaufgelöste vertikale Verteilungsprofile von jungen bis adulten Copepodit-Stadien der Spinocalanidae erstellt. Dies wäre anhand von morphologischen Eigenschaften nicht möglich gewesen. DNA-basierte Methoden hingegen sind derzeit zu kosten- und zeitintensiv für quantitative Planktonanalysen.

Um vorhersagekräftige Modelle zu entwickeln und Mesozooplankton in biogeochemische Modelle integrieren zu können, ist es unbedingt notwendig, den Stoffwechselbedarf bestimmter Schlüsselarten und den Energietransfer zwischen ihnen zu bestimmen, sowie die treibenden Faktoren, die die Zooplanktonbiomasse und -Gemeinschaftszusammensetzung beeinflussen, zu erfassen. Die genaue Erfassung dieser Interaktionen erfordert eine hohe taxonomische, räumliche und zeitliche Auflösung. Effiziente molekulare Techniken wie das proteomische Fingerprinting ermöglichen eine schnelle Durchführung bei gleichzeitiger detaillierterer Auflösung von Copepoden-Gemeinschaftsanalysen und gewähren so neue Erkenntnisse in Biodiversität, Plankton-Interaktionen, vertikale Verteilungsmuster und Phylogeographie. Dies ist insbesondere vielversprechend für morphologisch schwer identifizierbare Copepoden-Gruppen wie kryptische Arten, juvenile Stadien oder fragile Tiefseearten.

1 SCIENTIFIC BACKGROUND AND OBJECTIVES

The deep sea pelagic realms is at the same time the largest, but least known ecosystem on earth (Robison 2004, 2009; Ramirez-Llorda et al. 2010; Robinson et al. 2010). In particular, our knowledge about diversity and ecosystem function of the pelagic deep sea is still very fragmentary (Robinson et al. 2010). However, its enormous storage capacity for carbon (approx. 38,000 Gt C, 93% of total carbon is stored in the oceans) makes this zone very important in balancing the global carbon flux (Koppelmann and Frost 2008). Ecosystem functioning of the deep sea is largely influenced by pelagic organisms, i.e. zooplankton play a key role in mediating carbon fluxes from the surface to the ocean's interior (Longhurst and Harrison 1989; Longhurst et al. 1990; Steinberg et al. 2000; Ducklow et al. 2001; Turner 2015). Besides biomass and production of pelagic producers and consumers, the composition and richness of taxa and thus specific biological traits of key species influence the efficiency of the so-called biological carbon pump (Longhurst et al. 1990; Duffy and Stachowicz 2006; Steinberg et al. 2008, 2012). Especially in tropical and subtropical oceanic regions, knowledge about zooplankton distribution and community composition combined with trophic aspects and metabolic performance of key species is still rare. The present thesis contributes extensive data sets on the dynamics and diversity of copepod communities and their impact on the carbon flux throughout the tropical and subtropical eastern Atlantic Ocean between 24°N and 21°S, from the surface down to 2000 m, identifying key species and their specific ecophysiological characteristics.

1.1 The pelagic deep sea

Low temperatures, twilight to complete darkness, high pressure, high inorganic nutrient concentrations and low food supply pose major challenges for deep-sea organisms, in contrast to all other ecosystems on earth (Koppelmann and Frost 2008; Ramirez-Llorda et al. 2010; Robinson et al. 2010). While the mesopelagic zone (200-1000 m) is still influenced by strong gradients of environmental factors, chemical and physical parameters are rather stable in the dark zone below 1000 m (Koppelmann and Weikert 1999, 2007; Laakmann et al. 2012; Robinson et al. 2010). In total, the bathpelagic zone hosts 73% of the water in the oceans (Ramirez-Llorda et al. 2010). Around 90% of organic matter exported from the euphotic zone is respired as carbon dioxide as it sinks through the twilight zone (Armstrong et al. 2002; Koppelmann and Frost 2008). Nevertheless, changes in primary production and particle fluxes in the upper layers

usually propagate down to bathypelagic zones with time lags of several weeks to months (Voss et al. 1996; Holmes et al. 2002; Koppelmann and Weikert 2007). The mechanisms and remineralization processes that determine the export of organic matter from the euphotic zone to the deep sea remain poorly understood, as they are difficult to characterize and quantify (Laws et al. 2000). Only a few studies exist on seasonal and regional differences of mesozooplankton community structure impacting carbon flux in the deep sea, e.g. from the Northeast Pacific and Atlantic, and from the eastern Mediterranean and Arabian Seas (Sasaki et al. 1988; Yamaguchi et al. 2002; Koppelmann and Weikert 1999, 2007; Koppelmann et al. 2004; Homma et al. 2011).

While zooplankton abundance exponentially decreases with increasing depth, species diversity in the deep sea is relatively high with maxima in meso- to bathypelagic zones, despite the absence of physical barriers, which could trigger genetic isolation (Ward and Shreeve 2001; Ramirez-Llorda et al. 2010; Kosobokova et al. 2011; Laakmann et al. 2012). Mechanisms driving speciation processes and sustaining such a high biodiversity in the deep sea are not well understood, as data are especially rare for deep pelagic environments (Angel 1993; Robison et al. 2004; Duffy and Stachowicz 2006; Laakmann et al. 2012). Various mechanisms are likely to interact to reduce competition, e.g. fine-scale vertical partitioning of the water column (spatial niches) and the evolution of different life-cycle traits (e.g. prey size spectra, feeding behavior (trophic niches), migration patterns, metabolic demand and reproductive strategies), as well as physical-biological interactions, i.e. advection processes and continuous re-colonization of water masses (Ambler and Miller 1987; Weikert and Koppelmann 1993; Auel 1999; Matsuura et al. 2010; Laakmann et al. 2009a,b, 2012).

1.2 Hydrography of the tropical and subtropical eastern Atlantic

The eastern Atlantic Ocean is characterized by a complex current system forming regions with very different hydrographic conditions from the subtropical North Atlantic to the Benguela Current region (Fig. 1). The eastern part of the North Atlantic subtropical gyre consists of the Portugal Current, the Canary Current (CC) and the North Equatorial Current (NEC) centering at around 15°N (Aiken 2000). Likewise, the eastern part of the South Atlantic subtropical gyre comprises the South Atlantic Current, the Benguela Current (BC) and the South Equatorial Current (SEC), which passes across the equator. Both, the NEC and the SEC are broad uniform

westward currents north of 10°N and south of 3°N (to at least 15°S), respectively. In contrast, the eastward flowing North Equatorial Counter Current (NECC) is highly seasonal being strongest in boreal autumn between 9 and 3°N (to depths of 100 m; Aiken 2000). It transports low-salinity water affected by Amazon River outflow from west to east in the Atlantic Ocean. The CC and NECC separate the Eastern North Atlantic Central Water (ENACW) from the South Atlantic Central Water (SACW) generating the Cape Verde Frontal Zone (CVFZ) at around 20°N (Stramma and Schott 1999). A subsurface current centered on the equator at a depth of 100 m is the relatively strong westward-flowing Equatorial Undercurrent. The North and South Equatorial Undercurrents (NEU, SEU) are relatively narrow at ca. 200 m north and south of the equator, respectively. The South Equatorial Counter Current (SECC) is a rather weak current located between 7 and 9°S. These eastward flowing equatorial currents carry relatively oxygen-rich water masses. Branches of these are advected polewards forming cyclonic gyres known as the Guinea Dome located at around 10°N, 22°W in the northern and the Angola Dome centered at 10°S, 8°E in the southern hemisphere (Aiken 2000; Stramma and Schott 1999; Stramma et al. 2005).

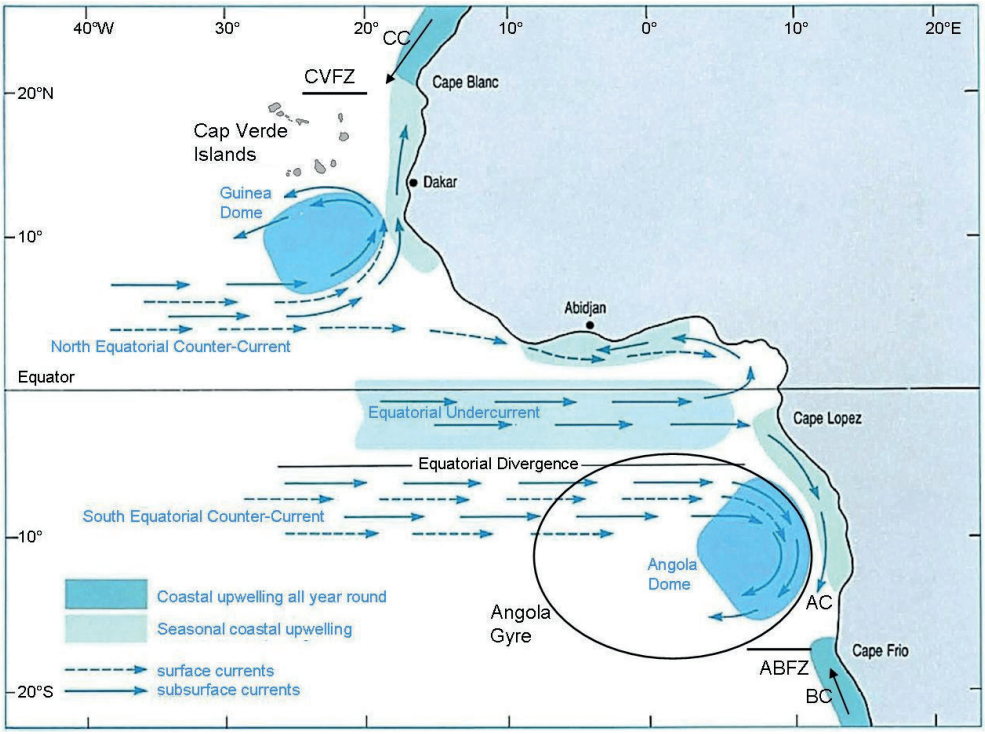

Figure 1: Eastward-flowing surface and subsurface currents in the equatorial current system of the eastern Atlantic Ocean, indicating positions of upwelling areas (after Brown et al. (2001) modified by Teuber (2014)). CVFZ: Cape Verde Frontal Zone, ABFZ: Angola-Benguela Frontal Zone, CC: Canary Current, AC: Angola Current, BC: Benguela Current, (Westward-flowing North and South Equatorial Currents not shown for clarity).

The Guinea and Angola Domes are associated with pronounced oxygen minimum zones (OMZ) in the eastern Atlantic due to stagnation of water transport in combination with continuous oxygen consumption (Stramma et al. 2008). The Angola Gyre is known to inject low-oxygen (< 45 µmol L^{-1}) and nutrient-rich SACW into surrounding regions such as the northern Benguela Current upwelling system (NBC), especially in austral summer (Mohrholz et al. 2008). In contrast, during winter the oxygen-rich Eastern SACW (ESACW) dominates and spreads northward in the NBC (Mohrholz et al. 2008). The northern boundary of the BC is marked by the Angola Benguela Frontal Zone (ABFZ) between 14 and 17°S to a depth of ~200 m, separating nutrient-poor, warmer and higher-saline Angola Current water from highly productive, colder and lower-saline waters of the BC (Shannon et al. 2006; Mohrholz et al. 2008). However, the ABFZ is not a strong barrier. The central Namibian region (19-24°S) is often affected by alongshore or onshore flows of warm waters from the North and oceanic waters from the West to Northwest (Boyd et al. 1987; Lass et al. 2000). To the south, at approx. 37°S, the BC is bordered by another warm current, the Agulhas Current and its retroflection zone (Shannon et al. 1987). Low salinity, 2-4°C cold Antarctic Intermediate Water occurs below the thermocline at average depths of 700-800 m in the BC and may be traced to at least 20°N in the Atlantic Ocean (Reid 1996; Talley 1996; Shannon and Nelson 1996).

Coastal upwelling of cold, nutrient-rich waters is responsible for the high productivity of the BC, supporting large, economically important fish stocks, which have been severely exploited since the 1950s (Boyer et al. 2000). The permanent upwelling cell at Lüderitz (27-28°S) divides the Benguela ecosystem into a northern and a southern subsystem. Upwelling-favourable, south-easterly trade winds are most pronounced during spring and summer (September to March) in the southern Benguela Current (SBC) system, but during winter and spring (July to November) in the northern Benguela Current (NBC) region (Shannon and O'Toole 2003).

1.3 Productivity and food web structures in the tropical and subtropical eastern Atlantic

Because of strong vertical stratification and thus limited nutrient supply from below the thermocline, regional primary production rates in the North and South Atlantic subtropical gyres are generally low with 18 to 362 mg C m^{-2} d^{-1} compared to 500-1000 mg C m^{-2} d^{-1} in upwelling regions (Longhurst et al. 1995; Marañón et al. 2000, 2003). Coastal upwelling systems such as the Canary Current and Benguela Current system comprise only <1% of the total ocean area, but

account for 5% of global primary production (11% of new primary production; Chávez and Toggweiler 1995) and 17% of global fish catch (Pauly and Christensen 1995; Heileman and O'Toole 2008). In contrast, open ocean ecosystems comprise 90% of the surface area of the world ocean and thus, despite their low areal production, they contribute more than 80% of global ocean primary production and 70% of total export production (Platt et al. 1989; Karl et al. 1996). The subtropical gyres alone comprise more than 60% of the total ocean surface and contribute more than 30% to global marine carbon fixation (Longhurst et al. 1995; Marañón et al. 2003). In total, the Atlantic trade wind biome produces about 4.6 Gt C y^{-1} due to its large regional expanse (Longhurst et al. 1995). Thus, understanding key processes of ecosystem functioning in these areas is crucial for quantifications and the establishment of predictive models of biogeochemical cycles (Marañón et al. 2000).

In contrast to highly seasonal mid- and high-latitude regions and coastal upwelling systems, the tropical ocean is characterized by continuous but generally low primary production rates, which results in small changes of phytoplankton and zooplankton biomass throughout the year (Longhurst 1995; Finenko et al. 2003). The most complex trophic networks are typically found in tropical waters, which are characterized by rather inefficient energy transfer, but high biodiversity (Woodd-Walker et al. 2002). Such complex networks may stabilize the community structure of tropical plankton, making them less susceptible to physical disturbances (Longhurst 1985; Post and Takimoto 2007; Giller et al. 2004). However, changes in environmental patterns such as water masses are often closely linked to variations of community structure (McGowan 1986; Painting et al. 1993; Longhurst 1995; Andersen et al. 2001; Ward and Shreeve 2001; Beaugrand et al. 2002; Beaugrand and Ibañez 2004; Loick et al. 2005).

Low concentrations of inorganic nitrogen restrict productivity in large areas of the subtropical and tropical oceans (Schlosser et al. 2014). Therefore, microbial N_2 fixation plays a crucial role in these regions by introducing bioavailable nitrogen to surface waters to fuel new primary production and sustain complex food webs (Hauss et al. 2013). In general, cyanobacteria may contribute up to 60% of the total primary production in offshore tropical oceans (Carpenter et al. 2004), while in more productive higher latitudes and upwelling regions diatoms and dinoflagellates represent typical primary producers with highly seasonal patterns (Anabalón et al. 2007; Montero et al. 2007; Barlow et al. 2009). Especially the eastern North Atlantic is regularly influenced by high iron input through Saharan dust deposition favoring high N_2 fixation (Voss et al. 2004; Capone et al. 2005; Montoya et al. 2007; Schlosser et al. 2014) and large areal

expanses of *Trichodesmium* blooms in fall and spring (Tyrrell et al. 2003; Westberry and Siegel 2006). In the oligotrophic Atlantic, the primary producer community is typically composed of cyanobacteria (*Synechococcus*, *Prochlorococcus*, *Trichodesmium*) and small autotrophic flagellates (≤5 µm) accounting for 70-90% of total photosynthetic biomass, while dinoflagellates and diatoms contribute only less than 4% and 2%, respectively, to total photosynthetic carbon (Calbet and Landry 1999; Marañón et al. 2000). Low chlorophyll *a* (chl *a*) concentrations between 20 and 40 mg chl *a* m^{-2} are usually found in oligotrophic waters of the Atlantic Ocean, with more than 60% attributed to picoplankon (<2 µm). In contrast, higher chl *a* values of 75-125 mg chl *a* m^{-2} were determined in the upwelling area off Northwest Africa, where diatoms usually dominated nutrient-rich, recently upwelled water (>10%, Marañón et al. 2000).

Hence, N_2 fixation by the filamentous cyanobacteria *Trichodesmium* or smaller diazotrophs may contribute significantly to the nitrogen pool in oligotrophic tropical and subtropical regions and oceanic environments (Voss et al. 2004; Capone et al. 2005; Staal et al. 2007). Especially in these regions, limited availability of phytoplankton is often compensated by feeding on heterotrophic protozoans (pico- and nanoflagellates) and microzooplankton (Calbet and Landry 2004; Calbet and Saiz 2005), which may directly ingest cyanobacteria. Consequently, diazotrophic nitrogen and trophic biomarkers may enter the metazoan food web (Sommer et al. 2006). Contrary to the rather complex and less efficient food webs in tropical and oceanic waters, classic food chains of coastal upwelling regions are usually shorter and more efficient, but have lower biodiversity (i.e. larger chain-forming diatoms as primary producers via small pelagic fish to top predators; Fenchel 1988; Cushing 1989). However, the trophic transfer is complex in highly dynamic upwelling regions as the planktonic community structure is strongly influenced by spatial and seasonal variability of the physical environment and microheterotrophic pathways are at times important components of food webs in these regions, especially in aging upwelled water masses and during non-upwelling seasons (Painting et al. 1993; Bode and Valera 1994; Vargas et 2007).

Opposing long-term trends in epipelagic mesozooplankton abundance and biomass were observed throughout the world's ocean: For example, zooplankton abundance in the SBC increased by more than two orders of magnitude and copepod biomass increased ten-fold from the 1950s to 1996 (Verheye and Richardson 1998, Verheye et al. 1998). Since 1995 zooplankton densities, particularly those of larger copepods have decreased again in the SBC, accompanied by an increase in anchovy biomass (Verheye et al. 1998; Hutchings et al. 2006). In contrast, zooplankton abundance in the NBC indicated a slight decrease from the 1950s to the early

1980s, whereas a marked increase appeared from 1983 onwards (Hutchings et al. 2006). Off Walvis Bay (23°S), total copepod densities increased six-fold between 1978 and 2004 followed by a decline after 2005 (Hutchings et al. 2006, 2009). Such changes were caused to a large extent by overfishing and thus by top-down mechanisms (Verheye et al. 1998; Hutchings et al. 2006), but also by environmental changes, as e.g. upwelling intensities also increased during this time period (Shannon et al. 1992), which may trigger regime shifts and alterations in species dominance at all trophic levels (Kraberg et al. 2011). In contrast, zooplankton biomass decreased by about 80% in the California Current from 1951 to 1993, while sea surface layers warmed by 1.5°C and stratification increased (Roemmich and McGowan 1995). In the North Pacific subtropical gyre a significant long-term increase in mesozooplankton biomass was documented from 1994 to 2005 (Sheridan and Landry 2004; Hannides et al. 2009). Mesozooplankton biomass also increased by 61% in the Sargasso Sea from 1994 to 2010 (Steinberg et al. 2012), while in the tropical Atlantic a nearly ten-fold decrease was observed from 1950-2000 (Piontkovski and Castellani 2009). The increase of epipelagic mesozooplankton biomass in the Sargasso Sea caused a significant, long-term increase of POC flux in the lower epipelagic zone. This was accompanied by increases in export fluxes of both passive carbon flux by fecal pellet export and active transport by diel vertical migration (DVM) (Steinberg et al. 2012). Concomitantly, smaller phytoplankton species increased in biomass and production in the Sargasso Sea (bottom-up), presumably translating organic matter into mesozooplankton biomass via the microbial food web (Steinberg et al. 2012). Decreasing predator abundance and/or the spreading of the tropical belt and thus distributional ranges of tropical species, as a result of warming, may also cause higher biomass in the subtropical regions, and lower biomass in the tropics (Hays et al. 2005; Piontkovski and Castellani 2009; Steinberg et al. 2012). Furthermore, in contrast to the Sargasso Sea, a decline in primary production was detected in the equatorial region due to thinning of the thermocline layer (Piontkovsi and Castellani 2009).

These contradictory trends exemplify how dynamic and variable environmental changes and responses of different ecosystems may be. An increase in zooplankton biomass underlines the vital role of this group in the energy transfer of different marine ecosystems. Understanding distributional patterns, diversity, trophodynamics and energetics of key species, thus ecosystem functioning, is crucial to predict ecosystem responses in a changing world. Therefore, this study focuses on these four major aspects of copepod communities with high species resolution in

different regions of the tropical and subtropical Atlantic Ocean from epi- to bathypelagic depths. Such data are particularly scarce for oceanic regions in lower latitudes.

1.4 The ecological role of copepods

Copepods are by far the most abundant (55-95%) and diverse components of mesozooplankton communities in all marine regions (Longhurst 1985; Turner 2004; Kosobokova et al. 2011). Thus, they play an important role in interlinking lower to higher trophic levels, i.e. sustaining marine fish stocks, as they are the principal food source of sardines, anchovies and other small pelagic fishes including ichthyoplankton (Heileman and O'Toole 2008). Trophic relationships are complex, as most copepod species do not merely interlink primary producers and higher trophic levels, but are usually opportunistic omnivorous feeders (Kleppel et al. 1993, 1996; Escribano and Pérez 2010; Calbet 2008; Schukat et al. 2014). However, to allow a high species diversity in the tropical Atlantic (Woodd-Walker et al. 2002; Schnack-Schiel et al. 2010), different specializations in feeding strategies are expected to exist. Yet, the natural diet of most copepod species and their trophic positions in these regions are largely unclear. To elucidate these aspects, the present study contributes a larger-scale data set on dietary preferences and trophic positions of dominant copepods along a latitudinal transect in the eastern Atlantic Ocean from 38°N to 21°S.

With their high abundance and diverse feeding habits and life strategies, copepods play an important role in the cycling of organic and inorganic matter through processes such as respiration, excretion, fecal pellet production, moulting, post-hatch and egg mortality (Longhurst and Harrison 1989; Frangoulis et al. 2005; Turner 2015). Especially under oligotrophic conditions, phytoplankton growth depends directly on the rate of nutrient regeneration by zooplankton, and indirectly on the release of dissolved organic matter providing substrates for bacterial colonization, mainly from "sloppy" feeding, excretion and feces release of zooplankton (Banse 1995). Zooplankton excretory products particularly contain high portions of inorganic and organic nutrients rapidly utilizable for primary producers (Frangoulis et al. 2005). Hence, the contribution of zooplankton excretion to nutrient regeneration is high in oligotrophic regions and may provide more than 40% of the nutrients required by phytoplankton. In contrast, this portion is lower in more productive upwelling regions (<40%), where nutrients in the euphotic

zone become replenished from deeper layers (Frangoulis et al. 2005). In general, the majority of nutrients are recycled through the microbial loop (Bode and Varela 1994).

An important component of the biological carbon pump is the total amount of carbon exported from the euphotic zone to deeper layers, the export flux. The transport of particulate and dissolved organic matter to deeper layers does not only depend on physical forcing (bottom-up), but also on the structure and function of the prevailing planktonic food web (top-down regulation) (Wassmann 1998). On its way through the water column, most of the carbon is modified by deep-living organisms into new dissolved or particulate matter (Ducklow et al. 2001). Thus, it is not necessarily removed from the ocean-atmosphere system by incorporation into the sea-floor sediment. However, once organic carbon sinks beneath the thermocline, it is effectively sequestered from the atmosphere for decades to several centuries (Bender and Heggie 1984). Meso- and bathypelagic zooplankton ingests sinking or suspended particles converting particulate organic carbon (POC) to CO_2 via respiration. Furthermore, they excrete dissolved organic matter and egest fecal pellets, fuelling microbial metabolism and mediating sinking POC flux (Steinberg et al. 2008a,b; Wilson et al. 2008). Diel vertical migrants significantly enhance the downward export of organic and inorganic carbon by consuming POC in the surface mixed layer, and metabolizing it at depth during the day (Longhurst and Harrison 1989; Longhurst et al. 1990; Steinberg et al. 2000, 2008b). At certain times and regions, respiratory carbon transported from the euphotic zone to the ocean's interior by diel migrant mesozooplankton represents the same order of magnitude as that of gravitationally sinking particles (Longhurst et al. 1990; Dam et al 1995). In the equatorial Pacific, carbon flux due to gravitational particle sinking was enhanced by 31% (March/April) and 44% (October) via diel migrant mesozooplankton (Zhang and Dam 1997). In addition, daily and ontogenetically migrating zooplankton transport organic carbon from the euphotic zone to the deep sea by predation losses and natural mortality at depth (Zhang and Dam 1997).

Changes in zooplankton biomass and community structure may significantly affect the efficiency of the biological carbon pump and thus the export of organic material to the deep ocean (Ducklow et al. 2001; Steinberg et al. 2012). Concomitantly, fluctuations in the magnitude of total and export production may strongly influence atmospheric CO_2 levels and hence climate on geological time scales. Thus, it is of utmost importance to understand key mechanisms connecting surface-water production to particle export to the deep ocean (Ducklow et al. 2001; Armstrong et al. 2002; Buesseler et al. 2007). More than one third of organic carbon flux in the

ocean appears to be channeled through mesozooplankton, which are responsible for the respiratory loss of 17-32% of photosynthetic carbon produced in the open ocean (41-77 Gt C y^{-1}; Hernández-Léon and Ikeda 2005). These estimates clearly identify mesozooplankton and thus copepods as major, but often neglected, component of the marine carbon cycle (Hernández-Léon and Ikeda 2005). Therefore, detailed research on a high-resolution taxonomic level in different regions and depth strata is necessary, in order to identify key species, their habitat preferences, metabolic demands and trophic pathways. The present study provides for the first time such a detailed data set in tropical and subtropical oceanic regions of the eastern Atlantic Ocean, elucidating the impact of different copepod assemblages on the carbon flux in discrete depth strata from surface layers down to 2000 m.

1.5 Copepods of the eastern tropical and subtropical Atlantic

Copepod biomass is usually dominated by species of the order Calanoida (Raymont 1963; Yamaguchi et al. 2002). Calanoid copepods are characterized by a wide variety of life-cycle strategies, i.e. distinct physiological and behavioral aspects such as vertical distribution. Subtropical and tropical oceanic waters sustain the highest species richness of copepods in the pelagic realm, while most of the species occur in low abundances (Wodd-Walker et al. 2002; Piontkovski et al. 2003; Rombouts et al. 2009). Horizontal distribution in tropical oceans is more or less unrestricted by physical barriers, which allows the co-occurrence and wide latitudinal ranges of many oceanic species (Schnack-Schiel et al. 2010). In contrast, strong vertical stratification, i.e. a pronounced thermocline and oxycline, effectively separates the mixed, oxygenated surface layer characterized by high temperatures from cooler, less oxygenated waters below. Hence, zooplankton communities may be structured vertically according to species-specific ecophysiological performances (Ekau et al. 2010; Stramma et al. 2010; Wishner et al. 2008, 2013). Typical epipelagic calanoids in the tropical Atlantic are small-sized species of the family Clausocalanidae and Paracalanidae, and medium-sized Calanidae, such as *Nannocalanus minor, Neocalanus gracilis, Neocalanus robustior* and *Undinula vulgaris* as well as *Euchaeta marina*, *Scolecithrix danae*, *Temora longicornis* and *Candacia* spp. (Paffenhöfer and Mazzochi 2003; Schnack-Schiel et al. 2010; Teuber et al. 2013). Fuelled by continuous, but low food supply, these species are characterized by high turnover, fast growth, intense reproduction and a short life span sustaining growth throughout the year (Kattner and Hagen 2009; Teuber et al. 2013). Other successful copepod families in all marine regions are Metridinidae and

Eucalanidae with wide distributional ranges from epi- to bathypelagic depths (Longhurst et al. 1990; Pavlova 1994; Steinberg et al. 2000; Schnack-Schiel et al. 2008; Escribano et al. 2009; Cass et al. 2011; Teuber et al. 2013; Schukat et al. 2014). In the meso- and bathypelagic zone of the tropical Atlantic, copepods commonly belong to the families Euchaetidae (e.g. *Paraeuchaeta* spp.) and Aetideidae (e.g. *Gaetanus* spp.), but also copepods such as *Megacalanus princeps* and *Gaussia princeps* are typical species of the mesopelagic copepod community (Bradford-Grieve et al. 1999; Teuber et al. 2013). However, most studies in the tropical oceanic Atlantic focused on the upper 300 m (e.g. Woodd-Walker 2001; Woodd-Walker et al. 2002; Piontkovski et al. 2003; Schnack-Schiel al. 2010). In consequence distributional patterns of copepods below the euphotic zone in these regions remain largely unknown. The present study sheds light on the variability of copepod abundance and community structure with a high species resolution, identifying key species in different regions and depths strata (0-2000 m) of the tropical and subtropical eastern Atlantic Ocean.

1.6 Copepod diversity and species identification

Recently, relationships between species composition and ecosystem functioning, i.e. production, element cycling, carbon flux and trophic transfer, have attracted more and more attention (Ducklow et al. 2001; Duffy and Stachowicz 2006). In past community structure analyses, usually the most prominent and well-known species were identified, while rare species were ignored, assuming their low abundance were equivalent to low ecological importance (Kosobokova et al. 2011). However, a high biodiversity may strongly contribute to ecosystems' resistance to environmental perturbations (Duffy and Stachowicz 2006), while the presence or absence of certain species may largely contribute to ecosystem functioning (e.g. diel migrants). Therefore, detailed explorations of zooplankton communities in various marine regions combined with species-specific biological and physiological traits have gained increasing importance to understand ecosystem functioning (Beaugrand et al. 2002; Steinberg et al. 2012; Schukat et al. 2013).

Calanoid copepods are known for their high taxonomic and ecological diversity (Mauchline 1998; Bradford-Grieve et al. 2010; Blanco-Bercial et al. 2011). Less-productive ecosystems such as epipelagic tropical regions are known for their usually high biodiversity (Woodd-Walker et al. 2002; MacPherson 2002; Rombouts et al. 2009). Biodiversity even increases in meso- to

bathypelagic layers (Yamaguchi et al. 2002; Homma et al. 2011; Kosobokova et al. 2011). The diversity of copepods is mainly regulated by environmental parameters and species-specific ecophysiological performances, while a high copepod biomass is usually accompanied by low biodiversity (Hooff and Peterson 2006).

Varying distributional patterns of certain species may serve as environmental indicators for changes in marine habitats (Beaugrand 2004, 2005). Thus, studying biodiversity and observing transitions in copepod communities can help to relate fluctuations in marine ecosystems to possible environmental changes (Beaugrand et al. 2002; Hays et al. 2005; Hooff and Peterson 2006). For that matter, accurate identification and quantification of key species are prerequisites for many ecological studies. However, both traditional morphological identification and genetic analyses perform at their limits in community studies. Classical morphological approaches usually fail to identify juvenile copepods or cryptic species, while the genetic analyses of specimens are still too time- and cost-intensive to quantify individuals in zooplankton samples. Also the application of next-generation sequencing techniques to analyze zooplankton communities is still very difficult and does not reproduce species diversity and abundance (Morhbeck et al. 2015).

Species identification and abundance analyses using dissecting microscopes are extremely tedious and require considerable experience. Identification of copepods is usually based on a few distinct characters, which are often secondary sexual characters only expressed in adult individuals, making it nearly impossible to identify juveniles by classical morphological studies. Even in adults, these diagnostic characters may be inconspicuous, may only be visible after detailed preparation of the organisms and identification is often complicated by incomplete or inconsistent taxonomic keys (e.g. Bucklin et al. 1999; Goetze 2003; Laakmann et al. 2013; Cornils and Held 2014). Moreover, high evolutionary conservation of morphological characters exacerbates accurate identification of sibling or cryptic species (Knowlton 2000; Bucklin et al. 2003, 2010; Goetze 2003). Slow rates of morphological evolution in relation to molecular evolution are common among copepods, indicating that speciation can occur without any associated morphological change (e.g. Lee and Frost 2002; Bucklin et al. 2003; Thum and Harrison 2009). This morphological stasis may be due to adaptive diversification focusing on physiological rather than on morphological traits (Knowlton 1993). This may especially be the case in non-visual invertebrates owing to the absence of sexual selection on morphology (Lee and Frost 2002). Due to these cryptic speciation processes, copepod diversity is largely

underestimated, making molecular systematic analyses particularly important (Bucklin et al. 2003).

To improve and overcome constraints of morphological species identification, molecular species discrimination methods were rapidly developed during the last decades. DNA sequence analyses of different gene fragments proved to resolve taxonomic relationships on many different levels (Bucklin et al. 2003, 2010; Blanco-Bercial et al. 2011). Analysis of a fragment of the mitochondrial cytochrome c oxidase subunit I (COI) gene proved to be a reliable tool for unambiguous species discrimination (Herbert et al. 2003a,b). Besides, DNA sequence analysis, species-specific PCR (Hill et al. 2001), restriction fragment length polymorphism (RFLP) analysis (Lindeque et al. 1999; Blanco-Bercial and Álvarez-Marqués 2007) and DNA hybridization (Kiesling et al. 2002) were successful in species delimitation. However, these DNA-based methods are still very time- and cost-intensive and require an *a priori* knowledge of species-specific sequences, i.e. accurate primer design (Feltens et al. 2010; Volta et al. 2012).

During the last two decades, protein mass fingerprinting, based on matrix-assisted laser desorption ionization time-of-flight mass spectrometry (MALDI-TOF MS), was discovered as a successful as well as time- and cost-efficient tool for microorganism identification and classification differentiating microorganisms on the genus, species and even subspecies level (Stackebrandt et al. 2005; Vargha et al. 2006). Simple sample handling, rapidity of analysis and species- or even strain-specific peak patterns in the associated mass spectra made this technology attractive for e.g. food quality control, environmental research, and veterinary and clinical diagnostics in pathogen identification (Lynn et al. 1999; Li et al. 2000; Fenselau and Demirev 2001; Tan et al. 2009). MALDI-TOF MS is particularly promising for ecological studies. As a routine and automated procedure, it may allow preparation and analysis of hundreds of individuals per day (Volta et al. 2012; Laakmann et al. 2013). Recent studies showed that MALDI-TOF MS was successful to discriminate also metazoans such as insects (Feltens et al. 2010; Kaufmann et al. 2011; Yssouf et al. 2013a,b, 2014; Uhlmann et al. 2014), fish (Volta et al. 2012), and zooplankton species such as shrimp (Salla and Murray 2013) and copepod species (Riccardi et al. 2012; Laakmann et al. 2013). The present study provides detailed information about the MALDI-TOF technology and how it may improve future copepod research. Its accuracy was tested by species identification of adults and juveniles of closely related copepods of the deep-sea family Spinocalanidae, investigating their diversity and vertical distributional patterns.

1.7 Objectives

In a changing world, with e.g. global warming, ocean acidification and expanding oxygen minimum zones, we need an improved understanding of ecological and biogeochemical interactions in the three-dimensional marine environment, considering temporal (seasonal and interannual) and spatial (horizontal and vertical) scales. The scale and scope of oceanic processes are often difficult to simulate in manipulative experiments. Therefore, detailed data collections are necessary from many different places, where naturally occurring variations in basic environmental parameters may reveal, by means of comparison, major driving forces and their effects on biological processes (Robison et al. 2004). Especially in tropical and subtropical oceanic regions, data are still too fragmentary to disentangle and predict biological, biogeochemical and physical interactions.

This thesis consists of large-scale studies on copepod distribution and ecophysiological aspects along a latitudinal transect from 24°N to 21°S in the eastern Atlantic Ocean and a longer-term data set of copepod distribution in the northern Benguela Current upwelling system. Copepod abundances, community composition and biodiversity as well as ecological niches and energetics of copepods are evaluated in relation to regional, vertical and environmental parameters in different tropical and subtropical regions of the eastern Atlantic Ocean. Knowledge about copepod distribution, community structure and their trophodynamics and energetics is still very limited in the tropical and subtropical Atlantic oceanic regions, especially below the euphotic zone. Based on energy requirements, dietary preferences, trophic levels and lipid storage patterns, different species- or taxa-specific life-history traits of copepods and how life strategies and community structure determine the efficiency of the biological carbon pump along the latitudinal transect are evaluated. These data provide the basis for the development of realistic carbon budgets and food-web models in different marine regions.

Furthermore, the applicability and potential of proteomic fingerprinting using MALDI-TOF MS is evaluated as a cost- and time-efficient method not only to identify adult and juvenile closely related copepods but also to quantify species in net samples. This may yield detailed horizontal and vertical distributional profiles of adults and developmental stages on a high taxonomic level and thus provide new insights into phylogeography, vertical niche partitioning, biodiversity and speciation processes, especially in the largely unknown pelagic deep sea. Therefore, taxonomy, species richness and distribution of the ecologically important, deep-living and largely unknown copepod family Spinocalanidae was investigated in the tropical eastern Atlantic Ocean

presenting MALDI-TOF MS as a valid tool in biodiversity research. Especially the genus *Spinocalanus* is a dominant component of meso- to abyssopelagic ecosystems at higher latitudes (Vinogradov 1972; Kosobokova et al. 2002; Yamaguchi et al. 2002; Homma et al. 2011; Kosobokova and Hopcroft 2010; Kosobokova et al. 2011) and also in the Arabian Sea (Wishner et al. 2008). In total, the family Spinocalanidae includes 59 species of 10 genera; however, many of these species names are not generally accepted or descriptions overlap and are inconsistent (Razouls et al. 2005-2015). Identification of these fragile, deep-sea species is usually exacerbated by missing morphological characters such as the first antenna and parts of the swimming legs, making molecular approaches essential in this context.

The four major working hypotheses investigated in this thesis are summarized below.

Hypothesis 1: *Copepod biomass increases with increasing primary production, with certain species characterizing different hydrographic regimes.*

Copepod distribution is mainly driven by temperature and water column stratification, thus availability of nutrients and ultimately primary production, food availability and seasonal gradients. Different copepod species with species specific life strategies thrive in different hydrographic regimes and may thus serve as indicator species. Tropical zooplankton communities are characterized by high species richness and complex trophic networks (Woodd-Walker 2001; Woodd-Walker et al. 2002; Schnack-Schiel et al. 2010). However, most previous studies were restricted to the upper 200-300 m and only worked with a low taxonomic resolution (zooplankton size classes instead of species, e.g. Huskin et al. 2001; Isla et al. 2004; San Martin et al. 2006; Calbet et al. 2009). Dynamics of copepod communities are highly variable on temporal and spatial scales. To identify their key drivers, high-resolution data sets are essential on all scales. In the present thesis, copepod abundance, biomass and community structure were investigated in different regions of the subtropical and tropical eastern Atlantic Ocean (24°N-21°S) from the surface down to 2000 m: in the Canary Basin in the subtropical North Atlantic (STNA), the Cape Verde, Sierra Leone, and Guinea basins in the tropical North Atlantic (TNA), near the Angola abyssal plains of the subtropical South Atlantic (STSA) and at the beginning of the Walvis Bay ridge in a region influenced by the Benguela Current (BCIR). Furthermore, a longer-term data set of copepod distribution and composition in the northern Benguela Current upwelling system (NBC) was analyzed and correlated with environmental

parameters. Key species and their habitat preferences were identified. In order to reliably model mechanisms of ecosystem functioning in the pelagic realm, it is a prerequisite to understand the dynamics of community structures and their respective key species, their feeding pressure and productivity (Wassmann 1998).

Hypothesis 2: *Copepod community structure has a major impact on the efficiency of the biological carbon pump.*

Copepod activities are a major but often neglected component in the carbon cycle. Metabolic demands of copepods may be used to assess their contribution to biogeochemical cycles, which is of particular importance under changing environmental conditions. Through respiration, excretion, fecal pellet production and special adaptations such as diel and ontogenetic migrations they may strongly enhance the vertical flux of inorganic carbon and organic matter from the epipelagic layers to the ocean's interior. Species-specific ecophysiological aspects such as metabolic performances, dietary preferences and predator avoidance strategies, i.e. diel and ontogenetic vertical migrations, have various impacts on the carbon flux. Thus, community structure determines the efficiency of the biological pump in certain areas (e.g. Ducklow et al. 2001; Wilson et al. 2008; Steinberg et al. 2012). In the present study, species-specific carbon consumption rates and community consumption were estimated from respiration rates of copepods in different regions of the eastern Atlantic Ocean from the surface down to 2000 m.

Hypothesis 3: *Less-productive ecosystems exhibit a high biodiversity of copepods with a large variety of feeding modes and life strategies in tropical epipelagic and pelagic deep-sea environments. Competition-minimizing mechanisms enhance pelagic biodiversity of copepods.*

Differences in trophic niches and life-cycle adaptations as well as vertical partitioning of the water column (spatial niche) are major diversity-enhancing mechanisms, allowing co-existence in the pelagic realm (Auel 1999; Laakmann et al. 2009a,b, 2012). Thus, co-existence of many different species implies a high variety of feeding modes and life strategies, even though regions of high biodiversity are generally characterized by low productivity. High biodiversity at the consumer level may also imply a corresponding high biodiversity of food items, which may be fueled in epipelagic oceanic tropical and subtropical environments by low but continuous primary production. In these regions heterotrophic micro- and picoplankton serve as crucial food

source for copepods and food webs are rather complex and inefficient (Gasol et al. 1997; Calbet and Lanry 1999; Calbet and Saiz 2005; Calbet 2008). To give new insights into prevailing mechanisms promoting high biodiversity in the pelagic deep sea, diversity of calanoid copepods combined with ecophysiological features such as trophodynamics, life strategies and nutritional demands were investigated along the latitudinal transect from 24°N to 21°S from the surface down to 2000 m to compare different types of ecosystems.

Hypothesis 4: *The analysis of species-specific proteome fingerprints gives new insights into the ontogenetic vertical distribution of closely related deep-sea copepods.*

Biodiversity in the deep sea is still likely underestimated. This is mainly due to difficulties of deep-sea sampling, morphological similarities of many closely related copepod species and incomplete identification keys. Juvenile copepodite stages usually lack distinct morphological characters. This makes identification and species-specific quantification based on morphology almost impossible.

To investigate species richness in the dominant deep-sea copepod family Spinocalanidae, an integrated taxonomic approach combining morphology (phenotype), DNA sequence analyses (genotype) of two gene fragments (18S rDNA, COI) and proteomic fingerprinting using MALDI-TOF MS was applied to adult females. As a unique feature of this study compared to previous studies, all three approaches were performed on fractions of the same specimen to allow direct comparison and test the accuracy of proteomic fingerprinting in identifying closely related and even cryptic species. The validated species-specific proteome fingerprints were then used to investigate ontogenetic vertical distribution of adult and juvenile copepodites stages. Hence, efficient molecular techniques such as proteomic fingerprinting may shed new light into distributional patterns of juveniles and taxonomically challenging species.

References

Aiken, J., Rees, N., Hooker, S., Holligan, P., Bale, A., Robins, D., Moore, G., Harris, R., Pilgrim, D., 2000. The atlantic meridional transect: Overview and synthesis of data. Prog. Oceanogr. 45, 257-312.

Ambler, J.W., Miller, C.B., 1987. Vertical habitat-partitioning by copepodites and adults of subtropical oceanic copepods. Mar. Biol. 94, 561-577.

Anabalón, V., Morales, C.E., Escribano, R., Veras, M.A., 2007. The contribution of nano- and micro-planktonic assemplages in the surface layer (0-30) under different hydrographic conditions in the upwelling area off Concepción, central Chile. Prog. Oceanogr. 75, 396-414.

Andersen, V., Nival, P., Caparroy, P., Gubanova, A., 2001. Zooplankton community during the transition from spring bloom to oligotrophy in the open NW Mediterranean and effects of wind events. 1. Abundance and specific composition. J. Plankt. Res. 23, 227-242.

Angel, M.V., 1993. Biodiversity of the pelagic ocean. Conserv. Biol. 7, 760-772.

Armstrong, R.A., Lee, C., Hedges, J.I., Honjo, S., Wakeham, S.G., 2002. A new mechanistic model for organic carbon fluxes in the ocean based on the quantitative association of POC with ballast minerals. Deep-Sea Res. II 49, 219-236.

Auel, H., 1999. The ecology of Arctic deep-sea copepods (Euchaetidae and Aetideidae). Aspects of their distribution, trophodynamics and effect on the carbon flux. Rep. Polar Res. 319, 1-97.

Banse, K., 1995. Zooplankton: Pivotal role in the control of ocean production. ICES J. Mar. Sci. 52, 265-277.

Barlow, R., Lamont, T., Mitchell-Innes, B., Lucas, M., Thomalla, S., 2009. Primary production in the Benguela ecosystem, 1999-2002. Afr. J. Mar. Sci. 31, 97-101.

Beaugrand, G., Ibañez, F., Lindley, J.A., Reid, P.C., 2002. Diversity of calanoid copepods in the North Atlantic and adjacent seas: Species associations and biogeography. Mar. Ecol. Prog. Ser. 232, 179-195.

Beaugrand, G., 2004. Monitoring marine plankton ecosystems. I: Description of an ecosystem approach based on plankton indicators. Mar. Ecol. Prog. Ser. 269, 69-81.

Beaugrand, G., Ibañez, F., 2004. Monitoring marine plankton ecosystems. II: Long-term changes in North Sea calanoid copepods in relation to hydro-climatic variability. Mar. Ecol. Prog. Ser. 284, 35-47.

Beaugrand, G., 2005. Monitoring pelagic ecosystems using plankton indicators. ICES J. Mar. Sci. 62, 333-338.

Bender, M.L., Heggie, D.T., 1984. Fate of organic carbon reaching the deep sea floor: A status report. Geochim. Cosmochim. Acta 48, 977-986.

Blanco-Bercial, L., Álvarez-Marqués, F., 2007. RFLP procedure to discriminate between *Clausocalanus* Giesbrecht, 1888 (Copepoda, Calanoida) species in the Central Cantabrian Sea. J. Exp. Mar. Biol. Ecol. 344, 73-77.

Blanco-Bercial, L., Bradford-Grieve, J.M., Bucklin, A., 2011. Molecular phylogeny of the Calanoida (Crustacea: Copepoda). Mol. Phylogenet. Evol. 59, 103-113.

Bode, A., Varela, M., 1994. Planktonic carbon and nitrogen budgets for the N-NW Spanish shelf: The role of pelagic nutrient regeneration during upwelling events. Sci. Mar. 58, 221-231.

Boyd, A.D., Salat, J., Masó, M., 1987. The seasonal intrusion of relatively saline water on the shelf off northern and central Namibia. S. Afr. J. Mar. Sci. 5, 107-120.

Boyer, D., Cole, J., Bartholomae, C., 2000. Southwestern Africa: Northern Benguela Current region. Mar. Pollut. Bull. 41, 123-140.

Bradford-Grieve, J.M., Markhaseva, E.L., Rocha, C.E.F., Abiahy, B., 1999. Copepoda. In: Boltovskoy, D. (Ed.), South Atlantic Zooplankton. Backhuys, Leiden, pp. 869-1098.

Bradford-Grieve, J.M., Boxshall, G.A., Ahyong, S.T., Ohtsuka, S., 2010. Cladistic analysis of the calanoid Copepoda. Invertebr. Syst. 24, 291-321.

Brown, E., Colling, A., Park, D., Phillips, J., Rothery, D., Wright, J., 2001. Chapter 5 - Other major current systems, Ocean Circulation. Butterworth-Heinemann, pp. 143-189.

Bucklin, A., Guarnieri, M., Hill, R.S., Bentley, A.M., Kaartvedt, S., 1999. Taxonomic assessment of planktonic copepods using mitochondrial COI sequence variation and competetive, species-specific PCR. Hydrobiol. 401, 239-254.

Bucklin, A., Frost, B.W., Bradford-Grieve, J.M., Allen, L.D., Copley, N.J., 2003. Molecular systematic and phylogenetic assessment of 34 calanoid copepod species of the Calanidae and Clausoalanidae. Mar. Biol. 142, 333-343.

Bucklin, A., Hopcroft, R.R., Kosobokova, K.N., Nigro, L.M., Ortman, B.D., Jennings, R.M., Sweetman, C.J., 2010. DNA barcoding of Arctic Ocean holozooplankton for species identification and recognition. Deep-Sea Res. II 57, 40-48.

Buesseler, K.O., Lamborg, C.H., Boyd, P.W., Lam, P.J., Trull, T.W., Bidigare, R.R., Bishop, J.K.B., Casciotti, K.L., Dehairs, F., Elskens, M., Honda, M., Karl, D.M., Siegel, D.A., Silver, M.W., Steinberg, D.K., Valdes, J., Van Mooy, B., Wilson, S., 2007. Revisiting carbon flux through the ocean's twilight zone. Science 316, 567-570.

Calbet, A., Landry, M.R., 1999. Mesozooplankton influences on the microbial food web: Direct and indirect trophic interactions in the oligotrophic open ocean. Limnol. Oceanogr. 44, 1370-1380.

Calbet, A., Landry, M.R., 2004. Phytoplankton growth, microzooplankton grazing, and carbon cycling in marine systems. Limnol. Oceanogr. 49, 51-57.

Calbet, A., Saiz, E., 2005. The ciliate-copepod link in marine ecosystems. Aquat. Microb. Ecol. 38, 157-167.

Calbet, A., 2008. The trophic roles of microzooplankton in marine systems. ICES J. Mar. Sci.: J. Cons. 65, 325-331.

Calbet, A., Atienza, D., Henriksen, C.I., Saiz, E., Adey, T.R., 2009. Zooplankton grazing in the Atlantic Ocean: A latitudinal study. Deep-Sea Res. II 56, 954-963.

Carpenter, E.J., Subramaniam, A., Capone, D.G., 2004. Biomass and primary productivity of the cyanobacterium, *Trichodesmium* spp., in the southwestern tropical N. Atlantic ocean. Deep-Sea Res. I 51, 173-203.

Cass, C.J., Wakeham, S.G., Daly, K.L., 2011. Lipid composition of tropical and subtropical copepod species of the genus *Rhincalanus* (Copepoda: Eucalanidae): A novel fatty acid and alcohol signature. Mar. Ecol. Prog. Ser. 439, 127-138.

Chàvez, F.P., Toggweiler, J.R., 1995. Physical estimates of global new production: The upwelling contribution. In: Summerhayes, C.P., Emeis, K.-C., Angel, M.V., Smith, R.L., Zeitzschel, B. (Eds.), Upwelling in the Ocean. Modern processes and acient records. Wiley, New York, pp. 313-320.

Cornils, A., Held, C., 2014. Evidence of cryptic and pseudocryptic speciation in the *Paracalanus parvus* species complex (Crustacea, Copepoda, Calanoida). Front. Zool. 11, 1-17.

Cushing, D.H., 1989. A difference in structure between ecosystems in strongly stratified waters and in those that are only weakly stratified. J. Plankt. Res. 11, 1-13.

Dam, H.G., Roman, M.R., Youngbluth, M.J., 1995. Downward export of respiratory carbon and dissolved inorganic nitrogen by diel-migrant mesozooplankton at the JGOFS Bermuda time-series station. Deep-Sea Res. I 42, 1187-1197.

Ducklow, H.W., Steinberg, D.K., Buesseler, K.O., 2001. Upper ocean carbon export and the biological pump. Oceanogr. 14, 50-58.

Duffy, J.E., Stachowicz, J.J., 2006. Why biodiversity is important to oceanography: Potential roles of genetic, species, and trophic diversity in pelagic ecosystem processes. Mar. Ecol. Prog. Ser. 311, 179-189.

Ekau, W., Auel, H., Pörtner, H.O., Gilbert, D., 2010. Impacts of hypoxia on the structure and processes in pelagic communities (zooplankton, macro-invertebrates and fish). Biogeosciences 7, 1669-1699.

Escribano, R., Hidalgo, P., Krautz, C., 2009. Zooplankton associated with the oxygen minimum zone system in the northern upwelling region of Chile during March 2000. Deep-Sea Res. II 56, 1083-1094.

Escribano, R., Pérez, C.S., 2010. Variability in fatty acids of two marine copepods upon changing food supply in the coastal upwelling zone off Chile: Importance of the picoplankton and nanoplankton fractions. J. Mar. Biol. Assoc. U. K. 90, 301-313.

Feltens, R., Gorner, R., Kalkhof, S., Groger-Arndt, H., von Bergen, M., 2010. Discrimination of different species from the genus *Drosophila* by intact protein profiling using matrix-assisted laser desorption ionization mass spectrometry. BMC Evol. Biol. 10.

Fenchel, T., 1988. Marine plankton food chains. Annu. Rev. Ecol. Syst. 19, 19-38.

Fenselau, C., Demirev, P.A., 2001. Characterization of intact microorganisms by MALDI mass spectrometry. Mass Spectrom. Rev. 20, 157-171.

Finenko, Z.Z., Piontkovski, S.A., Williams, R., Mishonov, A.V., 2003. Variability of phytoplankton and mesozooplankton biomass in the subtropical and tropical Atlantic Ocean. Mar. Ecol. Progr. Ser. 250, 125-144.

Frangoulis, C., Christou, E.D., Hecq, J.H., 2005. Comparison of marine copepod outfluxes: Nature, rate, fate and role in the carbon and nitrogen cycles. Adv. Mar. Biol. 47, 253-309.

Gasol, J.M., del Giorgio, P.A., Duarte, C.M., 1997. Biomass distribution in marine planktonic communities. Limnol. Oceanogr. 42, 1353-1363.

Goetze, E., 2003. Cryptic speciation on the high seas: Global phylogenetics of the copepod family Eucalanidae. Proc. R. Soc. Lond. B 270, 2321-2331.

Hannides, C.C.S., Landry, M.R., Benitez-Nelson, C.R., Styles, R.M., Montoya, J.P., Karl, D.M., 2009. Export stoichiometry and migrant-mediated flux of phosphorus in the North Pacific Subtropical Gyre. Deep-Sea Res. I 56, 73-88.

Hauss, H., Franz, J.M.S., Hansen, T., Struck, U., Sommer, U., 2013. Relative inputs of upwelled and atmospheric nitrogen to the eastern tropical North Atlantic food web: Spatial distribution of $\delta^{15}N$ in mesozooplankton and relation to dissolved nutrients dynamics. Deep-Sea Res. I 75, 135-145.

Hays, G.C., Richardson, A.J., Robinson, C., 2005. Climate change and marine plankton. Trends Ecol. Evol. 20, 337-344.

Heileman, S., O'Toole, M.J., 2008. Benguela Current LME. In: Sherman, K., Hempel, G. (Eds.), The UNEP Large Marine Ecosystem Report: A perspective of changing conditions in LMEs of the world's regional seas. UNEP Regional Seas Report and Studies No. 182. United Nations Environment Programme., Nairobi, Kenya, pp. 100-142.

Herbert, P.D.N., Ratnasingham, S., DeWaard, J.R., 2003a. Barcoding animal life: Cytochrome c oxidase subunit 1 divergences among closely related species. Proc. R. Soc. Lond. B (Suppl.) 270, 96-99.

Herbert, P.D.N., Cywinska, A., Ball, S.L., deWaard, J.R., 2003b. Biological identifications through DNA barcodes. Proc. R. Soc. Lond. B 270, 313-321.

Hernández-León, S., Ikeda, T., 2005. A global assessment of mesozooplankton respiration in the ocean. J. Plankt. Res. 27, 153-158.

Hill, R.S., Allen, L.D., Bucklin, A., 2001. Multiplexed species-specific PCR protocol to discriminate for N. Atlantic *Clanaus* species, with an mtCOI gene tree for ten *Calanus* species. Mar. Biol. 139, 279-287.

Holmes, E., Lavik, G., Fischer, G., Segl, M., Ruhland, G., Wefer, G., 2002. Seasonal variability of $\delta^{15}N$ in sinking particles in the Benguela upwelling region. Deep-Sea Res. I 49, 377-394.

Homma, T., Yamaguchi, A., Bower, J.R., Imai, I., 2011. Vertical changes in abundance, biomass, and community structure of copepods in the northern North Pacific and Bering Sea at 0-3000 m depth, and their role on the vertical flux of surface-produced organic material. Bull. Fish. Sci. Hokkaido Univ. 61, 29-47.

Hooff, R.C., Peterson, W.T., 2006. Copepod diversity as an indicator of changes in ocean and climate conditions of the northern California current ecosystem. Limnol. Oceanogr. 51, 2607-2620.

Huskin, I., Anadón, R., Woodd-Walker, R.S., Harris, R.P., 2001. Basin-scale latitudinal patterns of copepod grazing in the Atlantic Ocean. J. Plankt. Res. 23, 1361-1371.

Hutchings, L., Verheye, H.M.V., Hugget, J.A., Demarcq, H., Cloete, R., Barlow, R.G., Louw, D., da Silva, A., 2006. Variability of plankton with reference to fish variability in the Benguela Current Large Marine Ecosystem - An overview. In: Shannon, L.V., Hempel, G., Malanotte-Rizzoli, P., Moloney, C.L., Woods, J. (Eds.), Large Marine Ecosystems. Elsevier, Amsterdam, pp. 91-124.

Hutchings, L., van der Lingen, C.D., Shannon, L.J., Crawford, R.J.M., Verheye, H.M.S., Bartholomae, C.H., van der Plas, A.K., Louw, D., Kreiner, A., Ostrowski, M., Fidel, Q., Barlow, R.G., Lamont, T., Coetzee, J., Shillington, F., Currie, J.C., Monteiro, P.M.S., 2009. The Benguela Current: An ecosystem of four components. Prog. Oceanogr. 83, 15-32.

Isla, J.A., Llope, M., Anadon, R., 2004. Size-fractionated mesozooplankton biomass, metabolism and grazing along a 50°N-30°S transect of the Atlantic Ocean. J. Plankt. Res. 26, 1301-1313.

Karl, D.M., Christian, J.R., Dore, J.E., Hebel, D.V., Letelie, R.M., Tupas, L.M., Winn, C.D., 1996. Seasonal and interannual variability in primary production and particle flux at station ALOHA. Deep-Sea Res. II 43, 539-568.

Kattner, G., Hagen, W., 2009. Lipids in marine copepods: Latitudinal characteristics and perspectives to global warming. In: Arts, M.T., Brett, M., Kainz, M. (Eds.), Lipids in Aquatic Ecosystems. Springer, Berlin, pp. 377.

Kaufmann, C., Ziegler, D., Schaffner, F., Carpenter, S., Pfluger, V., Mathis, A., 2011. Evaluation of matrix-assisted laser desorption/ionization time-of-flight mass spectrometry for characterization of *Culicoides nubeculosus* biting midges. Med. Vet. Entomol. 25, 32-38.

Kiesling, T.L., Wilkinson, E., Rabalais, J., Ortner, P.B., McCabe, M.M., Fell, J.W., 2002. Rapid identification of adult and naupliar stages of copepods using DNA hybridization methodology. Mar. Bioltechnol. 4, 30-39.

Kleppel, G.S., 1993. On the diets of calanoid copepods. Mar. Ecol. Prog. Ser. 99, 183-195.

Kleppel, G.S., Burkart, C.A., Carter, K., Tomas, C., 1996. Diets of calanoid copepods on the West Florida continental shelf: Relationships between food concentration, food composition and feeding activity. Mar. Biol. 127, 209-217.

Knowlton, N., 1993. Sibling species in the sea. A. Rev. Ecol. Syst. 24, 189-216.

Knowlton, N., 2000. Molecular genetic analyses of species boundaries in the sea. Hydrobiol. 420, 73-90.

Koppelmann, R., Weikert, H., 1999. Temporal changes of deep-sea mesozooplankton abundance in the temperate NE Atlantic and estimates of the carbon budget. Mar. Ecol. Prog. Ser. 179, 27-40.

Koppelmann, R., Weikert, H., Halsband-Lenk, C., 2004. Mesozooplankton community respiration and its relation to particle flux in the oligotrophic eastern Mediterranean. Global Biogeochem. Cycles 18, GB1039.

Koppelmann, R., Weikert, H., 2007. Spatial and temporal distribution patterns of deep-sea mesozooplankton in the eastern Mediterranean - indications of a climatically induced shift? Mar. Ecol. 28, 259-275.

Koppelmann, R., Frost, J., 2008. The ecological role of zooplankton in the twilight and dark zones of the ocean. In: Mertens, L.P. (Ed.), Biological Oceanography Research Trends. Nova Science Publishers, Inc., New York, pp. 67-130.

Kosobokova, K.N., Hirche, H.-J., Scherzinger, T., 2002. Feeding ecology of *Spinocalanus antarcticus*, a mesopelagic copepod with a looped gut. Mar. Biol. 141, 503-511.

Kosobokova, K.N., Hopcroft, R.R., 2010. Diversity and vertical distribution of mesozooplankton in the Arctic's Canada Basin. Deep-Sea Res. II 57, 96-110.

Kosobokova, K.N., Hopcroft, R.R., Hirche, H.-J., 2011. Patterns of zooplankton diversity through the depths of the Arctic's central basins. Mar. Biodiv. 41, 29-50.

Kraberg, A.C., Wasmund, N., Vanaverbeke, J., Schiedek, D., Wiltshire, K.H., Mieszkowska, N., 2011. Regime shifts in the marine environment: The scientific basis and political context. Mar. Pollut. Bull. 62, 7-20.

Laakmann, S., Kochzius, M., Auel, H., 2009a. Ecological niches of Arctic deep-sea copepods: Vertical partitioning, dietary preferences and different trophic levels minimize inter-specific competition. Deep-Sea Res I 56, 741-756.

Laakmann, S., Stumpp, M., Auel, H., 2009b. Vertical distribution and dietary preferences of deep-sea copepods (Euchaetidae and Aetideidae; Calanoida) in the vicinity of the Antarctic Polar Front. Polar Biol. 32, 679-689.

Laakmann, S., Auel, H., Kochzius, M., 2012. Evolution in the deep sea: Biological traits, ecology and phylogenetics of pelagic copepods. Mol. Phylogenet. Evol. 65, 535-546.

Laakmann, S., Gerdts, G., Erler, R., Knebelsberger, T., Arbizu, P.M., Raupach, M.J., 2013. Comparison of molecular species identification for North Sea calanoid copepods (Crustacea) using proteome fingerprints and DNA sequences. Mol. Ecol. Resour. 13, 862-876.

Lass, H.U., Mohrholz, V., Nausch, G., 2000. Hydrographic and current measurements in the area of the Angola-Benguela front. J. Phys. Oceanogr. 30, 2589-2609.

Laws, E.A., Falkowski, P.G., Smith, W.O., Ducklow, H., McCarthy, J.J., 2000. Temperature effects on export production in the open ocean. Global Biogeochem. Cycles 14, 1231-1246.

Lee, C.E., Frost, B.W., 2002. Morphological stasis in the *Eurytemora affinis* species complex (Copepoda: Temoridae). Hydrobiol. 480, 111-128.

Li, T.Y., Liu, B.H., Chen, Y.C., 2000. Characterization of *Aspergillus* spores by matrix-assisted laser desorption/ionization time-of-flight mass spectrometry. Rapid Commun. Mass Spectrom. 14, 2393-2400.

Lindeque, P.K., Harris, R.P., Jones, M.B., Smerdon, G.R., 1999. Simple molecular method to distinguish the identity of *Calanus* species (Copepoda: Calanoida) at any developmental stage. Mar. Biol. 133, 91-96.

Loick, N., Ekau, W., Verheye, H.M., 2005. Water-body preferences of dominant calanoid copepod species in the Angola-Benguela frontal zone. Afr. J. Mar. Sci. 27, 597-608.

Longhurst, A.R., 1985. Relationship between diversity and the vertical structure of the upper ocean. Deep-Sea Res. I 32, 1535-1570.

Longhurst, A.R., Harrison, W.G., 1989. The biological pump: Profiles of plankton production and consumption in the upper ocean. Prog. Oceanogr. 22, 47–123.

Longhurst, A.R., Bedo, A.W., Harrison, W.G., Head, E.J.H., Sameoto, D.D., 1990. Vertical flux of respiratory carbon by oceanic diel migrant biota. Deep-Sea Res. I 37, 685-694.

Longhurst, A., Sathyendranath, S., Platt, T., Caverhill, C., 1995. An estimate of global primary production in the ocean from satellite radiometer data. J. Plankton Res. 17, 1245-1271.

Longhurst, A., 1995. Seasonal cycles of pelagic production and consumption. Progr. Oceanogr. 36, 77-167.

Lynn, E.C., Chung, M.C., Tsai, W.C., Han, C.C., 1999. Identification of Enterobacteriaceae bacteria by direct matrix-assisted laser desorption/ionization mass spectrometric analysis of whole cells. Rapid Comm. Mass Spectrom. 13, 2022-2027.

MacPherson, E., 2002. Large-scale-species-richness gradients in the Atlantic Ocean. Proc. R. Soc. Lond. B 269, 1715-1720.

Marañón, E., Holligan, P.M., Varela, M., Mourino, B., Bale, A.J., 2000. Basin-scale variability of phytoplankton biomass, production and growth in the Atlantic Ocean. Deep-Sea Res. I 47, 825-857.

Marañón, E., Behrenfeld, M.J., Gonzalez, N., Mourino, B., Zubkov, M.V., 2003. High variability of primary production in oligotrophic waters of the Atlantic Ocean: uncoupling from phytoplankton biomass and size structure. Mar. Ecol. Prog. Ser. 257, 1-11.

Matsuura, H., Nishida, S., Nishikawa, J., 2010. Species diversity and vertical distribution of the deep-sea copepods of the genus *Euaugaptilus* in the Sulu and Celebes Seas. Deep-Sea Res. II 57, 2098-2109.

Mauchline, J., 1998. The biology of calanoid copepods. Academic Press, San Diego, CA, 710 pp.

McGowan, J.A., 1986. The biogeography of pelagic ecosystems. UNESCO Tech. Pap. Mar. Sci. 49, 191-200.

Mohrbeck, I., Raupach, M.J., Arbizu, P.M., Knebelsberger, T., Laakmann, S., 2015. High-throughput sequencing - The key to rapid biodiversity assessment of marine metazoa? PLoS ONE 10, e0140342.

Mohrholz, V., Bartholomae, C.H., van der Plas, A.K., Lass, H.U., 2008. The seasonal variability of the northern Benguela undercurrent and its relation to the oxygen budget on the shelf. Cont. Shelf Res. 28, 424-441.

Montero, P., Daneri, G., Cuevas, L.A., Gonzáez, H.E., Jacob, B., Lizarraga, L., Menschel, E., 2007. Productivity cycles in the coastal upwelling area off Concepcion: The importance of diatoms and bacterioplankton in the organic carbon flux. Prog. Oceanogr. 75, 518-530.

Montoya, J.P., 2007. Natural abundance of ^{15}N in marine planktonic ecosystems. In: Michener, R., Lajtha, K. (Eds.), Stable isotopes in ecology and environmental science. Blackwell Publ., pp. 176-201.

Paffenhöfer, G.-A., Mazzocchi, M.G., 2003. Vertical distribution of subtropical epiplanktonic copepods. J. Plankt. Res. 25, 1139-1156.

Painting, S.J., Lucas, M.I., Peterson, W.T., Brown, P.C., Hutching, L., Mitchell-Innes, B.A., 1993. Dynamics of bacterioplankton, phytoplankton and mesozooplankton communities during the development of an upwelling plume in the southern Benguela. Mar. Ecol. Prog. Ser 100, 35-53.

Pauly, D., Christensen, V., 1995. Primary production required to sustain global fisheries. Nature 374, 255-257.

Pavlova, E.V., 1994. Diel changes in copepod respiration rates. Hydrobiologia 292/293, 333–339.

Piontkovski, S., Williams, R., Ignatyev, S., Boltachev, A., Chesalin, M., 2003. Structural-functional relationships in the pelagic community of the eastern tropical Atlantic Ocean. J. Plankt. Res. 25, 1021-1034.

Piontkovski, S.A., Castellani, C., 2009. Long-term declining trend of zooplankton biomass in the Tropical Atlantic. Hydrobiologia 632, 365-370.

Platt, T., Harrison, W.G., Lewis, M.R., Li, W.K.W., Sathyendranath, S., Smith, R.E., Vezina, A.F., 1989. Biological production of the oceans: The case for a consensus. Mar. Ecol. Prog. Ser 52, 77-88.

Post, D.M., Takimoto, G., 2007. Proximate structural mechanisms for variation in food-chain length. Oikos 116, 775-782.

Ramirez-Llorda, E., Brandt, A., Danovaro, R., De Mol, B., Escobar, E., German, C.R., Levin, L.A., Martinez-Arbizu, P., Menot, L., Buhl-Mortensen, P., Narayanaswamy, B.E., Smith, C.R., Tittensor, D.P., Tyler, P.A., Vanreusel, A., Vecchione, M., 2010. Deep, diverse and definitely different: Unique attributes of the world's largest ecosystem. Biogeosciences 7, 2851-2899.

Raymont, J.E.G., 1963. Plankton and productivity in the oceans. Pergamon Press, Oxford/New York, 660 pp.

Razouls, C., de Bovée, F., Kouwenberg, J., Desreumaux, N., 2005-2015. Diversity and geographic distribution of marine planktonic copepods. Available at http://copepodes.obs-banyuls.fr/en. Accessed December 15, 2015.

Reid, J.R., 1996. On the circulation of the South Atlantic Ocean. In: Wefer, G., Berger, W.H., Siedler, G., Webb, D.J. (Eds.), The South Atlantic: Present and past circulation. Spinger-Verlag, Berlin Heidelberg, pp. 13-44.

Riccardi, N., Lucini, L., Benagli, C., Welker, M., Wicht, B., Tonolla, M., 2012. Potential of matrix-assisted laser desorption/ionization time-of-flight mass spectrometry (MALDI-TOF MS) for the identification of freshwater zooplankton: A pilot study with three *Eudiaptomus* (Copepoda: Diaptomidae) species. J. Plankt. Res. 34, 484-492.

Robinson, C., Steinberg, D.K., Anderson, T.R., Arístegui, J., Carlson, C.A., Frost, J.R., Ghiglione, J.-F., Hernández-León, S., Jackson, G.A., Koppelmann, R., Quéguiner, B., Ragueneau, O., Rassoulzadegan, F., Robison, B.H., Tamburini, C., Tanaka, T., Wishner, K.F., Zhang, J., 2010. Mesopelagic zone ecology and biogeochemistry - a synthesis. Deep-Sea Res. II 57, 1504-1518.

Robison, B.H., 2004. Deep pelagic biology. J. Exp. Mar. Biol. Ecol. 300, 253-272.

Robison, B.H., 2009. Conservation of deep pelagic biodiversity. Conserv. Biol. 23, 847-858.

Roemmich, D., McGowan, J., 1995. Climatic Warming and the Decline of Zooplankton in the California Current. Science 267, 1324-1326.

Rombouts, I., Beaugrand, G., Ibañez, F., Gasparini, S., Chiba, S., Legendre, L., 2009. Global latitudinal variations in marine copepod diversity and environmental factors. Proc. R. Soc. B doi:10.1098/rspb.2009.0742.

Salla, V., Murray, K.K., 2013. Matrix-assisted laser desorption/ionization mass spectrometry for identification of shrimp. Anal. Chim. Acta 794, 55-59.

San Martin, E., Harris, R.P., Irigoien, X., 2006. Latitudinal variation in plankton size spectra in the Atlantic Ocean. Deep-Sea Res. II 53, 1560-1572.

Sasaki, H., Hattori, H., Nishizawa, S., 1988. Downward flux of particulate organic-matter and vertical-distribution of calanoid copepods in the Oyashio water in summer. Deep-Sea Res. I 35, 505-515.

Schlosser, C., Klar, J.K., Wake, B.D., Snow, J.T., Honey, D.J., Woodward, E.M.S., Lohan, M.C., Achterberg, E.P., Moore, C.M., 2014. Seasonal ITCZ migration dynamically controls the location of the (sub)tropical Atlantic biogeochemical divide. Proc. Natl. Acad. Sci. U.S.A. 111, 1438-1442.

Schnack-Schiel, S.B., Mizdalski, E., Cornils, A., 2010. Copepod abundance and species composition in the Eastern subtropical/tropical Atlantic. Deep-Sea Res. II 57, 2064-2075.

Schukat, A., Teuber, L., Hagen, W., Wasmund, N., Auel, H., 2013. Energetics and carbon budgets of dominant calanoid copepods in the northern Benguela upwelling system. J. Exp. Mar. Biol. Ecol. 442, 1-9.

Schukat, A., Auel, H., Teuber, L., Hagen, W., 2014. Complex trophic interactions of calanoid copepods in the Benguela upwelling system. J. Sea Res. 85, 186-196.

Shannon, L.V., Pillar, S.C., 1986. The Benguela ecosystem. Part III. Plankton. In: Barnes, M. (Ed.), Oceanography and Marine Biology. An annual review. University Press, Aberdeen, pp. 65-170.

Shannon, L.V., Agenbag, J.J., Buys, M.E.L., 1987. Large- and mesoscale features of the Angola-Benguela front. S. Afr. J. Mar. Sci. 5, 11-34.

Shannon, L.V., Crawford, R.J.M., Pollock, D.E., Hutchings, L., Boyd, A.D., Taunton-Clark, J., Badenhorst, A., Melville-Smith, R., Augustyn, C., Cochrance, K.L., Hampton, I., Nelson, G., Japp, D.W., Tarr, R.J.Q., 1992. The 1980s - A decade of change in the Benguela ecosystem. In: Payne, A.I.L., Brink, K.H., Mann, K.H., Hilborn, R. (Eds.), Benguela trophic functioning. S. Afr. J. Mar. Sc., pp. 271-276.

Shannon, L.V., Nelson, G., 1996. The Benguela: Large scale features and processes and system variability. In: Wefer, G., Berger, W.H., Siedler, G., Webb, D.J. (Eds.), The South Atlantic: Present and past circulation. Springer-Verlag, Berlin Heidelberg, pp. 163-210.

Shannon, L.V., O'Toole, M.J., 2003. Sustainability of the Benguela: *ex Africa semper aliquid novi*. In: Hempel, G., Sherman, K. (Eds.), Large marine ecosystems: trends in exploitation, protection and research. Elsevier, Amsterdam, pp. 227-253.

Shannon, L.V., Hempel, G., Malanotte-Rizzoli, P., Moloney, C.L., Woods, J., 2006. Benguela: Predicting a Large Marine Ecosystem. Large Marine Ecosystems 14. Elsevier, Amsterdam, 410 pp.

Sheridan, C.C., Landry, M.R., 2004. A 9-year increasing trend in mesozooplankton biomass at the Hawaii Ocean Time-Series Station ALOHA. ICES J. Mar. Sci. 61, 457-463.

Sommer, F., Hansen, T., Sommer, U., 2006. Transfer of diazotrophic nitrogen to mesozooplankton in Kiel Fjord, Western Baltic Sea: A mesocosm study. Mar. Ecol. Prog. Ser. 324, 105-112.

Staal, M., Hekkert, S.t.L., Brummer, G.J., Veldhuis, M., Sikkens, C., Persijn, S., Stal, L.J., 2007. Nitrogen fixation along a north-south transect in the eastern Atlantic Ocean. Limnol. Oceanogr. 52, 1305-1316.

Stackebrandt, E., Päuker, O., Erhard, M., 2005. Grouping Myxococci (*Corallococcus*) strains by matrix-assisted laser desorption/ionization time-of-flight (MALDI-TOF) mass spectrometry: Comparison with gene sequence phylogenies. Curr. Microbiol. 50, 71-77.

Steinberg, D.K., Carlson, C.A., Bates, N.R., Goldthwait, S.A., Madin, L.P., Michaels, A.F., 2000. Zooplankton vertical migration and the active transport of dissolved organic and inorganic carbon in the Sargasso Sea. Deep-Sea Res. I 47, 137-158.

Steinberg, D.K., Van Mooy, B.A.S., Buesseler, K.O., Boyd, P.W., Kobari, T., Karl, D.M., 2008a. Bacterial vs. zooplankton control of sinking particle flux in the ocean's twilight zone. Limnol. Oceanogr. 53, 1327-1338.

Steinberg, D.K., Cope, J.S., Wilson, S.E., Kobari, T., 2008b. A comparison of mesopelagic mesozooplankton community structure in the subtropical and subarctic North Pacific Ocean. Deep-Sea Res. II 55, 1615-1635.

Steinberg, D.K., Lomas, M.W., Cope, J.S., 2012. Long-term increase in mesozooplankton biomass in the Sargasso Sea: Linkage to climate and implications for food web dynamics and biogeochemical cycling. Global Biogeochem. Cycles 26.

Stramma, L., Schott, F., 1999. The mean flow field of the tropical Atlantic Ocean. Deep-Sea Res. II 46, 279-303.

Stramma, L., Huttl, S., Schafstall, J., 2005. Water masses and currents in the upper tropical northeast Atlantic off northwest Africa. J. Geophys. Res. 110, C12006.

Stramma, L., Brandt, P., Schafstall, J., Schott, F., Fischer, J., Kortzinger, A., 2008. Oxygen minimum zone in the North Atlantic south and east of the Cape Verde Islands. J. Geophys. Res. 113, C04014.

Stramma, L., Schmidtko, S., Levin, L.A., Johnson, G.C., 2010. Ocean oxygen minima expansions and their biological impacts. Deep-Sea Res. I 57, 587-595.

Talley, L.D., 1996. Antarctic Intermediate Water in the South Atlantic. In: Wefer, G., Berger, W.H., Siedler, G., Webb, D.J. (Eds.), The South Atlantic: Present and past circulation. Springer-Verlag, Berlin Heidelberg, pp. 219-238.

Tan, S.W.L., Wong, S.M., Kini, R.M., 2000. Rapid simultaneous detection of two orchid viruses using LC- and/or MALDI-mass spectrometry. J. Virol. Methods 85, 93-99.

Teuber, L., Kiko, R., Seguin, F., Auel, H., 2013. Respiration rates of tropical Atlantic copepods in relation to the oxygen minimum zone. J. Exp. Mar. Biol. Ecol. 448, 28-36.

Teuber, L., 2014. Ecology and physiology of calanoid copepods in relation to the oxygen minimum zone in the eastern tropical Atlantic. University of Bremen, Bremen, pp. 101.

Thum, R.A., Harrison, R.G., 2009. Deep genetic divergence among morphologically similar and parapatric *Skistodiaptomus* (Copepoda: Calanoida: Diaptomidae) challenge the hypothesis of Pleistocene speciation. Biol. J. Linnean. Soc. 96, 150-165.

Turner, J.T., 2004. The importance of small planktonic copepods and their roles in pelagic marine food webs. Zool. Stud. 43, 255-266.

Turner, J.T., 2015. Zooplankton fecal pellets, marine snow, phytodetritus and the ocean's biological pump. Progr. Oceanogr. 130, 205-248.

Tyrrell, T., Maranon, E., Poulton, A.J., Bowie, A.R., Harbour, D.S., Woodward, E.M.S., 2003. Large-scale latitudinal distribution of *Trichodesmium* spp. in the Atlantic Ocean. J. Plankt. Res. 25, 405-416.

Uhlmann, K.R., Gibb, S., Kalkhof, S., Arroyo-Abad, U., Schulz, C., Hoffmann, B., Stubbins, F., Carpenter, S., Beer, M., Von Bergen, M., Feltens, R., 2014. Species determination of *Culicoides* biting midges via peptide profiling using matrix-assisted laser desorption ionization mass spectrometry. Parasit. Vectors 7, 392.

Vargas, C.A., Martinez, R.A., Cuevas, L.A., Pavez, M.A., Cartes, C., Gonzalez, H.E., Escribano, R., Daneri, G., 2007. The relative importance of microbial and classical food webs in a highly productive coastal upwelling area. Limnol. Oceanogr. 52, 1495-1510.

Vargha, M., Takáts, Z., Konopka, A., Nakatsu, C.H., 2006. Optimization of MALDI-TOF MS for strain level differentiation of *Arthrobacter isolates*. J. Microbiol. Methods 66, 399-409.

Verheye, H.M.V., Richardson, A.J., Hutchings, L., Marska, G., Gianokouros, D., 1998. Long-term trends in the abundance and community structure of coastal zooplankton in the southern Benguela system, 1951-1996. S. Afr. J. Mar. Sci. 19, 317-332.

Verheye, H.M., Richardson, A.J., 1998. Long-term increase in crustacean zooplankton abundance in the southern Benguela upwelling region (1951-1996): Bottom-up or top-down control? ICES J. Mar. Sci. 55, 803-807.

Vinogradov, M.E., 1972. Vertical distribution of oceanic zooplankton. Israel Programm for Scientific Translations. Jerusalem, 1-339.

Volta, P., Riccardi, N., Lauceri, R., Tonolla, M., 2012. Discrimination of freshwater fish species by Matrix-Assisted Laser Desorption/Ionization-Time of Flight Mass Spectrometry (MALDI-TOF MS): A pilot study. J. Limnol. 71, 164-169.

Voss, M., Altabet, M.A., von Bodungen, B., 1996. $\delta^{15}N$ in sedimenting particles as indicator of euphotic-zone processes. Deep-Sea Res. I 43, 33-47.

Voss, M., Croot, P., Lochte, K., Mills, M., Peeken, I., 2004. Patterns of nitrogen fixation along 10°N in the tropical Atlantic. Geophys. Res. Lett. 31, 1-4.

Ward, P., Shreeve, R.S., 2001. The deep-sea copepod fauna of the Southern Ocean: patterns and processes. Hydrobiologia 453, 37-54.

Wassmann, P., 1998. Retention versus export food chains: processes controlling sinking loss from marine pelagic systems. Hydrobiol. 363, 29-57.

Weikert, H., Koppelmann, R., 1993. Vertical structural patterns of deep-living zooplankton in the NE Atlantic, the Levantine Sea and the Red Sea - A comparison. Oceanol. Acta 16, 163-177.

Westberry, T.K., Siegel, D.A., 2006. Spatial and temporal distribution of *Trichodesmium* blooms in the world's oceans. Global Biogeochem. Cycles 20, GB4016.

Wilson, S.E., Steinberg, D.K., Buesseler, K.O., 2008. Changes in fecal pellet characteristics with depth as indicators of zooplankton repackaging of particles in the mesopelagic zone of the subtropical and subarctic North Pacific Ocean. Deep-Sea Res. II 55, 14-15.

Wishner, K.F., Gelfman, C., Gowing, M.M., Outram, D.M., Rapien, M., Williams, R.L., 2008. Vertical zonation and distributions of calanoid copepods through the lower oxycline of the Arabian Sea oxygen minimum zone. Prog. Oceanogr. 78, 163-191.

Wishner, K.F., Outram, D.M., Seibel, B.A., Daly, K.L., Williams, R.L., 2013. Zooplankton in the eastern tropical north Pacific: Boundary effects of oxygen minimum zone expansion. Deep-Sea Res. I 79, 122-140.

Woodd-Walker, R.S., 2001. Spatial distributions of copepod genera along the Atlantic Meridional Transect. Hydrobiol. 453, 161-170.

Woodd-Walker, R.S., Ward, P., Clarke, A., 2002. Large-scale patterns in diversity and community structure of surface water copepods from the Atlantic Ocean. Mar. Ecol. Progr. Ser. 236, 189-203.

Yamaguchi, A., Watanabe, Y., Ishida, H., Harimoto, T., Furusawa, K., Suzuki, S., Ishizaka, J., Ikeda, T., Takahashi, M.M., 2002. Community and trophic structures of pelagic copepods down to greater depths in the western subarctic Pacific (WEST-COSMIC). Deep-Sea Res. I 49, 1007-1025.

Yssouf, A., Flaudrops, C., Drali, R., Kernif, T., Socolovschi, C., Berenger, J.M., Raoult, D., Parola, P., 2013a. Matrix-assisted laser desorption ionization time-of-flight mass spectrometry for rapid identification of tick vectors. J. Clin. Microbiol. 51, 522-528.

Yssouf, A., Socolovschi, C., Flaudrops, C., Ndiath, M.O., Sougoufara, S., Dehecq, J.S., Lacour, G., Berenger, J.M., Sokhna, C.S., Raoult, D., Parola, P., 2013b. Matrix-assisted laser desorption ionization time-

of-flight mass spectrometry: An emerging tool for the rapid identification of mosquito vectors. PLoS ONE 8, e72380.

Yssouf, A., Socolovschi, C., Leulmi, H., Kernif, T., Bitam, I., Audoly, G., Almeras, L., Raoult, D., Parola, P., 2014. Identification of flea species using MALDI-TOF/MS. Comp. Immunol. Microbiol. Infect. Dis. 37, 153-157.

Zhang, X.S., Dam, H.G., 1997. Downward export of carbon by diel migrant mesozooplankton in the central equatorial Pacific. Deep-Sea Res. II 44, 2191-2202.

2 PUBLICATIONS

Outline of Publications

The following overview illustrates the five publications and an additional chapter, which comprise the central part of my PhD thesis. The general idea for this PhD project was developed by PD Dr. H. Auel and Prof. Dr. W. Hagen, and extended by Dr. A. Cornils and Dr. S. Laakmann. The laboratory work and data analyses was done by myself at the department of Marine Zoology and partly at the Center for Environmental Research and Sustainable Technology (UFT) at the University of Bremen, the Alfred-Wegener-Institute (AWI) in Bremerhaven, the German Center for Marine Biodiversity Research (DZMB) at the Senckenberg am Meer in Wilhelmshaven and the National Marine Information and Research Centre (NatMIRC) in Swakopmund, Namibia.

CHAPTER I

Bode M, Kreiner A, van der Plas AK, Louw DC, Horaeb R, Auel H, Hagen W

Spatio-temporal variability of copepod abundance along the 20°S monitoring transect in the Northern Benguela upwelling system from 2005 to 2011

The data were compiled onboard RV *Welwitchia* between 2005 and 2011 by the scientists of the NatMIRC in Swakopmund, Namibia. I visited the NatMIRC in 2012 to analyze this longer-term data set. The manuscript was written by myself with scientific and editorial advice from all co-authors.

The manuscript was published in PLoS ONE 9(5): e97738 in May 2014.

CHAPTER II

Bode M, Hagen W, Schukat A, Teuber L, Fonseca-Batista D, Dehairs F, Auel H

Feeding strategies of tropical and subtropical calanoid copepods throughout the eastern Atlantic Ocean – Latitudinal and bathymetric aspects

The idea and concept of this manuscript was compiled by myself with assistance from H. Auel and W. Hagen. I conducted the field work together with H. Auel, L. Teuber, F. Dehairs and the students of the EUROPA training cruise (ANTXXIX/1) onboard *RV Polarstern* in 2012. I performed

the biochemical analyses of zooplankton at the department of Marine Zoology at the University of Bremen. D. Fonseca-Batista conducted the biochemical analyses of POM. I analyzed the data and wrote the manuscript with scientific advice from all co-authors.

The manuscript was published in Progress in Oceanography 138: 268-282 in October 2015.

CHAPTER III

Fonseca-Batista D, Dehairs F, Riou V, Fripiat F, Elskens M, Deman F, Brion N, Bode M, Auel H

Contribution of N_2 fixation to biological productivity along a meridional section in the Eastern Atlantic Ocean

I shared field work with H. Auel and F. Dehairs and provided scientific advice during the preparation of the manuscript.

The manuscript was submitted to Progress in Oceanography in November 2015.

CHAPTER IV

Bode M, Hagen W, Koppelmann R, Cornils A, Teuber L, Kaiser P, Auel H

Role of copepod communities in carbon budgets in the eastern Atlantic Ocean – Regional and vertical patterns from 24°N to 21°S

I developed the concept of the manuscript with advice from H. Auel and R. Koppelmann. I conducted the field work together with H. Auel, L. Teuber and the students of the EUROPA trainings cruise (ANTXXIX/1). A. Cornils introduced me to the taxonomy of small calanoid copepod species. The abundance and community analysis was conducted by myself with the help of P. Kaiser at the department of Marine Zoology at the University of Bremen. I performed the data analyses and wrote the manuscript with scientific advice from all co-authors.

The manuscript was submitted to Deep-Sea Research I in December 2015.

CHAPTER V

Bode M, Laakmann S, Kaiser P, Hagen W, Auel H, Cornils A

Unraveling diversity of deep-sea copepods using integrated morphological and molecular techniques

I developed the concept of this manuscript together with A. Cornils and S. Laakmann, who both introduced me to genetic analyses. S. Laakmann also introduced me to MALDI-TOF MS measurements which were performed by myself at the DZMB at the Senckenberg am Meer, Wilhelmshaven. The samples were collected during a research cruise with *RV Polarstern* in 2007. I sorted the samples at the AWI in Bremerhaven. Genetic analyses were performed at the department of Marine Zoology and partly at the UFT at the University of Bremen. P. Kaiser performed the analyses of the 18S rDNA sequence within the framework of a student research project. I performed the data analysis and wrote the manuscript with advice from all co-authors.

The manuscript was submitted to Molecular Phylogenetics and Evolution in January 2016.

CHAPTER VI

Kaiser P, Bode M, Cornils A, Hagen W, Auel H, Laakmann S

High-resolution community analysis of deep-sea copepods using proteomic fingerprinting

The data were compiled within the frame work of a Master Thesis by P. Kaiser. The idea was established by S. Laakmann together with A. Cornils and myself. I instructed and supervised the laboratory work and data analyses performed by P. Kaiser. The MALDI-TOF MS analysis was performed at the DZMB at the Senckenberg am Meer, Wilhelmshaven. The Master Thesis was written by P. Kaiser with scientific and editorial advice from all co-authors. In this chapter, I summarize the most important findings, which lead to the overall conclusion of the applicability and potential value of using proteomic fingerprinting in copepod biodiversity research.

P. Kaiser will prepare the manuscript for publication under the supervision of all co-authors.

CHAPTER I

Spatio-temporal Variability of Copepod Abundance along the 20°S Monitoring Transect in the Northern Benguela Upwelling System from 2005 to 2011

Bode M, Kreiner A, van der Plas AK, Louw DC, Horaeb R, Auel H and Hagen W

Published in PLoS ONE 9(5): e97738 (2014)

OPEN ACCESS Freely available online

PLOS ONE

Spatio-Temporal Variability of Copepod Abundance along the 20°S Monitoring Transect in the Northern Benguela Upwelling System from 2005 to 2011

Maya Bode[1]*, Anja Kreiner[2], Anja K. van der Plas[2], Deon C. Louw[2], Richard Horaeb[2], Holger Auel[1], Wilhelm Hagen[1]

1 BreMarE - Bremen Marine Ecology, Marine Zoology, University of Bremen, Bremen, Germany, **2** National Marine Information and Research Centre (NatMIRC), Swakopmund, Namibia

Abstract

Long-term data sets are essential to understand climate-induced variability in marine ecosystems. This study provides the first comprehensive analysis of longer-term temporal and spatial variations in zooplankton abundance and copepod community structure in the northern Benguela upwelling system from 2005 to 2011. Samples were collected from the upper 200 m along a transect at 20°S perpendicular to the coast of Namibia to 70 nm offshore. Based on seasonal and interannual trends in surface temperature and salinity, three distinct time periods were discernible with stronger upwelling in spring and extensive warm-water intrusions in late summer, thus, high temperature amplitudes, in the years 2005/06 and 2010/11, and less intensive upwelling followed by weaker warm-water intrusions from 2008/09 to 2009/10. Zooplankton abundance reflected these changes with higher numbers in 2005/06 and 2010/11. In contrast, zooplankton density was lower in 2008/09 and 2009/10, when temperature gradients from spring to late summer were less pronounced. Spatially, copepod abundance tended to be highest between 30 and 60 nautical miles off the coast, coinciding with the shelf break and continental slope. The dominant larger calanoid copepods were *Calanoides carinatus*, *Metridia lucens* and *Nannocalanus minor*. On all three scales studied, i.e. spatially from the coast to offshore waters as well as temporally, both seasonally and interannually, maximum zooplankton abundance was not coupled to the coldest temperature regime, and hence strongest upwelling intensity. Pronounced temperature amplitudes, and therefore strong gradients within a year, were apparently important and resulted in higher zooplankton abundance.

Citation: Bode M, Kreiner A, van der Plas AK, Louw DC, Horaeb R, et al. (2014) Spatio-Temporal Variability of Copepod Abundance along the 20°S Monitoring Transect in the Northern Benguela Upwelling System from 2005 to 2011. PLoS ONE 9(5): e97738. doi:10.1371/journal.pone.0097738

Editor: Hans G. Dam, University of Connecticut, United States of America

Received November 1, 2013; **Accepted** April 23, 2014; **Published** May 20, 2014

Funding: This study is embedded in the GENUS project (03F0650E), which is funded by the German Federal Ministry of Education and Research (BMBF). The funders had no role in study design, data collection and analysis, decision to publish, or preparation of the manuscript.

Competing Interests: The authors have declared that no competing interests exist.

* E-mail: mabode@uni-bremen.de

Introduction

The Benguela Current upwelling region, extending along the South West African coast from 17 to 34°S, belongs to the four major eastern boundary currents in the world [1]. It is one of the most productive marine ecosystems reaching an average annual primary production of about 400–900 g C m^{-2} yr^{-1} [2–4]. Coastal upwelling of cold, nutrient-rich waters is a prerequisite for its high productivity, supporting large, economically important fish stocks, which have been severely exploited since the 1950s [1,5]. As a unique feature, the Benguela Current upwelling system is bordered by warm, (sub-)tropical water masses, both at its northern and southern margins, i.e. by the Angola Current to the North and by the Agulhas Current and its retroflection zone to the South [6]. As part of the South Atlantic subtropical gyre, hypoxic, nutrient-rich South Atlantic central water (SACW) intrudes into the northern Benguela subsystem in summer, whereas oxygen-rich Eastern SACW is transported northwards during winter [7]. The permanent upwelling centre at Lüderitz (27–28°S) divides the Benguela ecosystem into a northern and a southern subsystem. Upwelling-favourable, south-easterly trade winds are most pronounced during spring and summer (September to March) in the southern Benguela Current (SBC) system and during winter and spring (July to November) in the northern Benguela Current (NBC) region [8]. The NBC region is characterized by highly variable upwelling intensities depending on local bathymetry, wind speed, wave action and frequent intrusions of tropical Angola Current waters [1]. Usually, the Angola-Benguela frontal zone (ABFZ) is situated between 14°S and 17°S, separating the oligotrophic tropical ecosystem from the nutrient-rich Benguela upwelling system [1]. The ABFZ is not a strong barrier, but periodically injects tropical waters into the surface layer of the NBC system [7,9]. The central Namibian region (19–24°S) is often affected by onshore or alongshore flows of tropical waters from the North and oceanic waters from the West to Northwest [10–12].

As dominant primary consumers, zooplankton provide an important link from lower to upper trophic levels [13]. Copepods are the most abundant (55–95%) and diverse components of mesozooplankton communities in all marine regions [13]. In the NBC region they usually dominate zooplankton communities by 70–85% [14]. Thus, they play an important role in sustaining

marine fish stocks, as they are the principal food source of sardines, anchovies and other pelagic fishes including their larval stages [2]. Long-term trends in, and relationships between, zooplankton, small pelagic fish stocks and environmental parameters have attracted growing interest in the context of climate change effects on marine ecosystems [15]. Due to its historical importance for Namibia's fishing industry, the area around Walvis Bay called "Walvis Bay routine area" (21–24°S) was studied most intensively in the past [16–18]. Between 1972 and 1982 the study area was expanded from 18 to 26°S during the South West African Pelagic Egg and Larval Surveys (SWAPELS) (for details see [19]). However, only a small fraction of these data have been analysed and published with regard to zooplankton, particularly copepod community composition [15].

The National Marine Information and Research Centre (NatMIRC) in Swakopmund, Namibia, is responsible for studying and managing the NBC ecosystem. In this context, they regularly monitor hydrographic parameters and plankton composition along several transects off the Namibian coast. Since March 2005, zooplankton samples were collected regularly along with oceanographic data, such as temperature, salinity, oxygen and chlorophyll *a* concentration in the upper 200 m along a transect at 20°S. This study provides the first analysis of these data with special reference to temporal and spatial variations in zooplankton abundance and copepod community structure from 2005 to 2011. The spatial and temporal distribution of total copepods as well as dominant calanoid copepod species was analysed and evaluated in relation to environmental factors.

Materials and Methods

Ethics Statement

Zooplankton samples have been collected by scientists from the National Marine Information and Research Centre (NatMIRC) in Swakopmund, which is part of the Ministry of Fisheries and Marine Resources and as such the responsible governmental agency for marine research in Namibia. This study on zooplankton does not include protected or endangered species. The deployment of WP2 nets has a negligible and non-measurable impact on the zooplankton community.

Sampling

Zooplankton samples were collected along a transect at 20°S off Namibia approximately every other month starting in March 2005. The stations were always located at the same positions at 2, 5, 10, 20, 30, 40, 50, 60, and 70 nm from the coast (Fig. 1). For this study, stations within 5 nm from shore are referred to as "inshore stations", while stations between 10 and 30 nm are on the continental shelf, thus "shelf stations", and stations beyond 40 nm from the coast are referred to as "offshore stations". Zooplankton samples were collected on board the research vessel "*Welwitchia*" using a WP2 net (0.25 m^2 mouth opening, 200 µm mesh size) deployed from 200 m (or 10 m above the bottom if bottom depth <200 m) to the surface. The flow was measured by a calibrated flowmeter mounted within the mouth of the net. In addition, oceanographic data such as temperature, salinity and oxygen profiles were measured concomitantly with a conductivity temperature depth (CTD) sensor (Fig. 2). At each station chlorophyll *a* concentration was calculated with a Model 10 Turner design fluorometer from water samples collected at four depth levels between 2 and 30 m. A mean value was taken for each station and converted to surface chlorophyll *a* concentration (mg m^{-2}). Zooplankton samples were preserved in 5% borax-buffered formaldehyde for subsequent taxonomic identification. Larger jelly-fish were removed from the samples before preservation. Mesozooplankton was identified and enumerated with special attention given to copepods. Several subsamples were taken using a Hensen Stempel pipette and analysed until about 500 individuals in total were counted from each station. Larger copepods (> 1.5 mm) were identified to genus or even species level if possible and counted separately. Smaller species, including *Clausocalanus arcuicornis*, *Paracalanus parvus*, *Paracalanus crassirostris*, *Ctenocalanus vanus* etc., were combined under the category "small calanoid copepods". Estimates of abundance per surface area (no. m^{-2}) were calculated from the respective water volume filtered and maximum sampling depth. The total copepod abundances reported here include adult and copepodite stages CI-CVI. The sampling map as well as three dimensional figures were created with Ocean Data View 4 [20] using *DIVA gridding* as gridding method. A general linear model (GLM) was applied to explore the relationship of log transformed copepod abundances (totals and individual species) with several physical, temporal and spatial variables, but revealed no conclusive results.

Principal component analysis

Variation in environmental data was explored applying principal component analysis (PCA) to identify environmental gradients throughout the study period. Potential environmental factors influencing copepod distribution were temperature, salinity, oxygen concentration (taken from the CTD data at 10 m depth) and chlorophyll *a*. Environmental parameters were standardized (log(x+1)) and normalized prior to PCA. Years were added as quantitative supplement, while the different months and sampling regions (inshore, shelf and offshore; for definition see above) were added as categorical supplement. The correlation

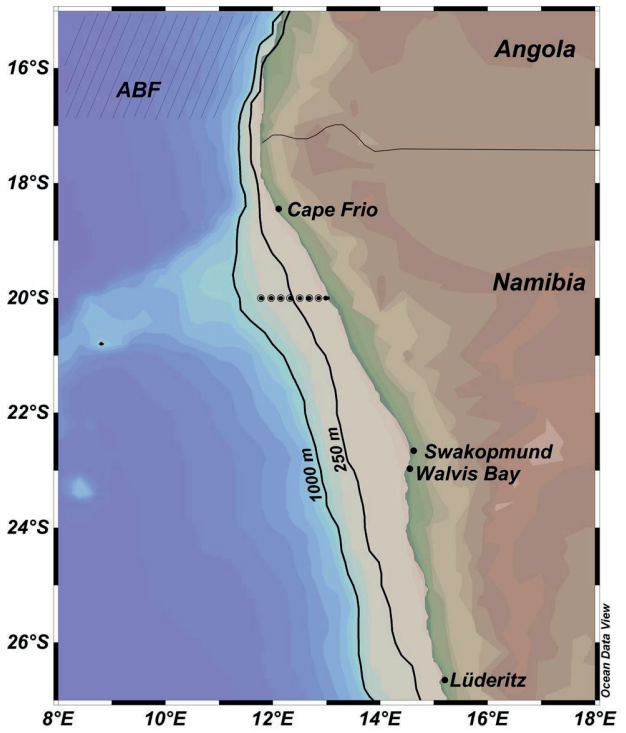

Figure 1. Location of the monitoring transect at 20°S off Namibia and approximate position of the Angola Benguela Front (ABF).
doi:10.1371/journal.pone.0097738.g001

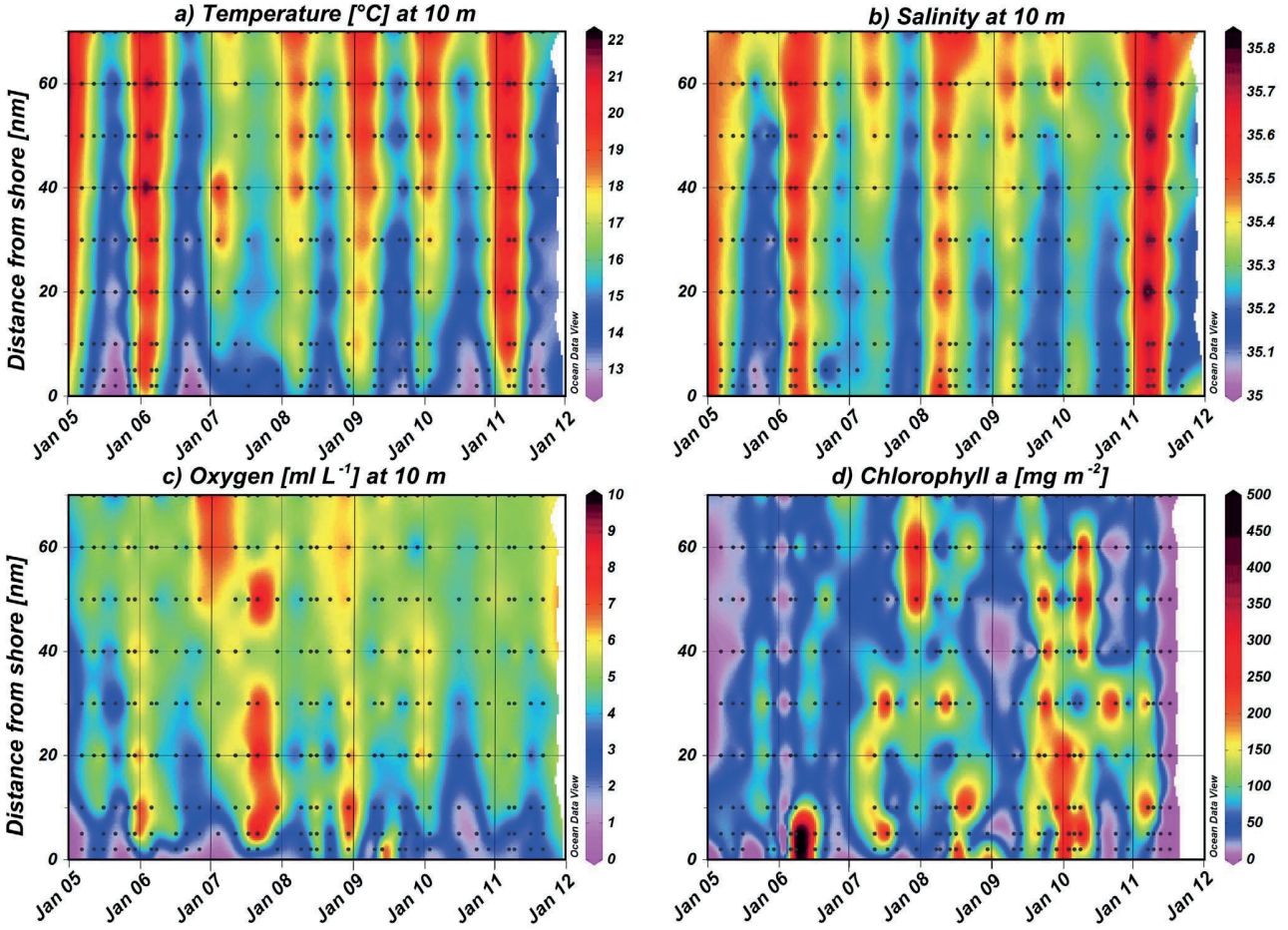

Figure 2. Horizontal and temporal distribution of a) temperature, b) salinity and c) oxygen concentration at 10 m and d) mean chlorophyll *a* concentration in the upper 30 m along the monitoring line at 20°S from March 2005 until September 2011. Black dots represent actual sampling positions and white areas indicate data gaps.
doi:10.1371/journal.pone.0097738.g002

matrix was used to calculate eigenvectors and principal components (PCs), which were ranked in order of significance. The contribution of each variable to each PC was estimated. In Figure 3, inshore, shelf and offshore stations are marked with different symbols (triangles, dots and squares, resp.), while months are pooled in quiescent (light grey: February-April), transition (dark grey: December and May), and upwelling (black: June-November) periods for a better overview (January was not monitored).

Results

Hydrography

At the 20°S transect, temperature and salinity showed a clear seasonal cycle with highest mean temperatures in March and lowest in September/October (Figs. 2 and 4). In March and April temperatures at 10 m depth ranged from 15° to 22°C. Coastal upwelling generally started in May or June with temperatures dropping below 15°C. From July to November temperatures were below 14°C, and coastal upwelling was strongest from September to November (<13°C). Cold, upwelled water was characterized by low salinities between 35.0 and 35.3, while maximum temperatures above 20°C were associated with salinities ≥35.7. Temperature generally increased from inshore to offshore stations by 3–4°C. However, there were substantial interannual variations in upwelling intensity and intrusions of tropical warm waters. Extensive warm-water intrusions of the Angola Current in late summer and autumn occurred in the same years as strong upwelling in spring. Therefore, years could be characterised according to the temperature amplitude with either high or low temperature gradients between spring and autumn. The years 2005/06 and 2010/11 showed comparatively wide temperature amplitudes (Figs. 2 and 5). In contrast, 2008/09 showed a rather weak gradient, with less intense upwelling in July and September 2008 accompanied by weak warm-water intrusions in April 2009 (Figs. 2 and 5). The years 2006/07, 2007/08 and 2009/10 cannot be clearly assigned to either of these two categories. Oceanographic data are missing in autumn 2007 and 2010, as well as in spring 2007 due to technical failure of the temperature and conductivity sensor of the CTD during these cruises. Because of these data gaps, the intensity of Angola Current intrusions in autumn 2007 is uncertain, but upwelling intensity was strong in spring 2006 and temperatures were below average in September and November 2006 (Figs. 2 and 5). In contrast, the upwelling intensity in spring 2007 was not recorded reliably, but the intrusion of tropical water in autumn 2008 was weak. However, temperatures in July 2007 were above average, whereas December 2007 and April 2008 were colder than usual (Fig. 5). Likewise,

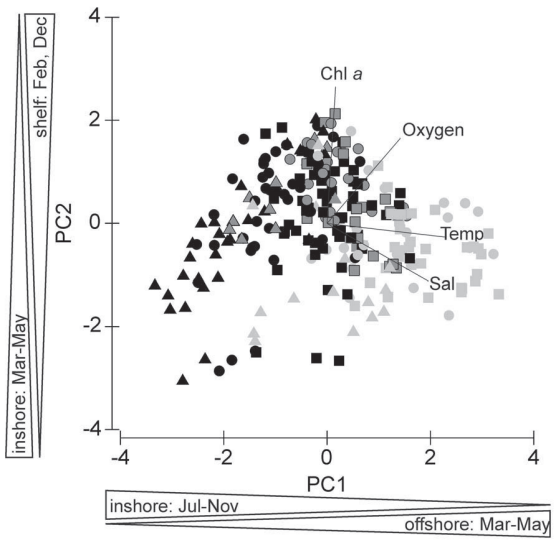

Figure 3. Inshore (triangles), shelf (circles) and offshore (squares) stations arranged according to the first two principal components. For a better overview, upwelling months (June-November) are black, while quiescent months (February to April) are light grey. Data of May and December are marked in dark grey, since these months showed a distinct oceanographic regime compared to the other months (start and end of upwelling period).
doi:10.1371/journal.pone.0097738.g003

temperatures were above average in spring 2008 and 2009, thus, reflecting weaker upwelling intensity, whereas temperatures in April 2009 were below average (Fig. 5). However, the extent of warm-water intrusions was not recorded properly during these years; especially in autumn 2010 data are missing. Besides indicators of either weak upwelling or weak warm-water intrusions, inshore temperatures above 14°C each July from 2007/08 until 2009/10 may indicate years of low temperature gradients. In contrast, inshore temperatures below 14°C were measured in July 2005, 2006, 2010 and 2011, years of high temperature gradients.

Oxygen concentration was generally low within the first 10 nm on the shelf and the permanent oxygen minimum zone (OMZ) ($<$ 1.4 ml L^{-1}) was more pronounced during quiescent months due to intrusions of low-oxygen Angola Current waters. The OMZ was usually observed between 40 and 60 m water depth, but oxygen concentrations below 1.4 ml L^{-1} even occurred at 10 m depth at 2 nm in March, September and November 2005, February 2007, April 2009 and November 2010 (Fig. 2). Chlorophyll *a* concentration in the upper 30 m was usually lower during the years 2005/06 and 2006/07, except for the peak value at 2 and 5 nm from shore in April 2006 of 540 mg Chl *a* m^{-2}. From the year 2007/08 onwards maximum concentrations of $>$200 mg Chl *a* m^{-2} were measured on the shelf in July 2007, April, May and July 2008, September 2009 throughout April 2010, September 2010 and March/April 2011. In contrast, such high concentrations were present in the offshore region only in December 2007, September 2009 and April 2010 (Fig. 2). In general, chlorophyll *a* concentration was higher in the inshore or shelf region compared to the offshore region and showed highest monthly means in February and April (Fig. 4).

Principal component (PC) analysis identified three main components, which were determined by temperature, salinity, oxygen and chlorophyll *a* concentration and accounted for 95% of the variance in the environmental data set (Fig. 3). The first PC mainly represents temperature and salinity followed by oxygen concentration (p-values $<$0.0001) with positive eigenvectors (47% of variance explained). In the first categorical dimension the offshore stations in March, April and May had positive, whereas inshore stations in the upwelling months from July to November had negative effects (p-values $<$0.0001, except May: p-value = 0.04). The second PC is mostly represented by chlorophyll *a*, oxygen concentration and salinity, for which chlorophyll *a* and oxygen content exhibited positive and salinity negative eigenvectors (p-values $<$0.0003; 28% of variance explained). Stations on the shelf in February and December were positively correlated with the second categorical dimension (p-values $<$0.004), while inshore stations in March, April and May showed negative effects (p-values $<$0.04). In Figure 3, inshore stations monitored from July to November coincided with colder temperatures and lower chlorophyll *a* concentrations, whereas inshore stations in December and May were associated with intermediate temperatures and higher oxygen and chlorophyll *a* concentrations. In contrast, inshore stations in February, March and April were characterized by warmer temperatures and lower chlorophyll *a* concentrations. In general, temperatures increased from inshore to offshore stations.

Mesozooplankton community structure, abundance and distribution

Total mesozooplankton abundance ranged from 3×10^3 m^{-2} at the 70 nm station in July 2010 to 943×10^3 m^{-2} at 30 nm in May 2011 (Fig. 6). In 2005/06 and 2006/07, zooplankton abundance was highest (Figs. 6 and 7), while 2005/06 was characterized by a pronounced temperature gradient from spring to late summer (Figs. 2 and 5). In contrast, zooplankton abundance was lowest in 2008/09 and 2009/10 (Figs. 6 and 7), which were characterized by low seasonal temperature amplitudes. In 2010/11, upwelling intensity increased again, followed by massive warm-water intrusions in autumn and high zooplankton abundances, particularly at 30 nm from shore (Figs. 6 and 7). Copepods usually dominated the zooplankton community and, on average, accounted for 78% of total zooplankton abundance. Hence, the distributional pattern of total copepods reflected that of total zooplankton (Figs. 4–7). The only exceptions were observed at the 10 nm station in September 2006 and March 2008, when echinoderm larvae dominated the zooplankton catch and between 2 and 10 nm from shore in May 2011, when cyclopoid copepods prevailed (Fig. 6). Apart from 2010/11, mean annual copepod abundance was generally higher in the offshore region, but was not significantly different from mean abundances on the shelf (Mann-Whitney U test, p-values $\geq$0.054). In contrast, annual copepod abundance averages were significantly lower at the 2 and 5 nm stations in the year 2006/07, 2008/09 and 2009/10 compared to the shelf and offshore stations in the same years (Mann-Whitney U test, p-values $\leq$0.018). In general, total copepod densities increased from inshore towards offshore regions with maxima usually occurring between 30 and 50 nm, albeit with strong interannual variations (Figs. 4, 6 and 8). Extremely high copepod densities were recorded at 30 nm from shore in September/December 2010 and July/September 2011 explaining the maximum value in Figure 8.

Total copepod abundance ranged from 3×10^3 m^{-2} at 70 nm from the coast in July 2010 to 857×10^3 m^{-2} at 30 nm in May 2011. Maxima of more than 500×10^3 m^{-2} were encountered in May 2007 and 2011 as well as in July 2006. Copepod densities of $300–500\times10^3$ m^{-2} occurred between March and May 2005, 2007, 2008, 2011, in July 2006, 2007, 2011 and in September 2011 as well as in November-December 2005 and 2010. No obvious seasonal cycles were observed throughout the year.

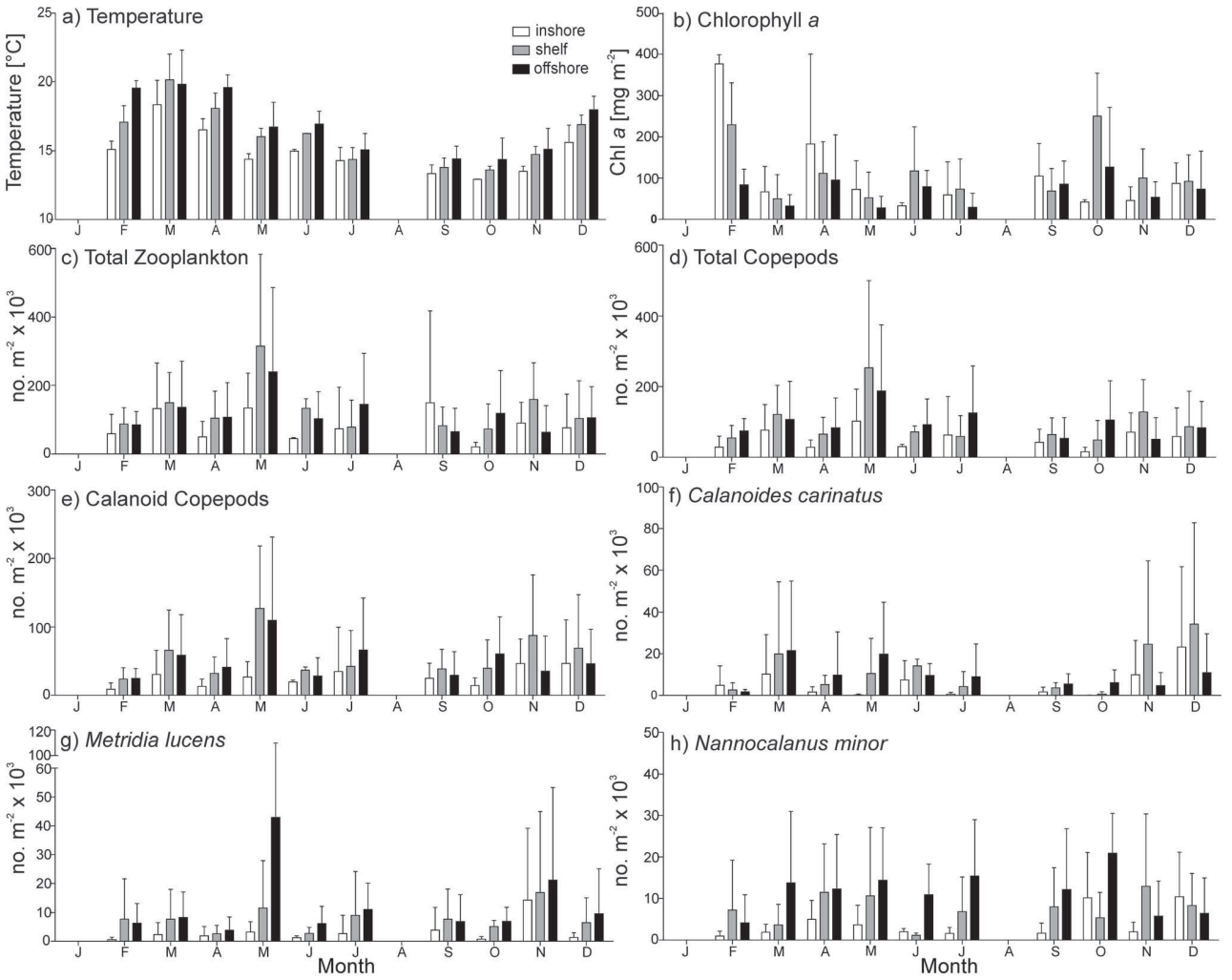

Figure 4. Monthly means (±SD) of a) temperature at 10 m, b) chlorophyll *a*, c) total zooplankton, d) total copepods, e) calanoid copepods, f) *Calanoides carinatus*, g) *Metridia lucens* and h) *Nannocalanus minor*. Note different scales.
doi:10.1371/journal.pone.0097738.g004

Abundances were usually highest in November and December and in March and May (Fig. 4), but the pattern varied from year to year. On average, the copepod community was dominated by calanoid copepods (56%), 40% belonged to cyclopoid copepods (of which 79% were *Oithona* spp. and 19% *Oncaea* spp.) and 4% were harpacticoid copepods. Maximum numbers of calanoid copepods reached 432×10^3 m^{-2} at 50 nm from shore in May 2007 and 338×10^3 m^{-2} at 30 nm in July 2011.

Calanoid community structure, abundance and distribution

Dominant species. Among the larger calanoid copepods, *Calanoides carinatus*, *Metridia lucens* and *Nannocalanus minor* clearly dominated. Spatial and temporal distribution patterns of the dominant and consistently abundant calanoid species are shown in Figure 9. The majority of *C. carinatus* was observed in patches between 10 and 50 nm from shore. Maximum numbers of 100–180×10^3 m^{-2} were observed inshore and on the shelf in December 2005, 2010 and in March 2006. High abundances between 20 and 90×10^3 m^{-2} were concentrated at 30–50 nm from shore in March 2005, April 2008, May 2007, 2011, November 2010 and at 5 nm from shore in December 2009. *C. carinatus* occurred regularly in large patches until the end of 2007/08 (Figs. 5 and 9). Annual abundance was highest in 2005/06, whereas the population decreased in 2008/09 and 2009/2010 and increased again from November 2010 onwards (Fig. 7). Generally, higher abundances across the transect were found in March and December as well as inshore and on the shelf in November, but also in the shelf and offshore region in May (Fig. 4). Maximum numbers occurred mainly during November and December, when temperatures were intermediate and chlorophyll *a* concentrations were high (Figs. 10 and 11). In some years high abundances also occurred in March (especially 2006 and 2008), when temperatures were high and chlorophyll *a* had already decreased (Figs. 10 and 11). During upwelling months (July to October), densities of *C. carinatus* were generally lower (Fig. 4).

The majority of *Metridia lucens* was found between 20 and 50 nm from the coast (Fig. 9). Maximum abundance of 223×10^3 m^{-2} was found 50 nm from shore in May 2007, whereas abundances of $50–100\times10^3$ m^{-2} were recorded at 30 nm in November 2005 and July 2011, as well as at 40 nm in December 2008. Highest annual abundances were observed in 2005/06 and 2006/07. From 2007/

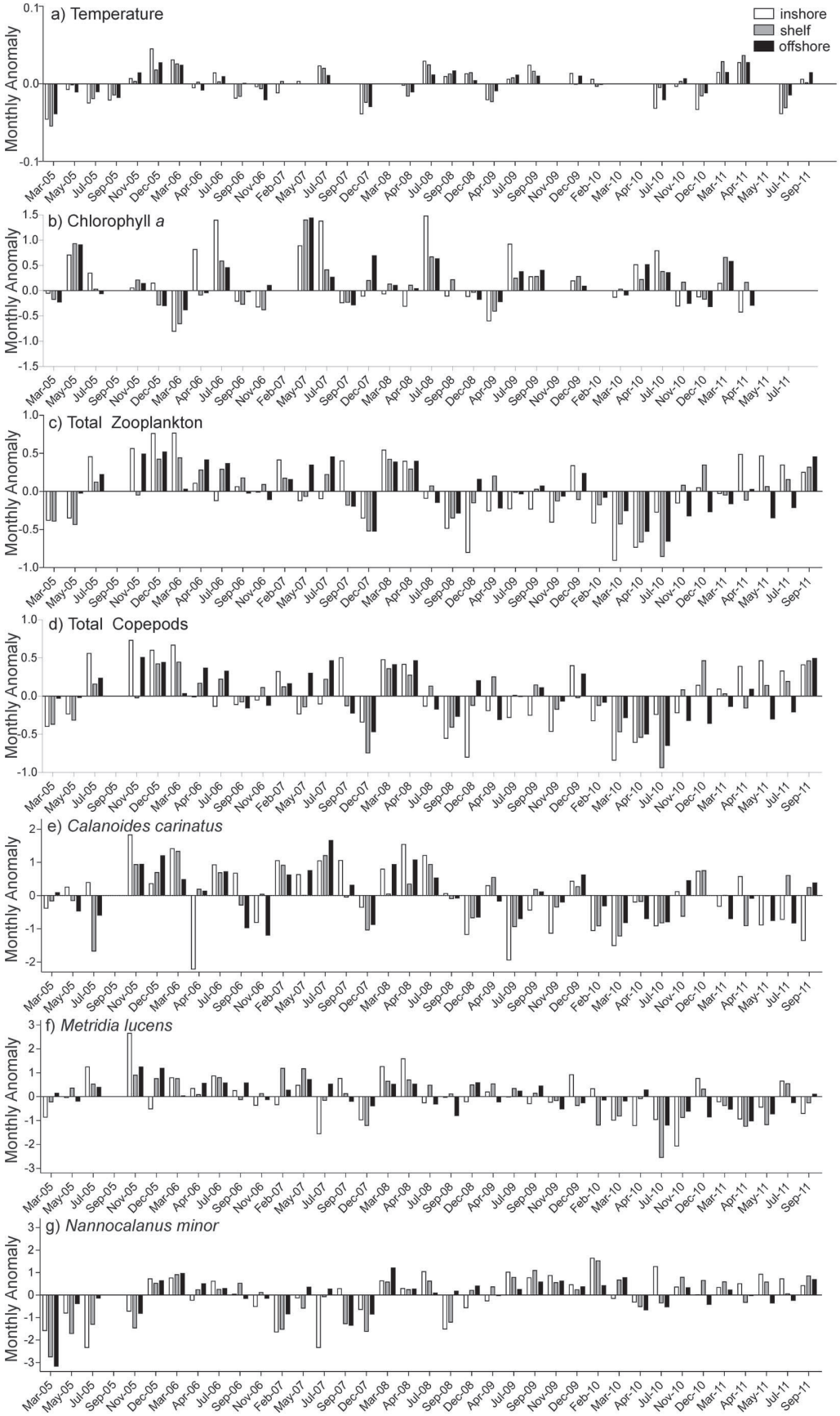
a) Temperature
inshore
shelf
offshore
b) Chlorophyll *a*
c) Total Zooplankton
d) Total Copepods
e) *Calanoides carinatus*
f) *Metridia lucens*
g) *Nannocalanus minor*
Monthly Anomaly

Figure 5. Log-transformed monthly anomalies between 2005 and 2011 of a) temperature at 10 m, b) chlorophyll *a*, and abundance (no. m^{-2}) of c) total zooplankton, d) total copepods, e) *Calanoides carinatus*, f) *Metridia lucens*, and g) *Nannocalanus minor*.
doi:10.1371/journal.pone.0097738.g005

08 onwards annual densities decreased, and in 2009/10 and 2010/2011 *M. lucens* was almost absent (Figs. 7 and 9). Only in July 2011 higher abundance occurred again at 30 nm from the coast (Figs. 5 and 9). No clear seasonal cycle was observed, but highest densities along the transect were usually observed in November and in the offshore region in May (Fig. 4). Highest abundances generally coincided with higher chlorophyll *a* concentrations and intermediate temperatures. However, higher densities also occurred during intensive upwelling in July and September, and throughout March and April, the warmest months (Fig. 10).

Nannocalanus minor was much more evenly distributed during the monitoring period (Fig. 7). Maximum abundances were present in the years 2005/06 and 2009/10, but mean annual abundance was more or less stable throughout the years (Figs. 7 and 9). Before 2007/08, the majority of the population was found between 40 and 70 nm from shore, whereas in 2008/09 and 2009/10 *N. minor* mainly occurred between 20 and 50 nm, which were years characterized by low temperature gradients between spring and late summer. From 2010/11 onwards, highest densities were caught at 30 nm and further offshore. In general, monthly abundances were higher offshore, except for November, December and February, when mean abundances were elevated on the shelf (Fig. 4). Maximum abundance of 62×10^3 m^{-2} was recorded at 30 nm from the coast in November 2010, while abundances between 50 and 60×10^3 m^{-2} were found at 50 to 60 nm from shore in March, April and July 2006. High densities of 20–50×10^3 m^{-2} co-occurred with warm-water intrusions in December 2005, 2008, 2010, February 2010 and March and April 2008 (Figs. 2 and 9). However, such high numbers of *N. minor* were also observed during upwelling months in July 2006, May and July 2007, July 2008, May-November 2009, and July and September 2011. Abundances were quite evenly distributed across the first two principal components without evidence of a seasonal cycle (Fig. 10).

Less abundant species. The distribution of *Centropages* spp. was patchy throughout the entire monitoring period except for the year 2006/07, when they were almost absent (Fig. 6). The majority of *Centropages* spp. was found between 20 and 50 nm from shore. However, maximum abundance of 20×10^3 m^{-2} was recorded at 5 nm from shore in December 2009. High abundances of 11×10^3 m^{-2} occurred at 30 nm in September 2007, while

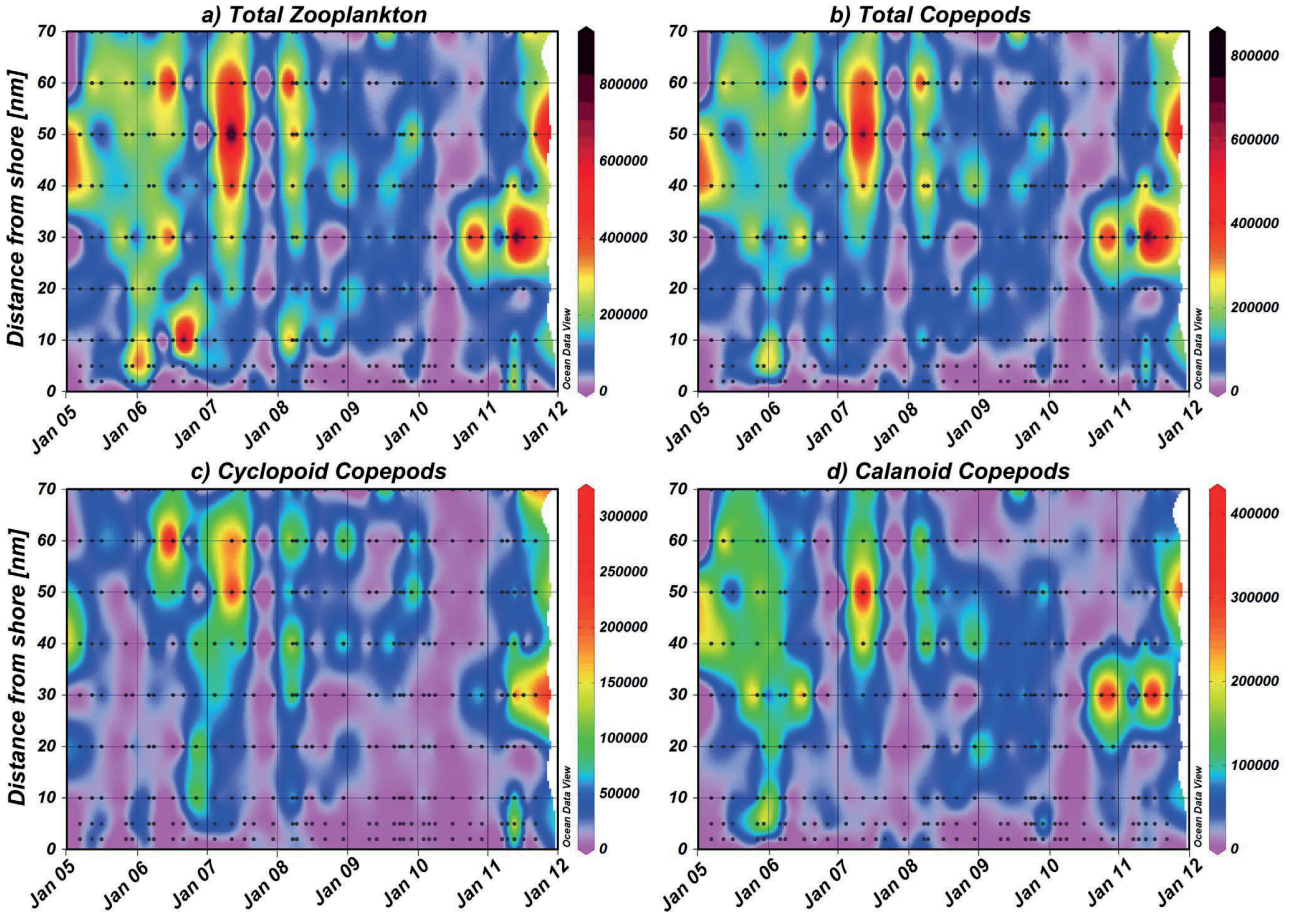

Figure 6. Abundance (no. m^{-2}) and distribution of a) total zooplankton, b) total copepods, c) cyclopoid copepods and d) calanoid copepods shown for each year along the transect.
doi:10.1371/journal.pone.0097738.g006

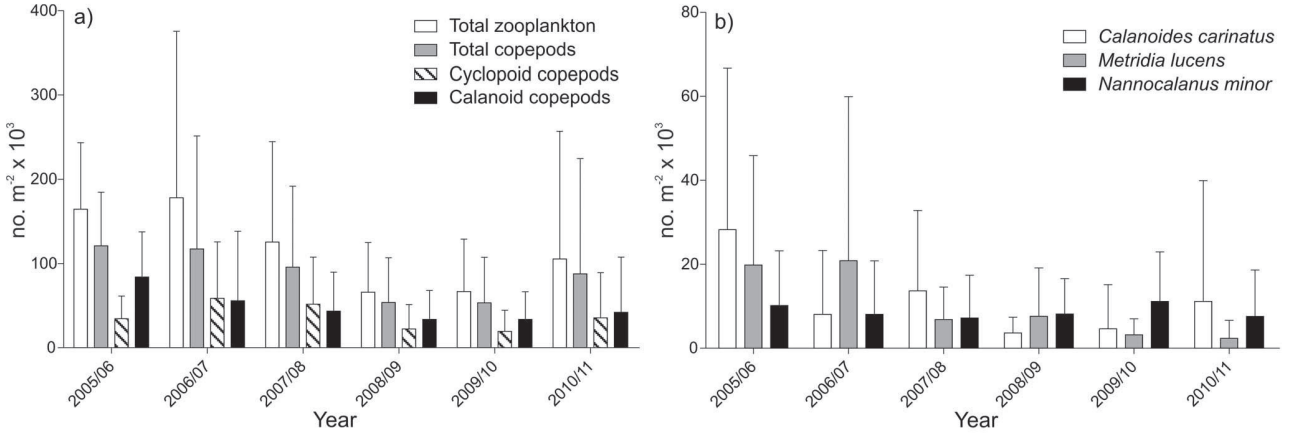

Figure 7. Mean annual abundance (no. $m^{-2} \times 10^3 \pm$SD) of a) total zooplankton, total copepods, cyclopoid and calanoid copepods and the dominant species b) *Calanoides carinatus*, *Metridia lucens* and *Nannocalanus minor* for each year recorded.
doi:10.1371/journal.pone.0097738.g007

9×10^3 m^{-2} were recorded around 40 nm from March-July 2005 and at 30 nm in July 2011. No clear seasonal cycle was observed. Generally, abundance was highest during upwelling months each year, and in some years in December (2005, 2009, 2010), when upwelled water was warming up. However, high densities also occurred between February and April (2005, 2006, 2008, 2009, 2010), when temperatures were higher but still ≤ 19.5°C.

The distribution of *Rhincalanus nasutus* was very patchy between 10 and 50 nm from shore throughout the whole monitoring period (Fig. 6). Maximum abundance of 10×10^3 m^{-2} occurred at 50 nm

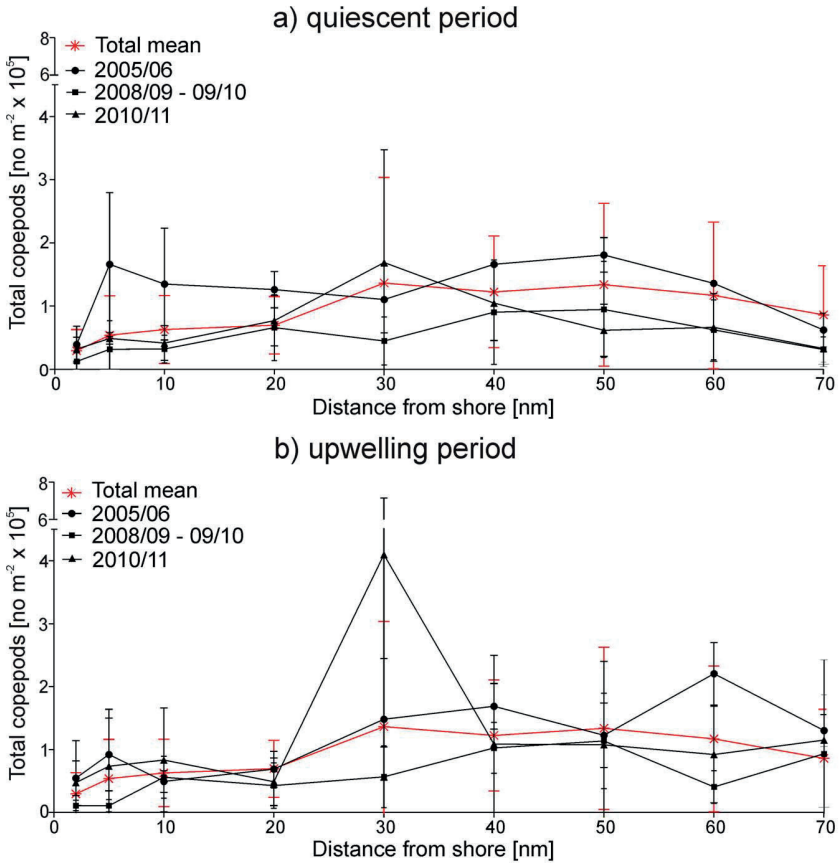

Figure 8. Mean abundance of total copepods (±SD) along the transect for upwelling (black) and quiescent (grey) months for the years 2005/06 and 2010/11 with extreme temperature gradients and the years 2008/09 and 2009/10 characterized by weak gradients. The total mean over all years was added (red).
doi:10.1371/journal.pone.0097738.g008

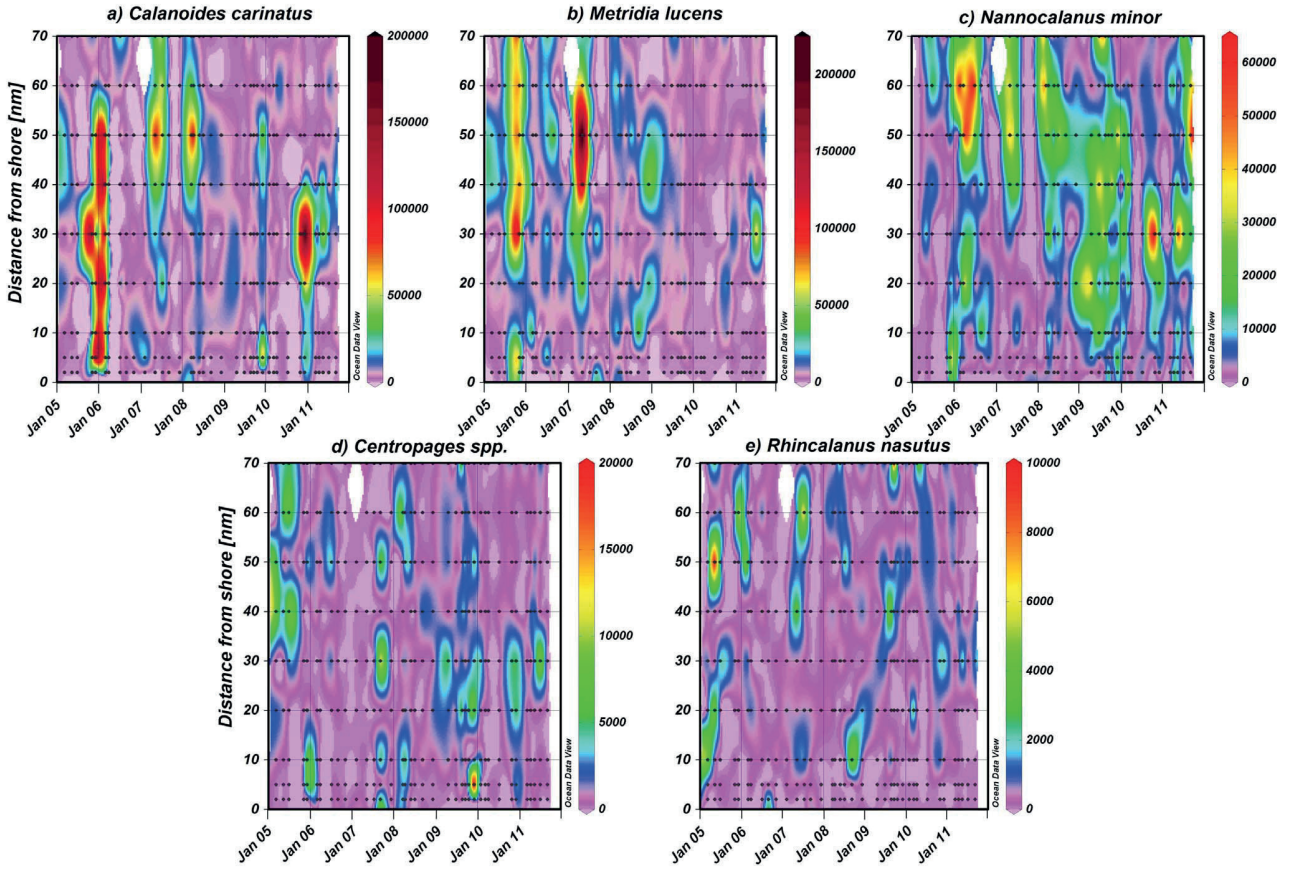

Figure 9. Monthly abundances (no. m^{-2}) of the dominant copepods a) *Calanoides carinatus*, b) *Metridia lucens*, c) *Nannocalanus minor*, d) *Centropages* spp. and e) *Rhincalanus nasutus* along the transect 20°S between March 2005 and September 2011. Note different scales.
doi:10.1371/journal.pone.0097738.g009

from shore in May 2005. Abundances between 3 and 6×10^3 m^{-2} were recorded on the shelf in March and May 2005 and September 2008 as well as offshore in December 2005, May and July 2007 and September 2009. From December 2009 onwards, densities did not exceed 3×10^3 m^{-2}. *R. nasutus* was associated with cooler, upwelled water from May to November each year and in some years with stratifying water masses in December (2005, 2008 and 2010). However, higher abundances were also recorded in March 2005, 2006, 2008 and 2010, when surface temperatures were high, but usually still below 20°C (only >20°C in March 2006).

Discussion

The Benguela Current is a highly productive eastern boundary current upwelling system [19]. Due to high seasonal and interannual variability in wind field structure and thus upwelling intensity, as well as strength and directions of ocean currents, the structure and dynamics of plankton communities are complex and may only be understood by continuous long-term monitoring [21]. In contrast to the southern Benguela Current system (SBC), plankton data are still scarce for the northern Benguela Current region (NBC), especially considering long-term dynamics [15]. This paper presents the first detailed study of a monitoring programme of temporal and spatial variability in zooplankton abundance and copepod community structure along a transect at 20°S, where at certain times the influence of tropical Angola Current waters can be strong [22]. Spatial, interannual and seasonal variations in copepod abundance and community structure were analyzed in context with changes of the environmental conditions.

Hydrographic regime

Hydrographic patterns reflected the general annual upwelling cycle in the northern Benguela Current region off Namibia, exhibiting a strong seasonal cycle with maximum temperatures in mid to late austral summer and lowest temperatures in mid to late spring [23,24]. This seasonality correlates with the general wind pattern with lowest velocities of southerly winds and a stronger westerly component in January and February, whereas highest wind velocities were generally recorded in October [23]. In the present study lowest temperatures (≤13°C) and salinities (≤35.3) were recorded inshore from July to November indicating maximum coastal upwelling, with increased chlorophyll *a* concentrations across the shelf during this time, except for spring 2009, when extremely high chlorophyll *a* values were also measured beyond the shelf. May and December were generally characterized by intermediate temperatures and salinities as well as high chlorophyll *a* concentrations. In contrast, March and April were the warmest months with highest temperatures and salinities, but lower chlorophyll *a* concentrations. During austral summer (December-March), oligotrophic waters from the Angola Current

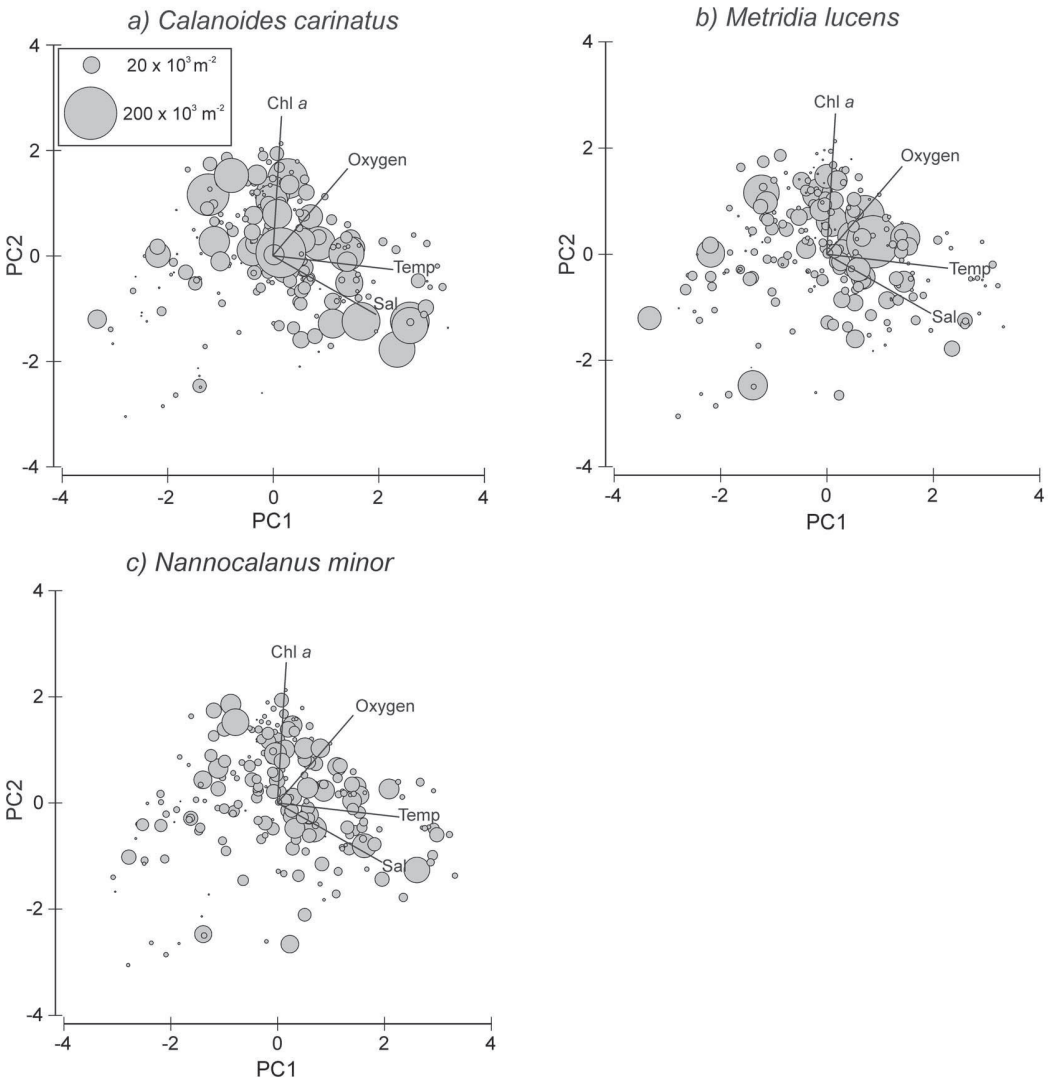

Figure 10. Abundances (no. m^{-2}) of a) *Calanoides carinatus*, b) *Metridia lucens*, and c) *Nannocalanus minor* for each station along the first two principal components PC1 and PC2 as shown in Fig. 3. The area of each circle is proportional to the abundance shown in the legend.
doi:10.1371/journal.pone.0097738.g010

intrude into the northern Benguela region, whereas during late winter and spring (July-September) cool, nutrient-rich waters may extend from the Benguela Current far north into Angola waters enhancing primary production [25].

Copepod abundance and distribution

With an average of 78%, copepods represented the most abundant component within the mesozooplankton community, which is in line with previous studies in the NBC [14,22]. Maximum copepod abundance was observed at 30 nm from shore in May 2011 reaching 857×10^3 m^{-2}, while typical values ranged from $300–500\times10^3$ m^{-2}, which is similar to published data [14,22,26]. In October 1979, maximum abundance of 700×10^3 m^{-2} was estimated at a cross-shelf transect between 20–21°S to 100 nm offshore using a WP-2 net [26]. In April 1986, total copepod abundances of $300–800\times10^3$ m^{-2} were recorded off Walvis Bay, while $100–300\times10^3$ m^{-2} were collected further north at 20°S using a multiple opening-closing rectangular midwater trawl (1 m^2 mouth opening) [22]. In December 2000, a maximum of 520×10^3 m^{-2} was reported at 20 nm off Walvis Bay (23°S) (WP-2 net with 200 μm mesh size; [14]).

Highest copepod abundances were generally observed between 30 and 50 nm from shore on the 20°S transect. This peak in zooplankton abundance over the shelf break and above the continental slope is in line with observations further south at 25° S [27]. However, in the present study, high abundances were also observed on the shelf during December, whereas lowest abundances generally occurred inshore from July to November. This agrees with observations made around Walvis Bay in 2000 [14], where highest abundances of copepods occurred around 40 nm from July to November and between 10 and 30 nm in December. Strikingly low densities of copepods were recorded within upwelling water masses at inshore stations from July to November [14]. Between 20 and 21°S, low abundances occurred closer inshore, increasing in the shelf region and peaking between 70–100 nm from shore between October and November 1979 [26]. In the present study, the coldest water masses occurring inshore from September to November were also depleted in copepods. In

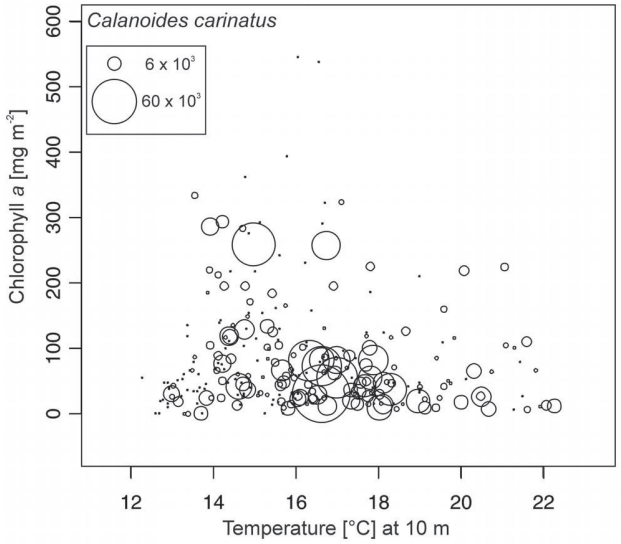

Figure 11. Abundances (no. m^{-2}) of *Calanoides carinatus* in relation to chlorophyll *a* concentration and temperature at 10 m depth. The area of each circle is proportional to the abundance shown in the legend.
doi:10.1371/journal.pone.0097738.g011

contrast, warmer water masses that had been transported further away from shore, exhibited higher copepod abundances during upwelling months. This is in line with the generally observed succession process from initial upwelling via phytoplankton blooms to subsequent zooplankton development [15]. Maximum phytoplankton abundance usually occurs two days after an upwelling event followed by increasing copepod abundance about 20–23 days after initial upwelling [26]. For example, the exceptionally low number of copepods in December 2007 may be explained by a delay of the upwelling period in this year. Temperatures in July 2007 were above and in December 2007 below average throughout the whole transect, while chlorophyll *a* concentration was unusually high in the offshore region in December 2007. Our study emphasises that zooplankton abundance is highly variable in space and time. This pronounced variability with its multiple peaks during each year seems to be affected by the influence of Angola Current water as well as by fluctuating, diffuse upwelling processes, which are often disrupted by plumes and filaments and have been observed especially in the NBC [14,22].

Total copepod abundance in the NBC was lower at the near-shore stations (usually 30×10^3 to 100×10^3 ind m^{-2}) than in the Humboldt Current Upwelling System off Chile (150×10^3 to 300×10^3 m^{-2}, [28]), where total copepod abundance was strongly dominated by the neritic species *Paracalanus parvus* (10×10^3 to 100×10^3 m^{-2}) and most of the species showed high abundances at the very near-shore stations [28]. In contrast to the Humboldt upwelling system, there was no pronounced cross-shelf gradient in total copepod abundance off Namibia [28]. The biomass species *Calanus chilensis*, however, occurred in numbers of several hundred to thousand individuals per square meter off northern Chile [28], also exhibiting lower abundances at the very near-shore stations during the upwelling season [29], similar to the ecologically comparable *Calanoides carinatus* off northern Namibia.

Interannual variability and seasonal cycles

Our study indicates a decline in copepod abundance for the years 2008/09 and 2009/10. This decrease coincided with low spring to late summer temperature gradients, thus, less pronounced upwelling in spring and only moderate warm-water intrusions in late summer (Figs. 2 and 6). In contrast, years with strong upwelling in spring and extensive warm-water intrusions in later summer, as in 2005/06 and 2010/11, were characterized by high copepod abundances suggesting a strong link between zooplankton distribution and physical forcing. By contrast, zooplankton abundance was positively correlated to upwelling intensity in the SBC [30]. A 100-fold increase in mesozooplankton abundance was reported in the SBC between 1950 and 1995 [30], while upwelling intensities also increased during this time period [31]. Since 1995 zooplankton densities, particularly those of larger copepods, have decreased again in the SBC, accompanied by an increase in anchovy biomass [15,30]. In contrast to the SBC, the NBC has not been studied regularly making long-term assessments difficult to date [14,16,18,21,22,26,27,32,33]. However, studies in the NBC indicate that zooplankton abundance decreased slightly from the 1950s to the early 1980s, whereas a long-term increase in zooplankton abundance was observed from 1983 onwards [15]. Total copepod densities increased 6-fold along a 70 nm transect off Walvis Bay (23° S) between 1978 and 2004 followed by a decline after 2005 [15,25]. Recently, contradictory long-term trends have been observed in the major upwelling regimes of the world. For example, macrozooplankton abundance decreased severely off southern California during the last half century, while sea surface layers warmed by 1.5°C and stratification increased [34,35]. However, no long-term decrease of calanoid copepods was observed off southern California from 1951 to 1999, while the calanoid species composition in spring remained stable over the entire monitoring period, except for six anomalous years [35].

The seasonal signal of total copepod abundance in the present study was similar to previously observed patterns, although much more diffuse and variable from year to year, despite the evident seasonal upwelling cycle. Maxima of total copepod abundance were mainly recorded in November and December (2005, 2008, 2009, 2010) and in March and May (2005, 2006, 2007, 2011). However, in 2006 and 2007 peaks were also observed in July. No direct correlation between upwelling intensity (temperature), phytoplankton activity (chlorophyll *a*) and zooplankton abundance emerged, which is in line with previous observations in the Walvis Bay region [15]. In the SBC at St. Helena Bay (32°S), a clear seasonal signal of zooplankton abundance was observed with a maximum abundance in late summer followed by a sharp decline in autumn [36]. Contrarily, in the "Walvis Bay routine area" (21–24°S), two annual peaks of zooplankton abundance were observed during a three year period in the 1950s: A primary peak from November to December in late spring to early summer, and a secondary peak from March to June during late summer and autumn [18], which corresponded to peaks in maximum phytoplankton concentrations [16]. In contrast, low copepod densities were observed off Walvis Bay from March to June in the year 2000, whereas abundances increased from July to December in the same year, indicating that seasonal cycles in the NBC are not as obvious as in the SBC [14].

Seasonal variations in abundance of the dominant copepods were also less pronounced in the Humboldt Current system [37]. Off southern California, most of the dominant copepods exhibited higher abundances in spring during the upwelling season than in winter, whereas *Metridia pacifica*, the second most dominant copepod in this region, occurred in comparable numbers throughout the two seasons [35]. Even during a 27 day time series at St Helena Bay in the southern Benguela Current system, daily changes of zooplankton biomass appeared to be uncorrelated with upwelling cycles [38]. Our study further clarifies, that

fluctuations in abundance of most species cannot be explained by upwelling processes alone, but that behavioural responses (e.g. diel vertical migrations) and biological interactions (e.g. predation and mortality) need to be considered to fully understand life cycles and distributional patterns of copepods in upwelling regions [37–39]. To disentangle these complex relationships, a much higher temporal resolution of biological and oceanographic data is suggested for future monitoring in the NBC region, including process studies of shorter duration with sampling coverage of days to weeks [38].

Copepod community structure

Long-term changes in copepod community structure and size composition have been observed for the southern Benguela system [30] and have been indicated for the NBC off Walvis Bay [14]. The eight dominant species described for the NBC were *Centropages brachiatus*, *Calanoides carinatus*, *Metridia lucens*, *Nannocalanus minor*, *Clausocalanus arcuicornis*, *Paracalanus parvus*, *Paracalanus crassirostris* and *Ctenocalanus vanus* [14,30]. Earlier studies in surface waters (100–0 m) of the "Walvis Bay routine area" in 1962–63 reported *P. crassirostris* and *Paracartia africana* as strictly neritic species, while *C. carinatus*, *P. parvus*, *M. lucens* and *C. brachiatus* dominated the cool-water community on the shelf in order of decreasing abundance (N70 net, 195 µm mesh size) [16,18]. In contrast, *N. minor* was most abundant in offshore warm-water communities [18]. Between 1985 and 1990, the four dominant species in Namibian waters were *C. carinatus*, *R. nasutus*, *M. lucens* and *C. brachiatus* in order of decreasing abundance (180 µm mesh size) [21,27], while in 2000 *M. lucens* prevailed over *Rhincalanus nasutus* (200 µm mesh size) [14]. In the present study area further north off Walvis Bay at 20°S, community composition was highly variable between years and months, but seven calanoid species always dominated the shelf and offshore region. The three larger species competing for the first rank were *C. carinatus*, *M. lucens* and *N. minor* followed by *Centropages* spp., *Calocalanus* spp. and, depending on the month, *Eucalanus hyalinus*, *Candacia* spp. and *Rhincalanus nasutus*. Off Oregon, in the California Current system, on- and off-shelf variations in copepod biomass and community structure reflected the origins of the source water currents while the copepod assemblage could be divided into a nearshore and a midshelf to outer shelf group [40]. In our study, no such clear zonation pattern was identified.

In general, *C. carinatus* prevailed especially on the shelf in March, November and December, whereas *M. lucens* and particularly *N. minor* were more evenly distributed and did not show seasonal patterns. Around Walvis Bay, *C. carinatus* exhibited higher abundances inshore between June and August at the onset of upwelling and peaked during October and December at the end of the upwelling season [14]. Species-specific temperatures ($<$ 13°C) and low salinity preferences were identified for *C. carinatus* characterizing recently upwelled waters [12]. Hence, this species was referred to as cold-water species [14,27]. However, our study does not show such a clear distributional pattern due to strong interannual variations (Fig. 9). Abundances of *C. carinatus* were generally high in May at the onset of the upwelling season and in November and December at the end of the upwelling season, but also in March during the quiescent season (Fig. 4). However, this pattern was not consistent over the years, e.g. extremely low densities occurred in December 2007 which may be due to delayed upwelling during this year. During upwelling months, high abundances of *C. carinatus* were correlated with intermediate temperatures and higher chlorophyll *a* concentrations above the shelf break and further offshore, which characterize stabilizing and sun-warmed offshore-moving, water masses sometime after the actual upwelling event (Figs. 10 and 11). In December, *C. carinatus* also occurred inshore and on the shelf, while temperatures were intermediate and chlorophyll *a* levels high. In March and April, *C. carinatus* was associated with high temperatures but lower chlorophyll *a* concentrations.

In contrast to previous studies mentioned above, *N. minor* represented one of the three dominant species. In the years 2008/09 and 2009/10, when *C. carinatus* and *M. lucens* populations had decreased, *N. minor* dominated the calanoid community. These years were characterised by weaker upwelling allowing stronger mixing with oceanic waters, which could explain the consistently higher densities of *N. minor* during this period. *N. minor* is usually considered a warm-water species with low abundances off Walvis Bay, where this species was associated with intrusions of warm oceanic waters onto the shelf in periods of weak upwelling [18,27,41]. During upwelling months, *N. minor* occurred only in low abundance at the most oceanic stations (160 nm) off Walvis Bay [41]. In contrast, in the northwesternmost part of the study area around Walvis Bay (~22°S), *N. minor* took over the dominant role in the copepod community [18]. During the Benguela Niño in 1963, when unusually high sea surface temperatures and salinities moved southwards from Angola into the northern Benguela region, abundances of *N. minor* increased considerably [17]. Along the monitoring line at 20°S, the influence of Angola Current water is even more pronounced than around Walvis Bay and generally higher abundances of *N. minor* are expected [19,22].

These observations underline that zooplankton dynamics in the NBC are highly complex and do not follow well-defined patterns. The present study elucidates that plankton dynamics in this region are driven by non-linear interactions between wind, upwelling events, solar radiation, regeneration and recycling of nutrients, biological interactions and species-specific response and development times of the organisms [15], which exacerbates attempts to model such a highly variable ecosystem. It emphasises the necessity of long-term studies with consistent high-resolution monitoring and analyses of the driving forces and key species to disentangle their interactions and dynamics. This is particularly important in order to understand ecosystem functioning and predict future changes with potentially severe impacts on such highly productive ecosystems.

Acknowledgments

We would like to thank the captain and crew of RV "Welwitchia" for their competent support during each cruise. Special thanks to Victor Hashoongo and Allie Samuel for helping with the sample analysis.

Author Contributions

Conceived and designed the experiments: AK HA WH. Performed the experiments: AK AKP DCL RH. Analyzed the data: MB. Contributed reagents/materials/analysis tools: AK AKP DCL. Wrote the paper: MB HA WH AK.

References

1. Boyer D, Cole J, Bartholomae C (2000) Southwestern Africa: Northern Benguela Current region. Mar Pollut Bull 41(1–6): 123–140.
2. Heileman S, O'Toole MJ (2008) Benguela Current LME. In: Sherman K, Hempel G, editors.The UNEP Large Marine Ecosystem Report: A perspective of changing conditions in LMEs of the world's regional seas UNEP Regional Seas Report and Studies No 182 United Nations Environment Programme. Nairobi, Kenya. pp. 100–142.

3. Monteiro PMS (2010) The Benguela Current System. In: Liu K-K, Atkinson L, Quinones R, Talaur-McManus L, editors.Carbon and nutrient-fluxes in the continental margins.Berlin: Springer. pp. 65–78.
4. Brown PC, Painting SJ, Cochrance KL (1991) Estimates of phytoplankton and bacterial biomass and production in the northern and southern Benguela ecosystems. S Afr J mar Sci 11: 537–567.
5. Crawford RJM, Shannon LV, Pollock DE (1987) The Benguela ecosystem part VI. The major fish and invertebrate resources. Oceangr Mar Biol Rev 25: 323–505.
6. Shannon LV, Agenbag JJ, Buys MEL (1987) Large- and mesoscale features of the Angola-Benguela front. S Afr J Mar Sci 5(1): 11–34.
7. Mohrholz V, Bartholomae CH, van der Plas AK, Lass HU (2008) The seasonal variability of the northern Benguela undercurrent and its relation to the oxygen budget on the shelf. Cont Shelf Res 28: 424–441.
8. Shannon LV, O'Toole MJ (2003) Sustainability of the Benguela*: ex Africa semper aliquid novi*. In: Hempel G, Sherman K, editors.Large marine ecosystems: trends in exploitation, protection and research. Amsterdam: Elsevier.
9. Shannon LV, Hempel G, Malanotte-Rizzoli P, Moloney CL, Woods J (2006) Benguela: Predicting a Large Marine Ecosystem. Large Marine Ecosystems 14. Amsterdam: Elsevier. 410 p.
10. Boyd AD, Salat J, Masó M (1987) The seasonal intrusion of relatively saline water on the shelf off northern and central Namibia. S Afr J mar Sci 5: 107–120.
11. Lass HU, Mohrholz V, Nausch G (2000) Hydrographic and current measurements in the area of the Angola-Benguela front. J Phys Oceanogr 30: 2589–2609.
12. O'Toole MJ (1980) Seasonal distribution of temperature and salinity in the surface waters off South West Africa. 1972-74. Investl Rep Sea Fish Inst South Africa 121–125.
13. Longhurst AR (1985) The structure and evolution of plankton communities. Prog Oceanogr 15: 1–35.
14. Hansen FC, Cloete RR, Verheye HMV (2005) Seasonal and spatial variability of dominant copepods along a transect off Walvis Bay (23°S), Namibia. Afr J Mar Sci 27(1): 55–63.
15. Hutchings L, Verheye HMV, Hugget JA, Demarcq H, Cloete R et al. (2006) Variability of plankton with reference to fish variability in the Benguela Current Large Marine Ecosystem - An overview. In: Shannon LV, Hempel G, Malanotte-Rizzoli P, Moloney CL, Woods J, editors.Large Marine Ecosystems. Amsterdam: Elsevier.
16. Kollmer WE (1963) The pilchard of South West Africa (*Sardinops ocellata*). Notes on zooplankton and phytoplankton collections made off Walvis Bay. Investl Rep mar Res Lab S W Afr 78 pp.
17. Stander GH, De Decker AHB (1969) Some physical and biological aspects of an oceanographic anomaly off South West Africa in 1963. Invest Rep Div Sea Fish S Afr 81: pp 46.
18. Unterüberbacher HK (1964) The pilchard of South West Africa (*Sardinops ocellata*). Zooplankton studies in the waters off Walvis Bay with special reference to the Copepoda. Investl Rep mar Res Lab S W Afr 11: 42 pp (+ Plates 42–36).
19. Shannon LV, Pillar SC (1986) The Benguela ecosystem. Part III. Plankton. In: Barnes M, editor.Oceanography and Marine Biology An annual review.Aberd-Aberdeen: University Press. pp. 65–170.
20. Schlitzer R (2013) Ocean Data View 4, http://odv.awi.de.
21. Timonin AG (1992) Zooplankton and environmental variability in the northern Benguela upwelling area. Russ J Aqua Ecol 1(2): 103–113.
22. Olivar M-P, Barangé M (1990) Zooplankton of the northern Benguela region in a quiescent upwelling period. J Plankt Res 12(5): 1023–1044.
23. Stander GH (1962)The pilchard of South West Africa (*Sardinops ocellata*). General hydrography of the waters off Walvis Bay, South West Africa 63 p.
24. Stander GH (1964) The Benguela Current of South West Africa. 43 p. +77 figures.
25. Hutchings L, van der Lingen CD, Shannon LJ, Crawford RJM, Verheye HMS et al. (2009) The Benguela Current: An ecosystem of four components. Prog Oceanogr 83: 15–32.
26. Postel L, Arndt EA, Brenning U (1995) Rostock zooplankton studies off West Africa. Helgoländer Meeresunters 49: 829–847.
27. Timonin AG (1991) Correlation between distribution of zooplankton and hydrologic conditions in the Benguela upwelling zone. Oceanology 31(2): 181–195.
28. Escribano R, Hidalgo P (2000) Spatial distribution of copepods in the north of the Humboldt Current region off Chile during coastal upwelling. J Mar Biol Ass UK 80: 283–290.
29. Escribano R (1998) Population dynamics of *Calanus chilensis* in the Chilean eastern boundary Humboldt Current. Fish Oceanogr 7(3/4): 245–251.
30. Verheye HMV, Richardson AJ, Hutchings L, Marska G, Gianakouras D (1998) Long-term trends in the abundance and community structure of coastal zooplankton in the southern Benguela system, 1951-1996. S Afr J mar Sci 19: 317–332.
31. Shannon LV, Crawford RJM, Pollock DE, Hutchings L, Boyd AD et al. (1992) The 1980s - A decade of change in the Benguela ecosystem. In: Payne AIL, Brink KH, Mann KH, Hilborn R, editors. Benguela trophic functioning. S Afr J Mar Sc 12: 271–276.
32. Barangé M (1989) Zooplankton size structure off Namibia in July 1983 and 1984. Colln scient Pap int Comm SE Atl Fish 16(1): 31–41.
33. Brenning U (1985) Structure and development of calanoid populations (Crustacea, Copepoda) in the upwelling regions off North West and South West Africa. Beitr Meeresk 53: 3–33.
34. Roemmich D, McGowan J (1995) Climatic warming and the decline of zooplankton in the California Current. Science 267: 1324–1327.
35. Rebstock GA (2002) Climatic regime shifts and decadal-scale variability in calanoid copepod populations off southern California. Global Change Biol 8: 71–89.
36. Verheye HM, Hutchings L, Huggett JA, Painting SJ (1992) Mesozooplankton dynamics in the Benguela ecosystem, with emphasis on the herbivorous copepods. In:Benguela trophic functioning. Payne, AIL, Brink, KH, Mann, KH and R Hilborn (Eds.). S Afr J mar Sci 12: 561–584.
37. Hidalgo P, Escribano R (2007) Coupling of life cycle of the copepods *Calanus chilensis* and *Centropages brachiatus* to upwelling induced variability in the central-southern region of Chile. Prog Oceanogr 75: 501–517.
38. Verheye HM (1991) Short-term variability during an anchor station study in the southern Benguela upwelling system: Abundance, distribution and estimated production of mesozooplankton with special reference to *Calanoides carinatus* (Krøyer, 1849). Prog Oceanogr 28: 91–119.
39. Peterson WT, Arcos DF, McManus GB, Dam H, Bellatoni D et al. (1988) The nearshore zone during coastal upwelling: Daily variability and coupling between primary and secondary production off Central Chile-. Prog Oceanogr 20: 1–40.
40. Morgan CA, Peterson WT, Emmett RL (2003) Onshore-offshore variations in copepod community structure off the Oregon coast during the summer upwelling season. Mar Ecol Prog Ser 249: 223–236.
41. Timonin AG, Arashkevich EG, Drits AV, Semenova TN (1992) Zooplankton dynamics in the northern Benguela ecosystem, with special reference to the copepod *Calanoides carinatus*. S Afr J Mar Sci 12(1): 545–560.

CHAPTER II

Feeding Strategies of Tropical and Subtropical Calanoid Copepods throughout the Eastern Atlantic Ocean – Latitudinal and Bathymetric aspects

Bode M, Hagen W, Schukat A, Teuber L, Fonseca-Batista D, Dehairs F and Auel H

Published in Progress in Oceanography 138: 268-282 (2015)

Progress in Oceanography 138 (2015) 268–282

Contents lists available at ScienceDirect

Progress in Oceanography

journal homepage: www.elsevier.com/locate/pocean

Feeding strategies of tropical and subtropical calanoid copepods throughout the eastern Atlantic Ocean – Latitudinal and bathymetric aspects

Maya Bode [a,*], Wilhelm Hagen [a], Anna Schukat [a], Lena Teuber [a], Debany Fonseca-Batista [b], Frank Dehairs [b], Holger Auel [a]

[a] BreMarE – Bremen Marine Ecology, Marine Zoology, University of Bremen, P.O. Box 330440, 28334 Bremen, Germany
[b] Analytical, Environmental and Geo – Chemistry, Earth System Sciences Research Group, Vrije Universiteit Brussel, Pleinlaan 2, 1050 Brussels, Belgium

ARTICLE INFO

Article history:
Received 28 February 2015
Received in revised form 15 October 2015
Accepted 15 October 2015
Available online 23 October 2015

ABSTRACT

The majority of global ocean production and total export production is attributed to oligotrophic oceanic regions due to their vast regional expanse. However, energy transfers, food-web structures and trophic relationships in these areas remain largely unknown. Regional and vertical inter- and intra-specific differences in trophic interactions and dietary preferences of calanoid copepods were investigated in four different regions in the open eastern Atlantic Ocean (38°N to 21°S) in October/November 2012 using a combination of fatty acid (FA) and stable isotope (SI) analyses. Mean carnivory indices (CI) based on FA trophic markers generally agreed with trophic positions (TP) derived from δ^{15}N analysis. Most copepods were classified as omnivorous (CI ~0.5, TP 1.8 to ~2.5) or carnivorous (CI $\geqslant$ 0.7, TP $\geqslant$ 2.9). Herbivorous copepods showed typical CIs of $\leqslant$0.3. Geographical differences in δ^{15}N values of epi- (200–0 m) to mesopelagic (1000–200 m) copepods reflected corresponding spatial differences in baseline δ^{15}N of particulate organic matter from the upper 100 m. In contrast, species restricted to lower meso- and bathypelagic (2000–1000 m) layers did not show this regional trend. FA compositions were species-specific without distinct intra-specific vertical or spatial variations. Differences were only observed in the southernmost region influenced by the highly productive Benguela Current. Apparently, food availability and dietary composition were widely homogeneous throughout the mesotrophic oceanic regions of the tropical and subtropical Atlantic. Four major species clusters were identified by principal component analysis based on FA compositions. Vertically migrating species clustered with epi- to mesopelagic, non-migrating species, of which only *Neocalanus gracilis* was moderately enriched in lipids with 16% of dry mass (DM) and stored wax esters (WE) with 37% of total lipid (TL). All other species of this cluster had low lipid contents (<10% DM) without WE. Of these, the tropical epipelagic *Undinula vulgaris* showed highest portions of bacterial markers. *Rhincalanus cornutus*, *R. nasutus* and *Calanoides carinatus* formed three separate clusters with species-specific lipid profiles, high lipid contents ($\geqslant$41% DM), mainly accumulated as WE ($\geqslant$79% TL). *C. carinatus* and *R. nasutus* were primarily herbivorous with almost no bacterial input. Despite deviating feeding strategies, *R. nasutus* clustered with deep-dwelling, carnivorous species, which had high amounts of lipids ($\geqslant$37% DM) and WE ($\geqslant$54% TL). Tropical and subtropical calanoid copepods exhibited a wide variety of life strategies, characterized by specialized feeding. This allows them, together with vertical habitat partitioning, to maintain high abundance and diversity in tropical oligotrophic open oceans, where they play an essential role in the energy flux and carbon cycling.

1. Introduction

The Atlantic Ocean is the second largest ocean on earth hosting diverse ecosystems from polar to tropical latitudes and oceanic to coastal regions (Aiken et al., 2000). The Atlantic trade wind biome alone produces about 4.6 Gt C y^{-1} (Longhurst et al., 1995). Due to strong vertical stratification and thus limited nutrient supply from below the thermocline, primary production rates in the North and South Atlantic subtropical gyres are generally low with 18–362 mg C m^{-2} d^{-1} compared to 500–1000 mg C m^{-2} d^{-1} in upwelling regions (Longhurst et al., 1995; Marañón et al., 2000). However,

* Corresponding author.
E-mail address: mabode@uni-bremen.de (M. Bode).

http://dx.doi.org/10.1016/j.pocean.2015.10.002
0079-6611/

more than 80% of global ocean production and 70% of total export production is contributed by oligotrophic oceanic regions due to their enormous regional expanse (Platt et al., 1989; Karl et al., 1996). The subtropical gyres alone comprise more than 60% of the total ocean surface and contribute more than 30% to the global marine carbon fixation (Longhurst et al., 1995). Thus, understanding key processes of ecosystem functioning in these areas is crucial for predictions of biogeochemical cycles (Marañón et al., 2000).

Copepods comprise 50–95% of mesozooplankton communities worldwide (Longhurst, 1985), and thus, they play a major role in shaping marine food webs and nutrient cycles (Longhurst and Harrison, 1989; Frangoulis et al., 2005). In oligotrophic open oceans, the contribution of zooplankton excretion to nutrient regeneration is high, providing more than 40% of the nutrients required by phytoplankton. In contrast, this portion is lower in more productive upwelling regions (<40%), where nutrients become replenished in the euphotic zone from deeper layers (Frangoulis et al., 2005). In general, the majority of nutrients are recycled through the microbial loop (Bode and Varela, 1994). Trophic relationships are complex, as most copepod species do not merely interlink primary producers and higher trophic levels, but are usually opportunistic omnivorous feeders (Kleppel, 1993; Kleppel et al., 1996; Escribano and Pérez, 2010; Calbet, 2008; Schukat et al., 2014). However, the natural diet of most copepod species and their trophic positions remain largely unclear. This is especially the case in oligotrophic tropical and subtropical environments, where the restricted availability of phytoplankton may often be compensated by feeding on heterotrophic protozoans and microzooplankton (Calbet and Saiz, 2005). Typical primary producers in the oligotrophic Atlantic are cyanobacteria (e.g. *Trichodesmium* or smaller diazotrophs) and small autotrophic flagellates ($\leqslant$5 μm) reaching 70–90% of total photosynthetic biomass, while only a small fraction is attributed to dinoflagellates and diatoms (Calbet and Landry, 1999; Marañón et al., 2000). Hence, nitrogen fixation may contribute significantly to the nitrogen pool entering the food webs in these regions (Voss et al., 2004; Capone et al., 2005; Staal et al., 2007).

In contrast to gut content analyses, trophic biomarkers such as stable isotopes and fatty acids integrate dietary information over several weeks to months providing information on trophic level, dietary preferences and life strategies (Minagawa and Wada, 1984; Graeve et al., 1994a,b; Hagen, 1999; Gentsch et al., 2009). Stable isotope ratios of nitrogen (δ^{15}N) and carbon (δ^{13}C) are commonly applied to trace pathways of organic matter in food webs (Minagawa and Wada, 1984; Hobson and Welch, 1992; Vander Zanden and Rasmussen, 2001; Post, 2002). Isotopic fractionation in animals leads to the accumulation of heavier isotopes in the body tissues of consumers, as lighter isotopes are preferentially metabolized and excreted. Previous studies revealed that δ^{15}N values of zooplankton reflected seasonal changes at the food-web base (Goering et al., 1990; Montoya, 1994; Rolff, 2000) and regional changes of the oceanographic regime (Schmidt et al., 2003; Montoya et al., 2002; Koppelmann et al., 2003, 2009; Hauss et al., 2013). In the central tropical Atlantic δ^{15}N values of size-fractionated mesozooplankton decreased, while trophic levels remained constant from east to west. This corresponded to the increasing abundance of *Trichodesmium* in the west (Montoya et al., 2002; McClelland et al., 2003), whose δ^{15}N values are as low as those of atmospheric nitrogen (Wada and Hattori, 1976). However, most of these studies consider only bulk size-fractionated zooplankton, which are often not suitable for spatial comparisons, as the community structure influences the δ^{15}N signal (Hauss et al., 2013). The pathways of nitrogen within food webs are not easy to assess. For a better understanding, more high-resolution studies on individual species reflecting spatial patterns of δ^{15}N are needed (Hauss et al., 2013).

Fatty acid trophic markers (FATM) specific for certain phytoplankton or zooplankton groups are incorporated largely unmodified into the consumers' body tissue and thus can be potentially traced through the food chain (Lee et al., 1971a,b; Graeve et al., 1994a,b; reviewed by Dalsgaard et al., 2003). In spite of rather low lipid levels and generally higher turnover rates of tropical copepods compared to those at higher latitudes, the validity of the FATM concept was confirmed also for subtropical and tropical regions (Lee et al., 1971b; Lee and Hirota, 1973; Kattner and Hagen, 2009; Schukat et al., 2014; Teuber et al., 2014). In higher latitudes and upwelling regions with pronounced seasonal and spatial gradients of food supply, seasonal (e.g. Sargent and Falk-Petersen, 1988; Kattner and Krause, 1989; Kattner and Hagen, 1995; El-Sabaawi et al., 2009; Escribano and Pérez, 2010) and regional (Kattner et al., 1989; Kattner and Hagen, 1995; Stevens et al., 2004) changes in phytoplankton population structure coincided with distinct changes of FATM in copepods. Similar data for tropical and subtropical regions are rare.

In general, copepods can be divided into three large groups, based on vertical distribution and certain life-strategy characteristics (Lee and Hirota, 1973; Lee et al., 2006). In most tropical epipelagic copepods, lipid deposition is almost absent and unnecessary because of low, but constant, year-round primary production. These copepods are characterized by high turnover, fast growth, intense reproduction and a short life span (Kattner and Hagen, 2009; Teuber et al., 2013). In contrast, deep-dwelling copepods are usually omnivorous or carnivorous with lower metabolic rates, longer life spans and pronounced lipid storage due to sporadic food availability and/or buoyancy aids (Laakmann et al., 2009a,b). Another group of copepods, predominantly inhabiting polar, boreal and upwelling regions, accumulates large energy reserves mainly as wax esters and undergoes ontogenetic vertical migrations entering different forms of dormancy to overcome periods of food shortage (Hagen, 1999; Verheye et al., 2005).

The present study provides a large data set on carbon and nitrogen stable isotopes for 30 species and lipid composition for 15 species of calanoid copepods throughout the tropical and subtropical eastern Atlantic Ocean. Widely distributed species were collected along a latitudinal transect through four hydrographical and biogeochemical provinces between 38°N and 21°S from the surface to 2000 m depth. The main objectives were to identify inter- and intra-specific differences in trophic interactions and dietary preferences between the different hydrographical regimes and from the surface down to bathypelagic depths. A new bacterial ratio was introduced as a first approach to estimate the proportional contribution of bacterial production to the nutritional basis of copepods, inspired by the fatty acid-based index of carnivory suggested by Schukat et al. (2014). The difference between the carnivory index (CI) and the bacterial ratio (BI) is that the CI refers to the carnivorous contribution to the diet of a given copepod, whereas the BI focuses on the bacterial contribution to the food-web base, on which a copepod relies. Hence, a copepod may have a high BI value, even if itself does not feed on bacteria at all, simply by incorporating FAs of bacterial origin via the food chain. Combining the fatty acid and stable isotope approaches, different life strategies were identified, characterized by specialized feeding modes.

2. Materials and methods

2.1. Sampling

Copepods were sampled during research cruise ANT-XXIX/1 on board RV *Polarstern* throughout the eastern Atlantic Ocean from 37° 49′N to 20° 59′S in October/November 2012 (Fig. 1). Stratified vertical hauls were conducted with a HydroBios Multinet Maxi

equipped with 9 nets (150 µm mesh size, 0.5 m^2 mouth opening). Specimens were usually collected during day light in discrete depth layers at nine stations from 800–700–600–500–400–300–200–100–50–0 m and at six stations from 2000–1500–1000–700–400–300–200–100–50–0 m. Copepod species and stages were identified alive immediately after each haul under a dissecting microscope. A large number of copepods (1–15 specimens per replicate, depending on size) were collected from the same stations and depth layers focusing on the dominant larger species that were abundant along the entire transect. Only apparently fit individuals were deep-frozen at −80 °C for further biochemical analyses.

Oceanographic parameters were measured underway in 5 m water depth by a thermosalinograph continuously recording sea surface temperature (SST) and sea surface salinity (SSS). At each station vertical profiles of temperature, salinity, oxygen concentration and fluorescence were recorded from the surface to maximum sampling depth (either 800 or 2000 m) with a conductivity temperature depth (CTD) sensor equipped with a rosette water sampler (Figs. 1 and 2; Rohardt and Wisotzki, 2013). Fluorescence provided a proxy for chlorophyll *a* (chl *a*) content in the upper 200 m.

2.2. Stable isotope analysis

After lyophilization (48 h) of the deep-frozen copepods, body dry mass was determined using a microbalance (Sartorius, NCII1S, precision ± 10 µg). Copepod samples (whole animals) of 0.5–5 mg dry mass were transferred into tin capsules. In case of smaller species, individuals were pooled to obtain sufficient biomass (>1 mg; e.g. 7–10 individuals of *Calanoides carinatus*, *Scolecithrix danae* and *Undinula vulgaris*; 4–7 *Euchaeta marina*, *Rhincalanus cornutus*, *Pleuromamma* spp.; 2–3 *Neocalanus gracilis, Pareucalanus* spp.; 1–2 *Eucalanus hyalinus*, *Rhincalanus nasutus*, *Euchirell*a spp.). Stable isotope analysis was performed by TÜV Rheinland Agroisolab GmbH in Jülich, Germany, using a mass spectrometer (EA NA1500 Series 2, Carlo Erba Instruments) and helium as carrier gas. Stable isotope ratios of carbon ($^{13}C/^{12}C$) and nitrogen ($^{15}N/^{14}N$) were measured against the IAEA-C1 and IAEA-N1 standards, respectively, and are expressed as $\delta^{13}C$ and $\delta^{15}N$ in ‰ with respect to VPDB for carbon and atmospheric air for nitrogen (Hobson et al., 2002). Lipids were not extracted prior to stable isotope analysis, due to generally low copepod biomass and to avoid any bias of $\delta^{15}N$ by lipid extraction (Hobson et al., 2002; Mintenbeck et al., 2008). To avoid bias of the $\delta^{13}C$ signal by varying lipid contents, $\delta^{13}C$ values of crustaceans were normalized to a common lipid content applying a lipid-normalization model, if C:N ratios exceeded 4 ($\delta^{13}C'$; McConnaughey and McRoy, 1979; Smyntek et al., 2007).

To assess trophic levels of different copepods within the food web, an isotopic baseline was established from particulate organic matter (POM) natural concentration and isotopic composition: $\delta^{15}N$-PN for particulate nitrogen and $\delta^{13}C$-POC for particulate organic carbon (D. Fonseca-Batista, pers. comm., 2015). Water samples (approx. 4.5 L) were taken of every CTD cast from four depth layers within the upper 100 m and filtered through precombusted GF/F filters (MGF, Sartorius, 0.7 µm nominal pore size). Weighted averages of POM-$\delta^{15}N$ ($\delta^{15}N_{base}$) were determined for each station in the upper 100 m stratum, taking into account particulate nitrogen content and sampling depth. $\delta^{15}N_{base}$ was defined as trophic level 1. The species-specific trophic level was calculated from station-specific $\delta^{15}N_{base}$ as follows:

$$\text{Trophic level} = 1 + (\delta^{15}N_{consumer} - \delta^{15}N_{base})/\Delta_n$$

where Δ_n is the enrichment of $\delta^{15}N$ per trophic level, applying an enrichment factor of 3.4‰ (Minagawa and Wada, 1984; Vander Zanden and Rasmussen, 2001; Post, 2002).

2.3. Lipid analysis

Body dry mass of the deep-frozen copepods was determined after lyophilization for 48 h. In case of small copepod species, several individuals were pooled to obtain sufficient biomass (>1 mg DM). Lipids were extracted with dichloromethane:methanol (2:1, v:v) and purified by adding a 0.88% aqueous KCl solution according to Folch et al. (1957). The total lipid content was determined gravimetrically (Hagen, 2000).

Lipids were converted to their fatty acid methyl ester (FAME) derivatives by transesterification in methanol with 3% concentrated sulfuric acid (Kattner and Fricke, 1986; Peters et al., 2007). Fatty acids (FA) and fatty alcohols (FAlc) were subsequently separated and quantified using a gas chromatograph (Agilent Technologies 7890A) equipped with a DB-FFAP column (30 m length, 0.25 mm diameter) operating with a programmable temperature vaporizer injector and helium as carrier gas. FAs and FAlcs were identified by comparing their retention times with those of natural standards (lipids of menhaden fish oil and *Calanus hyperboreus*) of known composition. The portion of wax esters was estimated based on FAlc content assuming equal masses of the FA and FAlc moieties in the wax ester molecules (Kattner et al., 2003).

According to the fatty acid trophic biomarker concept, 16:1($n-7$), 16:4($n-1$) and 18:1($n-7$) indicate a diatom-dominated food source, while 18:4($n-3$) is commonly used as a dinoflagellate biomarker (reviewed by Dalsgaard et al., 2003). The ratio 16:1($n-7$)/16:0 was applied as another index of diatom feeding (typically >1 for significant feeding on diatoms) (Dalsgaard et al.,

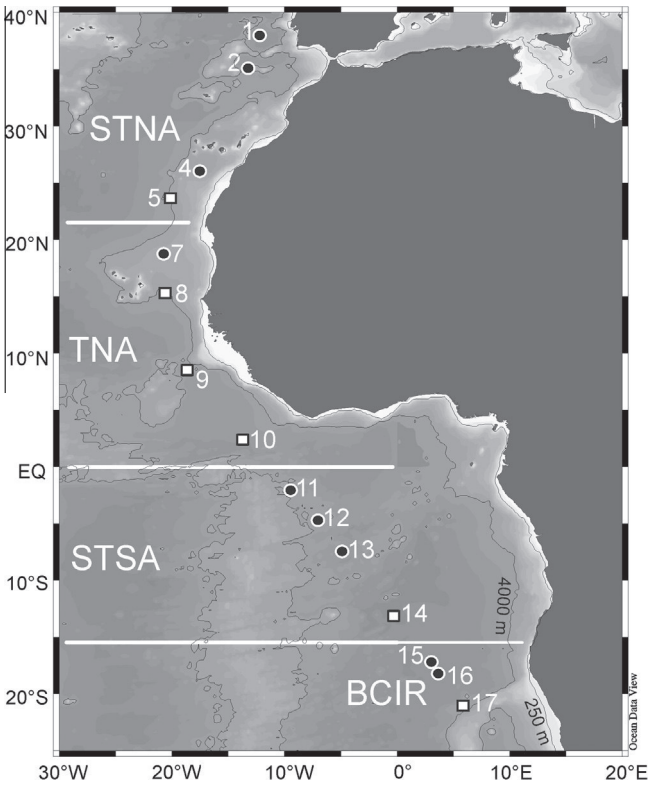

Fig. 1. Station Map showing all stations during ANT-XXIX/1 of RV *Polarstern* in October/November 2012. Stations marked as squares were sampled to a maximum depth of 2000 m, circles show stations with a maximum sampling depth of 800 m. Hydrographic provinces were identified based on oceanographic data (Fig. 2). The 250 and 4000 m bathymetry line are shown. STNA = subtropical North Atlantic, TNA = tropical North Atlantic, STSA = subtropical South Atlantic, BCIR = Benguela Current influenced region.

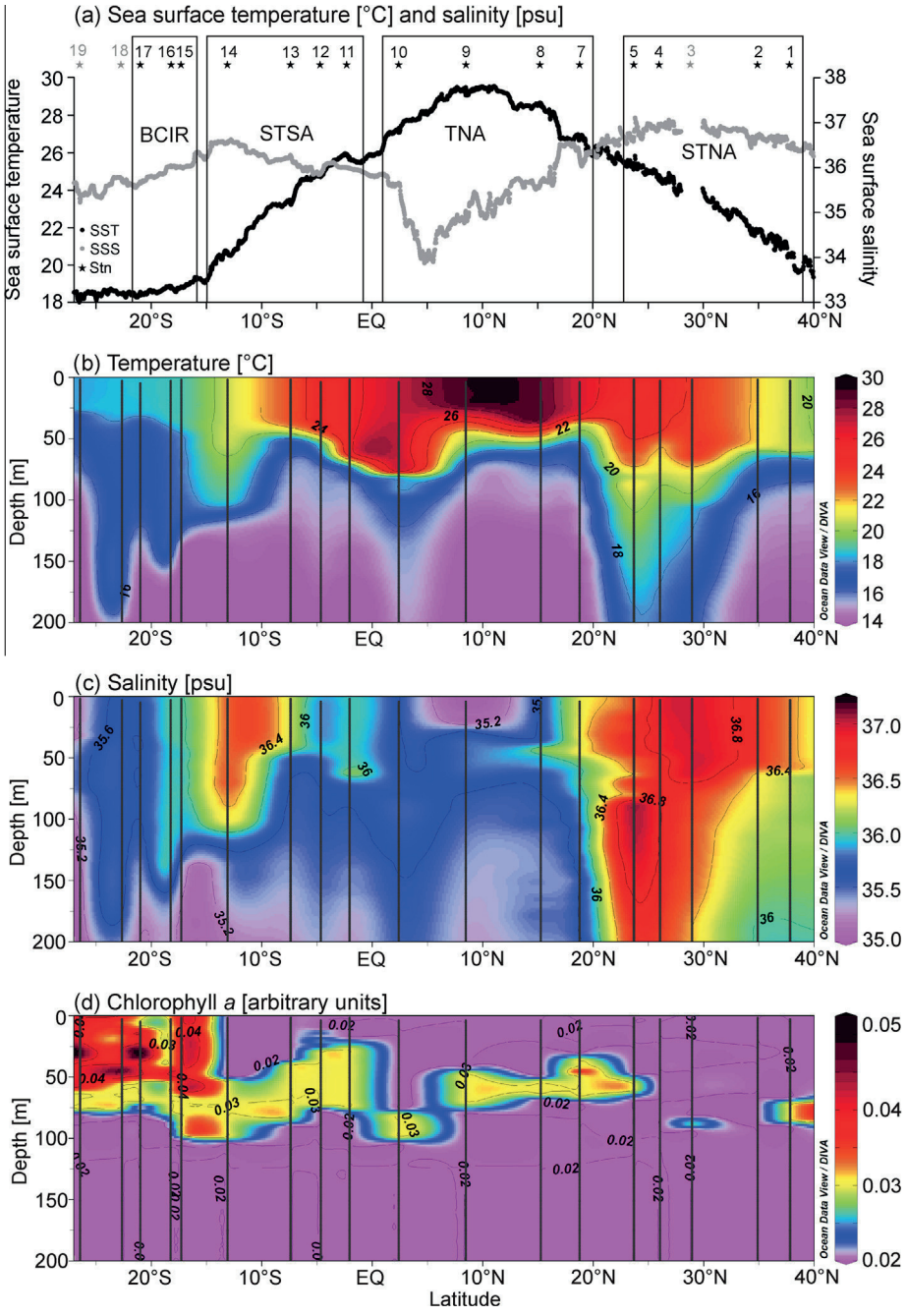

Fig. 2. (a) Sea surface temperature (SST) and sea surface salinity (SSS), (b) temperature, (c) salinity and (d) relative chlorophyll *a* values of the upper 200 m along the cruise track during ANT-XXIX/1. The lines represent respective station numbers marked above as asterisks, stations in gray only contributed CTD data. STNA = Subtropical North Atlantic, TNA = tropical North Atlantic, STSA = subtropical South Atlantic, BCIR = Benguela Current influenced region.

2003 and references therein). By contrast, 18:1($n-9$) is known as a carnivory biomarker (Sargent and Falk-Petersen, 1988). To provide a proportional measure of the carnivorous contribution to copepods' diets, the carnivory index of Schukat et al. (2014) was slightly modified by dividing the 18:1($n-9$) content by he sum of all herbivorous biomarkers and 18:1($n-9$), i.e. modified CI = 18:1($n-9$)/(16:1($n-7$) + 16:4($n-1$) + 18:1($n-7$) + 18:4($n-3$) + 18:1($n-9$)). In contrast to the original index, the modified CI ranges from 0 for herbivorous to 1 for most carnivorous feeding. In addition, a new proxy for the bacterial contribution (BI) to the nutrition of consumers was introduced as the sum of odd-numbered (15:0, 17:0) and *iso*-branched fatty acids (*iso* 15:0, *iso* 17:0) (Budge and Parrish, 1998), i.e. BI = Σbacterial markers/(Σherbivorous markers + bacterial markers). Thus, the BI ranges from 0 for no bacterial input to 1 for highest dietary bacterial contribution.

2.4. Statistical analysis

To identify species-specific and/or geographical and depth-related differences in the dietary composition and nutrition of copepods along the transect, a Principal Component Analysis (PCA) was conducted based on the lipid composition data. Copepod species varied in wax ester content and, hence, FAlc composition, but information on dietary origins is stored in specific FAs. Therefore, only FA data were used for the PCA, whereas FAlc data were

excluded from further analyses, as they are biosynthesized *de novo*, to avoid that the presence/absence of FAlcs interfered with or biased the outcome. Prior to PCA, proportions of FAs were transformed with arcsine-square-root transformation to correct deficiencies in normality and homogeneity of variance. The different regions and depths of occurrence were added as factors to the PCA (Primer v6 software, Clarke and Warwick, 1994). In addition, a cluster analysis based on a Bray–Curtis similarity matrix was performed on the same data set applying the group average linkage to better visualize this large data set (Fig. A, Appendix). To test for intra-specific differences a Man-Whitney *U*-test was applied using the Prism software package 5.0. Maps and hydrographic data were visualized using Ocean Data View 4 (Schlitzer, 2013).

3. Results

3.1. Hydrographic regime

The cruise track along the eastern side of the Atlantic Ocean from 38°N to 21°S crossed very different hydrographical regimes and climate zones. Based on sea surface temperature (SST), sea surface salinity (SSS) as well as CTD profiles of temperature, salinity, and fluorescence in the upper 200 m (Fig. 2; data derived from Rohardt and Wisotzki, 2013), the 15 stations sampled by Multinet were assigned to four different hydrographical provinces and grouped accordingly for further analyses.

Stations 1 to 5 between 38°N and 20°N were located in the subtropical North Atlantic (STNA) characterized by maximum salinities >36.5, warm SST >20 °C further increasing southwards and a pronounced layer of warm water extending to considerable depth. At stn. 5, the 20 °C isotherm reached down to 100 m, which was the maximum depth of this isotherm along the whole transect. A rather low fluorescence signal throughout the water column indicated oligotrophic conditions with low chlorophyll *a* (chl *a*) concentrations.

Stations 7 to 10 between 20°N and 2°N were situated in tropical waters (tropical North Atlantic, TNA). During the time of the cruise, the tropical zone was still shifted toward the northern hemisphere. The four tropical stations were characterized by the highest SST ranging from 26 °C to 30 °C and relatively low SSS <36.3 (min. 33.9 at 5°N). The thermocline was generally shallower (~20–35 m) and steeper compared to subtropical zones further north and south, except for stn. 10, where the 24 °C isotherm reached down to 80 m. Chl *a* concentrations were higher compared to the STNA and the chl *a* maximum usually occurred at intermediate depths around 60 m, except for stn. 10 (~90 m).

Stations 11–14 between 2°S and 14°S were located in the subtropical South Atlantic (STSA) with SST ranging from 26 °C at stn. 11 to 21 °C at stn. 14 and SSS usually >35.8 (max. 36.6 at stn. 14). The thermocline occurred at greater depths (~35–60 m) than in the tropical zone. Particularly, at stn. 14, there was a massive surface layer with high salinities >36.0 extending below 110 m depth. STSA stations had generally higher chl *a* concentrations than stations in the STNA. Compared to the TNA, the intermediate chl *a* maximum extended upwards into shallower depths of 25 m at stns. 11 and 12.

The three southernmost stations 15–17 between 17°S and 22°S were affected by relatively cold (<19 °C) and less saline (<36.0) waters originating from the Benguela Current coastal upwelling system and hence were classified as Benguela Current-influenced region (BCIR). At BCIR stations, there was almost no stratification by temperature or salinity down to 150 m depth. Presumably due to nutrient input from recently upwelled waters, chl *a* concentrations were highest in the BCIR, extending from the surface to 63 m depth with values at least 50% higher than in the TNA or STSA zones. Even between 70 and 98 m depth, BCIR stations still had chl *a* concentrations similar to those in the intermediate chl *a* maximum layers in the TNA.

3.2. Stable isotopic compositions and trophic levels

In general, the $\delta^{15}N$ signals of a copepod species collected at different stations within one of the four hydrological provinces did not differ from one another with regard to trophic positions (<±3.4‰). Therefore, results are presented as species-specific means ± standard deviation for each of the four regional clusters (Table 1). Mean $\delta^{15}N$ of calanoid copepods varied from 1.3‰ in mesopelagic *Pleuromamma abdominalis* from the BCIR to 10.8‰ in mesopelagic *Megacalanus princeps* from the STNA. $\delta^{15}N$ values of epi- to mesopelagic copepods increased from STNA (~2.0–4.6‰) to TNA (~2.9–7.3‰) and were highest in specimens from the STSA (~5.8–9.3‰). In contrast, lowest $\delta^{15}N$ values were measured in the BCIR (~1.3–5.9‰) in epi- to mesopelagic omnivorous species. $\delta^{13}C$ values were lipid-corrected ($\delta^{13}C'$), if C:N ratios were above 4.0 in copepods. Highest $\delta^{13}C'$ were measured for copepodids CV of *Calanoides carinatus* in the TNA (−17.5‰) and females of *Pareucalanus* spp. (−17.2‰) in the BCIR, while *Undeuchaeta major* from the TNA showed minimum $\delta^{13}C'$ values (−22.5‰). Distinct regional or vertical patterns of $\delta^{13}C'$ could not be observed.

While $\delta^{15}N$ values of epi-to mesopelagic species were lower in the BCIR, species-specific trophic levels generally tended to be higher in the BCIR. For example, *Rhincalanus cornutus* had a higher trophic position in the BCIR, although $\delta^{15}N$ decreased, compared to the other regions (Man-Whitney *U*-test, $p = 0.05$ compared to STNA). Intra-specific regional differences in $\delta^{15}N$ were most pronounced in epi- to mesopelagic copepods characterized by trophic levels between 1.5 and 3, e.g. for *Pleuromamm abdominalis*, *P. xiphias*, *Scolecithrix danae*, *Euchirella splendens*, *Neocalanus gracilis*, *Eucalanus hyalinus*, *R. cornutus* and *Pareucalanus* spp. (Table 1). $\delta^{15}N$ values of *P. abdominalis* decreased from around 4‰ in the STNA and TNA to 1.3‰ in the BCIR, whereas trophic levels significantly increased from 1.4 to 2.1 (Man-Whitney *U* test, $p = 0.01$). $\delta^{15}N$ of *S. danae* increased steadily from STNA (3.4‰) via TNA (5.2‰) to STSA (8.3‰), while trophic levels were constant around 2. This also holds true for *N. gracilis*. *E. splendens* from epi- and mesopelagic layers in the STSA showed $\delta^{15}N$ signatures around 8‰, while specimens from bathypelagic layers in the BCIR had much lower $\delta^{15}N$ values of 4.7‰, but mean trophic levels ranged from 2.1 to 2.6 throughout all regions. In contrast, regional differences in $\delta^{15}N$ were less pronounced or did not occur at all in meso- to bathypelagic copepods, which generally showed higher $\delta^{15}N$ (⩾7‰) than shallow-water species. For example, $\delta^{15}N$ values of *Gaetanus pileatus*, *Scottocalanus securifrons*, *Metridia princeps* and *Megacalanus princeps* were either constant or even increased in the BCIR compared to the other regions. These deep-living species exhibited extremely high trophic positions in the BCIR (4.2–5.8) indicating that the baseline and food resources may follow a different trend at depth.

With regard to depth-related changes, only *Pareucalanus* spp. showed pronounced increases in $\delta^{15}N$ and trophic level with increasing depth of occurrence in the TNA. Other species, e.g. *N. gracilis* from epipelagic layers had very similar $\delta^{15}N$ values (7.7‰) and trophic positions (1.9) as specimens from mesopelagic depths (7.6‰ and 1.9, resp.). In addition, *R. cornutus*, *E. hyalinus* and *Euchaeta marina* collected from different depth layers in the same region also showed no vertical differences in $\delta^{15}N$ and trophic level (Table 1). However, trophic levels calculated for specimens from below the upper 100 m should be treated with caution due to potentially different food sources at depth.

3.3. Fatty acid and fatty alcohol compositions

Details of the fatty acid (FA) and alcohol (FAlc) compositions of each species are presented in Table 2 and Fig. 3. FA compositions were species-specific and independent of region and depth of

Table 1
Stable carbon ($\delta^{13}C$) and nitrogen ($\delta^{15}N$) isotopic ratios, C:N atom ratios and trophic levels of calanoid copepods in the STNA, TNA, STSA and BCIR (see Fig. 1) from epi-, meso- and bathypelagic depths of occurrence (*E* = 200–0 m, *M* = 1000–200 m, *B* = 2000–1000 m). Trophic levels were calculated via station-specific $\delta^{15}N$ of particulate organic matter (POM) from the upper 100 m applying a $\delta^{15}N$ enrichment of 3.4‰ per trophic level. $\delta^{15}N$ of POM ranged from 0.9‰ to 2.9‰ in the STNA (1.9 ± 1.1‰), 0.5‰ to 2.6‰ in the TNA (1.7 ± 0.9‰), 2.1‰ to 4.7‰ in the STSA (3.9 ± 1.2‰), and to −2.9‰ to −0.6‰ in the BCIR (−2.0 ± 1.3‰). $\delta^{13}C$ was lipid-corrected ($\delta^{13}C'$), if C:N ratio ⩾ 4. $\delta^{13}C$ of POM ranged from −25.2‰ to −23.8‰ in the STNA (−24.7‰ ± 0.6‰), −24.3‰ to −21.4‰ in the TNA (−23.4 ± 1.4‰), −23.9 to −23.7 in the STSA (−23.8 ± 0.1‰), and −23.0 to −22.0 in the BCIR (−22.3 ± 1.2‰). Values are given as mean ± standard deviation, if *n* ⩾ 3 (f = female; CV = copepodid CV; *n* = number of replicates).

Species	Stage	Region	Depth	$\delta^{15}N$	$\delta^{13}C'$	C:N	Trophic level	*n*
Calanidae								
Undinula vulgaris	f	TNA	*E*	4.9 ± 1.1	−19.1 ± 0.9	3.4 ± 0	2.1 ± 0.5	7
Neocalanus gracilis	f	TNA	*E*	4.8 ± 0.2	−22.1 ± 0.1	3.8 ± 0.1	1.7 ± 0.1	5
		STSA	*E*	7.7 ± 0.3	−21.5 ± 0.1	3.9 ± 0.1	1.9 ± 0.1	7
			M	7.6 ± 0.8	−21.1 ± 0.4	3.8 ± 0.2	1.9 ± 0.2	5
		BCIR	*M*	3.8	−19.4	3.6	2.4	1
Calanoides carinatus	CV	STNA	*M*	6.3 ± 0.8	−18.5 ± 0.6	8 ± 0.2	2.6 ± 0.2	3
		TNA	*M*	6.7 ± 0.8	−18 ± 0.4	7.8 ± 0.2	2.3 ± 0.2	4
			B	6.9 ± 1.1	−17.5 ± 0.4	8.5 ± 0.5	2.6 ± 0.3	4
Candaciidae								
Candacia ethiopica	f	STNA	*E*	2.8 ± 0.3	−21.3 ± 0.1	3.7 ± 0	1.6 ± 0.1	3
Metridinidae								
Pleuromamma abdominalis	f	STNA	*E* − *M*	4.1 ± 0.4	−20.9 ± 0.4	3.6 ± 0.1	1.4 ± 0.2	5
		TNA	*M*	4.5/4.5	−20.4/−20.3	3.7/3.6	1.5/1.5	2
		STSA	*M*	8.1	−20.9	3.6	2.1	1
		BCIR	*M*	1.3 ± 0.3	−21 ± 0.1	3.6 ± 0	2.1 ± 0.1	5
Pleuromamma xiphias	f	TNA	*M*	6.6 ± 0.1	−22 ± 0.3	3.5 ± 0	2.5 ± 0	3
		STSA	*M*	8.4 ± 0.4	−21 ± 0.1	3.7 ± 0.1	2.2 ± 0.1	3
Metridia princeps	f	STNA	*M*	8 ± 0.6	−21.6 ± 0.5	5.7 ± 0.7	2.7 ± 0.2	6
		TNA	*B*	10.7/10.6	−20.9/−20.2	4.8/5.8	4/4	2
		STSA	*M*	12.2	−20.6	6.8	4.0	1
		BCIR	*M* − *B*	13.6/12.5	−22.6/−21.1	4.4/5.6	5.8/4.8	2
Gaussia princeps	f	TNA	*M*	14.5	−20.2	4.3	4.2	1
Eucalanidae								
Pareucalanus spp.	f	TNA	*E*	2.9 ± 0.8	−21.8 ± 0.1	3.7 ± 0.1	1.6 ± 0	5
			M	6.3 ± 0.8	−19.5 ± 1.0	7.1 ± 0.8	2.5 ± 0.4	8
			B	7.4 ± 0.8	−19.8 ± 0.4	7.2 ± 0.9	2.8 ± 0.2	4
		STSA	*B*	6.8 ± 2.1	−20.3 ± 1.4	5.6 ± 0.6	1.6 ± 0.6	3
		BCIR	*E*	3.2 ± 1.1	−17.2 ± 1.2	6.8 ± 2.1	2.3 ± 0	7
Rhincalanus cornutus		TNA	*E*	7.3 ± 1.1	−18.5 ± 0.2	9.8 ± 0.3	2.7 ± 0.3	3
			M	5.8 ± 0.7	−19 ± 0.3	8 ± 0.6	2.2 ± 0	4
			B	7.2 ± 0.5	−18.6 ± 0.5	9.7 ± 0.5	2.5 ± 0.3	5
		STSA	*M*	7.3 ± 1.2	−21 ± 1.9	8.1 ± 0.5	1.8 ± 0.3	7
		BCIR	*E*	5.9 ± 0.5	−22 ± 1.4	8.1 ± 0.7	3.6 ± 0.2	3
Eucalanus hyalinus	f	STNA	*M* − *B*	8.5 ± 1	−21.1 ± 0.7	4 ± 1	2.7 ± 0.3	6
		BCIR	*E*	4.8 ± 0.9	−20.3 ± 1.3	3 ± 0.2	3.2 ± 0.3	3
			M	4.4 ± 0.6	−20.2 ± 0.6	3.1 ± 0.1	3 ± 0.2	3
Scolecithrichidae								
Scolecithrix danae	f	STNA	*E*	3.4 ± 0.2	−20.7 ± 0.2	3.6 ± 0.1	1.7 ± 0.2	4
		TNA	*E*	5.1 ± 0.2	−20.2 ± 0.2	3.6 ± 0.1	2.4 ± 0.1	4
		STSA	*E*	8.3 ± 0.3	−21.3 ± 0.2	3.6 ± 0	2.1 ± 0.1	5
Scolecithricella sp.	CV	TNA	*B*	6.5 ± 0.5	−20.4 ± 0.2	8.5 ± 0.3	2.6 ± 0.1	6
Scottocalanus securifrons	f	STSA	*M*	8.7 ± 0.8	−20.3 ± 0.2	3.7 ± 0.1	2.2 ± 0.2	4
		BCIR		7.3/10.5	−19.8/−20.2	3.7/3.9	3.9/4.2	2
Scaphocalanus magnus	f	STNA	*M*	8.4	−21.4	4.2	3.2	1
Euchaetidae								
Euchaeta marina	f	STNA	*M*	6.2 ± 1.1	−21.8 ± 0.4	3.8 ± 0.3	2 ± 0.3	3
		TNA	*E*	6.1 ± 0.3	−20.6 ± 0.2	3.7 ± 0.1	2.6 ± 0.1	3
			M	5.5 ± 1.0	−22.7 ± 0.3	3.8 ± 0.1	2.3 ± 0.1	3
		STSA	*E*	8.6 ± 0.9	−21.3 ± 0.2	3.8 ± 0.2	2.1 ± 0.3	3
Paraeuchaeta gracilis	f	STNA	*M*	7.0	−21.0	7.0	2.8	1
		TNA	*M*	7.8 ± 0.9	−21.4 ± 0.1	5.3 ± 1.5	2.9 ± 0.1	4
	f + eggs	STSA	*M*	10.2 ± 1.5	−20.5 ± 0.5	6 ± 1.3	3 ± 0.4	5
	CV			9.5 ± 0.1	−20.4 ± 0.3	6.8 ± 1.8	2.5 ± 0	4
	f	BCIR	*M*	6.3 ± 0.5	−19.6 ± 1.4	6.4 ± 2.1	2.7 ± 0.8	3
Paraeuchaeta aequatorialis	f	STNA	*M* − *B*	9.1/8.5	−20.3/−20.0	7.7/7.9	2.8/2.7	2
Aetideidae								
Euchirella pulchra	f	STNA	*M*	4.6	−20.2	3.8	1.7	1

(*continued on next page*)

Table 1 (*continued*)

Species	Stage	Region	Depth	$\delta^{15}N$	$\delta^{13}C'$	C:N	Trophic level	*n*
		TNA	*E – M*	5.6/6.0	−20/−20.1	4.2/3.8	2/2.1	2
		STSA	*M*	6.8 ± 1.4	−20.5 ± 0.3	3.5 ± 0.0	1.9 ± 0.8	3
Euchirella splendens	f	STSA	*E*	8.1 ± 1	−20.5 ± 0.2	4.4 ± 0.2	2.1 ± 0.3	4
			M	8.2 ± 0.5	−20.5 ± 0.6	3.9 ± 0.6	2.1 ± 0.2	5
		BCIR	*B*	4.7 ± 0.7	−21.2 ± 0.2	4.2 ± 0.3	2.6 ± 0.2	3
Undeuchaeta major	f	STNA	*M*	6.1 ± 0.5	−22.2 ± 1	3.9 ± 0.4	2.2 ± 0.3	4
		TNA	*M*	7.7 ± 0.6	−22.5 ± 0.2	4.1 ± 0.2	2.9 ± 0.2	3
		STSA	*M*	9.3/9	−22.3/−22.4	4.4/4.5	3.1/3.0	2
Chirundina stretsii	f	STNA	*M*	7.5 ± 0.2	−21.7 ± 0.4	3.5 ± 0.2	2.4 ± 0	3
		TNA	*M*	9.5 ± 0.4	−21.0 ± 0.4	3.7 ± 0.5	2.7 ± 0.8	5
Gaetanus pileatus	f	STNA	*M*	6.8	−21.0	3.8	2.2	1
		STSA	*M*	10.0 ± 1.6	−20.3 ± 0.5	5 ± 1.4	2.9 ± 0.8	3
		BCIR	*M*	9.3 ± 3.5	−20.5 ± 0.4	4.8 ± 0.8	4.3 ± 0.8	3
Gaetanus kruppii	f	STNA	*M*	7.4	−20.9	3.7	2.3	1
			B	8.9	−20.4	4.0	2.8	1
		STSA	*M*	10.5	−19.8	6.7	2.8	1
Gaetanus miles	f	BCIR	*M*	9.0	−20.5	4.3	4.4	1
Gaetanus tenuispinus	f	STSA	*B*	12.1	−20.3	7.2	3.2	1
Pseudochirella obtusa	f	STNA	*M*	9.9	−20.6	3.6	3.1	1
Valdiviella sp.	f	BCIR	*M – B*	15.6/15.5	−19.5/−19.9	7.8/8.1	5.5/5.7	2
Heterorhabdidae								
Disseta palumbii	f	STNA	*B*	6.8/7.7	−21.7/−21.3	4.1/3.6	2.2/2.4	2
		TNA	*B*	11.7	−18.8	6.0	4.0	1
Megacalanidae								
Megacalanus princeps	f	TNA	*M*	10.8 ± 0.4	−19.2 ± 0.4	4.4 ± 0.6	3.5 ± 0.1	3
	CIII		*M*	8.9	−20.1	3.5	3.5	1
	CV		*B*	9.7	−21.5	4.1	3.4	1
	f	STSA	*M*	11.7	−20.8	3.5	3.1	1
		BCIR		11.3	−20.8	4.3	5.1	1
Augaptilidae	f	STNA	*M*	6.3	−20.9	5.6	3.0	1
		STSA	*M*	13/12	−20.6/−20.3	7.3/6.7	3.4/3.1	2
			B	10.9 ± 1.5	−21 ± 0.6	4.6 ± 0.7	2.8 ± 0.4	3

occurrence. Principal component analysis (PCA) based on FA compositions, grouped individuals of the same species closely together, even when they were collected from a wide latitudinal and vertical range throughout the eastern Atlantic Ocean. PCA produced four distinct species clusters (A, B, C and R, Fig. 3), but did not reveal intra-specific regional or vertical differences. Three main principal components (PC) were identified explaining 87% of the variance, with PC1 and PC2 together explaining 77% (Fig. 3). The first PC is mainly represented by positive values of 18:1($n-9$), 16:1($n-7$), the sum of 22:1 and 20:1 and 16:4($n-1$), and negative eigenvectors of 14:0, 16:0, 18:0, 22:6($n-3$) and the sum of bacterial markers, all mentioned in decreasing order of explanatory power (in total 40% of variance explained). The second PC is mostly represented by positive eigenvectors of 22:6($n-3$), 24:1($n-9$), 20:5 ($n-3$), 22:5($n-3$), 20:4($n-3$) and the sum of bacterial markers, and negative values of 14:0, 16:0, 16:4($n-1$), 16:1($n-7$) and 18:1($n-9$), again mentioned in decreasing order of explanatory power (in total 37% of variance explained).

One large cluster within the PC dimensions included the species *N. gracilis*, *P. robusta*, *P. xiphias*, *P. abdominalis*, *U. vulgaris*, *S. danae* and *E. pulchra* (cluster A, Fig. 3). Most of their FAs incorporated typical membrane components, e.g. 16:0, 20:5($n-3$) and 22:6($n-3$). In *N. gracilis*, *Pleuromamma* spp. and *U. vulgaris*, 16:0 comprised between 17% and 20% of total fatty acids (TFA), whereas *E. pulchra* had higher values of 26% TFA. In contrast, *Pleuromamma* spp. and *U. vulgaris* showed higher contents of 20:5($n-3$) and 22:6($n-3$) of around 12% and 32% TFA, respectively, whereas *S. danae* and *E. pulchra* had lower values around 9% and 20% TFA, respectively. Species in this group generally exhibited lowest total lipid (TL) contents per dry mass (DM; 9–14% DM) and only trace amounts of wax esters (WE; 2–5% TL). Only *N. gracilis* was distinguished by higher, but very variable amounts of TL (16% DM) and WE contents (37% TL). More than 90% of the FAlcs in *N. gracilis* were long-chain monounsaturated 22:1($n-11$, $n-9$, $n-7$) isomers, in descending order of importance and typically biosynthesized by calanid copepods. The sum of bacterial fatty acid markers (15:0, 17:0, iso 15:0, iso 17:0) ranged from 2.7% TFA in *S. danae* to a maximum of 4.3% TFA in *U. vulgaris*. The latter species revealed the highest bacterivory index (BI) compared to all other species studied. It ranged from 0.3 in *S. danae* to a maximum of 0.6 in *U. vulgaris*, while 16:1($n-7$)/16:0 approached zero ($\leqslant$0.2) within this group. In contrast, *U. vulgaris* showed minimum amounts of the carnivory marker FA 18:1($n-9$) with 3.4% TFA, whereas this marker FA was highest in *S. danae* and *E. pulchra* (around 11% TFA). The carnivory index (CI = 18:1($n-9$)/(Σherb. markers + 18:1($n-9$))) ranged around 0.5 and was highest with 0.6 in *N. gracilis*, *S. danae* and *E. pulchra* within this cluster (Table 2, Fig. 4).

Deep-dwelling copepodids CV of *C. carinatus* formed a separate cluster comprising high amounts of the long-chain-monounsaturated FA 20:1($n-9$) (11% TFA) and 22:1($n-11$) (13% TFA) typical of the family Calanidae (cluster C, Fig. 3). Besides, major FAs were the membrane components 14:0, 16:0, 20:5($n-3$) and 22:6($n-3$) and the diatom marker 16:1($n-7$). Total lipid levels were generally high with 41% DM, coinciding with maximum WE contents (84% TL) compared to all other copepods. WE were mainly composed of the typical calanid FAlcs 20:1($n-9$) (20% TFAlc) and 22:1($n-11$) (48% TFAlc), but also contained higher amounts of the short-chain FAlcs 14:0 (9.0% TFAlc) and 16:0 (16% TFAlc).

The dietary contribution of bacterial markers in *C. carinatus* was very low (0.1), whereas 16:1($n-7$)/16:0 was high with 1.9, coinciding with the lowest mean CI (0.3) in comparison to all other copepods.

Rhincalanus cornutus formed another separate cluster (R) due to extremely high concentrations of the FAs 14:0 and 16:0 and lower concentrations of 20:5($n-3$) and 22:6($n-3$) (Fig. 3, Table 2). More than 50% of TFA were 14:0 (25% TFA) and 16:0 (38% TFA), whereas the rest consisted of 16:1($n-7$), 18:1($n-9$), 20:5 ($n-3$) and 22:6($n-3$). *R. cornutus* and *R. nasutus* were the only species containing phytanic acid (3.1% TFA and 6.1% TFA, resp.). Both species were characterized by high TL (42% DM) and WE contents ($\geqslant$79% TL), while the FA and FAlc profiles of *R. cornutus* were markedly deviating from all other species. 90% of TFAlcs of *R. cornutus* were composed of the shorter-chain monounsaturated FAlcs 16:1 (21% TFAlc) and 18:1 (69% TFAlc). The sum of bacterial markers and the BI were slightly below the values measured for *S. danae* (2.2% TFA and 0.2, resp.), coinciding with an intermediate CI (0.5).

Within the PC dimensions, *R. nasutus*, *Paraeuchaeta* spp. and *L. wolfendeni* clustered closely together due to minimum amounts of the membrane FAs 14:0 and 16:0 and extraordinarily high amounts of 16:1($n-7$) and 18:1($n-9$) (cluster B, Fig. 3). In *R. nasutus,* 16:1($n-7$) comprised 26% TFA and 18:1($n-9$) 29% TFA. Total lipid compositions were very different compared to *R. cornutus*. More than 90% of TFAlcs were 14:0 (46% TFAlc) and 16:0 (48% TFAlc). In *R. nasutus*, bacterial contribution to their diet was almost zero. On the other hand, this species had a very high 16:1 ($n-7$)/16:0 ratio of 9.2. With high 18:1($n-9$), but also high 16:1($n-7$) amounts, the CI was around 0.5.

The FA composition of *Paraeuchaeta gracilis* was clearly dominated by the carnivory marker 18:1($n-9$) (49% TFA), while 16:1($n-7$) was present in moderate amounts (7.5% TFA). Particularly 16:1($n-7$) was much higher in *P. hanseni*, *P. barbata* and *P. aequatorialis* (18–21% TFA). In contrast to these three species and *L. wolfendeni*, *P. gracilis* exhibited high amounts of 20:5($n-3$) (7.4% TFA) and 22:6($n-3$) (17% TFA). *P. hanseni*, *P. barbata*, *P. aequatorialis* and *L. wolfendeni* contained moderate amounts of the calanid marker FAs 20:1($n-9$) and 22:1($n-11$). TL and WE contents were generally high in this group, with TL ranging from 42% DM in *P. gracilis* to 48% DM in *P. hanseni* and WE from 65% TL in *P. hanseni* to 78% TL in *P. barbata*. The dominant FAlcs were 14:0 and 16:0, comprising around 90% TFAlc in *P. gracilis* (17% and 73% TFAlc, resp.). Similar to their FA compositions, *P. hanseni*, *P. barbata*, *P. aequatorialis* and *L. wolfendeni* contained moderate amounts of the long-chain monounsaturated FAlcs 20:1($n-9$) and 22:1($n-11$). The sum of bacterial markers was low ranging from 1.6% TFA in *P. gracilis* to 2.8% TFA in *L. wolfendeni* with dietary contributions approaching zero (BI $\leqslant$ 0.2). The degree of carnivory was higher than in all other species ranging from 0.7 in *P. hanseni* to a maximum of 0.8 in *P. gracilis* (Fig. 4).

4. Discussion

The present study provides detailed insights into inter- and intra-specific differences in trophic characteristics of dominant calanoid copepods on a broad latitudinal scale in the tropical and subtropical eastern Atlantic Ocean. Stable nitrogen and carbon isotopes in combination with lipid compositions have proven to reliably resolve trophic levels and dietary relationships not only at high, but also at lower latitudes (Lee et al., 1971b; Lee and Hirota, 1973; Dalsgaard et al., 2003; Schukat et al., 2014; Teuber et al., 2014). In the present study, the carnivory index (CI) based on fatty acid trophic markers generally agreed with trophic levels (TP) derived from δ^{15}N analysis. Both classified most of the copepods as omnivorous (mean CI ~0.5, TP = 1.8–2.5) or carnivorous (mean CI $\geqslant$ 0.7, TP $\geqslant$ 2.9). This was further supported by lipid-corrected $\delta^{13}C'$ values, which were on average 2–3‰ higher than δ^{13}C of POM. However, δ^{13}C values are less useful than δ^{15}N for the identification of trophic levels, because the enrichment per trophic level is much weaker and more variable (usually ~1‰ per TP in δ^{13}C vs. 3.4‰ per TP in δ^{15}N; Hobson and Welch, 1992; Hobson et al., 2002).

4.1. Life strategies and specific feeding modes

The majority of the species, e.g. *Pleuromamma* spp., *Undinula vulgaris*, *Rhincalanus cornutus*, *Scolecithrix danae* and *Euchirella pulchra,* were opportunistic omnivorous feeders. This is typical of low chlorophyll environments also at higher latitudes, where particle-feeding copepods generally ingest the most abundant food items (Kattner et al., 1989). Fatty acid profiles of the different copepod species were generally in line with previous results from the tropical and subtropical eastern Atlantic Ocean (Teuber et al., 2014) and the Benguela Current upwelling system (Schukat et al., 2014). Four major species clusters (A, B, C and R), revealed by principal component analysis, reflected different life-strategy types characterized by specific dietary preferences. These generally agreed with the three large groups initially described by Lee and Hirota (1973): Group A comprised epipelagic to mesopelagic copepods with high turn-over rates (Teuber et al., 2013; Bode et al., 2013), while lipids were usually absent (except for *Neocalanus gracilis*). Group B consisted mainly of deep-living omnivorous to carnivorous species (except *Rhincalanus nasutus*) with lower metabolic rates (Teuber et al., 2013; Bode et al., 2013.) and high lipid storage. In contrast, group C and R (and *R. nasutus*) accumulated large lipid reserves undergoing ontogenetic vertical migrations.

The large group of constantly feeding, epi- to mesopelagic species (group A) was characterized by non-migrating, epipelagic *U. vulgaris*, *N. gracilis*, *S. danae*, *E. pulchra* as well as vertically migrating *P. robusta*, *P. xiphias*, and *P. abdominalis* (Ambler and Miller, 1987). These species exhibited fatty acid compositions dominated by the principal membrane components 16:0, 20:5 ($n-3$) and 22:6($n-3$). The extremely high amounts of 22:6 ($n-3$) may also derive from increased feeding of these epi- to mesopelagic species on dinoflagellates, which have neutral lipids high in this fatty acid and are usually more abundant in oceanic oligotrophic regions than larger phytoplankton species such as diatoms (for a detailed table showing the fatty acid biomarkers see Parrish, 2013). Furthermore, the dietary contribution of bacteria was more important in this group than in the other species, while low levels of phytoplankton biomarkers suggested minor phytoplankton uptake and/or immediate catabolism of ingested phytoplankton lipids. Epipelagic *S. danae* and mesopelagic *E. pulchra* were the most carnivorous species in this generally lipid- and wax ester-poor group. *U. vulgaris*, on the other hand, showed the highest proportion of bacterial contributions to their diet, which can be expected in this strictly epipelagic, tropical species (Ambler and Miller, 1987; Madhupratap and Haridas, 1990). However, it is not clear whether the bacterial fatty acids were directly derived from bacteria (e.g. feeding on suspended particles) or from feeding on ciliates or other small heterotrophic plankton (e.g. copepod nauplii), which themselves feed directly upon bacterioplankton and are very abundant in tropical oceanic waters (Calbet and Saiz, 2005; Ederington et al., 1995; Turner, 2004).

In general, epipelagic tropical copepods experience a year-round continuous, but poor food supply and therefore they do not accumulate large lipid deposits and their fatty acids are usually required to directly fuel metabolic processes (Lee and Hirota, 1973). However, *Neocalanus gracilis* exhibited moderate total lipid contents (16% DM) and significant, but quite variable amounts of wax esters (18–56% TL). These values were higher than those reported for *N. gracilis* by Kattner and Hagen (2009; TL and WE both 10%), while

Table 2
Dry mass (DM), total lipid (TL) and wax ester (WE) content of calanoid copepods from the eastern Atlantic Ocean listed with fatty acid and fatty alcohol compositions expressed as percentage of total fatty acids (TFA) and alcohols (TFAlc), the sum of bacterial markers (Σbact.), the proportion of bacterial marker input (Σbact./Σherb. + Σbact.), the diatom ratio (16:1($n-7$)/16:0) and the carnivory index (18:1($n-9$)/Σherb. + 18:1($n-9$)). Values are given as mean ± standard deviation, if $n \geqslant 3$ (f = female; CV = copepodid CV; n = number of replicates).

Species	*P. abdominalis*	*P. robusta*	*P. xiphias*	*U. vulgaris*	*S. danae*	*E. pulchra*	*N. gracilis*	*C. carinatus*	*R. cornutus*	*R. nasutus*	*P. gracilis*	*P. hanseni*	*P. aequatorialis*	*P. barbata*	*L. wolfendeni*
Stage	f	f	f	f	f	f	f	CV	f	f	f	f	f	f	f
DM (mg ind^{-1})	0.3 ± 0.1	1.7 ± 0.5	0.7 ± 0.2	0.2 ± 0.0	0.2 ± 0.0	1.7 ± 0.2	0.5 ± 0.1	0.1 ± 0.0	0.2 ± 0.0	0.5 ± 0.1	1.7 ± 0.9	1.4 ± 0.2	4.4 ± 2.4	5.9/5.2	1.8/2.9
TL (% DM)	9.0 ± 4.4	14.0 ± 2.6	9.2 ± 4.1	11.9 ± 3.7	13.8 ± 4.6	13.5 ± 5.9	15.6 ± 8.1	40.5 ± 3.5	41.8 ± 10.4	42.0 ± 10.1	42.7 ± 12.2	48.2 ± 2.6	36.9 ± 6.2	43.9/48.8	39.7/37.3
WE (% TL)	2.2 ± 1.6	3.4 ± 2.6	4.2 ± 3.4	1.8 ± 1.6	2.9 ± 1.9	3.2 ± 1.3	36.6 ± 15.4	84.4 ± 8.3	78.8 ± 8.7	81.4 ± 2.3	72.7 ± 10.3	64.7 ± 12.8	71.5 ± 2.4	77.7/77.1	53.9/57.9
n	14	17	24	8	8	11	14	10	41	10	3	4	5	2	2
Fatty acids (% TFA)															
14:0	2.0 ± 0.4	2.6 ± 1.2	3.0 ± 1.3	4.0 ± 1.2	1.4 ± 0.5	3.2 ± 0.8	3.3 ± 0.9	12.4 ± 2.5	24.8 ± 7.5	1.4 ± 0.5	0.5 ± 0.3	1.4 ± 1.0	0.4 ± 0.2	0.3/0.6	1.4/0.4
Phytanic acid	–	–	–	–	–	–	–	–	3.1 ± 1.3	6.1 ± 4.1	–	–	–	–	–
16:0	17.8 ± 1.0	18.1 ± 2.3	17.0 ± 2.5	20.3 ± 1.2	24.3 ± 2.2	26.2 ± 2.8	17.3 ± 1.5	7.5 ± 1.2	37.8 ± 4.2	2.9 ± 0.7	4.1 ± 2.7	6.0 ± 2.5	2.1 ± 1.0	1.9/1.8	3.7/5.6
16:1($n-9$)	0.5 ± 0.1	0.4 ± 0.1	0.6 ± 0.5	0.2 ± 0.1	0.4 ± 0.4	1.0 ± 0.3	0.4 ± 0.1	0.2 ± 0.1	0.4 ± 0.2	–	0.3 ± 0.1	0.3 ± 0.1	0.5 ± 0.0	0.5/0.6	0.8/0.6
16:1($n-7$)	1.8 ± 0.3	3.1 ± 0.9	3.0 ± 1.0	1.6 ± 0.4	5.0 ± 1.5	3.1 ± 0.5	1.9 ± 0.4	13.2 ± 2.7	3.4 ± 1.1	26.0 ± 2.8	7.4 ± 1.9	17.7 ± 4.5	20.9 ± 0.8	19.5/18.1	10.1/8
16:2($n-4$)	0.1 ± 0.1	0.5 ± 0.2	0.5 ± 0.2	0.2 ± 0.0	0.2 ± 0.0	0.7 ± 0.2	0.4 ± 0.2	1.3 ± 0.4	0.6 ± 0.3	2.3 ± 0.5	0.9 ± 0.1	1.1 ± 0.4	1.2 ± 0.1	1.8/2.1	0.0/0.4
16:3($n-4$)	0.3 ± 0.3	1.2 ± 0.7	0.5 ± 0.2	0.2 ± 0.1	0.5 ± 0.3	0.7 ± 0.2	0.7 ± 0.3	0.9 ± 0.5	0.8 ± 0.4	1.7 ± 0.6	0.9 ± 0.1	1.6 ± 0.4	2.0 ± 1.0	1.8/1.7	1.8/0.1
16:4($n-1$)	–	–	–	–	–	–	–	0.7 ± 0.3	1.2 ± 0.8	2.9 ± 1.0	0.5 ± 0.1	0.4 ± 0.1	1.0 ± 0.1	0.6/0.5	0.9/0.6
18:0	3.5 ± 0.6	3.7 ± 0.5	3.6 ± 0.6	7.2 ± 0.2	6.8 ± 0.8	4.9 ± 0.5	3.4 ± 0.3	1.6 ± 0.6	5.3 ± 1.0	0.6 ± 0.2	1.2 ± 0.7	0.7 ± 0.1	0.4 ± 0.2	0.4/0.3	0.0/1.2
18:1($n-9$)	5.4 ± 1.0	6.8 ± 3.2	6.1 ± 1.8	3.4 ± 0.2	11.4 ± 1.4	11.4 ± 1.2	7.0 ± 0.6	6.3 ± 1.4	7.9 ± 4.1	28.9 ± 2.1	48.0 ± 10.0	40.5 ± 9.7	51.5 ± 3.2	54.9/56.1	46.3/39.5
18:1($n-7$)	1.3 ± 0.2	1.7 ± 0.4	1.6 ± 0.3	1.0 ± 0.2	1.9 ± 0.2	1.7 ± 0.2	1.7 ± 0.3	0.8 ± 0.2	0.9 ± 0.1	1.1 ± 0.1	0.6 ± 0.2	1.7 ± 0.6	1.0 ± 0.2	0.8/0.8	1.7/2.9
18:2($n-6$)	1.7 ± 0.2	1.5 ± 0.3	1.5 ± 0.3	1.7 ± 0.2	1.6 ± 0.2	1.5 ± 0.2	1.9 ± 0.3	2.1 ± 0.7	0.5 ± 0.1	1.7 ± 0.3	1.3 ± 0.1	1.0 ± 0.3	1.2 ± 0.2	1.1/0.8	1.1/1.1
18:3($n-3$)	0.6 ± 0.1	0.7 ± 0.1	0.6 ± 0.2	0.6 ± 0.1	0.5 ± 0.1	0.7 ± 0.1	0.5 ± 0.1	1.1 ± 0.6	0.1 ± 0.1	0.4 ± 0.2	0.7 ± 0.0	0.3 ± 0.1	0.3 ± 0.1	0.3/0.2	0.0/0.2
18:4($n-3$)	1.8 ± 0.2	1.6 ± 0.3	1.7 ± 0.5	0.8 ± 0.2	1.4 ± 0.2	1.9 ± 0.5	1.5 ± 0.3	1.8 ± 0.7	0.8 ± 0.6	1.5 ± 0.9	1.5 ± 0.3	0.3 ± 0.1	0.3 ± 0.2	0.4/0.3	0.0/0.4
20:1($n-11$)	–	0.1 ± 0.1	0.1 ± 0.1	–	–	0.5 ± 0.1	0.3 ± 0.1	1.2 ± 0.1	–	0.5 ± 0.0	1.2 ± 0.3	1.2 ± 0.5	1.0 ± 0.2	1.8/1.8	0.9/1.2
20:1($n-9$)	0.9 ± 0.1	1.1 ± 0.2	1.1 ± 0.4	0.2 ± 0.0	0.4 ± 0.1	1.2 ± 0.2	0.9 ± 0.3	11.2 ± 1.8	0.1 ± 0.1	0.5 ± 0.2	0.3 ± 0.2	3.3 ± 3.9	0.8 ± 0.1	0.8/0.6	3.0/4.1
20:1($n-7$)	–	0.1 ± 0.1	0.1 ± 0.1	–	0.4 ± 1.1	0.1 ± 0.1	0.3 ± 0.1	0.4 ± 0.1	1.0 ± 0.5	0.1 ± 0.1	–	0.2 ± 0.1	0.2 ± 0.0	0.1/0.0	0.0/0.4
20:2($n-6$)	0.4 ± 0.2	0.3 ± 0.1	0.5 ± 0.5	0.2 ± 0.2	0.2 ± 0.1	1.0 ± 0.2	0.4 ± 0.1	1.1 ± 3.0	0.1 ± 0.6	0.1 ± 0.1	0.1 ± 0.1	0.3 ± 0.2	0.8 ± 1.5	0.2/0.1	0.0/0.2
20:4($n-6$)	1.1 ± 0.2	1.2 ± 0.2	1.3 ± 0.3	0.9 ± 0.1	0.8 ± 0.1	1.6 ± 0.4	0.9 ± 0.3	0.9 ± 0.2	0.6 ± 0.2	1.5 ± 0.3	0.7 ± 0.2	0.3 ± 0.1	0.2 ± 0.1	0.3/0.2	2.4/1.1
20:4($n-3$)	1.2 ± 0.3	0.7 ± 0.2	0.9 ± 0.2	0.6 ± 0.1	0.4 ± 0.1	0.5 ± 0.1	1.9 ± 0.3	0.6 ± 0.3	0.2 ± 0.2	0.5 ± 0.1	0.4 ± 0.2	0.1 ± 0.1	0.1 ± 0.1	0.1/0.1	0.0/0.4
20:5($n-3$)	12.6 ± 0.8	11.8 ± 1.4	11.6 ± 1.0	11.5 ± 0.4	8.8 ± 0.9	9.8 ± 1.6	10.7 ± 1.3	9.8 ± 4.5	5.7 ± 3.5	11.9 ± 3.2	7.4 ± 1.9	2.7 ± 0.9	2.6 ± 2.7	1.7/1.9	5.0/3.1
22:1($n-11$)	0.4 ± 0.5	0.3 ± 0.5	0.2 ± 0.3	0.1 ± 0.1	–	0.3 ± 0.2	5.8 ± 3.6	13.1 ± 2.6	–	0.2 ± 0.1	0.5 ± 0.3	6.5 ± 8.7	2.4 ± 0.6	1.7/1.5	1.9/4.9
22:1($n-9$)	0.2 ± 0.2	0.4 ± 0.1	0.3 ± 0.2	–	0.1 ± 0.1	0.2 ± 0.1	1.3 ± 0.7	0.7 ± 0.2	–	–	–	0.6 ± 0.2	0.6 ± 0.3	0.3/0.3	0.7/2.8
22:6($n-3$)	34.9 ± 2.2	29.7 ± 3.9	31.2 ± 5.7	34.1 ± 1.5	24.4 ± 2.2	17.7 ± 2.6	25.3 ± 3.5	5.9 ± 1.3	3.2 ± 0.8	4.2 ± 0.9	17.4 ± 5.7	7.3 ± 4.4	3.4 ± 1.2	3.8/4.5	12.7/10.7
24:1($n-9$)	5.2 ± 1.7	4.6 ± 1.6	5.1 ± 2.2	2.9 ± 0.8	3.4 ± 0.5	2.4 ± 0.8	3.5 ± 0.7	0.7 ± 0.2	0.5 ± 0.2	0.5 ± 0.1	1.4 ± 0.8	1.4 ± 0.8	0.9 ± 0.2	0.8/0.9	1.0/3.6
Fatty alcohols (% TFAlc)															
14:0	47.5 ± 29.5	33.9 ± 12.4	40.4 ± 23.4	29.7 ± 12.3	25.7 ± 9.6	81.9 ± 20.5	2.3 ± 1.7	9.0 ± 1.6	0.3 ± 0.2	46.1 ± 3.6	17.3 ± 10.1	21.9 ± 10.8	24.3 ± 2	38.7/44.3	13.3/8.6
16:0	34.5 ± 19.2	45.9 ± 11.2	39.6 ± 18.8	41.2 ± 6.2	35.7 ± 15.3	9.4 ± 11.4	1.8 ± 2.6	15.9 ± 2.3	5.0 ± 1.1	48.3 ± 3.6	73.2 ± 8.1	35.9 ± 8.1	50.1 ± 1.0	48.6/42.9	55.8/50
16:1($n-7$)	–	–	–	–	1.4 ± 3.2	–	0.1 ± 0.3	1.3 ± 0.2	21.1 ± 2.5	1.0 ± 0.2	1.5 ± 0.9	4.8 ± 3.7	3.8 ± 0.4	2.5/2.6	2.9/2.8
18:0	7.2 ± 9.3	9.9 ± 7.5	11.2 ± 7.3	27.8 ± 13.9	17.3 ± 8	1.6 ± 4.3	0.8 ± 1.1	1.5 ± 0.1	0.5 ± 0.2	3.9 ± 1.0	4.5 ± 1.1	1.4 ± 0.0	1.5 ± 0.2	1.6/1.7	4.6/5.6
18:1($n-9$)	2.0 ± 7.5	4.3 ± 8	2.1 ± 4.1	–	6.3 ± 11.7	–	0.4 ± 1.1	0.7 ± 0.2	69.3 ± 2.7	0.5 ± 0.2	1.2 ± 0.8	7 ± 7.8	3.7 ± 0.7	0.4/0.6	9.9/8.6
18:1($n-7$)	–	2.0 ± 4.2	–	–	2.0 ± 6.1	–	–	0.4 ± 0.2	1.3 ± 0.2	–	1.3 ± 0.4	5.7 ± 4	4.2 ± 0.4	2.6/2.3	5.2/5.4
20:1($n-9$)	0.7 ± 2.5	–	1.5 ± 7.4	–	1.7 ± 3.6	–	1.1 ± 0.6	20.2 ± 0.9	–	0.1 ± 0.1	0.4 ± 0.2	5.7 ± 4.4	1.4 ± 0.1	1.2/1.1	4.2/4.3
22:1($n-11$)	8.1 ± 17	1.1 ± 3.2	2.3 ± 4.9	1.3 ± 3.7	3.2 ± 9.5	7.1 ± 15.9	72.4 ± 7.3	48.1 ± 3.6	2.4 ± 0.8	–	0.4 ± 0.7	11.1 ± 11.6	3.7 ± 0.6	2.0/1.7	0/4.4
22:1($n-9$)	–	2.8 ± 11.7	1.4 ± 6.8	–	–	–	16.3 ± 2.5	2.2 ± 0.4	–	0.1 ± 0.2	0.2 ± 0.4	5.2 ± 3.4	5.9 ± 1.5	2.2/2.3	4.2/7.7
22:1($n-7$)	–	–	1.3 ± 6.1	–	6.7 ± 20.1	–	4.8 ± 2.0	0.3 ± 0.2	–	–	–	0.6 ± 0.7	1.1 ± 0.4	–	0/1.3
Bacterial markers															
Σbact. markers	3.6 ± 0.4	4.0 ± 0.4	4.3 ± 0.6	4.2 ± 0.2	2.7 ± 0.7	4.1 ± 0.4	3.8 ± 0.7	1.3 ± 0.3	2.2 ± 0.9	0.6 ± 0.1	1.6 ± 0.1	1.7 ± 0.7	2.7 ± 0.1	2.7/2.6	2.8/2.6
Σbact./Σherb.+Σbact.	0.4 ± 0.0	0.4 ± 0.0	0.4 ± 0.1	0.6 ± 0.1	0.3 ± 0.1	0.4 ± 0.0	0.4 ± 0.1	0.1 ± 0.0	0.2 ± 0.1	0.0 ± 0.0	0.1 ± 0.0	0.1 ± 0.0	0.1 ± 0.0	0.1/0.1	0.2/0.2
16:1($n-7$)/16:0	0.1 ± 0.0	0.2 ± 0.0	0.2 ± 0.0	0.1 ± 0.0	0.2 ± 0.1	0.1 ± 0.0	0.1 ± 0.0	1.9 ± 0.7	0.1 ± 0.0	9.2 ± 2.3	3.8 ± 4.7	4.3 ± 4.3	12.3 ± 6.3	10.1/9.9	2.8/1.4
Carnivory index															
Carn./Σherb. + carn.	0.5 ± 0.0	0.5 ± 0.1	0.5 ± 0.1	0.5 ± 0.1	0.6 ± 0.1	0.6 ± 0.0	0.6 ± 0.0	0.3 ± 0.1	0.5 ± 0.1	0.5 ± 0.0	0.8 ± 0.0	0.7 ± 0.1	0.7 ± 0.0	0.7/0.7	0.8/0.8

fatty acid compositions were similar. *N. gracilis* is known to perform ontogenetic vertical migrations (OVM) on a very small scale within the upper 300 m (Ambler and Miller, 1987; Shimode et al., 2009). Copepodids CI of *N. gracilis* apparently do not feed and carry a large oil droplet in their body as energy reserve, but do not enter dormancy (Shimode et al., 2009). Lipid and wax ester levels were significantly lower than those of their high-latitude congeners. They are known to perform extensive seasonal OVM including a developmental descent of late copepodids, which overwinter in diapause (Ohman, 1987; Tsuda et al., 2001; Lee et al., 2006; present study). However, maintaining the ability to accumulate energy reserves may be of evolutionary advantage for *Neocalanus sp.* also in highly competitive, oligotrophic environments.

Lipid and wax ester contents of CV copepodids of *C. carinatus* and females of *R. nasutus* and *R. cornutus* were much higher compared to *N. gracilis*. OVM including diapause is known for CV stages of *C. carinatus* in coastal upwelling systems (Verheye et al., 2005). CVs of *C. carinatus* were collected only below 500 m off the Northwest African and Angolan-Namibian coast obviously belonging to the offshore resting component of the population, which will eventually be transported back onto the shelf (Verheye et al., 2005). High concentrations of diatom markers and a minimum CI (0.3) indicate intensive feeding on diatoms as active stages at the surface during short periods of high productivity. *C. carinatus* exhibited the second lowest dietary contribution of bacteria compared to all other species. While wax esters are accumulated based on highly nutritious phytoplankton during short-term blooms (Verheye et al., 2005; Schukat et al., 2014), bacterivorous ciliates apparently do not cover nutritional demands for long-term survival (Ederington et al., 1995; present study). A CI of $\leqslant$0.3 seems to be typical for mostly herbivorous copepods, which is similar to 0.2 for *C. carinatus* in the Benguela Current System, calculated from Schukat et al. (2014) and Teuber et al. (2014). Even lower CIs of around 0.1 were calculated for herbivorous Arctic *Calanus* spp. from Graeve et al. (1994a). Although δ^{15}N values (6–7‰) and trophic levels of *C. carinatus* CVs were higher than expected, they were within the range of previous studies (Schukat et al., 2014; Teuber et al., 2014). The calculated trophic level may be somewhat biased, as the diapausing copepodids previously fed at different times at the surface, presumably with a different baseline δ^{15}N of POM. Furthermore, heavier ^{15}N isotopes may accumulate slowly over a long time period in these deep-dwelling, diapausing stages, depending on their residence time at depth. This is further supported by their unusually heavy $\delta^{13}C'$ signal compared to the other copepod species.

Large amounts of total lipids and wax esters were found in both *R. cornutus* and *R. nasutus*, which agrees with studies off southern California (Lee et al., 1971b), in the Arabian Sea (Schnack-Schiel et al., 2008), the tropical Atlantic (Cass et al., 2011; Teuber et al., 2014) and the Benguela upwelling system (Schukat et al., 2014). Dormancy of copepodids CV and females of *R. nasutus*, *R. rostrifrons* and other Eucalanidae occurred in tropical and subtropical, also non-upwelling oceanic regions, while dormant females were able to quickly respond to small-scale upwelling events (Ohman et al., 1998; Schnack-Schiel et al., 2008; Shimode et al., 2012a,b). Their quiescent stages seemed to be event-driven rather than seasonally determined by an internal clock (Ohman et al., 1998). Although dormancy has not been studied yet in *R. cornutus*, it is likely to be shared among tropical-subtropical *Rhincalanus* species (Shimode et al., 2012a). This is supported by our observation that some individuals were easily caught with a pipette showing no reactions, while other specimens were very active and hard to catch (data not shown). Furthermore, high lipid and wax ester levels in these species may provide neutral buoyancy and thus permit constantly low locomotion activity without sinking (Cass et al., 2011). This matches the generally sluggish life-style with low metabolic rates of eucalanid species (Flint et al., 1991; Ohman et al., 1998; Bode et al., 2013; Teuber et al., 2013).

However, lipid profiles and dietary preferences of *R. nasutus* (cluster B) and *R. cornutus* (cluster R) were very different from each other. *R. nasutus* seemed to be largely feeding on phytoplankton indicated by high levels of diatom markers, minimum bacterial contributions and considerable percentages of phytanic acid. The latter is derived from phytol, a component of chlorophyll, and thus either derived directly from feeding on phytoplankton or via phytodetritus (Sargent and Henderson, 1986). In contrast, *R. cornutus* was more omnivorous and diatoms were of minor dietary importance. These feeding preferences match the distributional pattern of the two species, as *R. nasutus* was caught only in the proximity of the Canary Current and Benguela Current, similar to *C. carinatus*, while *R. cornutus* was ubiquitously distributed along the cruise track. Furthermore, two alternative synthetic pathways of lipids have been suggested for *R. cornutus* and *R. rostrifrons,* on the one hand, and for *R. nasutus* and its Antarctic congener *R. gigas* on the other hand (see details in Cass et al., 2011). In addition to trophic influences, genetic predisposition likely plays a significant role in determining the principal lipid profile of copepods (Persson and Vrede, 2006; Cass et al., 2011), which is further supported by the results of the present study.

Deep-living *Lucicutia wolfendeni* and *Paraeuchaeta* spp. contained high amounts of total lipids and wax esters, together with the highest degree of carnivory (cluster B). Except for *P. gracilis*, high amounts of 16:1($n-7$) together with the calanid marker fatty acids 20:1 and 22:1 suggested preying on diapausing calanids such as *C. carinatus* (Hagen et al., 1995; Laakmann et al., 2009a,b). In case of *L. wolfendeni*, which can be a detrivore or opportunistic carnivore, feeding on *C. carinatus* could be either via direct predation or consumption of dead carcasses (Gowing and Wishner, 1998). This "trophic shortcut" from primary production in the surface layer to the deep sea via seasonally vertically migrating copepods was also found in polar oceans (e.g. for *P. barbata*) (Hagen et al., 1995; Laakmann et al., 2009a,b). Species of *Paraeuchaeta* and *Lucicutia* may synthesize 16:1($n-7$) *de novo* at least to a certain extent, indicated by elevated amounts of this fatty acid also in *P. gracilis*, which was hypothesized for euchaetid species by Hagen et al. (1995). The enrichment of 16:1($n-7$) biases the CI and thus should not be considered as a diatom marker in these clearly carnivorous species. Due to much higher concentrations of 16:1 ($n-7$) in *P. aequatorialis*, this species had a lower CI compared to *P. gracilis*, even though the trophic level of *P. aequatorialis* was higher than that of *P. gracilis*. *Lucicutia* aff. *L. grandis* in the Arabian Sea was described as primary detritivore and opportunistic carnivore, feeding on a wide variety of detrital material, prokaryotic and eukaryotic autotrophs, bacterial aggregates and metazoans (Gowing and Wishner, 1998). In contrast, *Paraeuchaeta* spp. are clearly rheotactic predators (Auel, 1999).

Copepods usually have trophic levels between 2 and 3, while a few species such as the very large *Gaussia princeps* reach TPs greater than 3 (Hobson et al., 2002; Schukat et al., 2014). Such a high trophic position coincides with a high CI of 0.85 in *G. princeps*, calculated from Teuber et al. (2014). Thus, copepods as a taxonomic group show very diverse feeding modes and dietary spectra, encompassing a wide range of trophic levels (Schukat et al., 2014).

4.2. Regional differences

Fatty acid compositions of the copepods were clearly species-specific and did not reveal remarkable intra-specific spatial differences between oceanic provinces. This coincided with the generally opportunistic feeding strategies and thus can be expected in low-latitude oceanic regions with constant, but low primary production. The only important exception was that the

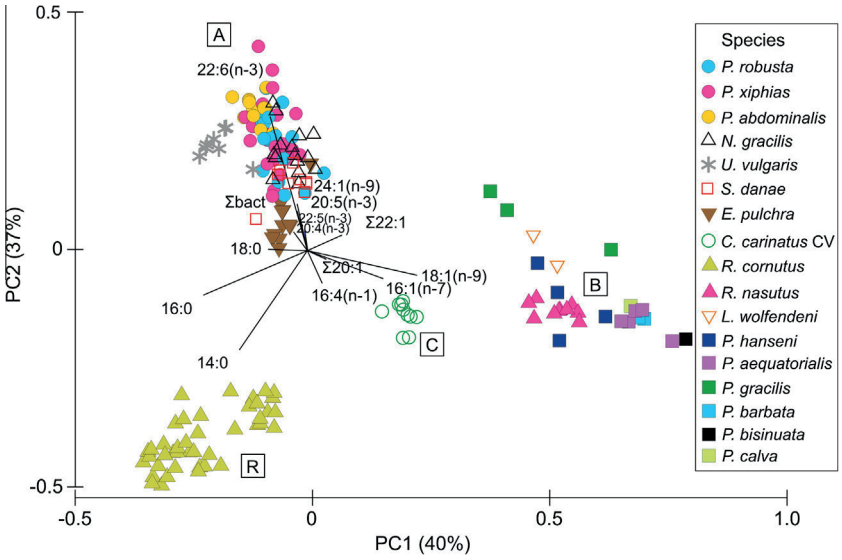

Fig. 3. Principal component analysis (PCA) based on fatty acid compositions. Copepod species (all females except copepodids CV of *C. carinatus*) are arranged along the first two principal components PC1 and PC2 resulting in four clusters (A, B, C, and R).

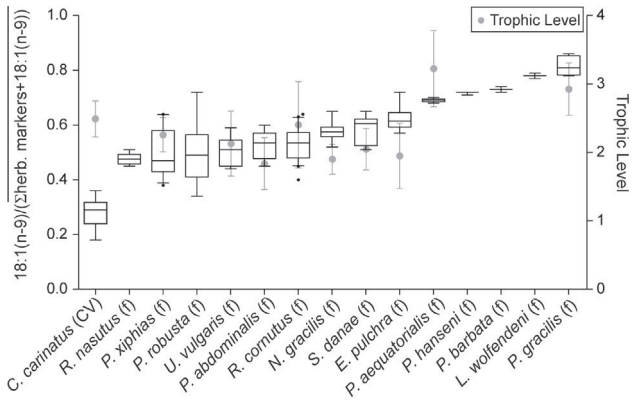

Fig. 4. Carnivory indices (18:1($n-9$)/Σherb. markers + 18:1($n-9$)) of the different copepods arranged as box plots according to increasing degree of carnivory. Boxes include the 5th and 95th percentiles, while whiskers show the variability outside the lower and the upper percentile. Black dots indicate outliers. Mean trophic levels derived from δ^{15}N stable isotope analysis were added as gray dots (± standard deviation) for each species along the right *y*-axis. CV = copepodid CV, f = female.

diatom ratio 16:1($n-7$)/16:0 in the two samples of *C. carinatus* CVs from the BCIR was higher (3.2) than in specimens from the TNA (1.6) and the STSA (1.4) (Fig. A, Appendix). Accordingly, the CI was lowest in the BCIR (0.2 compared to 0.3–0.4 at TNA and STSA). This agrees with findings indicating that the life cycle of herbivorous copepods is strongly linked to seasonal phytoplankton blooms occurring only during a short time period. Copepods responded to seasonal changes in phytoplankton assemblages at higher latitudes (Kattner et al., 1989; Stevens et al., 2004; Gentsch et al., 2009) and during upwelling blooms (Escribano and Pérez, 2010), as marker fatty acids mirrored available food items such as typical flagellates or diatoms. Furthermore, *P. abdominalis* and *R. cornutus* had significantly lower CIs in the BCIR (p-value $\leqslant 0.008$), while *P. xiphias* showed significantly lower proportions of bacterial feeding in the BCIR (p-value = 0.001) compared to all other regions. *R. cornutus* showed maximum bacterial indices in the TNA and STSA, which were higher than in the STNA (p-value $\leqslant 0.02$) and BCIR (p-value > 0.05). In contrast, *P. robusta* exhibited a significantly higher degree of carnivory in the BCIR (p-value = 0.01). Opportunistic copepods can obviously adapt their feeding toward herbivory, if phytoplankton is readily available (Landry, 1981; Gentsch et al., 2009; Escribano and Pérez, 2010). Other species (here *P. robusta*), however, may take advantage of potentially rich supplies of zooplankton prey during periods of high productivity.

Geographical differences in δ^{15}N values of the different epi- to mesopelagic copepod species reflected corresponding spatial differences in baseline δ^{15}N of POM (D. Fonseca-Batista, pers. comm., 2015). The observation that δ^{15}N of zooplankton follows seasonal (e.g. Goering et al., 1990; Montoya, 1994; Rolff, 2000) and regional (e.g. Montoya et al., 2002; McClelland et al., 2003; Schmidt et al., 2003; Hauss et al., 2013; Sandel et al., 2015) changes at the food-web base holds true on a large geographic scale. However, the majority of these studies were conducted on bulk, size-fractionated zooplankton samples, only few studies analyzed individual species (Schmidt et al., 2003; Hauss et al., 2013; Sandel et al., 2015). In the present study, δ^{15}N of POM was highest in the STSA region and severely decreased (<0‰) in the BCIR (D. Fonseca-Batista, pers. comm., 2015). Negative δ^{15}N signals of POM in the BCIR may be explained by preferential uptake of ^{14}N nitrate by phytoplankton, when nitrate is readily available upon mixing or injection of subsurface nutrients into the surface layer (Holmes et al., 2002; Montoya et al., 2002). The most intensive upwelling in the northern Benguela Current system generally takes place from September to November. Low SST and SSS together with low δ^{15}N of POM and elevated chl *a* signals in the BCIR during the time of sampling indicate the influence of the Benguela Current upwelling. Negative δ^{15}N values of POM (−2.8 to −0.2‰) were also reported after equatorial upwelling in the Atlantic Ocean in northern hemisphere spring (Montoya et al., 2002). Other biological processes, such as excreted ammonia and N_2-fixation processes, may also lead to decreased δ^{15}N signals of POM in respect to deep-water nitrate (global range: 3–6‰) (Mino et al., 2002). N_2-fixation extensively contributes to the nitrogen budget of the oligotrophic North Atlantic (Montoya et al., 2002), and, especially in the TNA, may be enhanced by atmospheric dust input (Sandel et al., 2015). Apparently, upwelling did not affect the other regions during the present study, as indicated by water column stratification, high SST and low chl *a* signals. Therefore, the intermediate δ^{15}N values of POM (0.9–2.9‰) in the TNA and STNA rather suggest the influence of excreted ammonia and/or N_2-fixation processes followed by remineralization and assimilation of this nitrogen. The higher δ^{15}N values in the STSA (2.1–4.7‰) suggested that these

contributions were lower or even absent during the time of sampling, while very low, but steady supply of advected nitrate rather fueled phytoplankton production (Mino et al., 2002; Montoya et al., 2002; D. Fonseca-Batista, pers. comm., 2015).

Unexpectedly, trophic levels of copepods, calculated from $\delta^{15}N$ differences between POM and consumer, strongly deviated between the BCIR and other regions (Table 1). On average, calculated trophic levels were 0.9 units higher in the BCIR as compared to other regions. It is not very likely that these differences indeed reflect real changes in feeding mode and dietary composition, as such a dramatic decrease of one unit TP would mean a change from carnivorous feeding ($TP \geqslant 3$) to herbivory ($TP = 2$). Moreover, respective shifts in the CI based on fatty acid profiles were not observed. Therefore, we assume that trophic positions in the BCIR have been overestimated by the $\delta^{15}N$ approach. In particular, finding an appropriate $\delta^{15}N$ baseline for the food web comprises a challenging task in such a highly dynamic system as the BCIR. Varying and not exactly known turnover and integration times of stable isotopic signatures in primary producers, protozoans and copepods can lead to delays, before periodic changes of baseline $\delta^{15}N$ are fully incorporated into body tissues of primary consumers (O'Reilly et al., 2002; Schmidt et al., 2006). This phenomenon may be even more pronounced in higher-level consumers, which applies to the majority of tropical and subtropical copepods (Hobson et al., 2002; Schukat et al., 2014; this study). Episodic upwelling usually leads to an initial decrease in the $\delta^{15}N$ of primary producers due strong phytoplankton discrimination toward the lighter nitrogen isotope, followed by an increase in $\delta^{15}N$ as nitrate becomes depleted again (Montoya et al., 2002). The extremely low $\delta^{15}N$ of POM in the BCIR suggests that a recent upwelling event triggered a new phytoplankton bloom with excess nitrate concentration (O'Reilly et al., 2002). Due to high turnover rates (growth rates of 1.2 d^{-1} or higher) and nitrogen uptake, phytoplankton stable isotope signatures respond within a few days (or faster) to the new upwelling signal (O'Reilly et al., 2002), whereas copepods, in particular deeper-dwelling species and/or higher trophic levels, will only change in stable isotope signature with a substantial time lag. Thus, spatial and seasonal changes in nutrient resources can drive significant and rapid fluctuations at the food-web base (Rolff, 2000), which are not immediately reflected in higher trophic levels due to their longer turnover times (Montoya et al., 2002; O'Reilly et al., 2002; Schmidt et al., 2006). Taking advantage of differences in ^{15}N enrichment in glutamic acid relative to phenylalanine, compound-specific isotope analysis of these amino acids may clarify the magnitude and time-scales, on which short-time variations of nutrient resources propagate into the food web and may lead to a more accurate determination of zooplankton trophic positions (McClelland and Montoya, 2002; McClelland et al., 2003; Hannides et al., 2009; Larsen et al., 2013).

4.3. Vertical differences

$\delta^{15}N$ values of copepod species in the different food webs of the eastern Atlantic Ocean were rather independent of their depth of occurrence. *Pareucalanus* was the only genus showing marked increases of $\delta^{15}N$ and trophic level from epi- to bathypelagic depths. However, at least two different species, similar to *Pareucalanus sewelli*, were pooled so that observed changes in $\delta^{15}N$ could be affected by species-specific differences, emphasizing the importance of individual species measurements. Due to extensive diel vertical migrations of species such as *Pleuromamma* spp. with night-time feeding at the surface and excretion and fecal pellet production at depth, copepods play an important role in the vertical flux of organic and inorganic matter from surface to deeper layers (Longhurst and Harrison, 1988, 1989; Longhurst et al., 1990; Zhang and Dam, 1997; Steinberg et al., 2002). They maintain a dynamic exchange with the euphotic zone and thus are actively involved in transforming the biochemical and stable isotope composition of POM (Laakmann and Auel, 2010). The fact that regional differences were observed among species from epi- to mesopelagic depth layers (e.g. *R. cornutus*, *N. gracilis*, *P. abdominalis*, *P. gracilis*) indicates that fractionation processes by primary producers in the euphotic zone propagate along the food chain to deeper layers (Koppelmann et al., 2009; Laakmann and Auel, 2010).

Species restricted to deeper layers below the euphotic zone, such as *Paraeuchaeta* spp., *Gaetanus* spp., *Chirundina streetsii*, *Scottocalanus securifrons*, *Metridia princeps* and *Megacalanus princeps*, had generally higher $\delta^{15}N$ values compared to species that also occurred in the euphotic zone. This agrees with the overall increasing tendency toward carnivory with greater depth for deep-sea species (Polunin et al., 2001; Auel and Hagen, 2005; Laakmann and Auel, 2010), due to the absence of phytoplankton and proportionally increased availability of detrital aggregates and secondary production (Sugisaki and Tsuda, 1995). The high degree of carnivorous feeding is further supported by high CIs of ~0.7 for *Paraeuchaeta* spp. (Teuber et al., 2014; present study) and even higher CIs of 0.8–0.9 for *L. wolfendeni* (present study), *Gaetanus pileatus* and *Megacalanus princeps*, calculated from Teuber et al. (2014). Concerning predatory *Paraeuchaeta* spp. (Auel, 1999), their increased $\delta^{15}N$ signals may be predominantly related to an increasing number of trophic steps between consumer and food web base. In species that rely to a greater extent on suspended particles than on predatory feeding such as *Lucicutia* (Gowing and Wishner, 1998; Koppelmann et al., 2009), increased $\delta^{15}N$ may be due to both, increase in trophic steps and ingestion of suspended POM enriched in $\delta^{15}N$ in the deep ocean. This is in line with findings from the oligotrophic Mediterranean, where $\delta^{15}N$ of size-fractionated zooplankton increased from meso- to bathypelagic depth by one trophic level, while $\delta^{15}N$ of sinking POM increased only slightly with depth (plus 0.3–1.3‰) (Koppelmann et al., 2003). Therefore, sinking and suspended POM need to be distinguished, as the stable isotope composition of sinking POM generally does not change much over depth compared to suspended POM, which becomes significantly enriched in ^{15}N with depth (Altabet, 1988). Such enrichment of suspended POM (up to 10‰) was observed at the lower limit of the euphotic zone due to decomposition by zooplankton and microbial processes as well as disaggregation of sinking particles (e.g. Saino and Hattori, 1980, 1987; Altabet and McCarthy, 1985; Altabet, 1988; Holmes et al., 1999; Mintenbeck et al., 2007; Koppelmann et al., 2009). Below 300 m, $\delta^{15}N$ of suspended POM remained constant (Holmes et al., 2002; Koppelmann et al., 2003, 2009). This explains why $\delta^{15}N$ in deep-sea organisms primarily feeding on suspended POM is expected to be generally higher than in surface organisms, but does not further increase with increasing depth.

The deep-sea community may rely to great extent on organic matter sinking out from the euphotic zone (Sasaki et al., 1988). For example, in the North Pacific sinking particulate organic carbon flux alone is potentially high enough down to 4000 m to meet nutritious needs of suspension feeding copepods, which themselves are an abundant food source for carnivorous copepods (Sasaki et al., 1988). Due to the time required for some particles to sink from the euphotic zone to greater depth, the seasonal pattern in $\delta^{15}N$ of sinking POM in the bathypelagic zone may be delayed by several weeks to months (Voss et al., 1996; Holmes et al., 2002). Both, the enrichment in $\delta^{15}N$ of suspended POM and delay of sinking POM, may explain why the $\delta^{15}N$ signals of deeper-living species (e.g. *Gaetanus pileatus*, *S. securifrons*, *Metridia princeps*) did not show the same regional trend as the epi- to mesopelagic species, since they rely to a large part on suspended and/or sinking particles. Furthermore, it is not certain if the $\delta^{15}N$ enrichment of 3.4‰ per trophic level can be reliably applied in

the deep-sea, as transfer efficiencies may be higher in food-limited environments (Childress and Thuesen, 1992; Koppelmann and Weikert, 2000). Copepods that feed at higher trophic levels and have lower metabolic rates and longer turn-over times, typical of deep-sea copepods (Koppelmann and Weikert, 2000), should generally show little response to temporal changes in $\delta^{15}N$ (Montoya, 2007). To establish an appropriate baseline for these deeper-dwelling species, $\delta^{15}N$ of sinking POM (sediment traps), suspended POM (water samples) and of individual species of the deep-sea food web from low to high trophic steps need to be more closely studied in future. This will be essential to truly understand trophic transfers and energetic processes in the deep sea.

5. Conclusions

As a prerequisite to understand the functioning of different food webs, we need to understand the roles of key species. Widely distributed copepod species seem to be useful indicators of differing nitrogen sources (Hauss et al., 2013) over wide latitudinal ranges. However, baseline $\delta^{15}N$ data, preferably from different nitrogen sources and depth layers, are essential for correct interpretations. More data on stable isotope compositions at species level with a high geographical resolution are needed, together with information on feeding behavior and $\delta^{15}N$ of organic matter, to better understand the pathways of nitrogen in the food webs. This is especially important for deep-sea zooplankton to gain new insights into life cycles, transfer efficiencies and trophic enrichment factors at great depth (Koppelmann and Weikert, 2000). During the period of our study, the only intra-specific differences in fatty acid profiles were observed in the BCIR, which was influenced by the Benguela Current upwelling. This suggests that food availability and composition is widely homogeneous throughout the tropical and subtropical open Atlantic. During other seasons, equatorial upwelling and/or shifts in the position of the ITCZ are likely to affect primary production, food availability, and hence, trophic biomarker profiles in zooplankton consumers (Schlosser et al., 2014). Nevertheless, tropical and subtropical calanoid copepods adopted a wide variety of life strategies with specific feeding, while the generally low concentrations of bacterial markers, even in species containing high amounts of storage lipids, indicate that bacterial fatty acids do not contribute substantially to copepod long-term nutrition (Ederington et al., 1995). Species-specific patterns of storage lipids at lower latitudes strongly resemble those of high-latitude congeners (e.g. *Calanoides*, *Rhincalanus*, *Neocalanus*, *Paraeuchaeta*), suggesting that dietary preferences and pathways are to a large extent genetically determined (Cass et al., 2011). For example, the evolutionary capacity to biosynthesize and deposit wax esters seems to be worth maintaining for some species, since small-scale variability and competition for food in tropical and subtropical waters can be high. The evolution of various life strategies, vertical habitat partitioning and specialized feeding appear to be major drivers of niche separation for copepod species, allowing such a high diversity and abundance also in tropical and subtropical oceanic regions (Ambler and Miller, 1987; present study). Finally, zooplankton community composition affects the energy transfer efficiency of food webs and ecosystem functioning. Species composition itself is most likely determined by the oceanographic regime, as it sets the general frame of the food web base to meet species-specific nutritional demands, which ensures growth, reproductive success and survival.

Acknowledgements

We would like to thank the captain and crew of RV *Polarstern* during ANT-XXIX/1 (PS81) for their competent support during the cruise. We would also like to thank the students of the EUROPA trainings cruise, who helped handling the nets and sampling. This study was partly supported by the GENUS project (03F0650E), which is funded by the German Federal Ministry of Education and Research (BMBF). Furthermore, part of this research was funded by Flanders Research Foundation (FWO) through grant G071512N and Strategic Research Plan (SRP-2) of the VUB research council.

Appendix A. Supplementary material

Supplementary data associated with this article can be found, in the online version, at http://dx.doi.org/10.1016/j.pocean.2015.10.002.

References

Aiken, J., Rees, N., Hooker, S., Holligan, P., Bale, A., Robins, D., Moore, G., Harris, R., Pilgrim, D., 2000. The Atlantic Meridional Transect: overview and synthesis of data. Progress in Oceanography 45, 257–312.

Altabet, M.A., McCarthy, J.J., 1985. Temporal and spatial variations in the natural abundance of ^{15}N in PON from a warm-core ring. Deep-Sea Research Part I 32, 755–772.

Altabet, M.A., 1988. Variations in nitrogen isotopic composition between sinking and suspended particles – implications for nitrogen cycling and particle transformation in the open ocean. Deep-Sea Research Part I 35, 535–554.

Ambler, J.W., Miller, C.B., 1987. Vertical habitat-partitioning by copepodites and adults of subtropical oceanic copepods. Marine Biology 94, 561–577.

Auel, H., 1999. The ecology of Arctic deep-sea copepods (Euchaetidae and Aetideidae). Aspects of their distribution, trophodynamics and effect on the carbon flux. Reports on Polar Research 319, 1–97.

Auel, H., Hagen, W., 2005. Body mass and lipid dynamics of Arctic and Antarctic deep-sea copepods (Calanoida, *Paraeuchaeta*): ontogenetic and seasonal trends. Deep-Sea Research Part I 52, 1272–1283.

Bode, M., Schukat, A., Hagen, W., Auel, H., 2013. Predicting metabolic rates of calanoid copepods. Journal of Experimental Marine Biology and Ecology 444, 1–7.

Bode, A., Varela, M., 1994. Planktonic carbon and nitrogen budgets for the N-NW Spanish shelf: the role of pelagic nutrient regeneration during upwelling events. Scientia Marina 58, 221–231.

Budge, S.M., Parrish, C.C., 1998. Lipid biogeochemistry of plankton, settling matter and sediments in Trinity Bay, Newfoundland. II. Fatty acids. Organic Geochemistry 29, 1547–1559.

Calbet, A., Landry, M.R., 1999. Mesozooplankton influences on the microbial food web: direct and indirect trophic interactions in the oligotrophic open ocean. Limnology and Oceanography 44, 1370–1380.

Calbet, A., Saiz, E., 2005. The ciliate-copepod link in marine ecosystems. Aquatic Microbial Ecology 38, 157–167.

Calbet, A., 2008. The trophic roles of microzooplankton in marine systems. ICES Journal of Marine Science: Journal du Conseil 65, 325–331.

Capone, D.G., Burns, J.A., Montoya, J.P., Subramaniam, A., Mahaffey, C., Gunderson, T., Michaels, A.F., Carpenter, E.J., 2005. Nitrogen fixation by *Trichodesmium* spp.: an important source of new nitrogen to the tropical and subtropical North Atlantic Ocean. Global Biogeochemical Cycles 19, 1–17.

Cass, C.J., Wakeham, S.G., Daly, K.L., 2011. Lipid composition of tropical and subtropical copepod species of the genus *Rhincalanus* (Copepoda: Eucalanidae): a novel fatty acid and alcohol signature. Marine Ecology Progress Series 439, 127–138.

Childress, J.J., Thuesen, E.V., 1992. Metabolic potential of deep-sea animals – regional and global scales. Deep-Sea Food Chains and the Global Carbon Cycle 360, 217–236.

Clarke, K.R., Warwick, R.M., 1994. Changes in Marine Communities: An Approach to Statistical Analysis and Interpretation. Plymouth Mar. Lab. NERC, Plymouth, UK.

Dalsgaard, J., St John, M., Kattner, G., Müller-Navarra, D., Hagen, W., 2003. Fatty acid trophic markers in the pelagic marine environment. Advances in Marine Biology 46, 225–340.

Ederington, M.C., McManus, G.B., Harvey, H.R., 1995. Trophic transfer of fatty acids, sterols, and a triterpenoid alcohol between bacteria, a ciliate, and the copepod *Acartia tonsa*. Limnology and Oceanography 40, 860–867.

El-Sabaawi, R., Dower, J.F., Kainz, M., Mazumder, A., 2009. Characterizing dietary variability and trophic positions of coastal calanoid copepods: Insight from stable isotopes and fatty acids. Marine Biology 156, 225–237.

Escribano, R., Pérez, C.S., 2010. Variability in fatty acids of two marine copepods upon changing food supply in the coastal upwelling zone off Chile: importance of the picoplankton and nanoplankton fractions. Journal of the Marine Biological Association of the United Kingdom 90, 301–313.

Folch, J., Lees, M., Sloane-Stanley, G.H., 1957. A simple method for the isolation and purification of total lipids from animal tissues. Journal of Biological Chemistry 226, 497–509.

Flint, M.V., Drits, A.V., Pasternak, A.F., 1991. Characteristic features of body composition and metabolism in some interzonal copepods. Marine Biology 111, 199–205.
Frangoulis, C., Christou, E.D., Hecq, J.H., 2005. Comparison of marine copepod outfluxes: nature, rate, fate and role in the carbon and nitrogen cycles. Advances in Marine Biology 47, 253–309.
Gentsch, E., Kreibich, T., Hagen, W., Niehoff, B., 2009. Dietary shifts in the copepod *Temora longicornis* during spring: evidence from stable isotope signatures, fatty acid biomarkers and feeding experiments. Journal of Plankton Research 31, 45–60.
Goering, J., Alexander, V., Haubenstock, N., 1990. Seasonal variability of stable carbon and nitrogen isotope ratios of organisms in a North Pacific bay. Estuarine, Coastal and Shelf Science 30, 239–260.
Gowing, M.M., Wishner, K.F., 1998. Feeding ecology of the copepod *Lucicutia* aff. *L. grandis* near the lower interface of the Arabian Sea oxygen minimum zone. Deep-Sea Research Part II 45, 2433–2459.
Graeve, M., Kattner, G., Hagen, W., 1994a. Diet-induced changes in the fatty acid composition of Arctic herbivorous copepods – experimental evidence of trophic markers. Journal of Experimental Marine Biology and Ecology 182, 97–110.
Graeve, M., Hagen, W., Kattner, G., 1994b. Herbivorous or omnivorous? On the significance of lipid compositions as trophic markers in Antarctic copepods. Deep-Sea Research Part I 41, 915–924.
Hagen, W., Kattner, G., Graeve, M., 1995. On the lipid biochemistry of polar copepods – compositional differences in the Antarctic calanoids *Euchaeta antarctica* and *Euchirella rostromagna*. Marine Biology 123, 451–457.
Hagen, W., 1999. Reproductive strategies and energetic adaptations of polar zooplankton. Invertebrate Reproduction & Development 36, 25–34.
Hagen, W., 2000. Lipids. In: Harris, R., Wiebe, P., Lenz, J., Skjøldal, H., Huntley, M. (Eds.), ICES Zooplankton Methodology Manual. Academic Press, San Diego, pp. 113–119.
Hannides, C.C.S., Popp, B.N., Landry, M.R., Graham, B.S., 2009. Quantification of zooplankton trophic position in the North Pacific Subtropical Gyre using stable nitrogen isotopes. Limnology and Oceanography 54, 50–61.
Hauss, H., Franz, J.M.S., Hansen, T., Struck, U., Sommer, U., 2013. Relative inputs of upwelled and atmospheric nitrogen to the eastern tropical North Atlantic food web: spatial distribution of $\delta^{15}N$ in mesozooplankton and relation to dissolved nutrients dynamics. Deep-Sea Research Part I 75, 135–145.
Hobson, K.A., Welch, H.E., 1992. Determination of trophic relationships within a high Arctic marine food web using $\delta^{13}C$ and $\delta^{15}N$ analysis. Marine Ecology Progress Series 84, 9–18.
Hobson, K.A., Fisk, A., Karnovsky, N., Holst, M., Gagnon, J.M., Fortier, M., 2002. A stable isotope ($\delta^{13}C$, $\delta^{15}N$) model for the North Water food web: implications for evaluating trophodynamics and the flow of energy and contaminants. Deep-Sea Research Part II 49, 5131–5150.
Holmes, E., Eichner, C., Struck, U., Wefer, G., 1999. Reconstruction of surface ocean nitrate utilization using stable nitrogen isotopes in sinking particles and sediments. In: Fischer, G., Wefer, G. (Eds.), The Use of Proxies in Paleoceanography: Examples from the South Atlantic. Springer, Berlin, pp. 447–468.
Holmes, E., Lavik, G., Fischer, G., Segl, M., Ruhland, G., Wefer, G., 2002. Seasonal variability of $\delta^{15}N$ in sinking particles in the Benguela upwelling region. Deep-Sea Research Part I 49, 377–394.
Karl, D.M., Christian, J.R., Dore, J.E., Hebel, D.V., Letelie, R.M., Tupas, L.M., Winn, C.D., 1996. Seasonal and interannual variablity in primary production and particle flux at statin ALOHA. Deep-Sea Res Part II 43, 539–568.
Kattner, G., Fricke, H.S.G., 1986. Simple gas-liquid-chromatographic method for the simultaneous determination of fatty acids and alcohols in wax esters of marine organisms. Journal of Chromatography 361, 263–268.
Kattner, G., Krause, M., 1989. Seasonal variation of lipids (wax esters, fatty acids and alcohols) in calanoid copepods from the North Sea. Marine Chemistry 26, 261–275.
Kattner, G., Hirche, H.J., Krause, M., 1989. Spatial variability in lipid composition of calanoid copepods from Fram Strait, the Arctic. Marine Biology 102, 473–480.
Kattner, G., Hagen, W., 1995. Polar herbivorous copepods – different pathways in lipid biosynthesis. ICES Journal of Marine Science 52, 329–335.
Kattner, G., Albers, C., Graeve, M., Schnack-Schiel, S.B., 2003. Fatty acids and alcohol composition of the small polar copepods, *Oithona* and *Oncaea*: indication on feeding modes. Polar Biology 26, 666–671.
Kattner, G., Hagen, W., 2009. Lipids in marine copepods: latitudinal characteristics and perspectives to global warming. In: Arts, M.T., Brett, M., Kainz, M. (Eds.), Lipids in Aquatic Ecosystems. Springer, Berlin, p. 377.
Kleppel, G.S., 1993. On the diets of calanoid copepods. Marine Ecology Progress Series 99, 183–195.
Kleppel, G.S., Burkart, C.A., Carter, K., Tomas, C., 1996. Diets of calanoid copepods on the West Florida continental shelf: relationships between food concentration, food composition and feeding activity. Marine Biology 127, 209–217.
Koppelmann, R., Weikert, H., 2000. Transfer of organic matter in the deep Arabian Sea zooplankton community: insights from $\delta^{15}N$ analysis. Deep-Sea Research Part II 47, 2653–2672.
Koppelmann, R., Weikert, H., Lahajnar, N., 2003. Vertical distribution of mesozooplankton and its $\delta^{15}N$ signature at a deep-sea site in the Levantine Sea (eastern Mediterranean) in April 1999. Journal Geophysics Research C 108, 1978–2012.
Koppelmann, R., Böttger-Schnack, R., Möbius, J., Weikert, H., 2009. Trophic relationships of zooplankton in the eastern Mediterranean based on stable isotope measurements. Journal of Plankton Research 31, 669–686.
Laakmann, S., Kochzius, M., Auel, H., 2009a. Ecological niches of Arctic deep-sea copepods: vertical partitioning, dietary preferences and different trophic levels minimize inter-specific competition. Deep-Sea Research Part I 56, 741–756.
Laakmann, S., Stumpp, M., Auel, H., 2009b. Vertical distribution and dietary preferences of deep-sea copepods (Euchaetidae and Aetideidae; Calanoida) in the vicinity of the Antarctic Polar Front. Polar Biology 32, 679–689.
Laakmann, S., Auel, H., 2010. Longitudinal and vertical trends in stable isotope signatures ($\delta^{13}C$ and $\delta^{15}N$) of omnivorous and carnivorous copepods across the South Atlantic Ocean. Marine Biology 157, 463–471.
Landry, M.R., 1981. Switching between herbivory and carnivory by the planktonic marine copepod *Calanus pacificus*. Marine Biology 65, 77–82.
Larsen, T., Ventura, M., Andersen, N., O'Brien, D.M., Piatkowski, U., McCarthy, M.D., 2013. Tracing carbon sources through aquatic and terrestrial food webs using amino acid stable isotope fingerprinting. PLoS ONE 8.
Lee, R.F., Nevenzel, J.C., Paffenhöfer, G.-A., 1971a. Importance of wax esters and other lipids in marine food chain: phytoplankton and copepods. Marine Biology 9, 99–108.
Lee, R.F., Barnett, A.M., Hirota, J., 1971b. Distribution and importance of wax esters in marine copepods and other zooplankton. Deep-Sea Research Part I 18, 1147–1165.
Lee, R.F., Hirota, J., 1973. Wax esters in tropical zooplankton and nekton and geographical distribution of wax esters in marine copepods. Limnology and Oceanography 18, 227–239.
Lee, R.F., Hagen, W., Kattner, G., 2006. Lipid storage in marine zooplankton. Marine Ecology Progress Series 307, 273–306.
Longhurst, A.R., 1985. The structure and evolution of plankton communities. Progress in Oceanography 15, 1–35.
Longhurst, A.R., Harrison, W.G., 1988. Vertical nitrogen flux from the oceanic photic zone by diel migrant zooplankton and nekton. Deep-Sea Research Part I 35, 881–889.
Longhurst, A.R., Harrison, W.G., 1989. The biological pump: profiles of plankton production and consumption in the upper ocean. Progress in Oceanography 22, 47–123.
Longhurst, A.R., Bedo, A.W., Harrison, W.G., Head, E.J.H., Sameoto, D.D., 1990. Vertical flux of respiratory carbon by oceanic diel migrant biota. Deep-Sea Research Part I 37, 685–694.
Longhurst, A., Sathyendranath, S., Platt, T., Caverhill, C., 1995. An estimate of global primary production in the ocean from satellite radiometer data. Journal of Plankton Research 17, 1245–1271.
Madhupratap, M., Haridas, P., 1990. Zooplankton, especially calanoid copepods, in the upper 1000 m of the south-east Arabian Sea. Journal of Plankton Research 12, 305–321.
Marañón, E., Holligan, P.M., Varela, M., Mouriño, B., Bale, A.J., 2000. Basin-scale variability of phytoplankton biomass, production and growth in the Atlantic Ocean. Deep-Sea Research Part I 47, 825–857.
McClelland, J.W., Montoya, J.P., 2002. Trophic relationships and the nitrogen isotopic composition of amino acids in plankton. Ecology 83, 2173–2180.
McClelland, J.W., Holl, C.M., Montoya, J.P., 2003. Relating low $\delta^{15}N$ values of zooplankton to N_2-fixation in the tropical North Atlantic: insights provided by stable isotope ratios of amino acids. Deep-Sea Research Part I 50, 849–861.
McConnaughey, T., McRoy, C.P., 1979. Food-web structure and the fractionation of carbon isotopes in the Bering Sea. Marine Biology 53, 257–262.
Minagawa, M., Wada, E., 1984. Stepwise enrichment of ^{15}N along food chains: further evidence and the relation between $\delta^{15}N$ and animal age. Geochimica et Cosmochimica Acta 48, 1135–1140.
Mino, Y., Saino, T., Suzuki, K., Maranon, E., 2002. Isotopic composition of suspended particulate nitrogen ($\delta^{15}N_{sus}$) in surface waters of the Atlantic Ocean from 50°N to 50°S. Global Biogeochemical Cycles 16, 1–7.
Mintenbeck, K., Jacob, U., Knust, R., Arntz, W.E., Brey, T., 2007. Depth-dependence in stable isotope ratio $\delta^{15}N$ of benthic POM consumers: the role of particle dynamics and organism trophic guild. Deep-Sea Research Part I 54, 1015–1023.
Mintenbeck, K., Brey, T., Jacob, U., Knust, R., Struck, U., 2008. How to account for the lipid effect on carbon stable isotope ratio ($\delta^{13}C$): sample treatment effects and model bias. Journal of Fish Biology 72, 815–830.
Montoya, J.P., 1994. Nitrogen isotope fractionation in the modern ocean: implications for the sedimentary record, carbon cycling in the glacial ocean. Constraints on the ocean's role in Global Change. Springer, pp. 259–279.
Montoya, J.P., Carpenter, E.J., Capone, D.G., 2002. Nitrogen fixation and nitrogen isotope abundances in zooplankton of the oligotrophic North Atlantic. Limnology and Oceanography 47, 1617–1628.
Montoya, J.P., 2007. Natural abundance of ^{15}N in marine planktonic ecosystems. In: Michener, R., Lajtha, K. (Eds.), Stable Isotopes in Ecology and Environmental Science. Blackwell Publ., pp. 176–201.
Ohman, M.D., 1987. Energy sources for recruitment of the sub-Antarctic copepod *Neocalanus tonsus*. Limnology and Oceanography 32, 1317–1330.
Ohman, M.D., Drits, A.V., Clarke, M.E., 1998. Differential dormancy of co-occurring copepods. Deep-Sea Research Part II 45, 1709–1740.
O'Reilly, C.M., Hecky, R.E., Cohen, A.S., Plisnier, P.D., 2002. Interpreting stable isotopes in food webs: recognizing the role of time averaging at different trophic levels. Limnology and Oceanography 47, 306–309.
Parrish, C.C., 2013. Lipids in marine ecosystems. ISRN Oceanography 2013, 16.
Persson, J., Vrede, T., 2006. Polyunsaturated fatty acids in zooplankton: variation due to taxonomy and trophic position. Freshwater Biology 51, 887–900.
Peters, J., Dutz, J., Hagen, W., 2007. Role of essential fatty acids on the reproductive success of the copepod *Temora longicornis* in the North Sea. Marine Ecology Progress Series 341, 153–163.

Platt, T., Harrison, W.G., Lewis, M.R., Li, W.K.W., Sathyendranath, S., Smith, R.E., Vezina, A.F., 1989. Biological production of the oceans: the case for a consensus. Marine Ecology Progress Series 52, 77–88.

Polunin, N.V.C., Morales-Nin, B., Pawsey, W.E., Cartes, J.E., Pinnegar, J.K., Moranta, J., 2001. Feeding relationships in Mediterranean bathyal assemblages elucidated by stable nitrogen and carbon isotope data. Marine Ecology Progress Series 220, 13–23.

Post, D.M., 2002. Using stable isotopes to estimate trophic position: models, methods, and assumptions. Ecology 83, 703–718.

Rohardt, G., Wisotzki, A., 2013. Physical oceanography during POLARSTERN cruise ANT-XXIX/1. Alfred Wegener Institute, Helmholtz Center for Polar and Marine Research, Bremerhaven. PANGAEA. http://dx.doi.org/10.1594/PANGAEA.817254.

Rolff, C., 2000. Seasonal variation in $\delta^{13}C$ and $\delta^{15}N$ of size-fractionated plankton at a coastal station in the northern Baltic proper. Marine Ecology Progress Series 203, 47–65.

Saino, T., Hattori, A., 1980. ^{15}N natural abundance in oceanic suspended particulate matter. Nature 283, 752–754.

Saino, T., Hattori, A., 1987. Geographical variation of the water column distribution of suspended particulate organic nitrogen and its ^{15}N natural abundance in the Pacific and its marginal seas. Deep-Sea Research Part I 34, 807–827.

Sandel, V., Kiko, R., Brandt, P., Dengler, M., Stemmann, L., Vandromme, P., Sommer, U., Hauss, H., 2015. Nitrogen fuelling of the pelagic food web of the tropical Atlantic. PLoS ONE 10.

Sargent, J.R., Henderson, R.J., 1986. Lipids. In: Corner, E.D.S., O'hara, S.C.M. (Eds.), The Biological Chemistry of Marine Copepods. Clarendon Press, Oxford, pp. 59–108.

Sargent, J.R., Falk-Petersen, S., 1988. The lipid biochemistry of calanoid copepods. Hydrobiologia 167 (168), 101–114.

Sasaki, H., Hattori, H., Nishizawa, S., 1988. Downward flux of particulate organic matter and vertical-distribution of calanoid copepods in the Oyashio Water in summer. Deep-Sea Research Part I 35, 505–515.

Schlitzer, R., 2013. Ocean Data View 4 <http://odv.awi.de>.

Schlosser, C., Klar, J.K., Wake, B.D., Snow, J.T., Honey, D.J., Woodward, E.M.S., Lohan, M.C., Achterberg, E.P., Moore, C.M., 2014. Seasonal ITCZ migration dynamically controls the location of the (sub)tropical Atlantic biogeochemical divide. Proceedings of the National academy of Sciences of the United States of America 111, 1438–1442.

Schmidt, K., Atkinson, A., Stübing, D., McClelland, J.W., Montoya, J.P., Voss, M., 2003. Trophic relationships among Southern Ocean copepods and krill: some uses and limitations of a stable isotope approach. Limnology and Oceanography 48, 277–289.

Schmidt, K., Atkinson, A., Petzke, K.J., Voss, M., Pond, D.W., 2006. Protozoans as a food source for Antarctic krill, *Euphausia superba*: complementary insights from stomach content, fatty acids, and stable isotopes. Limnology and Oceanography 51, 2409–2427.

Schnack-Schiel, S.B., Niehoff, B., Hagen, W., Böttger-Schnack, R., Cornils, A., Dowidar, M.M., Pasternak, A., Stambler, N., Stübing, D., Richter, C., 2008. Population dynamics and life strategies of *Rhincalanus nasutus* (Copepoda) at the onset of the spring bloom in the Gulf of Aqaba (Red Sea). Journal of Plankton Research 30, 655–672.

Schukat, A., Auel, H., Teuber, L., Hagen, W., 2014. Complex trophic interactions of calanoid copepods in the Benguela upwelling system. Journal of Sea Research 85, 186–196.

Shimode, S., Hiroe, Y., Hidaka, K., Takahashi, K., Tsuda, A., 2009. Life history and ontogenetic vertical migration of *Neocalanus gracilis* in the western North Pacific Ocean. Aquatic Biology 7, 295–306.

Shimode, S., Takahashi, K., Shimizu, Y., Nonomura, T., Tsuda, A., 2012a. Distribution and life history of two planktonic copepods, *Rhincalanus nasutus* and *Rhincalanus rostrifrons*, in the northwestern Pacific Ocean. Deep-Sea Research Part I 65, 133–145.

Shimode, S., Takahashi, K., Shimizu, Y., Nonomura, T., Tsuda, A., 2012b. Distribution and life history of the planktonic copepod, *Eucalanus californicus*, in the northwestern Pacific: mechanisms for population maintenance within a high primary production area. Progress in Oceanography 96, 1–13.

Smyntek, P.M., Teece, M.A., Schulz, K.L., Thackeray, S.J., 2007. A standard protocol for stable isotope analysis of zooplankton in aquatic food web research using mass balance correction models. Limnology and Oceanography 52, 2135–2146.

Staal, M., Hekkert, S.t.L., Brummer, G.J., Veldhuis, M., Sikkens, C., Persijn, S., Stal, L.J., 2007. Nitrogen fixation along a north-south transect in the eastern Atlantic Ocean. Limnology and Oceanography 52, 1305–1316.

Steinberg, D.K., Goldthwait, S.A., Hansell, D.A., 2002. Zooplankton vertical migration and the active transport of dissolved organic and inorganic nitrogen in the Sargasso Sea. Deep-Sea Research Part I 49, 1445–1461.

Stevens, C.J., Deibel, D., Parrish, C.C., 2004. Copepod omnivory in the North Water Polynya (Baffin Bay) during autumn: spatial patterns in lipid composition. Deep-Sea Research Part I 51, 1637–1658.

Sugisaki, H., Tsuda, A., 1995. Nitrogen and carbon stable isotopic ecology in the ocean: the transportation of organic materials through the food web. In: Sakai, H., Nozaki, Y. (Eds.), Biochemical Processes and Ocean Flux in the Western Pacific. Terra Scientific Publishing Company (TERRAPUB), Tokyo, pp. 307–317.

Teuber, L., Kiko, R., Seguin, F., Auel, H., 2013. Respiration rates of tropical Atlantic copepods in relation to the oxygen minimum zone. Journal of Experimental Marine Biology and Ecology 448, 28–36.

Teuber, L., Schukat, A., Hagen, W., Auel, H., 2014. Trophic interactions and life strategies of epi- to bathypelagic calanoid copepods in the tropical Atlantic Ocean. Journal of Plankton Research 36, 1109–1123.

Tsuda, A., Saito, H., Kasai, H., 2001. Life history strategies of subarctic copepods *Neocalanus flemingeri* and *N. plumchrus*, especially concerning lipid accumulation patterns. Plankton Biology and Ecology 48, 52–58.

Turner, J.T., 2004. The importance of small planktonic copepods and their roles in pelagic marine food webs. Zoological Studies 43, 255–266.

Vander Zanden, M.J., Rasmussen, J.B., 2001. Variation in $\delta^{15}N$ and $\delta^{13}C$ trophic fractionation: implications for aquatic food web studies. Limnology and Oceanography 46, 2061–2066.

Verheye, H.M., Hagen, W., Auel, H., Ekau, W., Loick, N., Rheenen, I., Wencke, P., Jones, S., 2005. Life strategies, energetics and growth characteristics of *Calanoides carinatus* (Copepoda) in the Angola-Benguela frontal region. African Journal of Marine Science 27, 641–651.

Voss, M., Altabet, M.A., vonBodungen, B., 1996. $\delta^{15}N$ in sedimenting particles as indicator of euphotic-zone processes. Deep-Sea Research Part I 43, 33–47.

Voss, M., Croot, P., Lochte, K., Mills, M., Peeken, I., 2004. Patterns of nitrogen fixation along 10°N in the tropical Atlantic. Geophysical Research Letters 31, 1–4.

Wada, E., Hattori, A., 1976. Natural abundance of ^{15}N in particulate organic matter in North Pacific Ocean. Geochimica et Cosmochimica Acta 40, 249–251.

Zhang, X.S., Dam, H.G., 1997. Downward export of carbon by diel migrant mesozooplankton in the central equatorial Pacific. Deep-Sea Research Part I 44, 2191–2202.

CHAPTER III

Contribution of N_2 fixation to Biological Productivity along a Meridional Section in the Eastern Atlantic Ocean

Fonseca-Batista D, Dehairs F, Riou V, Fripiat F, Elskens M, Deman F, Brion N,
Bode M and Auel H

Submitted to Progress in Oceanography in November 2015

Contribution of N_2 fixation to biological productivity along a meridional section in the Eastern Atlantic Ocean

Debany Fonseca-Batista, Frank Dehairs, Virginie Riou, François Fripiat, Marc Elskens, Florian Deman, Natacha Brion, Maya Bode and Holger Auel

Abstract

During the ANT XXIX/1 cruise (November 2012) along the Eastern Atlantic Ocean (38°N–21°S) we studied euphotic layer community N_2 fixation, ammonium, nitrate and bicarbonate uptake using incubation experiments based on ^{15}N and ^{13}C labelled substrates. This region is a hot spot for N_2 fixation, as it has been shown to be influenced by Saharan dust deposition and upwelling of waters with low N/P ratios in the equatorial region and near and/or within the Benguela Upwelling System. Using the $^{15}N_2$ dissolution method we measured substantial diazotrophic activities across the whole transect: averaged depth-integrated rates were relatively higher in the North ranging from 117–180 µmol m^{-2} d^{-1} in the Subtropical North Atlantic (STNA, 20–38°N) and Tropical North Atlantic (TNA, 0–20°N), respectively. Nevertheless, N_2 fixation activity in the Southern provinces, though slightly lower, was surprisingly close to observations in the North, with averaged rates of 74–75 µmol m^{-2} d^{-1} in the Benguela Current Influenced Region (BCIR, 15–21°S) and Tropical South Atlantic (TSA, 0–15°S), respectively. Maximal diazotrophic activity, up to 370 µmol m^{-2} d^{-1}, was found at 19°N within the Mauritanian Upwelling influenced region, where input of phosphorus excess to surface waters, combined with aeolian input of trace elements seemed to have triggered such activity. N_2 fixation accounted for up to 8% of total nitrogen uptake (considered as the sum of N_2 + NH_4^+ + NO_3^- uptake), more than 50% of new production, and to fuel as much as 11% of net primary production. Based on our N_2 fixation rates, we estimate an annual nitrogen input via N_2 fixation over the open Atlantic Ocean of ~35.2 Tg N yr^{-1}, of which 70% is accounted for by the region between 50°N and 10°S and 30% by the region between 10°S to 44°S. While these estimates are similar to the magnitude of N_2 fixation based on geochemical estimates, it appears important to expand the use of $^{15}N_2$ dissolution method to the Western boundary of the Atlantic Ocean to better constrain basin-wide estimates.

Keywords: nitrogen cycle; nitrogen fixation; new production; Atlantic Ocean

Introduction

Biological nitrogen fixation has been widely acknowledged as the dominant source of new nitrogen in the Ocean with minor though significant contributions from riverine and atmospheric inputs (Gruber & Sarmiento, 1997; Codispoti, 2007; Gruber, 2008). In tropical and subtropical regions where nitrogen availability limits primary productivity, microbial N_2 fixation introducing external nitrogen to surface waters indeed plays a critical role in the net sequestration of CO_2 into the deep ocean (Dugdale & Goering, 1967).

Assessing the global nitrogen input through N_2 fixation has long been debated, and significant uncertainties still persist today. Estimates based on geochemical parameters tend to converge to a range between 100 to 150 Tg N yr^{-1} (Gruber & Sarmiento, 1997 & 2002; Codispoti et al., 2001; Codispoti, 2007; Deutsch et al., 2007). Budget estimates based on *in-situ* measurements still require further harmonization. Luo et al. (2012) compiled worldwide *in-situ* measurements essentially based on the $^{15}N_2$ bubble-addition and determined an annual input of 140 Tg yr^{-1}. However, the latter method was shown to underestimate N_2 fixation rate as compared to the dissolution method (Mohr et al., 2010). Based on the average difference determined between the bubble-addition method and the new dissolution method during a fieldwork in the Atlantic, Großkopf et al. (2012) upscaled their N_2 fixation data obtained with the latter method and proposed a global N_2 fixation of about 177 Tg N yr^{-1}. In addition, a recent study highlighted the risks for potential over-estimation or erroneous detection of N_2 fixation resulting from the use of commercial $^{15}N_2$ gas containing ^{15}N-labeled contaminants such as nitrate, nitrite and ammonium (Dabundo et al., 2014) which could greatly bias past estimates. It is therefore essential to re-assess diazotrophic activity, using appropriate method and tools, while also increasing the spatial and temporal sampling resolution to better constrain global estimates.

The Atlantic Ocean is known to shelter substantial year round diazotrophic activity (Fernández et al., 2010; Sohm et al., 2011a), which makes it a key system for the global ocean nitrogen cycle. The Eastern North Atlantic under influence of high iron input through Saharan dust deposition observed to favor N_2 fixation (Mills et al., 2004; Langlois et al., 2012) has been intensively studied (Falcón et al., 2004; Voss et al., 2004; Capone et al., 2005; Montoya et al., 2007; Goebel et al., 2010; Benavides et al., 2011; 2013a & 2013b; Rijkenberg et al., 2011; Turk et al., 2011;

Fernández et al., 2012; Painter et al., 2013; Schlosser et al., 2014; Snow et al., 2015). On the contrary, South Atlantic regions, long considered as contributing little to global N_2 fixation due to limited iron availability, attracted much less sampling efforts, especially the south eastern region (Staal et al., 2007; Moore et al., 2009; Fernández et al., 2010; Mouriño-Carballido et al., 2011; Großkopf et al., 2012; Snow et al., 2015). Großkopf and colleagues (2012) recently showed using the $^{15}N_2$ dissolution method, that the Equatorial and South West Atlantic regions hosted intense N_2 fixation activity. We presently extended this data set to the South Eastern region of the Atlantic.

The present study contributes to the few published surveys of community N_2 fixation over a large latitudinal scale in the Eastern Atlantic Ocean (Staal et al., 2007; Moore et al., 2009; Fernández et al., 2010; Mouriño-Carballido et al., 2011; Großkopf et al., 2012;Schlosser et al., 2014; Snow et al., 2015) and is among the first ones using the latest $^{15}N_2$ dissolution method for this purpose. And more importantly, considering that inorganic nitrogen pool supporting production largely occurs as ammonium and nitrate (Gruber, 2008), we also investigated uptake rates of NH_4^+/NO_3^- and carbon in order to assess the contribution of N_2 fixation to nitrogen uptake, primary production and potential export production.

Material and methods

Field observations were carried out in the Eastern Atlantic Ocean along a transect from 38°N to 21°S between November 1st and 24th 2012 on board R/V Polarstern (ANT XXIX/1 expedition, Fig. 1). Hydrographic features were determined using a CTD profiler fitted with a 24–Niskin rosette system and a photosynthetically active radiation sensor (PAR, PNF-300, Biospherical Instruments Inc.). At each station, samples were taken from surface down to 700 m to characterize the physical structure of the water column and determine nutrient concentrations. Mixed layer depths (MLD) were estimated using a temperature threshold criterion of 0.2°C relative to the temperature at 10 m (de Boyer Montégut et al., 2004). For nitrogen and carbon incubations experiments, water was collected at depths equivalent to 50, 15, 3.5 and 0.5% of the PAR. Polycarbonate bottles pre-cleaned with acid (HCl reagent grade, Sigma-Aldrich) and ultrapure water (resistivity > 18 MΩ cm^{-1}, Sartorius) were used for the 24 h incubations in on-deck incubators wrapped with blue light filters (Rosco) reproducing *in-situ* PAR conditions, and equipped with a continuous surface water flow to maintain sea surface temperature.

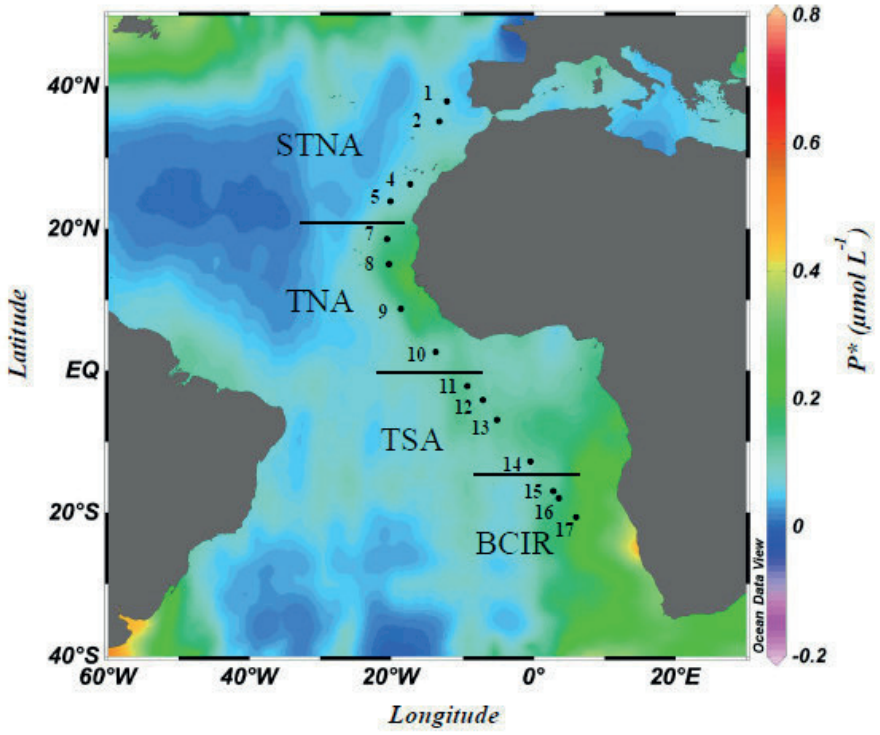

Figure 1: Location of sampling stations during ANT XXIX/1 cruise in November 2012 over a map of the annual average phosphate excess (P* = $[PO_4^{3-}]$ – $[NO_3^-]$/16) at 20 m depth (Garcia et al., 2014; World Ocean Atlas 2013). Oceanographic provinces according to physical and biogeochemical features are indicated: Subtropical North Atlantic (STNA), Tropical North Atlantic (TNA), Tropical South Atlantic (TSA) and Benguela Current Influenced Region (BCIR). Image provided by Schlitzer. R., Ocean Data View. http://odv.awi.de. 2014.

Nutrient concentrations

Ammonium (NH_4^+) and phosphate (PO_4^{3-}) concentrations were measured on-board while nitrate + nitrite (NO_3^- + NO_2^-, referred to afterwards as nitrate) were processed back at the lab. NH_4^+ concentrations were determined using the fluorimetric method by Holmes et al. (1999) with an uncertainty (standard error, SE) and a minimum detectable value (MDV) of 14 nmol L^{-1} and 44 nmol L^{-1} respectively. Fluorescence was detected at 425 nm with a 1 cm cell (LED LLS-365 light source and a Torus detector, Ocean Optics).

PO_4^{3-} was measured according to Grasshoff et al. (1983), with absorbance detected at 880 nm in a 10 cm cell (Spectronic Instruments). SE and MDV during analysis were 10 nmol L^{-1} and 42 nmol L^{-1}, respectively.

Seawater dedicated for NO_3^- + NO_2^- analyses was filtered over 0.2 µm porosity acrodiscs and stored at -20°C until analysis. Concentrations were determined based on the Griess colorimetric

reaction on a continuous flow QuAAtro auto-analyser (Seal Analytical). A copperized cadmium column converting NO_3^- into NO_2^- was used to measure NO_3^- + NO_2^- concentrations. For concentrations below 600 nmol L^{-1}, SE was 20 nmol L^{-1} and MDV 80 nmol L^{-1}, while for higher NO_3^- concentrations, SE was 220 nmol L^{-1}. N* was derived (according to Deutsch et al., 2007: N* = $[NO_3^-]$ – 16 x $[PO_4^{3-}]$) using nutrient data from the current study. Values were omitted when either nitrate or phosphate concentrations were below detection limit.

Nitrogen fixation rates

In the present study N_2 fixation was measured in duplicate for most stations (except stations 1, 14–17), and consistently at the 4 selected PAR levels, using the $^{15}N_2$-dissolution incubation method (Mohr et al., 2010; Großkopf et al., 2012). Briefly, $^{15}N_2$-enriched seawater was prepared prior to the expedition by degassing, in acid-cleaned conditions, prefiltered (0.2 µm) low nutrient seawater (natural Atlantic seawater, Osil) and injecting it with $^{15}N_2$ gas (98%+, Eurisotop). This spiked water was then stored in 2 L gastight polypropylene Tedlar bags (Sigma-Aldrich) until use on board. Acid-cleaned polycarbonate bottles (4.5 L) were filled with sampled seawater to which 250 mL of $^{15}N_2$ enriched seawater were added in order to reach a $^{15}N_2$ enrichment < 10%. All incubations bottles were also spiked with 3 mL $NaH^{13}CO3$ (99%, Eurisotop) of 202 mmol L^{-1} in order to simultaneously assess net primary production (net PP, Hama et al., 1983). Enrichments were measured as detailed in section 2.5, and these additions yielded initial ^{15}N Atom% of dissolved N_2 gas ($^{15}N\%$-N_2) of 1.23–8.28% (average ±standard error, avg ±SE, of 2.78 ±0.10%, n = 96) and ^{13}C Atom% of Dissolved Inorganic Carbon ($^{13}C\%$-DIC) of 5.74–6.99% (6.57 ±0.02%, n = 96). After 24 h incubation subsamples were taken in 12 mL Exetainers vials (Labco) poisoned with $HgCl_2$, by exerting a helium overpressure through the septum cap of the incubation bottles, in order to determine the substrates enrichments: $^{15}N\%$-N_2 and $^{13}C\%$-DIC. The remaining was filtered onto pre-combusted (450°C, > 4h) MGF filters (glass microfiber filters, 0.7 µm, Sartorius) for measurements of Particulate Organic Carbon and Particulate Nitrogen (POC/PN) concentration and isotopic composition. The natural nitrogen and carbon concentration and isotopic composition of POC/PN were assessed by filtering additional 4.5 L seawater from each depth. Afterwards, all filters were dried at 60°C for 24 h and kept at ambient temperature until further processing.

Prior to analysis the filters were fumed with HCL over night and finally pelletized in tin cups. POC/PN measurements were done using an Elemental Analyzer coupled to a continuous-flow Isotope Ratio Mass Spectrometer (EA-IRMS, Flash EA112 Delta V Plus, Thermo Scientific). Nitrogen and carbon analyses were calibrated against international certified reference materials (CRM): IAEA-N-1 Ammonium Sulfate (^{15}N Atom% of 0.37) and IAEA-305B Ammonium Sulfate (^{15}N Atom% of 0.50). Carbon was calibrated against IAEA-CH-6 Sucrose (^{13}C Atom% of 1.10) and IAEA-309B UL-D-glucose (^{13}C Atom% of 1.70). Precision during analysis, expressed as the standard deviation over all measurements of the enriched reference material, was 0.0002 Atom% and 0.0078 Atom% for N and C respectively.

Testing $^{15}N_2$ gas contamination

A recent study revealed that in some cases, commercial $^{15}N_2$ gas used during N_2 fixation incubation experiments potentially contained ^{15}N-labeled bioavailable nitrogen contaminants (NO_3^-/NO_2^-, NH_4^+ and N_2O) which caused the overestimation or false detection of N_2 fixation rates (Dabundo et al., 2014). Therefore the $^{15}N_2$ gas (Eurisotop, 98%+) used in the present study was tested in our laboratory post-cruise for contamination in $^{15}NO_3^-$, $^{15}NO_2^-$ and $^{15}NH_4^+$. Two test batches were made, one checking for contamination in $^{15}NO_3^-$ and ($^{15}NO_3^-$ + $^{15}NO_2^-$), based on the denitrifier method (Sigman et al., 2001; Casciotti et al., 2002; see section 2.4) previously treated or not with sulfamic acid to retrieve all traces of nitrite (Granger & Sigman, 2009); and the second batch checking for ($^{15}NH_4^+$+$^{15}NO_2^-$) with the hypobromite/azide method (McIlvin & Altabet, 2005; Zhang et al., 2007). For each method we investigated the influence of $^{15}N_2$ gas injection (1 mL) on the nitrogen isotopic composition of ~5 µM of international nitrate and ammonium reference solutions (IAEA N3; nitrate; δ^{15}N of 4.72‰ and IAEA N2; ammonium; δ^{15}N of 20.41‰) prepared in degassed low-nutrient Osil seawater (60 mL per treatment). Nitrogen isotopic signature of triplicate preparations for each technique were compared to signals of control standards prepared also in low nutrient seawater but not injected with $^{15}N_2$ gas. Student's paired t-test between average controls and treatments for both methods returned consistently no significant difference: for the sulfamic/denitrifier method (p-value = 0.40; control treatments δ^{15}N-NO_3^- of 4.81 ±0.02‰, avg ±SE, n = 3 versus labelled treatments δ^{15}N-NO_3^- of 4.75 ±0.04‰, avg ±SE, n = 9), for the denitrifier method only (p-value = 0.08; control treatments δ^{15}N-NO_3^- of 4.72 ±0.05‰, n = 5 versus labelled treatments δ^{15}N-NO_3^- of 4.87 ±0.05‰, n = 15) and for the hypobromite/azide method (p-value = 0.09; controls treatments δ^{15}N-NH_4^+ of 20.30

±0.10‰, n = 5 versus labelled treatments $\delta^{15}N\text{-}NH_4^+$ of 20.10 ±0.05‰, n = 15). We could therefore consider our labelled gas source free of contamination.

NH_4^+/NO_3^- uptake rates

Assimilation of ammonium and nitrate was determined at the same 4 PAR levels as for N_2 fixation. Per depth, and for both inorganic nitrogen forms, duplicate (initial + final) 1 L acid-cleaned polycarbonate bottles were filled with sample water, spiked with 1 mL of either $^{15}NH_4Cl$ (24 µM, 98%) or $Na^{15}NO_3$ (1 mM, 98%, Sigma-Aldrich). Exceptionally, at stations 9 to 13, nitrate incubations were spiked with 1 mL of a 22 µM $Na^{15}NO_3$. Net PP was measured for ammonium and nitrate incubations by spiking with 1 mL $NaH^{13}CO_3$ of 202 mM. These additions yielded calculated initial $^{15}N\%\text{-}NH_4^+$ enrichments of 4–52% (avg ±SE of 32 ±2%, n = 60), $^{15}N\%\text{-}NO_3^-$ of 0.5–95% (37 ±5%, n = 60) and $^{13}C\%$-DIC of 9.32–17.54% (10.15 ±0.22%, n = 60) and 8.87–11.06% (9.56 ±0.04%, n = 60) for NH_4^+ and NO_3^- incubations respectively. Note that tracer additions >> 10% of ambient concentration (Dugdale & Goering, 1967), will likely have stimulated phytoplankton N uptake, resulting in measurements of potential rather than real uptake rates (Allen et al., 1996; Harrison et al., 1996). After tracer addition, all bottles were gently shaken and $T_{initial}$ bottles were immediately filtered onto pre-combusted MGF filters (0.7 µm nominal pore size, Sartorius) to assess the initial concentration and isotopic enrichment of POC/PN, while T_{final} bottles were transferred to the on-deck incubators. After 24 h T_{final} bottles were filtered for POC/PN concentration and isotopic signature assessment. Before filtration nitrate incubations bottles were sampled to determine the initial concentration and nitrogen isotopic composition of nitrate ($^{15}N\%\text{-}NO_3^-$). Therefore subsamples (~50 mL) were taken from pre- incubation bottles then filtered over 0.2 µm acrodiscs and stored at -20°C for further analysis. POC/PN measurements were performed on the EA-IRMS as detailed previously, and calibrations involved the same CRM. $^{15}N\%\text{-}NO_3^-$ was assessed with the aim of comparing measured values to theoretical estimates of the initial enrichments. For this purpose, we applied the denitrifier method (Sigman et al., 2001; Casciotti et al., 2002) which consists in the bacterial transformation of NO_3^- into gaseous N_2O using a denitrifier bacteria (*Pseudomonas aureofaciens*) that lacks the nitrous oxide reductase activity. This procedure was then followed by the measurement on the IRMS of the isotopic composition of the N_2O gas produced. Analyses were calibrated against international reference materials: USGS32 Potassium Nitrate, USGS34 Potassium Nitrate and

USGS35 Sodium Nitrate with $\delta^{15}N$ values of 180‰, -1.8‰ and 2.7‰ with reference to N_2 air, respectively.

We acknowledge the fact that our nitrate and ammonium uptake rates could be potentially biased due to isotopic dilution during the incubations and overspiking, which are discussed and evaluated below. Underestimations of uptake rates due to isotopic dilution (due to ammonification and nitrification for NH_4^+ and NO_{3-}, respectively) during incubation experiments were corrected by applying a steady state model (Glibert et al., 1982) which assumes equal rates of uptake and regeneration for each nitrogen pool. For ammonium, the regression between corrected and raw uptake rates returned a slope of 1.69 ±0.08 (±SE, n = 48, r^2 = 0.90 ±0.03, p-value < 0.001). Such an underestimation factor of 1.69, fits within the range of values (1.5–2) reported by Rees et al., 1995, Elskens et al. (1997) and Slawyk et al., (1997). For nitrate, the impact of isotope dilution on the uptake rates, regarding experimental conditions (average ^{15}N% enrichment of nitrate of 37 ±38%, n = 60) was negligible (slope of 1.02 ±0.004, r^2 = 0.99 ±0.002, p-value < 0.001) although overspiking with ^{15}N-NO_3 renders the calculation of nitrate regeneration using the Glibert et al. (1982) approach unreliable. The Michaelis-Menten equation of saturation kinetics as presented in Elskens et al., (1997) was used to determine the stimulating effect of overspiking with $^{15}NO_3^-$ and $^{15}NH_4^+$ tracers ammonium and nitrate uptake rates. Using a half-saturation constant (K_s) ranging from 25 and 100 nM, as reported by Harrison et al., (1996), regressions between corrected and uncorrected uptakes rates all returned insignificant differences: for ammonium uptake rates with K_s = 25 nM, the slope was 0.98 ±0.01 (95% confidence interval between 0.96 and 1.00), p-value < 0.001, and with K_s = 100 nM, the slope was 0.95 ±0.02 (95% confidence interval between 0.92 and 0.98), p-value < 0.001. For nitrate uptake rates with a K_s of 25 nM, the slope was 0.96 ±0.03 (95% confidence interval between 0.91 and 1.02), p-value < 0.001, and with K_s of 100 nM, the slope was 0.93 ±0.05 (95% confidence interval between 0.83 and 1.03), p-value < 0.001. Since the stimulating effect due to overspiking is negligible, uptake rates are given without this correction.

Uptake rates calculations

Net nitrogen and carbon uptake rates were computed according to (Dugdale & Wilkerson, 1986), and uncertainties were expressed as propagated standard errors (SE) from ^{15}N-Atom% of substrate and particulate matter:

$$\text{Uptake rate X} = \frac{A_{particle}^{final} - A_{particle}^{t=0}}{A_{substrate} - A_{particle}^{t=0}} \times \frac{[Particle]}{\Delta t} \text{ (µmol m}^{-3}\text{ d}^{-1}\text{) (1)}$$

where $A_{particle}^{final}$ is the ^{15}N (or ^{13}C) Atom% measured in the particulate organic matter (POM) after incubation; $A_{particle}^{t=0}$ is, for N_2 incubation experiments, the natural abundance of ^{15}N (or ^{13}C) Atom% determined for the natural abundance POM and, for NH_4^+ and NO_3^- incubation experiments, the initial ^{15}N (or ^{13}C Atom%) determined after N and C spike additions. $A_{substrate}$ is the pre-incubation ^{15}N Atom% of the spiked nitrogen pool for NH_4^+ and NO_3^-. For dissolved N_2 gas and DIC $A_{substrate}$ is the ^{15}N% or ^{13}C% enrichment determined at the end of the incubation, based on the assumption that 24 h $^{15}N_2$ and $H^{13}CO_3^-$ fixation activities do not significantly affect these large N and C pool. $[Particle]$ is the PN or POC concentration after incubation (µmol L^{-1}) and Δt the incubation time (days). $A_{particle}^{final}$, $A_{particle}^{t=0}$, and $[Particle]$ were determined with the EA-IRMS by means of combustion of MGF filters on which POM was collected. $A_{substrate}$ was measured for $^{15}N_2$ and ^{13}C-DIC by injecting the sample gas in a custom made manual gas injection port connected to the EA-IRMS. Exetainers vials were first injected with helium to create the headspace to be sampled, and then equilibrated on a rotatory shaker with or without addition of phosphoric acid (99%, Sigma-Aldrich) for DIC and N_2 analyses, respectively. Injection of reference CO_2 gas, and correction for partitioning of the gas between the dissolved and the gaseous phase according to Miyajima et al. (1995) were applied for DIC enrichment measurements. $^{15}N_2$ enrichments were calibrated with atmospheric N_2 injection. Substrate ^{15}N enrichment for NH_4^+ incubations was calculated based on the isotopic mass balance determined from ambient ammonium concentration and natural ^{15}N% (0.37%, Rosman & Taylor, 1998) on the one hand; and the $^{15}NH_4^+$ spike concentration and its ^{15}N% (98%, Sigma-Aldrich) on the other hand. Since measured ^{15}N% of NO_3^- compared well with theoretical calculations (regression slope = 0.98 ±0.04, ±SE, r^2 = 0.95 ±3.78, n = 35, p-value < 0.001), theoretical $T_{initial}$ ^{15}N%-NO_3^- were used to compute nitrate uptake rates in cases where nitrate concentrations were too low to measure its isotopic composition. When NO_3^- or NH_4^+ concentrations were less than the MDV, the concentration considered to compute $T_{initial}$ ^{15}N% of the substrate was MDV/2 (assuming a continuous uniform distribution between zero and MDV). SE values from sample and CRM analyses of ^{15}N and ^{13}C-Atom% were used to propagate the measurement uncertainty to calculated uptake rates. Depth-integrated rates were calculated by non-uniform gridding trapezoidal integration for each station.

Results

Physical and biogeochemical features along the transect

The ANT XXIX/1 cruise went along the Northwest African coast within the Canary Current system, then crossed the Equatorial Upwelling System (EUS) to finally enter a region under influence of the Benguela Current system. Temperature, salinity, dissolved oxygen, fluorescence and nutrient profiles (Rohardt and Wisotzki, 2013) were used to delimit the four biogeographic provinces studied (Fig.2).

The subtropical North Atlantic (STNA, stations 1, 2, 4 and 5) between 20-38°N, was the most oligotrophic province as it had the lowest nutrient concentrations (NO_3^- < 1 µM and PO_4^{3-} < 0.10 µM; Fig.2e,f) and lowest fluorescence values (< 0.02, arbitrary units; Fig.2d) in the upper 100m. Temperature and salinity profiles indicated the presence of a relatively stratified water column (Fig.2a,b): in the upper 50 m sea surface temperature (SST) was > 20°C (average SST at 5 m depth, 25 ±1°C, ±SE, n = 4 stations) and salinity was > 36.5 psu, with maximal values at stations 4–5 (37.1 psu).

The tropical North Atlantic (TNA, 0–20°N, stations 7, 8, 9 and 10) appeared as the most stratified region, according to temperature profiles (average SST = 28 ±0.55°C, ±SE, n = 4). A surface salinity minimum (34.7 psu) was observed in this region, suggesting significant influence of precipitation prior to the time of sampling. The TNA province is impacted by the EUS, as shown by the doming in the nutrient and dissolved O_2 sections (Fig.2c, e & f): NO_3^- and PO_4^{3-} were depleted in the upper 25 m (concentrations were < MDV, being 80 and 42 nmol L^{-1}, respectively), except for phosphate at station 7 where a concentration as high as 0.10 µM was observed in the upper MLD (25 m). Below 25 m NO_3^- and PO_4^{3-} concentrations increased rapidly with depth.

As for the TNA, the tropical South Atlantic (TSA, 0–15°S, stations 11, 12, 13 and 14) also under influence of the EUS, was characterized similarly by significant O_2 depletion below 75–100 m depth (< 75 µmol L^{-1}), concomitant with higher nutrient levels at shallow depths (approx. 25 m depth for NO_3^-), and even at the surface for PO_4^{3-}.

The Benguela Current Influenced Region (BCIR, stations 15, 16 and 17) between 15–21°S, had a well homogenized surface water column (upper 50 m) and was the most nutrient replete region (NO_3^- > 5 µM and PO_4^{3-} > 0.50 µM in surface waters). As a result, BCIR showed maximal fluorescence (from surface to 50–60 m deep, ≥ 0.04 arbitrary unit). As for the TNA and TSA, the NH_4^+ profiles in the BCIR showed maximum values in subsurface waters (max of 0.6 µM between

50-100 m), mimicking the fluorescence profiles. Surface waters of BCIR were the coolest (average SST = 19 ±0.08°C, ±SE, n = 3) as a consequence of deep water upwelling to surface, which agrees with the southward shoaling of MLD: 42 m, 38 m and 29 m for stations 15, 16 and 17, respectively.

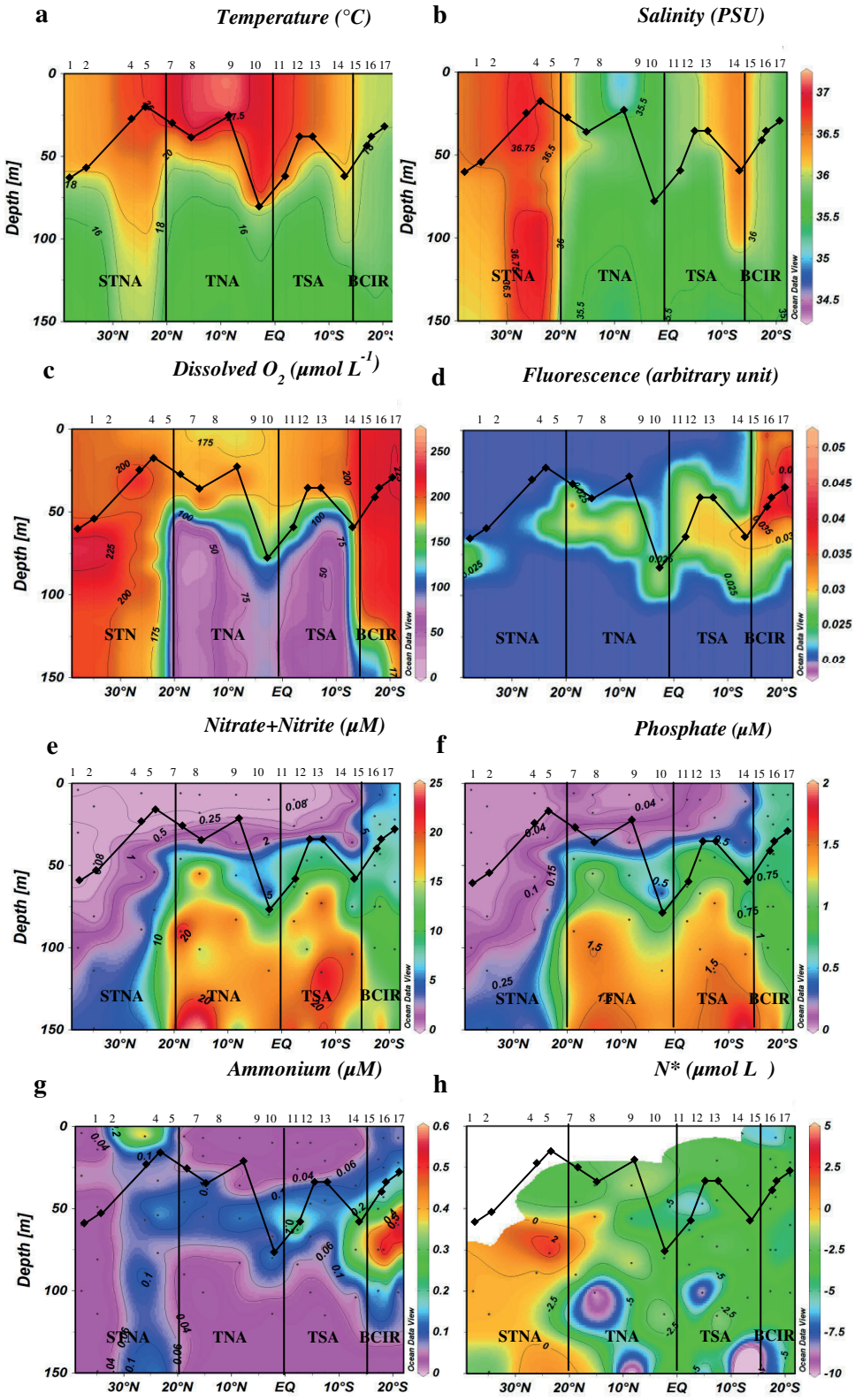
a
Temperature (°C)
b
Salinity (PSU)
c
Dissolved O2 (µmol L-1)
d
Fluorescence (arbitrary unit)
e
Nitrate+Nitrite (µM)
f
Phosphate (µM)
g
Ammonium (µM)
h
N* (µmol L)
Depth [m]
STNA
TNA
TSA
BCIR
STN
30°N
20°N
10°N
EQ
10°S
20°S
Ocean Data View

Figure 2: Spatial distribution of (a) temperature, (b) salinity, (c) dissolved O_2, (d) fluorescence (according to Rohardt and Wisotzki, 2013), (e) $NO_3^- + NO_2^-$, (f) PO_4^{3-} and (g) NH_4^+ concentrations along the ANT XXIX/1 transect. N* (h) = $[NO_3^-] - 16 \times [PO_4^{3-}]$, was derived using the current expedition nutrients data. Values were omitted when either nitrate or phosphate concentrations were below the minimum detectable value (MDV), respectively 0.08 and 0.042 µM. Biogeochemical provinces STNA, TNA, TSA and BCIR as defined in section 3.1, mixed layer depths (black lines connecting diamonds) and sampling stations are illustrated according to latitudinal range.

N_2 fixation

N_2 fixation activity was detected at all stations and at all investigated PAR levels in the euphotic layer. Results from duplicate incubations (duplicates uptake experiments were conducted at 9 out of the 14 stations studied) were well correlated (regression slope = 1.03 ±0.08, n = 36, r^2 = 0.82, p-value < 0.001) and average rates ranged from 0.10 ±0.02 (±SE) to 12.50 ±0.29 µmol m^{-3} d^{-1} (Fig. 3a–d & 4d). The highest N_2 fixation rates were measured in the Northern provinces with rates ranging from 0.25 to 3.98 µmol m^{-3} d^{-1} in the STNA (maximum fixation rate at station 5, 50% PAR) and from 0.39 to 12.50 µmol m^{-3} d^{-1} in the TNA (maximum rate at station 7, 50% PAR). In the southern provinces we also observed relatively high N_2 fixation rates ranging from 0.10 to 2.53 µmol m^{-3} d^{-1} in the TSA (maximum rate at station 11, 15% PAR) and from 0.11 to 3.29 µmol m^{-3} d^{-1} in the BCIR (maximum at station 15, 3.5% PAR).

The vertical distribution of N_2 fixation in the STNA, TNA and TSA generally indicated activity maxima in surface waters (upper 30 m), with values decreasing with depth (Fig. 3a–c & 4d). In the BCIR, N_2 fixation tended to be uniformly distributed over the upper water column, though significant subsurface maxima were observed (40–75 m depth), particularly at stations 15 and 16 (3.39 and 1.71 µmol m^{-3} d^{-1}, respectively Fig. 3d & 4d). Euphotic zone integrated N_2 fixation rates ranged from 47 µmol m^{-2} d^{-1} (station 14, TSA) to 370 µmol m^{-2} d^{-1} (station 7, TNA, Fig. 4a). Since duplicate N_2 fixation measurements yielded similar results, the averages of the two measurements were considered for further discussion. Average depth-integrated N_2 fixation rates for the different provinces were: 117 ±19 µmol m^{-2} d^{-1} (avg ±SE, n = 4, in the STNA), 180 ±92 µmol m^{-2} d^{-1} (n = 4, TNA), 75 ±16 µmol m^{-2} d^{-1} (n = 4, TSA) and 74 ±13 µmol m^{-2} d^{-1} (n = 3, BCIR).

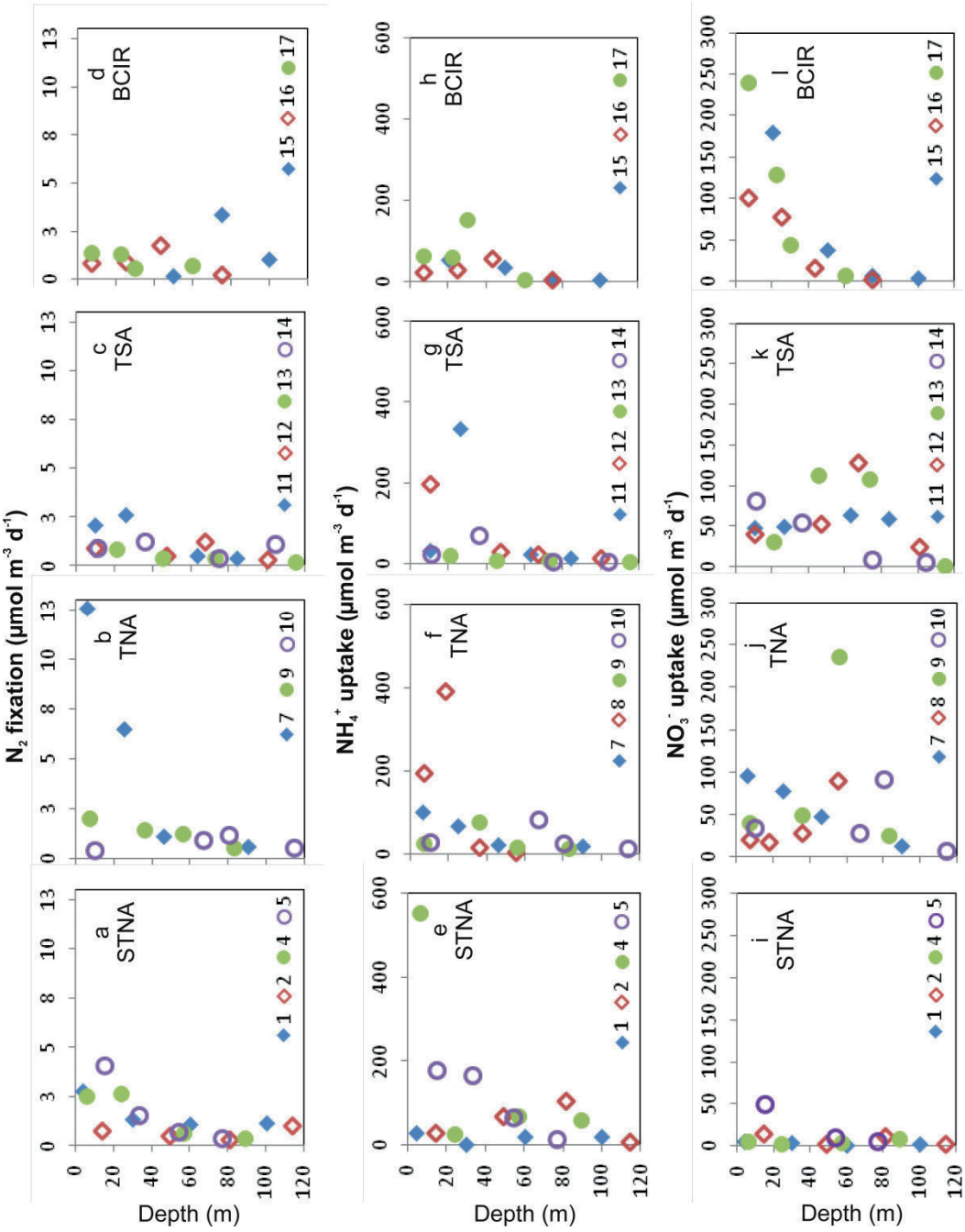

Figure 3: Vertical profiles of N_2 fixation (a – d), ammonium (e – h), and nitrate (i – l) uptake rates within the different biogeochemical provinces studied (see Fig. 1). Measurements were performed at 4 depths corresponding to 54%, 15%, 3.5% and 0.5% of surface irradiance.

NH_4^+ and NO_3^- uptake

NH_4^+ and NO_3^- uptake rates varied from undetectable to maxima of 550 ±104 µmol m^{-3} d^{-1} (±SE, station 4, 50% PAR) and 238 ±25 µmol m^{-3} d^{-1} (station 17, 50% PAR), respectively.

NH_4^+ uptake rates mainly described a decreasing trend southwards (Fig. 3e–h & 4e). Highest rates were found in the STNA (station 4, 50% PAR, 550 ±104 µmol m^{-3} d^{-1}), followed by the TNA (station 8, 15% PAR, 387 ±38 µmol m^{-3} d^{-1}), the TSA (station 12, 15% PAR, 331 ±52 µmol m^{-3} d^{-1}), and finally the BCIR (station 17, 3.5% PAR, 150 ±12 µmol m^{-3} d^{-1}). Vertical profiles of NH_4^+ uptake showed a deepening of the depth of maximal activity in southward direction although highest activities remained in the upper 30 m for all four provinces.

Inversely, NO_3^- uptake showed an overall increasing trend towards the south (Fig. 3i–l & 4f) with lowest rates in the STNA averaging 7 ±3 µmol m^{-3} d^{-1} (avg ±SE, n = 15), relatively similar rates in the TNA (55 ±14 µmol m^{-3} d^{-1}, n = 16) and in the TSA (53 ±10 µmol m^{-3} d^{-1}, n = 16) and finally highest rates in the BCIR (69 ±22 µmol m^{-3} d^{-1}, n = 12). However, local maxima in uptake rates were not only observed in the BCIR, where values ranged from 1.51 to 238 µmol m^{-3} d^{-1}, but also in the TNA, ranging from 5.29 to 234 µmol m^{-3} d^{-1} and in the TSA (from undetectable to 128 µmol m^{-3} d^{-1}). While NO_3^- uptake in the BCIR was concentrated in surface waters (upper 30 m depth), along most of the transect nitrate uptake rather peaked in the subsurface waters.

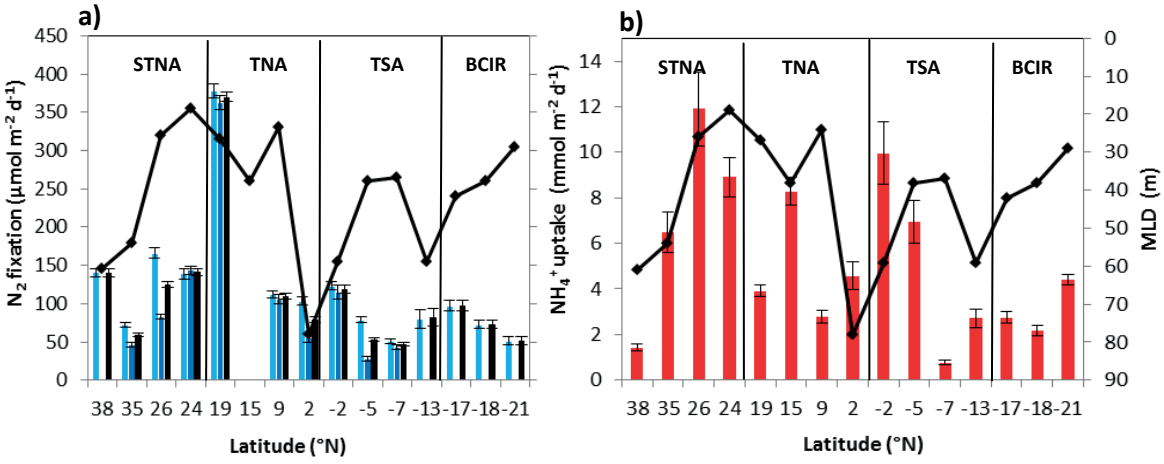

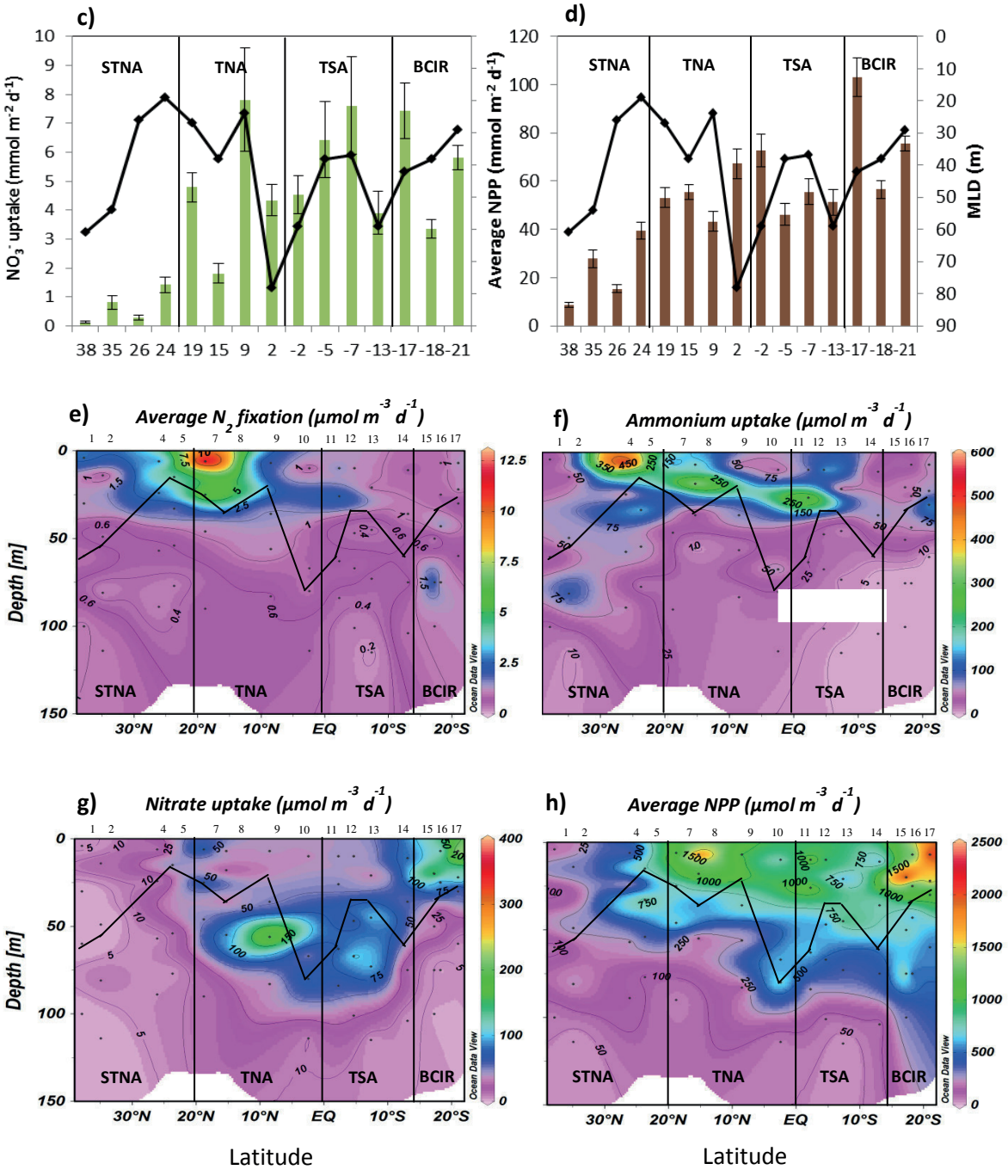

Figure 4: Spatial distribution (± SE) of depth-integrated (a) N_2 fixation rates (replicate A and B in light and dark blue, average of two in black), (b) NH_4^+, (c) NO_3^- and (d) carbon uptake rates; and profiled (e) average N_2 fixation rates, (f) NH_4^+, (g) NO_3^- and (h) carbon uptake rates. Mixed layer depths of each station are overwritten (MLD, black lines).

Net primary production

Carbon uptake measured simultaneously in all N_2, NH_4^+ and NO_3^- incubation experiments was not significantly different (Two Way Anova test returned no difference, p-value = 0.51). Therefore carbon uptake rates for the 3 different N-uptake experiments were averaged for further interpretation. Primary production rates ranged from 13 to 2276 µmol m^{-3} d^{-1} and showed a tendency to increase southwards (Fig. 4h). The oligotrophic province (STNA) was the least productive with rates ranging from 21 and 849 µmol m^{-3} d^{-1} (0.25–10.19 mg m^{-3} d^{-1}). The most productive province was the BCIR, where net PP rates ranged from 248 to 2276 µmol m^{-3} d^{-1} (2.97–27.31 mg m^{-3} d^{-1}). However, high net PP rates (> 1000 µmol m^{-3} d^{-1}) were also measured in the surface waters of the TNA (station 8 50% PAR, 2099 µmol m^{-3} d^{-1}) and TSA provinces (station 11 50% PAR, 1297 µmol m^{-3} d^{-1}). Net PP was generally highest in surface waters and decreased gradually with depth. However at some stations highest PP rates were observed in subsurface (36–80 m) waters: station 10, 80 m (936 ±129 µmol m^{-3} d^{-1}, avg ±SE, n = 4 incubations); station 13, 45 m (969 ±131 µmol m^{-3} d^{-1}, n = 4) and station 14, 36 m (753 ±5 µmol m^{-3} d^{-1}, n = 3).

Table 1: Comparison between present study and compiled published N_2 fixation measurements in the North East and South Atlantic Ocean. NL: Northern limit; SL: Southern limit; WL: Western limit; EL: eastern limit; n: Station counts; SE: standard error; DCM: deep chlorophyll maximum; <D.L.: below detection limit (Explanations of annotations see below).

Ocean basin	Method	Depth of integration	Reference	Time of sampling	NL (°N)	SL (°N)	WL (°E)	EL (°E)	n	Average Areal rate (µmol N m^{-2} d^{-1})	SE
Subtropical Eastern North Atlantic	Online C_2H_2 reduction	MLD	**Staal et al., 2007**	4 Jan. – 16 Feb. 2000	30	17	-20	-15	5	**< D.L**	
	C_2H_2 reduction & $^{15}N_2$ bubble-addition	DCM	**Benavides et al., 2011**	6 - 24 July & 16 Aug. to 5 Sept. 2009	42	31	-20	-9	33	**< 0.1**	
	$^{15}N_2$ bubble-addition	5 m	**Benavides et al., 2013b**	July – Sept. 2009	42	29	20	10	8	**1.2** [a]	
					31	31	11	10	8	**2.8** [b]	
		surface - intermediate - DCM	**Fernández et al., 2010**	16 Nov. – 16 Dec. 2007	26	17	-38	-28	4	**25**	3
				8 Apr. – 6 May 2008	29	17	-29	-28	4	**11**	2
		surface - intermediate - DCM	**Fernández et al., 2012**	17 – 22 Nov. 2007	26	26	-38	-17	6	**1.2**	0.2
				29 Apr. – 2 May 2008	29	29	-29	-15	4	**8.3**	1.7
		5 depths: surface - DCM	**Moore et al., 2009**	12 Oct. – 22 Nov. 2005	37	20	-45	-35	3	**<20** [c]	
		surface - intermediate - DCM	**Mouriño-Carballido et al., 2011**	14 Apr. – 2 May 2008	29	18	-29	-15	4	**11**	5
		5 depths: surface - < 1% irrandiance	**Painter et al., 2013**	11 Aug. – 12 Sept. 2011	27	25	-32	-30	8	**37**	10
		surface	**Rijkenberg et al., 2011**	26 Jan. – 26 Feb. 2006	30	20	-30	-25	4	**8.6** [d]	0.8
		surface	**Snow et al., 2015**	Oct. – Nov. 2011	50	24	-40	-8	-	**<20** [e]	
		Surface (15m)	**Turk et al., 2011**	Nov. – Dec. 2007	26	26	-24	-24	1	**38** [f]	
	$^{15}N_2$ pre-dissolved	surface (5 m)	**Benavides et al., 2013a**	27 Jan. – 15 Mar. 2011	28	24	-45	-13	20	**162** [g]	
		surface - 20 m - DCM	**Großkopf et al., 2012**	26 Oct. – 23 Nov 2009	25	25	-17	-17	1	**130** [h]	
		4 depths: surface - 0.5% irradiance	**Present study**	Nov. 2012	38	24	-20	-12	4	**117**	19

Table 1 continued:

Ocean basin	Method	Depth of integration	Reference	Time of sampling	NL (°N)	SL (°N)	WL (°E)	EL (°E)	n	Average Areal rate (µmol N m^{-2} d^{-1})	SE
Tropical Eastern North Atlantic	Online C_2H_2 reduction	MLD	**Staal et al., 2007**	4 Jan. – 16 Feb. 2000	14	-13	-20	5	20	**7.3**	1.5
	C_2H_2 reduction & $^{15}N_2$ bubble-addition	surface (5–15 m)	**Capone et al., 2005 & Montoya et al., 2007**	18 Mar. – 25 Apr. 1996	16	0	-40	-25	13	**72 –108** [i]	
		4 depths: surface - 1% irradiance	**Falcón et al., 2004**	summer 2001	12	7	-55	-45	3	**47**	
				spring 2002	12	7	-55	-45	18	**37**	
	$^{15}N_2$ Bubble-addition	surface - intermediate - DCM	**Fernández et al., 2010**	16 Nov. – 16 Dec. 2007	14	-9	-29	-28	7	**66**	6
		surface - intermediate - DCM		8 Apr. – 6 May 2008	14	-9	-29	-28	7	**55**	8
		4 depths: 5 - 200m	**Goebel et al., 2010**	18 June – 25 July 2006	17	15	-32	-25	2	**58** [j]	2
		Surface – 30 m – 60 m	**Krupke et al., 2013**	Dec. 2010	17	17	-25	-25	3	**21** [k]	12
		surface - intermediate - DCM	**Mouriño-Carballido et al., 2011**	14 Apr. – 2 May 2008	14	-9	-29	-28	7	**56**	19
		5 depths: surface - DCM	**Moore et al., 2009**	12 Oct. – 22 Nov. 2005	20	-10	-35	-25	3	**<100** [l]	
		surface	**Rijkenberg et al., 2011**	26 Jan. – 26 Feb. 2006	20	12	-30	-20	13	**39** [m]	4
		surface	**Schlosser et al., 2014**	Feb. – March 2011	20	-7	-28	-17	12	**~150**	23
		surface	**Snow et al., 2015**	Oct. – Nov. 2011	24	-10	-40	-25	-	**~100** [n]	
		1-6 depths within euphotic zone	**Subramaniam et al., 2013**	May – June 2009	3	-6	-23	5	24	**113** [o]	8
		Surface (15m)	**Turk et al., 2011**	Nov. – Dec. 2007	21	16	-25	-23	4	**86** [p]	21
		5 depths: surface - 0% irrandiance	**Voss et al., 2004**	12 Oct. – 17 Nov. 2002	10	0	-30	-17	6	**140**	32
	$^{15}N_2$ pre-dissolve	surface - 20 m - DCM	**Großkopf et al., 2012**	26 Oct. – 23 Nov 2009	15	-5	-23	-23	4	**194** [q]	12
		4 depths: surface - 0.5% irradiance	**Present study**	Nov. 2012	19	-13	-20	0	7	**123**	42

Table 1 continued:

Ocean basin	Method	Depth of integration	Reference	Time of sampling	NL (°N)	SL (°N)	WL (°E)	EL (°E)	n	Average Areal rate (µmol N m^{-2} d^{-1})	SE
South East Atlantic	Online C_2H_2 reduction	MLD	**Staal et al., 2007**	4 Jan. – 16 Feb. 2000	-14	-30	-20	3	13	**< D.L**	
South West Atlantic	$^{15}N_2$ bubble-addition	surface - intermediate - DCM	**Fernández et al., 2010**	16 Nov. – 16 Dec. 2007	-13	-33	-29	-28	6	**3**	0.4
				8 Apr. – 6 May 2008	-13	-31	-34	-28	6	**10**	0.8
		5 depths: surface - DCM	**Moore et al., 2009**	12 Oct. – 22 Nov. 2005	-10	-35	-25	10	4	**~10**	4
		surface - intermediate - DCM	**Mouriño-Carballido et al., 2011**	14 Apr. – 2 May 2008	-13	-31	-36	-28	6	**10**	13
		surface	**Snow et al., 2015**	March – May 2009	-22	-28	-34	15	26	**<20** [r]	
				Oct. – Nov. 2011	-10	-45	-50	-25	34	**<100** [s]	
South East Atlantic		5 depths: 0 - 110 m	**Sohm et al., 2011b**	Nov. – Dec. 2007	-10	-14	-30	15	2	**24**	
					-14	-24	12	12	1	**85**	
South West Atlantic	$^{15}N_2$ pre-dissolved	surface (11 m)	**Großkopf et al., 2012**	16 Oct. – 25 Nov 2009	-24	-44	-56	-29	4	**63** [t]	
South East Atlantic		4 depths: surface - 0.5% irradiance	**Present study**	Nov. 2012	-17	-21	3	6	3	**74**	13

Table 1 annotations:

[a & b] Hourly rates multiplied by 24 hours and by the own study average MLD over the 8 stations; [c] Depth-integrated N_2 fixation overestimated from published graph; [d] Depth-integrated rates resulting from surface measurements multiplied by the averaged 41 m mixed layer depth (MLD) determined during our study for the North Atlantic; [e] Depth-integrated N_2 fixation overestimated from published graph; [f] Averaged depth-integrated rates given by Luo et al., (2012) Maredat database; [g] Average daily N_2 fixation rates between the < 10 µM & > 10 µm size fraction for the Eastern fraction of the section (< 45°W), multiplied by the averaged MLD of 41 m determined during our study for the North Atlantic; [h] Depth-integrated N_2 fixation given by the correlation from the supplementary information of Großkopf et al. (2012) between surface N_2 fixation measurements and calculated areal rates. [i] Average range corresponding to measurements carried out using bulk water samples or isolated colonies of *Trichodesmium*. Average as given in the publication only considering the Eastern part (<40°W) of the whole set of sampling sites; [j & p] Averaged depth-integrated rates given by Luo et al., (2012) Maredat database; [k] Average rates measured for approx. 20h incubations multiplied by 41 m MLD for depth-integration; [l] Depth-integrated N_2 fixation overestimated from published graph; [m] Depth-integrated rates obtained by multiplying surface measurements by the average 43 m mixed layer depth during our study determined for the South Atlantic; [n] Depth-integrated N_2 fixation ranged from 0–250 µmol N m^{-2} d^{-1} , average was overestimated from published graph; [o] Average rate weighted according to the number of stations in each specific systems: upwelling, Gulf of Guinea, Equatorial Atlantic and river (as mentioned in the ref.); [q] Depth-integrated rates derived from 4 specific vertical profiles. SE: standard error computed as: (standard deviation) / √ (n); when not directly given in the publication; DCM: deep chlorophyll maximum. [r] Note that only the Eastern part (between 34°W to 15°E) of the JC32 oceanic transect was considered to be compared to data from the current study, since a very large localized maximum was found in the western border in the study of Snow et al. (2015); [s] Depth-integrated N_2 fixation ranged from 0–275 µmol N m^{-2} d^{-1}, average was overestimated from published graph; [t] Depth-integrated N_2 fixation given by the correlation from the Supplementary information of Großkopf et al. (2012) between surface N_2 fixation measurements and calculated areal rates.

Discussion

Importance of N_2 fixation in the different biogeochemical provinces

Diazotrophic activity distribution

During the present study (November 2012), *in-situ* N_2 fixation was highest in the northern part of the cruise track especially in the most stratified TNA province (0–20°N) where a maximal rate of 370 µmol m^{-2} d^{-1} was measured (station 7, 19°N). Großkopf et al. (2012) report a similar maximal N_2 fixation rate of 360 µmol m^{-2} d^{-1} for the eastern tropical Atlantic in Oct.-Nov. 2009, using the dissolution method we also used here. From Table 1, we deduce that the maximal N_2 fixation rates for the eastern tropical Atlantic reported by other studies (Voss et al., 2004; Staal et al., 2007; Moore et al., 2009; Fernández et al., 2010; Goebel et al., 2010; Mouriño-Carballido et al., 2011; Rijkenberg et al., 2011; Turk et al., 2011; Snow et al., 2015) are between 32 to 94% lower than our values and those of Großkopf et al. (2012), regardless of the sampling season. All those studies reporting lower fixation rates used the bubble-addition method to determine N_2 fixation rates. However, we are aware of two exceptions being the studies of Subramaniam et al. (2013) and Schlosser et al. (2014) also using the bubble-addition method, and which report maximum values of 424 and ~320 µmol m^{-2} d^{-1}, respectively. Großkopf et al. (2012) demonstrated that the bubble-addition method, used in most past studies, usually underestimates N_2 fixation in particular when performed by smaller diazotrophs (unicellular, symbiotic cyanobacteria and γ-proteobacteria) as compared to *Trichodesmium spp*. Applying both protocols (bubble-addition & dissolution method) Großkopf et al. (2012) showed, that in case *Trichodesmium* was dominating the diazotrophic community (5–15°N), the dissolution method returned N_2 fixation activities on average 62 % higher than the bubble-addition method. However, for situations where smaller diazotrophs were more abundant (between 4.5°N–5°S), the dissolution method yielded N_2 fixation rates on average 570% higher than the bubble-addition method. Those results are in agreement with findings from past studies investigating the composition of the diazotrophic community and/or size-fractionated N_2 fixation, which revealed for the tropical and subtropical North East Atlantic either an equal partitioning of N_2 fixation between *Trichodesmium* and smaller diazotrophs, (Montoya et al., 2007; Goebel et al., 2010; Subramaniam et al., 2013) or even a predominant contribution of smaller diazotrophs (Turk et al., 2011). We note for the tropical region (combining TNA and TSA provinces, between 19°N till 13°S), that published average fixation values obtained with the bubble-addition method are more similar to our average value of 123 ± 42 µmol m^{-2} d^{-1}. In view of the above discussion concerning the

dominating diazotrophs, this would then point towards *Trichodesmium* being the major player in the tropical region. In fact all studies (Table 1) converge in stating that N_2 fixation is generally highest in the tropical region of the eastern Atlantic Ocean where this activity has mostly been attributed to the presence of filamentous cyanobacteria *Trichodesmium spp*. (Falcón et al., 2004; Capone et al., 2005; Moore et al., 2009; Fernández et al., 2010; Mouriño-Carballido et al., 2011; Großkopf et al., 2012; Schlosser et al., 2014; Snow et al., 2015).

The results from the present study further expand the data set obtained by Großkopf et al. (2012) to the northern (24–38°N, STNA) and southern (17–21°S, BCIR) East Atlantic, where we observe substantial N_2 fixation rates of 117 ± 19 µmol m^{-2} d^{-1} and 74 ± 13 µmol m^{-2} d^{-1} (avg ±SE, n = 4 and 3), respectively. In these regions *Trichodesmium* abundance is known to be low to undetectable (Tyrrell et al., 2003; Moore et al., 2009; Fernández et al., 2010 ; Mouriño-Carballido et al., 2011; Schlosser et al., 2014; Snow et al., 2015). Therefore the high N_2 fixation rates we observe in the STNA and BCIR are likely due to the activity of other diazotrophs (unicellular and symbiotic cyanobacteria, γ-proteobacteria), which is better assessed using the $^{15}N_2$ dissolution method (Großkopf et al., 2012). The literature overview (Table 1) indeed reports integrated N_2 fixation rates which in general are 3 to more than 1000 times lower in the STNA (20–38°N) and 3–25 times lower in the BCIR (15–21°S) than observed in the present study. One exception is the recent work by Snow et al. (2015) who report rates (using the bubble-addition method) in the western margin of the South Atlantic reaching a maximum of ~150 µmol m^{-2} d^{-1} offshore (and ~600 µmol m^{-2} d^{-1} close to the shelf, both in March–May 2009) and up to ~275 µmol m^{-2} d^{-1} (Oct.–Nov. 2011) in the open ocean waters. The work of Benavides et al. (2013a) and Großkopf et al. (2012), both using the $^{15}N_2$ dissolution method, report similar values as the present study. Comparing results obtained with the $^{15}N_2$ dissolution method and bubble-addition methods from Table 1, we found N_2 fixation rates obtained with the former method to be higher by 87 ± 3% (avg ±SE, n = 12) for the North East (≥ 20°N) and by 85 ± 10% (n = 5) for the South (> 15°S) Atlantic than literature values based on the bubble addition method. The higher fixation rates returned from the dissolution method are likely related to the presence of small diazotrophs.

Very few data are presently available for the south eastern subtropical Atlantic. Sohm et al. (2011b) report integrated N_2 fixation rates of 25 µmol m^{-2} d^{-1}, using the bubble-addition method, for a region (11–13°S; 0–25°W) close to the area crossed during the present study. Such rates are lower than our measurements based on the dissolution method (average of 74 µmol m^{-}

^{2} d^{-1}; stations 15, 16, 17) On the other hand, Sohm et al. (2011b) observed higher rates, reaching up to 85 µmol m^{-2} d^{-1}, closer to the shelf within the Benguela Upwelling System (BUS), where N_2 fixation is supposedly stimulated. Snow et al. (2015), applying the bubble-addition method report N_2 fixation rates < 20 µmol m^{-2} d^{-1} for the Eastern South Atlantic. The present study corroborates the idea that N_2 fixation in the Southern Atlantic gyre, which has long been thought to be small with rates ≤ 10 µmol m^{-2} d^{-1} (Staal et al., 2007; Moore et al., 2009; Fernández et al., 2010; Mouriño-Carballido et al., 2011), is in fact similar in magnitude to the one observed in the tropical to subtropical North East Atlantic. In fact, no significant difference is found between the 4 provinces when their average N_2 fixation rates are considered (Two Way Anova p-value = 0.28). These findings would then be in agreement with results of Moore et al. (2014) pointing to equivalent rates of N_2 fixation in the North and South Atlantic, as determined from measurements of hydrogen supersaturations produced during biological nitrogen fixation.

Fixed-nitrogen and carbon uptake distribution

Euphotic layer integrated ammonium and nitrate uptake rates averaged over the STNA (24–38°N), tropical Atlantic (TNA+TSA, 19°N–13°S) and BCIR (17–21°S) were found very similar to previous values for the region (Fig. 4b, c & Table 2). Averaged ammonium uptake reached 6.39 ±2.15 mmol m^{-2} d^{-1} in the STNA (avg ±SE, n = 4 stations), 4.99 ±1.11 mmol m^{-2} d^{-1} (n = 8) in the tropical area and 3.12 ±0.67 mmol m^{-2} d^{-1} in the BCIR (n = 3); while nitrate uptake reached up to 0.67 ±0.29 mmol m^{-2} d^{-1}, 5.16 ±0.71 mmol m^{-2} d^{-1} and 5.53 ±1.18 mmol m^{-2} d^{-1} (n = 4, 8 and 3), respectively.

Averaged integrated net PP, for the STNA (23 ±7 mmol m^{-2} d^{-1}, avg ±SE, n = 4 stations, 274 ±81 mg m^{-2} d^{-1}) and for the tropical area (56 ±4 mmol m^{-2} d^{-1}, n = 8, 667 ±42 mg m^{-2} d^{-1}) were both in the range observed during previous Atlantic cruise which included several meridional transects (Fig. 4g & Table 2). In the BCIR, average primary production (78 ±14 mmol m^{-2} d^{-1}, n = 3; 942 ±162 mg m^{-2} d^{-1}) exceeded the 10–33 mmol m^{-2} d^{-1} range reported in earlier Atlantic studies values, However, sampling in the latter studies was mainly carried out either along the Western boundary of the South Atlantic basin or more to the center of the subtropical gyre (Poulton et al., 2006). This suggests that the present sampling area was under stronger influence of the Benguela Upwelling System (BUS).

Table 2: Comparison between present study and published data of NH_4^+ and NO_3^- uptake rates and primary production in the Atlantic Ocean.

	Depth-integrated NH_4^+ uptake rates (mmol m^{-2} d^{-1}) [a)]			**Depth-integrated NO_3^- uptake rates (mmol m^{-2} d^{-1}) [b)]**			**Depth-integrated Primary Production (mmol m^{-2} d^{-1}) [c)]**		
	Subtropical East Atlantic (40–25°N)	Tropical East Atlantic (25°N–10°S)	South Atlantic (10–40°S)	Subtropical East Atlantic (40–25°N)	Tropical East Atlantic (25°N–10°S)	South Atlantic (10–40°S)	Subtropical East Atlantic (40–25°N)	Tropical East Atlantic (25°N–10°S)	South Atlantic (10–40°S)
Range in past studies	0.7–6.5	1.7–7.9	2.2–7.9	0.1–5.7	0.1–27	0.6–15	6 –66	7–54	10–33
Average in present study (±SD)	6.4 ±4.3	5.0 ±3.1	3.1 ±1.2	0.7 ±0.6	5.2 ±2.0	5.5 ±2.0	23 ±14	56 ±10	78 ±23

a) Donald et al., 2001; Joint et al., 2001; Varela et al., 2005; Rees et al., 2006.
b) Donald et al., 2001; Joint et al., 2001; Varela et al., 2005; Rees et al., 2006; Fernández & Raimbault, 2007; Painter et al., 2008 & 2013.
c) Marañón et al., 2000; Donald et al., 2001; Joint et al., 2001; Varela et al., 2005; Pérez et al., 2006; Poulton et al., 2006; Painter et al., 2013.

Relative contribution of N_2 fixation to productivity

To the best of our knowledge, this is the first time that based on *in-situ* measurements, N_2 fixation is shown to contribute to such a large extent to productivity in the Atlantic Ocean. N_2 fixation could explain up to 8% of the combined N uptake (i.e, N_2 fixation + NH_4^+ uptake + NO_3^- uptake) in the STNA, 4% in the TNA and 1% in the TSA and BCIR. Note that the contribution of N_2 fixation to net PP was estimated as: [euphotic zone integrated N_2 fixation x (Redfield C/N)] / [euphotic zone integrated net PP], with 106/16 as the Redfield ratio. We observed that a maximum of 11% of net PP was fueled by N_2 fixation, while average contributions of N_2 fixation to net PP were 4.96 ±2.09% (avg ±SE, n = 4 stations) in the STNA, 2.35 ±1.15% (n = 3) in the TNA and 0.76 ±0.09% (n = 7) in the combined TSA and BCIR provinces.

We also estimated the contribution of N_2 fixation to new primary production (new PP), which is in fact equivalent to assessing the contribution to new nitrogen uptake (new NU). In order to do so, we used literature data for shallow nitrate regeneration in the Atlantic Ocean to evaluate the impact on our nitrate uptake calculations and thus on the contribution estimates of N_2 fixation to new nitrogen input. Fernández & Raimbault (2007) report that nitrification in the North Atlantic could account on average for 38% of nitrate uptake during February-March and for 20% during March-May. Benavides et al. (2013b) report a value of 25% for July-September 2009. However, Fawcett et al. (2015) found no evidence at all for nitrification in the euphotic layer of the north western Atlantic. To our knowledge no data on nitrification contribution to nitrate uptake are available for the South Atlantic, but the study of Clark et al., (2008) carried out in the same season as our study (September-October 2003) suggests that euphotic layer nitrification rates are equivalent for the North and South Atlantic gyres.

Therefore, we considered nitrification to contribute between 0 and 38% to total nitrate uptake at all our stations in the northern and southern hemisphere. The corrected new production is then given by: *f-ratio* × Net PP, where *f-ratio* = [N_2 fixation + (from 0.62 to 1) × total NO_3^- uptake] / (N_2 fixation + NH_4^+ uptake + total NO_3^- uptake) and the relative contribution of N_2 fixation is given by: N_2 fixation / [N_2 fixation + (from 0.62 to 1) × total NO_3^- uptake]. N_2 fixation was found to account for a maximum of 52–63% of new PP in the STNA province (considering a 0 to 38% contribution of nitrification, respectively), 7–10% in the TNA, 3–4% in the TSA and at 2–3% in the BCIR province. Such values are considerably higher than those reported in the STNA by Benavides et al. (2013b) for net and gross N_2 fixation (the latter including a ~60% release of fixed N_2 through DON release) and which indicated N_2 fixation to contribute to less than 1% of new

PP. Also in the STNA, Painter et al. (2013) report a maximum contribution of N_2 fixation to new NU (i.e., N_2 fixation / [N_2 fixation + total NO_3^- uptake]) of 19%. We note that our observations tend in fact to be more similar to estimates based on geochemical parameters (Table 3). For instance, based on a stable isotope budget of suspended particles in the tropical North West Atlantic, Capone et al. (2005) estimated a contribution of N_2 fixation to total nitrogen demand of about 36% and 68% for April and October 1996, respectively. Though these values are still larger than our estimates for the TNA, the tropical West Atlantic is known to have higher rates of N_2 fixation than the tropical East Atlantic (Capone et al., 2005; Montoya et al., 2007; Subramaniam et al., 2008). Based on nitrate isotopic mass balance calculations Bourbonnais et al. (2009) estimate that N_2 fixation in the subtropical North East Atlantic may account for close to 5% of the N required for total primary production, and 40% of export production, which is considered equivalent to new PP in the present study. However, it is important to note that atmospheric deposition of nitrogen compounds could also introduce isotopically light nitrogen to Atlantic Ocean surface waters (Baker et al., 2007) thereby affecting the nitrate and particulate nitrogen isotopic signatures, similarly than nitrogen input through N_2 fixation. Nevertheless, similarity in N_2 fixation magnitude between our measurements and calculations by Bourbonnais et al. (2009) suggest a predominant contribution of N_2 fixation relative to atmospheric input in the introduction of new nitrogen in this region.

Table 3: Comparison between present study and published estimates of the relative contribution (%) of N_2 fixation to, Nitrogen Uptake (N Uptake), Net Primary Production (Net PP) and New Primary Production (New PP) in the Atlantic Ocean.

					N_2 fixation contribution		
	Reference	**Method**	**Parameter**	**STNA**	**TNA**	**TSA**	**BCIR**
Direct measurements	Painter et al., 2013	$^{15}N_2$ Bubble-addition	% New N Uptake [a]	3–19%	-	-	-
	Benavides et al., 2013	$^{15}N_2$ Bubble-addition	% New PP	< 1%	-	-	-
	Present study	$^{15}N_2$ dissolution method	% N uptake	0.8–8.3%	0.9–4.1%	0.4–1.2%	0.5–1.3%
			% Net PP	1.4–10.7%	0.8–4.6%	0.6–1.1%	0.5–0.9%
			% New PP 0% nitrification	7–52%	1.4–7%	0.6–3%	0.9–2%
			% New PP 38% nitrification	10–63%	2–11%	1.0–4%	1.4–3%
Geochemical estimates	Capone et al., 2005	SPM isotopic mass balance	% N demand [b]	-	36–68%	-	-
	Bourbonnais et al., 2009	NO_3^- isotopic mass balance	% export production	~40%	-	-	-
			% Total PP	5%			

Relative contribution of N_2 fixation to new nitrogen uptake[a] (New N uptake) is equivalent to the contribution to new PP and thus to export production. Contribution to nitrogen demand [b] (N demand) is equivalent to the contribution to N uptake.

Revisiting the annual N_2 fixation rates

In order to compare our results with geochemical estimates, we calculated basin-wide annual N_2 fixation activities (Table 4). For that purpose we used published data for the Eastern Atlantic (essentially obtained with the $^{15}N_2$ bubble-addition method, see in Table 1) combined with data for the North West Atlantic (Goering et al., 1966; Orcutt et al., 2001; the western part of the region studied by Capone et al., 2005 and Montoya et al., 2007; Holl et al., 2007 and the open ocean data of Subramaniam et al., 2008). Indeed, to compute basin-wide N_2 fixation rates, we only considered open ocean data, representative of the whole ocean basin, and we did not take into account data for areas close to margins and shelves. The Caribbean (Capone et al., 2005), the Amazon River plume (Subramaniam et al., 2008; Snow et al., 2015) and the English Channel (Rees et al., 2009), for instance, have been observed to sustain quite high rates of N_2 fixation, but a correct assessment of the significance of margin and shelf areas at the global scale, clearly calls for more measurements. We thus calculate an annual input of 23.6 Tg N yr^{-1} and 5.7 Tg N yr^{-1} for the northern (50°N–10°S) and southern (10°S–44°S) areas of the Atlantic, respectively. These values are respectively 1.9 and 3.8 times higher than those reported by Großkopf et al. (2012) who also compiled literature data: 12.7 Tg N yr^{-1} in the North (50°N–5°S) and 1.5 Tg N yr^{-1} in the South (5°S–30°S) Atlantic basins. However, in the present study, we not only we took into account studies performed in the western Atlantic Ocean, known to shelter higher N_2 fixation activities compared to the eastern part of the basin (Capone et al., 2005; Montoya et al., 2007; Holl et al., 2007; Subramaniam et al., 2008), but we also used data from the most recent studies (Table 4). Additionally, ocean surfaces we considered for our computations were slightly different than those used by Großkopf et al. (2012). Considering exclusively the data from the present study we estimate N_2 fixation for the whole Atlantic Ocean to amount to 35.2 Tg N yr^{-1}, with 24.6 Tg N yr^{-1} for the northern and 10.7 Tg N yr^{-1} for the southern basin. Such rates fit the lower range of values proposed by Capone et al. (2005) for the North Atlantic, though we note that these authors only considered data for the tropical North West Atlantic where N_2 fixation rates are usually highest. However, our data are very similar to estimates made by Luo et al. (2012). The NW Atlantic is known to shelter not only large blooms of filamentous cyanobacteria but also a quite important community of symbiotic unicelullar cyanobacteria (Foster et al., 2007; Montoya et al., 2007). It thus appears important to expand westward N_2 fixation measurements using the dissolution method in order to reach more accurate yearly inputs at the whole basin-scale. Moreover, there is a need to perform these measurements during different seasons to

integrate any inter-season variability in diazotrophic activity. Overall our findings appear to be in agreement with geochemically estimated rates of N_2 fixation in the North Atlantic as well as the whole Atlantic Ocean (Table 4), which were commonly found to exceed *in-situ* measurements (Mahaffey et al., 2005; Codispoti, 2007; Gruber, 2008). Furthermore our findings suggest that the input of N through N_2 fixation in the South Atlantic (10.7 Tg N yr^{-1}) tends to exceed the loss of fixed N through the effect of anammox (1.4 Tg N yr^{-1}, Kuypers et al., 2005) and denitrification (~2.5 Tg N yr^{-1}, Nagel et al., 2013) within the Oxygen Minimum Zone of the BUS. It has been shown that upwelling systems (essentially by supplying waters with low N/P ratio) tend to stimulate N_2 fixation (Sohm et al., 2011b; Subramaniam et al., 2013), which would certainly lead to an upward evaluation once measurements with the dissolution method will be performed within the BUS.

Table 4: Estimates of N inputs to the open Atlantic Ocean.

	Reference	Method	N input (Tg N yr^{-1})	Basin
Direct measurements	**Capone et al., 2005**	Scaled in-situ measurements of *Trichodesmium* N_2 fixation	**22–34**	North Atlantic
	Großkopf et al., 2012	Scaled own N_2 fixation measurements	**24**	Whole Atlantic
	Luo et al., 2012	Scaled N_2 fixation measurements	**34**	
	Present study	Scaled N_2 fixation of past studies using the bubble-addition method in the North East and whole South Atlantic	**23.6**	North Atlantic
			5.7	South Atlantic
			29.3	Whole Atlantic
		Scaled present study N_2 fixation measurements	**24.6**	North Atlantic
			10.7	South Atlantic
			35.2	Whole Atlantic
Geochemical estimates	**Gruber and Sarmiento, 1997**	Thermocline N* = ($[NO_3^-]$ - 16 x $[PO_4^{3-}]$ + 2.90) x 0.87	**28**	North Atlantic
	Moore et al., 2009	Water column N* = $[NO_3^-]$ - 16 x $[PO_4^{3-}]$	**15–21**	
	Singh et al., 2013	Subsurface water column N* = $[NO_3^-]$ - 14.63 x $[PO_4^{3-}]$	**17**	
	Deutsch et al., 2007	Surface waters P* = $[PO_4^{3-}]$ - $[NO_3^-]$/16	**20**	Whole Atlantic
	Knapp et al., 2008	Water column nitrate isotopic composition	**21–34**	
	Lee et al., 2002	Carbon inventory assuming a C:N ratio of 7:1 for biomass	**28**	

Environmental control on N_2 fixation distribution

Diazotrophic activity in the eastern tropical North Atlantic is considered to be limited by iron (Moore et al., 2009) and phosphorus availability (Mills et al., 2004) and possibly by other trace compounds (Ho, 2013; Jacq et al., 2014). Also, maximal N_2 fixation rates in the eastern Tropical Atlantic appear well associated with areas of high Fe input (Moore et al., 2009; Schlosser et al., 2014). In the present study the most intense N_2 fixation activity was found at a location (station 7, 19°N) presenting relatively large surface phosphate concentrations (~0.10 µM in the upper 25m) contrasting somehow with the prevailing water column stratification and strong oligotrophic conditions (Fig. 2a, f). Since on the other hand nitrate was < MDV (80 nM) in the upper 25 m (Fig. 2e), station 7 was characterized by an excess of phosphate compared to nitrate (N/P ratio < 0.70), a condition believed to greatly stimulate N_2 fixation (Deutsch et al., 2007). According to Pradhan et al. (2006) the Mauritanian Upwelling System (MUS) extends from 10–25°N and from 30°W to the northwest African coast, thus covering the area where station 7 is located (19°N - 21°W). The high N_2 fixation rates at station 7, likely benefited from upward advection of waters having low nitrate/phosphate ratio, in combination with Fe input from wet and/or dry aeolian deposition. A possible influence of the MUS appears corroborated by the observed shoaling of the thermocline and mixed layer depth at station 7 (both ~27 m, Fig. 2a).

At all others stations, the euphotic zone integrated N_2 fixation activity was still important, although significantly lower than at station 7 (TNA, p-value < 0.05). Nevertheless, regionally integrated N_2 fixation rates are rather similar between provinces (STNA, TNA, TSA and BCIR), whether station 7 was included or not (p-value of 0.28 and 0.29, respectively).

Similar to the TNA, the STNA region is also known to be impacted by atmospheric input of nutrients capable of stimulating diazotrophic activity (Moore et al., 2009; Schlosser et al., 2014; Snow et al., 2015). This could explain the high N_2 fixation activity we observed in the STNA province (117 ±39 µmol m^{-2} d^{-1}, n = 4) which was almost as high as in the TNA (180 ±160 µmol m^{-2} d^{-1}, n = 4, Fig. 4a).

Despite some input of Namib desert dust into the Benguela Current region, the eastern South Atlantic region (TSA and BCIR provinces) overall receive far less atmospheric input of nutrients than the eastern North Atlantic, which is strongly affected by Saharan dust inputs (Mahowald et al., 2005; Luo et al., 2008; Moore et al., 2009; Schlosser et al., 2014). So the question remains —

how was N_2 fixation activity fueled in the TSA and BCIR provinces, to allow rates to reach levels quite as high as those for the STNA and TNA provinces?

The study of Subramaniam et al. (2013) in the TSA region and the Gulf of Guinea suggests that during active equatorial upwelling, advection of waters with low N/P ratios, and combined effect of aeolian and upwelled iron input sustains high N_2 fixation rates. Although, the EUS is reported to be weak in November (Verstraete, 1992), when our study took place, it appears that the phosphate excess signature in the eastern equatorial region could be maintained during longer timescale (see the annually averaged phosphate excess, Fig. 1). Sohm et al. (2011b) report N_2 fixation rates of 25–85 µmol m^{-2} d^{-1} near and within the Benguela Upwelling System. These authors suggest that the main source of dissolved iron (DFe) to surface waters in the region, was the resuspension and dissolution of metals from shelf sediments, citing Noble et al. (2012). Past studies have shown that wind forcing promotes upwelling during austral spring and summer in the southern part of the BUS (> ~30°S) and during autumn and spring in the northern Benguela region (~18° to 21°S); while the central Benguela region (~26° to 28°S) experiences perennially upwelling-favorable conditions (Shannon 1985, Shannon and Nelson 1996). In addition, the Benguela Upwelling System is known to host biologically mediated N loss processes (anammox and/or denitrification) in low oxygen environments and is characterized by P release from sediments (Kuypers et al., 2005; Nagel et al., 2013). Indeed, our results suggest that phosphate was locally in stoichiometric excess relative to nitrate within the TSA and BCIR ($N^* < -5$, Fig. 2h). We thus propose that upwelling of macro- and micro-nutrients within the BUS with a phosphorus excess, coupled to an offshore advection, via the Benguela and Angola Currents (Flohr et al., 2014) towards the subtropical gyre, were the major factors stimulating N_2 fixation in the TSA and BCIR provinces.

Previous studies have already pointed out the key role played by phosphate excess input to surface waters in regulating N_2 fixation intensity (Deutsch et al., 2007; Straub et al., 2013). Our study further corroborates the stimulating influence of phosphate excess on N_2 fixation activity, an excess which is suggested to originate in the Southern Ocean and is advected northwards associated with the Sub-Antarctic Mode Water and Antarctic Intermediate Water (Sarmiento et al., 2004; Moore et al., 2009; Straub et al., 2013). The present study suggests that this phosphate excess not only affects in the South East Atlantic in the proximity of the BUS and the EUS, but also in the North Atlantic near the MUS.

Conclusion

The present results add to the existing data set on community N_2 fixation measurements using the $^{15}N_2$ dissolution method in the Atlantic Ocean. Results presented here support the hypothesis that the use of the $^{15}N_2$ bubble-addition method in past studies led to an underestimation of N_2 fixation activity mainly by smaller diazotrophs as opposed to buoyant *Trichodesmium spp*. Differences in diazotrophic activity denoted in comparison to past studies in the Eastern Atlantic Ocean were significantly higher in the subtropical North Atlantic (20–38°N), tropical South Atlantic (0–15°S) and Benguela Current Influenced Region (15–21°S), regions where *Trichodesmium* abundance is either low or undetectable. According to our results, N_2 fixation could fuel up to ~11% of net primary production and more than 50% of new production in the subtropical North Atlantic. These computations are comparable to published geochemical estimates for the North Atlantic. Annual basin-scale N_2 fixation rates obtained in the present study are in the range of geochemical computations published during the past decade. However there is a need to investigate further the spatial and temporal variability in nitrogen fixation, using the dissolution method and including margin and shelf areas in order to better constrain basin wide N_2 fixation rates.

Acknowledgements

We are grateful towards Holger Auel (BreMarE, University of Bremen), Chief Scientist during the EUROPA expedition ANT-XXIX/1. We also thank the Captain and the crew of R/V Polarstern for their skillful support, and the Alfred Wegener Institute for Polar and Marine Research, Bremerhaven. This work was financed by the Flanders Research Foundation (FWO contract G071512N) and the Vrije Universiteit Brussel, R&D, Strategic Research Plan "Tracers of Past & Present Global Changes“. We thank D. Verstraeten, N. Brion and J. Aristegui for their assistance with experimental proceedings.

References

Allen, C. B., Kandat, J., & Laws, E. A. (1996). New production and photosynthetic rates within and outside a cyclonic mesoscale eddy in the North Pacific subtropical gyre. Deep-Sea Research Part I: Oceanographic Research Papers, 43(6), 917–936. http://doi.org/10.1016/0967-0637(96)00022-2

Baker, A. R., Weston, K., Kelly, S. D., Voss, M., Streu, P., & Cape, J. N. (2007). Dry and wet deposition of nutrients from the tropical Atlantic atmosphere: Links to primary productivity and nitrogen fixation.

Deep-Sea Research Part I: Oceanographic Research Papers, 54(10), 1704–1720. http://doi.org/10.1016/j.dsr.2007.07.001

Benavides, M., Agawin, N., Arístegui, J., Ferriol, P., & Stal, L. (2011). Nitrogen fixation by *Trichodesmium* and small diazotrophs in the subtropical northeast Atlantic. Aquatic Microbial Ecology, 65(1), 43–53. http://doi.org/10.3354/ame01534

Benavides, M., Bronk, D. A., Agawin, N. S. R., Pérez-Hernández, M. D., Hernández-Guerra, A., & Arístegui, J. (2013a). Longitudinal variability of size-fractionated N_2 fixation and DON release rates along 24.5°N in the subtropical North Atlantic. Journal of Geophysical Research: Oceans, 118(7), 3406–3415. http://doi.org/10.1002/jgrc.20253

Benavides, M., Arístegui, J., Agawin, N. S. R., Álvarez-Salgado, X. A., Álvarez, M., & Troupin, C. (2013b). Low contribution of N_2 fixation to new production and excess nitrogen in the subtropical northeast Atlantic margin. Deep Sea Research Part I: Oceanographic Research Papers, 81, 36–48. http://doi.org/10.1016/j.dsr.2013.07.004

Bourbonnais, A., Lehmann, M. F., Waniek, J. J., & Schulz-Bull, D. E. (2009). Nitrate isotope anomalies reflect N_2 fixation in the Azores Front region (subtropical NE Atlantic). Journal of Geophysical Research: Oceans, 114(3), 1–16. http://doi.org/10.1029/2007JC004617

Capone, D. G., Burns, J. A., Montoya, J. P., Subramaniam, A., Mahaffey, C., Gunderson, T., Michaels, A. F., & Carpenter, E. J. (2005). Nitrogen fixation by *Trichodesmium spp.*: An important source of new nitrogen to the tropical and subtropical North Atlantic Ocean. Global Biogeochemical Cycles, 19(2), 1–17. http://doi.org/10.1029/2004GB002331

Casciotti, K. L., Sigman, D. M., Hastings, M. G., Böhlke, J. K., & Hilkert, a. (2002). Measurement of the oxygen isotopic composition of nitrate in seawater and freshwater using the denitrifier method. Analytical Chemistry, 74(19), 4905–4912. http://doi.org/10.1021/ac020113w

Clark, D. R., Rees, A. P., & Joint, I. (2008). Ammonium regeneration and nitrification rates in the oligotrophic Atlantic Ocean: Implications for new production estimates. Limnology and Oceanography, 53(1), 52–62. http://doi.org/10.4319/lo.2008.53.1.0052

Codispoti, L. A., Brandes, J. A., Christensen, J. P., Devol, A. H., Naqvi, S. W. A., Paerl, H. W., & Yoshinari, T. (2001). The oceanic fixed nitrogen and nitrous oxide budgets : Moving targets as we enter the anthropocene? Scientia Marina, 65(2), 85–105. http://doi.org/10.3989/scimar.2001.65s285

Codispoti, L. A. (2007). An oceanic fixed nitrogen sink exceeding 400 Tg N a^{-1} vs the concept of homeostasis in the fixed-nitrogen inventory. Biogeosciences, 4, 233–253. http://doi.org/10.5194/bgd-3-1203-2006

Dabundo, R., Lehmann, M. F., Treibergs, L., Tobias, C. R., Altabet, M. A., Moisander, P. H., & Granger, J. (2014). The contamination of commercial $^{15}N_2$ gas stocks with ^{15}N-labeled nitrate and ammonium and consequences for nitrogen fixation measurements. PloS One, 9(10), e110335. http://doi.org/10.1371/journal.pone.0110335

De Boyer Montégut, C., Madec, G., Fischer, A. S., Lazar, A., & Iudicone, D. (2004). Mixed layer depth over the global ocean: An examination of profile data and a profile-based climatology. Journal of Geophysical Research C: Oceans, 109(12), 1–20. http://doi.org/10.1029/2004JC002378

Deutsch, C., Sarmiento, J. L., Sigman, D. M., Gruber, N., & Dunne, J. P. (2007). Spatial coupling of nitrogen inputs and losses in the ocean. Nature, 445(7124), 163–167. http://doi.org/10.1038/nature05392

Dugdale, R. C., & Goering, J. J. (1967). Uptake of new and regenerated forms of nitrogen in primary productivity. Limnology and Oceanography, 12(2), 196–206. http://doi.org/10.4319/lo.1967.12.2.0196

Dugdale, R. C., & Wilkerson, F. P. (1986). The use of ^{15}N to measure nitrogen uptake in eutrophic oceans; experimental considerations. Limnology and Oceanography, 31(4), 673–689. http://doi.org/10.4319/lo.1986.31.4.0673

Elskens, M., Baeyens, W., & Goeyens, L. (1997). Contribution of nitrate to the uptake of nitrogen by phyotplankton in an ocean marine environment. Hydrobiologia, 353, 139–152.

Falcón, L. I., Carpenter, E. J., Cipriano, F., Bergman, B., & Capone, D. G. (2004). N_2 Fixation by Unicellular Bacterioplankton from the Atlantic and Pacific Oceans : Phylogeny and In Situ. Society, 70(2), 765–770. http://doi.org/10.1128/AEM.70.2.765

Fawcett, S. E., Ward, B. B., Lomas, M. W., & Sigman, D. M. (2015). Vertical decoupling of nitrate assimilation and nitrification in the Sargasso Sea. Deep Sea Research Part I: Oceanographic Research Papers, 103, 64–72. http://doi.org/10.1016/j.dsr.2015.05.004

Fernández, A., Mouriño-Carballido, B., Bode, A., Varela, M., & Marañón, E. (2010). Latitudinal distribution of *Trichodesmium spp.* and N_2 fixation in the Atlantic Ocean. Biogeosciences Discussions, 7(2), 2195–2225. http://doi.org/10.5194/bgd-7-2195-2010

Fernández, A., Graña, R., Mouriño-Carballido, B., Bode, A., Varela, M., Domínguez-Yanes, J. F., Escánez, J., Armas, D., & Marañón, E. (2012). Community N_2 fixation and *Trichodesmium spp.* abundance along longitudinal gradients in the eastern subtropical North Atlantic. ICES Journal of Marine Science, 70(1), 223–231. http://doi.org/10.1093/icesjms/fst176

Fernández I., C., & Raimbault, P. (2007). Nitrogen regeneration in the NE Atlantic Ocean and its impact on seasonal new, regenerated and export production. Marine Ecology Progress Series, 337, 79–92. http://doi.org/10.3354/meps337079

Flohr, A., Van Der Plas, A. K., Emeis, K. C., Mohrholz, V., & Rixen, T. (2014). Spatio-temporal patterns of C : N : P ratios in the northern Benguela upwelling system. Biogeosciences, 11(3), 885–897. http://doi.org/10.5194/bg-11-885-2014

Glibert, P. M., Lipschultz, F., McCarthy, J. J., & Altabet, M. A. (1982). Isotope dilution models of uptake and remineralization of ammonium by marine plankton. Limnology and Oceanography. http://doi.org/10.4319/lo.1982.27.4.0639

Goebel, N. L., Turk, K. A., Achilles, K. M., Paerl, R., Hewson, I., Morrison, A. E., Montoya, J. P., Edwards, C. A., & Zehr, J. P. (2010). Abundance and distribution of major groups of diazotrophic cyanobacteria and their potential contribution to N_2 fixation in the tropical Atlantic Ocean. Environmental Microbiology, 12(12), 3272–3289. http://doi.org/10.1111/j.1462-2920.2010.02303.x

Goering, J. J., Dugdale, C., & Menzel, D. W. (1966). Estimates of in situ rates of nitrogen uptake by *Trichodesmium sp.* in the tropical Atlantic Ocean. Limnology & Oceanography, 11, 614–620.

Granger, J., & Sigman, D. M. (2009). Removal of nitrite with sulfamic acid for nitrate N and O isotope analysis with the denitrifier method. Rapid Communications in Mass Spectrometry : RCM, 23, 3753–3762. http://doi.org/10.1002/rcm

Grasshoff, K., Ehrhardt, M., & Kremling, K. (1983). Methods of Seawater Analysis. Second, Revised and Extended Edition. Methods of Seawater Analysis. Second, Revised and Extended Edition.

Großkopf, T., Mohr, W., Baustian, T., Schunck, H., Gill, D., Kuypers, M. M. M., Lavik, G., Schmitz, R. A., Wallace, D. W. R., & LaRoche, J. (2012). Doubling of marine dinitrogen-fixation rates based on direct measurements. Nature, 488(7411), 361–364. http://doi.org/10.1038/nature11338

Gruber, N., & Sarmiento, J. L. (1997). Global patterns of marine nitrogen fixation and denitrification. Global Biogeochemical Cycles, 11(2), 235. http://doi.org/10.1029/97GB00077

Gruber, N., & Sarmiento, J. L. (2002). Large scale biochemical/physical interactionsin elemental cycles. The Sea: biological-physical interactions in the oceans (Vol. 12), 337–399.

Gruber, N. (2008). The Marine Nitrogen Cycle: Overview and Challenges. Nitrogen in the Marine Environment. http://doi.org/10.1016/B978-0-12-372522-6.00001-3

Hama, T., Miyazaki, T., Ogawa, Y., Iwakuma, T., Takahashi, M., Otsuki, A., & Ichimura, S. (1983). Measurement of photosynthetic production of a marine phytoplankton population using a stable ^{13}C isotope. Marine Biology, 73, 31–36.

Harrison, W. G., Harris, L. R., & Irwin, B. D. (1996). The kinetics of nitrogen utilization in the oceanic mixed layer: Nitrate and ammonium interactions at nanomolar concentrations. Limnology and Oceanography, 41(1), 16–32. http://doi.org/10.4319/lo.1996.41.1.0016

Ho, T.-Y. (2013). Nickel limitation of nitrogen fixation in *Trichodesmium*. Limnology and Oceanography, 58(1), 112–120. http://doi.org/10.4319/lo.2013.58.1.0112

Holl, C. M., Clayton, T. D., & Montoya, J. P. (2007). *Trichodesmium* in the western Gulf of Mexico: $^{15}N_2$-fixation and natural abundance stable isotope evidence. Limnology & Oceanography, 52(5), 2249–2259.

Holmes, R. M., Aminot, A., Kérouel, R., Hooker, B. A., & Peterson, B. J. (1999). A simple and precise method for measuring ammonium in marine and freshwater ecosystems. Canadian Journal of Fisheries and Aquatic Sciences, 56(10), 1801–1808. http://doi.org/10.1139/f99-128

Jacq, V., Ridame, C., L'Helguen, S., Kaczmar, F., & Saliot, A. (2014). Response of the unicellular diazotrophic cyanobacterium Crocosphaera watsonii to iron limitation. PloS One, 9(1), e86749. http://doi.org/10.1371/journal.pone.0086749

Kuypers, M. M. M., Lavik, G., Woebken, D., Schmid, M., Fuchs, B. M., Amann, R., Jørgensen, B. B. & Jetten, M. S. M. (2005). Massive nitrogen loss from the Benguela upwelling system through anaerobic ammonium oxidation. Proceedings of the National Academy of Sciences of the United States of America, 102(18), 6478–83. http://doi.org/10.1073/pnas.0502088102

Langlois, R., Mills, M., Ridame, C., Croot, P., & LaRoche, J. (2012). Diazotrophic bacteria respond to Saharan dust additions. Marine Ecology Progress Series, 470, 1–14. http://doi.org/10.3354/meps10109

Luo, C., Mahowald, N., Bond, T., Chuang, P. Y., Artaxo, P., Siefert, R., Chen, Y., & Schauer, J. (2008). Combustion iron distribution and deposition. Global Biogeochemical Cycles, 22(1), 1–17. http://doi.org/10.1029/2007GB002964

Luo, Y.-W., Doney, S. C., Anderson, L. A., Benavides, M., Berman-Frank, I., Bode, A., … Zehr, J. P. (2012). Database of diazotrophs in global ocean: abundance, biomass and nitrogen fixation rates. Earth System Science Data, 4(1), 47–73. http://doi.org/10.5194/essd-4-47-2012

Mahaffey, C., Michaels, A. F., & Capone, D. G. (2005). The Conundrum of Marine N_2 Fixation. American Journal of Science, 305, 546–595. http://doi.org/10.2475/ajs.305.6-8.546

Mahowald, N. M., Baker, A. R., Bergametti, G., Brooks, N., Duce, R. A., Jickells, T. D., T. D., Kubilay, N., Prospero, J. M., & Tegen, I. (2005). Atmospheric global dust cycle and iron inputs to the ocean. Global Biogeochemical Cycles, 19(4). http://doi.org/10.1029/2004GB002402

McIlvin, M. R., & Altabet, M. A. (2005). Chemical conversion of nitrate and nitrite to nitrous oxide for nitrogen and oxygen isotopic analysis in freshwater and seawater. Analytical Chemistry, 77(17), 5589–5595. http://doi.org/10.1021/ac050528s

Mills, M. M., Ridame, C., Davey, M., La Roche, J., & Geider, R. J. (2004). Iron and phosphorus co-limit nitrogen fixation in the eastern tropical North Atlantic. Nature, 429(6989), 292–294. http://doi.org/10.1038/nature03632

Miyajima, T., Yamada, Y., Hanaba, Y. T., Yoshii, K., Koitabashi, K., & Wada, E. (1995). Determining the stable isotope ratio of total dissolved inorganic carbon in lake water by GC/C/IRMS. Limnology and Oceanography, 40(5), 994–1000. Retrieved from http://cat.inist.fr/?aModele=afficheN&cpsidt=3661524

Mohr, W., Großkopf, T., Wallace, D. W. R., & LaRoche, J. (2010). Methodological underestimation of oceanic nitrogen fixation rates. PLoS ONE, 5(9), 1–7. http://doi.org/10.1371/journal.pone.0012583

Montoya, J. P., Voss, M., & Capone, D. G. (2007). Spatial variation in N_2-fixation rate and diazotroph activity in the Tropical Atlantic. Biogeosciences, 4(3), 369–376. http://doi.org/10.5194/bg-4-369-2007

Moore, C. M., Mills, M. M., Achterberg, E. P., Geider, R. J., LaRoche, J., Lucas, M. I., McDonagh, E. L., Pan, X., Poulton, A. J,.Rijkenberg, M. J. A., Suggett, D. J., Ussher, S. J., & Woodward, E. M. S. (2009). Large-scale distribution of Atlantic nitrogen fixation controlled by iron availability. Nature Geoscience, 2(12), 867–871. http://doi.org/10.1038/ngeo667

Moore, R. M., Kienast, M., Fraser, M., Cullen, J. J., Deutsch, C., Dutkiewicz, S., … Somes, C. J. (2014). Extensive hydrogen supersaturations in the western South Atlantic Ocean suggest substantial underestimation of nitrogen fixation. Journal of Geophysical Research: Oceans, 119, 4340–4350. http://doi.org/10.1002/2014JC010017.Received

Mouriño-Carballido, B., Graña, R., Fernàndez, A., Bode, A., Varela, M., Domínguez, J. F., Follows, M. J., & Marañón, E. (2011). Importance of N_2 fixation vs. nitrate eddy diffusion along a latitudinal transect in the Atlantic Ocean. Limnology and Oceanography, 56(3), 999–1007. http://doi.org/10.4319/lo.2011.56.3.0999

Nagel, B., Emeis, K.-C., Flohr, A., Rixen, T., Schlarbaum, T., Mohrholz, V., & van der Plas, A. (2013). N-cycling and balancing of the N-deficit generated in the oxygen minimum zone over the Namibian shelf-An isotope-based approach. Journal of Geophysical Research: Biogeosciences, 118(1), 361–371. http://doi.org/10.1002/jgrg.20040

Noble, A. E., Lamborg, C. H., Ohnemus, D. C., Lam, P. J., Goepfert, T. J., Measures, C. I., Frame, C. H., Casciotti, K. L., DiTullio, G. R., Jennings, J, &Saito, M. A. (2012). Basin-scale inputs of cobalt, iron, and manganese from the Benguela-Angola front to the South Atlantic Ocean. Limnology and Oceanography, 57(4), 989–1010. http://doi.org/10.4319/lo.2012.57.4.0989

Orcutt, K. M., Lipschultz, F., Gundersen, K., Arimoto, R., Michaels, A. F., Knap, A. H., & Gallon, J. R. (2001). A seasonal study of the significance of N_2 fixation by *Trichodesmium spp.* at the Bermuda Atlantic Time-series Study (BATS) site. Deep-Sea Research Part II: Topical Studies in Oceanography, 48(8-9), 1583–1608. http://doi.org/10.1016/S0967-0645(00)00157-0

Painter, S. C., Patey, M. D., Forryan, A., & Torres-Valdes, S. (2013). Evaluating the balance between vertical diffusive nitrate supply and nitrogen fixation with reference to nitrate uptake in the eastern subtropical North Atlantic Ocean. Journal of Geophysical Research: Oceans, 118(10), 5732–5749. http://doi.org/10.1002/jgrc.20416

Poulton, A. J., Holligan, P. M., Hickman, A., Kim, Y. N., Adey, T. R., Stinchcombe, M. C., Holeton, C., Root, S., & Woodward, E. M. S. (2006). Phytoplankton carbon fixation, chlorophyll-biomass and diagnostic pigments in the Atlantic Ocean. Deep-Sea Research Part II: Topical Studies in Oceanography, 53(14-16), 1593–1610. http://doi.org/10.1016/j.dsr2.2006.05.007

Pradhan, Y., Lavender, S. J., Hardman-Mountford, N. J., & Aiken, J. (2006). Seasonal and inter-annual variability of chlorophyll-a concentration in the Mauritanian upwelling: Observation of an anomalous event during 1998-1999. Deep-Sea Research Part II: Topical Studies in Oceanography, 53(14-16), 1548–1559. http://doi.org/10.1016/j.dsr2.2006.05.016

Rees, A. P., Owens, N. J. P., Heath, M. R., Plummer, D. H., & Bellerby, R. S. (1995). Seasonal nitrogen assimilation and carbon fixation in a fjordic sea loch. Journal of Plankton Research, 17, 1307–1324. http://doi.org/10.1093/plankt/17.6.1307

Rees, A., Gilbert, J., & Kelly-Gerreyn, B. (2009). Nitrogen fixation in the western English Channel (NE Atlantic Ocean). Marine Ecology Progress Series, 374(1979), 7–12. http://doi.org/10.3354/meps07771

Rijkenberg, M. J. A., Langlois, R. J., Mills, M. M., Patey, M. D., Hill, P. G., Nielsdóttir, M. C., Compton, T. J., LaRoche, J., & Achterberg, E. P. (2011). Environmental forcing of nitrogen fixation in the Eastern Tropical and Sub-Tropical North Atlantic Ocean. PLoS ONE, 6(12). http://doi.org/10.1371/journal.pone.0028989

Rohardt, G., & Wisotzki, A. (2013). Physical oceanography during POLARSTERN cruise ANT-XXIX/1. Alfred Wegener Institute, Helmholtz Center for Polar and Marine Research, Bremerhaven, http:// doi.pangaea.de/10.1594/PANGAEA.817254

Rosman, K. J. R., & Taylor, P. D. P. (1998). Isotopic compositions of the elements 1997 (Commission on atomic weights and isotopic abundances * Technical Report). Pure and Applied Chemistry, 70(1), 217–235.

Sarmiento, J. L., Gruber, N., Brzezinski, M. a, & Dunne, J. P. (2004). High-latitude controls of thermocline nutrients and low latitude biological productivity. Nature, 427(6969), 56–60. http://doi.org/10.1038/nature10605

Schlosser, C., Klar, J. K., Wake, B. D., Snow, J. T., Honey, D. J., Woodward, E. M. S., Lohan, M. C., Achterberg, E. P., & Moore, C. M. (2014). Seasonal ITCZ migration dynamically controls the location of the (sub)tropical Atlantic biogeochemical divide. Proceedings of the National Academy of Sciences of the United States of America, 111(4), 1438–1442. http://doi.org/10.1073/pnas.1318670111

Shannon, L.V. (1985). The Benguela Ecosystem Part I. Evolution of the Benguela, physical features and processes. Oceanogr. Mar. Biol. Ann. Rev., 23, 105–182.

Shannon, L.V., & Nelson, G. (1996). The Benguela: large scale features and processes and system variability. In: The South Atlantic: Present and Past Circulation, Wefer, G., Berger, W.H., Siedler, G. and D.J. Webb (Eds), Berlin Heidelberg: Springer-Verlag, 163–210.

Sigman, D. M., Casciotti, K. L., Andreani, M., Barford, C., Galanter, M., & Böhlke, J. K. (2001). A bacterial method for the nitrogen isotopic analysis of nitrate in seawater and freshwater. Analytical Chemistry, 73(17), 4145–4153. http://doi.org/10.1021/ac010088e

Slawyk, G., Coste, B., Collos, Y., & Rodier, M. (1997). Isotopic and enzymatic analyses of planktonic nitrogen utilisation in the vicinity of Cape Sines (Portugal) during weak upwelling activity. Deep-Sea Research Part I: Oceanographic Research Papers, 44(1), 1–25. http://doi.org/10.1016/S0967-0637(96)00103-3

Snow, J. T., Schlosser, C., Woodward, E. M. S., Mills, M. M., Achterberg, E. P., Mahaffey, C., Bibby, T. S., & Moore, C. M. (2015). Environmental controls on the biogeography of diazotrophy and *Trichodesmium* in the Atlantic Ocean. Global Biogeochemical Cycles, 29, 865–884. http://doi.org/10.1002/2013GB004679.Received

Sohm, J. A., Webb, E. A., & Capone, D. G. (2011a). Emerging patterns of marine nitrogen fixation. Nature Reviews. Microbiology, 9(7), 499–508. http://doi.org/10.1038/nrmicro2594

Sohm, J. A., Hilton, J. A., Noble, A. E., Zehr, J. P., Saito, M. A., & Webb, E. A. (2011b). Nitrogen fixation in the South Atlantic Gyre and the Benguela Upwelling System. Geophysical Research Letters, 38(16), 1–6. http://doi.org/10.1029/2011GL048315

Staal, M., Lintel Hekkert, S. T., Brummer, G. J., Veldhuis, M., Sikkens, C., Persijn, S., & Stal, L. J. (2007). Nitrogen fixation along a north – south transect in the eastern Atlantic Ocean. Limnology and Oceanography, 52(4), 1305–1316.

Straub, M., Sigman, D. M., Ren, H., Martínez-García, A., Meckler, a N., Hain, M. P., & Haug, G. H. (2013). Changes in North Atlantic nitrogen fixation controlled by ocean circulation. Nature, 501(7466), 200–3. http://doi.org/10.1038/nature12397

Subramaniam, A., Yager, P. L., Carpenter, E. J., Mahaffey, C., Björkman, K., Cooley, S., Kustka, A. B., Montoya, J. P., Sañudo-Wilhelmy, S. A., Shipe, R., & Capone, D. G. (2008). Amazon River enhances diazotrophy and carbon sequestration in the tropical North Atlantic Ocean. Global Biogeochemical Cycles, 105, 10460–10465. http://doi.org/10.1029/2006GB002751

Subramaniam, A., Mahaffey, C., Johns, W., & Mahowald, N. (2013). Equatorial upwelling enhances nitrogen fixation in the Atlantic Ocean. Geophysical Research Letters, 40(9), 1766–1771. http://doi.org/10.1002/grl.50250

Turk, K. A., Rees, A. P., Zehr, J. P., Pereira, N., Swift, P., Shelley, R., Lohan, M., Woodward, E. M. S., & Gilbert, J. (2011). Nitrogen fixation and nitrogenase (nifH) expression in tropical waters of the eastern North Atlantic. The ISME Journal, 5(7), 1201–1212. http://doi.org/10.1038/ismej.2010.205

Tyrrell, T., Marañón, E., Poulton, A. J., Bowie, A. R., Harbour, D. S., & Woodward, E. M. S. (2003). Large-scale latitudinal distribution of *Trichodesmium spp.* in the Atlantic Ocean. Journal of Plankton Research, 25(4), 405–416. http://doi.org/10.1093/plankt/25.4.405

Verstraete, J.-M. (1992). The seasonal upwellings in the Gulf of Guinea. Progress in Oceanography, 29(1), 1–60. http://doi.org/10.1016/0079-6611(92)90002-H

Voss, M., Croot, P., Lochte, K., Mills, M., & Peeken, I. (2004). Patterns of nitrogen fixation along 10°N in the tropical Atlantic. Geophysical Research Letters, 31(23), 1–4. http://doi.org/10.1029/2004GL020127

Zhang, L., Altabet, M. A., Wu, T., & Hadas, O. (2007). Sensitive Measurement of NH_4^+ $^{15}N/^{14}N$ ($\delta^{15}NH_4^+$) at Natural Abundance Levels in Fresh and Saltwaters, 79(14), 5589–5595.

CHAPTER IV

Role of Copepod Communities in Carbon Budgets in the Eastern Atlantic Ocean – Regional and Vertical Patterns from 24°N to 21°S

Bode M, Hagen W, Koppelmann R, Cornils A, Teuber L, Kaiser P and Auel H

Submitted to Deep-Sea Research I in December 2015

Role of copepod communities in carbon budgets in the eastern Atlantic Ocean – Regional and vertical patterns from 24°N to 21°S

Maya Bode, Wilhelm Hagen, Rolf Koppelmann, Astrid Cornils, Lena Teuber,

Patricia Kaiser and Holger Auel

Abstract

Pelagic copepods play a key role in marine food webs as they transfer energy from lower to higher trophic level and are responsible for a substantial amount of organic matter cycling and flux. Vertical distribution and community structure of copepods were studied in nine separate depth layers down to 2000 m at six stations along a transect between 24°N and 21°S in the eastern Atlantic Ocean. The copepods' role in mediating vertical carbon flux in each layer was assessed. Usually, abundance and biomass was highest in the upper 100 m, exponentially decreasing with increasing depth, while species diversity was higher in the meso- and bathypelagic zones. Although there were certain differences in species composition between tropical and subtropical stations from north to south, depth had the strongest impact on the community structure of calanoids. In total, copepod community consumption varied between 202 to >604 mg C m^{-2} d^{-1}, with highest ingestion rates in the tropical North Atlantic. At each station, 75-90% of the particulate organic carbon (POC) ingested by copepods was consumed by calanoids. However, the relative contribution of cyclopoids (mostly Oncaeidae) increased with increasing depth. The total net loss rate of POC varied from 106-379 mg C m^{-2} d^{-1} for calanoids and 37-51 mg C m^{-2} d^{-1} for cyclopoids, corresponding to 16-58% and 5-9%, respectively, of surface primary production (PP). In total, 9-33% and 2-5% of PP were respired as inorganic carbon by calanoids and cyclopoids, respectively. Copepod ingestion and thus grazing impact was highly variable between stations and depth layers especially in the epi- and upper mesopelagic zone, while diel vertical migrants enhanced vertical flux to deeper layers. This effect was clearly evident in the Benguela Current influenced region, reflected by high biomass of *Pleuromamma* in the upper mesopelagic zone. The impact of copepod communities on incoming POC fluxes decreased below 1000 m and POC resources reaching the bathypelagic zone were far from being fully exploited by copepods. As key components, copepods are important mediators of carbon flux in the ocean. Their biomass, community composition and interactions strongly

affect the magnitude of organic carbon recycled or exported to deeper layers. High variability even at smaller vertical scales, emphasizes the complicated dynamics of marine ecosystem functioning.

Keywords: community structure; abundance; respiration; ingestion; grazing impact; deep sea; carbon flux

Introduction

Copepods comprise the majority of mesozooplankton communities in all marine regions. In tropical oceanic waters of the eastern Atlantic, copepods prevailed with 86-92% of total zooplankton abundance (Champalbert et al. 2005). Thus, they play a key role in marine food webs and for the cycling of organic and inorganic matter, i.e. for the energy flow from lower to higher trophic levels, in regenerating nutrients, and by enhancing downward fluxes of organic matter (Ketchum 1962; Longhurst and Harrison 1989). Especially under oligotrophic conditions, phytoplankton growth depends to a large extent on the grazing impact of micro- and mesozooplankton (top-down) and on the rate of nutrient regeneration by zooplankton (bottom up) via excretion, fecal pellet production and release of dissolved organic matter as e.g. by 'sloppy feeding' (Banse 1995; Wiggert et al 2005). In fact, more than 40% of the nutrient demands of phytoplankton can be contributed by zooplankton excretion to nutrient regeneration in oligotrophic open oceans (Frangoulis et al. 2005). The fraction of phytoplankton carbon leaving the euphotic zone may vary between 33-70%, depending on the trophic behavior and structure of the zooplankton community (Wassmann 1998).

Tropical zooplankton communities are characterized by high species richness and complex trophic networks (Woodd-Walker 2001; Woodd-Walker et al. 2002; Piontkovski et al. 2003; Schnack-Schiel et al. 2010). However, most previous studies were restricted to the upper 200-300 m working with a low taxonomic resolution (zooplankton size classes instead of species, e.g. Huskin et al. 2001; Isla et al. 2004; San Martin et al. 2006; Calbet et al. 2009). In order to reliably model mechanisms of ecosystem functioning in the pelagic realm, it is a prerequisite to understand the dynamics of community structures and their various key species, their feeding pressure and productivity (Wassmann 1998).

Due to strong vertical stratification and thus limited nutrient supply from below the thermocline, primary production rates in the North and South Atlantic subtropical gyres are generally low

with 18 to 362 mg C m^{-2} d^{-1} compared to 500-1000 mg C m^{-2} d^{-1} in upwelling regions (Longhurst et al. 1995; Marañón et al. 2000). Global photosynthetic carbon fixation by marine phytoplankton is estimated to yield around 45 Gt C a^{-1}, of which 16 Gt C a^{-1} are exported to the ocean's interior (Falkowski et al. 1998). Due to its enormous regional expanse, around 80% of this production occurs in the open ocean and 70% of the total export is contributed by oligotrophic oceanic regions (Martin et al. 1987; Platt et al. 1989; Karl et al. 1996). The Atlantic trade wind biome alone produces about 4.6 Gt C a^{-1} (Longhurst et al. 1995), while the contribution of the tropical zone to pelagic global carbon fixation in total exceeds that of the North Atlantic open ocean spring bloom (Longhurst 1993).

Fluxes of particulate organic matter depend on physical, biological and gravitational processes (Ducklow et al. 2001). On its way through the water column, most of the carbon is modified by deep-living organisms into new dissolved or particulate matter (Ducklow et al. 2001). Thus, it is not necessarily removed from the ocean-atmosphere system by incorporation into the sea-floor sediment. Once organic carbon sinks beneath the thermocline, it is effectively sequestered from the atmosphere for decades to several centuries (Bender and Heggie 1984). Changes in zooplankton biomass and community structure may significantly affect the efficiency of the biological carbon pump and thus the export of organic material to the deep ocean (Ducklow et al. 2001). Recent studies in the Sargasso Sea revealed that a decade-long increase of POC flux in the lower epipelagic zone was partly caused by increases in epipelagic mesozooplankton biomass accompanied by increases in fecal pellet export and migratory fluxes (Steinberg et al. 2012). Thus, it is of utmost importance to understand key mechanisms connecting surface-water production to particle export to the deep ocean (Armstrong et al. 2002; Buesseler et al. 2007).

On a global scale, 34-63% of carbon produced by global primary production is consumed by epipelagic mesozooplankton communities (Hernández-Léon and Ikeda 2005). Lower estimates were reported from oligotrophic regions, where 21-50% of primary production was ingested (Lenz et al. 1993; Dam et al. 1995; Hernández-Léon et al. 1999, 2001; Calbet 2001). In these regions, 59-75% of primary production was grazed by microzooplankton, which is then channeled to higher trophic levels (Calbet and Landry 2004). More than one third of organic carbon flux in the ocean appears to be channeled through mesozooplankton, which are responsible for the respiratory loss of 17-32% of photosynthetic carbon produced in the open ocean (41-77 Gt C y^{-1}; Hernández-Léon and Ikeda 2005). These estimates clearly identify

mesozooplankton as an integral, but often neglected, part of the carbon cycle in the world's ocean (Hernández-Léon and Ikeda 2005).

The pelagic deep sea is largely under-represented in global datasets (Webb et al. 2010) and knowledge about diversity and function below the euphotic zone is still very fragmentary (Robinson et al. 2010). However, its enormous storage capacity for carbon (approx. 38,000 Gt C, 93% of total carbon stored in the oceans) makes this zone very important in balancing the global carbon flow (Koppelmann and Frost 2008). While the mesopelagic or so-called "twilight zone" (200-1000 m) is still influenced by strong gradients in environmental factors, chemical and physical parameters are rather stable in the bathypelagic zone below 1000 (Koppelmann and Frost 2008; Robinson et al. 2010). Around 90% of organic matter resulting from the euphotic zone is remineralized as it sinks through the twilight zone (Koppelmann and Frost 2008). Nevertheless, changes in primary production and particle fluxes in the upper layers usually propagate down to bathypelagic zones with time lags of several weeks to months (Voss et al. 1996; Holmes et al. 2002). The mechanisms and remineralization processes that determine how organic matter is exported from the euphotic zone to the deep sea remain poorly understood, as they are difficult to observe and characterize (Laws et al. 2000). Only a few studies exist on seasonal and regional differences of mesozooplankton community structure impacting carbon flux in the deep sea, e.g. in the Northeast Pacific and Atlantic, the eastern Mediterranean and Arabian Sea (Sasaki et al. 1988; Yamaguchi et al. 2002; Koppelmann and Frost 2008; Homma et al. 2011).

The present study provides detailed insights into the distribution and community structure of copepods at six stations along a latitudinal transect in the eastern Atlantic Ocean from 24°N to 21°S from surface down to 2000 m. Minimal food requirements of copepods were estimated from respiration rates, with a special focus on calanoid copepod species to estimate their role in the cycling of organic matter and evaluate the relationship between copepod biomass and community structure to particle flux in the deep eastern open Atlantic Ocean.

Materials and Methods

Sampling

Zooplankton was collected during the research cruise ANTXXIX/1 on board of RV *Polarstern* along a transect in the eastern Atlantic Ocean from 37° 49'N to 20° 59'S in October/November

2012. Sampling was carried out during daylight between 8:00 and 12:00 a.m. local time by vertical hauls with a HydroBios Multinet Maxi (0.5 m^2 mouth opening) equipped with nine nets of 150 µm mesh size. The volume of seawater filtered was measured with a flow-meter attached to the net frame (hauling speed 0.5 m s^{-1}). Mesozooplankton was sampled from discrete depth layers at six stations from 2000-1500-1000-700-400-300-200-100-50-0 m (Fig. 1). Due to technical problems onboard, net samples are missing from 50-100 m at stn. 8 and 300-400 m at stn. 14, while the depth layers at stn. 17 deviate slightly from the other stations as 2000-1500-1000-700-500-400-200-100-50-0 m was sampled. The samples were preserved in a 4% borax-buffered formaldehyde and seawater solution. Profiles of temperature, salinity and oxygen concentration were obtained at each station with a conductivity temperature depth (CTD) sensor attached to a rosette water sampler (Fig. 2, Rohardt and Wisotzki 2013). Surface primary production was measured at each station (see details in Fonseca-Batista et al., subm.).

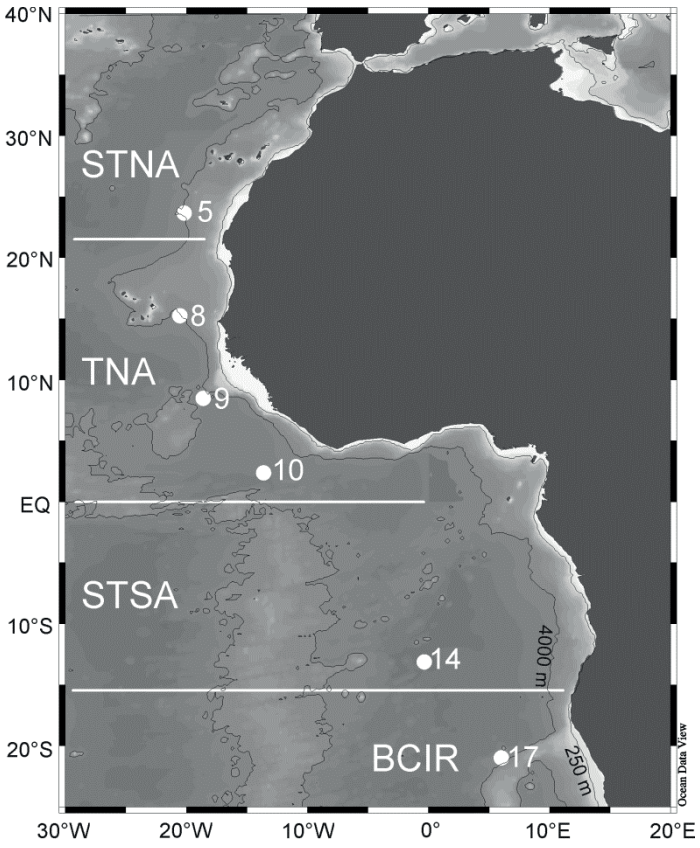

Figure 1: Station map showing all deep stations (0-2000 m) during ANT-XXIX/1 of RV *Polarstern* in October/November 2012. The 250 m and 4000 m bathymetry lines are indicated as black lines. Hydrographic provinces were identified based on oceanographic data (Fig. 2). STNA: Subtropical North Atlantic, TNA: Tropical North Atlantic, STSA: Subtropical South Atlantic, BCIR: Benguela Current Influenced Region.

Abundance analysis

Mesozooplankton samples were transferred into a sorting fluid consisting of 0.5% propylene-phenoxetol, 5% propylene glycol and 94.5% fresh water (Steedman 1976) and split into subsamples (1/2 to 1/32) using a Motoda plankton splitter. Rare species (< 100 individuals per sample) were counted from the entire sample. Calanoid copepods were counted and identified to genus level or, if possible, to species level under a dissecting microscope. The animals were separated into adult females, adult males and copepodids (CI-CV). Cyclopoid copepods were identified to either family or genus level. Species diversity H' was calculated according to Shannon (1948):

$$H' = -\Sigma p_i \ln(p_i)$$

where p_i is the proportion of the *i*th ranked species in the calanoid community in each sampling layer. Multidimensional scaling (MDS) plots were created using the Primer software based on the Bray-Curtis similarity matrix of the log(x+1) transformed abundance data (Primer v6; Clarke and Gorley 2006). Similarities between depth layers were statistically tested for significance using a one-way analysis of similarities test (ANOSIM). Similarity percentages (SIMPER) analysis was conducted to analyze similarities within and between depth-layer specific groups more closely and to identify the contribution of each species/genus to observed similarities or dissimilarities between samples.

Respiration

Calanoid copepods used for onboard respiration experiments were identified to species and stage under a dissecting microscope immediately after each haul. Only apparently healthy individuals were selected. Oxygen consumption was measured by optode respirometry using a 10-Channel Fiber-Optic Oxygen Meter (OXY-10, PreSens, Precision Sensing GmbH) under simulated *in situ* temperatures (see Köster et al. 2008; Bode et al. 2013). Copepods were transferred into gas-tight glass bottles containing 13 ml of UV-treated, 0.2 µm filtered and oxygenated seawater. Usually, one or two individuals were used per bottle. In case of smaller body size, such as copepodite stages of *Rhincalanus cornutus* or *Calanoides carinatus*, 3-6 individuals were incubated together. In each experimental run, two bottles without copepods were monitored as animal-free controls to correct for unspecific microbial respiration. At least three replicates were measured for each species and stage. The bottles were connected to

oxygen minisensors and kept in a water bath in a temperature-controlled refrigerator. After each experiment, copepods were frozen at -80°C for subsequent determination of dry mass using a Sartorius microbalance (Sartorius, NCII1S, precision ± 10 µg) after lyophilization for 48 h (Auel et al. 2005). Respiration rates of deep- and shallow-living copepods were standardized to a temperature of 15°C and to a standard body dry mass of 0.7 mg ind^{-1} assuming a Q_{10} value of 2 and a scaling coefficient of 0.76 (Ikeda et al. 2001, 2006) to allow for physiological comparisons. To test for intra-specific differences unpaired t-tests were performed using the GraphPadPrism software package 5.0.

Community respiration

To assess the energy demand of the total calanoid copepod community, respiration rates of species, whose respiration rates were not measured directly onboard, were calculated from dry mass and water temperature at the respective depth of occurrence. Metabolic rates are strongly correlated with body mass, habitat temperature and the general activity level (Ikeda et al. 2001; Bode et al. 2013). Species- and/or genera-specific dry mass data were calculated from median total length (TL) for adult females, adult males and copepodids (Chisholm and Roff 1990; Homma et al. 2011).

$$\text{Ln DM} = 2.74 \times \text{Ln TL} - 16.41$$

A regression model was applied after Bode et al. (2013) based on dry mass, habitat temperature and activity level. Equations were fitted to our data by adding measured respiration rates and dry mass values. Respiration rates were calculated separately for slow-moving (species of the copepod family Eucalanidae) and fast-moving (all other) copepods (see details in Bode et al. 2013). The following equations were applied, where R is the individual respiration rate for a) slow- (R_s) and b) fast-moving (R_f) copepods, DM represents copepod dry mass in mg and T temperature at mid sampling depth in °C:

a) $\text{Ln } R_s \text{ (µL } O_2 \text{ ind}^{-1} \text{ h}^{-1}) = -2.18 + 0.787 \ln(\text{DM}) + 0.131 \text{ T } (r^2 = 0.71)$

b) $\text{Ln } R_f \text{ (µL } O_2 \text{ ind}^{-1} \text{ h}^{-1}) = -0.890 + 0.646 \ln(\text{DM}) + 0.094 \text{ T } (r^2 = 0.53)$

Because corresponding data compilations of respiration rates for cyclopoid copepods are still lacking, we applied a global respiration model from Ikeda et al. (2001) to estimate the metabolic rates of *Oithona* and Oncaeidae:

$$\text{Ln } R_c \text{ (µL } O_2 \text{ ind}^{-1} \text{ h}^{-1}) = -0.399 + 0.801 \ln(\text{DM}) + 0.069 \text{ T}$$

Carbon budget

Respiration rates (R=µL O_2 ind^{-1} d^{-1}) of copepod species were converted to carbon units (µg C ind^{-1} d^{-1}) assuming that 1 ml O_2 equals 0.44 mg of organic carbon assuming a respiration quotient (RQ) of 0.82 for a mixed diet (Winberg 1956; Gnaiger 1983). Ingestion (I) and egestion (E) rates (µg C ind^{-1} d^{-1}) were estimated according to Ikeda and Motoda (1978) assuming an average digestive efficiency of 70% (U=0.7) and gross growth efficiency of 30% (K_1=0.3) in marine zooplankton, regardless of species and food availability:

$$\text{I} = (\text{R x C x RQ}) \text{ x } \frac{1}{\text{U} - \text{K}_1}$$

$$\text{E} = (1 - 0.7) \text{ x I}$$

where C equals carbon mass per mole (12 g C/22.4 L). I and E were calculated on a daily basis and converted to total community requirement of copepods at each station and depth interval. Diapausing copepodids CV of *C. carinatus* were excluded from ingestion estimates, as they were inactive and rely on their internal lipid reserves.

The particulate organic carbon (POC) flux to each sampling layer was calculated using surface primary production values for each station applying the equation published by Suess (1980):

$$C_{flux} = C_{prod}/(0.0238 \text{ Z} + 0.212)$$

where C_{flux} is the POC flux (mg C m^{-2} d^{-1}) at depth Z, C_{prod} is the primary production (mg C m^{-2} d^{-1}) and Z is the water depth (≥ 50 m).

To quantify the role of copepod ingestion and egestion in the vertical carbon flux, a box model similar to that of Sasaki et al. (1988) and Yamaguchi et al. (2002) was applied. The following relationships were assumed:

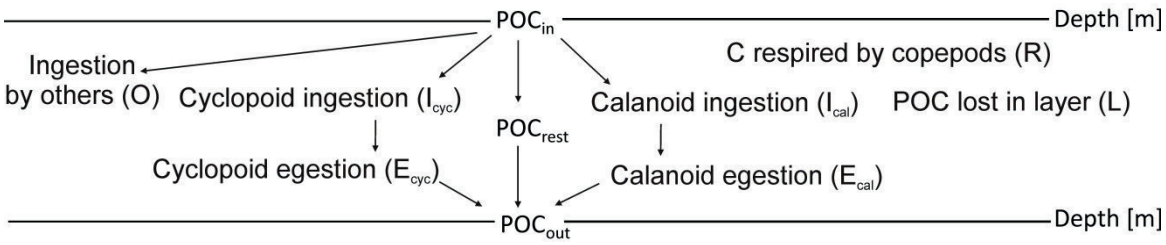

1) Incoming POC (POC_{in}) is the available POC by primary production (measured) for the top layer or the sedimented POC for lower layers estimated according to the equation by Suess (1980). 2) The amount of organic carbon lost within a depth layer ($L = POC_{in} - POC_{out}$) is either consumed by calanoid copepods (I_{cal} derived from respiration measurements), cyclopoid copepods (I_{cyc} estimated after Ikeda et al. 2001), or is available for others inhabiting this depth layer either by direct consumption or after disaggregation as suspended POC ($O = L – I_{cal} - I_{cyc} + E_{cal} + E_{cyc}$). 3) The assimilation efficiency of copepods (70%) was assumed to be constant throughout the water column and 4) the carbon egested by copepods ($E = 0.3 \times I$) within a layer potentially contributes to the outgoing POC (POC_{out}) into the depth layer below. 5) Residual POC ($POC_{rest} = POC_{out} – E$) may be aggregating POC not ingested, thus directly sinking, or POC egested by other consumers inhabiting the respective depth layer. 6) The carbon respired by copepods (R) is lost as inorganic carbon in the respective depth layer.

Results

Hydrography and primary production

The six stations were located in different hydrographical provinces of the eastern Atlantic Ocean, and accordingly, differed in their oceanographic conditions (Figs. 1, 2). Temperature, salinity and oxygen profiles are shown for each station in Fig. 2 (data derived from Rohardt and Wisotzki 2013). Station 5 (23.7°N) was located in the subtropical North Atlantic (STNA) with high sea surface salinity (SSS) of 36.6 and high sea surface temperature (SST) of 25°C. The 20°C isotherm reached deep down to 100 m. According to the fluorescence signal chlorophyll *a* (chl *a*) concentration was low, and primary production was lowest (445 mg C m^{-2} d^{-1}) compared to the other stations (for details see Fonseca-Batista et al., in prep.). Oxygen concentrations were always >60 O_2 µmol L^{-1}. Below 800 m stn. 5 was influenced by Mediterranean Outflow Water, characterized by temperatures of 4-8°C and elevated salinities between 35.1 and 35.2.

Stations 8, 9 and 10 (15°N - 2°N) were situated in the tropical North Atlantic (TNA). These stations were characterized by the highest SST ranging from 27°C at stn. 10 to 29° C at stn. 9 and relatively low SSS of 35.6 (stns. 8 and 10) and 35.0 (stn. 9). Chl *a* concentration was slightly higher than at stn. 5, while primary production was relatively high with 650 mg C m^{-2} d^{-1} at stn. 8, 563 mg C m^{-2} d^{-1} at stn. 9, and 907 mg C m^{-2} d^{-1} at stn. 10. An extensive oxygen minimum zone (OMZ, < 60 µmol O_2 L^{-1}) occurred between 60 m and 750 m at stn. 8 (min. 14 µmol O_2 L^{-1} at 400

m). The OMZ at stn. 9 was narrower, between 250 m and 600 m (min. 13 µmol O_2 L^{-1} at 400 m), and very thin at stn. 10 between 240 m and 290 m (min. 30 µmol O_2 L^{-1} at 250 m). Down to 500 m, South Atlantic Central Water (SACW) was detected throughout stns. 8 to 17. A tongue of Antarctic Intermediate Water (AIW) was observed approx. between 600 and 1200 m from stns. 9 to 17. Below 1200 m North Atlantic Deep Water (NADW) was evident. At stn. 8 only NADW but no AIW was identified.

Station 14 (14°S) was located in the subtropical South Atlantic (STSA) in direct vicinity of the Angola Gyre with lower SST (21°C) but higher SSS of 36.5 compared to the TNA. The intermediate chl *a* maximum was located between 50 and 100 m, while primary production was moderately high with 665 mg C m^{-2} d^{-1}.

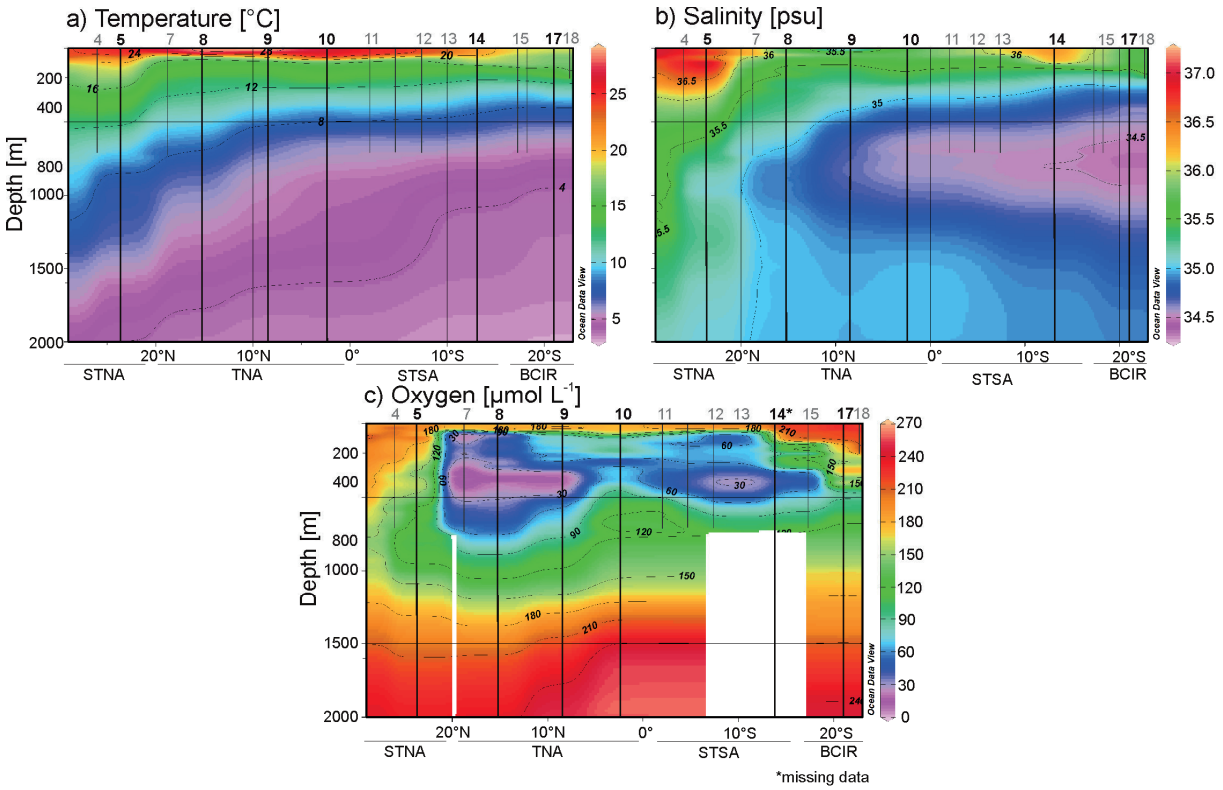

Figure 2: a) Temperature, b) salinity and c) oxygen concentration along the cruise track during ANT-XXIX/1 (Rohardt and Wisotzki 2013). The lines and numbers above represent respective stations where CTD sampling was conducted to either 800 m or 2000 m. Copepod community structure was analyzed at all deep stations with max. sampling depth of 2000 m (bold black, see Fig. 1). For stn. 14 oxygen data were not available (created with Ocean Data View 4 using *DIVA gridding* as gridding method, Schlitzer 2013). STNA = Subtropical North Atlantic, TNA = Tropical North Atlantic, STSA = Subtropical South Atlantic, BCIR = Benguela Current Influenced Region.

Station 17 (21°S) was situated in the Benguela Current influenced region (BCIR), thus, characterized by relatively cold SST (18.5°C) and low SSS (35.6). There was only weak stratification by temperature or salinity down to 150 m depth. The dominant water mass was oxygen-rich Eastern SACW (ESACW) (max. 20% SACW at 160 m). No OMZ was detected. Presumably due to nutrient input from recently upwelled waters, chl *a* concentrations were highest in this region, as was primary production with 930 mg C m^{-2} d^{-1}.

Abundance and biomass

Copepod biomass was generally highest in the euphotic zone (Fig. 3). In the upper 100 m, copepod biomass ranged from 1.7 mg DM m^{-3} between 50-100 m at stn. 5 to 22.5 mg DM m^{-3} in the surface layer of stn. 8, while biomass below 1000 m did not exceed 0.4 mg DM m^{-3}. At stns. 10 and 14, maximum copepod biomass was found between 50-100 m (12.4 mg DM $m^{-3}$and 6.9 mg DM m^{-3}, resp.). A second, less pronounced peak was often observed between 200-400 m. In contrast, at stns. 5 and 17, copepod biomass reached maxima between 100-200 m (4.1 mg DM m^{-3}) and 200-400 m (8.6 mg DM m^{-3}), respectively. In terms of biomass, calanoids dominated on average with 77-80% total copepod biomass in all depth zones (mean 78%).

Both, abundance and biomass generally decreased exponentially with increasing depth. Linear regression analyses of logarithmically (ln) transformed total copepod biomass and abundance gave significant slopes (-0.002 and -0.003, resp., p-values < 0.0001; r^2 = 0.83 and 0.86, resp.). In the upper 100 m, total copepod abundance was highest ranging from 371 ind m^{-3} at stn. 14 to 1348 ind m^{-3} at stn. 8 in the upper 50 m, and decreasing with increasing depth to 1.6 ind m^{-3} at stn. 17 or 12.1 ind m^{-3} at stn. 9 below 1500 m. In the upper 100 m, calanoid copepods usually outnumbered cyclopoid copepods with a minimum dominance of 55% at stn. 17 and maximum dominance of 88% at stn. 5. Abundance of calanoid copepods in the upper 50 m ranged from 254 ind. m^{-3} at stn 14 to 933 ind m^{-3} at stn 8, and decreased to minimum values of 1-3 ind. m^{-3} below 1500 m (Fig. 3, Table A). *Oithona* was usually the most abundant cyclopoid copepod in the upper 100 m ranging from 52 ind. m^{-3} at stn. 5 to 466 ind. m^{-3} at stn. 17. Exceptions were stns. 8 and 10, where Oncaeidae prevailed over *Oithona* in all depth layers with maximum abundances of 269 and 177 ind m^{-3}, respectively (Fig. 3, Table A).

Below the euphotic zone, cyclopoid copepods generally prevailed in terms of numbers (57-88% of total copepod abundance) and Oncaeidae usually dominated the cyclopoid population at

these depths. In the TNA, Oncaeidae exhibited a bimodal abundance distribution, where a surface peak of 130-269 ind m^{-3} was observed. A second peak, either as high or lower, occurred between 200-400 m. In contrast, in the STNA, STSA and BCIR only one deeper abundance maximum was observed between 100-300 m. Maximum abundances of Oncaeidae reached 276 ind m^{-3} between 200-300 m at stn. 8, while numbers generally decreased below 400 m with depth to a minimum value of 0.9 ind m^{-3} below 1500 m at stn. 17 (Fig. 3, Table A).

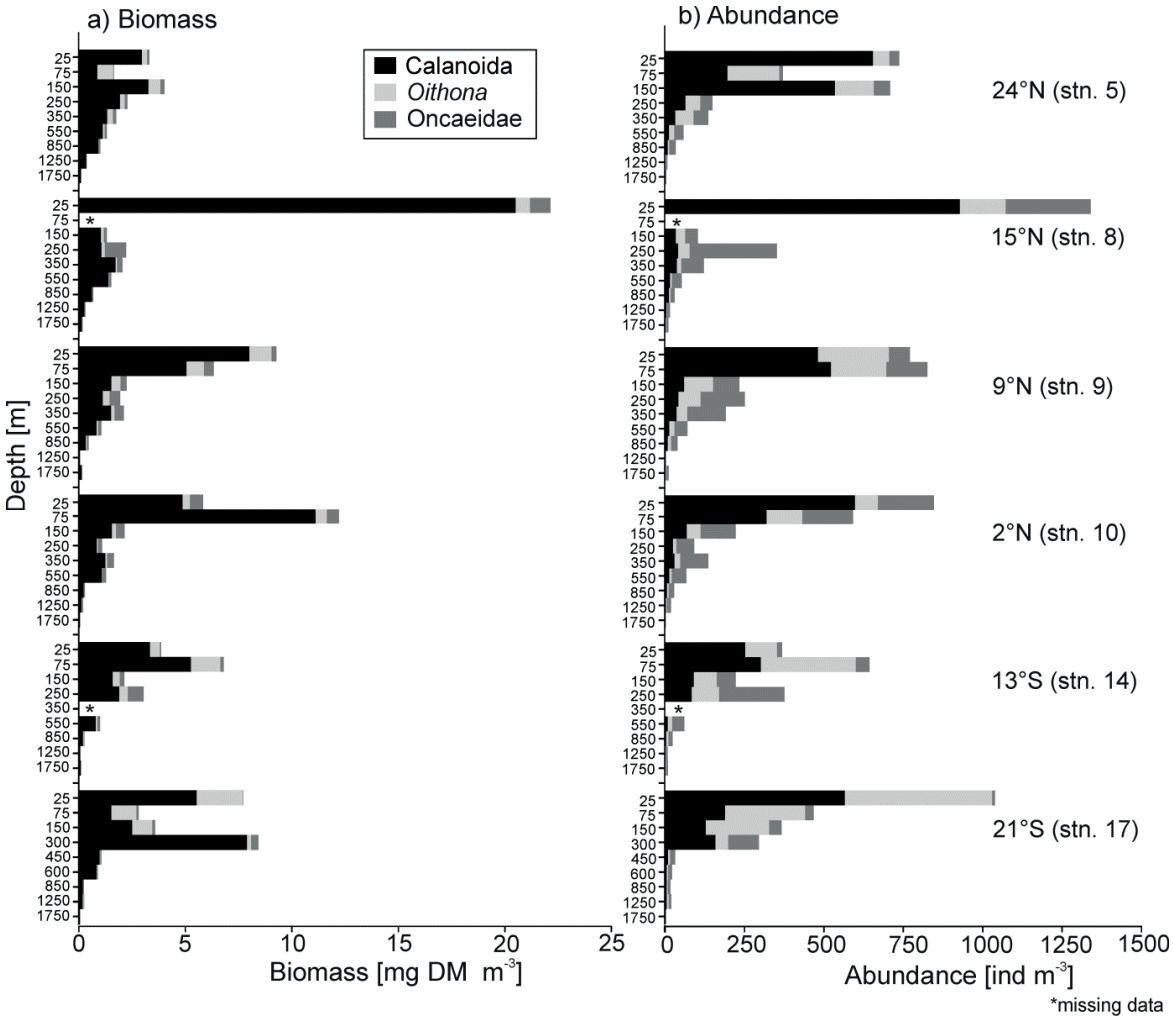

Figure 3: Vertical distribution of a) biomass (mg DM m^{-3}) and b) abundance (ind m^{-3}) of calanoid (black) and cyclopoid (*Oithona*: light grey, Oncaeidae: dark grey) copepods at each station (Fig. 1).

Diversity

Among calanoid copepods, 26 families, 79 genera and at least 172 species were identified (Table A). In general, the number of genera and species increased with increasing depth (Fig. 4). The TNA differed from the subtropical and BCIR stations. At the northern (stn. 5) and southernmost

stations (stns. 14 and 17), diversity was highest in the mesopelagic zone between 400-700 m (H' ≥2.9, max. 3.2 at stn. 17). In the TNA, maximum species diversity occurred shallower between 100-200 m (H'=2.8-2.9), while at stn. 9 a similar species diversity (H'=2.9) was determined between 300-700 m. In general, diversity slightly decreased again below these depths, but remained much higher than in the epipelagic zone (Fig. 4).

Within the euphotic zone, diversity increased towards the equator, while the most northerly and southerly stations 5 and 17 showed lowest Shannon indices in the euphotic zone (1.0-1.5) compared to the tropical stations (0.9-2.9) (Fig. 4). The low H' value of 0.9 was found in the upper 50 m at stn. 10, but below 50 m H' was similar to the other TNA stns. 8 and 9 (2.3 and 2.9).

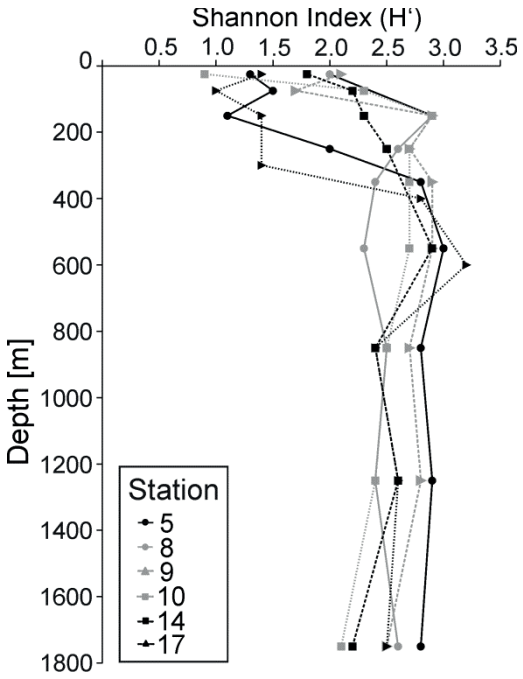

Figure 4: Vertical distribution of Shannon diversity (H') for each station indicated at mid-sampling depth based on abundance of calanoid species.

Community structure of calanoid copepods

Total abundance and community structure integrated over the whole 0-2000 m water column was very similar between stations (71-82%). In general, depth rather than station location was more important in determining community structure and distributional patterns of calanoid copepods (Fig. 5). Based on depth layer-specific species abundance and community structure, the water column could be divided into an upper (0-50-100 m, one-way ANOSIM, factor depth layer, R-value=0.14, significance level= 2%) and lower (100-200 m) epipelagic, an upper (200-

300-400 m, R-value=0.12, significance level=12%) and lower (400-700-1000 m, R-value=0.38, significance level=0.2%) mesopelagic zone, and a bathypelagic zone (1000-1500-2000 m, R-value=0.00, significance level=46%) (Fig. 5a). Divided into these depth zones, community structures were significantly different from each other with R-values generally ≥ 0.69 (one-way ANOSIM, factor depth zone, significance level=0.1%).

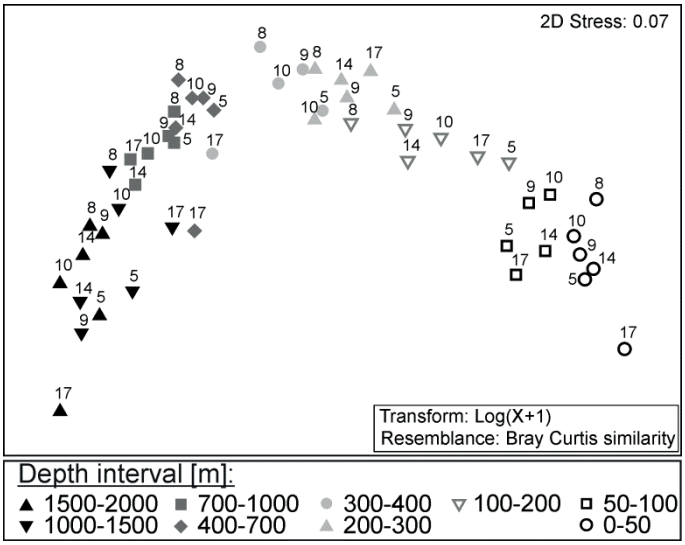

Figure 5: MDS analysis based on Bray-Curtis similarity indices of transformed abundances of calanoid species at each depth layer. Numbers next to the symbols indicate the respective station.

Epipelagic Zone (0-200 m)

In terms of total calanoid biomass (TCB), *Clausocalanus* (max. 68% TCB, 0-50 m, stn. 10), *Acartia* (max. 44% TCB, 0-50 m, stn. 17)*, Euchaeta* (max. 51% TCB, 50-100 m, stn. 10)*, Neocalanus* (max. 32% TCB, 50-100 m, stn. 14) and *Nannocalanus minor* (max. 26% TCB, 0-50 m, stn. 14) were usually the major taxa in the upper epipelagic zone. At stn. 8, *Undinula vulgaris* contributed 16% to TCB (0-50 m), while at stn. 17 *Mecynocera clausi* and *Eucalanus hyalinus* comprised 13-16% and 7-10% of TCB, respectively (Fig. 6a). The lower epipelagic zone was generally dominated by *Clausocalanus* (max. 26% TCB, stn. 5)*, Haloptilus* (max. 19% TCB, stn. 14)*, Heterorhabdus* (max. 17% TCB, stn. 8) and *Pleuromamma* (max. 59% TCB, stn. 17). In terms of biomass, *Delibus* was only important at stn. 5, contributing 14% to TCB.

Clausocalanus, Delibus and *Calocalanus* were generally the most abundant genera in the euphotic zone. They occurred with highest densities in the upper 50 m: *Clausocalanus* with a maximum density of 541 ind m^{-3} at station 8, and *Delibus* with a maximum of 405 ind m^{-3} at stn.

5, while *Calocalanus* showed highest numbers of 105 ind m^{-3} at stn. 17 (Table A, appendix). At stn. 17, *Acartia* and *Mecynocera clausi* were found in exceptionally high numbers in the upper 50 m (262 ind m^{-3} and 149 ind m^{-3}, resp.), while *Pleuromamma* occurred with very high densities of 84 ind m^{-3} between 100-200 m. Various genera reached their maximum abundances in the upper 50 m layer of stn. 8, i.e. *Nannocalanus minor* (79 ind m^{-3}), *Acrocalanus* (48 ind m^{-3}), *Temora stylifera* (46 ind m^{-3}), *Undinula vulgaris* (23 ind m^{-3}) and *Subeucalanus* (16 ind m^{-3}). At stn. 10, *Euchaeta* and *Ctenocalanus* cf. *vanus* reached maximum abundances of 38 ind m^{-3} and 19 ind m^{-3}, respectively, while *Paracalanus* exhibited highest numbers of 36 ind m^{-3}at stn. 14 between 50-100 m.

Station 5 in the STNA was quite different from the other stations in the epipelagic zone with dominance of *Delibus* cf. *nudus* ranging from 59 to 73% of total calanoid abundance (TCA) (Fig. 6b). Portions of *Clausocalanus* varied from 16% TCA at 100-200 m to 22% TCA at 0-50 m, while *Calocalanus* was most abundant (14% TCA) at 50-100 m and *Acartia* was only present in the upper 100 m (2-10% TCA). In contrast, the tropical North Atlantic stations were dominated by *Clausocalanus* with 47-76% TCA in the upper 50 m. Between 50-100 m, *Delibus* cf. *nudus* was most abundant at stn. 9 (45% TCA) and *Calocalanus* at stn. 10 (27% TCA). Further south at stn. 14 in the STSA, *Clausocalanus* prevailed down to 200 m contributing 40% TCA (Fig. 6b). The most southerly stn. 17 in the BCIR was distinct from all other stations. The upper 50 m layer differed from the water layers below with highest concentrations of *Acartia* (46% TCA), *M. clausi* (26% TCA) and *Calocalanus* (19% TCA). In contrast, the 50-100 m layer was dominated by *Clausocalanus* (76% TCA), while in the lower epipelagic zone *Pleuromamma* prevailed with 64% TCA, and *Clausocalanus* decreased to 24% TCA (Fig. 6).

Mesopelagic Zone (200-1000 m)

In terms of biomass, *Pleuromamma* (max. 85% TCB, stn. 17, 200-400 m), *Subeucalanus* (max. 51% TCB, stn. 8, 300-400 m), *Eucalanus hyalinus* (max. 48% TCB, stn. 5, 700-1000 m), *Euaugaptilus* (max. 35% TCB, stn. 10, 400-700 m), *Spinocalanus* (max. 26%, TCB stn. 14, 200-300 m), *Haloptilus* (max. 21% TCB, stn. 5, 200-300 m), *Metridia* (max. 19%, TCB stn. 14, 700-1000 m) and *Rhincalanus* (max. 12% TCB, stn 8, 400-700 m) generally accounted for the majority of TCB in the mesopelagic zone (Fig. 6a). At stn. 5 *Clausocalanus* prevailed down to 200-300 m (28% TCB),

while *C. carinatus* (35% TCB) and *Megacalanus princeps* (35% TCB) dominated in the lower mesopelagic zone at stns. 8 and 14, respectively (Fig. 6a).

In general, *Microcalanus* and *Spinocalanus* were the most abundant genera below the euphotic zone contributing at least 20% to TCA in one depth layer per station (mean 19 and 16% TCA, resp., Fig. 6b). Highest densities were found at stn. 14 between 200-300 m with 24 ind m^{-3} of *Microcalanus* and 19 ind m^{-3} of *Spinocalanus*. Only at stn. 5, *Microcalanus* was almost absent, instead *Clausocalanus* prevailed with 32 ind m^{-3} between 200-300 m (49% TCA), which was unusually deep for this genus. *Subeucalanus* occurred with a maximum of 13 ind m^{-3} between 300-400 m at stn. 8, while *Pleuromamma* was found in exceptionally high abundances at stn. 17 (max. 109 ind m^{-3}, 200-400 m).

The lower mesopelagic zone especially was dominated by *Spinocalanus* with usually 25-35% TCA. At stn. 8, copepodids CV of *C. carinatus* prevailed with 28% TCA between 700-1000 m, while the water layers above (300-700 m) were dominated by *Subeucalanus* with 35-46% TCA. Station 17 was characterized by maximum portions of *Pleuromamma* (68% TCA) in the upper mesopelagic, and *Microcalanus* (34% TCA) in the lower mesopelagic zone. Other abundant genera were *Metridia, Temoropia, Scaphocalanus* and *Scolecithricella* (max. 10-20% TCA). *Metridia* contributed most to TCA at stn. 17 (17% TCA) and stn. 14 (13% TCA) between 400-700 m, while *Temoropia* represented a maximum of 12% TCA at stn. 8 between 300-400 m (Fig. 6b).

Bathypelagic Zone (1000-2000 m)

In terms of biomass, *Rhincalanus* (max. 34% TCB, stn. 8, 2000-1500 m), *Euaugaptilus* (max. 29% TCB, stn. 17, 1500-1000 m), *Spinocalanus* (max. 25% TCB, stn. 10, 1500-1000 m), *Pareucalanus* (max. 23% TCB stn. 10, 1500-1000 m), *Metridia* (max. 21% TCB, stn. 17, 2000-1500 m) and *Lucicutia* (max. 21% TCB, stn. 10, 2000-1500 m) were usually dominant in the bathypelagic zone (Fig. 6a). Occasionally, other species occurred with higher biomass proportions, such as *Eucalanus hyalinus* (max. 41% TCB, 1000-1500 m) at stn. 5, *C. carinatus* copepodids CV (36% TCB, 1000-1500 m) at stn. 8, *Hemirhabdus* (19% TCB) and Aetideidae CI-III (12% TCB) between 1500-2000 m at stn. 9, *Haloptilus* (13% TCB, 1000-1500 m) and *Mospicalanus* (12% TCB, 1500-2000 m) at stn. 14, *Pleuromamma* (10% TCB, 1000-1500 m) and *Scaphocalanus* (11% TCB, 1500-2000 m) at stn. 17 (Fig. 6a).

Similar to the mesopelagic zone, *Spinocalanus* and *Microcalanus* were the most numerous genera below 1000 m, however with much lower abundances of usually < 1 ind m^{-3}. Maxima

were found between 1000-1500 m with 3 ind m^{-3} of *Spinocalanus* (stn. 10) and 1.1 ind m^{-3} of *Microcalanus* (stn. 17). In general, the calanoid community was composed of 16-43% TCA *Spinocalanus* and 8-16% TCA *Microcalanus*. Exceptions were stn. 8, where copepodids CV of *C. carinatus* occurred at highest densities of 1.6 ind m^{-3} (30% TCA) between 1000-1500 m, and stn. 5, where *Microcalanus* was almost absent. At stn. 17, *Clausocalanus* was caught unusually deep at 1000-1500 m reaching 15% TCA. Furthermore, Aetideidae CI-III*, Lucicutia, Subeucalanus, Temoropia* and *Disco* were usually abundant at such great depths (max. 10-15% TCA), whereas *Mospicalanus* occurred with higher proportions of 16% TCA only at stn. 14 (1500-2000 m).

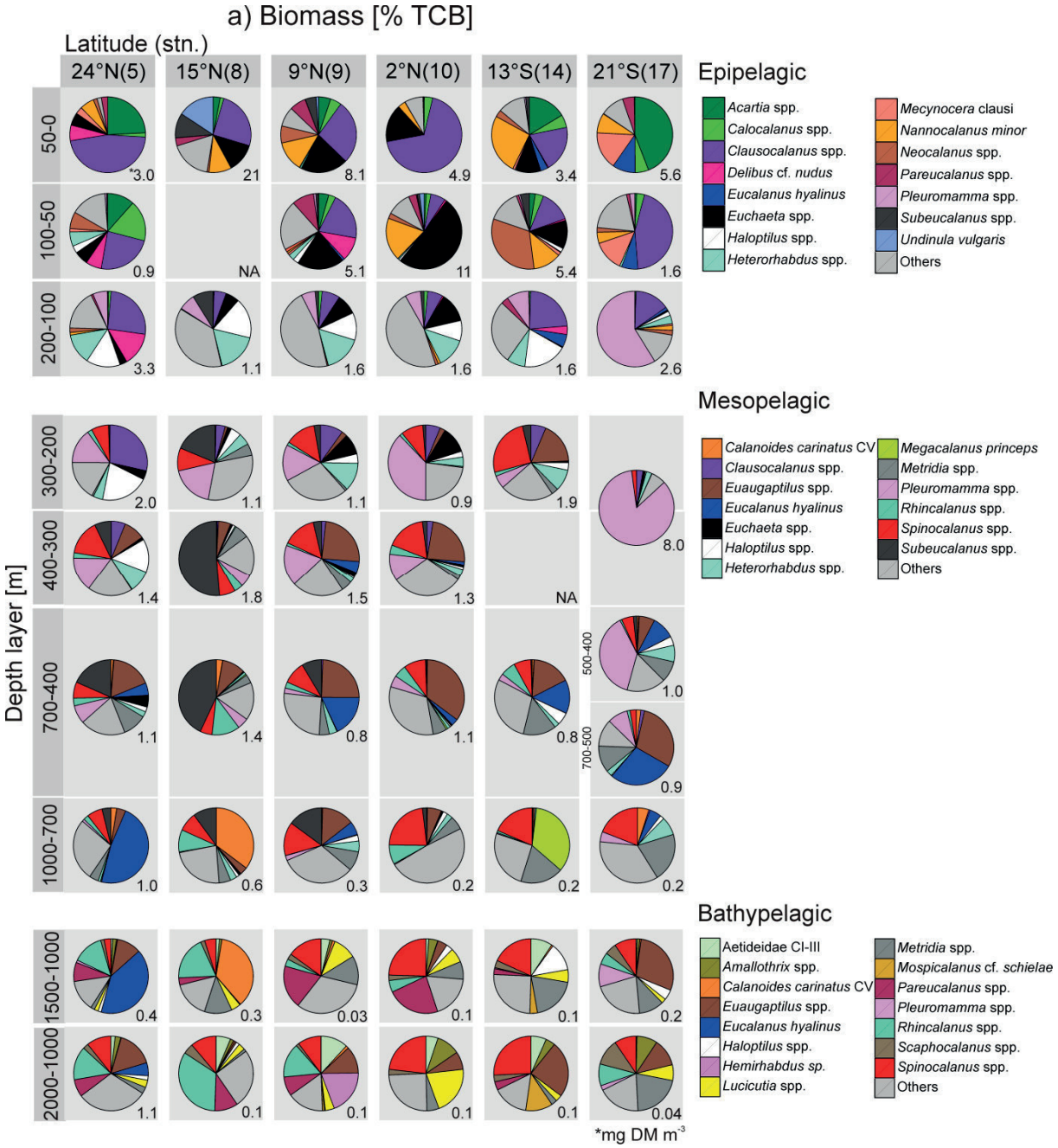
a) Biomass [% TCB]
Latitude (stn.)
24°N(5)
15°N(8)
9°N(9)
2°N(10)
13°S(14)
21°S(17)
Depth layer [m]
50-0
100-50
200-100
300-200
400-300
700-400
1000-700
1500-1000
2000-1000
500-400
700-500
*3.0
21
8.1
4.9
3.4
5.6
0.9
NA
5.1
11
5.4
1.6
3.3
1.1
1.6
1.6
1.6
2.6
2.0
1.1
1.1
0.9
1.9
8.0
1.4
1.8
1.5
1.3
NA
1.1
1.4
0.8
1.1
0.8
1.0
0.9
1.0
0.6
0.3
0.2
0.2
0.2
0.4
0.3
0.03
0.1
0.1
0.2
1.1
0.1
0.1
0.1
0.1
0.04
*mg DM m-3
Epipelagic
Acartia spp.
Calocalanus spp.
Clausocalanus spp.
Delibus cf. nudus
Eucalanus hyalinus
Euchaeta spp.
Haloptilus spp.
Heterorhabdus spp.
Mecynocera clausi
Nannocalanus minor
Neocalanus spp.
Pareucalanus spp.
Pleuromamma spp.
Subeucalanus spp.
Undinula vulgaris
Others
Mesopelagic
Calanoides carinatus CV
Clausocalanus spp.
Euaugaptilus spp.
Eucalanus hyalinus
Euchaeta spp.
Haloptilus spp.
Heterorhabdus spp.
Megacalanus princeps
Metridia spp.
Pleuromamma spp.
Rhincalanus spp.
Spinocalanus spp.
Subeucalanus spp.
Others
Bathypelagic
Aetideidae CI-III
Amallothrix spp.
Calanoides carinatus CV
Euaugaptilus spp.
Eucalanus hyalinus
Haloptilus spp.
Hemirhabdus sp.
Lucicutia spp.
Metridia spp.
Mospicalanus cf. schielae
Pareucalanus spp.
Pleuromamma spp.
Rhincalanus spp.
Scaphocalanus spp.
Spinocalanus spp.
Others

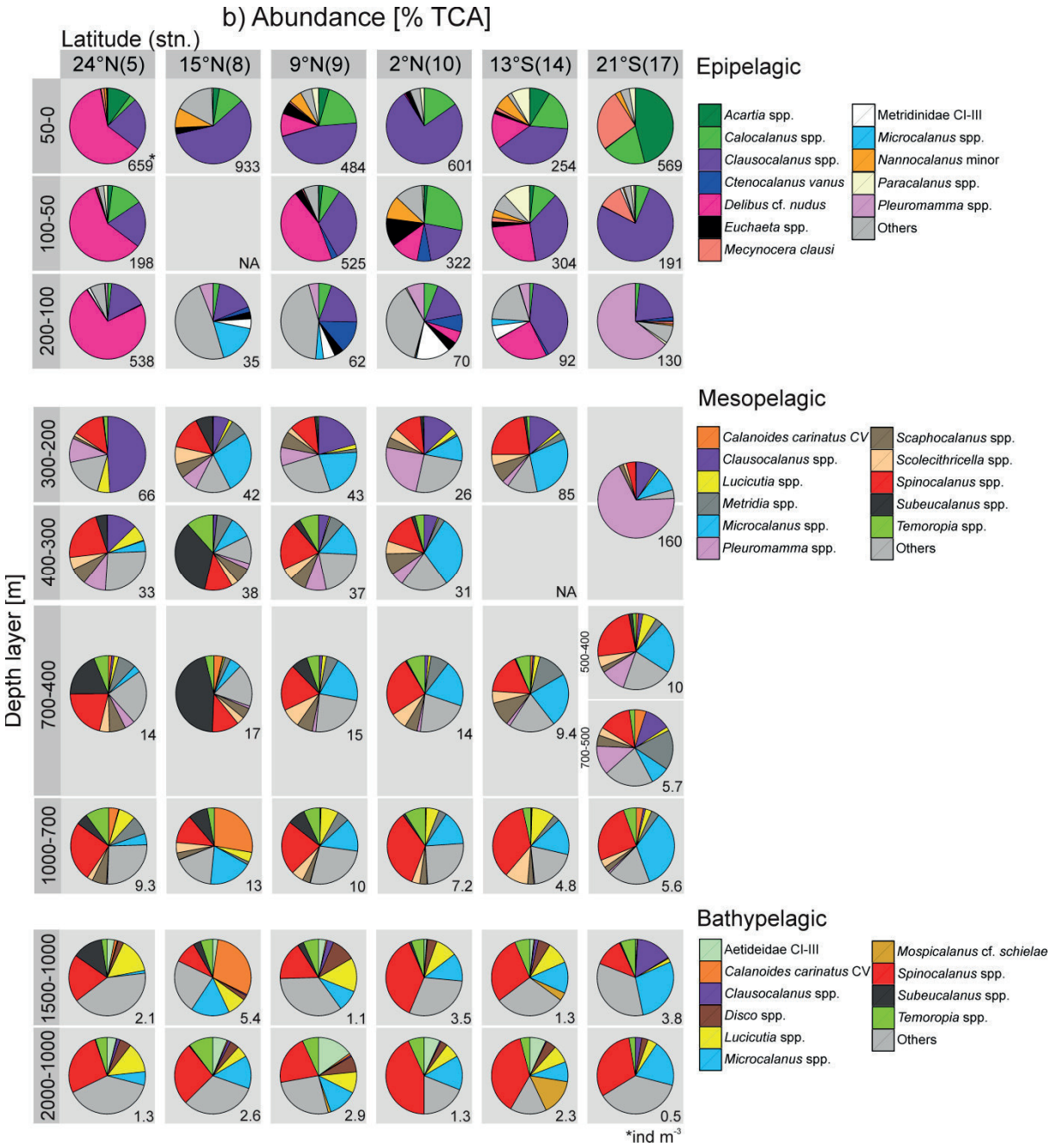

Figure 6: Vertical changes in community composition of calanoid copepods in terms of a) biomass (mg DM m^{-3}) and b) abundance (ind m^{-3}) given as percentages of total calanoid biomass (TCB) and total calanoid abundance (TCA), respectively, in each sampling layer in the epi-, meso- and bathypelagic zones of each station (Fig. 1). Numbers below the pies indicate a) total biomass (mg DM m^{-3}) and b) total abundance (ind m^{-3}) of calanoids at the respective depth layer and station.

Respiration

A total of 202 respiration measurements were conducted with 28 calanoid copepod species (Table 1). Dry mass-specific respiration rates ranged from 0.3 µL O_2 mg dry mass (DM)$^{-1}$ h^{-1} in deep-dwelling females of *Rhincalanus cornutus* and CVs of *Gaetanus brevicornis* and *Pareucalanus* spp. to 16 µL O_2 mg DM^{-1} h^{-1} in epipelagic *Undinula vulgaris* (Table 1). Significant differences in adjusted metabolic rates (AMR, 15°C and 0.7 mg DM) were determined. All eucalanid species, diapausing CVs of *Calanoides carinatus* and females of *Paraeuchaeta aequatorialis* and *Metridia princeps* had lowest mean AMRs between 0.5 and 0.8 µL O_2 mg DM^{-1} h^{-1}. Typical mesopelagic species such as *Scottocalanus securifrons, Chirundina streetsii, Euchirella pulchra, E. splendens, E. curticauda, Gaetanus pileatus, G. krupii,* and *Megacalanus princeps* showed generally low AMRs of 1-2 µL O_2 mg DM^{-1} h^{-1}. Highest mean AMRs of > 4 µL O_2 mg DM^{-1} h^{-1} were measured in epipelagic *U. vulgaris, Candacia pachydactyla, C. ethiopica* and *Euchaeta marina*. Males showed generally lower respiration rates than females ($p = 0.05$ for *C. ethiopica* and *U. vulgaris*). Epipelagic *E. splendens* and *E. marina* exhibited significantly higher AMRs than specimens caught at mesopelagic depths ($p \leq 0.02$). In contrast, mesopelagic *Pleuromamma xiphias* had a slightly, but not significantly increased AMR compared to epipelagic specimens (Table 1).

Individual *in situ* oxygen consumption rates were converted to minimal carbon requirements for each species. Minimum individual carbon demands were 0.7 and 0.9 µg C ind^{-1} d^{-1} for CVs and females of *R. cornutus* and 1.1 µg C ind^{-1} d^{-1} for diapausing CVs of *C. carinatus*. Highest carbon demands of > 20 µg C ind^{-1} d^{-1} were measured in the upper 100 m for E*. splendens, U. vulgaris, C. pachydactyla, E. marina, P. xiphias* and *Neocalanus robustior* (Table 1). *E. splendens* caught in the upper 100 m exhibited a maximum mean daily ingestion rate of 115 µg C ind^{-1} d^{-1}, while females of *U. vulgaris, C. pachydactyla* and *E. marina* from the epipelagic zone ingested on average 70-75 µg C ind^{-1} d^{-1}. Minimum daily ingestion rates of <10 µg C ind^{-1} d^{-1} were measured in deep-dwelling females of *E. pulchra, E. curticauda, Eucalanus hyalinus, Pareucalanus* spp., *Rhincalanus nasutus* and copepodids of *G. pileatus* and *G. brevicornis*, with minima of 1.7 and 2.3 µg C ind^{-1} d^{-1} in CVs and females of *R. cornutus*.

Table 1: Sampling depth, experimental temperature (T), mass-specific respiration rates (R), daily individual R and daily ingestion rates (I) for 28 calanoid species from the eastern tropical and subtropical Atlantic (mean ± SD). AMR is the adjusted metabolic rates to 15°C and 0.7 mg dry mass (DM). f: female, m: male, C: copepodite stage, n: number of replicate measurements.

Species	Stage	n	Depth [m]	T [°C]	DM [mg ind^{-1}]	Mass-specific R [µL O_2 mg DM^{-1} h^{-1}]		Daily R (*in situ*)		Daily I (*in situ*)
						in situ	AMR	µL O_2 ind^{-1} d^{-1}	µg C ind^{-1} d^{-1}	µg C ind^{-1} d^{-1}
Calanidae										
U. vulgaris	f	6	0-50	25	0.18 ± 0.01	16.4 ± 3.4	6.1 ± 1.4	68.7 ± 12.8	30.2 ± 5.6	75.6 ± 14.1
U. vulgaris	m	4	0-50	25	0.12 ± 0.01	12.8 ± 1.8	4.4 ± 0.6	37.3 ± 2.8	16.4 ± 1.2	41 ± 3.1
N. gracilis	f	3	50-100	20	0.56 ± 0.04	2.7 ± 0.8	1.8 ± 0.5	37 ± 12.5	16.3 ± 5.5	40.7 ± 13.8
N. gracilis	CV	4	0-50	27	0.15 ± 0.04	11 ± 3.1	3.3 ± 0.7	37.1 ± 1.1	16.3 ± 0.5	40.8 ± 1.2
N. robustior	f	4	50-100	20	0.47 ± 0.07	2.9 ± 0.1	1.8 ± 0	32.2 ± 4.1	14.2 ± 1.8	35.4 ± 4.5
N. robustior	CV	3	0-50	27	0.23 ± 0.01	8.1 ± 0.7	2.7 ± 0.2	45.1 ± 3.3	19.8 ± 1.5	49.6 ± 3.6
C. carinatus	CV	9	500-700	8.5	0.18 ± 0.06	0.6 ± 0.3	0.7 ± 1.3	2.6 ± 0.9	1.1 ± 0.4	-
Candaciidae										
C. pachydactyla	f	6	50-100	24	0.19 ± 0.01	14 ± 2.8	5.6 ± 1.2	63.9 ± 10.6	28.1 ± 4.7	70.3 ± 11.6
C. ethiopica	f	4	0-200	16	0.16 ± 0.04	7.2 ± 1.1	4.8 ± 0.8	27.9 ± 7.2	12.3 ± 3.2	30.7 ± 7.9
C. ethiopica	m	4	0-200	16	0.14 ± 0.03	4.2 ± 4.2	2.7 ± 1.6	14.2 ± 7.8	6.3 ± 3.4	15.6 ± 15.6
Scolecithrichidae										
S. danae	f	4	0-50	20	0.17 ± 0	4.3 ± 2.1	2.3 ± 1.1	17.9 ± 8.9	7.9 ± 3.9	19.7 ± 9.8
S. danae	m	4	0-50	20	0.15 ± 0.03	4.7 ± 1.7	2.4 ± 0.8	17.1 ± 6	7.5 ± 2.7	18.8 ± 6.7
S.securifrons	f	5	400-700	8.5	0.97 ± 0.13	1.2 ± 0.1	2 ± 0.2	29 ± 6	12.8 ± 2.6	31.9 ± 6.6
Eucalanidae										
E. hyalinus	f	3	400-1000	8	0.66 ± 0.24	0.5 ± 0.1	0.8 ± 0.3	8.2 ± 4.6	3.6 ± 2	9 ± 5.1
Pareucalanus spp.	f	2	0-200	24	0.25/0.15	1.0/2.0	0.4/0.8	5.9/6.8	2.6/3.0	6.5/7.4
Pareucalanus spp.	CV	4	600-700	8	0.88 ± 0.13	0.3 ± 0.1	0.5 ± 0.1	6.5 ± 1.3	2.9 ± 0.6	7.2 ± 1.4
R. cornutus	f		500-800	9	0.22/0.22	0.7/0.4	0.74/0.44	3.4/2.0	1.5/0.9	2.7/1.6
R. cornutus	CV	6	500-800	9	0.12 ± 0.03	0.5 ± 0.3	0.5 ± 0.3	1.6 ± 1.1	0.7 ± 0.5	1.7 ± 1.2
R. cornutus	f	7	1500-2000	4	0.32 ± 0.07	0.3 ± 0.2	0.5 ± 0.3	2.1 ± 1.4	0.9 ± 0.6	2.3 ± 1.5
R. nasutus	f	4	600-700	8	0.56 ± 0.23	0.4 ± 0.1	0.6 ± 0.1	5.4 ± 1.8	2.4 ± 0.8	5.9 ± 2
Metridinidae										
P. abdominalis	f	5	400-700	9	0.28 ± 0.05	1.7 ± 0.5	2.2 ± 0.6	12.4 ± 6.8	5.5 ± 3	13.7 ± 7.4
P. robusta	f	5	0-100	23	0.27 ± 0.02	3.2 ± 0.8	1.6 ± 0.3	20.7 ± 4	9.1 ± 1.8	22.8 ± 4.4
P. xiphias	f	3	50-100	23	0.6 ± 0.27	3 ± 0.9	1.7 ± 0.6	46.7 ± 28.8	20.6 ± 12.7	51.4 ± 31.7
P. xiphias	f	13	400-700	9	0.57 ± 0.18	2 ± 0.8	2.8 ± 1.1	28.4 ± 17.2	12.5 ± 7.6	31.3 ± 19
P. xiphias	m	3	500-700	8	0.73 ± 0.01	0.8 ± 0.3	1.4 ± 0.5	14.8 ± 5.7	6.5 ± 2.5	16.3 ± 6.2
M.princeps	f	4	500-700	7.5	1.41 ± 0.27	0.4 ± 0.1	0.8 ± 0.3	14.7 ± 6.4	6.5 ± 2.8	16.1 ± 7.1
M. princeps	m	3	600-700	8	0.57 ± 0.26	0.8 ± 0.6	1.2 ± 1	12.8 ± 14.7	5.6 ± 6.5	14.1 ± 16.2
Aetideidae										
E. rostrata	f	2	50-100	20	1.35/0.95	3.6/3.5	2.94/2.67	116/80	50.8/34.9	91.0/62.5
E. rostrata	f	2	400-700	7	0.78/0.56	1.1/1.0	2.1/1.49	21/14	9.1/6.1	16.3/10.9
Euchirella sp.	CV	5	50-100	25	0.4 ± 0.16	8.1 ± 1.7	3.5 ± 0.6	74.9 ± 18.1	33 ± 8	82.4 ± 19.9
E. splendens	f	3	50-100	25	0.99 ± 0.14	4.4 ± 0.5	2.4 ± 0.3	104.5 ± 18.3	46 ± 8.1	114.9 ± 20.2
E. splendens	f	5	400-700	8.5	1.42 ± 0.44	0.9 ± 0.2	1.7 ± 0.3	31 ± 6.8	13.7 ± 3	34.1 ± 7.5
E. pulchra	f	6	500-700	6	0.51 ± 0.07	0.9 ± 0.4	1.5 ± 0.5	10.9 ± 3.3	4.8 ± 1.5	12 ± 3.7
E.curticauda	f	3	500-700	7	0.65 ± 0.04	0.6 ± 0.1	1 ± 0.2	9.5 ± 2.2	4.2 ± 1	10.4 ± 2.5
C. streetsii	f	8	500-700	6.5	1.36 ± 0.25	0.9 ± 0.3	1.8 ± 0.6	29.5 ± 10.5	13 ± 4.6	32.5 ± 11.5
G. pileatus	f	2	500-600	7.5	1.4/1.3	1.0/0.6	1.9/1.1	33/19	14/8.3	36/21
G. pileatus	CIII	3	400-500	8	0.29 ± 0.05	0.9 ± 0.3	1.2 ± 0.4	6 ± 1.4	2.7 ± 0.6	6.7 ± 1.5
G. krupii	f	2	500-1000	7.5	0.8/1.4	0.7/0.8	1.1/1.5	12/26	5.3/11	13/28
G.brevicornis	CIII	3	400-700	8.	0.81 ± 0.15	0.3 ± 0.2	0.5 ± 0.3	5.3 ± 2.6	2.3 ± 1.2	5.8 ± 2.9
Euchaetidae										
E. marina	f+eggs	8	50-100	24.	0.12 ± 0.02	13.8 ± 3.1	4.9 ± 1.1	39.8 ± 8.5	17.5 ± 3.8	43.7 ± 9.4
E.marina	f	3	0-200	24	0.28 ± 0.07	9.8 ± 1.3	4.9 ± 1.1	63.7 ± 11.7	28 ± 5.2	70.1 ± 12.9
E.marina	f	3	400-700	8	0.3 ± 0.03	2 ± 0.2	2.6 ± 0.3	14.7 ± 2.1	6.5 ± 0.9	16.2 ± 2.3
P.gracilis	f+eggs	2	400-700	7	2.09/1.97	1.1/1.0	2.42/2.27	55.0/49.2	24.2/21.7	43.3/38.8
P. gracilis	f	7	400-700	9	1.68 ± 0.59	0.9 ± 0.3	1.8 ± 0.5	33.1 ± 9.2	14.6 ± 4.1	36.4 ± 10.1
P.gracilis	CV	7	400-500	8	1.08 ± 0.26	1 ± 0.4	1.6 ± 0.7	22.8 ± 6.6	10 ± 2.9	25.1 ± 7.3
P. aequatorialis	f	4	400-1500	8	1.66 ± 0.27	0.4 ± 0	0.8 ± 0.1	16.8 ± 1.7	7.4 ± 0.7	18.5 ± 1.8
Megacalanidae										
M. princeps	f	2	700-1000	8	5.1/6.0	0.3/0.5	0.8/1.3	38/74	17/32	42/81

Community consumption and carbon budget

Total community consumption of all copepods integrated over the entire 0-2000 m water column varied from 202 mg C m^{-2} d^{-1} at stn. 14 to 604 mg C m^{-2} d^{-1} at stn. 8, potentially ingesting 30-93% of the carbon produced by surface primary production (PP) (Fig. 7). 75-90% of carbon ingested by copepods per station was consumed by calanoids, while the vertical distribution of maximum carbon ingestion was similar between cyclopoids and calanoids. Highest ingestion rates of calanoid communities were found in the TNA (323 to >541 mg C m^{-2} d^{-1}, 45-83% PP), while consumption was intermediate in the BCIR (301 mg C m^{-2} d^{-1}, 32% PP) and lowest in the STNA (266 mg C m^{-2} d^{-1}, 60% PP) and STSA (151 mg C m^{-2} d^{-1}, 23% PP). In general, highest carbon consumption coincided with the biomass maximum of copepods, thus, at stns. 8 and 9 in the upper 50 m, stns. 10 and 14 between 50-100 m and deeper at the northern- and southernmost stns. 5 and 17 between 100-200 m and 200-400 m, respectively. However, the deep maximum at stn. 17 was only valid for calanoid copepods; both, biomass and ingestion maxima of cyclopoids were located in the upper 50 m at this station. Ingestion rates of cyclopoids and calanoids approached each other with increasing depth, so that in the bathypelagic zone 54-73% of carbon consumed by copepods was ingested by calanoids.

Community consumption of cyclopoids and calanoids in the epipelagic zone ranged from 3.9 to 32 mg C m^{-2} d^{-1} and 11 to 490 mg C m^{-2} d^{-1}, respectively (Fig. 7). Both minimum and maximum values occurred at stn. 8 between 100-200 m and 0-50 m, respectively. In the upper mesopelagic zone, calanoid community ingestion showed a clear maximum at stn. 17 with 157 mg C m^{-2} d^{-1} due to extremely high abundance of *Pleuromamma*. The second highest ingestion rate of calanoids in the upper mesopelagic zone was much lower with 31 mg C m^{-2} d^{-1} between 200-300 m at stn. 5, while a minimum value of 8.1 mg C m^{-2} d^{-1} was estimated at stn. 10 (300-400 m). Maximum consumption of cyclopoids in the upper mesopelagic zone was 15 mg C m^{-2} d^{-1} at stn. 8 (200-300 m), which was actually the only location where cyclopoid carbon consumption exceeded calanoid ingestion (10 mg C m^{-2} d^{-1}). In the bathypelagic zone, copepod community ingestion was low, ranging from 0.2-2.3 mg C m^{-2} d^{-1} for cyclopoids and 0.6-3.0 mg C m^{-2} d^{-1} for calanoids (Fig. 7). The contribution of each calanoid copepod genus is shown in detail in Fig. 8.

a) Impact of copepod communities on vertical POC flux

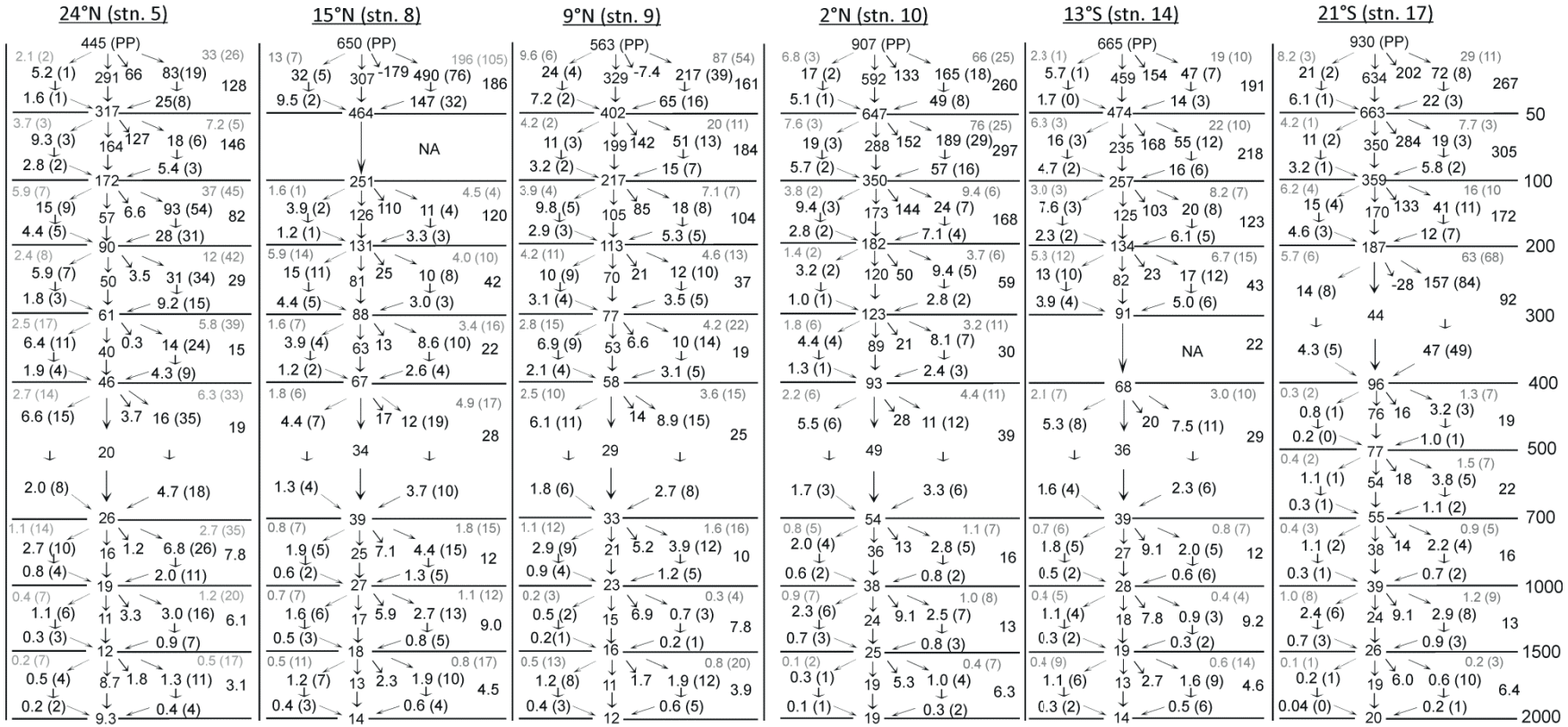

Station totals (%PP)

Cyclopoida	Calanoida	Cyclopoida	Calanoida	Cyclopoida	Calanoida	Cyclopoida	Calanoida	Cyclopoida	Calanoida	Cyclopoida	Calanoida	
53 (12%)	266 (60%)	63 (10%)	541 (83%)	73 (13%)	323 (57%)	63 (7%)	412 (45%)	51 (8%)	151 (23%)	66 (7%)	301 (32%)	BI
37 (8%)	186 (42%)	45 (7%)	378 (58%)	51 (8%)	226 (40%)	44 (5%)	288 (32%)	36 (5%)	106 (16%)	47 (5%)	211 (23%)	NI
21 (5%)	106 (24%)	25 (4%)	217 (33%)	25 (4%)	129 (23%)	21 (2%)	165 (18%)	21 (3%)	60 (9%)	27 (3%)	121 (13%)	R

b) Schematic description:

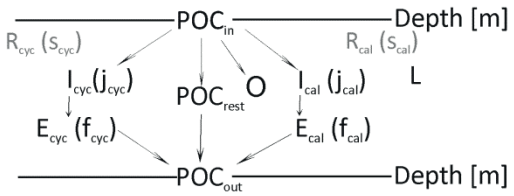

Absolute values [mg C m^{-2} d^{-1}]:

POC_{in}: available POC by primary production (PP, measured) for top layer or sedimentation for lower layers (calculated)

POC_{rest}: residual POC sinking out of layer $POC_{rest} = POC_{out} - E_{cal} - E_{cyc} = POC_{in} - I_{cal} - I_{cyc} - O$

POC_{out}: outgoing POC, calculated after Suess (1980)

L: POC removed in layer (lost) $L = POC_{in} - POC_{out} = O + I_{cal} + I_{cyc} - E_{cal} - E_{cyc}$

R: Respiration rates of calanoids (R_{cal} estimated from measurements) and cyclopoids (R_{cyc} estimated from Ikeda et al. (2001))

I: Ingestion rates of calanoids (I_{cal}) and cyclopoids (I_{cyc}) (based on R after Ikeda and Motoda (1978))

E: Egestion rates of calanoids (E_{cal}) and cyclopoids (E_{cyc})(E = 0.3 x I, Ikeda and Motoda (1978))

O: Consumptions by other consumers $O = POC_{in} - POC_{out} - I_{cal} - I_{cyc} + E_{cal} + E_{cyc}$

Percentages:

j: Relative ingestion of POC_{in} by calanoids (j_{cal}) and cyclopoids (j_{cyc}) ($j = I/POC_{in} \times 100$)

f: Potential contribution of egestion to POC_{out} of calanoids (f_{cal}) and cyclopoids (f_{cyc}) ($f = E/POC_{out} \times 100$)

s: Portion of carbon lost by copepod respiration of calanoids (s_{cal}) and cyclopoids (s_{cyc}) ($s = R/L \times 100$)

Figure 7: a) Box model diagram showing particulate organic carbon flux (mg C m^{-2} d^{-1}) in the 0-2000 m water column via nine depth strata at each station in the eastern tropical and subtropical Atlantic ocean. Downward POC flux was estimated from surface primary production rates based on the equation of Suess (1980). Community ingestion (I) and egestion (E) of cyclopoids and calanoids are shown for each depth layer. The potential impact of ingestion on incoming POC, the potential contribution of egestion to outgoing POC and carbon lost as inorganic carbon by respiration are given as percentages. BI: brutto ingestion, NI: netto ingestion (=I-E), R: Respiration. b) Schematic description and legend of a).

The mass balance between cyclopoid and calanoid copepod ingestion and egestion as well as POC flux is summarized in Fig. 7. According to Suess (1980), around 20% of primary production in the surface layers reaches the upper mesopelagic zone (POC_{in} at 200 m). In layers of maximum community consumption, calanoid copepods consumed 12% (50-100 m, stn. 14) to 84% (200-400 m, stn. 17) of incoming POC (POC_{in}), while cyclopoids consumed only 2% (0-50 m, stn. 17) to 9% POC_{in} (100-200 m, stn. 5). Minimum potential ingestion of POC_{in} by calanoids was found between 400-500 m at stn. 17 and between 1000-1500 m at stns. 9 and 14 with 3% POC_{in} consumed. Since in our model copepod egestion depended on their ingestion, the two parameters followed a similar distributional pattern. Potential contribution of copepod egestion to outgoing POC flux was 0.4-5% for cyclopoids and 2-32% for calanoids in the epipelagic zone, 0.3-8% for cyclopoids and 1-49% for calanoids in the mesopelagic zone, 0.2-3% for cyclopoids

and 1-7% for calanoids in the bathypelagic zone. Below the euphotic zone, 5-68% of the carbon lost within a depth layer was potentially respired as inorganic carbon by calanoid copepods and additionally 1-17% by cyclopoid copepods (Fig. 7).

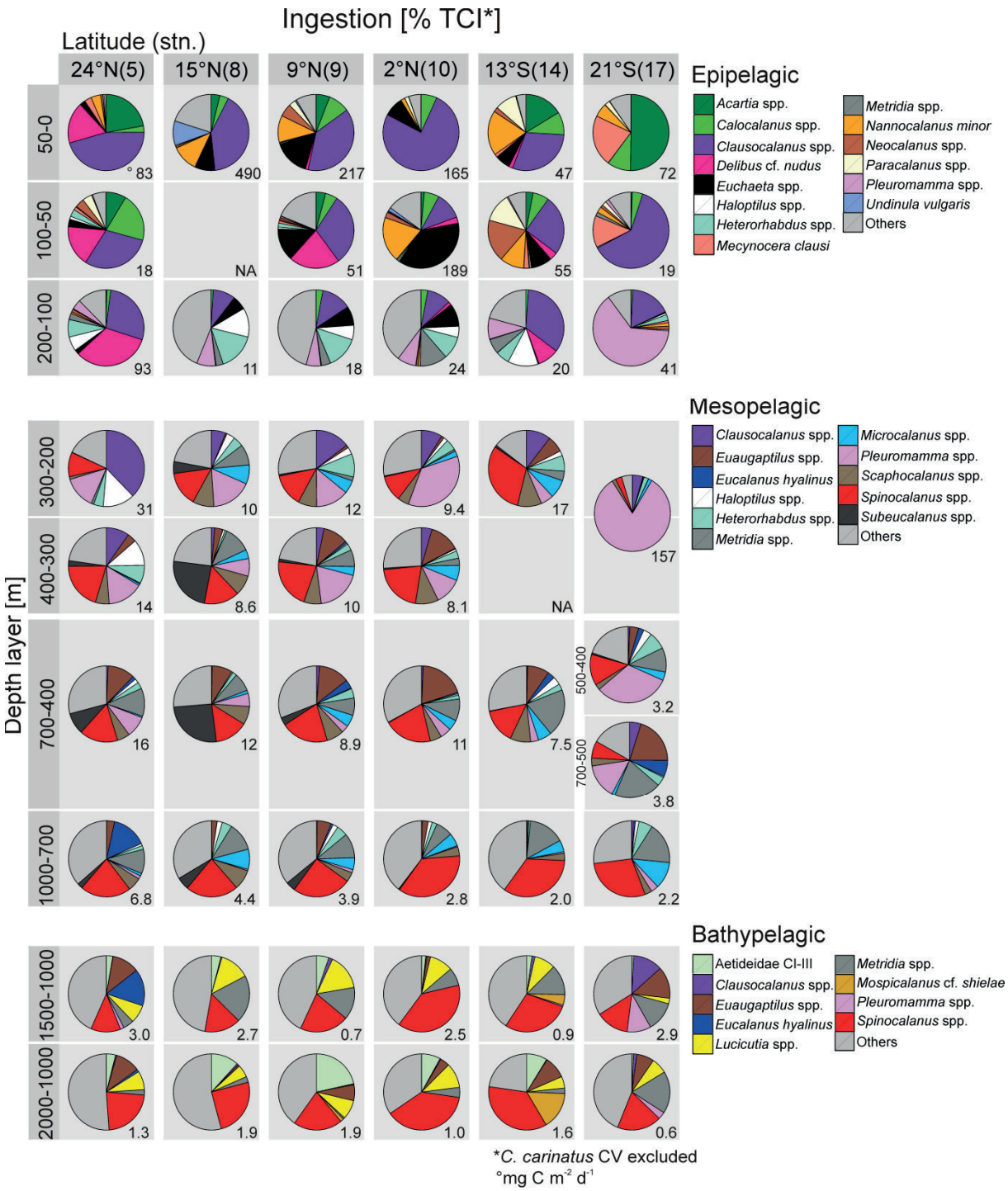

Figure 8: Vertical changes in the contribution of calanoid genera to daily community consumption of calanoid copepods in specific depth layers from epi-, meso- to bathypelagic zones at each station. Numbers below the pies indicate total calanoid ingestion (TCI, mg C m^{-2} d^{-1}) in the respective depth layer.

The total net loss of POC by copepods varied from 142 mg C m^{-2} d^{-1} in the STSA to 423 mg C m^{-2} d^{-1} in the TNA, which is equivalent to 21 and 65% of primary production (Figs. 7 and 9). In the upper 200 m, the net loss rate of POC by calanoids was highest in the TNA with 200-351 mg C m^{-2} d^{-1} (29-54% PP), while lowest estimates were found in the BCIR and STSA with 92 mg C m^{-2} d^{-1} and 86 mg C m^{-2} d^{-1} corresponding to 10% and 13% PP, respectively. In contrast, net loss mediated by cyclopoids was rather low and uniform ranging from 20-33 mg C m^{-2} d^{-1}, i.e. 3-6% PP in the epipelagic and 11-15 mg C m^{-2} d^{-1} (6-17% POC_{in}) in the mesopelagic zone. The net loss by calanoids in the mesopelagic zone was 19-25 mg C m^{-2} d^{-1} in the TNA and STSA (12-22% POC_{in}), 47 mg C m^{-2} d^{-1} in the STNA (53% POC_{in}) and 116 mg C m^{-2} d^{-1} in the BCIR (62% POC_{in}). In the bathypelagic zone, net loss of POC by calanoid ingestion was rather steady varying from 1.8-3.2 mg C m^{-2} d^{-1} (6-16% POC_{in}), while cyclopoids accounted for 1.1-2.0 mg C m^{-2} d^{-1} (5-8% POC_{in}) of the net loss at these depths.

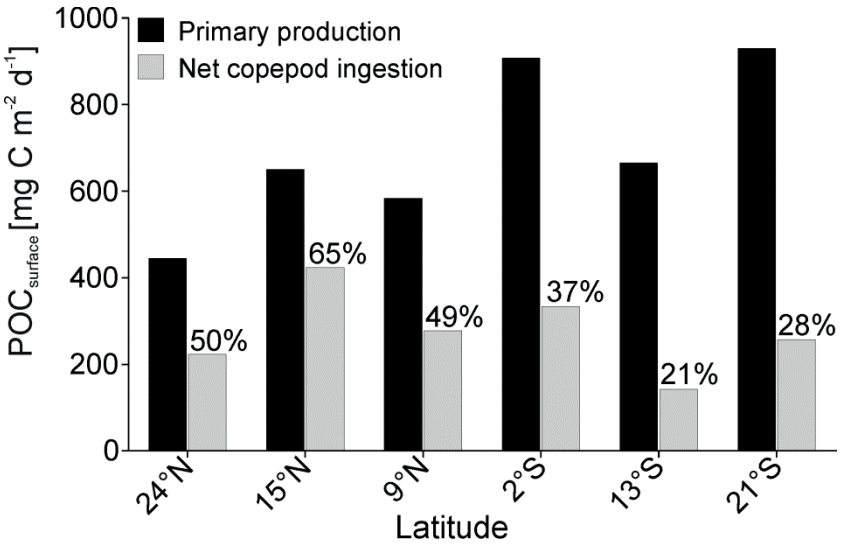

Figure 9: Net loss of POC via copepod ingestion at each station from 0-2000 m. Total net copepod ingestion in relation to primary production are indicated as percentages.

Discussion

The present study provides detailed insights in the vertical distribution and community structure of copepods at six different sites in the tropical and subtropical eastern Atlantic Ocean. Total abundance of copepods calculated for the upper 300 m (348-491 ind m^{-3}) were well within the range of a previous study on a similar latitudinal transect (*Polarstern* cruise ANTXXI/1 in 2002) studying copepod community composition in the upper 300 m applying similar sampling gear

and mesh size (173-842 ind m^{-3}) (Schnack-Schiel et al. 2010). Despite distinct differences between sampling sites, variations in abundance, biomass and species composition were much more affected by depth than by regional differences, which seems to be a common feature of pelagic ecosystems worldwide (Auel and Hagen 2002; Kosobokova et al. 2011).

Community distribution

Total copepod abundance and biomass generally decreased exponentially with increasing depth, which is a common feature of pelagic open ocean environments observed in higher latitudes (Deevey and Brooks 1977; Koppelmann and Weikert 1992; Auel and Hagen 2002; Yamaguchi et al. 2002; Kosobokova et al. 2011). In terms of abundance, the major part (47-66%) of the copepod community inhabited the epipelagic zone, while a smaller portion of 30-47% existed in the mesopelagic zone and only 4-9% of total copepod abundance occurred between 1000-2000 m. Larger fractions of copepod abundance in the epipelagic zone (74-87%) were found in the Arabian Sea (Böttger-Schnack 1996) and North Pacific (Homma et al. 2011 and references therein), while portions in the bathypelagic zone also comprised 4-9%. However, these studies include averages over day and night-time sampling, while sampling in the present study was performed only during daylight. Therefore, we assume that copepod abundance and also biomass were higher during night in the epipelagic zone due to diel vertical migrations.

Calanoids usually dominate the copepod community in terms of biomass in all depth layers (Yamaguchi et al. 2002; Homma et al. 2011; this study). For abundance, this picture is generally different, as calanoids usually dominated the epipelagic zone with a mean of 54% of total copepod abundance and Oncaeidae prevailed below 200 m with a mean of 56% and abundance peaks generally between 200-700 m. This is similar to findings in the North Pacific (Yamaguchi et al. 2002, mesh 90 µm; Homma et al. 2011; mesh 66 µm) and Arabian Sea (Böttger-Schnack 1996, mesh 55 µm) and typical of this taxon usually feeding on suspended or sinking detritus (Steinberg et al. 2008). However, numbers of small cyclopoid copepods as well as early copepodite stages of small calanoid species might still be underestimated in the present study due to the mesh size of 150 µm (Paffenhöfer and Mazzocchi 2003; Homma et al. 2011).

Community structure of calanoid copepods

The generally high similarities between stations are typical of tropical oceans, due to generally unrestricted exchange without physical barriers and thus wide latitudinal distributions of many oceanic species in these regions (Schnack-Schiel et al. 2010). In contrast, vertical gradients are more important in limiting species distribution (Angel 1997; Woodd-Walker et al. 2002; Kosobokova et al. 2011; this study). The calanoid community structure could be divided into three main depth zones: epipelagic (0-200 m), mesopelagic (200-1000 m) and bathypelagic (1000-2000 m). Similar divisions based on copepod community structure were obtained in the Red Sea (Weikert 1982), Arabian Sea (Böttger-Schnack 1996), Mediterranean Sea (Weikert and Trinkaus 1990), North Atlantic (Roe 1972; Deevey and Brooks 1977), Greenland Sea (Richter 1994) and the Arctic (Auel and Hagen 2002; Kosobokova and Hopcropft 2010; Kosobokova et al. 2011). In the western subarctic Pacific, boundaries between these three depth zones were located between 200-500 m and 1500-2000 m (Yamaguchi et al. 2002).

Clausocalanidae (mostly *Clausocalanus*) and Paracalanidae (mostly *Delibus* and *Calocalanus*) numerically dominated the calanoid community of the epipelagic zone, accounting on average for 36% and 33% of calanoid abundance, respectively. This observation agrees well with studies from tropical and subtropical epipelagic waters (Paffenhöfer and Mazzocchi 2003; Schnack-Schiel et al. 2010). In contrast, Clausocalanidae (*Microcalanus*), Spinocalanidae (mostly *Spinocalanus*), Metridinidae (*Pleuromamma* and *Metridia*) and Scolecithrichidae (mostly *Scolecithricella* and *Scaphocalanus*) were numerically dominant in the mesopelagic zone (mean: 23%, 20%, 14% and 12%, resp.). In the bathypelagic zone, Spinocalanidae (mostly *Spinocalanus*) and Clausocalanidae (*Microcalanus*) were dominant families in terms of abundance (mean: 30% and 15%, resp.). The high abundance and biomass contribution of *Spinocalanus* agrees with findings in polar regions, stressing their successful colonization of the world's ocean with wide regional and vertical distribution ranges (Kosobokova et al. 2002). For example, in the Northwest Pacific, *Spinocalanus* dominated copepod abundance even at abyssopelagic depths between 6000-8000 m (Vinogradov 1972). In terms of biomass larger species became important, such as *Euchaeta, Nannocalanus minor* and *Neocalanus* in the upper epipelagic, *Heterorhabdus* and *Haloptilus* in the lower epipelagic, and *Metridia, Euaugaptilus, Pareucalanus*, *Rhincalanus* (esp. *R. cornutus*) and *Eucalanus hyalinus* in the meso- to bathypelagic zones. Likewise, numerically dominant genera such as *Microcalanus, Paracalanus* and *Pseudocalanus* in the North Pacific were less important considering biomass, whereas species of *Eucalanus* and *Neocalanus* were

major biomass taxa (Yamaguchi et al. 2002). Many of the species encountered in the epi- to mesopelagic zone were typically found in oxygen minimum zones (OMZ) in different regions of the world (Gowing and Wishner 1998; Ohman et al. 1998; Wishner et al. 2000; Loick et al. 2005; Auel and Verheye 2007; Schnack-Schiel et al. 2008; Wishner et al. 2008; Teuber et al. 2013). Tropical oceans are known for their extensive horizontal and vertical expansion of OMZs (Ekau et al. 2010; Stramma et al. 2010). Thus, only species adapted to such hypoxic conditions can attain dominance in these areas.

Diversity

A total of 110-130 calanoid species were identified at each station (gamma diversity: 2.4-3.0). The lower species diversity in the epipelagic zone contrasted with a high diversity in the meso- and bathypelagic zones. Because species-rich families such as Clausocalanidae, Scolecithrichidae, Lucicutiidae, Heterorhabdidae, Augaptilidae and Spinocalanidae were mostly identified to genus level, the number of species was clearly underestimated in the present study. In comparison, a maximum of 120 calanoid species were identified by Schnack-Schiel et al. (2010) considering only the upper 300 m of the tropical and subtropical eastern Atlantic. They also found lower species numbers (72-93) in the subtropical North and South Atlantic regions. In the present study, species richness and diversity in the upper 200 m was highest in the TNA (59-70 species) as compared to the subtropics and the BCIR (47-56 species). Typical of an upwelling system, the Benguela region is known for its rather low diversity in surface waters (Angel 1997; Woodd-Walker et al. 2002). In general, species diversity increases from the poles to the equator also in pelagic environments (MacPherson 2002; Kosobokova et al. 2011).

The high species numbers observed in the present study emphasize the high diversity and abundance of small calanoids in tropical and subtropical oceanic regions not only in surface waters (Woodd-Walker 2001; Woodd-Walker et al. 2002; Schnack-Schiel et al. 2010), but also at depth. In general, species diversity was higher in the meso- and bathybelagic zones than in the euphotic zone. Increasing species diversity with depth is a common feature of the pelagic realm (e.g. Deevey and Brooks 1977; Auel 1999; Kosobokova and Hopcroft 2010; Kosobokova et al. 2011). A bimodal copepod diversity pattern was found in the Mediterranean with peaks between 50-200 m and 500-800 m (Scotto di Carlo et al. 1984), and in the North Pacific between 500-1000 m and 2000-3000 m (Yamaguchi et al. 2002). However, little information is available

for tropical and subtropical regions. In the present study, peaks of species diversity seemed to occur shallower in stratified tropical waters than in less stratified subtropical waters, which may be related to the depth of the thermocline (Cornils et al. 2005).

Copepod grazing impact

Total copepod ingestion rates per station varied from 202 to >604 mg C m^{-2} d^{-1} (31-93% of primary production (PP)). These values are within ranges for copepod communities in the subarctic western Pacific calculated for the 0-2000 m water column: 276 mg C m^{-2} d^{-1} (Yamaguchi et al. 2002), 426 and 637 mg C m^{-2} d^{-1} (Homma et al. 2011). Highest ingestion rates of calanoid communities were found in the TNA (323 to >541 mg C m^{-2} d^{-1}, 45-83% PP) and lowest in the STNA (266 mg C m^{-2} d^{-1}, 60% PP) and STSA (151 mg C m^{-2} d^{-1}, 23% PP). Carbon consumption of cyclopoids was less variable ranging from 51-73 mg C m^{-2} d^{-1} (7-13% PP), but also lowest in the STNA and STSA. However, the cyclopoid community structure was not analyzed in detail and data compilations of respiration rates of cyclopoids are still lacking to accurately predict their metabolic rates. Therefore, our calculations may provide only rough estimates. Recent studies suggested that mass-specific metabolic rates of cyclopoids are lower than those of calanoids (Castellani et al. 2005). For example, *Oithona similis* showed eight times lower respiration rates than a calanoid copepod of equivalent body mass (Castellani et al. 2005). More accurate models need to be established for cyclopoid copepods in the future.

The potential grazing impact of copepod communities in the epipelagic zone varied from 19% at the BCIR station to >83% at stn. 8 in the TNA (this study). Grazing impact in tropical oligotrophic regions is usually higher than at higher latitudes and systems with a pronounced seasonality (e.g. Dam et al. 1993; Le Borgne and Rodier 1997; Barquero et al. 1998; Huskin et al. 2001). For example, during an extensive bloom in subarctic waters, zooplankton removed <5% (Atkinson 1996), whereas during a weaker bloom zooplankton consumed 25-56% of daily PP (Ward et al. 1995). The highest grazing impact (102% PP) was associated with lowest primary production rates (Pakhomov et al. 1997). In the Benguela Current upwelling system, mean grazing impact was around 40% of daily PP (45% of cells >2 µm), while copepods ingested up to 60% of PP and even >100% of large (>2 µm) phytoplankton production in the equatorial upwelling regions of the Atlantic (Huskin et al. 2001). This may be explained by the time lag of growth of copepod populations compared to the much faster growth rates of phytoplankton and the large

phytoplankton biomass in recently upwelled waters. Only when copepods reach a population peak and phytoplankton decays due to nutrient depletion, copepod feeding may significantly reduce further phytoplankton growth (Barquero et al. 1998). Thus, zooplankton grazing is assumed to be one of the main reasons for the steady state in phytoplankton biomass usually found in oligotrophic regions (Cullen et al. 1992; Banse et al. 1995; Huskin et al. 2001), and also in late stages of upwelling events (Painting et al. 1993; Barquero et al. 1998).

Oligotrophic conditions as encountered in the subtropical gyres (PP typically < 300-400 mg C m^{-2} d^{-1}; Longhurst et al. 1995) were absent during our time of sampling, when primary production rates were relatively high. The lowest primary production was found in the STNA with 445 mg C m^{-2} d^{-1}, where the grazing impact of copepods was quite high with 50% of the PP potentially ingested in the euphotic zone, although copepod community ingestion was rather low. In the TNA, primary production was relatively high (563-907 mg C m^{-2} d^{-1}) with high copepod biomass and ingestion in the euphotic zone, indicating that equatorial upwelling may have recently influenced this region, although this was not reflected any more by the hydrographic data. However, it has to be emphasized, that a part of the carbon ingested by copepods is not directly derived from phytoplankton (Dam et al. 1995). The contribution of ciliates as carbon source to copepod ingestion may be as high as 30% of daily copepod ration, especially in regions of poor phytoplankton growth (Calbet and Saiz 2005).

Role of copepods in the carbon flux

The total net loss rate of POC from 0-2000 m varied from 106-379 mg C m^{-2} d^{-1} for calanoids and 37-51 mg C m^{-2} d^{-1} for cyclopoids, corresponding to 16-58% and 5-9%, respectively, of primary carbon introduced into the system by surface primary production. Thus, copepods accounted for 21 to >65% of total net loss of POC. Similar estimates were made in the western subarctic Pacific, where suspension-feeding copepods consumed on average 32% (Yamaguchi et al. 2002) and 38% (Sasaki et al. 1988) of sinking particles throughout 0-4000 m and 150-1000 m, respectively. Off California, zooplankton consumed 6-43% of discarded larvacean houses in the upper mesopelagic zone (Steinberg et al. 1997). Zooplankton community composition and biomass may significantly determine the fate of organic carbon and potential export efficiencies of an ecosystem, which has been demonstrated in different regions of the world's ocean

(Koppelmann and Frost 2008; Wilson et al. 2008; Homma et al. 2011; Steinberg et al. 2012; this study).

High variations in copepod ingestion rates and thus grazing impact were found between the different sampling layers, even at the same sampling sites reflecting high variability of copepod community structure and biomass. Applying the equation by Suess (1980) around 80% of primary production was recycled in the upper 200 m, where maximum net loss rates by calanoids were found, being highest in the TNA with 29-54% of PP and lowest in the BCIR and STSA with 10 and 13% PP, respectively. Epipelagic layers associated with high biomass species such as *Pleuromamma* in the BCIR, *Euchaeta* and calanid copepods such as *Nannocalanus minor, Neocalanus gracilis* and *Undinula vulgaris* in the TNA seemed to be most "efficient" as biological carbon pump components. In contrast, relative net loss of POC mediated by cyclopoids was low in the euphotic zone with 3-6% of PP but higher in the mesopelagic zone with 6-17% of incoming POC (POC_{in}), due to the usually larger biomass of Oncaeidae. Total net loss of POC_{in} in the mesopelagic zone by calanoids was between 12 and 22% POC_{in} in the TNA and STSA, and was highest with 53 and 62% of POC_{in} in the STNA and BCIR, respectively. Active carbon transport was highest in the BCIR resulting in maximum net loss by calanoids of 116 mg C m^{-2} d^{-1} in the mesopelagic zone, while the majority of this carbon was probably consumed in shallower water layers during the night, as *Pleuromamma* alone was responsible for the net loss of 90 mg C m^{-2} d^{-1} between 200-400 m. However, a large part of the fecal pellet production (50 mg C m^{-2} d^{-1}) and respiration (66 mg C m^{-2} d^{-1}) happened at depth, thus transporting carbon actively to deeper layers and potentially increasing the efficiency of the biological carbon pump between the euphotic and mesopelagic zones. To a certain but much lower extent this active carbon flux also occurred at the other sampling sites, as *Pleuromamma* and other vertically migrating species such as *Temoropia* were present at all stations. Both respiratory carbon and POC transfer via DVM can be highly significant (Longhurst et al. 1990; Steinberg et al. 2000).

The amount of sinking particles gradually decreases with depth due to consumption by copepods and other consumers and disaggregation into suspended particles, so that around 4% PP reaches the 1000 m layer after Suess (1980). Thus, highest amounts of POC reaching the bathypelagic zone were found at stns. 10 and 17, which were characterized by highest surface primary production rates. In contrast, net loss by calanoid ingestion was rather steady (1.8-3.2 mg C m^{-2} d^{-1}), while maximum values did not coincide with highest incoming POC amounts. Maximum net consumption actually occurred at stns. 5 and 8, corresponding to 16% and 12%

POC_{in}, respectively. In general, previous studies also indicated that depth rather than surface primary production affects deep-sea zooplankton biomass to a much larger extent (Wishner 1980). However, more extreme seasonal changes in primary production rates usually propagate down to bathypelagic depths with a certain time lag and may be detectable in zooplankton biomass (Wishner 1980; Koppelmann and Weikert 1999; Koppelmann et al. 2004). For example, the coupling between surface production and deep particulate matter flux at 3200 m was within a month or less in the Sargasso Sea (Deuser and Ross 1980). Therefore, one has to keep in mind that by sampling the bathypelagic zones, we sample past surface POC conditions, as POC may be delayed by several weeks to months sinking from the surface (Voss et al. 1996; Holmes et al. 2002).

In the bathypelagic zone, differences between cyclopoid and calanoid ingestion rates were much smaller. Net ingestion of total copepods corresponded to 10-22% POC_{in} below 1000 m, indicating that POC fluxes exceeded by far the minimal food requirements of copepod communities and providing sufficient quantities of sinking particles as potential food source at these depths. A decreasing impact of copepod communities on incoming POC flux below 1000 m were also reported in the North Pacific, suggesting that repeated repackaging of POC in the upper layers may reduce the nutritional value of POC (Reinthaler et al. 2006; Homma et al. 2011). However, deep-sea detritivores such as *Spinocalanus* may have evolved efficient digestive systems like elongated guts (Kosobokova et al. 2002). Thus, transfer efficiencies may be higher in food-limited environments (Childress and Thuesen 1992; Koppelmann and Weikert 2000). However, our knowledge on these mechanisms is still too superficial to allow integration in ecosystem models. Nevertheless, the copepod family Spinocalanidae seemed to be of great importance in the cycling of organic matter and deep-sea food webs below the euphotic zone down to bathypelagic depths, as this copepod family primarily feeds on components of vertical flux and suspended matter (Kosobokova et al. 2002; Wishner et al. 2008; this study).

Conclusions

There are still major uncertainties regarding quantitative data from the meso- and bathypelagic zones of the ocean (Koppelmann and Frost 2008; Buesseler et al. 2007). We need a better understanding of regional variability of transfer efficiencies of POC to the deep sea and their primary drivers such as oceanographic parameters and biological activities to be included into

biogeochemical models. Regional and temporal differences in particle flux may be attributed, e.g. to differences in the pelagic food web structure, the proportion of fecal pellets to phytoplankton aggregates, their quantity and quality, presence and absence of ballast minerals (silicate, carbonate, dust), the nutrient and oceanographic regime, and the carbon demand of mesopelagic bacteria and zooplankton communities (Buesseler et al. 2007). Higher zooplankton biomass and the presence of certain species (e.g. *Pleuromamma*) greatly affect carbon transfer via feeding, metabolism, fecal pellet production and diel vertical migrations (Buesseler et al. 2007; Steinberg et al. 2012; this study).

The carbon flux model indicated that incoming POC resources in the deep sea were far from being fully exploited by copepods. However, we do not know to what extent decreasing nutritional value through constant repackaging of POM arriving at greater depth affects copepod growth (Robinson et al. 2010). It may not contain enough energy to support large population sizes, as biomass in the deep sea seems to be similarly restricted in all marine regions. However, the generally high carbon ingestion rates obtained in the present study indicate that copepods substantially influence oceanic carbon fluxes, mediating processes in the biological carbon pump and enhancing carbon sequestration by the deep ocean. The tropical and subtropical oceanic ecosystems in the eastern Atlantic Ocean are highly diverse and productive, while grazing pressure of copepods can be very variable even on smaller vertical scales, depending on abundance, biomass and community structure of the copepod assemblage. With special regard to their huge regional expanse, these regions play an important role in the carbon cycling of the ocean.

Appendices

For Table A please see supplementary data.

Acknowledgements

We would like to thank the captain and crew of RV *Polarstern* during ANT-XXIX/1 (PS81) for their competent support during the cruise. We would also like to thank the students of the EUROPA trainings cruise, who helped handling the nets and sampling as well as coordinating respiration measurements onboard.

References

Angel, M.V., 1997. Pelagic biodiversity. In: Ormond, R.G.F., Gage, J.D., Angel, M.V. (Eds.), Marine biodiversity: Patterns and processes. Cambridge University Press, Cambridge, pp. 35-68.

Armstrong, R.A., Lee, C., Hedges, J.I., Honjo, S., Wakeham, S.G., 2002. A new mechanistic model for organic carbon fluxes in the ocean based on the quantitative association of POC with ballast minerals. Deep-Sea Res. II 49, 219-236.

Atkinson, A., 1996. Subantarctic copepods in an oceanic, low chlorophyll environment: Ciliate predation, food selectivity and impact on prey population. Mar. Ecol. Prog. Ser 130, 85-96.

Auel, H., 1999. The ecology of Arctic deep-sea copepods (Euchaetidae and Aetideidae). Aspects of their distribution, trophodynamics and effect on the carbon flux. Rep. Polar Res. 319, 1-97.

Auel, H., Hagen, W., 2002. Mesozooplankton community structure, abundance and biomass in the central Arctic Ocean. Marine Biology 140, 1013-1021.

Auel, H., Hagen, W., Verheye, H.M., 2005. Metabolic adaptations and reduced respiration of the copepod *Calanoides carinatus* during diapause at depth in the Angola-Benguela Front and northern Benguela upwelling regions. Afr. J. Mar. Sci. 27, 653–657.

Auel, H., Verheye, H.M., 2007. Hypoxia tolerance in the copepod Calanoides carinatus and the effect of an intermediate oxygen minimum layer on copepod vertical distribution in the northern Benguela Current upwelling system and the Angola-Benguela Front. J. Exp. Mar. Biol. Ecol. 352, 234-243.

Banse, K., 1995. Zooplankton: Pivotal role in the control of ocean production. Ices J. Mar. Sci. 52, 265-277.

Barquero, S., Cabal, J.A., Anadón, R., Fernández, E., Varela, M., Bode, A., 1998. Ingestion rates of phytoplankton by copepod size fractions on a bloom associated with an off-shelf front off NW Spain. J. Plankt. Res. 20, 957-972.

Bender, M.L., Heggie, D.T., 1984. Fate of organic carbon reaching the deep sea floor: A status report. Geochim. Cosmochim. Acta 48, 977-986.

Bode, M., Schukat, A., Hagen, W., Auel, H., 2013. Predicting metabolic rates of calanoid copepods. J. Exp. Mar. Biol. Ecol. 444, 1-7.

Böttger-Schnack, R., 1996. Vertical structure of small metazoan plankton, especially non-calanoid copepods. I. Deep Arabian Sea. J. Plankt. Res. 18, 1073-1101.

Buesseler, K.O., Lamborg, C.H., Boyd, P.W., Lam, P.J., Trull, T.W., Bidigare, R.R., Bishop, J.K.B., Casciotti, K.L., Dehairs, F., Elskens, M., Honda, M., Karl, D.M., Siegel, D.A., Silver, M.W., Steinberg, D.K., Valdes, J., Van Mooy, B., Wilson, S., 2007. Revisiting carbon flux through the ocean's twilight zone. Science 316, 567-570.

Calbet, A., 2001. Mesozooplankton grazing effect on primary production: A global comparative analysis in marine ecosystems. Limnol. Oceanogr. 46, 1824-1830.

Calbet, A., Landry, M.R., 2004. Phytoplankton growth, microzooplankton grazing, and carbon cycling in marine systems. Limnol. Oceanogr. 40.

Calbet, A., Saiz, E., 2005. The ciliate-copepod link in marine ecosystems. Aquat. Microb. Ecol. 38, 157-167.

Calbet, A., Atienza, D., Henriksen, C.I., Saiz, E., Adey, T.R., 2009. Zooplankton grazing in the Atlantic Ocean: A latitudinal study. Deep-Sea Res. II 56, 954-963.

Castellani, C., Robinson, C., Smith, T., Lampitt, R.S., 2005. Temperature affects repiration rate of *Oithona similis*. Mar. Ecol. Prog. Ser 285, 129-135.

Champalbert, G., Pagano, M., Kouamé, B., Riandey, V., 2005. Zooplankton spatial and temporal distribution in a tropical oceanic area off West Africa. Hydrobiol. 548, 251-265.

Childress, J.J., Thuesen, E.V., 1992. Metabolic potential of deep-sea animals: Regional and global scales. In: Rowe, G.T., Pariente, V. (Eds.), Deep-sea food chains and the global carbon cycle. Kluwer Academics Publishers, pp. 217-236.

Chisholm, L.A., Roff, J.C., 1990. Abundances, growth rates, and production of tropical neritic copepods off Kingston, Jamaica. Mar. Biol. 106, 79-89.

Clarke, A., Gorley, R.N., 2006. PRIMER v6: User manual/tutorial. PRIMER-E. Plymouth. 192 pp.

Cornils, A., Schnack-Schiel, S.B., Hagen, W., Dowidar, M.M., Stambler, N., Plähn, O., Richter, C., 2005. Spatial and temporal distribution of mesozooplankton in the Gulf of Aquaba and the northern Red Sea in February/March 1999. J. Plankt. Res. 27, 505-518.

Cullen, J.J., Lewis, M.R., Davis, C.O., Barber, R.T., 1992. Photosynthetic characteristics and estimated growth rates indicate grazing is the proximate control of primary production in the Equatorial Pacific. J. Geophys. Res. 97, 639-654.

Dam, H.G., Miller, C.A., Jonasdottir, S.H., 1993. The trophic role of mesozooplankton at 47°N, 20°W during the North Atlantic Bloom Experiment. Deep-Sea Res. I 40, 197-212.

Dam, H.G., Zhang, X.S., Butler, M., Roman, M.R., 1995. Mesozooplankton grazing and metabolism at the equator in the central Pacific - Implications for carbon and nitrogen fluxes. Deep-Sea Res. II 42, 735-756.

Deevey, G.B., Brooks, A.L., 1977. Copepods of the Sargasso Sea off Bermuda: Species composition, and vertical and seasonal deistribution between the surface and 2000 m. Bull. Mar. Sci. 27, 256-291.

Deuser, W.G., Ross, E.H., 1980. Seasonal change in the flux of organic carbon to the deep Sargasso Sea. Nature 283, 364-365.

Ducklow, H.W., Steinberg, D.K., Buesseler, K.O., 2001. Upper ocean carbon export and the biological pump. Oceanogr. 14, 50-58.

Ekau, W., Auel, H., Pörtner, H.-O., Gilbert, D., 2010. Impacts of hypoxia on the structure and processes in pelagic communities (zooplankton,macro-invertebrates and fish). Biogeosci. 7, 1669-1699.

Falkowski, P.G., Barber, R.T., Smetacek, V., 1998. Biogeochemical controls and feedbacks on ocean primary production. Science 281, 200-206.

Fonseca-Batista, D., Dehairs, F., Riou, V., Fripiat, F., Elskens, M., Deman, F., Bode, M., Auel, H., Contribution of N_2 fixation to biological productivity along a meridional section in the eastern Atlantic Ocean. submitted to Prog. Oceanogr.

Frangoulis, C., Christou, E.D., Hecq, J.H., 2005. Comparison of marine copepod outfluxes: Nature, rate, fate and role in the carbon and nitrogen cycles. Adv. Mar. Biol. 47, 253-309.

Gnaiger, E., 1983. Calculation of energetic and biochemical equivalents of respiratory oxygen consumption. Polarographic oxygen sensors. Springer Berlin Heidelberg, pp. 337-345.

Gowing, M.M., Wishner, K.F., 1998. Feeding ecology of the copepod *Lucicutia* aff. *L. grandis* near the lower interface of the Arabian Sea oxygen minimum zone. Deep-Sea Res. II 45, 2433-2459.

Hernández-León, S., Postel, S., Arístegui, J., Gómez, M., Montero, M.F., Santiago, T., Almeida, C., Kühner, E., Brenning, U., Hagen, E., 1999. Large-scale and mesoscale distribution of plankton biomass and metabolic acitivty in the northeastern Central Atlantic. J. Oceanogr. 55.

Hernández-León, S., Ikeda, T., 2005. A global assessment of mesozooplankton respiration in the ocean. J. Plankt. Res. 27, 153-158.

Holmes, E., Lavik, G., Fischer, G., Segl, M., Ruhland, G., Wefer, G., 2002. Seasonal variability of $\delta^{15}N$ in sinking particles in the Benguela upwelling region. Deep-Sea Res. I 49, 377-394.

Homma, T., Yamaguchi, A., Bower, J.R., Imai, I., 2011. Vertical changes in abundance, biomass, and community structure of copepods in the northern North Pacific and Bering Sea at 0-3000 m depth, and their role on the vertical flux of surface-produced organic material. Bull. Fish. Sci. Hokkaido Univ. 61, 29-47.

Huskin, I., Anadón, R., Woodd-Walker, R.S., Harris, R.P., 2001. Basin-scale latitudinal patterns of copepod grazing in the Atlantic Ocean. J. Plankt. Res. 23, 1361-1371.

Ikeda, T., Motoda, S., 1978. Estimated Zooplankton Production and Their Ammonia Excretion in Kuroshio and Adjacent Seas. Fish. Bull. 76, 357-367.

Ikeda, T., Kanno, Y., Ozaki, K., Shinada, A., 2001. Metabolic rates of epipelagic marine copepods as a function of body mass and temperature. Mar.Biol. 139, 587–596.

Ikeda, T., Sano, F., Yamaguchi, A., Matsuishi, T., 2006. Metabolism of mesopelagic and bathypelagic copepods in the wetsren North Pacific Ocean. Mar. Ecol. Prog. Ser 322, 199-211.

Isla, J.A., Llope, M., Anadon, R., 2004. Size-fractionated mesozooplankton biomass, metabolism and grazing along a 50°N-30°S transect of the Atlantic Ocean. J. Plankt. Res. 26, 1301-1313.

Karl, D.M., Christian, J.R., Dore, J.E., Hebel, D.V., Letelie, R.M., Tupas, L.M., Winn, C.D., 1996. Seasonal and interannual variability in primary production and particle flux at station ALOHA. Deep-Sea Res. II 43, 539-568.

Ketchum, B.H., 1962. Regeneration of nutrients zooplankton. Rapp. P. V. Reun., Cons. Int. Explor. Mer. 153, 142-147.

Koppelmann, R., Weikert, H., 1992. Full-depth zooplankton profiles over the deep bathyal of the NE Atlantic. Mar. Ecol. Prog. Ser 86, 263-272.

Koppelmann, R., Weikert, H., 1999. Temporal changes of deep-sea mesozooplankton abundance in the temperate NE Atlantic and estimates of the carbon budget. Mar. Ecol. Prog. Ser. 179, 27-40.

Koppelmann, R., Weikert, H., 2000. Transfer of organic matter in the deep Arabian Sea zooplankton community: insights from $\delta^{15}N$ analysis. Deep-Sea Res. II 47, 2653-2672.

Koppelmann, R., Weikert, H., Halsband-Lenk, C., 2004. Mesozooplankton community respiration and its relation to particle flux in the oligotrophic eastern Mediterranean. Global Biogeochem. Cycles 18, GB1039.

Koppelmann, R., Frost, J., 2008. The ecological role of zooplankton in the twilight and dark zones of the ocean. In: Mertens, L.P. (Ed.), Biological Oceanography Research Trends. Nova Science Publishers, Inc., New York, pp. 67-130.

Kosobokova, K.N., Hirche, H.-J., Scherzinger, T., 2002. Feeding ecology of *Spinocalanus antarcticus*, a mesopelagic copepod with a looped gut. Mar. Biol. 141, 503-511.

Kosobokova, K.N., Hopcroft, R.R., 2010. Diversity and vertical distribution of mesozooplankton in the Arctic's Canada Basin. Deep-Sea Res. II 57, 96-110.

Kosobokova, K.N., Hopcroft, R.R., Hirche, H.-J., 2011. Patterns of zooplankton diversity through the depths of the Arctic's central basins. Mar. Biodiv. 41, 29-50.

Köster, M., Krause, C., Paffenhöfer, G., 2008. Time-series measurements of oxygen consumption of copepod nauplii. Mar. Ecol. Prog. Ser. 353, 157-164.

Laws, E.A., Falkowski, P.G., Smith, W.O., Ducklow, H., McCarthy, J.J., 2000. Temperature effects on export production in the open ocean. Global Biogeochem. Cycles 14, 1231-1246.

Le Borgne, R., Rodier, M., 1997. Net zooplankton and the biological pump: A comparison between the oligotrophic and mesotrophic equatorial Pacific. Deep-Sea Res. II 44, 2003-2023.

Lenz, J., Morales, A., Gunkel, J., 1993. Mesozooplankton standing stock during the North Atlantic sping bloom study 1989 and its potential grazing pressure on phytoplankton: a comparison between low, medium and high latitudes. Deep-Sea Res. II 40, 559-572.

Loick, N., Ekau, W., Verheye, H.M., 2005. Water-body preferences of dominant calanoid copepod species in the Angola-Benguela frontal zone. Afr. J. Mar. Sci. 27, 597-608.

Longhurst, A.R., Harrison, W.G., 1989. The biological pump: Profiles of plankton production and consumption in the upper ocean. Prog. Oceanogr. 22, 47–123.

Longhurst, A.R., Bedo, A.W., Harrison, W.G., Head, E.J.H., Sameoto, D.D., 1990. Vertical flux of respiratory carbon by oceanic diel migrant biota. Deep-Sea Res. I 37, 685-694.

Longhurst, A., 1993. Seasonal cooling and blooming in tropical oceans. Deep-Sea Res. I 40, 2145-2165.

Longhurst, A., Sathyendranath, S., Platt, T., Caverhill, C., 1995. An estimate of global primary production in the ocean from satellite radiometer data. J. Plankton Res. 17, 1245-1271.

MacPherson, E., 2002. Large-scale-species-richness gradients in the Atlantic Ocean. Proc. R. Soc. Lond. B 269, 1715-1720.

Marañón, E., Holligan, P.M., Varela, M., Mourino, B., Bale, A.J., 2000. Basin-scale variability of phytoplankton biomass, production and growth in the Atlantic Ocean. Deep-Sea Res. I 47, 825-857.

Martin, J.H., Knauer, G.A., Karl, D.M., Broenkow, W.W., 1987. VERTEX: carbon cycling in the northeast Pacific. Deep-Sea Res I 34, 267-285.

Morales, C.E., Harris, R.P., Head, R.N., Tranter, P.R.G., 1993. Copepod grazing in the oceanic northeast atlantic during a 6 week drifting station - the contribution of size classes and vertical migrants. J. Plankt. Res. 15, 185-211.

Ohman, M.D., Drits, A.V., Clarke, M.E., 1998. Differential dormancy of co-occurring copepods. Deep-Sea Res. II 45, 1709–1740.

Paffenhöfer, G.-A., Mazzocchi, M.G., 2003. Vertical distribution of subtropical epiplanktonic copepods. J. Plankt. Res. 25, 1139-1156.

Painting, S.J., Lucas, M.I., Peterson, W.T., Brown, P.C., Hutching, L., Mitchell-Innes, B.A., 1993. Dynamics of bacterioplankton, phytoplankton and mesozooplankton communities during the development of an upwelling plume in the southern Benguela. Mar. Ecol. Prog. Ser 100, 35-53.

Pakhomov, E.A., Verheye, H.M., Atkinson, A., Laubscher, R.K., Taunton-Clark, J., 1997. Structure and grazing impact of the mesozooplankton community during late summer 1994 near South Georgia, Antarctica. Polar Biol. 18, 180-192.

Piontkovski, S., Williams, R., Ignatyev, S., Boltachev, A., Chesalin, M., 2003. Structural-functional relationships in the pelagic community of the eastern tropical Atlantic Ocean. J. Plankt. Res. 25, 1021-1034.

Platt, T., Harrison, W.G., Lewis, M.R., Li, W.K.W., Sathyendranath, S., Smith, R.E., Vezina, A.F., 1989. Biological production of the oceans: the case for a consensus. Mar. Ecol. Prog. Ser 52, 77-88.

Reinthaler, T., van Aken, H., Veth, C., Arístegui, J., Robinson, C., Williams, P., Lebaron, P., Herndl, G.J., 2006. Prokaryotic respiration and production in the meso- and bathypelagic realm of the eastern and western North Atlantic basin. Limnol. Oceanogr. 51, 1262-1273.

Richter, C., 1994. Regional and seasonal veriability in the vertical distribution of mesozooplankton in the Greenland Sea. Ber. Polarforsch. 154, 1-87.

Robinson, C., Steinberg, D.K., Anderson, T.R., Arístegui, J., Carlson, C.A., Frost, J.R., Ghiglione, J.-F., Hernández-León, S., Jackson, G.A., Koppelmann, R., Quéguiner, B., Ragueneau, O., Rassoulzadegan, F., Robison, B.H., Tamburini, C., Tanaka, T., Wishner, K.F., Zhang, J., 2010. Mesopelagic zone ecology and biogeochemistry - a synthesis. Deep-Sea Res. II 57, 1504-1518.

Roe, H.S.J., 1972. The vertical distributions and diurnal migrations of calanoid copepods collected on the SOND cruise, 1965. I. The total population and general discussion. J. Mar. Biol. Ass. U.K. 52, 277-314.

Rohardt, G., Wisotzki, A., 2013. Physical oceanography during POLARSTERN cruise ANT-XXIX/1. Alfred Wegener Institute, Helmholtz Center for Polar and Marine Research, Bremerhaven. PANGAEA.

San Martin, E., Harris, R.P., Irigoien, X., 2006. Latitudinal variation in plankton size spectra in the Atlantic Ocean. Deep-Sea Res. II 53, 1560-1572.

Sasaki, H., Hattori, H., Nishizawa, S., 1988. Downward flux of particulate organic matter and vertical distribution of calanoid copepods in the Oyashio water in summer. Deep-Sea Res. I 35, 505-515.

Schlitzer, R., 2013. Ocean Data View 4, http://odv.awi.de.

Schnack-Schiel, S.B., Niehoff, B., Hagen, W., Böttger-Schnack, R., Cornils, A., Dowidar, M.M., Pasternak, A., Stambler, N., Stübing, D., Richter, C., 2008. Population dynamics and life strategies of Rhincalanus nasutus (Copepoda) at the onset of the spring bloom in the Gulf of Aqaba (Red Sea). J. Plankt. Res. 30, 655–672.

Schnack-Schiel, S.B., Mizdalski, E., Cornils, A., 2010. Copepod abundance and species composition in the Eastern subtropical/tropical Atlantic. Deep-Sea Res. II 57, 2064-2075.

Scotto di Carlo, B., Ianora, A., Fresi, E., Hure, J., 1984. Vertical zonation patterns for Mediterranean copepdos from the surface to 3000 m at a fixed station in the Tyrrhenian Sea. J. Plankt. Res. 6, 1031-1056.

Shannon, C.E., 1948. A mathematical theory of communications. Bell Syst. Tech. J. 27, 379-423.

Steedman, H.F., 1976. General and applied data formaldehyde fixation and preservation of marine zooplankton. In: Steedman, H.F. (Ed.), Zooplankton fixation and preservation. Monographs on oceanographic methodology 4. UNESCO Press, Vendome, pp. 103-154.

Steinberg, D.K., Silver, M.W., Pilskaln, C.H., 1997. Role of mesopelagic zooplankton in the community metabolism of giant larvacean house detritus in Monterey Bay, California, USA. Mar. Ecol. Prog. Ser 147, 167-179.

Steinberg, D.K., Carlson, C.A., Bates, N.R., Goldthwait, S.A., Madin, L.P., Michaels, A.F., 2000. Zooplankton vertical migration and the active transport of dissolved organic and inorganic carbon in the Sargasso Sea. Deep-Sea Res. I 47, 137-158.

Steinberg, D.K., Cope, J.S., Wilson, S.E., Kobari, T., 2008. A comparison of mesopelagic mesozooplankton community structure in the subtropical and subarctic North Pacific Ocean. Deep-Sea Res. II 55, 1615-1635.

Steinberg, D.K., Lomas, M.W., Cope, J.S., 2012. Long-term increase in mesozooplankton biomass in the Sargasso Sea: Linkage to climate and implications for food web dynamics and biogeochemical cycling. Global Biogeochem. Cycles 26.

Stramma, L., Johnson, G., Sprintall, J., Mohrholz, V., 2008. Expanding oxygen minimum zones in the tropical oceans. Science 320, 655-658.

Suess, E., 1980. Particulate organic carbon flux in the oceans - surface productivity and oxygen utilization. Nature 288, 260-263.

Teuber, L., Kiko, R., Seguin, F., Auel, H., 2013. Respiration rates of tropical Atlantic copepods in relation to the oxygen minimum zone. J. Exp. Mar. Biol. Ecol. 448, 28-36.

Vinogradov, M.E., 1972. Vertical distribution of oceanic zooplankton. Israel Programm for Scientific Translations. Jerusalem.

Voss, M., Altabet, M.A., von Bodungen, B., 1996. $\delta^{15}N$ in sedimenting particles as indicator of euphotic-zone processes. Deep-Sea Res. I 43, 33-47.

Ward, P., Atkinson, A., Murray, A.W.A., Wood, A.G., Williams, R., Poulet, S.A., 1995. The summer zooplankton community at South Georgia: biomass, vertical migration and grazing. Polar Biol. 15, 195-208.

Wassmann, P., 1998. Retention versus export food chains: processes controlling sinking loss from marine pelagic systems. Hydrobiol. 363, 29-57.

Webb, T.J., Vanden Berghe, E., O`Dor, R., 2010. Biodiversity's big wet secret: The global distribution of marine biological records reveals chronic under-exploration of the deep pelagic ocean. PLoS ONE 5, e10223.

Weikert, H., 1982. The vertical distribution of zooplankton in relation to habitat zones in the area of the Atlantis II Deep, Central Red Sea. Mar. Ecol. Prog. Ser 8, 129-143.

Weikert, H., Trinkaus, S., 1990. Vertical mesozooplankton abundance and distribution in the deep eastern Mediterranean Sea SE of Crete. J. Plankt. Res. 12, 601-628.

Wiggert, J.D., Haskell, A.G.E., Paffenhöfer, G.-A., Hofmann, E.E., Klinck, J.M., 2005. The role of feeding behavior in sustaining copepod populations in the tropical ocean. J. Plankt. Res. 27, 1013-1031.

Wilson, S.E., Steinberg, D.K., Buesseler, K.O., 2008. Changes in fecal pellet characteristics with depth as indicators of zooplankton repackaging of particles in the mesopelagic zone of the subtropical and subarctic North Pacific Ocean. Deep-Sea Res. II 55, 14-15.

Winberg, G.G., 1956. Rate of metabolism and requirements of fishes. Beloruss State University, Minsk. Fish. Res. Bd. Can. Transl. Ser. No. 194, 1960, 253 pp.

Wishner, K.F., 1980. The biomass of the deep-sea benthopelagic plankton. Deep-Sea Res. I 27A, 203-216.

Wishner, K.F., Gowing, M.M., Gelfman, C., 2000. Living in suboxia: Ecology of an Arabian Sea oxygen minimum zone copepod. Limnol. Oceanogr. 45, 1576-1593.

Wishner, K.F., Gelfman, C., Gowing, M.M., Outram, D.M., Rapien, M., Williams, R.L., 2008. Vertical zonation and distributions of calanoid copepods through the lower oxycline of the Arabian Sea oxygen minimum zone. Prog. Oceanogr. 78, 163-191.

Woodd-Walker, R.S., 2001. Spatial distributions of copepod genera along the Atlantic Meridional Transect. Hydrobiol. 453, 161-170.

Woodd-Walker, R.S., Ward, P., Clarke, A., 2002. Large-scale patterns in diversity and community structure of surface water copepods from the Atlantic Ocean. Mar. Ecol. Progr. Ser. 236, 189-203.

Yamaguchi, A., Watanabe, Y., Ishida, H., Harimoto, T., Furusawa, K., Suzuki, S., Ishizaka, J., Ikeda, T., Takahashi, M.M., 2002. Community and trophic structures of pelagic copepods down to greater depths in the western subarctic Pacific (WEST-COSMIC). Deep-Sea Res. I 49, 1007-1025.

CHAPTER V

Unraveling Diversity of Deep-sea Copepods using Integrated Morphological and Molecular Techniques

Bode M, Laakmann S, Kaiser P, Hagen W, Auel H, Cornils A

Submitted to Molecular Phylogenetics and Evolution in January 2016

Unraveling Diversity of Deep-Sea Copepods Using Integrated Morphological and Molecular Techniques

Maya Bode, Silke Laakmann, Patricia Kaiser, Wilhelm Hagen, Holger Auel and Astrid Cornils

Abstract

Copepods dominate mesozooplankton communities in all marine regions. Their species identification is usually based on a few and often inconspicuous diagnostic characters. Many morphological features in copepods are highly conserved and thus, species richness is still largely underestimated in many copepod families. However, accurate identification of zooplankton organisms is crucial for ecological studies. Rapid advances in molecular techniques have largely improved traditional morphological species identification methods. We applied both, morphological and molecular identification techniques to assess species richness in the deep-sea copepod family Spinocalanidae. Representatives of this family are particularly abundant below the euphotic zone down to abyssopelagic depths. Thus, they play an important ecological role in deep-sea ecosystems worldwide. Their species identification based on morphological features represents a very challenging to impossible task. Therefore, their diversity in the tropical Atlantic was elucidated applying an integrated taxonomic approach combining morphology, DNA sequence analyses (18S, COI) and proteomic fingerprinting using matrix-assisted laser desorption/ionization time-of-flight mass spectrometry (MALDI-TOF MS). These three methodologies were performed on different fractions of each individual copepod specimen. Species clusters were similar for DNA sequence analyses and MALDI-TOF MS, revealing more putative species than derived from morphological identifications. In total, 40 putative species of Spinocalanidae were detected, while only 28 species could be discriminated based on morphological characters. Even cryptic species were discriminated based on MALDI-TOF MS. As a very time- and cost-efficient technique, MALDI-TOF MS provides a suitable tool to simplify and accelerate future studies of biodiversity and distributional patterns of copepods with a high taxonomic resolution.

Keywords: COI, 18S, proteomic fingerprinting, MALDI-TOF, species delimitation, Spinocalanidae

Introduction

Calanoid copepods are well-known for their enormous biological and ecological diversity (Mauchline 1998; Bradford-Grieve 2002; Blanco-Bercial et al. 2011). Accurate species identification is a prerequisite for meaningful ecological studies. However, identification of copepods is often based on only a few distinct characters. In many species, these diagnostic features are inconspicuous, may only be visible after detailed preparation of the organisms. In addition, identification is often complicated by incomplete or inconsistent taxonomic keys (e.g. Knowlton 1993, 2000; Goetze 2003; Wilson et al. 2007; Jörger et al. 2012; Cornils and Held 2014). Furthermore, morphological characters may be highly conserved, which exacerbates accurate identification of sibling or cryptic species (Knowlton 2000; Bucklin et al. 1999; 2003). Cryptic speciation without any associated morphological change is a common phenomenon in copepods (e.g. Bucklin et al. 1998, 1999, 2003; Rocha-Olivares et al. 2001; Lee and Frost 2002; Goetze 2003; Thum and Harrison 2009) and may hinder identification of species, especially when they co-occur (e.g. Bucklin et al. 1998; Laakmann et al. 2013; Aarbakke et al. 2014). Thus, species richness is still underestimated in many copepod families.

In the last decades, molecular techniques have been supplementing traditional identification methods based on morphological characters. DNA sequencing of different gene fragments and PCR-based methods proved to resolve taxonomic relationships at many different levels (Hill et al. 2001; Kiesling et al. 2002; Blanco-Bercial and Àlvarez-Marqués 2007; Bucklin et al. 2003, 2010; Blanco-Bercial et al. 2011). DNA barcoding using the mitochondrial cytochrome c oxidase subunit I (COI) gene is especially valuable for unambiguous species discrimination in metazoans (Herbet et al. 2003) and was verified for calanoid copepods (e.g. Bucklin et al. 2003, 2010; Götze 2003; Laakmann et al., 2012, 2013; Aarbakke et al. 2014; Cornils and Held 2014). Nevertheless, these DNA-based methods are still time- and cost-intensive. Moreover, *a priori* knowledge of species-specific sequences is required for accurate primer design (Feltens et al., 2010; Volta et al., 2012; Laakmann et al. 2013).

Major improvements of mass spectrometric techniques to analyze even large and fragile molecules such as proteins using “soft” ionization methods resulted in an increasing popularity of proteomics methods for species discrimination (Pappin et al. 1993; Holland et al. 1996; Krishnamurthy et al. 1996; Claydon et al. 1996; Feltens et al. 2010). Applying matrix-assisted laser desorption/ionization time-of-flight mass spectrometry (MALDI-TOF MS), protein fingerprinting successfully differentiates microorganisms on the genus, species and even

subspecies level (e.g. Stackebrandt et al. 2005; Vargha et al. 2006). Low cost, simple sample handling, speed of analysis and species- or even strain-specific patterns in the associated mass spectra made this technology attractive for e.g. food quality control, environmental research, as well as veterinary and clinical diagnostics in pathogen identification (Lynn et al. 1999). This technique has also great potential to improve and simplify ecological studies, as routine and automated procedures would allow preparation and analyses of hundreds of individuals per day (Volta et al. 2012). Recent studies showed that MALDI-TOF MS successfully discriminated metazoans such as insects (Feltens et al. 2010; Kaufmann et al. 2011; Yssouf et al. 2013a,b, 2014; Uhlmann et al. 2014), fish (Volta et al. 2012), and also zooplankton species such as shrimp (Salla and Murray 2013) and copepod species (Riccardi et al. 2012; Laakmann et al. 2013).

The copepod family Spinocalanidae, especially the genus *Spinocalanus*, is a dominant component of meso- to abyssopelagic ecosystems from tropical to polar oceans (Vinogradov 1972; Kosobokova et al. 2002; Yamaguchi et al. 2002; Homma et al. 2011; Kosobokova and Hopcroft 2010; Bode et al. submitted). Spinocalanid species are usually omnivorous feeding on a large spectrum of particle sizes (Kosobokova et al. 2002). Thus, this copepod family may be of great ecological importance for the cycling of organic matter, deep-sea food webs and carbon flux (Wishner et al. 2008; Bode et al. submitted). Spinocalanidae include about 59 known species of ten genera (Razouls et al. 2005-2015). However, many of these species names are not generally accepted or descriptions overlap and/or are inconsistent (Razouls et al. 2005-2015; WoRMS Editorial Board 2015). Thus, taxonomy, species richness and distribution of this species complex are not well understood.

After first detailed descriptions of the genus *Spinocalanus* by Brodsky (1950), Grice and Hülsemann (1965), Park (1970) and Grice (1971), the most common genera *Spinocalanus* and *Mimocalanus* from the Arctic Ocean were reviewed only once by Damkaer (1975), followed by some additional work on some pelagic species from New Zealand waters by Bradford-Grieve (1994), from the eastern North Atlantic and Antarctic waters by Schulz (1989; 1996). Exact morphological identification is often exacerbated by missing morphological characters, such as lost antennules and swimming legs, due to net sampling from greater depths. Thus, molecular species identification techniques are of special importance for taxonomically challenging copepod groups, and particularly promising for small and fragile deep-sea species.

We therefore applied an integrated taxonomic approach by combining 1) morphological diagnostics, 2) DNA-sequence analyses of the nuclear 18S rDNA gene and mitochondrial COI, and

3) proteomic fingerprinting based on MALDI-TOF MS, performing all three methods on fractions of the same spinocalanid specimens. We tested, if the MALDI-TOF technology can be applied for rapid and efficient identification even of closely related copepod species by exploring the diversity of the spinocalanid species complex with focus on the most abundant genus *Spinocalanus* in the tropical and subtropical eastern Atlantic Ocean.

Materials and Methods

Sampling

Copepods were sampled during the research cruise ANTXXIV/1 with RV *Polarstern* throughout the tropical and subtropical eastern Atlantic Ocean from 25°N to 24°S in October/November 2007 (Fig. 1). Sampling was conducted using different net types and net-specific sampling depths. Vertical hauls were performed with a Multinet (HydroBios Multinet Maxi: 9 nets, 0.5 m^2 mouth opening, 150 µm mesh size) with standard sampling depths from 1000-800-600-500-400-300-200-100-50-0 m. Tows were conducted with two types of multiple opening/closing net and environmental sensing systems: 1 m^2 MOCNESS (9 nets, 335 µm) from 1000-800-600-400-200-100-50-0 m and 10 m^2 MOCNESS (5 nets, 335 µm) from 5000-4000-3000-2000-1000-0 m. The samples were fixed in pure ethanol (96% ETOH).

Intact-looking females of Spinocalanidae were sorted from bulk ethanol samples. Individuals were isolated in pure ethanol and identified to species level, if possible, using the identification guides by Brodksy (1950), Park (1970), Grice (1971), Damkaer (1975), Schulz (1989; 1996) and Razouls et al. (2005-2015). Furthermore, prosome and urosome length, total length, body shape and striking morphological characteristics, which were visible under the dissecting microscope, were noted prior to further analysis. This pre-identification was carried out rather quickly under the dissecting microscope to avoid damage of the DNA by light or temperature. Some important diagnostic characters can only be seen under a light microscope. Due to net sampling, however, specimens usually lacked distal parts of swimming legs, which made accurate species identification nearly impossible. At least 3-5 individuals per putative species were selected, if available. In total, 193 individuals were sorted and cut in half, leaving one half (cephalosome) for DNA extraction and the other (last metasomal segments/urosome) for protein mass fingerprinting. Some intact individuals were included into the analyses to test whether peak patterns were affected when analyzing only half of the animal by MALDI-TOF MS. The exuviae (exoskeletons), retained from the DNA extraction (see below), were analyzed in detail under the

microscope and further identified to species level, if possible, using notes and total length measurements from initial sorting and the above mentioned identification guides. Two species bear a double name as they share morphological characters described for both species (*S. longispinus/stellatus*, *S. neospinosus/hoplites*). Species, that have a number after the species name, could not be distinguished from congeners based on morphological features (e.g. the *S. dispar* species complex).

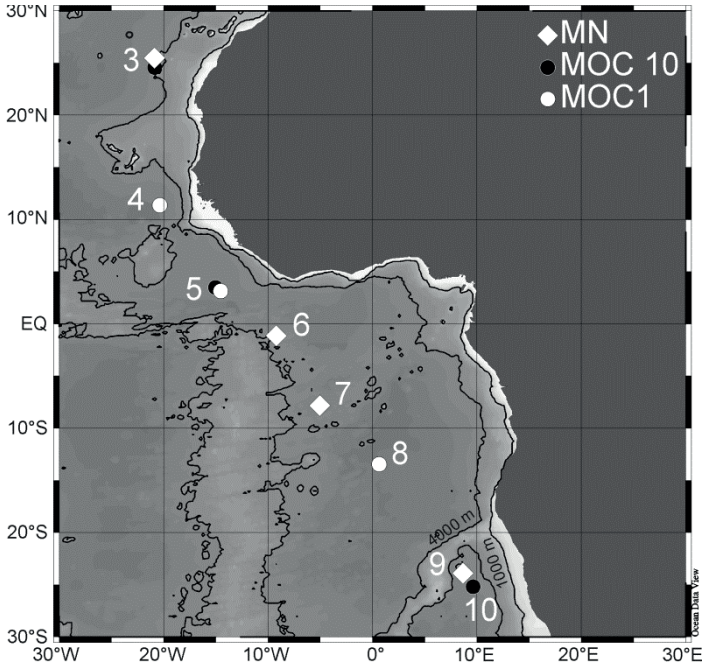

Figure 1: Map showing the stations, where spinocalanid copepods were sampled during ANTXXIV/1 on RV *Polarstern* in the tropical and subtropical eastern Atlantic Ocean in November 2007. Different sampling net types are indicated as MN: multinet, MOC10: 10m^2 MOCNESS, MOC1: 1m^2 MOCNESS.

Molecular genetic analyses

Genomic DNA was extracted from the cephalosomes of the adult spinocalanid females using Chelex (Chelex resin, Bio-Rad) to preserve the exuviae of the specimens. The samples were incubated in 40 µL of a 10% Chelex solution for 20 min at 95°C. After centrifugation, the supernatant was stored at -20°C. The remaining exuviae were kept in absolute ethanol at -20°C for later morphological analyses. PCR amplifications were carried out by using *illustra PuReTaq Ready-to-Go PCR* Beads (GE Healthcare) applying 2 µL DNA templates in 23 µL reaction mixture. Cytochrome c oxidase subunit I (COI) was amplified and sequenced using the primer pair LCO1490 (Folmer et al. 1994) and C1-N-2191 (alias Nancy; Simon et al. 1994). The thermal profile was 5 min at 95°C, followed by 40 cycles of 30 s at 95°C, 60 s at 42°C, 60 s at 72°C and one final

elongation step of 7 min at 72°C. Complete 18S rDNA amplification was accomplished using the primer pair 18A1 mod and 1800 mod (Raupach et al. 2009). The thermal profile was 5 min at 95°C, followed by 40 cycles of 45 s at 95°C, 50 s at 50°C, 200 s at 72°C and one final elongation step of 10 min at 72°C at an annealing temperature of 50°C (50 s) for 40 cycles. For sequencing, the primers F1, CF2, CR1 and R2 were additionally applied to receive the complete 18S rRNA gene sequence (Laakmann et al. 2013). PCR products were visualized using gel electrophoresis in a 1% agarose gel with ethidium bromide staining.

All PCR products were sent to Macrogen, Amsterdam, for purification and sequencing. Sequences were assembled, edited, checked for errors, and in case of COI for reading frames using the software Geneious (version 7.1.7). The *Spinocalanus* COI sequence deposited in GenBank (HQ150073 *Spinocalanus abyssalis*) was added to the present data set. No complete 18S sequence of Spinocalanidae was found in GenBank (until November 2015). Three sequences of *Pseudocalanus elongatus* of COI (JX995271, JX995272, JX995275) and complete 18S (JX995319, JX995320, JX995321), respectively, were added as outgroup to the data sets from GenBank, as Clausocalanidae are phylogenetically closest to Spinocalanidae (Blanco-Bercial et al. 2011). Sequences were aligned by MUSCLE using the software Geneious 7.1.7. All sequences were uploaded in GenBank (accession numbers KU247605-KU247866). The COI alignment comprised 173 sequences of 667 bp length, while the 18S alignment comprised 95 sequences each of 1674 bp length. The alignments were analyzed with RAxML-VI-HPC (version 8, Stamatakis 2014) inferring Maximum Likelihood trees with GTRGAMMA + I nucleotide substitution model using the bootstopping criteria, which automatically determine, if enough bootstrap replicates were conducted (Stamatakis 2014; Pattengale et al 2014). Pairwise genetic distances (*p* distance) were calculated with MEGA (version 6, Tamura et al. 2013). Species cluster based on *p* distances were tested by analysis of similarity (ANOSIM) with 999 permutations using the PRIMER software (version 6.1.1; Clarke and Gorley 2006).

The Automatic Barcode Gap Discovery (ABGD) algorithm is a method of species delimitation, sorting sequences into hypothetical species based on the barcode gap detecting significant differences between intra- and interspecific variations of the individuals' *p* distances. The *p* distance matrix derived from aligned COI sequences of all individuals was uploaded to the ABGD website http://wwwabi.snv.jussieu.fr/public/abgd/abgdweb.html and was run with the default settings applying a relative gap width (X) of 1. All available models (Jukes-Cantor (JC86), Kimura (K80)) were tested.

Proteomic fingerprinting using MALDI-TOF MS

The last metasomal segment/urosomes of 193 spinocalanid adult females were analyzed applying the MALDI-TOF MS technology according to the protocols by Riccardi et al. (2012) and Laakmann et al. (2013). Seven whole animals were added to the analyses to test whether they clustered correctly with the urosome only samples. Single specimens were incubated in 5 µL of matrix solution for 10 min at room temperature and dark conditions. The matrix solution consisted of saturated alpha-cyano-4-hydroxycinnamic acid (HCCA) in 50% acetonnitrile and 2.5% trifluoroacetic acid. After incubation, the sample-matrix mix was vortexed for 10 s and centrifuged for 30 s at 13000 RMP. In three replicates, 1µL of sample-matrix extract was placed on a target plate. After evaporation at room temperature for a few minutes, each spot was measured three times receiving nine mass spectra per specimen (technical replicates). Analyses were performed with the compact linear-mode bench-top microflex LT system (Bruker Daltonics) at a laser frequency of 60 Hz. To create one spectrum, 240 laser shots were generated at fixed optical laser energy and a pulse of 3 ns. Prior to each measurement cycle, calibration was performed using a bacterial test standard (Bruker Daltonics) containing a protein extract of *Escherichia coli* DH5alpha.

MALDI-TOF data analyses were performed in R (version 3.1.3, R core team, 2015). Raw spectra were imported into R using the MALDIquantForeign R package (version 0.9; Gibb 2014). Further processing and analyses of mass spectra were carried out using the MALDIquant package (version 1.12; Gibb and Strimmer 2012) after Gibb and Strimmer (2014). Mass spectra between 2-20 kDa were square root transformed and smoothed using the Savitzky-Golay-Filter. Baseline correction was conducted applying the SNIP algorithm with 20 iterations. To equalize intensities across spectra, normalization was performed with the Total-Ion-Current-calibration (TIC). Peak detection was applied to the averaged spectra of the technical replicates, while peaks that occurred in less than 100% of technical replicates were removed and the remaining peaks were binned. All replicates were averaged for each individual. Finally, a binary peak matrix was generated.

The binary peak matrix was used to calculated pairwise distances between the spectra. Hierarchical cluster analysis was based on a Euclidean distance matrix using Ward's minimum variance method and a bootstrapping analysis (n=1000) applying the vegan R package (version 2.3-0; Oksanen et al. 2015) and pvclust R package (version 1.3-2; Suzuki and Shimodaira 2014). Distances within and between species were tested for significance by analysis of similarity

(ANOSIM) with 999 permutations using the PRIMER software (version 6.1.6; Clarke and Gorley, 2006).

Results

Based on morphology, 28 spinocalanid species were identified from the sample material of the present study. The most prominent morphological features are listed in Table 1. *Spinocalanus longispinus/stellatus* and *S. neospinosus/hoplites* bear morphological characteristics of both species. For example, *S. longispinus/stellatus* had very conspicuous ventrolateral edges of the cephalosome ("shoulders") and metasomal spinules on the left side of the cephalosome, as described for *S. longispinus* (Brodsky 1950; Razouls et al. 2005-2015). In contrast, the spine comb on the coxa of the maxilliped was clearly on a protrusion, similar to descriptions of *S. stellatus* (Brodsky 1950; Razouls et al. 2005-2015). These two species are currently not generally accepted and ranked among *Spinocalanus horridus* (WoRMS Editorial Board 2015). However, *S. horridus* was much more spinulose on both sides of the cephalosome and had very long spines on the basis of the maxilliped (Table 1). *Spinocalanus dispar* carried four posterior setae on the first inner lobe, which is contrary to descriptions of *Spinocalanus longicornis*, and a fringe of hair was missing on the supra-anal plate, which was described for *Spinocalanus abyssalis* (Schulz 1989). *S. magnus*, *S. antarcticus* and *S. angusticeps* are characterized by distinctively different body shapes and morphological characters (see Damkaer 1975). *S. magnus* and *S. antarcticus* could only be distinguished based on their body shape.

Table 1: List of the species revealed by COI and MALDI-TOF analyses. Sampling depth, sampling locations, total length and most prominent morphological characters are listed, if species identification was ambiguous (n: number of specimens; TL: total length, U/Pr: ratio of urosome to prosome length). Otherwise see Grice (1971), Damkaer (1975) and Schulz (1989; 1996). Morphological features are summarized for putative cryptic in a species complex, since only molecular and no morphological differences were hitherto found. A: antenna, Mx: maxilla, Li: inner lobe, Mxp: maxilliped, C: coxa, B: basis, Exp: exopodite, End: endopodite, P: pedigerous segment, CR: caudal rami.

Species	n	Depth [m]	Latitude	TL [mm]	U/Pr	Most prominent morphological characters (if identification was ambiguous; after Grice (1971), Damkaer (1975) and Schulz (1989; 1996)
Spinocalanus						
Group A (Damkaer 1975)						
without metasomal spinules:						
S. dispar						A2 Exp1 with 1 seta, A1 broken
1	8	400-1000	24-11°N	0.95-1.20	2.7-3.9	Mx1 Li1 with 4 posterior setae
2	2	600-800	13°S	1.00/1.02	3.3/3.1	Mxp C spine comb absent on C, present on
3	4	2000-5000	25°S	1.12-1.22	3.1-3.7	B (not in all samples visible)
4	10	800-4000	11°N-13°S	0.99-1.34	2.4-3.3	
5	9	600-2000	3°N-13°S	1.00-1.23	2.7-3.4	Mxp End3 with 3 setae
6	1	4000-5000	25°S	1.12	3.9	P1 Exp distal spines long and slender, exceeding next Exp P2 Exp1 outer spine rather long P2/3 C with 3 rows of spinules No fringe of hair on supra-anal plate Slightly asymmetrical CR
S. elongatus						A2 Exp1 with 1 seta
1	3	2000-3000	3°N	1.58-1.66	3.0-3.2	Mx1 Li1 with 4 posterior setae
2	2	2000-4000	25°S	1.60/1.90	NA/2.8	Mxp C with 3 transverse spine combs (*S. elongatus* 2: 1st row inconspicuous)
3	4	800-1000	13°S-25°S	1.08-1.20	3.1-3.7	Mxp B with 1 spine comb with long spines Mxp End3 with 2 setae P1 Exp distal spines rather long and slender (not exceeding next Exp) P2/3 C with 3 rows of spinules P3 End3 with long spinules
S. similis	2	2000-3000	25°S	1.63/1.76	4.0/3.6	A2 Exp1 with 1 seta Mxp C with very fine rows of spines on C, B with 1 spine comb with long spines
S. brevicaudatus	13	400-5000	3°N-25°S	1.31-1.72	2.7-3.9	Mxp C without spines comb, B with 1 spine comb P1 Exp3 without spinules P2/3 C rather nude
S. terranovae	2	2000-3000	25°S	1.80/1.82	3.3/3.6	Mxp C without spines comb, B with 1 spine comb P1 Exp3 with spinules P2/3 C with 3 row of spinules P4 C with 2 rows of spinules
S. aspinosus	6	2000-3000	3°N-25°S	1.19-1.74	3.0-4.1	Mxp C and B with 1 spine comb, of C on protrusion, spines of equal length P2/3 C with 4 rows of spinules P4 with at least 3 rows of spinules
with metasomal spinules:						
S. horridus	11	800-1000	11°N-25°S	2.33-2.50	2.0-2.8	Spinules on Th1-Th4, strikingly spinulose Mxp spine comp on C and B, of C not on protrusion with very short spines (almost half as long as on B), very long spines on B
S. hoplites	4	2000-5000	25°S	1.53-1.98	3.1-4.5	Spinules on Th1-Th4 Cephalosome with conspicuous shoulders Mxp spine comp on C and B, of C on protrusion, spines of equal length (at least 10 spines per comb)
S. usitatus	6	800-5000	3°N-25°S	1.76-1.98	2.3-3.1	Spinules on Th1-Th4, very few on Th4, less spinulose than *S. horridus* Cephalosome with conspicuous shoulders Mx2 base of 5th lobe with 7 (?) spines Mxp spine comb on C and B, of C on protrusion, spines on C much shorter (half as long) than on B

Species	n	Depth [m]	Latitude	TL [mm]	U/Pr	Most prominent morphological characters (if identification was ambiguous; after Grice (1971), Damkaer (1975) and Schulz (1989; 1996)
S. stellatus	2	2000-5000	25°S	2.23/2.25	2.6/2.5	Spinules on Th1-Th4, more distinct on the left side, very inconspicuous on right side Cephalosome with conspicuous shoulders Spine comb on C and B of Mxp, of C on protrusion, on B very inconspicuous P2/3 C with 4 rows of spinules, very spinulose P4 3 rows of spinules
S. longispinus/stellatus	8	2000-5000	3°-25°S	2.53-3.00	2.2-4.3	Spinules on Th1-Th4, more distinct on left side, but clearly visible on both sides Cephalosome with conspicuous shoulders, on the left side more pronounced Mxp spine comb on C and B, of C on protrusion, approx. equal in length Mxp C with additional spinules P2/3 C with 4 rows of spinules, very spinulose P4 3 rows of spinules
S. spinosus						
1	17	400-1000	24°N-13°S	1.83-2.03	2.8-4.1	
2	1	600-800	13°S	1.90	3.8	
S. neospinosus/hoplites	5	800-2000	24-3°N	1.72-1.95	2.2-3.1	Spinules on at least on the left side Th1-4 Cephalosome with conspicuous shoulders Mxp spine comb on C and B, of C on large protrusion, spines on C longer than on B, but only few spines: C 3-5 spines, B 2-3 spines P2-4 1-3 rows of spinules, less spinulose
S. neospinosus	3	400-1000	24°N-13°S	1.48-1.70	2.1-2.7	Spinules only on left Th1-Th4 (very conspicuous) Mxp spine comb on C and B, not on protrusion, very small on C P2/3 C with 3 rows of spinules
Group B (Damkaer 1975)						
S. magnus	13	200-1000	11°N-13°S	2.20-2.55	2.8-3.8	
S. antarcticus	3	2000-3000	25°S	2.55-2.83	3.4-3.9	
S. angusticeps	2	1000-3000	25°S	2.33/2.60	3.9/3.7	
Mospicalanus						
M. schielae	6	2000-5000	25°S	1.95-2.10	3.4-4.7	
Mospicalanus sp.	4	2000-4000	3°N	1.12-1.17	3.8-3.9	Similar to *M. schielae*, but smaller
Mimocalanus						
P1 End with outer lobe:						
M. nudus	3	600-1000	2°N	2.40-2.58	3.5-40	P1 Exp2 outer spine rather short, not longer than two thirds of Exp3 P2 End2 with 1 outer seta P2/3 C with inner seta Th5 reaching approx. to mid-genital segment
M. heronae						P2 End2 with 1 outer seta
1	9	600-1000	11-3°N	1.62-1.80	3.3-4.6	P2/3 C with 1 inner seta
2	1	4000-5000	25°S	1.72	4.4	(*M. heronae 2&3*: P2 End2 all missing)
3	2	4000-5000	25°S	1.38/1.40	3.9/3.7	
M. cultrifer						P2 End2 no outer seta
1	5	2000-5000	3°N-25°S	1.36-1.62	3.3-4.7	P2/P3 C with 1 inner seta
2	5	600-1000	11°N	1.05-1.40	2.8-4.4	(*M. cultrifer 2*: P2 End all missing)
M. crassus	5	800-1000	3°N-13°S	1.05-1.17	3.2-3.9	
Mimocalanus sp. 1	1	2000-3000	25°S	1.88	3.9	P2/3 C with inner seta Th5 very long (longer than *M. nudus*) (all other Exps and Ends missing) *M. sulcifrons?*

Species	n	Depth [m]	Latitude	TL [mm]	U/Pr	Most prominent morphological characters (if identification was ambiguous; after Grice (1971), Damkaer (1975) and Schulz (1989; 1996)
Mimocalanus sp. 2	1	4000-5000	25°S	2.10	4.3	P2 End2 with no outer seta P2 C without inner seta? P3 C with inner seta Similar *M. cultrifer* (much larger)
Monacilla						
M. typica	14	400-2000	11°N-13°S	2.05-2.58	2.5-3.7	
M. tenera	2	1000-2000	25°S	2.28/2.40	2.8/2.6	
Teneriforma						
Teneriforma naso						Rostral cone apically rounded
1	1	200-400	7°S	0.86	3.1	P1 End in total with 4 setae
2	2	600-800	23°S	0.99/1.01	3.2/2.9	

Monophyly of the family Spinocalanidae was supported by 100% bootstrap value based on the analyses of the 18S rDNA (1674 bp) with *Pseudocalanus elongatus* (Clausocalanidae) as outgroup taxon (Fig. 2). In total, five genera of Spinocalanidae were identified morphologically from the zooplankton samples prior to molecular analyses and from the exuviae: *Spinocalanus, Mimocalanus, Monacilla, Teneriforma* and *Mospicalanus*. Apart from the genus *Spinocalanus*, all other genera were monophyletic clades. The genera were supported by high bootstrap values (89-99%). Minimum uncorrected *p* distances between the genera differed between 0.4 and 1.5% (Table 2). The genus *Spinocalanus*, however, was polyphyletic: One clade consisted of *S. magnus* and *S. antarcticus*, being closest to *Monacilla*, a second clade was formed by a singleton sequence of *S. angusticeps,* and a third large clade contained all other identified species, being closest to *Mospicalanus*. The large *Spinocalanus* clade showed the largest difference with a mean p distance of 2.1% to the *S. magnus* and *S. antarcticus* group. It comprised six clusters with *S. brevicaudatus*, *S. elongatus 1* and *S. elongatus 2* as separate clusters and three larger clusters consisting of 1) *S. dispar* 1-6, 2) *S. longispinus/stellatus, S. neospinosus/hoplites, S. usitatus, S. similis and S. spinosus 2*, and 3) *S. aspinosus, S. elongatus 3, S. hoplites, S. horridus, S. stellatus, S. neospinosus, S. spinosus* and *S. terranovae*. Thus, the species within these three species complexes could not be discriminated based on their 18S rDNA sequence indicating a very close relationship of these species. However, aside from the *S. dispar* sub-cluster, the other two sub-clusters were rather random demonstrating the deficiency of 18S rDNA for a high taxonomic resolution.

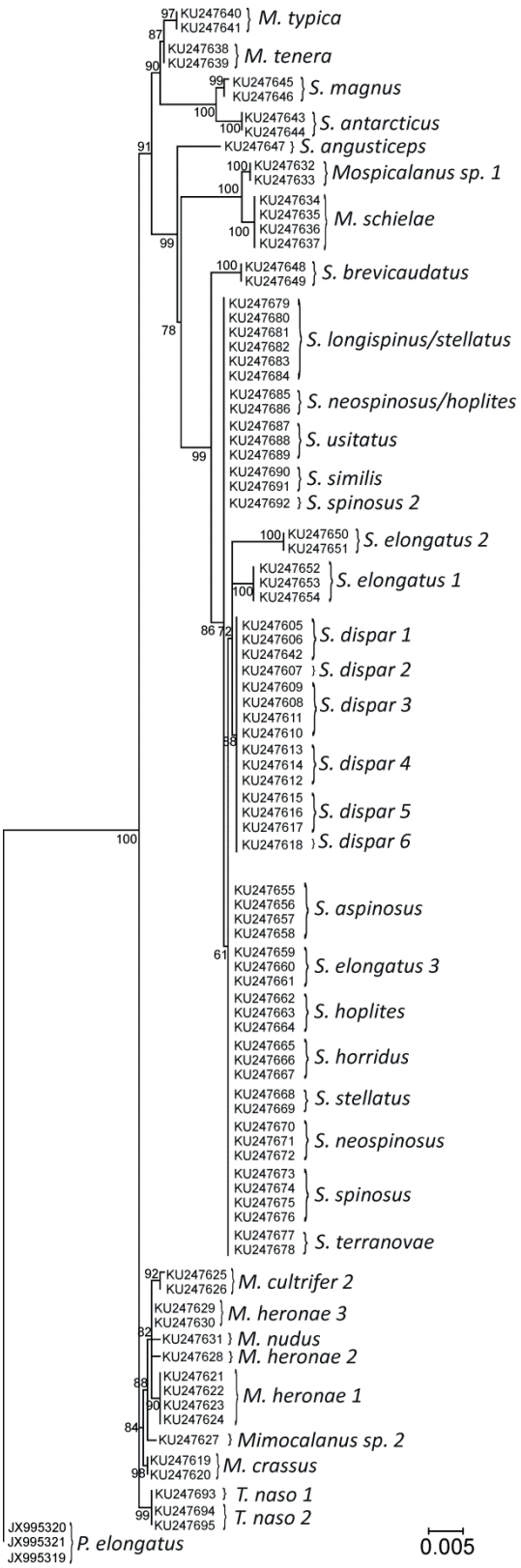

Figure 2: Reconstruction of evolutionary relationships among Spinocalanidae. RAxML Maximum Likelihood tree for the 18S rDNA fragments (1674 bp alignment). Numbers at the nodes represent the percentage bootstrap values >50%.

Table 2: Test for distinctiveness of genera based on 1674 bp of the 18S rDNA (n: no. of specimens).

Species group/genus	n	Mean p-distance within group	Closest group	Mean p-distance to closest group
Mospicalanus	6	0.002	*S. angusticeps*	0.015
Spinocalanus	62	0.002	*S. angusticeps*	0.013
S. magnus/antarcticus	4	0.004	*Monacilla*	0.012
S. angusticeps	1	-	*Monacilla*	0.012
Monacilla	4	0.001	*Teneriforma*	0.006
Teneriforma	3	0.000	*Mimocalanus*	0.004
Mimocalanus	13	0.002	*Teneriforma*	0.004
Outgroup				
P. elongatus	3	0.000	*Teneriforma*	0.020

The species delimitation methods ABGD revealed 39 spinocalanid lineages based on COI divergence (Tables 2 and 3, Fig. 3a). The 18S and MALDI-TOF results suggest one more species, *Monacilla tenera*, which could not be sequenced for COI. Thus, 40 lineages of Spinocalanidae were identified in total, most of which belonged to the genus *Spinocalanus* (Tables 1 and 3). Molecular analyses revealed 22 lineages of *Spinocalanus*, plus *S. magnus*, *S. antarcticus* and *S. angusticeps,* which seem to represent separate genera. Levels of mtCOI variations within lineages ranged from 0.3-3.8% and, based in ABGD results, were significantly lower than minimum interspecific variation to the closest neighboring species ranging from 9.6-18.6% (maximum 27%) (Table 3, Fig. 3a).

Table 3: Tests for species distinctiveness of 667 bp for COI (n: number of specimens).

Species	n	Mean p-distance within group	Closest group	Mean p-distance	
				closest group	most distant group
Spinocalanus					
S. dispar 1		0.008	*S. dispar 2*	0.156	0.229
S. dispar 2	1	-	*S. dispar 3*	0.124	0.228
S. dispar 3	1	-	*S. dispar 4/5/6**	0.122	0.227
S. dispar 4	10	0.009	*S. dispar 3*	0.122	0.234
S. dispar 5	3	0.019	*S. dispar 3*	0.122	0.228
S. dispar 6	1	-	*S. dispar 3*	0.122	0.231
S. brevicaudatus	12	0.010	*S. dispar 6*	0.186	0.244
S. elongatus 1	3	0.002	*S. elongatus 3*	0.139	0.225
S. elongatus 2	2	0.008	*S. elongatus 1*	0.143	0.221
S. elongatus 3	3	0.003	*S. elongatus 1*	0.139	0.231
S. aspinosus	5	0.016	*S. stellatus/S. longspinus/stellatus*	0.163	0.265
S. horridus	10	0.014	*S. stellatus/S. neospinosus/holpites*	0.172	0.243
S. stellatus	3	0.009	*S. stellatus*	0.148	0.243
S. hoplites	4	0.015	*S. similis*	0.157	0.249

Species	n	Mean p-distance within group	Closest group	Mean p-distance	
				closest group	most distant group
S. neospinosus	3	0.003	*S. elongatus 1*	0.165	0.228
S. terranovae	2	0.000	*S. stellatus*	0.172	0.274
S. spinosus	13	0.007	*S. longispinus/stellatus*	0.155	0.239
S. spinosus 2	1	-	*S. stellatus*	0.180	0.265
S. usitatus	2	0.005	*S. stellatus /S. spinosus*	0.160	0.245
S. neospinosus/hoplites	2	0.025	*S. longispinus/stellatus*	0.169	0.262
S. longispinus/stellatus	6	0.019	*S. stellatus*	0.148	0.274
S. similis	2	0.038	*S. stellatus*	0.155	0.249
S. angusticeps	1	-	*S. elongatus* 3	0.153	0.220
S. magnus	13	0.000	*S.antarcticus*	0.096	0.251
S.antarcticus	4	0.000	*S. magnus*	0.096	0.262
Mimocalanus					
M. heronae 1	8	0.003	*M. heronae* 3	0.114	0.248
M. heronae 2	1	-	*M. heronae* 3	0.116	0.265
M. heronae 3	2	0.009	*M. heronae* 1	0.114	0.256
M. crassus	5	0.009	*Mimocalanus sp. 1*	0.136	0.247
M. nudus	2	0.012	*Mimocalanus sp.* 2	0.140	0.268
M. cultrifer 1	4	0.024	*M. cultrifer* 2	0.123	0.230
M. cultrifer 2	4	0.035	*M. cultrifer* 1	0.123	0.254
Mimocalanus sp. 1	1	-	*M. crassus*	0.136	0.258
Mimocalanus sp. 2	1	-	*M. heronae* 3	0.133	0.265
Mospicalanus					
M. schielae	6	0.005	*S. angusticeps*	0.155	0.229
Mospicalanus sp.	4	0.001	*S. elongatus* 3	0.146	0.242
Monacilla					
M. typica	7	0.008	*S. elongatus* 3	0.186	0.247
M. tenera	-	-	-	-	-
Teneriforma					
*Teneriforma sp.*1	1	-	*Teneriforma sp.*2	0.154	0.268
*Teneriforma sp.*2	2	0.018	*Teneriforma sp.*1	0.154	0.274
Outgroup					
P. elongatus	1	-	*Mimocalanus sp. 1*	0.195	0.288

*similar distance

Species clusters revealed by mtCOI were generally in line with species clusters based on MALDI-TOF mass spectra (Figs. 3 and 4). However, species clusters with ≤3 specimens were difficult to discriminate based on proteome profiles alone. Thus, groups were assigned based on the COI results. The ANOSIM based on these 40 species groups revealed highly significant differences between the groups and thus significantly lower intraspecific differences than distances between species (global R-value = 0.95; significance level = 0.1%). In total, 31 species could be clearly discriminated with high R-values usually ≥0.7, whereas nine species were only

represented by one individual. Only *S. elongatus 1* showed lower R-values between 0.3-0.6, compared to the samples of an ambiguous cluster containing almost all samples with n=1. This low R-value resulted from the fact that one *S. elongatus 1* sample (M41/KU247816) wrongly clustered in this ambiguous group (Fig. 3b). This group comprised *Mimocalanus sp.* 1 and 2, *M. heronae* 2, *Mospicalanus sp., S. spinosus* 2 and *S. elongatus* 2, of which only one MALDI-TOF sample was available, and also the two samples of *S. stellatus*. *Teneriforma sp.* 1 (also n=1) clustered nearby *Teneriforma sp.* 2. *Spinocalanus dispar 3* and *S. dispar 6* clustered nearby two other samples, of which no gene sequences were available, but were morphologically described as *S. dispar* (Fig. 3b).

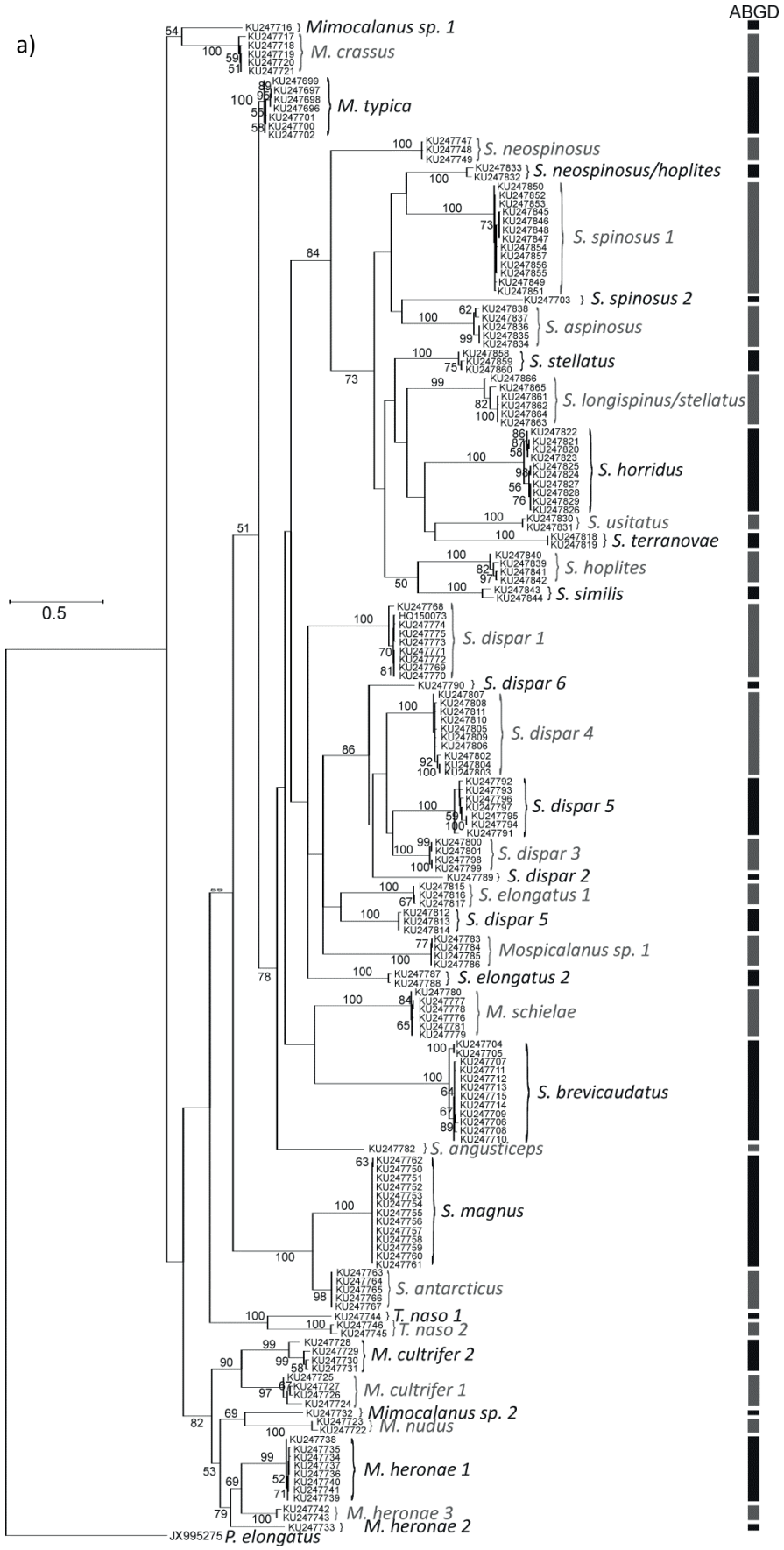
a)
ABGD
0.5
Mimocalanus sp. 1
M. crassus
M. typica
S. neospinosus
S. neospinosus/hoplites
S. spinosus 1
S. spinosus 2
S. aspinosus
S. stellatus
S. longispinus/stellatus
S. horridus
S. usitatus
S. terranovae
S. hoplites
S. similis
S. dispar 1
S. dispar 6
S. dispar 4
S. dispar 5
S. dispar 3
S. dispar 2
S. elongatus 1
S. dispar 5
Mospicalanus sp. 1
S. elongatus 2
M. schielae
S. brevicaudatus
S. angusticeps
S. magnus
S. antarcticus
T. naso 1
T. naso 2
M. cultrifer 2
M. cultrifer 1
Mimocalanus sp. 2
M. nudus
M. heronae 1
M. heronae 3
M. heronae 2
JX995275 P. elongatus

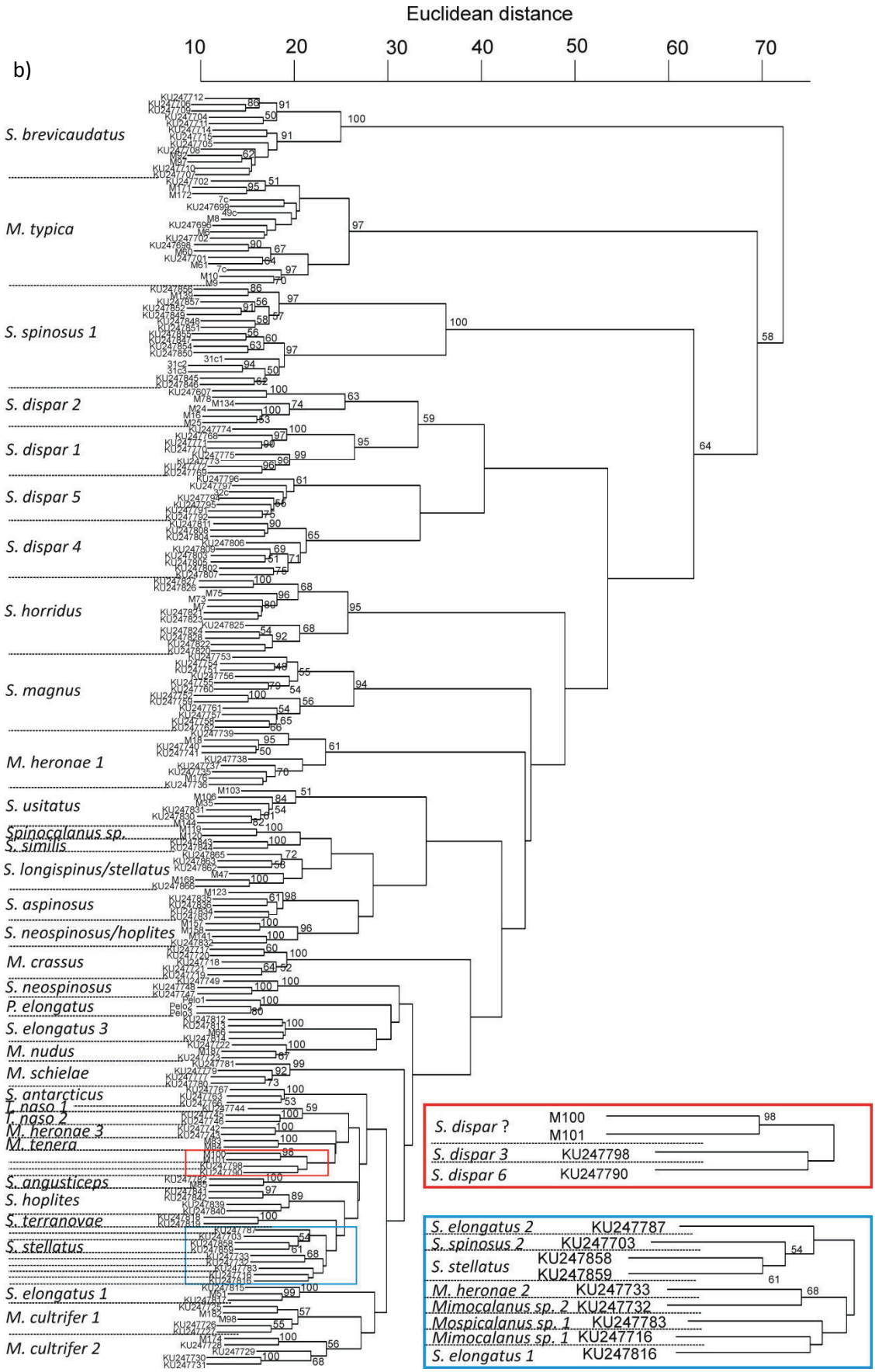
Euclidean distance
10
20
30
40
50
60
70
b)
S. brevicaudatus
M. typica
S. spinosus 1
S. dispar 2
S. dispar 1
S. dispar 5
S. dispar 4
S. horridus
S. magnus
M. heronae 1
S. usitatus
Spinocalanus sp.
S. similis
S. longispinus/stellatus
S. aspinosus
S. neospinosus/hoplites
M. crassus
S. neospinosus
P. elongatus
S. elongatus 3
M. nudus
M. schielae
S. antarcticus
L. naso 1
L. naso 2
M. heronae 3
M. tenera
S. angusticeps
S. hoplites
S. terranovae
S. stellatus
S. elongatus 1
M. cultrifer 1
M. cultrifer 2
S. dispar ?
M100
M101
S. dispar 3
KU247798
S. dispar 6
KU247790
S. elongatus 2
KU247787
S. spinosus 2
KU247703
S. stellatus
KU247858
KU247859
M. heronae 2
KU247733
Mimocalanus sp. 2
KU247732
Mospicalanus sp. 1
KU247783
Mimocalanus sp. 1
KU247716
S. elongatus 1
KU247816

Figure 3: a) RAxML maximum Likelihood tree for the COI mtDNA fragments (667 bp alignment). Numbers at the nodes represent the percentage bootstrap values >50%. Results of the species delimitation method ABGD (Automatic Barcode Gap Discovery) method are indicated as alternating black and grey boxes. b) Cluster analyses of the MALDI-TOF mass spectra based on Euclidean distance. Numbers at the nodes represent the percentage bootstrap values >50%.

Discussion

The present study provides first insights into the molecular diversity of the morphologically challenging and ecologically important copepod family Spinocalanidae by analyzing mitochondrial and nuclear gene fragments, as well as protein mass fingerprints. These methods agreed well in the number of lineages found within this copepod family. The molecular results provide evidence that this meso- to abyssopelagic copepod family is much more diverse than previously described based on morphological characters alone. Furthermore, the genus *Spinocalanus* appears to be polyphyletic, which is supported by the morphological separation of species-groups within this genus by Damkaer (1975). The large differences in the 18S rDNA gene and distinct body shapes and morphological characters even suggest two separate genera for the *S. magnus* and *S. antarcticus* complex and for *S. angusticeps*. To verify this separation of *S. angusticeps,* a detailed study comprising more specimens is needed.

Analysis of 18S rDNA sequence variation confirmed the highly conservative state of this region, as some species could not be discriminated. Hence, this gene region proves to be useful as a phylogenetic marker for higher taxonomic levels (Hillis and Dixon, 1991; Bucklin et al., 2003; Laakmann et al., 2013). 18S rDNA of copepods was previously described to differ by <1-6% among genera; however, this referred to a much shorter region of this gene (660 bp; Bucklin et al. 2003). Genetic distances between the spinocalanid genera (0.4-1.5%) were well within this range. There was no variability of 18S rDNA sequences for individuals of a given species, which is a consequence of concerted evolution of ribosomal DNA (Hillis et al. 1991; Eickbush and Eickbush 2007) and has been demonstrated for other calanoid copepods (Bucklin et al. 2003; Laakmann et al. 2013). However, between certain spinocalanid species no differences were found, indicating either a close genetic relationship of these species or at least no differences of the 1674 bp sequence: 1) *S. dispar* 1-6, 2) *S. longispinus/stellatus, S. neospinosus/hoplites, S. usitatus, S. similis and S. spinosus 2*, and 3) *S. aspinosus, S. elongatus 2, S. hoplites, S. horridus, S. stellatus, S. neospinosus, S. spinosus* and *S. terranovae* (Fig. 2). Analyzing large 18S rDNA fragments (i.e. 1844 bp) resulted in differences between species within the same copepod genus

as observed in *Centropages*, *Pseudocalanus* and *Acartia* (Laakmann et al. 2013), whereas on a much shorter fragment (667 bp), closely related species of *Paraeuchaeta* could not be discriminated (Laakmann et al. 2012).

Genetic species delimitation

In total, 40 putative species of the spinocalanid family were identified based on cladistic analyses (maximum likelihood) of the mtCOI and the ABGD algorithm. These methods are independent from *a priori* defined groups and were congruent with each other. Speciation processes in marine copepods are apparently completed when COI sequence distinctiveness between two specimens are approximately ≥8-9% (Bucklin et al. 1999, 2003; Hill et al. 2001). This agrees well with species discrimination in the present study, as the minimum interspecific variation to the neighboring species was 9.6%.

Especially the *Spinocalanus* genus, which was most abundant, comprised more species than previously described by Park (1970), Grice (1971), Damkaer (1975) and Schulz (1989; 1996) based on morphological characters. Some of these, such as the *S. dispar* complex, may even be cryptic species, which is a common phenomenon in marine copepods (Bucklin et al. 1999; Hill et al. 2001; Goetze 2003; Bucklin and Frost 2009; Cornils and Held 2014). High morphological similarities explain why species initially described as *S. stellatus* and *S. longispinus* are currently all summarized to *S. horridus* and species such as *S. pteronus* is synonymous with *S. usitatus* (Damkaer 1975; WoRMS Editorial Board 2015). As Spinocalanidae have only been reviewed in detail by Damkaer (1975), who only considered Arctic specimens, a new morphological review of this family from other latitudes is necessary. However, second exo- and endopodites as well as the first antennae are often missing, due to the stressful net sampling procedure from greater depths. This makes molecular species identification methods indispensible for fragile, deep-sea copepod families.

Proteomic fingerprinting

In general, the species discrimination based on mtCOI agreed well with the species clusters based on MALDI-TOF mass spectra, even for putative cryptic species. The cluster analysis of MALDI-TOF mass spectra showed species-specific peak patterns between 2 and 20 kDa with significantly lower intraspecific differences than distances between species, resulting in similar

species clusters as identified by COI analyses. Thus, species identification of closely related or even putative cryptic species with MALDI-TOF MS is possible. Besides, this method proved to be as simple and fast as indicated by previous studies (Feltens et al. 2012; Laakmann et al. 2013). These results complement studies that demonstrated successful discriminations of zooplankton species such as shrimp (Salla and Murray 2013) and copepod species (Riccardi et al. 2012; Laakmann et al 2013). However, sample size was often insufficient to conduct robust statistical analyses and at least three to five individuals of one species were needed to establish clear species clusters. In this context, routine application and the establishment of mass spectral data bases for zooplankton, as already available for microorganisms, will be essential to establish MALDI-TOF MS as a routine species identification method, as it is already established in diagnostic bacteriology (e.g. Seng et al. 2009; Saffert et al. 2011; Laakmann et al. 2013).

The database of diversity and distribution of marine planktonic copepods of the Observatoire Océanologique de Banyuls (Razouls et al. 2005-2015) only lists 17 *Spinocalanus,* 6 *Mimocalanus,* 3 *Monacilla* and 4 *Teneriforma* species in subtropical and/or temperature waters of the Atlantic Ocean, while most studies focused on polar regions (Damkaer 1975; Razouls et al. 2005-2015). Only one species of *Mospicalanus* (*M. schielae*) was described, which was found in the Antarctic Weddell Sea (Schulz 1989). In contrast, our study demonstrates that many of the spinocalanid species have much wider distributional ranges than previously thought. For example, *M. crassus, M. cultrifer*, *S. aspinosus, S. hoplites* and *S. oligospinosus* were found so far only in Caribbean waters, while *S. usitatus* was reported in temperate waters in the NW Atlantic and *S. terranovae* in the SW Atlantic. In contrast, *S. sulcifrons*, *S. elongatus, S. antarcticus, S. horridus, S. longispinus* and *S. stellatus* were mainly found in Arctic or Antarctic waters, the latter three also in the NE and NW Pacific. *S. horridus* (=*longispinus*) and *S. elongatus* were even classified as Arctic endemic species (Kosobokova et al. 2011). Hence, molecular comparisons of populations from tropical and polar regions may reveal interesting insights into the true diversity and phylogeography of this copepod family.

The present study analyzed a few, non-quantitative samples of Spinocalanidae from the subtropical and tropical eastern Atlantic Ocean (24°N-25°S). Considering the high number of species found in these rather limited samples (~200 specimens), the true species richness of this copepod family considered world-wide seems to be underestimated. Given the high abundance and important ecological role of Spinocalanidae in deep-sea ecosystems in almost all marine regions (Kosobokova et al. 2002; Wishner et al. 2008; Bode et al. submitted), knowledge about

their diversity and distributional patterns will shed new light on deep-sea biodiversity and ecosystem functioning. Due to its time- and cost-efficiency, MALDI-TOF MS represents a very promising tool in zooplankton biodiversity research, simplifying and accelerating future research. This molecular technique offers new prospects and opportunities for zooplankton studies with high taxonomic resolution of adults and possibly even juvenile stages.

Acknowledgments

We are grateful for the support of the captain, the crew, and the scientific participants of RV *Polarstern* during ANT-XXIV/1 (PS71). Furthermore, we would like to thank Janne Timm for allowing us to use the laboratory facilities for parts of the genetic analyses at the Center for Environmental Research and Sustainable Technology (UFT), and Thomas Knebelsberger for his support and helpful advices during handling of the MALDI-TOF MS at the German Center for Marine Biodiversity Research (DZMB). Finally, our special thanks go to Sebastian Gibb, who helped establishing the R scripts. This study is a contribution from the Census of Marine Zooplankton (CMarZ, see www.CMarZ.org), a field project of the Census of Marine Life.

References

Aarbakke, O.N.S., Bucklin, A., Halsband, C., Norrbin, F., 2014. Comparative phylogeography and demographic history of five sibling species of *Pseudocalanus* (Copepoda: Calanoida) in the North Atlantic Ocean. J. Exp. Mar. Biol. Ecol. 461, 479-488.

Blanco-Bercial, L., Àlvarez-Marqués, F., 2007. RFLP procedure to discriminate between *Clausocalanus* Giebrecht, 1988 (Copepoda, Calanoida) species in the Central Cantabrian Sea. J. Exp. Mar. Biol. Ecol. 344, 73-77.

Blanco-Bercial, L., Bradford-Grieve, J.M., Bucklin, A., 2011. Molecular phylogeny of the Calanoida (Crustacea: Copepoda). Mol. Phylogenet. Evol. 59, 103-113.

Bode, M., Hagen, W., Koppelmann, R., Cornils, A., Teuber, L., Kaiser, P., Auel, H., submitted. Role of copepod communities in carbon budgets in the eastern Atlantic Ocean - Regional and vertical patterns from 24°N to 21°S. Deep-Sea Res. I.

Bradford-Grieve, J.M., 1994. The marine fauna of New Zealand: Pelagic Calanoid Copepoda: Magacalanidae, Calanidae, Paracalanidae, Mecynoceridae, Eucalanidae, Spinocalanidae, Clausocalanidae. New Zealand Oceanographic Institute, Wellington, 101 pp.

Bradford-Grieve, J.M., 2002. Colonization of the pelagic realm by calanoid copepods. Hydrobiol. 485, 223-244.

Brodsky, K.A., 1950. Calanoida of the far-eastern seas and polar basin of the USSR. Veslonogie rachki (Calanoida) dalnevostochnykh morei SSSR i pol'yarnogo basseina. Opredeliteli po Faune SSSR, Nauka, Leningrad 35, 1-442 (Russian). (English translation see Brodsky, 1967).

Bucklin, A., Bentley, A.M., Franzen, S.P., 1998. Distribution and relative abundance of Pseudocalanus moultoni and P-newmani (Copepoda: Calanoida) on Georges Bank using molecular identification of sibling species. Mar. Biol. 132, 97-106.

Bucklin, A., Guarnieri, M., Hill, R.S., Bentley, A.M., Kaartvedt, S., 1999. Taxonomic assessment of planktonic copepods using mitochondrial COI sequence variation and competetive, species-specific PCR. Hydrobiol. 401, 239-254.

Bucklin, A., Frost, B.W., Bradford-Grieve, J.M., Allen, L.D., Copley, N.J., 2003. Molecular systematic and phylogenetic assessment of 34 calanoid copepod species of the Calanidae and Clausoalanidae. Mar. Biol. 142, 333-343.

Bucklin, A., Hopcroft, R.R., Kosobokova, K.N., Nigro, L.M., Ortman, B.D., Jennings, R.M., Sweetman, C.J., 2010. DNA barcoding of Arctic Ocean holozooplankton for species identification and recognition. Deep-Sea Res. II 57, 40-48.

Clarke, A., Gorley, R.N., 2006. PRIMER v6: User manual/tutorial. PRIMER-E. Plymouth. 192 pp.

Claydon, M.A., Davey, S.N., Edwards-Jones, V., Gordon, D.B., 1996. The rapid identification of intact microorganisms using mass spectrometry. Nat. Biotechnol. 14, 1584-1586.

Cornils, A., Held, C., 2014. Evidence of cryptic and pseudocryptic speciation in the *Paracalanus parvus* species complex (Crustacea, Copepoda, Calanoida). Front. Zool. 11, 1-17.

Damkaer, D.M., 1975. Calanoid copepods of the genera *Spinocalanus* and *Mimocalanus* from the central Arctic Ocean, with a review of the Spinocalanidae. NOAA Tech Rep NMFS CIRC-391, 88 pp.

Eickbush, T.H., Eickbush, D.G., 2007. Finely orchestrated movements: evolution of the ribosomal RNA genes. Genetics 175, 477-485.

Feltens, R., Gorner, R., Kalkhof, S., Groger-Arndt, H., von Bergen, M., 2010. Discrimination of different species from the genus *Drosophila* by intact protein profiling using matrix-assisted laser desorption ionization mass spectrometry. BMC Evol. Biol. 10.

Gibb, S., Strimmer, K., 2012. MALDIquant: A versatile R package for the analysis of mass spectrometry data. Bioinformatics 28, 2270-2271.

Gibb, S., Strimmer, K., 2014. Species identification using MALDIquant.

Gibb, S., 2014. MALDIquantForeign: Import/Export routines for MALDIquant. R pack. ver. 0.9. http://CRAN.R-project.org/package=MALDIquantForeign.

Goetze, E., 2003. Cryptic speciation on the high seas: Global phylogenetics of the copepod family Eucalanidae. Proc. R. Soc. Lond. B 270, 2321-2331.

Grice, G.D., Hulsemann, K., 1965. Abundance, vertical distribution and taxonomy of calanoid copepods at selected stations in the northeast Atlantic. J. Zool. 146, 213-262.

Grice, G.D., 1971. Deep water calanoid copepods from the Mediterranean Sea. Family Spinocalanidae (I). Cah. Biol. Mar. 12, 273-281.

Herbert, P.D.N., Cywinska, A., Ball, S.L., deWaard, J.R., 2003. Biological identifications through DNA barcodes. Proc. R. Soc. Lond. B 270, 313-321.

Hill, R.S., Allen, L.D., Bucklin, A., 2001. Multiplexed species-specific PCR protocol to discriminate for N. Atlantic *Clanaus* species, with an mtCOI gene tree for ten *Calanus* species. Mar. Biol. 139, 279-287.

Hillis, D.M., Dixon, M.T., 1991. Ribosomal DNA: Molecular Evolution and phylogenetic inference. Q. Rev. Biol. 66, 411-453.

Hillis, D.M., Moritz, C., Porter, C.A., Baker, R.J., 1991. Evidence for biased gene conversion in concerted evolution of ribosomal DNA. Science 228, 308-311.

Holland, R.D., Wilkes, J.G., Rafii, F., Sutherland, J.B., Persons, C.C., Voorhees, K.J., Lay, J.O., 1996. Rapid identification of intact whole bacteria based on spectral patterns using matrix-assisted laser desorption/ionization with time-of-flight mass spectrometry. Rapid Comm. Mass Spectrom. 10, 1227-1232.

Jörger, K.M., Norenburg, J.L., Wilson, N.G., Schrödl, M., 2012. Barcoding against a paradox? Combined molecular species delineations relveal multiple cryptic lineages in elusive meiofaunal sea slugs. BMC Evol. Biol. 12, 245.

Kaufmann, C., Ziegler, D., Schaffner, F., Carpenter, S., Pfluger, V., Mathis, A., 2011. Evaluation of matrix-assisted laser desorption/ionization time-of-flight mass spectrometry for characterization of *Culicoides nubeculosus* biting midges. Med. Vet. Entomol. 25, 32-38.

Kiesling, T.L., Wilkinson, E., Rabalais, J., Ortner, P.B., McCabe, M.M., Fell, J.W., 2002. Rapid identification of adult and naupliar stages of copepods using DNA hybridization methodology. Mar. Bioltechnol. 4, 30-39.

Knowlton, N., 1993. Sibling species in the sea. A. Rev. Ecol. Syst. 24, 189-216.

Knowlton, N., 2000. Molecular genetic analyses of species boundaries in the sea. Hydrobiol. 420, 73-90.

Kosobokova, K.N., Hirche, H.-J., Scherzinger, T., 2002. Feeding ecology of *Spinocalanus antarcticus*, a mesopelagic copepod with a looped gut. Mar. Biol. 141, 503-511.

Kosobokova, K.N., Hopcroft, R.R., 2010. Diversity and vertical distribution of mesozooplankton in the Arctic's Canada Basin. Deep-Sea Res. II 57, 96-110.

Kosobokova, K.N., Hopcroft, R.R., Hirche, H.-J., 2011. Patterns of zooplankton diversity through the depths of the Arctic's central basins. Mar. Biodiv. 41, 29-50.

Krishnamurthy, T., Ross, P.L., Rajamani, U., 1996. Detection of pathogenic and nonpathogenic bacteria by matrix-assisted laser desorption/ionization time-of-flight mass spectrometry. Rapid Comm. Mass Spectrom. 10, 883-888.

Laakmann, S., Auel, H., Kochzius, M., 2012. Evolution in the deep sea: Biological traits, ecology and phylogenetics of pelagic copepods. Mol. Phylogenet. Evol. 65, 535-546.

Laakmann, S., Gerdts, G., Erler, R., Knebelsberger, T., Arbizu, P.M., Raupach, M.J., 2013. Comparison of molecular species identification for North Sea calanoid copepods (Crustacea) using proteome fingerprints and DNA sequences. Mol. Ecol. Resour. 13, 862-876.

Lee, C.E., Frost, B.W., 2002. Morphological stasis in the *Eurytemora affinis* species complex (Copepoda: Temoridae). Hydrobiol. 480, 111-128.

Lynn, E.C., Chung, M.C., Tsai, W.C., Han, C.C., 1999. Identification of Enterobacteriaceae bacteria by direct matrix-assisted laser desorption/ionization mass spectrometric analysis of whole cells. Rapid Comm. Mass Spectrom. 13, 2022-2027.

Mauchline, J., 1998. The biology of calanoid copepods. Academic Press, San Diego, CA.

Oksanen, J., Blanchet, F.G., Kindt, R., Legendre, P., Minchin, P.R., O'Hara, R.B., Simpson, G.L., Solymos, M., Stevens, H.H., Wagner, H., 2015. vegan: Community Ecology Package. R packag. ver. 2.3-0. http://CRAN.R-project.org/package=vegan.

Pappin, D.J.C., Hojrup, P., Bleasby, A.J., 1993. Rapid Identification of Proteins by Peptide-Mass Finger Printing. Curr. Biol. 3, 327-332.

Pappin, D.J.C., Rahman, D., Hansen, H.F., Jeffery, W., Sutton, C.W., 1995. Peptide-mass fingerprinting as a tool for the rapid identification and mapping of cellular proteins. In: Atassi, M.Z., Appella, E. (Eds.), Methods in Protein Structure Analysis, pp. 161-173.

Park, T.S., 1970. Calanoid copepods from the Carribean Sea and Gulf of Mexico. 2. New species and new records from plankton samples. Bull. Mar. Sci. 20, 472-546.

Perkins, D.N., Pappin, D.J.C., Creasy, D.M., Cottrell, J.S., 1999. Probability-based protein identification by searching sequence databases using mass spectrometry data. Electrophoresis 20, 3551-3567.

Razouls, C., de Bovée, F., Kouwenberg, J., Desreumaux, N., 2005-2015. Diversity and geographic distribution of marine planktonic copepods. Available at http://copepodes.obs-banyuls.fr/en. Accessed December 15, 2015.

R Core Team, 2015. R: A language and environment for statistical computing. R Foundation for Statistical Computing, Vienna, Austria. URL http://www.R-project.org/

Riccardi, N., Lucini, L., Benagli, C., Welker, M., Wicht, B., Tonolla, M., 2012. Potential of matrix-assisted laser desorption/ionization time-of-flight mass spectrometry (MALDI-TOF MS) for the

identification of freshwater zooplankton: A pilot study with three *Eudiaptomus* (Copepoda: Diaptomidae) species. J. Plankt. Res. 34, 484-492.

Rocha-Olivares, A., Fleeger, J.W., Foltz, W., 2001. Decoupling of molecular and morphological evolution in deep lineages of a meiobenthic harpacticoid copepod. Mol. Biol. Evol. 18, 1088-1102.

Saffert, R.T., Cunningham, S.A., Ihde, S.M., Monson Jobe, K.E., Mandrekar, J., Patel, R., 2011. Comparison of Bruker Biotyper matrix-assisted laser desorption ionization time-of-flight mass spectrometer to BD Pheonix Automated Microbiology System for identification of gram-negative bacilli. J. Clin. Microbiol. 49, 887-892.

Salla, V., Murray, K.K., 2013. Matrix-assisted laser desorption/ionization mass spectrometry for identification of shrimp. Anal. Chim. Acta 794, 55-59.

Seng, P., Drancourt, M., Gouriet, F., La Scola, B., Fournier, P.-E., Rolain, J.M., Raoult, D., 2009. Ongoing revolution in bacteriology: Routine identification of bacteria by matrix-assisted laser desoprtion ionization time-of-flight mass spectrometry. Clin. Infect. Dis. 49, 543-551.

Schulz, K., 1989. Notes on rare spinocalanid copepods from the eastern North Atlantic, with desriptions of new species of the genera *Spinocalanus* and *Teneriforma* (Copepoda: Calanoida). Mitt. ham. zool. Mus. Inst. Band 86, 185-208.

Schulz, K., 1996. *Mospicalanus schielae*, a new genus and species of calanoid copepod (Crustacea: Spinocalanidae) from deep Antarctic water. Polar Biol. 16, 595-600.

Stackebrandt, E., Päuker, O., Erhard, M., 2005. Grouping Myxococci (*Corallococcus*) strains by matrix-assisted laser desorption/ionization time-of-flight (MALDI-TOF) mass spectrometry: Comparison with gene sequence phylogenies. Curr. Microbiol. 50, 71-77.

Stamatakis, A., 2014. RAxML Version 8: A tool for phylogenetic analysis and post-analysis of large phylogenies. Bioinformatics 30, 1312-1313.

Suzuki, R., Shimodaira, H., 2014. pvclust: Hierarchical clustering with p-values via multiscale bootstrap resampling. R packag. ver. 1.3-2. http://CRAN.R-project.org/package=pvclust.

Tamura, K., Stecher, G., Peterson, D., Filipski, A., Kumar, S., 2013. MEGA6: Molecular Evolutionary Genetics Analysis version 6.0. Mol. Biol. Evol. 30, 2725-2729.

Thum, R.A., Harrison, R.G., 2009. Deep genetic divergence among morphologically similar and parapatric *Skistodiaptomus* (Copepoda: Calanoida: Diaptomidae) challenge the hypothesis of Pleistocene speciation. Biol. J. Linnean. Soc. 96.

Uhlmann, K.R., Gibb, S., Kalkhof, S., Arroyo-Abad, U., Schulz, C., Hoffmann, B., Stubbins, F., Carpenter, S., Beer, M., Von Bergen, M., Feltens, R., 2014. Species determination of *Culicoides* biting midges via peptide profiling using matrix-assisted laser desorption ionization mass spectrometry. Parasit. Vectors 7, 392.

Vargha, M., Takáts, Z., Konopka, A., Nakatsu, C.H., 2006. Optimization of MALDI-TOF MS for strain level differentiation of *Arthrobacter isolates*. J. Microbiol. Methods 66, 399-409.

Vinogradov, M.E., 1972. Vertical distribution of oceanic zooplankton. Israel Programm for Scientific Translations. Jerusalem.

Volta, P., Riccardi, N., Lauceri, R., Tonolla, M., 2012. Discrimination of freshwater fish species by Matrix-Assisted Laser Desorption/Ionization - Time of Flight Mass Spectrometry (MALDI-TOF MS): A pilot study. J. Limnol. 71, 164-169.

Wilson, N.G., Hunter, R.L., Lockhart, S.J., Halanych, K.M., 2007. Multiple lineages and absence of panmixia in the "circumpolar" crinoid *Promachocrinus kerguelensis* from the Atlantic sector of Antarctica. Mar. Biol. 152, 895-904.

Wishner, K.F., Gelfman, C., Gowing, M.M., Outram, D.M., Rapien, M., Williams, R.L., 2008. Vertical zonation and distributions of calanoid copepods through the lower oxycline of the Arabian Sea oxygen minimum zone. Prog. Oceanogr. 78, 163-191.

WoRMS Editorial Board, 2015. World register of marine species. Available from http://www.marinespecies.org at VLIZ. Accessed 2015-12-15. WoRMS Editorial Board.

Yamaguchi, A., Watanabe, Y., Ishida, H., Harimoto, T., Furusawa, K., Suzuki, S., Ishizaka, J., Ikeda, T., Takahashi, M.M., 2002. Community and trophic structures of pelagic copepods down to greater depths in the western subarctic Pacific (WEST-COSMIC). Deep-Sea Res. I 49, 1007-1025.

Yssouf, A., Flaudrops, C., Drali, R., Kernif, T., Socolovschi, C., Berenger, J.M., Raoult, D., Parola, P., 2013a. Matrix-assisted laser desorption ionization time-of-flight mass spectrometry for rapid identification of tick vectors. J. Clin. Microbiol. 51, 522-528.

Yssouf, A., Socolovschi, C., Flaudrops, C., Ndiath, M.O., Sougoufara, S., Dehecq, J.S., Lacour, G., Berenger, J.M., Sokhna, C.S., Raoult, D., Parola, P., 2013b. Matrix-assisted laser desorption ionization time-of-flight mass spectrometry: An emerging tool for the rapid identification of mosquito vectors. PLoS ONE 8, e72380.

Yssouf, A., Socolovschi, C., Leulmi, H., Kernif, T., Bitam, I., Audoly, G., Almeras, L., Raoult, D., Parola, P., 2014. Identification of flea species using MALDI-TOF/MS. Comp. Immunol. Microbiol. Infect. Dis. 37, 153-157.

CHAPTER VI

High-resolution Community Analysis of Deep-sea Copepods Using Proteomic Fingerprinting

Kaiser P, Bode M, Cornils A, Hagen W, Auel H, Laakmann S

In preparation by P. Kaiser

High-resolution Community Analysis of Deep-sea Copepods Using Proteomic Fingerprinting

Patricia Kaiser, Maya Bode, Astrid Cornils, Wilhelm Hagen,
Holger Auel and Silke Laakmann

Abstract

The majority of copepod communities is often comprised of juvenile stages. Juvenile copepodite stages usually lack distinct morphological characters and thus make identification and species-specific quantification based on morphology, almost impossible. Even in adult copepods, many morphological features are highly conserved and thus species richness is still largely underestimated in many copepod families. Distributional patterns of such taxonomically challenging species remain unknown. The time- and cost-effectiveness of the analysis of proteome fingerprints using matrix-assisted laser desorption/ionization time-of-flight mass spectrometry (MALDI-TOF MS) make this method superior to DNA-sequence analyses for mere species identification purposes and even applicable for abundance analyses. In the present study, MALDI-TOF MS was applied to identify and quantify adult and juvenile copepods of the ecologically important deep-sea copepod family Spinocalanidae. Therefore, vertical distribution of this little-known copepod family in stratified depth samples (0-1000 m) from two stations in the eastern tropical Atlantic was analysed. The analysis of proteome fingerprints yielded valid species identification and fine-scale vertical profiles with a high species and stage resolution, even of putative cryptic species and young copepodite stages. In total, 25 different spinocalanid species were identified with a correct identification of 94% of all 1549 analyzed specimens. Thus, proteomic fingerprinting has great potential in accelerating and improving copepod community structure analyses. This is particularly promising for taxonomically challenging copepod groups, juvenile stages and fragile deep-sea organisms to give new insights into biodiversity as well as phylogeographic and vertical patterns.

Key words: juvenile copepodids, species identification, MALDI-TOF MS, ontogenetic vertical distribution, cryptic species, Spinocalanidae

Introduction

Copepods are by far the most abundant (55-95%) and diverse components of mesozooplankton communities in all marine regions (e.g. Longhurst 1985; Turner 2004; Kosobokova et al. 2011). Due to their extremely high abundance and biomass, calanoid copepods play a key role in marine food webs and the cycling of organic and inorganic matter. Copepods are by far the most abundant (55-95%) and diverse components of mesozooplankton communities in all marine regions (Longhurst and Harrison 1989; Frangoulis et al. 2005; Schukat et al. 2014; Turner 2015). Species composition and abundances often reflect responses of an ecosystem to hydro-climatic forcing, i.e. changes in temperature, hydrodynamics, stratification and seasonal variability (Beaugrand et al. 2002; Beaugrand and Ibañez 2004). Such changes in zooplankton community structure may severely impact the cycling of organic matter and/or propagate along the food chain, as zooplankton plays a key role in transferring energy from lower to higher trophic levels (Verheye et al. 1998; Steinberg et al. 2012). In some cases, certain copepod species may be used as indicators for severe shifts in marine ecosystems as response to environmental changes (Beaugrand 2004, 2005; Hays et al. 2005; Hooff and Peterson 2006).

Accurate and efficient species identification and quantification are crucial for many ecological studies (McManus and Katz 2009). Morphological identification of copepods is based on a few distinct characters, which are usually expressed only in adult individuals. Thus, the identification of juvenile copepods is extremely challenging or even impossible (Blanco-Bercial et al. 2007; McManus and Katz 2009; Riccardi et al. 2012). Even in adults these diagnostic characters may be inconspicuous, may only be visible after detailed preparation of the organisms and identification is often complicated by incomplete or inconsistent taxonomic keys (e.g. Bucklin et al. 1999; Goetze 2003; Laakmann et al. 2013; Cornils and Held 2014). Moreover, the presence of cryptic species lacking any morphological differences is very common among copepods (Knowlton 2000; Bucklin et al. 2003, 2010; Goetze 2003). Therefore, copepod diversity was largely underestimated in the past, while mechanisms of ecosystem structuring and functioning may remain hidden the coarser the taxonomic resolution, thus making molecular systematic analyses particularly promising for copepod studies (Bucklin et al. 2003). During the last decades, DNA sequences analyses such as the analysis of a fragment of the mitochondrial cytochrome c oxidase subunit I (COI) gene, known as the DNA barcode gene, proved to be a reliable tool for unambiguous species discrimination (Bucklin et al. 2003, 2010; Herbert et al. 2003a,b; Goetze 2003). However,

DNA-based methods are still very time- and cost-intensive and require an *a priori* knowledge of species-specific sequences, i.e. accurate primer design (Feltens et al. 2010; Volta et al. 2012).

Improvements of mass spectrometric techniques to analyze even large and fragile molecules such as proteins using "soft" ionization methods lead to increasing usability of the proteome for species discrimination (Pappin et al. 1993; Holland et al. 1996; Krishnamurthy et al. 1996; Claydon et al. 1996; Feltens et al. 2010). In this context, the matrix-assisted laser desorption ionization time-of-flight mass spectrometry (MALDI-TOF MS) method was particularly promising. Its discriminatory power based on species-specific patterns of peptide and protein masses was successful for the discrimination of microorganisms on the species (Cladyon et al. 1996; Krishnamurthy et al. 1996; Jarman et al. 1999) and even on the subspecies level (Arnold and Reilly 1998; Stackebrandt et al. 2005; Vargha et al. 2006; Diekmann et al. 2008; Seng et al. 2010). During the last two decades, MALDI-TOF MS became an established method for the identification of bacteria, viruses and fungi in clinical diagnostics (e.g. Li et al. 2000; Fenselau and Demirev 2001; Maier and Kostrzewa 2007; Marklein et al. 2009; van Veen et al. 2010; Wieser et al. 2012).

Applying MALDI-TOF MS, samples can be analyzed after one simple protein extraction step without further preparation. The sample extract then co-crystallizes with a matrix on a target plate. The matrix is usually acidic containing a chromophore (e.g. α-cyano-4-hydroxycinnamic acid). This acts as a proton source to assist the transition of large molecules from the solid crystalline state into intact molecular ions in the gas phase (Hillenkamp et al. 1991). Hence, the sample-matrix mix is shot by laser pulses causing desorption and finally ionization of the protein molecules (Pappin et al. 1993; Holland et al. 1996; Krishnamurthy et al. 1996; Claydon et al. 1996; Feltens et al. 2010). The charged molecules are accelerated in an electric field and their time of flight is measured in a vacuum flight tube. Finally, the different masses of the single molecules are represented as peaks, depending on their time of flight (Hillenkamp et al. 1991; Cotter 1992). Specimens are then identified based on their species-specific protein mass spectra. The high potential of applying MALDI-TOF MS for ecological studies, as routine and automated procedure, allows the preparation and analysis of hundreds of individuals per day (Volta et al. 2012). Recent studies showed that MALDI-TOF MS was successful to discriminate also metazoans such as insects (Feltens et al. 2010; Kaufmann et al. 2011; Yssouf et al. 2013a,b, 2014; Uhlmann et al. 2014), fish (Volta et al. 2012), and zooplankton species such as shrimp (Salla and Murray 2013) and copepod species (Riccardi et al. 2012; Laakmann et al. 2013).

To evaluate the potential of proteomic fingerprinting in zooplankton biodiversity and ecology research, MALDI-TOF MS was applied not only to identify but also to quantify adult and juvenile copepods in deep-sea multinet samples from the eastern tropical Atlantic. Therefore, species richness and vertical distribution patterns of the ecologically important, but taxonomically challenging and little-known deep-sea copepod family Spinocalanidae was investigated.

Materials and Methods

Sampling

Samples were collected during the ANTXXIV/1 cruise with R/V *Polarstern* in the eastern tropical Atlantic in 2007. Vertical hauls were conducted with a Multinet (HydroBios Multinet Maxi: 9 nets, 0.5 m^2 mouth opening, 150 µm mesh size) with standard sampling depths from 1000-800-600-500-400-300-200-100-50-0 m. Immediately after the haul, the samples were split, with one half being preserved in absolute ethanol (96%) and the other half in 4% formaldehyde seawater solution. In the present study, stations 6 (1ºS, 9ºW) and 7 (7ºS, 4ºW) in the tropical East Atlantic Ocean were analyzed (see Chapter V for station map). All spinocalanid copepods were quantitatively sorted from the ethanol-preserved samples at both stations using a dissecting microscope. Total length of each specimen was measured and notes about it's morphology were taken. Individuals were divided into five ontogenetic stages: CI-III, CIV, CV, CVI-female and CVI-male. Copepodids CI-III were pooled, as they were hard to distinguish. Each specimen was stored separately in a plastic cup with absolute ethanol and subsequently analyzed with MALDI-TOF MS.

MALDI-TOF MS measurements

Single specimens were placed in 2-5 µL of matrix solution consisting of saturated alpha-cyano-4-hydroxycinnamic acid (HCCA) as matrix in 50% acetonnitrile, 47% nuclease-free water and 2.5% trifluoroacetic acid. For smaller individuals (<0.6 mm), the amount of matrix was reduced to increase the protein concentration in the sample to receive robust mass spectra: For CIV, CV and CVI specimens 5 µl, for CI-III >0.6 mm 4 µl, for CI-III between 0.5 and 0.6 mm 3 µl and for CI-III <0.5 mm 2 µl of matrix solution were used. The sample-matrix mix was then incubated for 10 min at room temperature and dark conditions. After incubation, it was vortexed for 10 s and centrifuged for 30 s at 13000 RMP. Finally, 1 µl of extract was placed on a target plate and al-

lowed to evaporate at room temperature. Depending on the amount of matrix used, one to three pseudoreplicates per sample were measured. Each spot was measured three times receiving three to nine mass spectra per specimen (technical replicates). Calibration was performed using a bacterial test standard (Bruker Daltonics) containing a protein extract of *Escherichia coli* DH5alpha. Analyses were performed with the compact linear-mode bench-top microflex LT system (Bruker Daltonics) at a laser frequency of 60 Hz. To create one spectrum, 240 laser shots were generated at fixed optical laser energy and a pulse of 3 ns.

Spectra processing and data analysis

MALDI-TOF data analyses were performed in R (version 3.1.3, R core team, 2015). Raw spectra were imported into R using the MALDIquantForeign R package (version 0.9; Gibb 2014b). Further processing and analyses of mass spectra were carried out using the MALDIquant package (version 1.12; Gibb and Strimmer 2012) after Gibb and Strimmer (2014). Mass spectra between 2-20 kDa were square root transformed and smoothed using the Savitzky-Golay-Filter. Baseline correction was conducted applying the SNIP algorithm with 20 iterations. Normalization was performed with the Total-Ion-Current-calibration. Peak detection was applied to the averaged spectra of all technical replicates with a signal-to-noise ratio of 3 and half window size of 8. Peaks that occurred in less than 100% of technical replicates were removed and the remaining peaks were binned. Finally, the average spectra of technical replicates were merged with pseudoreplicate measurements of the specimens generating one mass spectral profile per sample.

Specimens were identified based on their species-specific mass spectra with the help of the reference females verified by morphology and DNA sequence analysis in a previous study (see Chapter V). Dendrograms of the merged mass spectra were computed by hierarchical cluster analysis based on a Euclidean distance matrix using the ward method with 1000 bootstrap replicates. Averaged distances were visualized as a heatmap using the 'gplots' package in R (Warnes et al. 2015). A linear discriminant analysis (LDA) was conducted to detect species-specific peaks and cross-validation to find the number of peaks necessary for reliable species discrimination. Both analyses were conducted in R, using the 'sda.ranking' (Ahdesmaki et al. 2015) and 'crossval' function (Strimmer 2014), respectively. The distances between the different species as well as stages were tested for significance by analysis of similarity (ANOSIM) with 999 permutations

using the software PRIMER6 (version 6.1.6; Clarke and Gorley 2006). Non-metric multidimensional scaling (nMDS) plots were generated with PRIMER6 for the visualization of distances between developmental stages.

Weighted mean depths (WMD) for each species and their developmental stages were computed using the following equation:

$$WMD = \frac{\sum(n_i \cdot z_i \cdot d_i)}{\sum(n_i \cdot z_i)}$$

where n_i is the number of individuals per m^3 in depth stratum, z_i the depth range of the sampling interval i in m and d_i the mean depth of the sampling interval i in m (Andersen et al. 2001).

Results

Identification of adult and juvenile copepods

Spinocalanid species and their developmental stages were identified based on the reference females and notes of morphology (Chapter V). In total, 1178 spinocalanid individuals were classified to 25 different species of the four genera: *Spinocalanus*, *Mimocalanus*, *Monacilla* and *Teneriforma*. One species shared morphological characters described for two species and thus was named after the two, *S. nerospinosus/hoplites*. Putative cryptic species, which could not be distinguished from congeners based on morphological characteristics, carry a number after the species name, such as *Spinocalanus dispar 1*, *S. dispar 2*, *S. dispar 4*, *S. dispar 5* and *S. elongatus 3* (see details in Chapter V). For *S. dispar 7*, *S. dispar 8* and *Monacilla gracilis* no reference females were available.

Averaged Euclidean distances within and between the different species of Spinocalanidae are visualized in Fig. 1. Intraspecific variability was smaller than interspecific variability. The largest intraspecific difference was observed in *Teneriforma sp*.; however, these contained two separate species *T. naso 1* and *T. naso 2* but the number of specimens was too low for statistical validation. Analysis of similarity (ANOSIM) revealed significant differences between all species with low p-values (≤0.002) and high R-values (≥0.605), indicating a good separation of the species. Species groups with less than six specimens were excluded from this analysis (*M. gracilis*, *S. angusticeps*, *S. stellatus*, *S. neospinosus/hoplites*, *Mimocalanus heronae 2* and *Mimocalanus sp. 3*). The R and p-values are given in Table 1.

Table 1: Analysis of similarity (ANOSIM) between 18 spinocalanid species based on pairwise tests with 999 permutations. Numbers represent the R-values. All p-values were ≤0.002. Sd5: *Spinocalanus dispar* 5, Mt: *Monacilla typica*, Sb: *Spinocalanus brevicaudatus*, Sd2: *S. dispar* 2, Sd4: *S. dispar* 4, Ss: *S. spinosus*, Sd1: *S. dispar* 1, M2: *Mimocalanus* sp. 2, Su: *Spinocalanus usitatus*, Se3: *S. elongatus* 3, Sh: *S. horridus*, Sd7: *S. dispar 7*, Sn: *S. neospinosus*, Sm: *S. magnus*, Mc2: *Mimocalanus cultrifer 2*, Sd8: *S. dispar* 8, Mh: *Mimocalanus heronae*, T: *Teneriforma* sp.

	Sd5	Mt	Sb	Sd2	Sd4	Ss	Sd1	M2	Su	Se3	Sh	Sd7	Sn	Sm	Mc2	Sd8	Mh	T
Sd5																		
Mt	1.0																	
Sb	0.9	1.1																
Sd2	0.9	1.0	0.9															
Sd4	0.6	1.0	0.9	0.9														
Ss	0.9	1.0	1.0	1.0	1.0													
Sd1	0.8	1.0	0.9	0.9	0.9	0.9												
M2	1.0	1.0	1.0	1.0	1.0	1.0	0.9											
Su	0.8	1.0	0.9	0.9	0.9	1.0	0.8	1.0										
Se3	0.9	0.9	0.9	1.0	1.0	1.0	0.8	1.0	1.0									
Sh	1.0	1.0	1.0	1.0	1.0	1.0	0.9	1.0	1.0	1.0								
Sd7	0.8	1.0	0.8	0.8	0.8	0.9	0.8	0.9	0.9	0.9	0.9							
Sn	0.8	1.0	0.9	1.0	0.9	1.0	0.8	0.9	0.8	0.9	1.0	0.8						
Sm	0.8	1.0	0.8	0.8	0.9	1.0	0.8	1.0	0.9	0.9	1.0	0.7	0.9					
Mc2	0.8	1.0	0.9	0.9	0.9	0.9	0.8	0.8	0.8	0.9	0.8	0.9	0.8	0.8				
Sd8	0.8	1.0	0.8	1.0	0.9	1.0	0.8	1.0	0.9	0.9	0.9	0.7	0.9	0.8	0.8			
Mh	1.0	1.0	1.0	1.0	1.0	1.0	0.9	1.0	1.0	1.0	1.0	1.0	0.9	1.0	0.9	1.0		
T	1.0	1.0	1.0	1.00	1.0	0.9	1.0	0.8	0.6	0.9	0.7	1.0	0.7	1.0	0.9	1.0	0.8	
Mcr	1.0	1.0	1.0	1.0	1.0	1.0	1.0	1.0	1.0	1.0	1.0	1.0	1.0	1.0	0.9	1.0	1.0	0.7

In total, 1549 individuals were measured, of which 371 specimens, mainly CI-III, did not belong to the copepod family Spinocalanidae based on their mass spectral profiles, but were initially selected due to their morphological similarity to this family. Measurements of 59 individuals (only CI-IIIs smaller than 0.55 mm) failed, thus, no mass spectrum was obtained. Depth-specific dendograms showed ambiguous clustering for some specimens of *S. dispar 2*, *S. dispar 4-8*, *S. magnus*, *S. brevicaudatus*, *S. neospinosus, Mimocalanus cultrifer 2* and *Mimocalanus heronae 2*. Most of those falsely clustered individuals (81%) were copepodids CI-III and thereof 75% were smaller than 0.55 mm. For clear and unambiguous identification all spinocalanid specimens from both stations had to be included to the cluster analyses and species assignments were double-checked with notes on morphology.

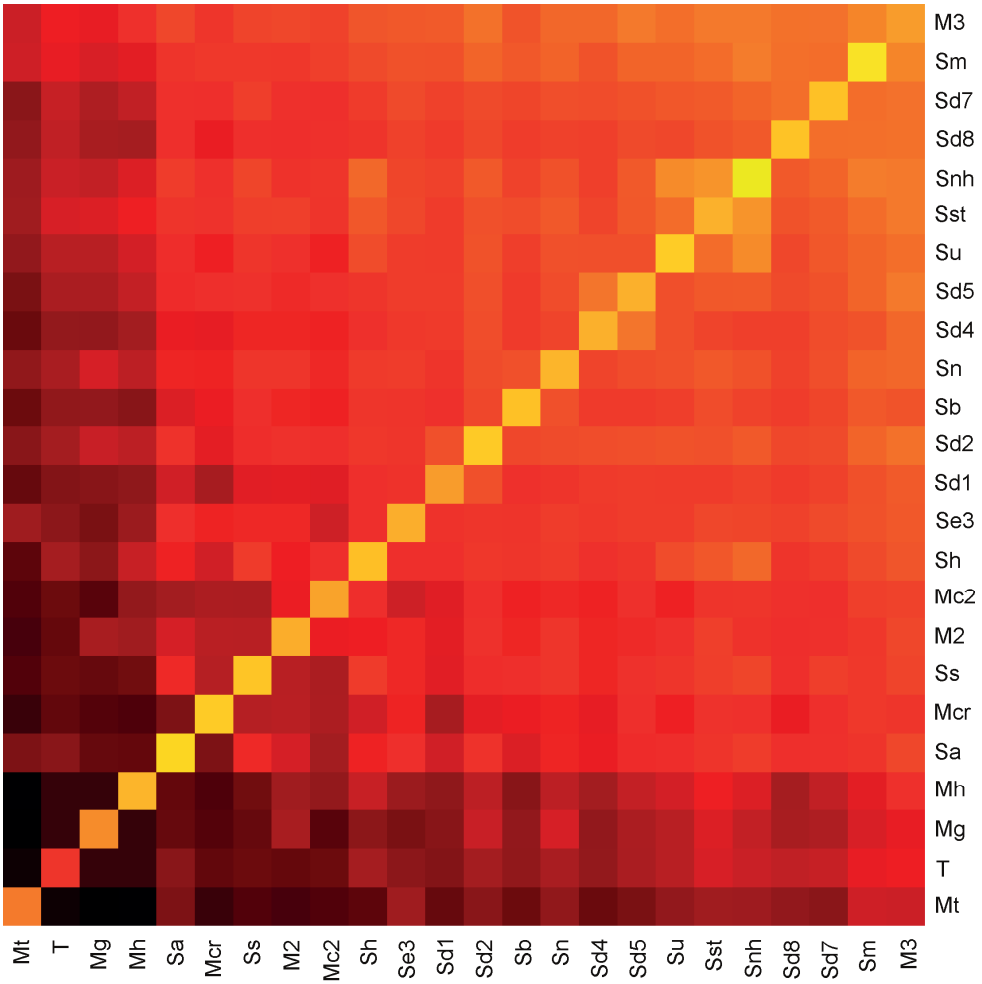

Figure 1: Heatmap visualizing averaged Euclidean distances of protein mass spectra between spinocalanid species. Bright colors (yellow) indicate low, dark colors (black) large distances. For most species abbreviations see Tab. 3. Mg: *Monacilla gracilis*, Sa: *Spinocalanus angusticeps*, Sst: *S. stellatus*, Snh: *S. neospinosus/hoplites*, M3: *Mimocalanus sp. 3,* Mt: *Monacilla tenera*.

The degree of intraspecific similarity varied among the species. One reason for this was that significant differences with variable R-values of spectral profiles of developmental stages were observed within species clusters (Fig. 2; one-way ANOSIM, factor 'stage'). In general, lower R-values were observed for developmental stages that were closer to each other on developmental time-scales, i.e. CI-III to CIV, CIV to CV and CV to CVI. Hence, CI-III and CIV generally showed the lowest, while CI-III and CVI the highest R-values and thus the greatest differences between stages. R and p-values between developmental stages are shown in Table 2 for two abundant species, *S. dispar* 2 and *S. brevicaudatus*. Distances between developmental stages are visualized as nMDS plot for these two species (Fig. 2).

Table 2: Analysis of similarity (ANOSIM) between developmental stages of *S. dispar 2* and *S. brevicaudatus* based on pairwise tests with 999 permutations. Numbers represent the R values. All p-values were ≤ 0.015. CI-V: copepodids CI-V, f: female.

S. dispar 2

	CI-III	CIV	CV
CI-III			
CIV	0.25		
CV	0.55	0.07	
f	0.83	0.38	0.28

S. brevicaudatus

	CI-III	CIV	CV
CI-III			
CIV	0.40		
CV	0.66	0.20	
f	0.88	0.69	0.30

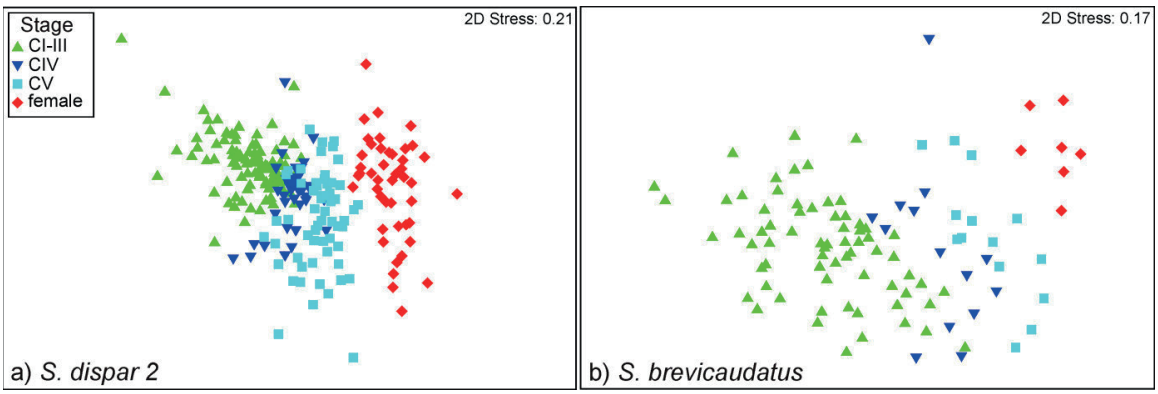

Figure 2: Non-metric multidimensional scaling plots of a) *S. dispar* 2 and b) *S. brevicaudatus* developmental stages based on Euclidean distance matrices of their MALDI-TOF protein mass spectra.

To identify genus- or species-specific peaks in the mass spectra, linear discriminant analysis (LDA) was performed. LDA resulted in a ranked peak list with the top 40 peaks ordered based on their calculated correlation-adjusted t-scores (CAT score). The higher the CAT score was, the stronger the influence of this peak on the discrimination of the species became. No species- or genus-specific peaks were identified. Nevertheless, a few prominent characteristics were found. *S. dispar* 4 and *S. dispar* 5 had similar discriminant peaks, sharing four of their six peaks with highest CAT scores. *Mimocalanus sp. 3* on the other hand did not exhibit one distinct peak among the top 40 features. *Monacilla gracilis*, *Mimocalanus heronae 2*, *S. brevicaudatus* and *S. dispar* 8 only showed peaks with low CAT scores. The other species had between three and nine peaks with high scores. Cross validation revealed that with all 3020 peaks, discrimination between species is to 98% reliable. The reliability increases rapidly with the number of peaks, reaching 96% already with only ninety peaks.

Abundance and vertical distribution of Spinocalanidae

The identified adult and juvenile stages were finally quantified obtaining high-resolution vertical distribution profiles of abundance, species richness and community composition of Spinocalanidae over nine distinct depth intervals from the surface down to 1000 m. These profiles were similar at both stations (Fig. 3). Only a few species occurred in very low abundance in the euphotic zone (0-200 m). Species richness of the spinocalanid family increased steadily with depth until 450 m, and, after a distinct drop between 500-600 m, reached a maximum between 600-800 m with 13 species at stn. 7 and 15 species at stn. 6 (Fig. 3a). In contrast, maximum abundance of spinocalanid copepods was found in the upper mesopelagic zone (Fig. 3b). Highest abundance occurred between 300-400 m at station 6 with 8 ind m^{-3} and between 200-300 m at station 7 with 4 ind m^{-3}.

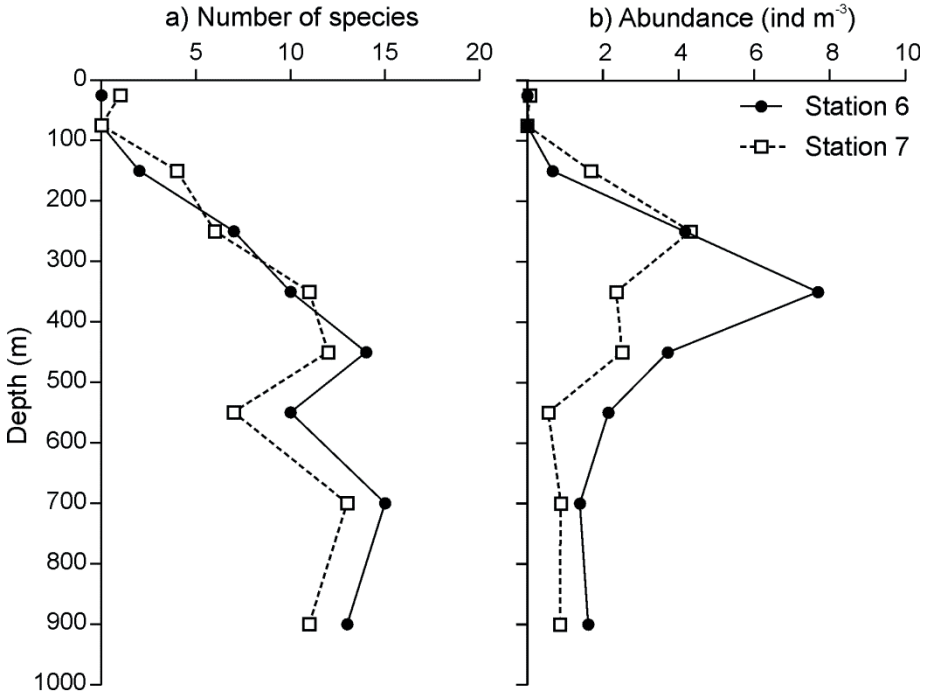

Figure 3: Vertical distribution from 0-1000 m of a) species richness and b) abundance (ind m^{-3}) of Spinocalanidae at two stations in tropical eastern Atlantic.

Copepodids (CI-V) outnumbered adult CVIs by far, contributing 80% to the spinocalanid community. Only 1-2 % of the adults were males. At both stations, CI-III stages were the dominant component with 40 and 45%. Stages CIV and CV contributed between 13-26% to the spinocalanid community, with CV being more abundant at both stations. *Spinocalanus dispar* 2 was the most abundant species at both stations, with 304 ind m^{-2} (stn. 7) and 504 ind m^{-2} (stn. 6). Followed by *S. dispar* 7 with 253 ind m^{-2} (stn 7) and 383 ind m^{-2} (stn 6) and *S. dispar 4* with 239 ind m^{-2} (stn 7)

and 218 ind m^{-2} (stn 6). Further abundant species were *S. brevicaudatus*, *S. dispar 8*, *S. dispar 5* and *S. magnus*. Vertical profiles of species-specific abundances of the 14 most abundant species at stn. 6 and the 13 most abundant species at stn. 7 revealed distinct vertical distribution patterns at both stations (Fig. 4). Species were divided into the following three groups, depending of their preferred habitat depth (Fig. 4): Group A consisted of *S. horridus*, *S. elongatus 3*, *S. dispar 4* and *S. dispar 5*, which preferred the lower mesopelagic zone. WMDs were below 600 m at stn. 6 and below 500 m at stn. 7. Group B consisted of *Teneriforma* sp., *S. dispar 1*, *M. typica*, *S. dispar 2*, *S. spinosus*, *S. brevicaudatus* and *Mimocalanus cultrifer 2*, which showed generally wider distributional patterns throughout the entire 200-1000 m water column. WMDs were between 271 and 800 m. Group C comprised *S. magnus*, *S. dispar* 7 and *S. dispar* 8, which inhabited the upper meso- to epipelagic zones. Individuals were usually found between 100-500 m, being concentrated in the upper mesopelagic zone. WMDs were between 330 and 150 m, except for males, which occurred slightly deeper.

Beside these species-specific differences in vertical distribution, some species also showed ontogenetic vertical partitioning of different types (Fig. 4). Only *S. elongatus 3*, *Teneriforma* sp., *Mimocalanus* sp. *3*, *S. magnus*, *S. dispar 7* and *S. dispar 8* showed a rather uniform distribution of all stages but the males, which occurred considerably deeper than the other stages. In most species, adult females resided in deeper layers, as e.g. for *S. dispar 1*, *S. dispar 2* and *M. typica* at stn. 7 and in *S. brevicaudatus* and *S. spinosus* at stn 6. In *S. horridus*, *S. dispar 4*, *S. dispar 5* and *S. brevicaudatus* (only stn. 6) copepodids CI-III inhabited the same deep layers as the females, while copepodids CIV and CV prevailed at shallower depths.

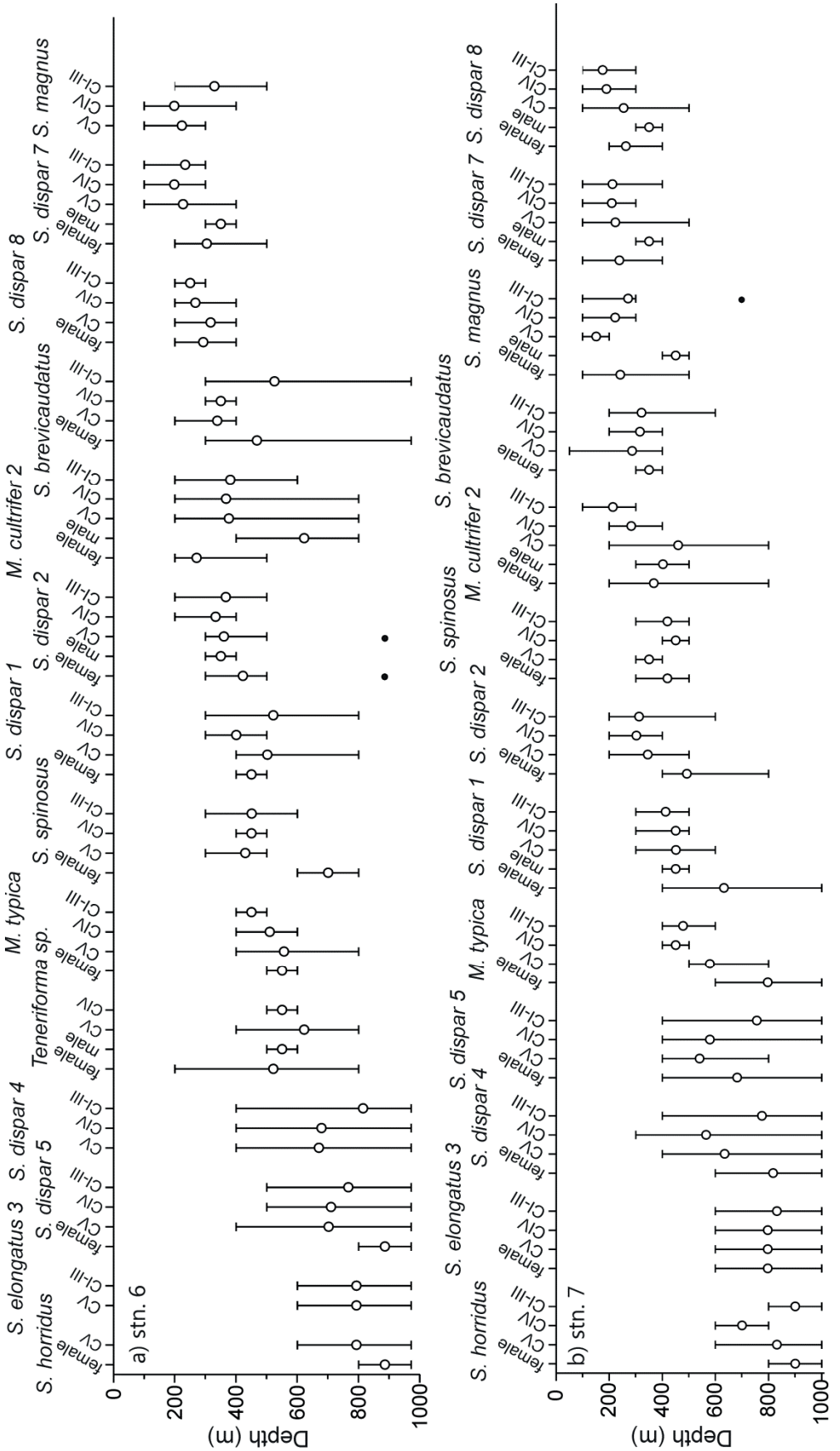

Figure 4: Vertical distribution of the most abundant Spinocalanidae a) at stn. 6 and b) at stn. 7 in the tropical eastern Atlantic Ocean. Open circles represent weighted mean depths. Bars indicate the vertical range in which the respective species occurred. Black dots indicate that only one individual was found at the respective depth.

Discussion

The present study provides the first large-scale data set demonstrating proteomic fingerprinting using MALDI-TOF MS as an efficient method to reliably identify and quantify copepod species and their developmental stages. Fine-scale vertical profiles of Spinocalanidae with a high species and stage resolution were yielded applying species identification on the basis of species-specific proteome mass spectra, even of putative cryptic species and young copepodite stages. MALDI-TOF measurements proved to be as simple and fast as indicated by several studies (e.g. Holland et al. 1996; Haag et al. 1998; Campbell 2005; Perera et al. 2005; Laakmann et al. 2013). The high sample throughput (hundreds of samples per day) and cost-effectiveness (~0.30 Euro per sample) makes it superior to DNA-sequence analyses for mere species identification purposes and even applicable for ecological studies, when a large portion of highly abundant individuals has to be analyzed. However, similar to DNA barcoding based on cytochrome c oxidase subunit I (COI), proteomic fingerprinting does not seem to reveal any phylogenetic relationships (Chapter V; Yssouf et al. 2013b, Dieme et al. 2014).

Although often termed proteomic fingerprinting, only a very limited fraction of the whole proteome is represented by MALDI-TOF MS (Müller et al. 2013). It detects the most abundant proteins and peptides of low molecular weight, which tend to be alkaline and originate in the cytosol (Ryzhov and Fenselau 2001; Sandrin et al. 2013). In bacterial diagnostics, the majority of proteins generating a spectral profile are likely ribosomal (Ryzhov and Fenselau 2001). However, for mere species identification purposes, the protein identities of the spectral profiles are not important, but the species-specific peak patterns as a whole are crucial. To determine the identity of an unknown species/specimen via MALDI-TOF MS, it is necessary to measure spectra of reference samples first. Ideally, this reference sample is validated based on both, morphological and molecular genetic species identification methods (Chapter V). Afterwards, no additional species-specific *a priori* knowledge is necessary (Feltens et al. 2010).

In general, intraspecific variability of spectral profiles was significantly lower than interspecific variability. Stage-specific differences in the protein patterns increased during ontogenetic development with strongest deviation between the youngest copepodids CI-III and adults. Nevertheless, those differences between developmental stages were significantly smaller within a given species than between species, allowing a clear species discrimination of both adults and early stages. Hence, the primary determinant for the mass spectra profiles is the species, followed by

the developmental stage (Karger et al. 2012; Dieme et al. 2014). Phylogenetic relationships were not revealed by protein mass fingerprints (Chapter V; Yssouf et al. 2013b, Dieme et al. 2014).

Only 4% of all measurements failed, which applied solely to copepodids CI-III <0.55 mm. Of the remaining 1178 spinocalanid specimens, 94% were correctly identified to species level with unambiguous clustering. Even higher percentages (97-100%) of correct species identification were reported by MALDI-TOF MS studies on shrimps and insects (Salla and Murray, 2013; Yssouf et al., 2013b; Dieme et al., 2014). Greatest discrepancies in identification were detected for young copepodite stages (CI-III) of the relatively small *S. dispar* species complex (see details in Kaiser 2015). These specimens were mainly <0.55 mm and at the same time relatively similar due to their close relationship (Chapter V). Therefore, a higher protein concentration may be necessary to obtain robust mass spectra of such small samples by further concentrating the sample extract. In the present study, at least 90 peaks were necessary to achieve 96% accurate species identification. Previously it was suggested that the sensitivity of MALDI-TOF MS allows identification of single individuals <1/10 of the size of *Drosophila melanogaster* (Campbell 2005). Laakmann et al. (2013) were able to successfully identify young copepodids and even nauplii with this method. Even the use of mosquito and tick legs was sufficient to discriminate between different species (Yssouf et al. 2013a, b).

The identification of closely related and even putative cryptic copepod species is possible with MALDI-TOF MS. Several studies reported the successful delimitation of closely related metazoan species based on MALDI-TOF MS (Chapter V; Kaufmann et al. 2012; Riccardi et al. 2012; Laakmann et al. 2013; Dieme et al. 2014). It was even possible to discriminate between two cryptic mosquito species (Müller et al. 2013; Yssouf et al. 2013b). In contrast, difficulties were reported to differentiate between congeners of two closely related *Drosophila* spp. (Feltens et al. 2010) and cryptic species of sand flies (Mathis et al. 2015).

Despite their morphological homogeneity, *S. dispar* 1 to 5 exhibit genetic distances large enough to be considered different species, indicating the presence of several cryptic species within this species complex (Chapter V). Since reference females were unavailable for *S. dispar* 7 and 8, no statement about their genetic diversity can be made, but they were morphologically similar to *S. dispar*. As MALDI-TOF MS clearly distinguished between *S. dispar* 1 to 5, *S. dispar* 7 and 8 seem to be two more cryptic species in the *S. dispar* species complex. The large genetic distances of the COI sequences as well as large distances of protein patterns indicate that those sympatric cryptic species are reproductively isolated (Chapter V). The high numbers of lineages in many

deep-sea copepod families with high portions of putative cryptic species exemplify reproductive isolation even in physically rather homogenous deep-sea environments (Chapter V; Auel 1999; Kuriyama and Nishida 2006; Matsuura et al. 2010; Laakmann et al. 2012). This may be achieved by spatial (distinct depth strata) and temporal differences in reproductive activity to avoid a mixture of the different populations even if cross-fertilization is possible and produces fertile offspring (Palumbi 1994; Levitan et al. 2004). Due to the morphological homogeneity of cryptic species and the absence of visual perception, sexual selection based on morphological traits is limited, suggesting that rather species-specific chemical signaling plays an essential role in reproduction (e.g. Lonsdale et al. 1998; Weissburg et al. 1998; Yen et al. 1998; Bagøien and Kiørboe 2005). Cryptic speciation is a common phenomenon among copepods, and with steady progress in molecular techniques discoveries are constantly increasing (e.g. Chapter V; Bucklin et al. 1996, 2000, 2003; Rocha-Olivares et al. 2001; Goetze 2003; Blanco-Bercial et al. 2007; Chen and Hare 2008; Cornils and Held 2014). Their divergence is assumed to be very recent so that morphological traits have not yet evolved (Bickford et al. 2006; Thum and Harrison 2009). However, it has been questioned whether this is indeed universally applicable to copepods (Rocha-Olivares 2001), suggesting that copepod speciation may occur with little or no morphological change (Thum and Harrison 2009). This may be due to favoring adaptive diversification on physiological rather than on morphological traits (Knowlton, 1993), especially in non-visual invertebrates due to the absence of sexual selection on morphological features (Lee and Frost 2002).

Juvenile copepodids made up the majority of all spinocalanid specimens (80%) at both stations. CI-III stages contributed between 40 and 45% to the total community, stressing the importance of being able to identify the younger stages correctly to fully understand ecological and trophic interactions within the pelagic zone. Juvenile copepodids are often the dominant component of copepod communities outnumbering adults by far. Studies on copepod abundance often ignore especially young copepodite stages (CI-III), as a correct species or genus identification is very complicated, if not impossible. Abundance analyses based on the MALDI-TOF MS results, yielded high-resolution vertical profiles of distributional patterns of the different spinocalanid species and their developmental stages. Species of group A preferred the lower mesopelagic, group C the upper mesopelagic and species of group B were rather evenly distributed over the whole mesopelagic zone. Such a habitat partitioning serves as niche diversification mechanisms in many zooplankton taxa to avoid competition among species with similar trophic niches

(Longhurst 1985; Ambler and Miller 1987; Auel 1999; Kuriyama and Nishida 2006; Matsuura 2010; Laakmann et al. 2009a,b, 2012).

Some species also exhibited ontogenetic vertical partitioning, thus, distinct stage-specific vertical patterns indicating ontogenetic vertical migrations (OVM). Females of *S. dispar 1*, *S. dispar 2*, *S. spinosus* and *M. typica* and males of *S. dispar 7*, *S. dispar 8* and *Mimocalanus cultrifer 2* resided at deeper layers than corresponding copepodite stages. Such an ontogenetic descent of adults in pelagic copepods is believed to serve as a predator evasion (Ambler and Miller 1987; Yamaguchi et al. 2004). Besides, feeding is of minor importance in male copepods as their main purpose is reproduction. Hence, males may benefit bioenergetically by staying in deeper, cooler layers (Verheye and Field 1992; Yamaguchi and Ikeda 2002). Furthermore, younger copepodids find higher concentrations of prey at shallower depths (Laakmann et al. 2009a,b). In *S. horridus*, *S. dispar 4*, *S. dispar 5* and *S. brevicaudatus* both females and CI-III occurred in deeper layers, indicating a developmental ascent of copepodids CIV and CV. This is similar to patterns found in e.g. *Neocalanus gracilis*, *Gaetanus variabilis* and *Paraeuchaeta birostrata* (Yamaguchi et al. 2007; Shimode et al. 2009; Abe et al. 2012). Thus, this behavior reduces mortality due to predation for both, adults and younger copepodids (Shimode et al. 2009). Altogether, these wider distributional patterns may reduce intraspecific competition between the different developmental stages.

Conclusions

Species composition and abundances often reflect ecosystem responses to hydro-climatic forcing, e.g. changes in temperature, stratification and seasonal variability (Beaugrand et al. 2002; Beaugrand and Ibañez 2004). Therefore, accurate and improved species identification methods are needed to study zooplankton communities with high taxonomic resolution, and finally not only identify, but also quantify taxonomically challenging specimens to receive new insights into the structure and functioning of the pelagic realm. The analysis of proteome fingerprints using MALDI-TOF MS offers new prospects and opportunities for copepod studies on a whole new level. This method is superior to genetic analyses as it is much more time- and cost-efficient. Furthermore, it is much more accurate than traditional morphological analyses, as it identifies even cryptic species and juvenile copepods, which usually lack morphological diagnostic characters, and finally allows abundance analyses with much higher species resolution of all develop-

mental stages. Thus, it is very promising to give new insights into biodiversity as well as phylogeographic patterns and vertical habitat partitioning. Distribution patterns with such high taxonomic resolution even of cryptic species may contribute to understand speciation processes and ecosystem processes and to efficiently detect ecosystem changes and relate them to possible environmental parameters. Since other metazoans such as insects (Feltens et al. 2010; Kaufmann et al. 2011; Yssouf et al. 2013a,b, 2014; Uhlmann et al. 2014), fish (Volta et al. 2012), and also zooplankton species such as shrimp (Salla and Murray 2013) have successfully been discriminated by MALDI-TOF MS, the applicability of this technology may be expanded to other zooplankton organisms. However, to apply MALDI-TOF MS as a routine method in species identification, abundance and community analyses, the generation of a mass spectra database for zooplankton as already available for microorganisms will be essential, which allows immediate comparison and analysis of the mass spectra by a standard pattern matching algorithm against the reference data base (BioTyper database) (Seng et al. 2009; Saffert et al. 2011). This would revolutionize metazoan species identification, providing a straightforward result within minutes and thus being a powerful alternative to morphological and genetic analyses.

References

Abe, Y., Ishii, K., Yamaguchi, A., Imai, I., 2012. Short-term changes in population structure and vertical distribution of mesopelagic copepods during the srping phytoplankton bloom in the Oyashio region. Deep-Sea Res. I 65, 100-112.

Ahdesmaki, M., Zuber, V., Gibb, S., Strimmer, K., 2015. sda: Shrinkage discriminant analysis and CAT score variable selection. R package version 1.3.6. http://CRAN.R-project.org/package=sda.

Ambler, J.W., Miller, C.B., 1987. Vertical habitat-partitioning by copepodites and adults of subtropical oceanic copepods. Mar. Biol. 94, 561-577.

Andersen, V., Gubanova, A., Nival, P., Ruellet, T., 2001. Zooplankton community during the transition from spring bloom to oligotrophy in the open NW Mediterranean and effects of wind events. 2. Vertical distributions and migrations. J. Plankt. Res. 23, 243-261.

Arnold, R.J., Reilly, J.P., 1998. Fingerprint matching of *E. coli* strains with matrix-assisted laser desorption ionization time-of-flight mass spectrometry of whole cells using a modified correlation approach. Rapid Commun. Mass Spectrom. 12, 630-636.

Auel, H., 1999. The ecology of Arctic deep-sea copepods (Euchaetidae and Aetideidae). Aspects of their distribution, trophodynamics and effect on the carbon flux. Rep. Polar Res. 319, 1-97.

Bagøien, E., Kiørboe, T., 2005. Blind dating - mate finding in planktonic copepods. I. Tracking the pheromone trail of *Centropages typicus*. Mar. Ecol. Prog. Ser. 300, 105-115.

Beaugrand, G., Ibañez, F., Lindley, J.A., Reid, P.C., 2002. Diversity of calanoid copepods in the North Atlantic and adjacent seas: species associations and biogeography. Mar. Ecol. Prog. Ser. 232, 179-195.

Beaugrand, G., Ibanez, F., 2004. Monitoring marine plankton ecosystems. II: Long-term changes in North Sea calanoid copepods in relation to hydro-climatic variability. Mar. Ecol. Prog. Ser. 284, 35-47.

Beaugrand, G., 2004. Monitoring marine plankton ecosystems. I: Description of an ecosystem approach based on plankton indicators. Mar. Ecol. Prog. Ser. 269, 69-81.

Beaugrand, G., 2005. Monitoring pelagic ecosystems using plankton indicators. ICES J. Mar. Sci. 62, 333-338.

Bickford, D., Lohman, D.J., Sodhi, N.S., Ng, P.K.L., Meier, R., Winker, K., Ingram, K.K., Das, I., 2007. Cryptic species as a window on diversity and conservation. Trends Ecol. Evol. 22, 148-155.

Blachowiak-Samolyk, K., Kwasniewski, S., Dmoch, K., Hop, H., Falk-Petersen, S., 2007. Trophic structure of zooplankton in the Fram Strait in spring and autumn 2003. Deep-Sea Res. II 54, 2716-2728.

Blanco-Bercial, L., Álvarez-Marqués, F., 2007. RFLP procedure to discriminate between *Clausocalanus* Giesbrecht, 1888 (Copepoda, Calanoida) species in the Central Cantabrian Sea. J. Exp. Mar. Biol. Ecol. 344, 73-77.

Bucklin, A., LaJeunesse, T.C., Curry, E., Wallinga, J., Garrison, K., 1996. Molecular diversity of the copepod, *Nannocalanus minor*: Genetic evidence of species and population structure in the North Atlantic Ocean. J. Mar. Res. 54, 285-310.

Bucklin, A., Guarnieri, M., Hill, R.S., Bentley, A.M., Kaartvedt, S., 1999. Taxonomic assessment of planktonic copepods using mitochondrial COI sequence variation and competetive, species-specific PCR. Hydrobiol. 401, 239-254.

Bucklin, A., Astthorsson, O.S., Gislason, A., Allen, L.D., Smolenack, S.B., Wiebe, P.H., 2000. Population genetic variation of *Calanus finmarchicus* in Icelandic waters: Preliminary evidence of genetic differences between Atlantic and Arctic populations. ICES J. Mar. Sci. 57, 1592-1604.

Bucklin, A., Frost, B.W., Bradford-Grieve, J.M., Allen, L.D., Copley, N.J., 2003. Molecular systematic and phylogenetic assessment of 34 calanoid copepod species of the Calanidae and Clausoalanidae. Mar. Biol. 142, 333-343.

Campbell, P.M., 2005. Species differentiation of insects and other multicellular organisms using matrix-assisted laser desorption/ionization time of flight mass spectrometry protein profiling. Syst. Entomol. 30, 186-190.

Chen, G., Hare, M.P., 2008. Cryptic ecological diversification of a planktonic estuarine copepod, *Acartia tonsa*. Mol. Ecol. 17, 1451-1468.

Clarke, A., Gorley, R.N., 2006. PRIMER v6: User manual/tutorial. PRIMER-E. Plymouth. 192 pp.

Claydon, M.A., Davey, S.N., Edwards-Jones, V., Gordon, D.B., 1996. The rapid identification of intact microorganisms using mass spectrometry. Nat. Biotechnol. 14, 1584-1586.

Cornils, A., Schnack-Schiel, S.B., Böer, M., Graeve, M., Struck, U., Al-Najjar, T., Richter, C., 2007. Feeding of Clausocalanids (Calanoida, Copepoda) on naturally occurring particles in the northern Gulf of Aqaba (Red Sea). Mar. Biol. 151, 1261-1274.

Cornils, A., Held, C., 2014. Evidence of cryptic and pseudocryptic speciation in the *Paracalanus parvus* species complex (Crustacea, Copepoda, Calanoida). Front. Zool. 11, 1-17.

Cotter, R.J., 1992. Time-of-Flight Mass-Spectrometry for the Structural-Analysis of Biological Molecules. Anal. Chem. 64, A1027-a1039.

Diekmann, R., Helmuth, R., Erhard, M., Malorny, B., 2008. Rapid classification and identification of salmonellae at the species and subspecies levels by whole-cell matrix-assisted laser desorption ionization-time of flight mass spectrometry. Appl. Environ. Microbiol. 74, 7767-7778.

Dieme, C., Yssouf, A., Vega-Rua, A., Berenger, J.M., Failloux, A.B., Raoult, D., Parola, P., Almeras, L., 2014. Accurate identification of Culicidae at aquatic developmental stages by MALDI-TOF MS profiling. Parasit. Vectors 7.

Feltens, R., Gorner, R., Kalkhof, S., Groger-Arndt, H., von Bergen, M., 2010. Discrimination of different species from the genus *Drosophila* by intact protein profiling using matrix-assisted laser desorption ionization mass spectrometry. BMC Evol. Biol. 10.

Fenselau, C., Demirev, P.A., 2001. Characterization of intact microorganisms by MALDI mass spectrometry. Mass Spectrom. Rev. 20, 157-171.

Frangoulis, C., Christou, E.D., Hecq, J.H., 2005. Comparison of marine copepod outfluxes: Nature, rate, fate and role in the carbon and nitrogen cycles. Adv. Mar. Biol. 47, 253-309.

Gibb, S., Strimmer, K., 2012. MALDIquant: A versatile R package for the analysis of mass spectrometry data. Bioinformatics 28, 2270-2271.

Gibb, S., 2014. MALDIquantForeign: Import/Export routines for MALDIquant. R pack. ver. 0.9. http://CRAN.R-project.org/package=MALDIquantForeign.

Gibb, S., Strimmer, K., 2014. Species identification using MALDIquant.

Goetze, E., 2003. Cryptic speciation on the high seas: Global phylogenetics of the copepod family Eucalanidae. Proc. R. Soc. Lond. B 270, 2321-2331.

Haag, A.M., Taylor, S.N., Johnston, K.H., Cole, R.B., 1998. Rapid identification and speciation of *Haemophilus* bacteria by matrix-assisted laser desorption/ionization time-of-flight mass spectrometry. J. Mass Spectrom. 33, 750-756.

Hays, G.C., Richardson, A.J., Robinson, C., 2005. Climate change and marine plankton. Trends Ecol. Evol. 20, 337-344.

Herbert, P.D.N., Ratnasingham, S., DeWaard, J.R., 2003a. Barcoding animal life: Cytochrome c oxidase subunit 1 divergences among closely related species. Proc. R. Soc. Lond. B (Suppl.) 270, 96-99.

Herbert, P.D.N., Cywinska, A., Ball, S.L., deWaard, J.R., 2003b. Biological identifications through DNA barcodes. Proc. R. Soc. Lond. B 270, 313-321.

Hillenkamp, F., Karas, M., Beavis, R.C., Chait, B.T., 1991. Matrix-assisted laser desorption ionization mass - spectrometry of biopolymers. Anal. Chem. 63, A1193-a1202.

Holland, R.D., Wilkes, J.G., Rafii, F., Sutherland, J.B., Persons, C.C., Voorhees, K.J., Lay, J.O., 1996. Rapid identification of intact whole bacteria based on spectral patterns using matrix-assisted laser desorption/ionization with time-of-flight mass spectrometry. Rapid Comm. Mass Spectrom. 10, 1227-1232.

Hooff, R.C., Peterson, W.T., 2006. Copepod diversity as an indicator of changes in ocean and climate conditions of the northern California current ecosystem. Limnol. Oceanogr. 51, 2607-2620.

Jarman, K.H., Daly, D.S., Petersen, C.E., Saenz, A.J., Valentine, N.B., Wahl, K.L., 1999. Extracting and visualizing matrix-assisted laser desorption/ionization time-of-flight mass spectral fingerprints. Rapid Communications in Mass Spectrometry 13, 1586-1594.

Kaiser, P., 2015. MALDI-TOF mass spectrometry - a novel method for the identification of pelagic copepods. Universität Bremen, Bremen, pp. 62.

Karger, A., Kampen, H., Bettin, B., Dautel, H., Ziller, M., Hoffmann, B., Suss, J., Klaus, C., 2012. Species determination and characterization of developmental stages of ticks by whole-animal matrix-assisted laser desorption/ionization mass spectrometry. Ticks Tick Borne Dis. 3, 78-89.

Kaufmann, C., Ziegler, D., Schaffner, F., Carpenter, S., Pfluger, V., Mathis, A., 2011. Evaluation of matrix-assisted laser desorption/ionization time-of-flight mass spectrometry for characterization of *Culicoides nubeculosus* biting midges. Med. Vet. Entomol. 25, 32-38.

Knowlton, N., 1993. Sibling species in the sea. A. Rev. Ecol. Syst. 24, 189-216.

Kosobokova, K.N., Hirche, H.-J., Scherzinger, T., 2002. Feeding ecology of *Spinocalanus antarcticus*, a mesopelagic copepod with a looped gut. Mar. Biol. 141, 503-511.

Kosobokova, K.N., Hopcroft, R.R., Hirche, H.-J., 2011. Patterns of zooplankton diversity through the depths of the Arctic's central basins. Mar. Biodiv. 41, 29-50.

Krishnamurthy, T., Ross, P.L., Rajamani, U., 1996. Detection of pathogenic and nonpathogenic bacteria by matrix-assisted laser desorption/ionization time-of-flight mass spectrometry. Rapid Comm. Mass Spectrom. 10, 883-888.

Kuriyama, M., Nishida, S., 2006. Species diversity and niche-partitioning in the pelagic copepods of the family Scolecitrichidae (Calanoida). Crustaceana 79, 293-317.

Laakmann, S., Kochzius, M., Auel, H., 2009a. Ecological niches of Arctic deep-sea copepods: Vertical partitioning, dietary preferences and different trophic levels minimize inter-specific competition. Deep-Sea Res Part I 56, 741-756.

Laakmann, S., Stumpp, M., Auel, H., 2009b. Vertical distribution and dietary preferences of deep-sea copepods (Euchaetidae and Aetideidae; Calanoida) in the vicinity of the Antarctic Polar Front. Polar Biol. 32, 679-689.

Laakmann, S., Auel, H., Kochzius, M., 2012. Evolution in the deep sea: Biological traits, ecology and phylogenetics of pelagic copepods. Mol. Phylogenet. Evol. 65, 535-546.

Laakmann, S., Gerdts, G., Erler, R., Knebelsberger, T., Arbizu, P.M., Raupach, M.J., 2013. Comparison of molecular species identification for North Sea calanoid copepods (Crustacea) using proteome fingerprints and DNA sequences. Mol. Ecol. Resour. 13, 862-876.

Lee, C.E., Frost, B.W., 2002. Morphological stasis in the *Eurytemora affinis* species complex (Copepoda: Temoridae). Hydrobiol. 480, 111-128.

Levitan, D.R., Fukami, H., Jara, J., Kline, D., McGovern, T.M., McGhee, K.E., Swanson, C.A., Knowlton, N., 2004. Mechanisms of reproductive isolation among sympatric broadcast-spawning corals of the *Montastraea annularis* species complex. Evolution 58, 308-323.

Li, T.Y., Liu, B.H., Chen, Y.C., 2000. Characterization of *Aspergillus* spores by matrix-assisted laser desorption/ionization time-of-flight mass spectrometry. Rapid Commun. Mass Spectrom. 14, 2393-2400.

Longhurst, A.R., 1985. Relationship between diversity and the vertical structure of the upper ocean. Deep-Sea Res. I 32, 1535-1570.

Longhurst, A.R., 1985. Relationship between diversity and the vertical structure of the upper ocean. Deep-Sea Res. I 32, 1535-1570.

Longhurst, A.R., Harrison, W.G., 1989. The biological pump: Profiles of plankton production and consumption in the upper ocean. Prog. Oceanogr. 22, 47–123.

Lonsdale, D.J., Frey, M.A., Snell, T.W., 1998. The role of chemical signaling in copepod reproduction. J. Mar. Syst. 15.

Maier, T., Kostrzewa, M., 2007. Fast and reliable MALDI-TOF MS-based microorganism identification. Chim. Oggi 25, 68-71.

Marklein, G., Josten, M., Klanke, U., Muller, E., Horre, R., Maier, T., Wenzel, T., Kostrzewa, M., Bierbaum, G., Hoerauf, A., Sahl, H.G., 2009. Matrix-assisted laser desorption ionization-time of flight mass spectrometry for fast and reliable identification of clinical yeast isolates. J. Clin. Microbiol. 47, 2912-2917.

Mathis, A., Depaquit, J., Dvořák, V., Tuten, H., Bañuls, A.L., Halada, P., Zapata, S., Lehrter, V., Hlavačková, K., Prudhomme, J., Volf, P., Sereno, D., Kaufmann, C., Pflüger, V., Schaffner, F., 2015. Identification of phlebotomine sand flies using one MALDI-TOF MS reference database and two mass spectrometer systems. Parasit. Vectors 8.

Matsuura, H., Nishida, S., Nishikawa, J., 2010. Species diversity and vertical distribution of the deep-sea copepods of the genus *Euaugaptilus* in the Sulu and Celebes Seas. Deep-Sea Res. II 57, 2098-2109.

McManus, G.B., Katz, L.A., 2009. Molecular and morphological methods for identifying plankton: What makes a successful marriage? J. Plankt. Res. 31, 1119-1129.

Müller, P., Pflüger, V., Wittwer, M., Ziegler, D., Chandre, F., Simard, F., Lengeler, C., 2013. Identification of cryptic *Anopheles* mosquito species by molecular protein profiling. PLoS ONE 8, e57486.

Palumbi, S.R., 1994. Genetic divergence, reproductive isolation, and marine speciation. Annu. Rev. Ecol. Syst. 25, 547-572.

Pappin, D.J.C., Hojrup, P., Bleasby, A.J., 1993. Rapid Identification of Proteins by Peptide-Mass Finger Printing. Curr. Biol. 3, 327-332.

Peralba, A., Mazzocchi, M.G., 2004. Vertical and seasonal distribution of eight *Clausocalanus* species (Copepoda: Calanoida) in oligotrophic waters. ICES J. Mar. Sci. 61, 645-653.

Perera, M.R., Vargas, R.D.F., Jones, M.G.K., 2005. Identification of aphid species using protein profiling and matrix-assisted laser desorption/ionization time-of-flight mass spectrometry. Entomol. Exp. Appl. 117, 243-247.

R core team, 2015. R: A language and environment for statistical computing. R Foundation for Statistical Computing, Vienna, Austria. URL http://www.R-project.org/

Riccardi, N., Lucini, L., Benagli, C., Welker, M., Wicht, B., Tonolla, M., 2012. Potential of matrix-assisted laser desorption/ionization time-of-flight mass spectrometry (MALDI-TOF MS) for the identification of freshwater zooplankton: A pilot study with three *Eudiaptomus* (Copepoda: Diaptomidae) species. J. Plankt. Res. 34, 484-492.

Rocha-Olivares, A., Fleeger, J.W.F., D.W., 2001. Decoupling of molecular and morphological evolution in deep lineages of a meiobenthic harpacticoid copepod. Mol. Biol. Evol. 18, 1088-1102.

Ryzhov, V., Fenselau, C., 2001. Characterization of the protein subset desorbed by MALDI from whole bacterial cells. Anal. Chem. 73, 746-750.

Saffert, R.T., Cunningham, S.A., Ihde, S.M., Monson Jobe, K.E., Mandrekar, J., Patel, R., 2011. Comparison of Bruker Biotyper matrix-assisted laser desorption ionization - time of flight mass spectrometer to BD Pheonix Automated Microbiology System for identification of gram-negative bacilli. J. Clin. Microbiol. 49, 887-892.

Salla, V., Murray, K.K., 2013. Matrix-assisted laser desorption/ionization mass spectrometry for identification of shrimp. Anal. Chim. Acta 794, 55-59.

Sandrin, T.R., Goldstein, J.E., Schumaker, S., 2013. MALDI TOF MS profiling of bacteria at the strain level: A review. Mass Spectrom. Rev. 32, 188-217.

Sano, M., Maki, K., Nishibe, Y., Nagata, T., Nishida, S., 2013. Feeding habits of mesopelagic copepods in Sagami Bay: Insights from integrative analysis. Prog. Oceanogr. 110, 11-26.

Sano, M., Nishibe, Y., Tanaka, Y., Nishida, S., 2015. Temporally sustained dietary niche partitioning in two mesopelagic copepod species and their mouthpart morphology. Mar. Ecol. Prog. Ser. 518, 51-67.

Schukat, A., Auel, H., Teuber, L., Hagen, W., 2014. Complex trophic interactions of calanoid copepods in the Benguela upwelling system. J. Sea Res. 85, 186-196.

Seng, P., Drancourt, M., Gouriet, F., La Scola, B., Fournier, P.-E., Rolain, J.M., Raoult, D., 2009. Ongoing revolution in bacteriology: Routine identification of bacteria by matrix-assisted laser desorption ionization time-of-flight mass spectrometry. Clin. Infect. Dis. 49, 543-551.

Shimode, S., Hiroe, Y., Hidaka, K., Takahashi, K., Tsuda, A., 2009. Life history and ontogenetic vertical migration of *Neocalanus gracilis* in the western North Pacific Ocean. Aquat. Biol. 7, 295-306.

Stackebrandt, E., Päuker, O., Erhard, M., 2005. Grouping Myxococci (*Corallococcus*) strains by matrix-assisted laser desorption/ionization time-of-flight (MALDI-TOF) mass spectrometry: Comparison with gene sequence phylogenies. Curr. Microbiol. 50, 71-77.

Steinberg, D.K., Lomas, M.W., Cope, J.S., 2012. Long-term increase in mesozooplankton biomass in the Sargasso Sea: Linkage to climate and implications for food web dynamics and biogeochemical cycling. Global Biogeochem. Cycles 26.

Strimmer, K., 2014. crossval: Generic functions for cross validation. R package version 1.0.2. http://CRAN.R-project.org/package=crossval.

Thum, R.A., Harrison, R.G., 2009. Deep genetic divergence among morphologically similar and parapatric *Skistodiaptomus* (Copepoda: Calanoida: Diaptomidae) challenge the hypothesis of Pleistocene speciation. Biol. J. Linnean. Soc. 96.

Turner, J.T., 2004b. The importance of small planktonic copepods and their roles in pelagic marine food webs. Zool. Stud. 43, 255-266.

Turner, J.T., 2015. Zooplankton fecal pellets, marine snow, phytodetritus and the ocean's biological pump. Progr. Oceanogr. 130, 205-248.

Uhlmann, K.R., Gibb, S., Kalkhof, S., Arroyo-Abad, U., Schulz, C., Hoffmann, B., Stubbins, F., Carpenter, S., Beer, M., Von Bergen, M., Feltens, R., 2014. Species determination of *Culicoides* biting midges via

peptide profiling using matrix-assisted laser desorption ionization mass spectrometry. Parasit. Vectors 7, 392.

van Veen, S.Q., Class, E.C.J., Kuijper, J., 2010. High-throughput identification of bacteria and yeast by matrix-assisted laser desorption ionization-time of flight mass spectrometry in conventional medical microbiology laboratories. J. Clin. Microbiol. 48, 900-907.

Vargha, M., Takáts, Z., Konopka, A., Nakatsu, C.H., 2006. Optimization of MALDI-TOF MS for strain level differentiation of *Arthrobacter isolates*. J. Microbiol. Methods 66, 399-409.

Verheye, H.M., Field, J.G., 1992. Vertical distribution and diel vertical migration of *Calanoides carinatus* (Kroyer, 1849) developmental stages in the southern Benguela upwelling region. J. Exp. Mar. Biol. Ecol. 158, 123-140.

Verheye, H.M., Richardson, A.J., 1998. Long-term increase in crustacean zooplankton abundance in the southern Benguela upwelling region (1951-1996): Bottom-up or top-down control? ICES J. Mar. Sci. 55, 803-807.

Volta, P., Riccardi, N., Lauceri, R., Tonolla, M., 2012. Discrimination of freshwater fish species by Matrix-Assisted Laser Desorption/Ionization-Time of Flight Mass Spectrometry (MALDI-TOF MS): A pilot study. J. Limnol. 71, 164-169.

Warnes, G.R., Bolker, B., Bonebakker, L., Gentleman, R., Huber, W., Liaw, A., Lumley, T., Maechler, M., Magnusson, A., Moeller, S., Schwartz, M., Venables, B., 2015. gplots: Various R programming tools for plotting data. R package version 2.17.0. http://CRAN.R-project.org/package=gplots.

Weissburg, M.J., Doall, M.H., Yen, J., 1998. Following the invisible trail: Kinematic analysis of mate-tracking in the copepod *Temora longicornis*. Phil. Trans. Royal Soc. Lond. B 353, 701-712.

Wieser, A., Schneider, L., Jung, J.T., Schubert, S., 2012. MALDI-TOF MS in microbiological diagnostics - identification of microorganisms and beyond (mini review). Appl. Microbiol. Biotechnol. 93, 965-974.

Wishner, K.F., Gelfman, C., Gowing, M.M., Outram, D.M., Rapien, M., Williams, R.L., 2008. Vertical zonation and distributions of calanoid copepods through the lower oxycline of the Arabian Sea oxygen minimum zone. Prog. Oceanogr. 78, 163-191.

Yamaguchi, A., Ikeda, T., 2002. Vertical distribution patterns of three mesopelagic Paraeuchaeta species (Copepoda: Calanoida) in the Oyashio region, western subarctic Pacific Ocean. Bull. Fish. Sci. Hokkaido Univ. 53, 1-10.

Yamaguchi, A., Ikeda, T., Watanabe, Y., Ishizaka, J., 2004. Vertical distribution patterns of pelagic copepods as viewed from the predation pressure hypothesis. Zoological Studies 43, 475-485.

Yamaguchi, A., Ohtsuka, S., Hirakawa, K., Ikeda, T., 2007. Vertical distribution and feeding ecology of a copepod *Gaetanus variabilis* in the southern Japan Sea during winter. La Mer 45, 47-58.

Yen, J., Weissburg, M.J., Doall, M.H., 1998. The fluid physics of signal perception by mate-tracking copepods. Phil. Trans. Royal Soc. Lond. B 353, 787-804.

Yssouf, A., Flaudrops, C., Drali, R., Kernif, T., Socolovschi, C., Berenger, J.M., Raoult, D., Parola, P., 2013a. Matrix-assisted laser desorption ionization - time of flight mass spectrometry for rapid identification of tick vectors. J. Clin. Microbiol. 51, 522-528.

Yssouf, A., Socolovschi, C., Flaudrops, C., Ndiath, M.O., Sougoufara, S., Dehecq, J.S., Lacour, G., Berenger, J.M., Sokhna, C.S., Raoult, D., Parola, P., 2013b. Matrix-assisted laser desorption ionization - time of flight mass spectrometry: an emerging tool for the rapid identification of mosquito vectors. PLoS ONE 8, e72380.

Yssouf, A., Socolovschi, C., Leulmi, H., Kernif, T., Bitam, I., Audoly, G., Almeras, L., Raoult, D., Parola, P., 2014. Identification of flea species using MALDI-TOF/MS. Comp. Immunol. Microbiol. Infect. Dis. 37, 153-157.

3 SYNOPTIC DISCUSSION

The eastern Atlantic Ocean comprises very different ecosystems in terms of oceanographic and biogeochemical conditions (Aiken 2000). While upwelling regions are highly variable ecosystems regarding productivity, oxygen concentration and water temperature, oceanic tropical and subtropical ecosystem are rather stable with high temperatures, strong stratification and low nutrient supply and thus low, but constant productivity throughout the year (Longhurst et al. 1995; Aiken 2000; Marañon et al. 2000, 2003). Besides regional differences, strong vertical gradients are present in the pelagic realm (Longhurst 1985; Longhurst and Harrison 1989; Kosobokova et al. 2011).

The mesopelagic zone (200-1000 m) is a transition zone between the euphotic zone and the deep sea. It is still influenced by strong gradients of chemical and physical parameters such as e.g. decreasing light intensities, permanent thermoclines and oxygen minimum zones (OMZ) (Koppelmann and Frost 2008; Robinson et al. 2010). In contrast, the bathypelagic environment (>1000 m) is characterized by rather uniform environmental conditions such as low temperatures, complete darkness, high pressure, high inorganic nutrient concentrations and generally low food availability, posing specific challenges for organisms inhabiting the deep sea (Koppelmann and Frost 2008; Robinson et al. 2010; Laakmann et al. 2012). However, food supply may significantly vary temporally and spatially, depending on the productivity regime in the corresponding euphotic layer (Koppelmann and Weikert 2007), usually with a delay of sinking particles in the bathypelagic zone (1500-3000 m) by several weeks to months (Voss et al. 1996; Holmes et al. 2002).

As key representatives of mesozooplankton communities, copepods are important mediators of vertical carbon flux in the ocean (Chapter IV; Longhurst et al. 1990). Their biomass, community composition and interactions strongly affect the magnitude of organic carbon recycled in the epipelagic realm or exported to deeper layers (Chapter IV; Sasaki et al. 1988; Ducklow et al. 2001; Yamaguchi et al. 2002; Hannides et al. 2009; Homma et al. 2011; Steinberg et al. 2008a,b, 2012). In order to reliably model biogeochemical cycles and ecosystem processes, e.g. the contribution of different ecosystems to the carbon cycle, it is a prerequisite to understand the dynamics of community composition, distributional patterns and ecological roles of various key species (Chapters I, II and IV; Ducklow et al. 2001; Armstrong et al. 2002; Yamaguchi et al. 2002;

Buesseler et al. 2007; Hannides et al. 2009; Burd et al. 2010; Robinson et al. 2010; Steinberg et al. 2012).

This thesis provides an extensive and detailed data set on ecological and physiological aspects of copepod communities in different regions of the tropical and subtropical eastern Atlantic in relation to spatial, i.e. regional and vertical, distribution and environmental parameters. Copepod abundance, biomass and community structure were analyzed at six sites along a latitudinal transect in the eastern Atlantic Ocean (24°N to 21°S) from the surface down to 2000 m: the Canary basin, Cape Verde basin, Sierra Leone basin, Guinea basin, the Angola basin and near the Walvis Ridge. Based on hydrological and biogeochemical features, the regions were divided into four large provinces: the subtropical North Atlantic (STNA), tropical North Atlantic (TNA), subtropical South Atlantic (STSA) and a region influenced by the Benguela Current (BCIR). Furthermore, a time series on seasonal, interannual and spatial variations of copepod abundance and their community composition was analyzed in the northern Benguela Current upwelling system (NBC) at 20°S for the period 2005 to 2011.

The following section (section 3.1) provides a detailed overview of copepod abundance, biomass and community structures in relation to the different hydrographic regimes. Furthermore, ecophysiological features of key copepod species along the latitudinal transect in the eastern Atlantic Ocean were investigated during this study. In particular, lipid contents, fatty acid profiles, stable isotope signatures and metabolic rates were determined for dominant calanoid copepods to elucidate dietary preferences, trophic positions, nutritional requirements and life-cycle adaptations. In section 3.2 the impact of different copepod communities and the contribution of certain key copepod species to the vertical carbon flux down to 2000 m depth are assessed. Ecophysiological aspects are related to species-specific distributional patterns and concepts of biodiversity in tropical regions and deep-sea environments, supported by the results from proteomic fingerprinting using matrix-assisted laser desorption/ionization time-of-flight mass spectrometry (MALDI-TOF MS). Finally, the potential value of proteomic fingerprinting to copepod biodiversity research is evaluated in section 3.4.

3.1 Copepod biomass and community structure in relation to space and time

Copepod distribution in relation to primary productivity regimes

In the present study rather mesotrophic conditions persisted along the latitudinal transect in the eastern tropical and subtropical regions. Lowest primary production rates (PP) were 445 mg C m^{-2} d^{-1} in the STNA. Relatively high PP between 563-907 mg C m^{-2} d^{-1} occurred in the TNA, while maximum PP of 930 mg C m^{-2} d^{-1} was encountered in the BCIR (Chapters III and IV). Oligotrophic conditions usually occur in centers of the subtropical gyres with PP typically < 300-400 mg C m^{-2} d^{-1} (Longhurst et al. 1995). The general dominance of picophytoplankton in tropical and subtropical oceanic regions emphasizes the importance of microbial loop organisms and their significance in trophic pathways in these regions (Calbet and Landry 1999; Steinberg et al. 2001; Marañón et al. 2003; Arístegui et al. 2005, Calbet 2008). Especially in the eastern tropical Atlantic, N_2-fixation is enhanced by atmospheric dust input and extensively contributes to the nitrogen budget and thus to PP, which is then channeled towards higher trophic levels (Chapters II and III; Montoya et al. 2002; Hauss et al. 2013; Sandel et al. 2015). However, even though usually uniform growth conditions prevail in the subtropical gyres, a remarkable variability of PP (18-362 mg C m^{-2} d^{-1}) can be present due to significant changes of nutrient supply and in the composition of the picophytoplankton community (Marañón et al. 2003). Time-series studies demonstrated significant seasonal and interannual variability in phytoplankton and bacterioplankton production, biomass and community structure in subtropical regions of the Atlantic and Pacific (Karl et al. 2001; Steinberg et al. 2001).

Maximum biomass of calanoid copepods integrated from the surface to 2000 m (2.7 g dry mass (DM) m^{-2}) occurred in the BCIR, coinciding with highest surface PP in the euphotic zone (Chapters III and IV). However, highest copepod biomass did not necessarily coincide with highest primary production rates. A closer look into the specific depth strata was necessary, as copepod communities exhibited very different vertical structures. In the BCIR, the largest copepod biomass prevailed as diel vertical migrants in the upper mesopelagic zone (200-400 m: 8.0 mg DM m^{-3}) (Chapter IV). In contrast, highest biomass in the TNA was found in the surface layer (0-50 m: 21 mg DM m^{-3}) coinciding with highest PP in this layer, but also with a very pronounced oxygen minimum zone (OMZ) (stn. 8; Chapters III and IV). The relatively shallow OMZ may have restrained species preferring higher oxygen concentrations in water layers above the OMZ. This phenomenon was also observed at stations in the Angola Dome (Teuber et al.

2013). Tropical oceans are known for their enormous horizontal and vertical expansion of permanent OMZs (Ekau et al. 2010; Stramma et al. 2010).

Due to the upwelling of cold, nutrient-rich waters, coastal upwelling regions such as the NBC support much higher regional primary and secondary production rates compared to the less productive open ocean environments (Hutchings et al. 1995; Gasol et al. 1997; Le Borgne and Rodier 1997; Isla et al. 2004). For example, in the southern Benguela Current system (SBC) the annual mean of copepod biomass is around 2.1 g C m^{-2} (years 1988-2003; Hugget et al. 2009). In contrast, the highest estimated copepod biomass was 1.3 g DM m^{-2} in the epipelagic zone of the TNA, which equals ca. 0.5 g C m^{-2}, assuming carbon was 40% of dry mass after Peterson et al. (1990) (Chapter IV). Copepod abundance in the epipelagic zone of the NBC typically ranged from 300 to 500 x 10^3 m^{-2} (max. 857 x 10^3 m^{-2}), in contrast to 50-127 x 10^3 m^{-2} in the tropical and subtropical Atlantic (Chapters I and IV). In the NBC, highest copepod densities were neither correlated with coldest sea surface temperatures (upwelling) nor highest chlorophyll *a* concentrations, due to the clear offset between physical changes, phytoplankton growth and zooplankton development (Chapter I; Hutchings et al. 2006). Even during a 27-day time series at St. Helena Bay in the SBC, daily changes of zooplankton biomass appeared to be uncorrelated with upwelling cycles (Verheye 1991). Plankton dynamics are driven by non-linear interactions between upwelling events, water column stratification, regeneration and recycling of nutrients, biological interactions and species-specific responses as well as ontogenetic development times (Chapter I; Andersen et al. 2001a; Arístegui et al. 2005; Hutchings et al. 2006; Abe et al. 2012; Hansen et al. 2014). This clearly exacerbates the establishment of reliably predictive model of plankton dynamics.

However, copepod abundance, biomass and community structure are certainly connected to upwelling intensities (Chapters I and IV; Roemmich and McGowan 1995; Verheye et al. 1998; Hutchings et al. 2006). Interannually, lowest copepod abundances occurred in the NBC during the years 2008/09 and 2009/10, which coincided with low spring to late summer temperature gradients, thus, less pronounced upwelling in spring and only moderate warm-water intrusions in late summer (Chapter I). In contrast, years with strong upwelling in spring and intensive warm-water intrusions in later summer, as in 2005/06 and 2010/11, were characterized by high copepod abundances, suggesting a strong link between zooplankton distribution and physical forcing (Chapter I). In the SBC, a 100-fold increase in mesozooplankton abundance was reported between 1950 and 1995 (Verheye et al. 1998), while upwelling intensities also increased during

this time period (Shannon et al. 1992). Since 1995 zooplankton densities, particularly those of larger copepods have decreased again in the SBC, accompanied by an increase in anchovy biomass indicating that top-down mechanisms may also be important drivers of copepod abundance (Verheye et al. 1998; Hutchings et al. 2006).

It is still unclear, whether ecosystems are bottom-up and/or top-down controlled and to which degree these mechanisms interact (Ware and Thomson 2005). Zooplankton size structure may be influenced by the dominant size of their prey, as e.g. an increase in phytoplankton size may lead to an increase in the size of the zooplankton grazers (Kiørboe 1993; Legendre and Michaud 1998; Steinberg et al. 2012). Likewise, planktivorous fish feeding primarily on larger zooplankton may lead to dominance of small-sized zooplankton species, and, as a consequence to less intense grazing on larger phytoplankton species (Carpenter et al. 1995; Verheye et al. 1998; Clark et al. 2001; Steinberg et al. 2012). To truly disentangle ecosystem functioning and reliably predict ecosystem changes, it is apparently not sufficient to study zooplankton size-classes (e.g. Dam et al. 1993, 1995; Boyd and Newton 1999; Huskin et al. 2001; Isla et al. 2004; Koppelmann et al. 2004; San Martin et al. 2006; Calbet et al. 2009). More detailed studies on species distribution and community structures coupled with ecophysiological performance and high taxonomic resolution are necessary, as many species of similar sizes have completely different life strategies and feeding behaviors. This is addressed in detail in the following sections.

Community structure in different hydrographic regimes and vertical strata

Copepod abundance and biomass typically decreases exponentially with increasing depth in tropical regions (Chapter IV; Le Borgne et al. 2003; Champalbert et al. 2005; Teuber et al. 2013), as well as at higher latitudes (Koppelmann and Weikert 1992; Auel and Hagen 2002; Yamaguchi et al. 2002; Kosobokovo and Hopcroft 2010; Homma et al. 2011; Kosobokova et al. 2011). Variations in species composition in the pelagic realm are usually much more affected by depth than by regional differences (Chapter IV; Auel and Hagen 2002; Kosobokova et al. 2011; Yamaguchi et al. 2015). Significant differences in depth layer-specific species abundance and community structure confirmed the general vertical partitioning of the ocean into an upper (0-100 m) and lower (100-200 m) epipelagic stratum, an upper (200-400 m) and lower (400-1000 m) mesopelagic zone, and a bathypelagic zone (>1000 m) (e.g. Chapter IV; Deevey and Brooks 1977; Weikert and Trinkaus 1990; Yamaguchi et al. 2002; Kosobokova and Hopcroft 2010), while

maximum sampling depth in the present study was 2000 m. Nevertheless, the abundance of certain key species with different life-history traits varied between hydrographic provinces in the eastern tropical and subtropical Atlantic, indicating differences in the role of copepod communities in biogeochemical cycles and in the functioning of different marine ecosystems (see section 3.2). In following sections the differences of copepod community structures between the different hydrographic provinces are elaborated and schematically presented in Fig. 1.

Oceanic tropical and subtropical regions (STNA, TNA and STSA)

Calanoid copepods are the dominant biomass component of zooplankton communities in most marine regions (Chapter IV; Yamaguchi et al. 2002; Homma et al. 2011). In the upper epipelagic zone, small calanoids such as *Clausocalanus, Delibus*, *Calocalanus* and *Acartia* usually contribute large portions of copepod biomass in the euphotic zone, due to their enormously high abundances, especially in tropical and subtropical oceanic waters, and owing to the absence of large, herbivorous calanoids from less-productive warm waters (Chapter IV; Woodd-Walker 2001; Paffenhöfer and Mazzocchi 2003; Schnack-Schiel et al. 2010). Especially in the STNA, where PP was lowest, these small species prevailed down to 200 m (Chapter IV). In contrast, in the TNA and STSA, larger biomass species such as *Euchaeta marina, Undinula vulgaris, Nannocalanus minor* and *Neocalanus* spp. (mainly *N. gracilis*) were important components of the copepod communities, whereas *E. marina* clearly dominated in the TNA, and *N. minor* and *Neocalanus* spp. in the STSA (Chapter IV). Of the tropical epipelagic Calanidae, the genus *Neocalanus* is known to accumulate moderately high amounts of wax esters, performing ontogenetic vertical migrations (OVM) on a very small scale within the upper 300 m but without any dormant stages (Chapter II; Shimode et al. 2009).

Eucalanidae such as *Pareucalanus* spp., *Subeucalanus* spp. and, to a lesser extent *Rhincalanus cornutus* were also important in epipelagic layers of the TNA, and additionally *Eucalanus hyalinus* in the STSA. Eucalanid species are known for their sluggish life style with generally low locomotory activities, reduced metabolic rates, high wax ester levels and OVM (Chapter II; Cass et al. 2011; Bode et al. 2013; Schukat et al. 2014; Teuber 2014). They conduct a rather event-driven form of quiescence, presumably responding to increases in phytoplankton production (Ohman et al. 1998; Shimode et al. 2012a,b). *R. rostrifrons* and on rare occasions also *R. nasutus*

occur in both upwelling and non-upwelling regions in the tropical Pacific Ocean, with dormant individuals being able to respond quickly to small-scale upwelling events (Ohman et al. 1998; Schnack-Schiel et al. 2008; Shimode et al. 2012a,b). Although dormancy has not been studied yet in the Atlantic species *R. cornutus*, it is likely to be shared among tropical-subtropical *Rhincalanus* species (Shimode et al. 2012a).

Large numbers of *Subeucalanus monachus/pileatus*, *Pareucalanus* spp., *R. cornutus* and *E. hyalinus* occurred in the mesopelagic or even bathypelagic layers in all regions, the STNA, TNA and STSA, and additionally *R. nasutus* in the STNA. These deep-water populations apparently survive in dormant stages "waiting" to be transported to more favorable conditions (Chapters II and IV; Ohman et al. 1998; Schnack-Schiel et al. 2008; Shimode et al. 2012a,b). Metabolic rates of deep-dwelling eucalanid species may be reduced by 47% to 62% compared to surface-dwelling individuals (Schukat et al. 2013; Teuber 2014). Due to this metabolic reduction, they can easily cope with low oxygen concentrations and frequently occur in OMZs (Flint et al. 1991; Ohman et al. 1998; Wishner et al. 2000, 2008, 2013; Teuber et al. 2013).

In general, the dominant species encountered in the lower epipelagic and upper mesopelagic zone in the eastern Atlantic were typically found in OMZs in different regions of the world (Chapter IV; Gowing and Wishner 1998; Ohman et al. 1998; Wishner et al. 2000, 2008; Loick et al. 2005; Auel and Verheye 2007; Schnack-Schiel et al. 2008; Escribano et al. 2009; Teuber et al. 2013). For example, besides the group of Eucalanidae, *Scolecithricella*, *Scaphocalanus, Heterorhabdus lobatus/papilliger* and *Haloptilus longicirrus/longicornis* were present in all layers of the OMZ, with generally maximum abundances between 50-400 m (Chapter IV). Diel vertical migrations (DVM) with night-time feeding in the surface layers and residence in deeper layers during the day are common among many epi- and mesopelagic copepods such as species of the genera *Scaphocalanus, Scottocalanus*, *Temoropia*, *Metridia*, *Pleuromamma* (Longhurst and Williams 1979; Weikert 1982; Peterson 1998; Steinberg et al. 2000; Sano et al. 2013). In general, amplitudes of DVMs are within the range of about 100 m (Weikert 1982) and presumably serve as a purpose avoid predators in the sun-lit surface layers during the day and reduce metabolic demands in cooler deep water layers (Chapter IV; Ambler and Miller 1987; Pavlova 1994; Wishner et al. 2008). *Metridia* and *Pleruomamma* are rapid and permanent swimmers (Mazzocchi and Paffenhöfer 1999) with an estimated migration speed e.g. of 130-145 m h^{-1} for *P. xiphias* and thus they undergo extensive DVMs as some individuals migrate down to even lower mesopelagic depths (Weikert 1982). These two genera were particularly abundant during the

present study. *Pleuromamma robusta*, *P. gracilis/piseki and P. abdominalis* were most common in the lower epipelagic and upper mesopelagic zone in the TNA, while *M. effusa* was the dominant *Metridia* species in the TNA and STSA and, together with *M. curticauda, M. brevicauda, M. venusta* and *M. princeps*, it was present throughout all oceanic regions in the tropical and subtropical Atlantic (Appendix Table A; Chapter IV). Partial DVMs, where only a part of the population migrates into shallower layers at dusk, were observed in aetideid species such as *Chirundina streetsii*, *Euchirella rostrata*, *Undeuchaeta major* (Sano et al. 2013). Aetideidae occurred with very diverse and often abundant species, although genera rarely played a dominant role in terms of total copepod biomass in the present study (Appendix Table A; Chapter IV; Teuber et al. 2013).

In general, species of the copepod families Lucicutiidae, Heterorhabdidae, Scolecithrichidae, Augaptilidae and Spinocalanidae prevailed below 100 m (Chapter IV; Yamaguchi et al. 2002; Koppelmann and Frost 2008; Wishner et al. 2008; Laakmann et al. 2009a,b; Kosobokova and Hopcroft 2010; Homma et al. 2011; Kosbokova et al. 2011). In particular, *Spinocalanus* and *Euaugaptilus* were dominant in meso- and bathypelagic layers exhibiting high abundances from the upper OMZ down to 2000 m (Chapter IV; Wishner et al. 2000, 2008). Due to the general depletion of zooplankton, rather uniform environmental conditions and dim light to complete darkness, these meso- to bathypelagic species usually perform little or no DVMs at all (Weikert 1982; Kosobokova et al. 2002; Matsuura et al. 2010). Representatives of these deep sea copepods usually contain large amounts of storage lipids, with particularly high amounts of wax esters usually detected in Euchaetidae, Aetideidae, Lucicutiidae, Heterorhabdidae and Augaptilidae (Chapters II; Lee et al. 1971; Kosobokova et al. 2002; Laakmann et al. 2009a,b; Teuber 2014).

Calanoides carinatus occurred only as deep-dwelling copepodids CV (>500 m) off the NW and SW African coast with highest abundances at the northernmost station in the TNA (Chapter IV). *C. carinatus* conduct OVM with a typical bimodal distribution pattern. They reproduce on the shelf in nutrient-rich, recently upwelled surface waters (Auel et al. 2005). A part of the population is transported towards the open ocean by Ekman drift and later descends as copepodids CV to greater depths, where they endure periods of food shortage in diapause, partially relying on their large wax ester reservoirs (Chapters II and IV; Auel et al. 2005; Verheye et al. 2005; Schukat et al. 2014). Metabolic reduction during diapause is extreme up to 96% compared to surface-dwelling active individuals (Arashkevich et al. 1996; Auel et al. 2005;

Schukat et al. 2013). Obviously, the CVs found in the present study belonged to the offshore resting component of the population, which will eventually be transported back onto the shelf by new upwelling events (Chapters II and IV; Verheye et al. 1991; Peterson 1998; Verheye et al. 2005).

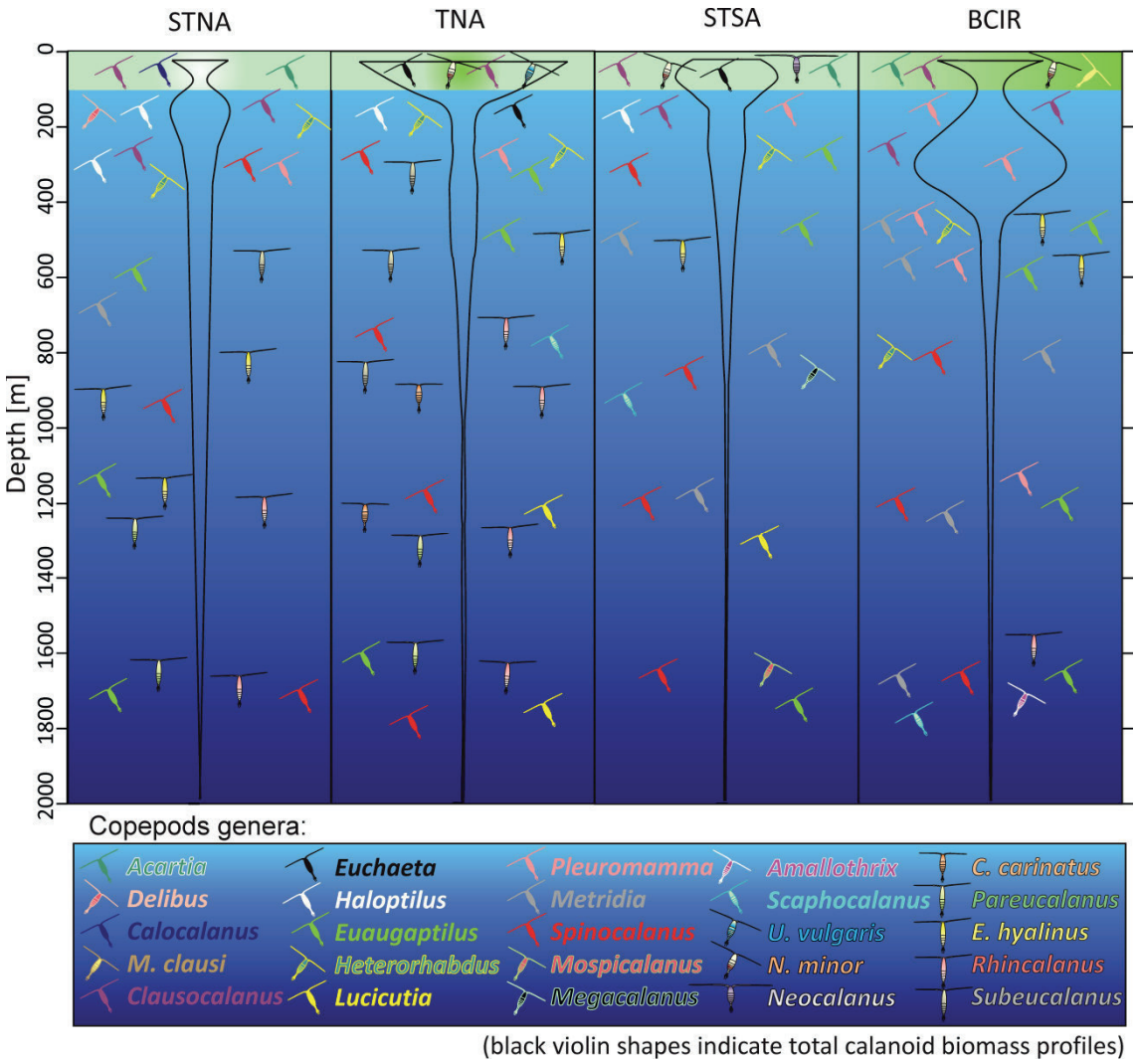

Figure 1: Schematic overview of the most dominant calanoid copepod genera, which contributed the major portions of total copepod biomass in the different hydrographic provinces from the surface down to 2000 m. Total calanoid biomass profiles are indicated as violin shapes in each region (STNA: Subtropical North Atlantic; TNA: Tropical North Atlantic; STSA: Subtropical South Atlantic; BCIR: Benguela Current influenced region). Higher intensities of green in the surface layer indicate higher primary production in this region.

The Benguela Current influenced region (BCIR)

The most striking difference of the BCIR in contrast to the other regions was the extreme dominance of *Pleuromamma* in the lower epipelagic and upper mesopelagic zone, which mainly

consisted of *P. xiphias*, *P. abdominalis* and *P. borealis* (Chapter IV). *M. lucens*, a key species in the offshore region of the Benguela Current upwelling system, was found in the upper mesopelagic only in the STSA and BCIR (Appendix Table A). They usually inhabit water layers below 200 m during daylight and migrate into shallower water layers (100-200 m) during the night (Timonin 1997). As sampling was conducted exclusively during daylight, it is assumed that populations of diel vertical migrants in these layers moved up into the euphotic zone during the night to feed (Chapter IV). Vertical migrations presumably ensure the maintenance of their populations within the productive upwelling area, which are exposed to a strong offshore Ekman-transport at rates of up to several km day^{-1} (Timonin 1991, 1997; Verheye and Field 1992; Peterson 1998; Weisberg et al. 2000; Escribano et al. 2001; Schukat et al. 2013). Such advection processes severely impact population dynamics and distribution patterns of epipelagic species by transporting individuals away from the productive upwelling area. Hence, species that undergo DVMs may be particularly successful in upwelling areas, as they may compensate their night drift by migrating between water layers moving in opposite directions (Peterson et al. 1979; Verheye and Field 1992).

C. carinatus, R. nasutus and *E. hyalinus* occurred only in very low concentrations, with maximum abundances found in the vicinity of the NW and SW African coast (Chapter IV). In oceanic regions of the tropical and subtropical Atlantic other congeners of these copepod families were dominant (see above). These three species are well-known, large-biomass species associated with the upwelling systems (Chapters I, II, and IV; Kollmer 1963; Unterüberbacher 1964; Timonin 1991; Hansen et al. 2005; Schukat et al. 2013). *C. carinatus* and to a lesser extent *R. nasutus* were the only mainly herbivorous species found in the present study (Chapter II). Their dormant or diapausing stages aid them to overcome periods of food paucity, which is particularly important in highly pulsed ecosystems. *C. carinatus* CVs occurred only as diapausing, deep-dwelling (400-1000 m) offshore resting population in the BCIR. This specialized life-cycle adaption ensures the dominance of *C. carinatus* as key species in the Benguela Current upwelling system, where it occurs with high abundance throughout the year (Chapter I; Arashkevich et al. 1996; Loick et al. 2005; Verheye et al. 2005; Schukat et al. 2013). With their more opportunistic and event-driven dormant stages, *E. hyalinus* and *R. nasutus* showed higher abundances and a bimodal distribution in the BCIR with presumably active females occurring in the epipelagic zone (Chapter IV; Schukat et al. 2013; Teuber et al. 2013).

The northern Benguela Current upwelling system (NBC)

In upwelling systems smaller species such as *Clausocalanus* spp.*, Paracalanus* spp.*, Acartia* spp., *Mecynocera clausi* and *Ctenocalanus vanus* are also abundant, but they are usually less dominant in terms of biomass than in oligotrophic regions (Chapter IV; Timonin 1991, 1992; Kollmer 1963; Verheye et al. 1998; Hansen et al. 2005). Dominant biomass-richer calanoid species in the NBC are *C. carinatus, M. lucens* and *N. minor* followed by *Centropages* spp. (mostly *C. brachiatus*), and, depending on the month, *Eucalanus hyalinus*, *Candacia* spp. and *Rhincalanus nasutus* (Chapter I; Timonin 1991, 1992; Kollmer 1963; Verheye et al. 1998; Hansen et al. 2005). Earlier studies in surface waters (0-100 m) of the "Walvis Bay routine area" in 1962-63 reported that *C. carinatus*, *M. lucens* and *C. brachiatus* dominated the cool-water community on the shelf, in order of decreasing abundance (N70 net, 195 µm mesh size) (Kollmer 1963; Unterüberbacher 1964; Timonin 1991; Hansen et al. 2005). In contrast, *N. minor* is usually considered a warm-water species with high abundances in oceanic regions of the tropical and subtropical Atlantic (Chapter IV) and low abundances off Walvis Bay, where this species was associated with intrusions of warm oceanic, tropical waters transported onto the shelf in periods of weak upwelling (Unterüberbacher 1964; Timonin 1991; Timonin et al. 1992). In the area at 20°S no such clear discrimination could be made, since *N. minor* co-occurred in high abundances on the shelf within the same water masses as the presumed cold-water species *C. carinatus* (Chapter I). High abundances of *C. carinatus* were rather correlated with intermediate temperatures and higher chlorophyll *a* concentrations above the shelf break and further offshore, which characterize stabilizing and sun-warmed offshore-moving water masses some time after the actual upwelling event. Along the monitoring line at 20°S, the influence of Angola Current water is more pronounced than around Walvis Bay (Olivar and Barangé 1990) and generally higher abundances of *N. minor* are expected (Chapter I; Shannon and Pillar 1986). *N. minor* was particularly dominant during years characterized by less pronounced upwelling in spring and only moderate warm-water intrusions in late summer, thus, suggesting stronger mixing with oceanic waters. In contrast, years with strong spring to late summer temperature gradients were dominated by the typical upwelling species *C. carinatus* and *M. lucens*, indicating a close link between copepod community structure and the hydrographic regime (Chapter I).

In conclusion, copepod abundance, biomass and community structure were quite variable, even in oceanic regions of the tropical and subtropical Atlantic (Chapter IV). Similarly, higher than expected variability of phytoplankton and bacterioplankton communities in tropical and

subtropical communities were found (Karl et al. 2001; Steinberg et al. 2001; Marañón et al. 2003). Besides physical forcing, fluctuations of species abundance are also affected by species-specific life-history strategies, metabolic performances, behavioural responses (e.g. diel or ontogenetic vertical migrations) and biological interactions (e.g. predation and mortality) (Peterson et al. 1988; Verheye 1991; Hidalgo and Escribano 2007). Key species associated with the different biogeochemical provinces can be very different in their ecological role, even though they may be of similar size. Thus, they have a quite different impact on ecosystem functioning, as for example species undergoing DVM, OVM or without any migration behaviour at all differently affect the efficiency of the biological carbon pump (see section 3.2; Chapter IV; Longhurst and Harrison 1989; Zhang and Dam 1997; Steinberg et al. 2000, 2008a, 2012). For example, the three key species in the NBC are quite similar in size, with adult females of *N. minor* being slightly smaller with ~1.8-2.3 mm and adult females of *C. carinatus* and *M. lucens* varying from ~2.3-2.9 mm (Bradford-Grieve et al. 1999). However, each species is characterized by very different life strategies, which result in different mechanisms of ecosystem functioning operating during their dominance (see also Schukat et al. 2013; Teuber 2014). Therefore, a high species resolution and a high temporal and spatial coverage of biological and oceanographic data are necessary to complement existing data and disentangle species-specific dynamics of zooplankton communities. This is particularly important for our ability to predict future changes in different marine ecosystems, with potentially severe impacts especially on highly productive regions. Species-specific life strategies are described in more detail in relation to their vertical distribution and biodiversity patterns in section 3.3.

Hypothesis 1: *Copepod biomass increases with increasing primary production, with certain species characterizing different hydrographic regimes.*

Summary:

- In general, copepod biomass is higher in more productive upwelling regions compared to tropical oceanic regions. However, highest copepod biomass does not directly correlate with primary production rates, chlorophyll *a* concentrations or water temperature due to the general offset of copepod production to primary production.
- Certain species may be associated with major oceanographic regimes, while copepod communities are even stronger structured in the vertical dimension.

- Species with special life strategies, such as high wax ester amounts and OVM including dormant stages are particularly adapted to highly variable upwelling regions.
- Copepod dynamics are driven by interactions between upwelling events, water column stratification, biological interactions, species-specific life strategies (e.g. energy storage patterns, dormant stages, metabolic performances, feeding strategies), response times and ontogenetic development times. It emphasizes the necessity of combined long-term high resolution monitoring of oceanographic and biological processes to disentangle these relationships.

3.2 Impact of copepod communities on the vertical carbon flux

The rising CO_2 concentrations in the atmosphere create a growing interest in better understanding the role of the ocean in the carbon cycle (Field et al. 2000). As a prerequisite factors that control the transport of fixed carbon to the deep ocean need to be understood (Falkowski et al. 1998; Laws et al. 2000; Grunewald et al. 2002). With special regard to their huge regional expanse, tropical and subtropical oceanic regions play an important role in the carbon cycling of the ocean (Longhurst et al. 1995; Marañón et al. 2003). In general, primary producers in the surface layers convert inorganic carbon into organic carbon, which is then transferred to the deep sea via advection or vertical mixing of dissolved organic matter, sinking particles and active transport by vertically migrating organisms. This downward export of organic matter, the so-called “biological pump”, is a key component in sequestering carbon towards the deep sea (Longhurst and Harrison 1989; Steinberg et al. 2012). The majority of particulate organic carbon (POC) that sinks below the thermocline, is remineralized or modified by microbial and zooplankton organisms and thus is redistributed as inorganic or organic carbon (Steinberg et al. 2008a). An annual removal of >10 billion tons of carbon from epipelagic waters by means of the biological pump was estimated (Buesseler and Boyd 2009), of which around 10% reach the 1000 m layer (Martin et al. 1987; Turner 2015). The consumption of sinking particle fluxes by zooplankton largely contributes to degradation and remineralization processes in the meso- and bathypelagic zones, while estimates of losses of sinking carbon flux attributed to zooplankton are highly variable ranging from 4% to as much as 86% at different deep sea sites (Koppelmann et al. 2004 and references therein). To understand the causes of such high variability, detailed knowledge about the interaction between POM and key organisms are necessary (Koppelmann et al. 2004). As major representatives of marine pelagic ecosystems, copepods are a key

component of the biological carbon pump (e.g. Chapter IV; Longhurst et al. 1990; Zhang and Dam 1997; Steinberg et al. 2000; Wilson and Steinberg 2010).

In the present study, the total net loss rate of POC from 0-2000 m varied between 16% and 58% of primary production (PP) for calanoids and between 5% and 9% PP for cyclopoids. Thus, copepods accounted for 21 to >65% of total net loss of POC (Chapter IV). Similar estimates were made in the western subarctic Pacific, where suspension-feeding copepods consumed on average 32% (Yamaguchi et al. 2002) and 38% (Sasaki et al. 1988) of sinking particles throughout 0-4000 m and 150-1000 m, respectively. Applying the equation by Suess (1980), around 80% of primary production is recycled in the upper 200 m, while around 3% PP reaches the bathypelagic zone (Chapter IV). In general, it was estimated that about 5-25% of net primary production (nPP) is exported from the euphotic zone and <3% nPP reaches bathypelagic depths (De La Rocha and Passow 2007). However, the export varies with different regions from usually <10% nPP in central gyres and may be even 30-100% nPP in polar regions (Buesseler 1998; Neuer et al. 2002; Turner 2015).

In the present study, depth layers of high biodiversity are not necessarily associated with high biomass and productivity (Chapter IV). Rather the abundance of certain key species with different life-history traits was crucial in determining the role of copepod communities in the biological pump and its efficiency (Chapter IV; Longhurst and Harrison 1989; Steinberg et al. 2008a,b, 2012; Wilson et al. 2008). Relatively high PP, high temperatures and high abundances of biomass-rich species such as *E. marina, Neocalanus* spp., *N. minor* and *U. vulgaris* increased the efficiency of the biological carbon pump in the TNA. Strong net grazing impact (mean 44% PP) and high potential amounts of fecal pellets contributed to the outgoing POC flux (POC_{out}) from the epipelagic zone (mean 93% POC_{out}) (Fig. 2; Chapter IV). Furthermore, variations in zooplankton size and composition and thus their fecal pellet characteristics may significantly impact transfer efficiencies of sinking POC (Wilson et al. 2008). For example, passive POC flux (due to fecal pellets) was four to five times higher in the mesopelagic zone at a mesotrophic station (K2) in the Pacific Ocean than at an oligotrophic station (ALOHA), as fecal pellets were much larger at K2 reflecting differences in zooplankton community structure at the two sites (Wilson et al. 2008).

In contrast, in the STNA and BCIR, active carbon transport was of particular importance, as carbon export from the euphotic zone to mesopelagic layers was clearly enhanced via increased abundances of biomass-rich diel vertical migrants such as *Pleuromamma* spp. (Chapter IV). The

relative impact was similar in both regions, but absolute values were much higher in the BCIR with higher PP and much higher abundances of these species (Fig. 2; Chapter IV). Vertical migrants may feed on a variety of phytoplankton and microzooplankton during the night at the surface, whereas they reduce their metabolic demands, respire and defecate in cooler waters at depths during the day and thus significantly enhance the vertical carbon export (Longhurst et al. 1990; Steinberg et al. 2000, 2008, 2012; Fernández-Àlmano and Färber-Lorda 2006; Wishner et al. 2008; Robinson et al. 2010).

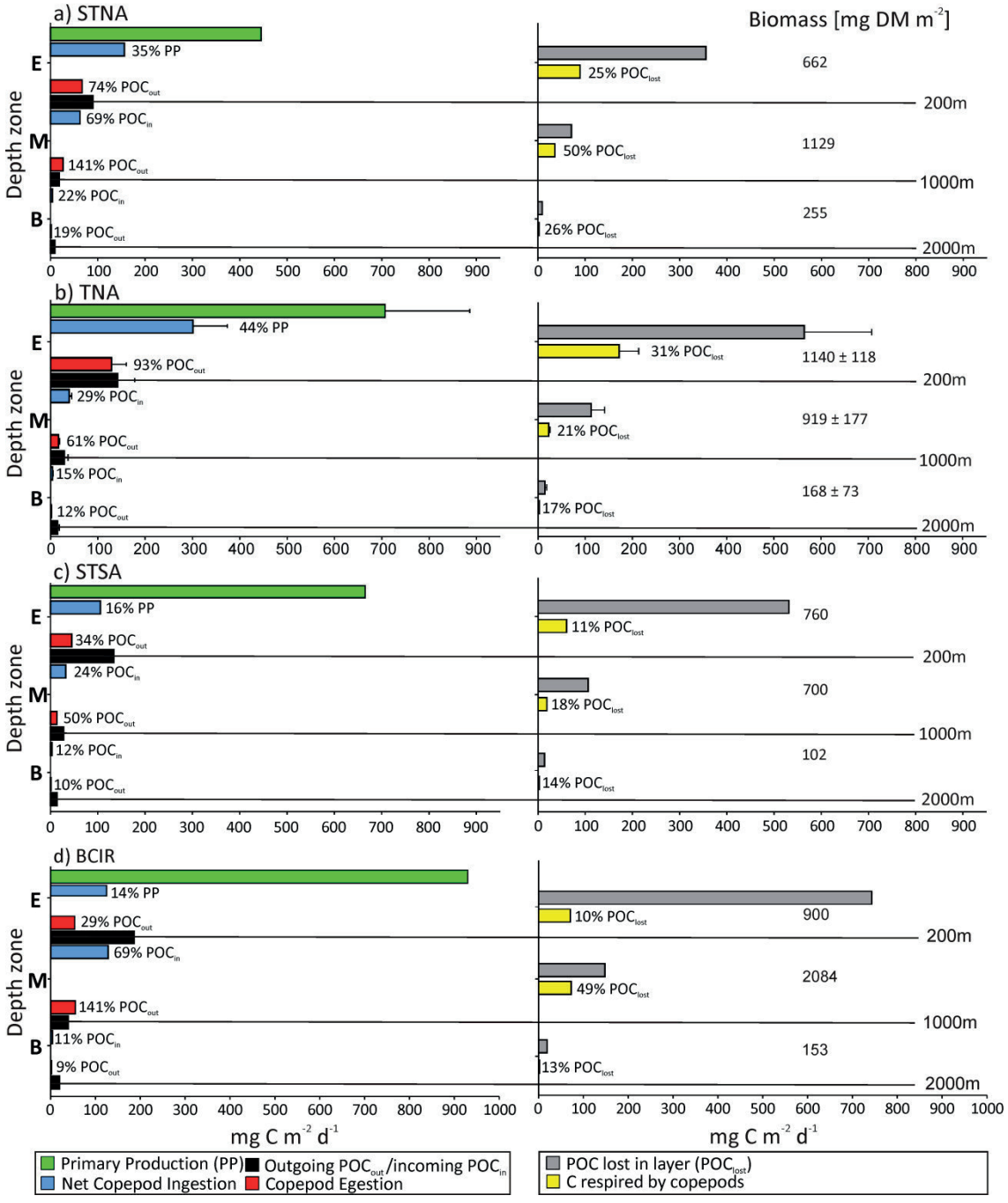

Figure 2: Left: Impact of net copepod ingestion (blue bars) on primary production and incoming POC (black bars). Potential contribution of copepod egestion (red bars) on outgoing POC (=incoming POC for the adjacent layer below=black bars) in respective depth zones and regions. Right: Potential carbon of POC lost in a depth zone (grey bars) respired as inorganic carbon by copepods (yellow bars). Total copepod biomass per depth zone (mg dry mass m^{-2}) is indicated on the right. E: Epipelagic (0-200 m), M: Mesopelagic (200-1000 m), B: Bathypelagic (1000-2000 m), STNA: Subtropical North Atlantic, TNA: Tropical North Atlantic; STSA: Subtropical South Atlantic, BCIR: Benguela Current influenced region.

Abundant species feeding directly on POC such as Spinocalanidae or Scolecithrichidae, may be especially important in remineralization, repackaging and redistribution of POC below the euphotic zone (Chapter IV; Yamaguchi et al. 2002; Homma et al. 2011). For example, *Spinocalanus antarcticus* fed primarily on components of the vertical flux and suspended matter in the Arabian Sea (Wishner et al. 2008). Due to the dominance of spinocalanid species in meso- to abyssopelagic depths in all marine regions, this copepod family is of major importance in the cycling of organic matter and deep-sea food webs (Chapters IV-VI; Kosobokova et al. 2002; Wishner et al. 2008). In contrast, predatory *Euaugaptilus* have a large biomass and thus contribute to POC flux via the production of large fecal pellets. For example, the annual contribution of fecal pellets to carbon fluxes was about three times that of active carbon transport by diel vertical migrations in the Sargasso Sea (Steinberg et al. 2012). Thus, carbon flux is significantly mediated by copepod communities, while species-specific body size, ecophysiological performance, feeding behavior and dietary preferences determine the role of different copepod species in the carbon flux (Chapter IV; Longhurst et al. 1990; Ducklow et al. 2001; Steinberg et al. 2000, 2008, 2012). In consequence, variations in zooplankton community biomass and composition over time, as e.g. increasing or decreasing biomass of large diel vertical migrants such as *Pleuromamma*, may significantly impact the fate of organic carbon and transfer efficiencies of sinking POC (Chapter IV; Ducklow et al. 2001; Wilson et al. 2008; Homma et al. 2011). For instance, higher diel migrant biomass increases the removal rates of primary production in the surface layers during the day and at the same time enhances the active transport of carbon and nutrients to the ocean's interior at night. This was already observed in the Sargasso Sea, where an overall increase of epipelagic mesozooplankton biomass and in particular an increase of diel vertical migrant biomass caused a significant, long-term increase of POC flux in the lower epipelagic zone and thus enhanced both passive and active vertical flux (Steinberg et al. 2012).

In general, net loss rates of sinking POC by copepods decrease with increasing depth (Fig. 2; Chapter IV; Sasaki et al. 1988; Yamaguchi et al. 2002; Koppelmann and Frost 2008; Homma et al. 2011). The greatest variability of feeding impacts was found in the epi- and mesopelagic zone, while in bathypelagic depth layers impacts of copepods were more uniform ranging from 11% to 22% net loss of incoming POC flux (Chapter IV; Koppelmann and Frost 2008). Nevertheless, even though the deep is generally seen as a relatively uniform and stable environment, POC fluxes vary temporally and regionally depending on the overlaying primary productivity (Voss et al.

1996; Holmes et al. 2002; Koppelmann and Weikert 2007). There is evidence that deep-sea biota respond within months to these environmental changes (e.g. seasonally increased POC flux) and that such changes persist for a certain time period (Danovaro et al. 2001, 2004; Koppelmann and Weikert 2007; Koppelmann and Frost 2008). For example, in the upper bathypelagic zone in the eastern Atlantic Ocean, higher remineralization rates were found after a spring phytoplankton bloom, when mesozooplankton abundance was clearly increased after the sinking of phytodetritus (Koppelmann und Weikert 1999). Hence, if changes in the euphotic zone are large enough, they penetrate down to the bathypelagic zone. Yet, deep-sea communities may be particularly sensitive to a wide range of disturbances, due to the general and long-term stability of the deep sea (Gage and Tyler 1991; Danovaro et al. 2004; Koppelmann and Frost 2008). Therefore, more detailed knowledge about seasonal and regional differences of POC fluxes and responses of deep-sea communities as well as the dominant components of these communities and their role in biogeochemical cycles is crucial for predicting potential consequences of environmental changes.

Hypothesis 2: *Copepod community structure has a major impact on the efficiency of the biological carbon pump.*

Summary:

- Higher copepod biomass and the presence of key species (e.g. *Pleuromamma*) greatly affect carbon transfer and thus the efficiency of the biological carbon pump via species-specific body size, feeding, metabolism, fecal pellet production and vertical migration.
- Changes in copepod biomass and species composition over time lead to variations in removal of primary production, fecal pellet export and active transport of carbon via vertical migrants. For instance, an increase of biomass-rich, daily vertically migrating *Pleuromamma* significantly enhances the active carbon transport to the ocean's interior.
- Dominant particle feeders such as *Spinocalanus* are particularly important in repackaging suspended and sinking POC below the euphotic zone.
- The impact of copepod communities on vertical POC fluxes decreased in the bathypelagic zone. It yet has to be determined to what extent potentially decreasing nutritional value

(quality) through constant repackaging of POM arriving at greater depth affects copepod growth and thus population sizes.

3.3 Biodiversity and ecological niches of calanoid copepods

Latitudinal and vertical copepod biodiversity patterns

Changes in environmental patterns such as water masses are often closely linked to changes in community structure (Chapters I and IV; McGowan 1986; Painting et al. 1993; Longhurst 1998; Andersen et al. 2001a; Ward and Shreeve 2001; Beaugrand et al. 2002; Beaugrand and Ibañez 2004; Loick et al. 2005). Complex networks in highly diverse ecosystems seem to stabilize the community structure of tropical plankton, making them less susceptible to physical disturbances (Giller et al. 2004). This has been formulated as “insurance hypothesis”, as putatively redundant species may contribute to ecosystem resilience, when environmental conditions change (McNaughton 1977; Barnett et al. 2007).

Epipelagic zooplankton communities show a general increase of species richness from the poles to the tropics with highest biodiversity in equatorial regions (Chapter IV; Woodd-Walker et al. 2002; MacPherson 2002; Rombouts et al. 2009; Schnack-Schiel et al. 2010). In general, less-productive ecosystems are known for their high biodiversity compared to high productive systems such as coastal upwelling regions (Angel 1993; Woodd-Walker et al. 2002). Low but continuous production throughout the year in the tropics and subtropics lead to retentive systems with typically high biodiversity, where primary and secondary production is closely coupled (Chapter IV; Conover 1979; Longhurst and Pauly 1987; Gasol et al. 1997; Wassmann 1998; Woodd-Walker et al. 2002). In contrast, highly productive regions such as the Benguela Current coastal upwelling system are characterized by lower diversity but usually higher biomass (Chapters I and IV; Wood-Walker 2001).

It was proposed (evolutionary speed hypothesis by Rohde (1992)) that high temperatures in tropical, epipelagic waters accelerates evolutionary processes promoting mutation rates and hence speciation and extinction of population via short generation times and high metabolic rates of copepods in these regions (Allen et al. 2002, 2007; Rombouts et al. 2009). Furthermore, the distribution of plankton organisms in tropical and subtropical regions is often more or less unrestricted by physical barriers allowing wide latitudinal ranges and co-occurrence of many oceanic species (Angel 1993; Schnack-Schiel et al. 2010). Only the strong decrease in species

richness near 50°N and 40°S in the Atlantic was associated with clear transitional zones, i.e. the subtropical convergence and polar fronts, according to the large expanse of the subtropical gyres such as the warm-water Gulf Stream reaches far north in the North Atlantic (Ward and Shreeve 2001; MacPherson 2002).

In contrast to epipelagic environments, information on abundance and species diversity with a high taxonomic resolution is still very limited in the pelagic deep-sea (Yamaguchi et al. 2015), especially considering tropical ecosystems (Teuber et al. 2013). Although deep-sea biodiversity has gained increasing scientific attention over the last decades, most research focused on benthic communities (e.g. Brandt et al. 2007; Danovaro et al. 2010) or higher latitudes (Auel 1999; Ward and Shreeve 2001; Yamaguchi et al. 2002; Matsuura et al. 2010; Homma et al. 2011; Kosobokova et al. 2011; Laakmann et al. 2012). The pelagic deep sea is generally assumed to be an almost homogeneous environment without any physico-chemical barriers, sustaining higher biodiversity than corresponding diversity in the euphotic zone (Deevey and Brooks 1977; Ward and Shreeve 2001; Yamaguchi et al. 2002; Homma et al. 2011; Kosobokova et al. 2011), even in highly diverse tropical ecosystems (Chapter IV). A biodiversity maximum is usually observed in the mesopelagic zone with a second deeper peak occasionally occurring in the bathypelagic zone below 2000 m (Chapter IV; Scotto di Carlo 1984; Ward and Shreeve 2001; Yamaguchi et al. 2002; Homma et al. 2011; Kosobokova et al. 2011;).

Mechanisms promoting high biodiversity in the deep sea have been a major concern in zooplankton ecology. Three major hypotheses attempting to explain high biodiversity were formulated at the end of the 1960s and during the 1970s. Decades later, the underlying mechanisms are still not disentangled yet (reviewed by Danovaro et al. 2010; Ramirez-Llorda et al. 2010 and McClain and Schlacher 2015 for benthic deep-sea diversity), especially for the pelagic deep sea (Laakmann et al. 2012; Sano et al. 2013). The stability-time hypothesis (Hessler and Sanders 1967) claims that stable environmental conditions of the deep sea allow species to evolve and become highly specialized for a particular microhabitat or food source, creating intense niche partitioning to fine levels. Thus, the currently observed co-existence of deep sea species reflects competitive interactions of the past (Hessler and Sanders 1967; Sanders 1968). However, since specialization was difficult to imagine among species in the generally food-limited deep sea, it was suggested that deep sea animals are generalists feeding with little selection on anything they encounter (Dayton and Hessler 1972). Thus, high diversity is maintained by intense feeding at all trophic levels, preventing any species to develop large

population sizes, so that abundances remain constantly at such a low level that competition may not occur (disturbance or cropper theory; Dayton and Hessler 1972). The species-area hypothesis is a generally positive correlation between species numbers and ecosystem size (MacArthur et al. 1966; Rosenzweig 1992). However, diversity increases rather in the shape of a parabolic curve with maxima at intermediate depths rather than a continuous increase with depths in both benthic and pelagic environments (Deevey and Brooks 1977; Rex et al. 1981; Yamaguchi et al. 2012; Kososbokova et al. 2011). For benthic deep-sea communities, patterns of diversity are likely generated by multiple factors such as e.g. biologically generated habitat heterogeneity (microhabitat diversification), productivity (energy input), biological interactions (e.g. competition, predation), succession and disturbances, while all these mechanisms may operate at different scales of time and space (Rex et al. 2005; McClain and Schlacher 2015 and references therein). Likewise, in the pelagic deep sea the proposed hypotheses each may not be adequate to explain diversity patterns, and high biodiversity is a result of interacting factors. The following sections describe to what extent competition regulates structure and thus promote high copepod biodiversity in pelagic environments.

Competition in the pelagic realm

Co-occurring copepod species usually differ in either spatial niches, trophic niches or other life-cycle adaptations assuming that these mechanisms minimize inter-specific competition. In consequence, these are major factors in structuring copepod communities (Chapters II, IV and VI; Auel 1999; Laakmann et al. 2009a,b, 2012). Vertical habitat partitioning of the water column results in fine-scale vertical arrangement of species with similar trophic demands and/or life-cycle adaptations (Chapters IV and VI; Ambler and Miller 1987; Auel 1999; Laakmann et al. 2009a,b, 2012). In contrast, species that occur within the same depth stratum are usually characterized by different trophic niches, i.e. distinct trophic levels, body size (= dietary spectra), feeding behavior (chemotaxis vs. rheotactic predators) and degree of carnivory, and/or modes of energy storage and reproductive strategies (life cycle adaptations) (Chapter II; Ambler and Miller 1987; Auel 1999; Laakmann et al. 2009a,b, 2012). These mechanisms were largely confirmed in the present study, as life-cycle adaptations and/or differences in dietary preferences of copepod species, which comprised a wide range of trophic levels, often coincided with their vertical distributional ranges (Chapters II, IV and VI). The highly structured pelagic realm indicates that competition does takes place, at least to a certain extent, promoting high diversity in both

tropical epipelagic and deep-sea environments (Chapters IV and VI; Auel 1999; Kuriyama and Nishida 2006; Matsuura et al. 2010; Laakmann et al. 2012).

Species inhabiting the same depth differ in their trophic niches or other life-history traits

High biodiversity is usually accompanied by a wide spectrum of dietary preferences and life strategies (Chapters II and IV; Mauchline 1998; Teuber et al. 2014). Although the majority of the copepod species found throughout the tropical and subtropical eastern Atlantic Ocean were omnivorous, co-occurring dominant species within the same depth strata usually exhibited different life strategies, prey size spectra and/or dietary preferences. For example, strictly epipelagic females of the tropical *Scolecitrhix danae* and *Undinula vulgaris* of similar size occurred in the same depth layers in the TNA (Chapters II and IV). While *S. danae* had a higher degree of carnivory, *U. vulgaris* exhibited higher dietary bacterial contributions. Thus, they obviously fed on different microzooplankton organisms and/or types of particulate organic matter (POM), potentially minimizing interspecific competition with only slightly different trophic levels (Chapter II). Species of Scolecithrichidae are usually omnivorous and specialized to detect suspended or sinking POM as food items using chemoreceptors on their feeding appendages (Nishida and Ohtsuka 1997). Selective utilization of POM was recently observed in omnivorous/detritivorous copepods, even in deep sea specimens (Wishner et al. 2008; Laakmann et al. 2009a,b; Sano et al. 2013). Thus, even mainly particle-feeding copepod species appear to be more specialized than initially assumed when food is readily available, indicating the importance of different types of marine snow aggregates in all depth zones (e.g. Silver and Aldredge 1981; Steinberg 1995; Nishida and Ohtsuka 1996, 1997; Matsuura and Nishida 2000; Kiørboe 2000, 2001; Nishida et al. 2002; Wiggert et al. 2005; Wishner et al. 2008; Sano et al. 2013).

The dominant deep-living copepod families found in the present studies were usually omnivorous/detritivorous or carnivorous applying various specialized feeding tactics. For instance, carnivorous *Heterorhabdus*, which are usually abundant in the lower epipelagic and upper mesopelagic zone, may inject venom into their prey via a mandible tooth (Chapter IV; Nishida and Ohtsuka 1996; Ohtsuka et al. 1997; Wishner et al. 2008). *Euaugaptilus* spp. are usually carnivorous and some species are ambush predators preying on small copepods by using specialized “button setae” on their maxilla and maxilliped to catch prey (Boxshall 1985;

Matsuura and Nishida 2000; Matsuura et al. 2010). In contrast, *Paraeuchaeta* spp. are rheotactic predators with extremely strong maxillipeds and feeding appendages, which even allow them to feed on large, diapausing calanids, applying a “drift and wait” feeding strategy (Auel and Hagen 2005; Laakmann et al. 2009a,b). Thereby, they take advantage of a so-called “trophic shortcut” from primary production in the surface layer to the deep sea via seasonally vertically migrating copepods (Chapter II; Hagen et al. 1995; Auel 1999; Laakmann et al. 2009a,b; Teuber et al. 2014). In contrast, *Lucicutia* specimens were described as primary detritivores and opportunistic carnivores, feeding on a wide variety of detritus, prokaryotic and eukaryotic autotrophs, bacterial aggregates and metazoans (Chapter II; Gowing and Wishner 1998). Spinocalanid species are usually omnivorous feeding on a wide spectrum of vertical flux items and suspended matter (Kosobokova et al. 2002; Wishner et al. 2008). Some species contain high lipid contents (e.g. *S. antarcticus* 54% DM) and have evolved particularly efficient digestive systems with severely elongated and looped mid-guts (Kosobokova et al. 2002). Similar adaptations to efficiently utilize POM are also described for other deep sea detritivores such as *Chiridiella sp.* (Vinogradov 1972) and *Lophothrix frontalis* (Nishida et al. 1991). *Lophothrix* spp., amongst other deeper-living scolecithrichid genera such as *Scolecithricella, Brodskius, Scaphocalanus* and *Scottocalanus* were also very common in the present study (Appendix Table A; Chapter IV).

In addition to differences in feeding strategies, different reproductive modes are known in deep sea species, i.e. broadcast spawning (Heterorhabdidae, Spinocalanidae, Scolecithrichidae, Tharybidae and Bathypontiidae) or egg-carrying (Euchaetidae, Augaptilidae) (Kosobokovae et al. 2007). Different genera of Aetideidae vary in their reproductive modes with both broadcast spawning and egg-carrying species (Kosobokova et al. 2007; Laakmann et al. 2012). In general, clutch size and egg diameter may strongly differ between species to improve survival potential of their offspring (Kosobokova et al. 2007); reproductive strategies may even vary among congeneric *Paraeuchaeta* species (Auel 1999). Deeper-living species usually produce larger, more energy-rich eggs, at the expense of total egg numbers in both broadcast spawners (Kosobokova et al. 2007) and egg-brooders (Auel 1999) to reduce or eliminate feeding during naupliar stages and thus make them rather independent of the low food concentrations in bathypelagic zones (Auel 1999; Kosobokova et al. 2007).

Closely related species occurring in the same depth strata were usually different in body size. For instance, *S. danae* and S*. bradyi* co-occurred throughout the epipelagic zone in the TNA, and *E. marina* and *E. paraconcinna* were found in the same depth strata at one TNA station (Chapter IV;

Appendix Table A). Similarly, mesopelagic *Spinocalanus horridus* and *S. dispar 4* occurred together in the lower mesopelagic zone. These two species are very different in their size and morphological features, since *S. dispar* 4 is very small and *S. horridus* is much bigger with enlarged maxillipeds. Apparently, copepod species with large morphological differences of feeding appendages and body sizes prey on food items of different type and/or size (Chapter VI; Laakmann et al. 2012).

Species of similar trophic niches differ in spatial niches or other life-history traits

Neocalanus gracilis exhibited only a slightly lower trophic level and similar dietary preferences as *S. danae*. Yet, they co-occurred in the epipelagic zone throughout the TNA and STSA (Chapters II and IV). However, these two species differ in their reproductive strategies as well as in their mode of energy storage and feeding tactics. *S. danae* does not store lipids and searches for food via chemotaxis (Nishida and Ohtsuka 1997). In contrast, *N. gracilis* is known to perform OVMs on a small scale within the upper 300 m including a non-feeding copepodite stage CI, which contains a large oil droplet as energy reserve (Ambler and Miller 1987; Shimode et al. 2009). Adult females of *N. gracilis* have moderately high total lipid (TL) contents (16% DM) and significant, but quite variable amounts of wax esters (18-56% TL) (Chapter II). These levels were significantly lower than those of their high-latitude congeners, which are known to perform extensive seasonal OVM including a developmental descent and diapause of the late copepodids (Ohman 1987; Tsuda et al. 2001; Lee et al. 2006). In general, epipelagic tropical copepods experience a year-round continuous but low food supply and therefore, they do not accumulate large lipid deposits, while dietary lipids directly fuel metabolic processes (Lee et al. 1971; Lee and Hirota 1973). However, maintaining the ability to accumulate energy reserves may be of evolutionary advantage also for tropical, epipelagic species indicating high competition pressure in these environments.

On the contrary, closely related species of similar size with similar trophic niches and life strategies usually occur in separate depth strata resulting in a fine vertical partitioning of the water column (Chapter IV; Ambler and Miller 1987; Auel 1999; Kuriyama and Nishida 2006; Laakmann et al. 2009a,b; Matsuura et al. 2010). For example, adult females of the same genera such as *Scolecithrichopsis tenuipes* and *S. ctenopus* as well as *Euchaeta marina* and *E. acuta* occurred in different depth strata of the epipelagic zone in the TNA (Appendix Table A; Chapter

IV). Furthermore, a temporal offset of the starting and endpoint of DVMs is another form of creating spatial niches, which may be an important mechanism of co-occurring and closely related diel vertical migrants of similar size, such as females of *Pleuromamma gracilis/piseki* and *P. borealis*, as well as *P. robusta* and *P. abdominalis* (Appendix Table A; Chapter IV; Ambler and Miller 1987).

Below the euphotic zone, spinocalanid copepods exhibited three distinct vertical distribution patterns with certain species being mainly concentrated either in the upper or lower mesopelagic, while others were rather evenly distributed throughout the whole mesopelagic zone (Chapter VI). Fine-scale differences in vertical distribution even of developmental stages and putative cryptic species were observed (Chapter VI). Vertical habitat partitioning is also common in deep sea species of Euchaetidae and Aetideidae in polar regions (Auel 1999; Laakmann et al. 2009a,b, 2012). Due to the exponential decrease of both copepod abundance and food availability and at the same time largely increasing habitat size, vertical habitat partitioning appears to be a particularly effective mechanism to avoid competition in meso- and bathypelagic zones. Apparently, these fine-scale, species-specific vertical separations are also an important aspect of speciation processes in the deep sea (Chapters IV and VI; Laakmann et al. 2012).

Different types of ontogenetic vertical partitioning were observed in several spinocalanid species (Chapter VI). On the one hand, ontogenetic ascent of young copepodids (CI-CIV or CI-CV) with a corresponding descent of adults (e.g. *S. dispar* 2 *and Monacilla typica*) was observed (Chapter VI). Similarly, developmental ascent of young copepodids CI-CIV was detected in different deep sea *Paraeuchaeta* spp. (Laakmann et al. 2009a,b). On the other hand, ontogenetic ascent of copepodids CIV and CV with both adults and copepodids CI-III residing at deeper layers (e.g. *S. dispar* 4, S. *dispar 5*, and *S. brevicaudatus*) were detected (Chapter VI). This ontogenetic migration pattern is similar in epipelagic *Neocalanus gracilis* as well as meso- to bathypelagic *Spinocalanus antarcticus*, *Gaetanus variabilis* and *Paraeuchaeta birostrata*, suggesting that reproduction of these species takes place at these depths (Kosobokova et al. 2002; Yamaguchi et al. 2007; Shimode et al. 2009; Abe et al. 2012). In general, ontogenetic vertical partition may reduce intraspecific competition. In particular, the ontogenetic ascent of younger copepodids may ensure that they find higher concentrations of prey at shallower depths (Laakmann et al. 2009a,b). In contrast, ontogenetic descent of copepodite stages is believed to mainly serve as predator avoidance strategy, indicating that predation pressure is important in structuring the

pelagic realm (Longhurst 1985; Ambler and Miller 1987; Yamaguchi et al. 2004). Furthermore, individuals also benefit bioenergetically by staying in deeper, cooler layers (Verheye and Field 1992; Yamaguchi and Ikeda 2002).

The pelagic deep sea: Not so food-limited and not so uniform?

Exceptions of closely related species of similar size and trophic niches co-occurring in the same depth layer are observed occasionally in both epipelagic and mesopelagic environments, suggesting lower competition pressure at certain times and places (Appendix Table A; Chapters IV and VI; Ambler and Miller 1987; McClain and Schlacher 2015). For example in the epipelagic zone, adult females of *N. gracilis* and *N. robustior* in the STSA, *E. acuta* and *E. media* in the STNA as well as *Aetideus armatus*, *A. bradyi* and *A. giesbrechti* in the TNA occasionally co-occurred in the same depth layers (Appendix Table A; Chapter IV). In meso- and bathypelagic depths, sampling depth strata are usually too coarse to reveal vertical partitioning mechanisms (Chapter IV). However, disentangling species diversity of Spinocalanidae revealed the co-occurrence of several cryptic species in mesopelagic depth layers (Chapter VI). For example, *S. dispar 4* and *5* as well as *S. dispar 7* and *8* inhabited the same strata in the lower and upper mesopelagic zone, respectively, showing no apparent differences in morphology or size (Chapters V and VI). Different mechanisms may explain such co-existence: 1) one species has not yet outcompeted the other, 2) individuals of both species are constantly replenished due to continuous re-colonization of the pelagic realm from their original habitat (Ambler and Miller 1987; Auel 1999; Laakmann et al. 2009b, 2012), and 3) competition pressure may locally and/or temporally be low.

Based on the results of this study, it is not possible to make assumptions about the “evolutionary state” of the community or the respective habitats of origin, where the species reproduce. Co-existence of closely related and ecologically similar species was also found in deep-dwelling Euchaetidae, Scolecithrichidae and Aetideidae (Auel 1999; Kuriyama and Nishida 2006; Laakmann et al. 2009a,b). In Arctic waters, co-occurring *Paraeuchaeta glacialis* and *P. norvegica* were related to opposing current systems in the Fram Strait: each species was initially associated with a different current explaining the overlapping distribution by continuous advection of individuals from their origin and thus continuously replacing the population (Auel 1999; Laakmann et al. 2009a,b). The current system in the equatorial region is very complex and thus

continuous re-colonization of the pelagic realm may be an important mechanism ensuring the co-existence of many species. However, to identify such habitats of origin and follow changes of community structures over time, continuous monitoring and detailed phylogeographic distribution patterns at different depth horizons are necessary.

At last, low copepod abundances and limited exploitation of possible food sources by copepods in the deep sea indicate that competition pressure may be lower than initially assumed, as food supply may be locally and/or temporally not as limited (Chapter IV). POC resources were far from being fully exploited by copepods in most meso- and especially bathypelagic layers of the tropical and subtropical eastern Atlantic, and also in higher latitudes of the Pacific Ocean (see section 3.2; Chapter IV; Sasaki et al. 1988; Yamaguchi et al. 2002; Homma et al. 2011). The net loss of POC via copepod communities in bathypelagic depth strata was only between 2% and 15% (Chapter IV). This may be especially important considering omnivorous, particle-feeding species (Chapters IV and VI; Sasaki et al. 1988; Yamaguchi et al. 2002; Homma et al. 2011). Furthermore, omnivorous, opportunistic species of copepod families such as Aetideidae (Laakmann et al. 2009a,b) and Spinocalanidae (Chapter V-VI; Kosobokova et al. 2002; Wishner et al. 2008) may be able to switch feeding to other food source and/or size classes, as soon as food becomes limited. This is also common in epipelagic omnivorous copepods (Chapter II; Landry 1981; Cornils et al. 2007; Gentsch et al. 2009; Escribano and Pérez 2010).

The twilight zone: A special habitat to be

Similar to tropical epipelagic zones, food webs in mesopelagic waters are rather complex, offering a wide spectrum of prey items for omnivorous consumers. These may include dead and living zooplankton as well as particle aggregates of various sizes and compositions (i.e. POC, viruses, bacteria/archaea, flagellates, ciliates, migrating and resident mesozooplankton, etc.; Silver and Alldredge 1981; Arístegui et al. 2009; Robinson et al. 2010). Several decades ago, the deep ocean sea floor was revealed as a much more heterogeneous environment than initially thought, e.g. due to spatially localized or temporally pulsed food imports and creation of biogenic structures of bioturbation. These features together with the generally high physical stability lead to the creation of patchily distributed microhabitats increasing diversity (Rex et al. 1981; Thistle 1983; Grassle 1989). Similarly in the pelagic deep sea, suspended and sinking

particulate organic matter (POM) is suitable for microhabitat formations, which may be very heterogeneously distributed in this vast realm.

The mesopelagic zone receives various forms of POM from the euphotic zone originating mostly from phytoplankton and zooplankton grazing activities (Kepkay 2000; Verdugo et al. 2004; Robinson et al. 2010). Most intense modifications of organic matter usually occur in the mesopelagic zone (and not cycling within the euphotic zone) strongly affecting organic matter composition of deep-sea suspended particles (Arístegui et al. 2009). This alteration of POM is caused by direct degradation and by the aggregation and mixing of phytodetritus with material derived from microbial and zooplankton activities (Sheridan et al. 2002; Arístegui et al. 2009). Thus, marine snow aggregates may be of very different chemical and biological composition depending on its origin and the associated bacterial and zooplankton community (Kiørboe 2000, 2001; Kiørboe et al. 2002, 2004; Arístegui et al. 2009), while zooplankton organisms may actively search for different types of these aggregates (Kiørboe 2000). In consequence, fine-scale trophic niche separations and diverse types of marine snow seem to be crucial mechanisms promoting and sustaining high biodiversity in the mesopelagic zone (Sano et al. 2013). Another important factor permitting the development and “evolution” of these microhabitats may be time and thus the general physical stability of the mesopelagic environment (McClain and Schlacher 2015). This was further supported, as biodiversity peaks were observed at greater depth (400-700 m) in subtropical regions with deeper thermoclines, thus seemed to be related to surface stratification and hence stability (Chapter IV).

Even though tropical, epipelagic oceanic environments and the deep sea could not be more different in environmental conditions, as for instance temperature, pressure, and inorganic nutrient concentrations, some attributes, such as large ecosystem size, high physical stability and constant but low energy supply are similar, which seem to be important drivers of high biodiversity in these two ecosystems. As unique features, the deep-sea comprises by far the largest ecosystem on earth, both in horizontal and vertical dimensions, offering countless, patchily distributed potential microenvironments and thus trophic and spatial niche possibilities (Kiørboe 2000; Arístegui et al. 2009; Robinson et al. 2010; Sano et al. 2013). This vast realm may therefore allow an even higher biodiversity as compared to tropical epipelagic ecosystems (Chapter IV). In particular, the twilight zone fulfils unique preconditions, which may account for the usual biodiversity maxima as found in this zone: 1) close interaction with the euphotic zone: constant energy supply from above, high diversity of food items and potential microhabitats,

thus high biologically generated heterogeneity, 2) physical stability, 3) dim light (protection), 4) low zooplankton abundances (population sizes) and 5) large ecosystem size.

Hypothesis 3: *Less-productive ecosystems exhibit a high biodiversity of copepods with a large variety of feeding modes and life strategies in tropical epipelagic and pelagic deep-sea environments. Competition-minimizing mechanisms enhance pelagic biodiversity of copepods.*

Summary:

- Dominant copepod species usually differed either in their dietary preferences (trophic niche), life-cycle adaptations or spatial niches. This complex species-specific vertical and ecological structure indicates that competition-minimizing or -avoiding mechanisms are prominent in both epipelagic, tropical environments and in the pelagic deep sea.
- Due to low copepod abundance, low food availability but an enormous ecosystem size, vertical habitat partitioning is particularly effective to avoid competition in meso- and bathypelagic zones.
- Temporally and spatially, the pelagic deep sea may be not be as food-limited as previously assumed resulting in lower competition pressure at certain times and places.
- The vast pelagic deep sea offers countless, patchily distributed microhabitats and thus is biologically more heterogeneous than previously assumed. These microhabitats can be very different from each other and hence competition pressure may differ largely between these microhabitats.
- The twilight zone fulfils unique preconditions promoting biodiversity peaks: 1) close interaction with the euphotic zone, thus high biologically mediated heterogeneity, 2) physical stability, 3) dim light (protection), 4) low organism abundances, and 5) large ecosystem size.

3.4 The potential benefit of proteomic fingerprinting in copepod biodiversity research

The majority of copepod communities usually comprise large portions of young developmental stages, which are often impossible to identify, and also many undiscovered cryptic species. For these it was up to now not possible to receive detailed distribution patterns on a quantitative basis. Applying proteomic fingerprinting using MALDI-TOF MS yielded valid species identification and fine-scale vertical profiles of Spinocalanidae with a high species and stage resolution, even of putative cryptic species and young copepodite stages (Chapters V and VI). Hence, this method is particularly promising for high throughput analyses of taxonomically challenging copepod groups, e.g. juvenile stages, fragile deep-sea copepods and even cryptic species. Due to the higher taxonomic resolution, it may provide new insights into biodiversity, phylogeographic patterns and vertical habitat partitioning, and finally provide more detailed knowledge about mechanisms promoting high biodiversity and speciation processes (see section 3.3; Chapters V and VI).

Small species, as for example Clausocalanidae or Paracalanidae in the epipelagic and Spinocalanidae in the deep sea, are often ignored in zooplankton studies, even though they are important both in terms of abundance and biomass in all oceans (Chapter IV; Kosobokova et al. 2002; Blanco-Bercial et al. 2007; Schnack-Schiel et al. 2010). Pooled together with other species of the same size in an entire small-size fraction, their ecological features are blurred as distinct trophic relationships and behavior as well as seasonal and vertical patterns remain unnoticed (Peralba and Mazzocchi 2004; Turner 2004; Blanco-Bercial et al. 2007; Cornils et al. 2007). Thus, to track or even predict changes in zooplankton communities and their ecological consequences, detailed knowledge on community structures is necessary. Applying proteomic fingerprinting to efficiently identify and quantify copepod species opens new prospects and possibilities for long-term monitoring studies of copepod communities.

The high sample throughput and cost-effectiveness made MALDI-TOF MS a well-established technology in microorganism identification based on their specific proteome fingerprints, e.g. in food quality control, environmental research, and veterinary and clinical diagnostics in pathogen identification (Lynn et al. 1999; Li et al. 2000; Tan et al. 2009; Fenselau and Demirev 2001). This involved the establishment of routine identification methods by software development, such as the BioTyper software (Bruker Daltonik GmbH). Raw spectra may be imported and analyzed by standard pattern matching against a reference data base (BioTyper database), allowing immediate comparison and discrimination of bacterial spectral profiles (Seng et al. 2009; Saffert

et al. 2011). The generation of a mass spectral database applying a standard pattern matching algorithm for species identification based on mass spectral profiles, as already available for microorganisms and similar also to existing algorithms (e.g. Basic Local Alignment Search Tool) for comparing DNA sequences, will be essential. Establishing proteomic fingerprinting using MALDI-TOF MS as a routine procedure in copepod biodiversity research will make it a powerful alternative for species identification. In particular, it may even be superior to morphological and genetic analyses, as it allows detailed phylogeographic studies and abundance analyses with a higher species resolution than previously achieved by morphological identification and similar to taxonomic resolution achieved by genetic analyses (Chapters V and VI). This allows plankton studies at new levels, leading to a better understanding of the structure and function of the pelagic realm and the detection of qualitative and quantitative changes in marine ecosystems, while it's potential may even be expanded for other zooplankton organisms (Chapter VI).

Hypothesis 4: *The analysis of species-specific proteome fingerprints gives new insights into the ontogenetic vertical distribution of closely related deep-sea copepods.*

Conclusions:

- Species richness of the deep sea copepod family Spinocalanidae was largely underestimated by mere morphological identification. Even cryptic species and juvenile copepods were discriminated based on their species-specific proteome fingerprints.
- The community analyses applying proteome fingerprinting for quantitative species identification yielded fine-scale species-specific and ontogenetic vertical distribution profiles of Spinocalanidae.
- The high sample throughput and cost-effectiveness of proteomic fingerprinting using MALDI-TOF MS allow rapid and accurate species identification and community analyses on a quantitative basis at a high taxonomic resolution. This is particularly promising for taxonomically challenging copepod groups such as cryptic species, juvenile stages and fragile deep-sea species, to provide new insights into biodiversity, phylogeographic patterns and vertical habitat partitioning.

4 Outlook

Yet, great uncertainties exist concerning carbon budgets throughout the world's ocean, especially in the upper 1000 m, due to accuracy issues of different sediment trap types and procedures. Furthermore, active carbon transport is usually not considered by most sediment traps (Buesseler et al. 2007; Burd et al. 2010). As a prerequisite to understand the functioning of different ecosystems, we need to 1) develop more accurate and standardized methods measuring POC fluxes at various depths, and 2) understand the roles of key species and identify their qualitative (e.g. energy storage, predator avoidance, habitat or food preference, feeding behavior and reproductive processes) and quantitative traits (e.g. body mass, metabolic rates such as respiration, ingestion, egestion and growth rates) (Barnett et al. 2007). Species composition and abundances often reflect responses of an ecosystem to hydro-climatic forcing, e.g. changes in temperature, stratification and seasonal variability (Beaugrand et al. 2002; Beaugrand and Ibañez 2004). Such changes in zooplankton community structure will propagate along the food chain, as zooplankton plays a key role in transferring energy from lower to higher trophic levels (Verheye et al. 1998; Steinberg et al. 2012). Therefore, I encourage a sharper focus on how species composition and biodiversity, at both producer and consumer level, is interlinked to pelagic ecosystem processes such as primary and secondary production, carbon cycling and sequestration and trophic transfer efficiencies.

To disentangle major underlying environmental and ecological forces regulating copepod dynamics and generating high biodiversity in the deep sea and in general, community structures of high taxonomic resolution need to be routinely monitored. In addition, high spatial and temporal resolution of community analyses are necessary to identify species-specific regional and vertical patterns and to relate changes in community structure and/or biodiversity to major driving mechanisms. Thereby, we may be able to better predict shifts in zooplankton communities and their consequences on ecosystem processes and element cycles upon environmental changes (Norberg 2004; Duffy and Stachowicz 2006; Barnett et al. 2007).

Yet, such high-resolution monitoring at all scales seems to be an almost impossible task up to now. In this context, advances in molecular techniques such as high-throughput species identification and community analyses based on proteomic fingerprinting using MALDI-TOF MS are of special importance, allowing rapid species identification and detailed community analyses to shed new light on biodiversity, distributional patterns and phylogeography.

References

Abe, Y., Ishii, K., Yamaguchi, A., Imai, I., 2012. Short-term changes in population structure and vertical distribution of mesopelagic copepods during the spring phytoplankton bloom in the Oyashio region. Deep-Sea Res. I 65, 100-112.

Aiken, J., Rees, N., Hooker, S., Holligan, P., Bale, A., Robins, D., Moore, G., Harris, R., Pilgrim, D., 2000. The Atlantic meridional transect: Overview and synthesis of data. Prog. Oceanogr. 45, 257-312.

Allen, A.P., Brown, J.H., Gillooly, J.F., 2002. Global biodiversity, biochemical kinetics, and the energetic-equivalence rule. Science 297.

Allen, A.P., Gillooly, J.F., Brown, J.H., 2007. Recasting the species-energy hypothesis: The different roles of kinetic and potential energy in regulating biodiversity. Cambridge University Press, New York, 283-299 pp.

Ambler, J.W., Miller, C.B., 1987. Vertical habitat-partitioning by copepodites and adults of subtropical oceanic copepods. Mar. Biol. 94, 561-577.

Andersen, V., Nival, P., Caparroy, P., Gubanova, A., 2001a. Zooplankton community during the transition from spring bloom to oligotrophy in the open NW Mediterranean and effects of wind events. 1. Abundance and specific composition. J. Plankt. Res. 23, 227-242.

Andersen, V., Gubanova, A., Nival, P., Ruellet, T., 2001b. Zooplankton community during the transition from spring bloom to oligotrophy in the open NW Mediterranean and effects of wind events. 2. Vertical distributions and migrations. J. Plankt. Res. 23, 243-261.

Angel, M.V., 1993. Biodiversity of the pelagic ocean. Conserv. Biol. 7, 760-772.

Arashkevich, E.G., Drits, A.V., Timonin, A.G., 1996. Diapause in the life cycle of *Calanoides carinatus* (Krøyer), (Copepoda, Calanoida). Hydrobiologia 320, 197–208.

Arístegui, J., Montero, M.F., 2005. Temporal and spatial changes in plankton respiration and biomass in the Canary Islands region: the effect of mesoscale variability. J.f Mar. Syst. 54, 65-82.

Arístegui, J., Gasol, J.M., Duarte, C.M., Herndl, G.J., 2009. Microbial oceanography of the dark ocean's pelagic realm. Limnol. Oceanogr. 54, 1501-1529.

Armstrong, R.A., Lee, C., Hedges, J.I., Honjo, S., Wakeham, S.G., 2002. A new mechanistic model for organic carbon fluxes in the ocean based on the quantitative association of POC with ballast minerals. Deep-Sea Res. II 49, 219-236.

Auel, H., 1999. The ecology of Arctic deep-sea copepods (Euchaetidae and Aetideidae). Aspects of their distribution, trophodynamics and effect on the carbon flux. Rep. Polar Res. 319, 1-97.

Auel, H., Hagen, W., 2002. Mesozooplankton community structure, abundance and biomass in the central Arctic Ocean. Marine Biology 140, 1013-1021.

Auel, H., Hagen, W., Verheye, H.M., 2005. Metabolic adaptations and reduced respiration of the copepod *Calanoides carinatus* during diapause at depth in the Angola-Benguela Front and northern Benguela upwelling regions. Afr. J. Mar. Sci. 27, 653–657.

Auel, H., Verheye, H.M., 2007. Hypoxia tolerance in the copepod *Calanoides carinatus* and the effect of an intermediate oxygen minimum layer on copepod vertical distribution in the northern Benguela Current upwelling system and the Angola-Benguela Front. J. Exp. Mar. Biol. Ecol. 352, 234-243.

Barnett, A.J., Finlay, K., Beisner, B.E., 2007. Functional diversity of crustacean zooplankton communities: towards a trait-based classification. Freshw. Biol. 52, 796-813.

Beaugrand, G., Ibañez, F., Lindley, J.A., Reid, P.C., 2002. Diversity of calanoid copepods in the North Atlantic and adjacent seas: Species associations and biogeography. Mar. Ecol. Prog. Ser. 232, 179-195.

Beaugrand, G., Ibañez, F., 2004. Monitoring marine plankton ecosystems. II: Long-term changes in North Sea calanoid copepods in relation to hydro-climatic variability. Mar. Ecol. Prog. Ser. 284, 35-47.

Blanco-Bercial, L., Álvarez-Marqués, F., 2007. RFLP procedure to discriminate between *Clausocalanus* Giesbrecht, 1888 (Copepoda, Calanoida) species in the Central Cantabrian Sea. J. Exp. Mar. Biol. Ecol. 344, 73-77.

Boxshall, G.A., 1985. The comparative anatomy of two copepods, a predatory calanoid and a particle-feeding mormonilloid. Phil. Trans. R. Soc. (Ser. B) 311, 303-377.

Boyd, P.W., Newton, P.P., 1999. Does planktonic community structure determine downward particulate organic carbon flux in different oceanic provinces? Deep-Sea Res. I 46, 63-91.

Bradford-Grieve, J.M., Markhaseva, E.L., Rocha, C.E.F., Abiahy, B., 1999. Copepoda. In: Boltovskoy, D. (Ed.), South Atlantic Zooplankton. Backhuys, Leiden, pp. 869-1098.

Brandt, A., Gooday, A.J., Brandao, S.N., Brix, S., Brokeland, W., Cedhagen, T., Choudhury, M., Cornelius, N., Danis, B., De Mesel, I., Diaz, R.J., Gillan, D.C., Ebbe, B., Howe, J.A., Janussen, D., Kaiser, S., Linse, K., Malyutina, M., Pawlowski, J., Raupach, M., Vanreusel, A., 2007. First insights into the biodiversity and biogeography of the Southern Ocean deep sea. Nature 447, 307-311.

Buesseler, K.O., 1998. The decoupling of production and particulate export in the surface ocean. Global Biogeochem. Cycles 12, 297-310.

Buesseler, K.O., Lamborg, C.H., Boyd, P.W., Lam, P.J., Trull, T.W., Bidigare, R.R., Bishop, J.K.B., Casciotti, K.L., Dehairs, F., Elskens, M., Honda, M., Karl, D.M., Siegel, D.A., Silver, M.W., Steinberg, D.K., Valdes, J., Van Mooy, B., Wilson, S., 2007. Revisiting carbon flux through the ocean's twilight zone. Science 316, 567-570.

Buesseler, K.O., Boyd, A.D., 2009. Shedding light on processes that control parcticle export and flux attenuation in the twilight zone of the open ocean. Limnol. Oceanogr. 54, 1210-1232.

Burd, A.B., Hansell, D.A., Steinberg, D.K., Anderson, T.R., Aristegui, J., Baltar, F., Beaupre, S.R., Buesseler, K.O., DeHairs, F., Jackson, G.A., Kadko, D.C., Koppelmann, R., Lampitt, R.S., Nagata, T., Reinthaler, T., Robinson, C., Robison, B.H., Tamburini, C., Tanaka, T., 2010. Assessing the apparent imbalance between geochemical and biochemical indicators of meso- and bathypelagic biological activity: What the @$#! is wrong with present calculations of carbon budgets? Deep-Sea Res. II 57, 1557-1571.

Calbet, A., Landry, M.R., 1999. Mesozooplankton influences on the microbial food web: Direct and indirect trophic interactions in the oligotrophic open ocean. Limnol. Oceanogr. 44, 1370-1380.

Calbet, A., 2008. The trophic roles of microzooplankton in marine systems. ICES J. Mar. Sci.: J. Cons. 65, 325-331.

Calbet, A., Atienza, D., Henriksen, C.I., Saiz, E., Adey, T.R., 2009. Zooplankton grazing in the Atlantic Ocean: A latitudinal study. Deep-Sea Res. II 56, 954-963.

Carpenter, S.R., Christensen, D.L., Cole, J.J., Cottingham, K.L., He, X., Hodgson, J.R., Kitchell, J.F., Knight, S.E., Pace, M.L., Post, D.M., Schindler, D.E., Voichick, N., 1995. Biological control of eutrophication in lakes. Environmental Sci. Technol. 29, 784-786.

Cass, C.J., Wakeham, S.G., Daly, K.L., 2011. Lipid composition of tropical and subtropical copepod species of the genus *Rhincalanus* (Copepoda: Eucalanidae): A novel fatty acid and alcohol signature. Mar. Ecol. Prog. Ser. 439, 127-138.

Champalbert, G., Pagano, M., Kouamé, B., Riandey, V., 2005. Zooplankton spatial and temporal distribution in a tropical oceanic area off West Africa. Hydrobiol. 548, 251-265.

Clark, D.R., Aazem, K.V., Hays, G.C., 2001. Zooplankton abundance and community structure over a 4000 km transect in the north-east Atlantic. J. Plankt. Res. 23, 365-372.

Conover, R.J., 1979. Secondary production as an ecological phenomenon. In: van der Spoel, S., Pierrot-Bults, A.C. (Eds.), Zoogeography and diversity of plankton. Bunge Scientific Publishers, Utrecht, pp. 50-86.

Cornils, A., Schnack-Schiel, S.B., Böer, M., Graeve, M., Struck, U., Al-Najjar, T., Richter, C., 2007. Feeding of Clausocalanids (Calanoida, Copepoda) on naturally occurring particles in the northern Gulf of Aqaba (Red Sea). Mar. Biol. 151, 1261-1274.

Dam, H.G., Miller, C.A., Jonasdottir, S.H., 1993. The trophic role of mesozooplankton at 47°N, 20°W during the North Atlantic Bloom Experiment. Deep-Sea Res. I 40, 197-212.

Dam, H.G., Zhang, X.S., Butler, M., Roman, M.R., 1995. Mesozooplankton grazing and metabolism at the equator in the central Pacific - Implications for carbon and nitrogen fluxes. Deep-Sea Res. II 42, 735-756.

Danovaro, R., Dell'Anno, A., Fabiano, M., Pusceddu, A., Tselepides, A., 2001. Deep-sea ecosystem response to climate changes: the eastern Mediterranean case study. Trends Ecol. Evol. 16, 505-510.

Danovaro, R., Dell'Anno, A., Pusceddu, A., 2004. Biodiversity response to climate change in a warm deep sea. Ecol. Lett. 7, 821-828.

Danovaro, R., Company, J.B., Corinaldesi, C., D'Onghia, G., Galil, B., Gambi, C., Gooday, A.J., Lampadariou, N., Luna, G.M., Morigi, C., Olu, K., Polymenakou, P., Ramirez-Llodra, E., Sabbatini, A., Sarda, F., Sibuet, M., Tselepides, A., 2010. Deep-Sea Biodiversity in the Mediterranean Sea: The Known, the Unknown, and the Unknowable. PloS ONE 5.

Dayton, P., Hessler, R.H., 1972. The role of biological disturbance in mainting diversity in the deep sea. Deep-Sea Res. I 19, 199-208.

De La Rocha, C., Passow, U., 2007. Factor influencing the sinking POC and the efficiency of the biological carbon pump. Deep-Sea Res. II 54, 639-658.

Deevey, G.B., Brooks, A.L., 1977. Copepods of the Sargasso Sea off Bermuda: Species composition, and vertical and seasonal deistribution between the surface and 2000 m. Bull. Mar. Sci. 27, 256-291.

Ducklow, H.W., Steinberg, D.K., Buesseler, K.O., 2001. Upper ocean carbon export and the biological pump. Oceanogr. 14, 50-58.

Duffy, J.E., Stachowicz, J.J., 2006. Why biodiversity is important to oceanography: Potential roles of genetic, species, and trophic diversity in pelagic ecosystem processes. Mar. Ecol. Prog. Ser. 311, 179-189.

Ekau, W., Auel, H., Portner, H.O., Gilbert, D., 2010. Impacts of hypoxia on the structure and processes in pelagic communities (zooplankton, macro-invertebrates and fish). Biogeosciences 7, 1669-1699.

Escribano, R., Marin, V.H., Hidalgo, P., 2001. The influence of coastal upwelling on the distribution of *Calanus chilensis* in the Mejillones Peninsula (northern Chile): implications for its population dynamics. Hydrobiologia 453, 143-151.

Escribano, R., Hidalgo, P., Krautz, C., 2009. Zooplankton associated with the oxygen minimum zone system in the northern upwelling region of Chile during March 2000. Deep-Sea Res. II 56, 1083-1094.

Escribano, R., Pérez, C.S., 2010. Variability in fatty acids of two marine copepods upon changing food supply in the coastal upwelling zone off Chile: Importance of the picoplankton and nanoplankton fractions. J. Mar. Biol. Assoc. U. K. 90, 301-313.

Falkowski, P.G., Barber, R.T., Smetacek, V., 1998. Biogeochemical controls and feedbacks on ocean primary production. Science 281, 200-206.

Fenselau, C., Demirev, P.A., 2001. Characterization of intact microorganisms by MALDI mass spectrometry. Mass Spectrom. Rev. 20, 157-171.

Fernández-Álamo, M.A., Färber-Lorda, J., 2006. Zooplankton and the oceanography of the eastern tropical Pacific: A review. Progr. Oceanogr. 69, 318-359.

Field, J.G., Ducklow, H.W., Hanson, R.B., 2000. Some conclusions and highlight of JGOFS mid-project achievements. In: Hanson, R.B., Ducklow, H.W., Field, J.G. (Eds.), The changing global ocean carbon cycle. International Geosphere-Biosphere Programme Book Series 5. Cambridge University Press, Cambridge, pp. 493-499.

Flint, M.V., Drits, A.V., Pasternak, A.F., 1991. Characteristic features of body composition and metabolism in some interzonal copepods. Mar. Biol. 111, 199-205.

Gage, J.D., Tyler, P.A., 1991. Deep-sea Biology: A natural history of organisms at the deep-sea floor. Cambridge University Press, Cambrige, 504 pp.

Gasol, J.M., del Giorgio, P.A., Duarte, C.M., 1997. Biomass distribution in marine planktonic communities. Limnol. Oceanogr. 42, 1353-1363.

Gentsch, E., Kreibich, T., Hagen, W., Niehoff, B., 2009. Dietary shifts in the copepod *Temora longicornis* during spring: Evidence from stable isotope signatures, fatty acid biomarkers and feeding experiments. J. Plankton Res. 31, 45-60.

Giller, P.S., Hillebrand, H., Berninger, U.G., Gessner, M.O., Hawkins, S., Inchausti, P., Inglis, C., Leslie, H., Malmqvist, B., Monaghan, M.T., Morin, P.J., O'Mullan, G., 2004. Biodiversity effects on ecosystem functioning: emerging issues and their experimental test in aquatic environments. Oikos 104, 423-436.

Gowing, M.M., Wishner, K.F., 1998. Feeding ecology of the copepod *Lucicutia* aff. *L. grandis* near the lower interface of the Arabian Sea oxygen minimum zone. Deep-Sea Res. II 45, 2433-2459.

Grassle, J.F., 1989. Species diversity in deep-sea communities. Trends Ecol. Evol. 4, 12-15.

Grunewald, A.C., Morales, C.E., Gonzalez, H.E., Sylvester, C., Castro, L.R., 2002. Grazing impact of copepod assemblages and gravitational flux in coastal and oceanic waters off central Chile during two contrasting seasons. J. Plankt. Res. 24, 55-67.

Hagen, W., Kattner, G., Graeve, M., 1995. On the lipid biochemistry of polar copepods - Compositional differences in the Antarctic calanoids *Euchaeta antarctica* and *Euchirella rostromagna*. Mar. Biol. 123, 451-457.

Hagen, W., 1999. Reproductive strategies and energetic adaptations of polar zooplankton. Invertebr. Reprod. Dev. 36, 25-34.

Hannides, C.C.S., Landry, M.R., Benitez-Nelson, C.R., Styles, R.M., Montoya, J.P., Karl, D.M., 2009. Export stoichiometry and migrant-mediated flux of phosphorus in the North Pacific Subtropical Gyre. Deep-Sea Res. I 56, 73-88.

Hansen, F.C., Cloete, R.R., Verheye, H.M.V., 2005. Seasonal and spatial variability of dominant copepods along a transect off Walvis Bay (23°S), Namibia. Afr. J. Mar. Sci. 27, 55-63.

Hansen, A., Ohde, T., Wasmund, N., 2014. Succession of micro- and nanoplankton groups in ageing upwelled waters of Namibia. J. Mar. Syst. 140, 130-137.

Hauss, H., Franz, J.M.S., Hansen, T., Struck, U., Sommer, U., 2013. Relative inputs of upwelled and atmospheric nitrogen to the eastern tropical North Atlantic food web: Spatial distribution of $\delta^{15}N$ in mesozooplankton and relation to dissolved nutrients dynamics. Deep-Sea Res. I 75, 135-145.

Hessler, R.R., Sanders, H.L., 1967. Faunal diversity in the deep. Deep-Sea Res. I 14, 65-78.

Hidalgo, P., Escribano, R., 2007. Coupling of life cycle of the copepods *Calanus chilensis* and *Centropages brachiatus* to upwelling induced variability in the central-southern region of Chile. Prog Oceanogr 75, 501-517.

Holmes, E., Lavik, G., Fischer, G., Segl, M., Ruhland, G., Wefer, G., 2002. Seasonal variability of $\delta^{15}N$ in sinking particles in the Benguela upwelling region. Deep-Sea Res. I 49, 377-394.

Homma, T., Yamaguchi, A., Bower, J.R., Imai, I., 2011. Vertical changes in abundance, biomass, and community structure of copepods in the northern North Pacific and Bering Sea at 0-3000 m depth, and their role on the vertical flux of surface-produced organic material. Bull. Fish. Sci. Hokkaido Univ. 61, 29-47.

Hugget, J., Verheye, H., Escribano, R., Fairweather, T., 2009. Copepod biomass, size composition and production in the Southern Benguela: Spatio-temporal patterns of variation, and comparison with other eastern boundary upwelling systems. Progr. Oceanogr. 83, 197-207.

Huskin, I., Anadón, R., Woodd-Walker, R.S., Harris, R.P., 2001. Basin-scale latitudinal patterns of copepod grazing in the Atlantic Ocean. J. Plankt. Res. 23, 1361-1371.

Hutchings, L., Verheye, H.M., Mitchell-Innes, B.A., Peterson, W.T., Huggett, J.A., Painting, S.J., 1995. Copepod production in the southern Benguela system. ICES J. Mar. Sci. 52, 439-455.

Hutchings, L., Verheye, H.M.V., Hugget, J.A., Demarcq, H., Cloete, R., Barlow, R.G., Louw, D., da Silva, A., 2006. Variability of plankton with reference to fish variability in the Benguela Current Large

Marine Ecosystem - An overview. In: Shannon, L.V., Hempel, G., Malanotte-Rizzoli, P., Moloney, C.L., Woods, J. (Eds.), Large Marine Ecosystems. Elsevier, Amsterdam, pp. 91-124.

Isla, J.A., Llope, M., Anadon, R., 2004. Size-fractionated mesozooplankton biomass, metabolism and grazing along a 50°N-30°S transect of the Atlantic Ocean. J. Plankt. Res. 26, 1301-1313.

Karl, D.M., Bidigare, R.R., Letelie, R.M., 2001. Long-term changes in plankton community structure and productivity in the North Pacific subtropical gyre: The domain shift hypothesis. Deep-Sea Res. II 48, 1449-1470.

Kepkay, P.E., 2000. Colloids and the ocean carbon cycle. In: Wangersky, P. (Ed.), Handbook of environmental chemistry. Springer, pp. 35-56.

Kiørboe, T., 1993. Turbulence, phytoplankton cell size, and the structure of pelagic food webs. Adv. Mar. Biol. 29, 1-72.

Kiørboe, T., 2000. Colonization of marine snow aggregates by invertebrate zooplankton: abundance, scaling, and possible role. Limnol. Oceanogr. 45.

Kiørboe, T., 2001. Formation and fate of marine snow: small-scale processes with large-scale implications. Sci. Mar. 65 (suppl. 2), 57-71.

Kiørboe, T., Tang, K., Grossart, H.-P., Ploug, H., 2003. Dynamics of microbial communities on marine snow aggregates: colonization, growth, detachment and grazing mortality of attached bacteria. Appl. Environ. Microbiol. 69, 3036-3047.

Kiørboe, T., Grossart, H.-P., Ploug, H., Tang, K., Auer, B., 2004. Particle associated flagellates: swimming patterns, colonization rates, and grazing on attached bacteria. Aquat. Microbiol. Ecol. 35, 141-152.

Kollmer, W.E., 1963. The pilchard of South West Africa (*Sardinops ocellata*). Notes on zooplankton and phytoplankton collections made off Walvis Bay. Investl Rep. mar. Res. Lab. S. W. Afr. 8, 78.

Koppelmann, R., Weikert, H., 1992. Full-depth zooplankton profiles over the deep bathyal of the NE Atlantic. Mar. Ecol. Prog. Ser 86, 263-272.

Koppelmann, R., Weikert, H., 1999. Temporal changes of deep-sea mesozooplankton abundance in the temperate NE Atlantic and estimates of the carbon budget. Mar. Ecol. Prog. Ser. 179, 27-40.

Koppelmann, R., Weikert, H., Halsband-Lenk, C., 2004. Mesozooplankton community respiration and its relation to particle flux in the oligotrophic eastern Mediterranean. Global Biogeochem. Cycles 18, GB1039.

Koppelmann, R., Weikert, H., 2007. Spatial and temporal distribution patterns of deep-sea mesozooplankton in the eastern Mediterranean - indications of a climatically induced shift? Mar. Ecol. 28, 259-275.

Koppelmann, R., Frost, J., 2008. The ecological role of zooplankton in the twilight and dark zones of the ocean. In: Mertens, L.P. (Ed.), Biological Oceanography Research Trends. Nova Science Publishers, Inc., New York, pp. 67-130.

Kosobokova, K.N., Hirche, H.-J., Scherzinger, T., 2002. Feeding ecology of *Spinocalanus antarcticus*, a mesopelagic copepod with a looped gut. Mar. Biol. 141, 503-511.

Kosobokova, K.N., Hirche, H.J., Hopcroft, R.R., 2007. Reproductive biology of deep-water calanoid copepods from the Arctic Ocean. Mar. Biol. 151, 919-934.

Kosobokova, K.N., Hopcroft, R.R., 2010. Diversity and vertical distribution of mesozooplankton in the Arctic's Canada Basin. Deep-Sea Res. II 57, 96-110.

Kosobokova, K.N., Hopcroft, R.R., Hirche, H.-J., 2011. Patterns of zooplankton diversity through the depths of the Arctic's central basins. Mar. Biodiv. 41, 29-50.

Kuriyama, M., Nishida, S., 2006. Species diversity and niche-partitioning in the pelagic copepods of the family Scolecitrichidae (Calanoida). Crustaceana 79, 293-317.

Laakmann, S., Kochzius, M., Auel, H., 2009a. Ecological niches of Arctic deep-sea copepods: Vertical partitioning, dietary preferences and different trophic levels minimize inter-specific competition. Deep-Sea Res. I 56, 741-756.

Laakmann, S., Stumpp, M., Auel, H., 2009b. Vertical distribution and dietary preferences of deep-sea copepods (Euchaetidae and Aetideidae; Calanoida) in the vicinity of the Antarctic Polar Front. Polar Biol. 32, 679-689.

Laakmann, S., Auel, H., Kochzius, M., 2012. Evolution in the deep sea: Biological traits, ecology and phylogenetics of pelagic copepods. Mol. Phylogenet. Evol. 65, 535-546.

Laakmann, S., Gerdts, G., Erler, R., Knebelsberger, T., Arbizu, P.M., Raupach, M.J., 2013. Comparison of molecular species identification for North Sea calanoid copepods (Crustacea) using proteome fingerprints and DNA sequences. Mol. Ecol. Resour. 13, 862-876.

Landry, M.R., 1981. Switching between herbivory and carnivory by the planktonic marine copepod *Calanus pacificus*. Mar. Biol. 65, 77-82.

Laws, E.A., Falkowski, P.G., Smith, W.O., Ducklow, H., McCarthy, J.J., 2000. Temperature effects on export production in the open ocean. Global Biogeochem. Cycles 14, 1231-1246.

Le Borgne, R., Rodier, M., 1997. Net zooplankton and the biological pump: A comparison between the oligotrophic and mesotrophic equatorial Pacific. Deep-Sea Res. II 44, 2003-2023.

Le Borgne, R., Champalbert, G., Gaudy, R., 2003. Mesozooplankton biomass and composition in the equatorial Pacific along 180°. J. Geophys. Res. C 108, C128143.

Lee, R.F., Barnett, A.M., Hirota, J., 1971. Distribution and importance of wax esters in marine copepods and other zooplankton. Deep-Sea Res. I 18, 1147-1165.

Lee, R.F., Hirota, J., 1973. Wax esters in tropical zooplankton and nekton and geographical distribution of wax esters in marine copepods. Limnol. Oceanogr. 18, 227-239.

Lee, R.F., Hagen, W., Kattner, G., 2006. Lipid storage in marine zooplankton. Mar. Ecol. Prog. Ser. 307, 273-306.

Legendre, L., Michaud, J., 1998. Flux of biogenic carbon in oceans: size-dependent regulation by pelagic food webs. Mar. Ecol. Prog. Ser. 164, 1-11.

Li, T.Y., Liu, B.H., Chen, Y.C., 2000. Characterization of *Aspergillus* spores by matrix-assisted laser desorption/ionization time-of-flight mass spectrometry. Rapid Commun. Mass Spectrom. 14, 2393-2400.

Loick, N., Ekau, W., Verheye, H.M., 2005. Water-body preferences of dominant calanoid copepod species in the Angola-Benguela frontal zone. Afr. J. Mar. Sci. 27, 597-608.

Longhurst, A., 1967. Vertical distribution of zooplankton in relation to the eastern Pacific oxygen minimum. Deep-Sea Res. I 14, 51-63.

Longhurst, A., Williams, R., 1979. Materials for plankton modelling: Vertical distribution of Atlantic zooplankton in summer. J. Plankt. Res. 1, 1-28.

Longhurst, A.R., 1985. Relationship between diversity and the vertical structure of the upper ocean. Deep-Sea Res. I 32, 1535-1570.

Longhurst, A., 1985. Relationship between diversity and the vertical structure of the upper ocean. Deep-Sea Res. I 32, 1535-1570.

Longhurst, A., Pauly, D., 1987. The ecology of the tropical oceans. Academic Press, San Diego.

Longhurst, A.R., Harrison, W.G., 1989. The biological pump: Profiles of plankton production and consumption in the upper ocean. Prog. Oceanogr. 22, 47–123.

Longhurst, A.R., Bedo, A.W., Harrison, W.G., Head, E.J.H., Sameoto, D.D., 1990. Vertical flux of respiratory carbon by oceanic diel migrant biota. Deep-Sea Res. I 37, 685-694.

Longhurst, A., Sathyendranath, S., Platt, T., Caverhill, C., 1995. An estimate of global primary production in the ocean from satellite radiometer data. J. Plankton Res. 17, 1245-1271.

Longhurst, A., 1995. Seasonal cycles of pelagic production and consumption. Progr. Oceanogr. 36, 77-167.

Lynn, E.C., Chung, M.-C., Tsai, W.-C., Han, C.-C., 1999. Identification of Enterobacteriaceae bacteria by direct matrix-assisted laser desorption/ionization mass spectreometrc analysis of whole cells. Rapid Commun. Mass Spectrom. 13, 2022-2027.

MacArthur, R.H., Recher, H., Cody, M.L., 1966. On the relation between habitat selection and species diversity Am. Nat. 100, 319-332.

MacPherson, E., 2002. Large-scale-species-richness gradients in the Atlantic Ocean. Proc. R. Soc. Lond. B 269, 1715-1720.

Marañón, E., Holligan, P.M., Varela, M., Mourino, B., Bale, A.J., 2000. Basin-scale variability of phytoplankton biomass, production and growth in the Atlantic Ocean. Deep-Sea Res. I 47, 825-857.

Marañón, E., Behrenfeld, M.J., Gonzalez, N., Mourino, B., Zubkov, M.V., 2003. High variability of primary production in oligotrophic waters of the Atlantic Ocean: uncoupling from phytoplankton biomass and size structure. Mar. Ecol. Prog. Ser. 257, 1-11.

Martin, J.H., Knauer, G.A., Karl, D.M., Broenkow, W.W., 1987. VERTEX: carbon cycling in the northeast Pacific. Deep-Sea Res. I 34, 267-285.

Matsuura, H., Nishida, S., 2000. Fine structure of the "button setae" in the deep-sea pelagic copepods of the genus *Euaugaptilus* (Calanoida: Augaptilidae). Mar. Biol. 137, 339-345.

Matsuura, H., Nishida, S., Nishikawa, J., 2010. Species diversity and vertical distribution of the deep-sea copepods of the genus *Euaugaptilus* in the Sulu and Celebes Seas. Deep-Sea Res. II 57, 2098-2109.

Mauchline, J., 1998. The biology of calanoid copepods. Academic Press, San Diego, CA, 710 pp.

Mazzocchi, M.G., Paffenhöfer, G.-A., 1999. Swimming and feeding behaviour of the planktonic copepod *Clauscocalanus furcatus*. J. Plankt. Res. 21, 1501-1518.

McClain, C.R., Schlacher, T.A., 2015. On some hyptheses of diversity of animal life at great depths on the sea floor. Mar. Ecol. 36, 849-872.

McGowan, J.A., 1986. The biogeography of pelagic ecosystems. UNESCO Tech. Pap. Mar. Sci. 49, 191-200.

McNaughton, S.J., 1977. Diversity and stability of ecological communities - Comment on role of empiricism in ecology. Am. Nat. 111, 515-525.

Montoya, J.P., Carpenter, E.J., Capone, D.G., 2002. Nitrogen fixation and nitrogen isotope abundances in zooplankton of the oligotrophic North Atlantic. Limnol. Oceanogr. 47, 1617-1628.

Neuer, S., Davenport, R., Fredenthal, T., Wefer, G., Llinás, O., Rueda, M.-J., Steinberg, D.K., Karl, D.M., 2002. Differences in the biological carbon pump at three subtropical ocean sites. Geophys. Res. Lett. 49, 3561-3576.

Nishida, S., Oh, B.O., Nemoto, T., 1991. Midgut structure and food habits of the mesopelagic copepods *Lophothrix frontalis* and *Scottocalanus securifrons*. In: Proc. 4th Int. Conf. Copepoda. Bull. Plankt. Soc. Spec. 527-534.

Nishida, S., Ohtsuka, S., 1996. Specialized feeding mechanism in the pelagic copepod genus *Heterorhabdus* (Calanoida: Heterorhabdidae), with special reference to the mandibular tooth and labral glands. Mar. Biol. 126, 619-632.

Nishida, S., Ohtsuka, S., 1997. Ultrastructure of the mouthpart sensoray setae in mesopelagic copepods of the family Scolecithrichidae. Plankton Biol. Ecol. 44, 81-90.

Nishida, S., Ohtsuka, S., Parker, A.R., 2002. Functional morphology and food habits of deep-sea copepods of the genus *Cephalophanes* (Calanoida: Phaennidae): Perception of bioluminescence as a strategy for food detection. Mar. Eco. Prog. Ser. 227, 157-171.

Norberg, J., 2004. Biodiversity and ecosystem functioning: A complex adaptive systems approach. Limnol. Oceanogr. 49, 1269-1277.

Ohman, M.D., 1987. Energy sources for recruitment of the sub-Antarctic copepod *Neocalanus tonsus*. Limnol. Oceanogr. 32, 1317-1330.

Ohman, M.D., Drits, A.V., Clarke, M.E., 1998. Differential dormancy of co-occurring copepods. Deep-Sea Res. II 45, 1709–1740.

Ohtsuka, S., Soh, H.Y., Nishida, S., 1997. Evolutionary switching from suspension feeding to carnivory in the calanoid family Heterorhabdidae (Copepoda). J. Crustac. Biol. 17, 577-595.

Olivar, M.-P., Barangé, M., 1990. Zooplankton of the northern Benguela region in a quiescent upwelling period. J. Plankt. Res. 12, 1023-1044.

Paffenhöfer, G.-A., Mazzocchi, M.G., 2003. Vertical distribution of subtropical epiplanktonic copepods. J. Plankt. Res. 25, 1139-1156.

Painting, S.J., Lucas, M.I., Peterson, W.T., Brown, P.C., Hutching, L., Mitchell-Innes, B.A., 1993. Dynamics of bacterioplankton, phytoplankton and mesozooplankton communities during the development of an upwelling plume in the southern Benguela. Mar. Ecol. Prog. Ser 100, 35-53.

Pavlova, E.V., 1994. Diel changes in copepod respiration rates. Hydrobiologia 292/293, 333–339.

Peralba, A., Mazzocchi, M.G., 2004. Vertical and seasonal distribution of eight *Clausocalanus* species (Copepoda: Calanoida) in oligotrophic waters. ICES J. Mar. Sci. 61, 645-653.

Peterson, W.T., Miller, C.B., Hutchinson, A., 1979. Zonation and maintenance of copepod populations in the Oregon upwelling zone. Deep-Sea Res. I 26, 467-494.

Peterson, W.T., Arcos, D.F., McManus, G.B., Dam, H., Bellatoni, D., Johnson, T., Tiselius, P., 1988. The nearshore zone during coastal upwelling: Daily variability and coupling between primary and secondary production off Central Chile-. Prog Oceanogr 20, 1-40.

Peterson, W.T., Painting, S.J., Hutchings, L., 1990. Diel variations in gut pigment content, diel vertical migration and estimates of grazing impact for copepods in the southern Benguela upwelling region in October 1987. J. Plankt. Res. 12, 259-281.

Peterson, W., 1998. Life cycle strategies of copepods in coastal upwelling zones. J. Mar. Syst. 15, 313-326.

Ramirez-Llorda, E., Brandt, A., Danovaro, R., De Mol, B., Escobar, E., German, C.R., Levin, L.A., Martinez-Arbizu, P., Menot, L., Buhl-Mortensen, P., Narayanaswamy, B.E., Smith, C.R., Tittensor, D.P., Tyler, P.A., Vanreusel, A., Vecchione, M., 2010. Deep, diverse and definitely different: Unique attributes of the world's largest ecosystem. Biogeosciences 7, 2851-2899.

Rex, M.A., 1981. Community structure in the deep sea benthos. Ann. Rev. Ecol. Sys. 12, 331-353.

Rex, M.A., McClain, C.R., Johnson, N.A., Etter, R.J., Allen, J.A., 2005. A source-sink hypothesis for abyssal biodiversity. Am. Soc. Nat. 165, 163-178.

Robinson, C., Steinberg, D.K., Anderson, T.R., Arístegui, J., Carlson, C.A., Frost, J.R., Ghiglione, J.-F., Hernández-León, S., Jackson, G.A., Koppelmann, R., Quéguiner, B., Ragueneau, O., Rassoulzadegan, F., Robison, B.H., Tamburini, C., Tanaka, T., Wishner, K.F., Zhang, J., 2010. Mesopelagic zone ecology and biogeochemistry - A synthesis. Deep-Sea Res. II 57, 1504-1518.

Roemmich, D., McGowan, J., 1995. Climatic warming and the decline of zooplankton in the California Current. Science 267, 1324-1326.

Rohde, K., 1992. Latitudinal gradients in species diversity: The search for the primary cause. Oikos 65, 514-527.

Rosenzweig, M.L., 1992. Species diversity gradients: We know more and less than we thought. J. Mamm. 73, 715-7130.

Saffert, R.T., Cunningham, S.A., Ihde, S.M., Monson Jobe, K.E., Mandrekar, J., Patel, R., 2011. Comparison of Bruker Biotyper matrix-assisted laser desorption ionization - time of flight mass spectrometer to BD Pheonix Automated Microbiology System for identification of gram-negative bacilli. J. Clin. Microbiol. 49, 887-892.

San Martin, E., Harris, R.P., Irigoien, X., 2006. Latitudinal variation in plankton size spectra in the Atlantic Ocean. Deep-Sea Res. II 53, 1560-1572.

Sandel, V., Kiko, R., Brandt, P., Dengler, M., Stemmann, L., Vandromme, P., Sommer, U., Hauss, H., 2015. Nitrogen fuelling of the pelagic food web of the tropical Atlantic. PLoS One 10.

Sanders, H.L., 1968. Marine benthic diversity, a comparative study. Amer. Nat. 102, 243-282.

Sano, M., Maki, K., Nishibe, Y., Nagata, T., Nishida, S., 2013. Feeding habits of mesopelagic copepods in Sagami Bay: Insights from integrative analysis. Prog. Oceanogr. 110, 11-26.

Sasaki, H., Hattori, H., Nishizawa, S., 1988. Downward flux of particulate organic matter and vertical distribution of calanoid copepods in the Oyashio water in summer. Deep-Sea Res. I 35, 505-515.

Schnack-Schiel, S.B., Niehoff, B., Hagen, W., Böttger-Schnack, R., Cornils, A., Dowidar, M.M., Pasternak, A., Stambler, N., Stübing, D., Richter, C., 2008. Population dynamics and life strategies of *Rhincalanus nasutus* (Copepoda) at the onset of the spring bloom in the Gulf of Aqaba (Red Sea). J. Plankt. Res. 30, 655–672.

Schnack-Schiel, S.B., Mizdalski, E., Cornils, A., 2010. Copepod abundance and species composition in the Eastern subtropical/tropical Atlantic. Deep-Sea Res. II 57, 2064-2075.

Schukat, A., Teuber, L., Hagen, W., Wasmund, N., Auel, H., 2013. Energetics and carbon budgets of dominant calanoid copepods in the northern Benguela upwelling system. J. Exp. Mar. Biol. Ecol. 442, 1-9.

Schukat, A., Auel, H., Teuber, L., Hagen, W., 2014. Complex trophic interactions of calanoid copepods in the Benguela upwelling system. J. Sea Res. 85, 186-196.

Scotto di Carlo, B., Ianora, A., Fresi, E., Hure, J., 1984. Vertical zonation patterns for Mediterranean copepods from the surface to 3000 m at a fixed station in the Tyrrhenian Sea. J. Plankt. Res. 6, 1031-1056.

Seng, P., Drancourt, M., Gouriet, F., La Scola, B., Fournier, P.-E., Rolain, J.M., Raoult, D., 2009. Ongoing revolution in bacteriology: Routine identification of bacteria by matrix-assisted laser desorption ionization time-of-flight mass spectrometry. Clin. Infect. Dis. 49, 543-551.

Shannon, L.V., Pillar, S.C., 1986. The Benguela ecosystem. Part III. Plankton. In: Barnes, M. (Ed.), Oceanography and Marine Biology. An annual review. University Press, Aberdeen, pp. 65-170.

Shannon, L.V., Crawford, R.J.M., Pollock, D.E., Hutchings, L., Boyd, A.D., Taunton-Clark, J., Badenhorst, A., Melville-Smith, R., Augustyn, C., Cochrance, K.L., Hampton, I., Nelson, G., Japp, D.W., Tarr, R.J.Q., 1992. The 1980s - A decade of change in the Benguela ecosystem. In: Payne, A.I.L., Brink, K.H., Mann, K.H., Hilborn, R. (Eds.), Benguela trophic functioning. S. Afr. J. Mar. Sc., pp. 271-276.

Sheridan, C.C., Lee, C., Wakeham, S.G., Bishop, J.K.B., 2002. Suspended particle organic composition and cycling in surface and midwaters of the equatorial Pacific Ocean. Deep-Sea Res. I 49.

Shimode, S., Hiroe, Y., Hidaka, K., Takahashi, K., Tsuda, A., 2009. Life history and ontogenetic vertical migration of *Neocalanus gracilis* in the western North Pacific Ocean. Aquat. Biol. 7, 295-306.

Shimode, S., Takahashi, K., Shimizu, Y., Nonomura, T., Tsuda, A., 2012a. Distribution and life history of two planktonic copepods, *Rhincalanus nasutus* and *Rhincalanus rostrifrons*, in the northwestern Pacific Ocean. Deep-Sea Res. Part I 65, 133-145.

Shimode, S., Takahashi, K., Shimizu, Y., Nonomura, T., Tsuda, A., 2012b. Distribution and life history of the planktonic copepod, *Eucalanus californicus*, in the northwestern Pacific: Mechanisms for population maintenance within a high primary production area. Prog. Oceanogr. 96, 1-13.

Silver, M.W., Alldredge, A.L., 1981. Bathypelagic marine snow: Deep-sea algal and detrital community. J. Mar. Res. 39, 501-530.

Steinberg, D.K., 1995. Diet of copepods (*Scopalatum vorax*) associated with mesopelagic detritus (giant larvacean houses) in Monterey Bay, California. Mar. Biol. 122, 571-584.

Steinberg, D.K., Carlson, C.A., Bates, N.R., Goldthwait, S.A., Madin, L.P., Michaels, A.F., 2000. Zooplankton vertical migration and the active transport of dissolved organic and inorganic carbon in the Sargasso Sea. Deep-Sea Res. I 47, 137-158.

Steinberg, D.K., Carlson, C.A., Bates, N.R., Johnson, G.C., Michaels, A.F., Knap, A.H., 2001. Overview of the US JGOFS Bermuda Atlantic Time-series Study (BATS): a decadal-scale look at ocean biology and biogeochemistry. Deep-Sea Res. II 48, 1405-1447.

Steinberg, D.K., Van Mooy, B.A.S., Buesseler, K.O., Boyd, P.W., Kobari, T., Karl, D.M., 2008a. Bacterial vs. zooplankton control of sinking particle flux in the ocean's twilight zone. Limnol. Oceanogr. 53, 1327-1338.

Steinberg, D.K., Cope, J.S., Wilson, S.E., Kobari, T., 2008b. A comparison of mesopelagic mesozooplankton community structure in the subtropical and subarctic North Pacific Ocean. Deep-Sea Res. II 55, 1615-1635.

Steinberg, D.K., Lomas, M.W., Cope, J.S., 2012. Long-term increase in mesozooplankton biomass in the Sargasso Sea: Linkage to climate and implications for food web dynamics and biogeochemical cycling. Global Biogeochem. Cycles 26.

Stramma, L., Schmidtko, S., Levin, L.A., Johnson, G.C., 2010. Ocean oxygen minima expansions and their biological impacts. Deep-Sea Res. I 57, 587-595.

Suess, E., 1980. Particulate organic carbon flux in the oceans - surface productivity and oxygen utilization. Nature 288, 260-263.

Tan, S.W.L., Wong, S.M., Kini, R.M., 2000. Rapid simultaneous detection of two orchid viruses using LC- and/or MALDI-mass spectrometry. J. Virol. Methods 85, 93-99.

Teuber, L., Kiko, R., Seguin, F., Auel, H., 2013. Respiration rates of tropical Atlantic copepods in relation to the oxygen minimum zone. J. Exp. Mar. Biol. Ecol. 448, 28-36.

Teuber, L., Schukat, A., Hagen, W., Auel, H., 2014. Trophic interactions and life strategies of epi- to bathypelagic calanoid copepods in the tropical Atlantic Ocean. J. Plankton Res. 36, 1109-1123.

Teuber, L., 2014. Ecology and physiology of calanoid copepods in relation to the oxygen minimum zone in the eastern tropical Atlantic. University of Bremen, Bremen, pp. 101.

Thistle, D., 1983. The role of biologically produced habitat heterogeneity in deep-sea diversity maintenance. Deep-Sea Res. I 30, 1235-1245.

Timonin, A.G., 1991. Correlation between distribution of zooplankton and hydrologic conditions in the Benguela upwelling zone. Oceanology 31, 181-195.

Timonin, A.G., 1992. Zooplankton and environmental variability in the northern Benguela upwelling area. Russ. J. Aqua. Ecol. 1, 103-113.

Timonin, A.G., Arashkevich, E.G., Drits, A.V., Semenova, T.N., 1992. Zooplankton dynamics in the northern Benguela ecosystem, with special reference to the copepod *Calanoides carinatus*. S. Afr. J. Mar. Sci. 12, 545–560.

Timonin, A.G., 1997. Diel vertical migrations of *Calanoides carinatus* and *Metridia lucens* (Copepoda: Calanoida) in the northern Benguela upwelling area. Oceanology 37, 782-787.

Tsuda, A., Saito, H., Kasai, H., 2001. Life history strategies of subarctic copepods *Neocalanus flemingeri* and *N. plumchrus*, especially concerning lipid accumulation patterns. Plankton Biol. Ecol. 48, 52-58.

Turner, J.T., 2004. The importance of small planktonic copepods and their roles in pelagic marine food webs. Zool. Stud. 43, 255-266.

Turner, J.T., 2015. Zooplankton fecal pellets, marine snow, phytodetritus and the ocean's biological pump. Progr. Oceanogr. 130, 205-248.

Unterüberbacher, H.K., 1964. The pilchard of South West Africa (*Sardinops ocellata*). Zooplankton studies in the waters off Walvis Bay with special reference to the Copepoda. Investl Rep. mar. Res. Lab. S. W. Afr. 11, 42 (+ Plates 42-36).

Verdugo, P., Alldredge, A.L., Azam, F., Kirchman, D.L., Passow, U., Santschi, P.H., 2004. The oceanic gel phase: a bridge in the DOM-POM continuum. Mar. Chem. 92, 67-85.

Verheye, H.M., 1991. Short-term variability during an anchor station study in the southern Benguela upwelling system: Abundance, distribution and estimated production of mesozooplankton with special reference to *Calanoides carinatus* (Kroyer, 1849). Prog. Oceanogr. 28, 91-119.

Verheye, H.M., Hutchings, L., Peterson, W.T., 1991. Life history and population maintenance strategies of *Calanoides carinatus* (Copepods: Calanoida) in the southern Benguela ecosystem. S. Afr. J. mar. Sci. 11, 179-191.

Verheye, H.M., Field, J.G., 1992. Vertical distribution and diel vertical migration of *Calanoides carinatus* (Kroyer, 1849) developmental stages in the southern Benguela upwelling region. J. Exp. Mar. Biol. Ecol. 158, 123-140.

Verheye, H.M.V., Richardson, A.J., Hutchings, L., Marska, G., Gianokouros, D., 1998. Long-term trends in the abundance and community structure of coastal zooplankton in the southern Benguela system, 1951-1996. S. Afr. J. Mar. Sci. 19, 317-332.

Verheye, H.M., Hagen, W., Auel, H., Ekau, W., Loick, N., Rheenen, I., Wencke, P., Jones, S., 2005. Life strategies, energetics and growth characteristics of *Calanoides carinatus* (Copepoda) in the Angola-Benguela frontal region. Afr. J. Mar. Sci. 27, 641–651.

Vinogradov, M.E., 1972. Vertical distribution of oceanic zooplankton. Israel Programm for Scientific Translations. Jerusalem.

Voss, M., Altabet, M.A., von Bodungen, B., 1996. $\delta^{15}N$ in sedimenting particles as indicator of euphotic-zone processes. Deep-Sea Res. I 43, 33-47.

Ward, P., Shreeve, R.S., 2001. The deep-sea copepod fauna of the Southern Ocean: patterns and processes. Hydrobiologia 453, 37-54.

Ware, D.M., Thomson, R.E., 2005. Bottom-up ecosystem trophic dynamics determine fish production in the northeast Pacific. Science 308, 1280-1284.

Wassmann, P., 1998. Retention versus export food chains: processes controlling sinking loss from marine pelagic systems. Hydrobiologia 363, 29-57.

Weikert, H., 1982. The vertical distribution of zooplankton in relation to habitat zones on the area of the Atlantic II Deep, Central Red Sea. Mar. Ecol. Prog. Ser 8, 129-143.

Weikert, H., Trinkaus, S., 1990. Vertical mesozooplankton abundance and distribution in the deep eastern Mediterranean Sea SE of Crete. J. Plankt. Res. 12, 601-628.

Weikert, H., Koppelmann, R., 1996. Mid-water zooplankton profiles from the temperate ocean and partially landlocked seas. A re-evaluation of interoceanic differences. Oceanol. Acta 19, 657-664.

Weisberg, R.H., Black, B.D., Li, Z.J., 2000. An upwelling case study on Florida's west coast. J. Geophys. Res. C 105, 11459-11469.

Wiggert, J.D., Haskell, A.G.E., Paffenhöfer, G.-A., Hofmann, E.E., Klinck, J.M., 2005. The role of feeding behavior in sustaining copepod populations in the tropical ocean. J. Plankt. Res. 27, 1013-1031.

Wilson, S.E., Steinberg, D.K., Buesseler, K.O., 2008. Changes in fecal pellet characteristics with depth as indicators of zooplankton repackaging of particles in the mesopelagic zone of the subtropical and subarctic North Pacific Ocean. Deep-Sea Res. II 55, 14-15.

Wishner, K.F., Gowing, M.M., Gelfman, C., 2000. Living in suboxia: Ecology of an Arabian Sea oxygen minimum zone copepod. Limnol. Oceanogr. 45, 1576-1593.

Wishner, K.F., Gelfman, C., Gowing, M.M., Outram, D.M., Rapien, M., Williams, R.L., 2008. Vertical zonation and distributions of calanoid copepods through the lower oxycline of the Arabian Sea oxygen minimum zone. Prog. Oceanogr. 78, 163-191.

Wishner, K.F., Outram, D.M., Seibel, B.A., Daly, K.L., Williams, R.L., 2013. Zooplankton in the eastern tropical north Pacific: Boundary effects of oxygen minimum zone expansion. Deep-Sea Res. I 79, 122-140.

Woodd-Walker, R.S., 2001. Spatial distributions of copepod genera along the Atlantic Meridional Transect. Hydrobiol. 453, 161-170.

Woodd-Walker, R.S., Ward, P., Clarke, A., 2002. Large-scale patterns in diversity and community structure of surface water copepods from the Atlantic Ocean. Mar. Ecol. Progr. Ser. 236, 189-203.

Yamaguchi, A., Watanabe, Y., Ishida, H., Harimoto, T., Furusawa, K., Suzuki, S., Ishizaka, J., Ikeda, T., Takahashi, M.M., 2002. Community and trophic structures of pelagic copepods down to greater depths in the western subarctic Pacific (WEST-COSMIC). Deep-Sea Res. I 49, 1007-1025.

Yamaguchi, A., Ikeda, T., 2002. Vertical distribution patterns of three mesopelagic Paraeuchaeta species (Copepoda: Calanoida) in the Oyashio region, western subarctic Pacific Ocean. Bull. Fish. Sci. Hokkaido Univ. 53, 1-10.

Yamaguchi, A., Ikeda, T., Watanabe, Y., Ishizaka, J., 2004. Vertical distribution patterns of pelagic copepods as viewed from the predation pressure hypothesis. Zoological Studies 43, 475-485.

Yamaguchi, A., Matsuno, K., Homma, T., 2015. Spatial changes in the vertical distribution of calanoid copepods down to great depths in the North Pacific. Zool. Stud. 54.

Zhang, X.S., Dam, H.G., 1997. Downward export of carbon by diel migrant mesozooplankton in the central equatorial Pacific. Deep-Sea Res. II 44, 2191-2202.

5 APPENDIX

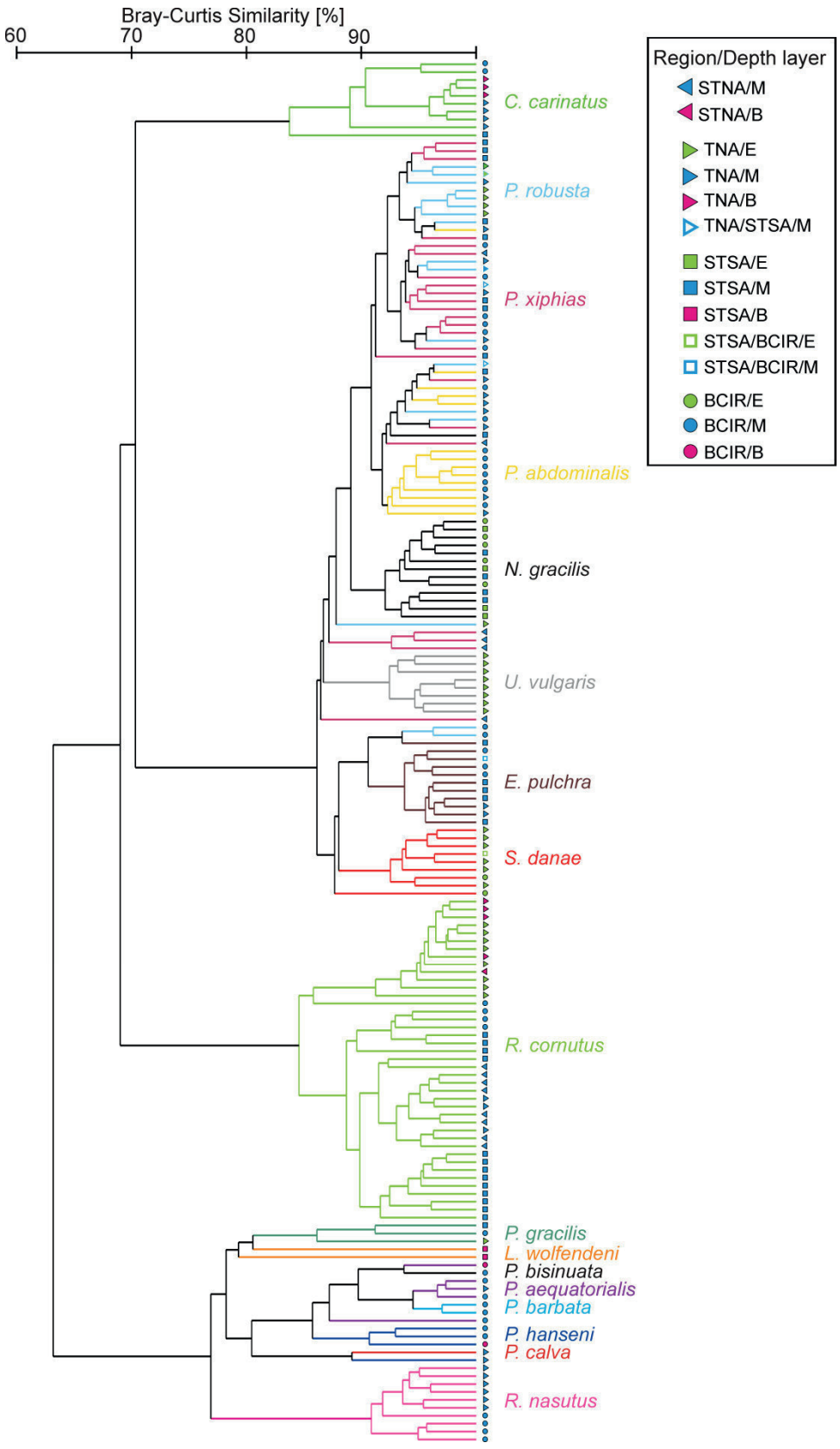
Bray-Curtis Similarity [%]
60
70
80
90
Region/Depth layer
STNA/M
STNA/B
TNA/E
TNA/M
TNA/B
TNA/STSA/M
STSA/E
STSA/M
STSA/B
STSA/BCIR/E
STSA/BCIR/M
BCIR/E
BCIR/M
BCIR/B
C. carinatus
P. robusta
P. xiphias
P. abdominalis
N. gracilis
U. vulgaris
E. pulchra
S. danae
R. cornutus
P. gracilis
L. wolfendeni
P. bisinuata
P. aequatorialis
P. barbata
P. hanseni
P. calva
R. nasutus

Figure A: Cluster analysis based on fatty acid compositions of the copepod species (all females except copepodids CV of *C. carinatus*). The four hydrographic provinces (STNA: Subtropical North Atlantic; TNA: Tropical North Atlantic; STSA: Subtropical South Atlantic; BCIR: Benguela Current influenced region) and different depth zones (E: 200-0 m, M: 1000-200 m, B: 2000-1000 m) are distinguished by different symbols (online supplementary material of Chapter II).

Table A: Copepod abundance ranges (ind m^{-3}) at six station in the eastern (sub)tropical Atlantic Ocean along the cruise track ANT-XXIX/1 of RV *Polarstern* in October/November 2012 (see Fig. 1 for station positions), separated in epi- (0-200 m), meso- (200-1000 m) and bathypelagic (1000-2000 m) depth zones. Abund.: Abundance. (+ indicates species was present)

Depth zone	**Epipelagic**						**Mesopelagic**						**Bathypelagic**					
Station	**5**	**8**	**9**	**10**	**14**	**17**	**5**	**8**	**9**	**10**	**14**	**17**	**5**	**8**	**9**	**10**	**14**	**17**
Latitude	24°N	15°N	9°N	2°N	13°S	21°S	24°N	15°N	9°N	2°N	13°S	21°S	24°N	15°N	9°N	2°N	13°S	21°S
Order Calanoida																		
Total Abund. [ind. m^{-3}]	198-659	35-933	62-484	70-601	92-304	130-569	9.3-66	13-42	10-43	7.2-31	4.8-85	5.6-160	1-3-2.1	2.6-5.4	1.1-2.9	1.3-3.5	1.3-2.3	0.5-3.6
No. of species	19-40	43-44	36-48	29-46	23-44	19-47	40-65	45-65	42-59	42-72	43-71	49-55	42-47	39-41	32-34	33-44	30-38	27-54
Family Acartiidae																		
Genus *Arcartia*																		
Acartia spp.	0.82-67	0.02-25	0-21	0-4.3	0-22	0.02-262	0-0.04					0-0.02	0-0.007				0-0.003	0-0.01
A. danae	+	+	+	+	+	+	+					+	+					+
A. negligens	+	+			+	+											+	
Family Aetideidae																		
unident. copepodites	0-0.35	0-0.22	0-0.62	0-0.59	0-0.06	0-0.3	0.1-0.69	0.09-0.38	0.18-0.76	0.15-0.77	0.07-0.72	0.04-0.59	0.05-0.07	0.003-0.007	0.04-0.44	0.04-0.09	0.02-0.16	0-0.02
Genus *Aetideopsis*																		
A. carinata									0-0.02		0-0.02							
A. rostrata								0-0.006						0-0.007				
Aetideopsis sp.								0-0.02					0-0.004					
Genus *Aetideus*																		
A. acutus	0-1.2		0-0.04				0-0.07											
A. arcuatus			0-1		0-1.7		0-0.03	0-0.05	0-0.3	0-0.08	0-0.46	0.006-0.02		0-0.02				0-0.01
A. armatus		0-0.39	0-0.88	0-2.3	0-0.35	0-0.04	0-0.04	0-0.25	0.006-0.45	0-0.92	0-0.31	0-0.03						
A. bradyi		0-0.69	0-1.1	0-0.93	0-0.15						0-0.02							
A. giesbrechti		0-0.04	0-0.19	0-0.11	0-0.12				0-0.1	0-0.04	0-0.02							
Genus *Chiridiella*																		
C. smoki										0-0.006	0-0.005						0-0.003	
Chiridiella sp.																	0-0.003	
Genus *Chiridius*																		
C. poppei		0-0.07	0-0.21			0-0.02	0-0.1	0-0.16	0-0.24	0-0.04	0-0.005	0-0.08	0-0.007	0-0.003				0-0.007
Genus *Chirundina*																		
C. streetsii									0-0.02			0-0.009						
Genus *Euchirella*																		
E. amoena									0-0.006						0-0.003			
E. curticauda										0-0.006								
E. pulchra									0-0.02	0-0.08		0-0.04	0-0.004					
E. rostrata		0-0.06	0-0.3		0-0.03							0-0.02	0-0.007					
E. splendens			0-0.44								0-0.04							
Euchirella spp.			0-0.26	0-0.14	0-0.05	0-0.13	0-0.04	0-0.07	0-0.38	0-0.42	0-0.12	0-0.37				0.003-0.007		

Depth zone	Epipelagic						Mesopelagic						Bathypelagic					
Latitude	24°N	15°N	9°N	2°N	13°S	21°S	24°N	15°N	9°N	2°N	13°S	21°S	24°N	15°N	9°N	2°N	13°S	21°S
Genus *Gaetanus*																		
G. armiger								0-0.006								0-0.003		
G. brevicornis									0-0.01		0-0.05							
G. brevispinus							0-0.006							0-0.04	0-0.003			
G. krupii							0-0.01						0-0.007					
G. latifrons											0-0.005							
G. miles						0-0.02				0-0.006	0-0.02	0-0.23						
G. minor	0-0.08	0-0.15					0-0.27	0-0.28	0-0.3	0-0.4	0-0.05	0-0.39						0-0.01
G. pileatus							0-0.02	0-0.09		0-0.03	0-0.02	0-0.02						0-0.003
G. tenuispinus								0-0.02		0-0.04	0-0.01	0-0.02	0-0.007		0-0.006	0-0.01	0-0.01	
Gaetanus spp.			0-0.17	0-0.03		0-0.04	0-0.07	0-0.04	0-0.21	0-0.08	0-0.03	0-0.09		0.08-0.16		0-0.007		0-0.003
Genus *Pseudochirella*																		
Pseudochirella sp.										0-0.006	0-0.005	0-0.03		0-0.003		0-0.003	0-0.003	0-0.003
Genus *Undeuchaeta*																		
Undeuchaeta cf. *major*							0-0.01	0-0.01		0-0.02		0-0.009						
Genus *Valdiviella*																		
Valdiviella sp.													0-0.003	0-0.003		0-0.003		
Family Arietellidae																		
Genus *Arietellus*																		
Arietellus spp.			0-0.02		0-0.03		0-0.05	0-0.05	0-0.02	0-0.02	0-0.05	0-0.02						
Genus *Paraugaptilus*																		
Paraugaptilus sp.										0-0.006		0-0.02						
Family Augaptilidae																		
unidentified							0-0.02		0-0.006	0-0.02		0-0.009	0-0.007					
Genus *Augaptilus*																		
A. longicaudatus				0-0.02			0-0.02	0-0.02		0-0.03		0-0.02						
A. megalurus										0-0.1		0-0.02				0-0.003		
Augaptilus spp.		0-0.06	0-0.02	0-0.08	0-0.07		0-0.04	0-0.11	0.006-0.02			0-0.02		0.003-0.007				
Genus Centraugaptilus																		
Centraugaptilus sp.					0-0.02			0-0.006	0-0.006	0-0.02								
Genus *Euaugaptilus*																		
Euaugaptilus spp.	0-0.03	0-0.06	0-0.11		0-0.03		0-0.2	0.01-0.15	0.04-0.42	0.02-0.62	0.005-0.57	0-0.14	0.02-0.03	0-0.003	0-0.02	0.003-0.007	0-0.02	0.007-0.06
Genus *Haloptilus*																		
H. acutifrons			0-0.07					0-0.006					0-0.003					
H. austini								0-0.02		0-0.05								
H. fons																		0-0.003
H. longicirrus/longicornis	0-3.8	0-0.94	0-0.79	0-0.69	0.06-3.7	0-0.17	0-3.9	0.02-0.47	0.02-0.51	0.03-0.23	0-0.51	0-0.29	0.02-0.02	0.01-0.02		0-0.02		0-0.003
H. mucronatus				0-0.02														
H. oxycephalus	0-0.04		0-0.04	0-0.05		0-0.07	0-0.1		0-0.02	0-0.006	0-0.005	0-0.009					0-0.006	
H. plumulosus										0-0.006								
H. spiniceps	0-0.07			0-0.04			0-0.006	0-0.02					0-0.007					0-0.003
Haloptilus spp.	0-0.27	0-0.39	0-0.17	0-0.07	0.03-0.06	0-0.02	0.006-0.14	0-0.02	0-0.01		0-0.04	0-0.03				0-0.01	0-0.01	
Genus *Pseudhaloptilus*																		
Pseudhaloptilus sp.	0-0.1			0-0.05				0-0.02		0-0.02	0-0.03							

Family Bathypontiidae																		
Genus *Temorites*																		
T. brevis								0-0.02	0-0.05	0-0.03	0-0.06	0-0.06		0-0.02	0-0.003	0-0.01	0.003-0.006	
T. elongata											0-0.005	0-0.006						
T. minor								0-0.006				0-0.02		0-0.003				0-0.01
T. sarsi							0-0.02				0-0.005		0-0.003			0-0.003		
Temorites spp.							0-0.01		0-0.03	0-0.02	0-0.01	0-0.03	0-0.01	0-0.003	0-0.003	0-0.003	0-0.006	
Genus *Undinella*																		
Undinella spp.							0-0.01	0-0.02	0-0.02	0-0.006	0-0.005						0-0.003	0-0.003
Family Calanidae																		
unident. copepodites		0.75-1.5	0-1.6	0.07-4.3	0-2			0-0.88	0-0.98		0-2.2			0-0.003				
Genus *Calanoides*																		
C. carinatus		0-0.03			0-0.02		0-0.39	0.07-3.7	0-0.02	0-0.006	0-0.1	0.009-0.28	0.003-0.03	0.01-1.6	0.006-0.03	0-0.003	0-0.006	0-0.02
Genus *Calanus*																		
Calanus sp.							0-0.17						0-0.004					
Genus *Mesocalanus*																		
M. tenuicornis	0.04-1.8	0-0.2	0-1.6	0-0.71		0.89-17	0-0.05					0-0.009						
Genus *Nannocalanus*																		
N. minor	0-6.7	0-79	0-27	0.32-32	0-17	0.96-14	0-0.02	0-0.04	0-0.02	0-0.05		0-0.09						
Genus *Neocalanus*																		
N. gracilis	0.81-1.1	0-2.3	0.03-8	0.07-4.1	0-6.7	0.18-0.74	0-0.23	0-0.04	0-0.05	0-0.04		0-0.36						
N. robustior		0-0.04	0-0.3		0-0.97			0-0.006	0-0.08			0-0.006						
Genus *Undinula*																		
U. vulgaris		0-23	0-0.3	0-1.3				0-0.04										
Family Candaciidae																		
Genus *Candacia*																		
Candacia spp.	0.07-1.3	0.04-1.5	0.31-2.4	0.56-1.7	0.03-0.44	0.04-0.28	0-0.33	0-0.03	0-0.03	0-0.04	0-0.005	0-0.24						
C. bipinnata		+			+													
C. bispinosa	+																	
C. catula			+															
C. cheirura						+						+						
C. curta		+	+	+														
C. elongata											+							
C. ethiopica	+																	
C. longimana							+											
C. pachydactyla		+	+	+			+		+									
C. tenuimana				+														
C. truncata					+													
Family Centropagidae																		
Genus *Centropages*																		
C. bradyi		0-0.47	0-1.4	0.07-1.7		0.2-2.4												

Depth zone	Epipelagic						Mesopelagic						Bathypelagic					
Latitude	24°N	15°N	9°N	2°N	13°S	21°S	24°N	15°N	9°N	2°N	13°S	21°S	24°N	15°N	9°N	2°N	13°S	21°S
Family Clausocalanidae																		
Genus *Clausocalanus*																		
Clausocalanus spp.	39-148	5.6-541	12-226	11-456	37-109	0.25-145	0.02-32	0.006-2.8	0.03-8.9	0.02-3.4	0.02-12	0.05-15	0.007-0.02	0.03-0.03	0.02-0.03	0.007-0.01	0.01-0.02	0.01-0.58
Genus *Ctenocalanus*																		
C. vanus	0-2.1	0.78-2.3	0.85-14	0.15-19	0-0.98	0.54-2.2	0-0.07	0-0.02	0-0.62	0-0.33	0-0.05						0-0.003	
Genus *Farrania*																		
Farrania spp.									0-0.02	0-0.02	0-0.02		0-0.003	0-0.003	0.003-0.003	0-0.003	0.003-0.003	0-0.003
Farrania frigida													+	+	+	+		
Farrania oblonga																		
Genus *Microcalanus*																		
Microcalanus spp.		0-6	0.03-2	0-0.31	0-2.7	0-0.02	0.02-1.5	0.82-11	1.3-9	1.1-9.6	0.74-24	0.46-16	0.03-0.08	0.37-0.89	0.1-0.36	0.19-0.42	0.17-0.19	0.1-1.1
Family Discoidae																		
Genus *Disco*																		
Disco spp.	0-0.02		0-0.05	0-0.03			0.05-0.48	0.02-0.19	0.05-0.7	0.04-0.32	0.07-0.43	0.04-0.11	0.05-0.07	0.1-0.11	0.11-0.2	0.04-0.14	0.07-0.1	0.01-0.02
Family Eucalanidae																		
Genus *Eucalanus*																		
Eucalanus hyalinus		0-0.03	0-0.04		0.03-0.06	0.02-0.57	0-0.26		0-0.1	0-0.05	0-0.07	0.006-0.14	0.003-0.08					
Genus *Pareucalanus*																		
P. cf. *sewelli*	0-0.11	0.02-2.8	0-2.5	0-0.86	0-0.25	0-0.57	0.02-0.07	0.02-0.11	0-0.05	0-0.07	0-0.005	0-0.02	0.007-0.05	0.02-0.03	0.006-0.03	0-0.06	0.003-0.003	
Genus *Rhincalanus*																		
R. cornutus	0.02-0.1	0.04-5.3	0.03-0.26	0-0.08	0-0.15	0-0.02	0.09-0.19	0-0.88	0.006-0.1	0.08-0.22	0.005-0.21	0-0.04	0.05-0.18	0.16-0.17	0.003-0.06	0-0.03		0.003-0.007
R. nasutus						0-0.02	0-0.02	0-0.02				0-0.009	0-0.02					0-0.01
Genus *Subeucalanus*																		
S. mucronatus		0-14																
S. pileatus/monachus	0-0.08	1.4-1.7	0-0.22	0.04-0.9	0-0.03		0.24-2.6	1.1-13	0.48-1.1	0.08-0.4	0-0.97	0-0.17	0.003-0.28	0.01-0.17	0-0.03	0-0.04		0-0.02
S. subtenuis			0-3.5	0-0.96	0-3		0-0.02	0-0.02	0-0.02	0-0.08								
Family Euchaetidae																		
unident. copepodites										0-0.13		0-0.07		0.003-0.01				
Genus *Euchaeta*																		
E. acuta			0-0.03				0-0.14		0-0.05	0-0.1								
E. marina	0-1.6	0-3.2	0-0.3	0.07-38	0-6.9			0-0.07	0-0.02			0-0.43				0-0.007		
E. media							0-0.01											
E. paraconcinna		0-1.2																
Euchaeta spp.	0-1.7	1-20	2.3-25	0.25-10	0-0.12	0-0.3	0-1.3	0.06-0.21	0-1.3	0.03-0.85	0-0.23	0-0.02	0-0.004			0-0.003		0-0.007
Genus *Paraeuchaeta*																		
P. aequatorialis							0-0.01	0-0.006					0-0.007			0-0.007		
P. exigua/pseudodontosa								0-0.05		0-0.02	0-0.005							
P. gracilis								0-0.006		0-0.02								
Paraeuchaeta sp.		0-0.03					0-0.006	0-0.03			0-0.005				0.003-0.003	0-0.003		0.003-0.007
Family Fosshageniidae																		
Genus *Temoropia*																		
T. mayumbaensis	0-2	0-0.98	0-2.6	0-2.2	0-0.2	0-0.07	0-1.1		0-0.25	0-0.12	0-0.06	0-0.25						

T. minor	0-0.03						0-0.93	0.07-4.4	0-3.1	0-1.2	0.16-1.1	0-0.31	0.05-0.07	0.27-0.28	0.07-0.2	0.09-0.19	0.08-0.09	0.01-0.24
Family Heterorhabdidae																		
Genus *Disseta*																		
D. palumbii							0-0.04	0-0.02	0-0.01	0-0.006		0-0.006	0-0.004					
Genus *Hemirhabdus*																		
Hemirhabdus sp.															0-0.003			
Genus *Heterorhabdus*																		
H. lobatus/papilliger	0-0.31	0.2-0.78	0.33-2.2	0.05-1.2	0-0.47	0-1.8	0-2.3	0-0.14	0-0.85	0-1.2	0-0.03	0-0.54		0.01-0.04		0-0.007		0-0.03
H. spiniceps	0-0.06	0-0.04	0-0.05				0-0.02		0-0.03	0-0.06		0-0.006						0-0.007
Heterorhabdus spp.	0-5.2	0-2.1	0-3	0-2.6	0-1.4	0-0.18	0-0.95	0-0.55	0-1.5	0-0.35	0.02-1.5	0.07-1.3	0.03-0.03	0.02-0.03	0.006-0.01	0.003-0.01	0.01-0.02	0.007-0.07
Genus *Heterostylites*																		
H. major													0-0.003					
Genus Paraheterorhabdus																		
P. cf. compactus		0-0.02	0-0.04	0-0.02	0-0.02		0-0.08	0-0.006	0-0.05	0-0.006	0-0.06	0-0.02	0-0.03			0-0.01		0.003-0.007
Family Lucicutiidae																		
Genus *Lucicutia*																		
L. aurita												0-0.02						
L. bicornuta							0-0.006	0-0.02										
L. curta										0-0.02				0-0.007				
L. grandis														0-0.003				
L. lucida								0-0.05										
L. macrocera						0-0.13						0-0.04						
L. magna										0-0.04	0-0.01	0-0.006						0.003-0.007
L. wolfendeni																0-0.003		
Lucicutia spp. < 2mm	0.04-13	0.98-1	0.85-13	0.22-8.8	0.09-2	0-3.1	0.26-3.4	0-0.66	0.22-0.83	0.11-0.73	0.21-1.4	0.09-1.5	0.17-0.32	0.12-0.44	0.16-0.26	0.08-0.32	0.12-0.17	0.01-0.06
Family Mecynoceridae																		
Genus *Mecynocera*																		
M. clausi	0.14-9.1		0.02-3.8	0-0.54	0.08-6.1	1.4-149			0-0.02		0-0.03	0-0.11						0-0.003
Family Megacalanidae																		
Genus *Megacalanus*																		
M. princeps								0-0.006		0-0.006	0-0.01			0-0.007				
Family Metridinidae																		
Genus *Gaussia*																		
G. princeps										0-0.006								
Genus *Metridia*																		
M. brevicauda				0-0.07			0-0.34	0-0.12	0-0.37	0-0.99	0-0.23	0-0.11	0.003-0.03	0.06-0.44	0.003-0.07	0.01-0.1		0-0.003
M. curticauda							0-0.01	0-0.02	0-0.41	0-0.02		0-0.23	0-0.007	0-0.003		0-0.003	0-0.02	0-0.003
M. discreta								0-0.04			0-0.4	0-0.52			0-0.006	0.007-0.007	0.003-0.03	0.01-0.02
M. effusa					0-0.03		0-0.07	0-3	0-2.3	0-0.73	0-2.3	0-0.006						0-0.11
M. lucens							0.02-0.59				0-0.16	0-0.13	0-0.02				0-0.003	0-0.06
M. princeps							0-0.02	0-0.006		0-0.02	0-0.01	0-0.04	0-0.003	0-0.007		0-0.003	0-0.003	0.003-0.007

Depth zone	Epipelagic						Mesopelagic						Bathypelagic					
Latitude	24°N	15°N	9°N	2°N	13°S	21°S	24°N	15°N	9°N	2°N	13°S	21°S	24°N	15°N	9°N	2°N	13°S	21°S
M. venusta							0-0.27	0-0.4	0-0.12	0-0.12	0.005-0.13	0-0.05	0-0.01					0-0.02
unident. copepodites	0-6.7	0-1.5	0-3.1	0-10	0-5.6	0-2.1	0-1.1	0-1.6	0-0.41	0-0.37	0.07-0.85	0-0.43						0.01-0.18
Genus *Pleuromamma*																		
P. abdominalis	0-0.03	0-0.13	0.06-0.48	0-0.54	0.03-0.4	0-2.5	0.01-1.3	0.006-0.78	0.01-0.85	0.006-0.85	0-0.34	0.02-4.7	0-0.004					0-0.03
P. borealis	0-0.1			0-0.07	0.12-3.7	0.18-1	0-0.13	0-0.6	0-1.7	0-0.27	0.005-1.7	0-103						0-0.01
P. gracilis/piseki	0-0.02	0.03-2	0-0.22	0-0.12		0-0.15	0.01-0.52	0-1.1	0-0.67	0-5.4	0-0.005	0.02-0.22						0-0.14
P. quadrungulata	0-1.3	0-0.02	0-0.12		0-0.25		0-1.3	0-0.03	0-0.32	0-0.03	0-0.35	0-1.1						
P. robusta						0-0.04	0-0.02	0-0.02	0-0.02	0-0.08	0-0.02	0-0.02					0-0.003	
P. xiphias						0-0.04	0-0.08	0-0.08	0-0.006	0-0.04	0-0.01	0-0.41	0-0.004					0-0.01
Pleuromamma spp. < 2 mm	0-4.3		0-1.9	0-4.9		0-81	0-4.1	0-0.59	0-1.7	0-0.27	0-0.01	0-0.44					0-0.003	
Family Nullostigeridae																		
Genus *Nullosetigera*																		
N. bidendata								0-0.02		0-0.006	0-0.005	0-0.05						
N. helgae		0-0.03					0-0.22	0-0.18	0-0.16	0-0.05	0-0.09		0.003-0.004					
N. impar							0-0.006	0-0.02			0-0.03		0-0.003	0-0.01				
N. mutica											0-0.005			0-0.003				
Nullosetigera spp.						0-0.02	0-0.2	0-0.1	0-0.13			0-0.006		0-0.007	0-0.009	0.003-0.007	0-0.003	0-0.02
Family Paracalanidae																		
Genus *Acrocalanus*																		
Acrocalanus spp.		0-48	0-1.1	0.02-17					0-0.02									
Genus *Calocalanus*																		
Calocalanus spp.	8.8-27	0.94-101	3.4-93	4.1-91	1.4-45	2.4-105	0-0.12	0-0.12	0-0.05	0-0.15	0-0.06	0-0.18	0.004-0.007		0-0.003	0-0.003	0-0.02	0-0.01
Genus *Delibus*																		
D. cf. *nudus*	117-405		0.16-236	3.3-39	22-78	0-0.04	0-0.8		0-0.02		0.06-0.77		0-0.04		0.006-0.03	0-0.003	0.02-0.03	0-0.003
Genus *Paracalanus*																		
Paracalanus spp.	1.1-3.2	0-5.2	0-14	0.37-11	0.18-35	1.3-15	0-0.1	0-0.14	0-0.13	0-0.08	0-0.08	0-0.04	0.02-0.04					0-0.003
Family Phaennidae																		
unidentified											0-0.02	0-0.006			0-0.009	0-0.003		
Genus *Cephalophanes*																		
Cephalophanes spp.								0-0.01			0.005-0.03	0-0.006						
C. frigidus																		
C. refulgens																		
Genus *Onchocalanus*																		
Onchocalanus sp.							0-0.006			0-0.006								
Genus *Phaenna*																		
P. spinifera	0-0.02	0.02-0.13	0-0.1				0-0.04		0-0.02		0-0.08							
Family Pontellidae																		
Genus *Lapidocera*																		
Lapidocera spp.		0-0.28	0-0.45															

Genus *Pontellina*																		
Pontellina spp.		0-0.25	0-0.36	0-0.33	0-0.03	0-0.18												
Family Scolecithrichidae																		
unidentified			0-0.69				0-0.68		0.3-0.67	0-0.23	0-0.005	0-0.07		0-0.01	0-0.03		0.003-0.003	0.02-0.04
Genus *Amallothrix*																		
Amallothrix spp.	0-0.03	0.03-0.65		0-0.04			0-0.04	0.006-0.64	0-0.05	0.02-0.03	0.01-0.02	0.02-0.38	0.007-0.02	0.003-0.01	0-0.003	0.02-0.02	0-0.02	0.02-0.02
Genus *Brodskius*																		
B. cf. *paululus*								0-0.18	0-0.35	0-0.13	0-0.02	0-0.02		0.003-0.07	0.009-0.03	0.003-0.07	0-0.003	
Genus *Falsilandrumius*																		
Falsilandrumius sp.										0-0.006		0-0.02						
Genus *Heteramella*																		
Heteramella sarsi											0-0.005		0-0.003				0-0.003	
Genus *Lophothrix*																		
L. frontalis								0-0.02			0-0.01							
L. humilifrons										0-0.01		0-0.02		0-0.003	0-0.01	0-0.003		
L. latipes		0.02-0.06	0-0.02				0-0.29		0-0.03									0-0.007
L. quadrispinosa											0-0.02							
L. similis											0-0.01							
Lophothrix spp.							0-0.006	0-0.006	0-0.02	0-0.08	0-0.01	0-0.009	0-0.004	0-0.007				
Genus *Pseudoamallothrix*																		
Pseudoamallothrix spp.		0-0.06					0-0.02		0-0.05	0-0.12	0-0.04	0-0.17	0.003-0.01	0-0.003	0-0.003	0-0.007	0-0.02	
Genus *Scaphocalanus*																		
S. cf. *magnus*								0-0.03	0-0.02	0-0.01	0-0.02	0-0.04	0-0.007	0.003-0.003		0.003-0.003	0-0.003	0.007-0.007
Scaphocalanus spp.	0-0.96	0.03-1.4	0-3.8	0.04-4.8	0-2.2	0-0.91	0.57-2.4	0.38-2.6	0.31-3	0.23-2.8	0.12-6.6	0.13-3.1	0.05-0.08	0.07-0.09	0.02-0.05	0.01-0.09	0.03-0.05	0.003-0.16
Genus *Scolecithricella*																		
S. maritima	0-0.11	0-0.2			0-0.58		0-0.03	0-0.35	0-0.73	0-0.54	0.12-1.5	0-0.06	0-0.01	0-0.03	0.01-0.05	0.04-0.09	0.01-0.04	
S. vittata					0-0.27	0-0.04		0-0.02	0-0.08		0-0.11							
Scolecithricella spp.	0-2.3	0-2.1	0.03-1.8	0-2.7	0-2.4	0-0.44	0.2-1.8	0.23-3.2	0.22-1.8	0.03-1.7	0.23-2.5	0.13-2.1	0.02-0.05	0.06-0.15	0.03-0.08	0.03-0.18	0.05-0.08	0.02-0.17
Genus *Scolecithrichopsis*																		
S. ctenopus		0-0.78	0-0.03	0-0.11					0-0.01									
S. tenuipes		0-0.2	0-1.3	0-1.1	0-0.23	0-0.04		0-0.05	0-1.7	0-0.35	0-0.29	0-0.009						
Scolecithrichopsis sp.								0-0.04		0-0.006		0-0.006						
Genus *Scolecithrix*																		
S. bradyi		0-0.34	0.48-5	0.04-0.89	0-0.02	0-1.3	0-0.07		0-0.06	0-0.02								
S. danae	0-0.33	0-5.3	0-3	0.12-3.3	0.1-6	0-1.1		0-0.04	0-0.03	0-0.06	0-0.03							
Genus *Scottocalanus*																		
S. helenae									0-0.05									
S. persecans							0-0.01		0-0.02	0-0.07	0-0.005	0-0.009						
S. securifrons							0-0.02	0-0.05			0-0.02							
Family Spinocalanidae																		
Genus *Mimocalanus*																		
Mimocalanus spp.		0-0.15			0-0.03	0-0.04	0-0.2	0.1-0.19	0.05-0.55	0.02-0.47	0.1-0.92	0-0.15	0.02-0.03	0.06-0.14	0.01-0.06	0-0.05	0.03-0.03	0.01-0.01

Depth zone	Epipelagic						Mesopelagic						Bathypelagic					
Latitude	24°N	15°N	9°N	2°N	13°S	21°S	24°N	15°N	9°N	2°N	13°S	21°S	24°N	15°N	9°N	2°N	13°S	21°S
Genus *Monacilla*																		
M. tenera										0-0.006			0.007-0.02	0-0.01	0.003-0.02	0.007-0.02	0-0.003	
M. typica							0-0.03	0-0.23	0-0.09	0-0.1	0.02-0.08	0-0.03		0-0.007	0-0.006	0-0.01		0-0.007
Genus *Mospicalanus*																		
Mospicalanus cf. *schielae*											0-0.005				0-0.03		0.04-0.35	
Genus *Spinocalanus*																		
Spinocalanus spp.		0-1.6	0-0.84	0-0.32	0-0.67	0-0.02	2.4-8.8	1.6-6	2.2-7.7	2.5-4.5	1.6-19	0.79-6.4	0.36-0.43	0.52-0.7	0.18-0.61	0.57-1.3	0.38-0.85	0.15-0.47
Genus *Teneriforma*																		
Teneriforma spp.							0-0.09	0.03-0.14	0.04-0.17	0-0.1	0.02-0.04	0.009-0.03	0.01-0.01	0-0.007	0-0.02	0-0.02	0.01-0.02	0-0.02
Family Temoridae																		
Genus *Temora*																		
T. stylifera		0-46	0-0.55	0-0.18				0-0.02						0-0.003				
Family Tharybidae																		
Genus *Tharybis*																		
Tharybis sp.									0-0.006						0.003-0.003	0-0.007		
Unident. copepodites	0-0.34	0-0.61		0-0.78		0-0.19	0-1.8	0.09-1.1	0-0.53	0.36-0.79	0.07-0.23	0-0.09	0.03-0.1	0.03-0.14	0.1-0.28	0.05-0.18	0.03-0.03	0-0.003
Order Cyclopoida																		
Family Oithonidae																		
Genus *Oithona*	52-164	30-146	92-225	43-113	72-300	201-466	5.2-58	5.3-36	10-71	5-18	7-87	3.7-41	0.14-1.2	1.6-2.1	0.78-2	0.29-3.9	1.4-1.4	0.2-8.8
Family Oncaeidae	11-52	41-269	67-130	112-177	16-60	9.3-39	20-47	13-276	21-140	18-89	14-207	9.1-97	3.9-5.4	6.9-9.6	2.7-7.2	2.1-12	6.7-6.8	0.93-8.3

ACKNOWLEDGEMENTS

At first, I would like to express my special appreciation and thanks to my supervisors, Prof. Dr. Wilhelm Hagen and PD Dr. Holger Auel, for providing me an excellent working place at the Marine Zoology department of the University of Bremen. Thank you for your constant support, scientific guidance and valuable and constructive comments on early drafts of my work, which contributed significantly to this dissertation. Thank you, Willy for offering me the opportunity to conduct my thesis at the University of Bremen, for thorough proof-reading and supporting me during the whole time. Thank you, Holger for many valuable and fruitful discussions during the past years, which were essential to achieve progress during this thesis.

I would also like to thank my second referee Dr. Werner Ekau for his time and expertise. Also thanks to the member of my GLOMAR Thesis Committee, Prof. Dr. Wilhelm Hagen, PD Dr. Holger Auel, Dr. Reinhard Saborowski, Dr. Rolf Koppelmann, Dr. Astrid Cornils and Dr. Silke Laakmann, for their guidance, valuable assistance and proof-reading during this study.

I am very grateful to Dr. Astrid Cornils and Dr. Silke Laakmann, who initiated a major part of my thesis and inspired me. Thank you, Astrid, for assisting me with taxonomic and genetic expertise. Thank you, Silke, for introducing me to genetic analyses and handling the MALDI-TOF MS. Thank you, both, for your kindness, constant support and constructive help, which significantly contributed to the accomplishment of this study.

I really appreciate the time I spent at the NatMIRC in Swakopmund, Namibia. My special thanks go to Dr. Anja Kreiner, who gave me the possibility to work with this very valuable long-term data set and kindly supported me during my research stay. Thank you also Anja, Deon and Richard for your warm welcome and support during this time.

I want to thank the Federal Ministry of Education and Research (BMBF), who financially supported parts of this thesis embedded into the GENUS project (03F0650E).

Furthermore, I would like to thank the captain and crew of the RV *Polarstern* for their competent and friendly support during the fieldwork, and the chief scientist PD Dr. Holger Auel for a fantastic cruise. Special thanks go the students of the EUROPA trainings cruise, who helped with handling the nets, copepod sorting and respiration measurements. I would also like to thank Dr. Lena Teuber for supervising the respiration measurements and for her scientific and mental

support during the cruise, Thomas Kanitz for providing me with food and coffee in the cold container, Michael Ginzburg for “decorating” my container, and all of them for an unforgettable cruise.

I am very grateful for the time in the Marine Zoology department, embedded in the BreMarE Institute at the University of Bremen. Thank you all for proving scientific and mental support during the past years. It was a great team offering help and advice any time. Dr. Lena Teuber, Dr. Anna Schukat, Dr. Sabine Schründer, Marina Giunio, Joy N. Smith, Dr. Karin Boos, Simon Jungblut, Timothy Thomson, Hagen Buckwiese and Patricia Kaiser: I could not imagine having better colleagues, thank you for a pleasant atmosphere, all the help and inspiring kitchen talks.

Especially I would like to thank Anna, Lena and Sabine for all your help, proof reading and support during the whole time.

I would also like to thank Prof. Dr. Pedro Martínez Arbizu for offering their laboratory facilities and the valuable MALDI-TOF MS at the DZMB, Senckenberg am Meer, in Wilhelmshaven. My sincere thanks go also to Rebekka Schüller, Dr. Thomas Knebelsberger and Dr. Silke Laakmann for their help and warm support during my work.

Furthermore, I would like to thank Dr. Janne Timm for allowing me to use the laboratory facilities for parts of the genetic analyses at the UFT at the University of Bremen.

My special thanks go to Sebastian Gibb, who supported me to establish the R scripts for the MALDI-TOF analyses, with an exemplary willingness to help, although we have never met.

Last but not least, I would like to sincerely thank all my friends and family for their endless encouragement, patience and believe in me during the past years.

Thank you, Jonas that you are there!

ERKLÄRUNG

Eidestattliche Erklärung

(Gem. § 6(5) Nr. 1-3 PromO)

Hiermit versichere ich, dass ich die vorliegende Arbeit mit dem Titel:

„Pelagic Biodiversity and Ecophysiology of Copepods in the Eastern Atlantic Ocean - Latitudinal and Bathymetric Aspects“

- ohne unerlaubte, fremde Hilfe angefertigt habe,
- keine anderen, als die von mir im Text angegebenen Quellen und Hilfsmittel benutzt habe,
- die den benutzten Werken wörtlich oder inhaltlich entnommenen Stellen als solche kenntlich gemacht habe.

Des Weiteren erkläre ich hiermit, dass es sich bei den drei abgegebenen Exemplaren dieser Arbeit um drei identische Ausführungen handelt.

Bremen, den 01.02.2015

Maya Bode

Maya Bode

February 2016